SafeG

(Project Number: 945 041)

DELIVERABLE D5.2

Proceedings of the Advanced modelling techniques workshop

Lead Beneficiary: University of Cambridge

Due date: 01/09/2023 Released on: 01/09/2023

Authors:	Congjin Ding

For the Lead Beneficiary	**Reviewed by Work package Leader**	**Approved by Coordinator**
Eugene SHWAGERAUS	**Eugene SHWAGERAUS**	**Branislav HATALA**

Start date of project: **01/10/2020** Duration: **48 Months**
Project Coordinator: **Branislav Hatala**
Project Coordinator Organisation: **VUJE, a. s.** VERSION: **0.1**

Project co-funded by the European Commission under the Euratom Research and Training Programme on Nuclear Energy within the Horizon 2020 Programme		
Dissemination Level		
PU	Public	**X**
RE	Restricted to a group specified by the Beneficiaries of the MEET-CINCH project	
CO	Confidential, only for Beneficiaries of the MEET-CINCH project	

Version control table

Version number	Date of issue	Author(s)	Brief description of changes made
0.1	17.08.2023	Congjin Ding	First version (not reviewed)
1.0	04.09.2023	Eugene Shwageraus	Reviewed by WP leader
1.1	05.09.2023	Michaela Velckova	Reviewed by MST Final version

Project information

Project full title:	Safety of GFR through innovative materials, technologies and processes
Acronym:	SafeG
Funding scheme:	Research and innovation action
ECGA number:	945041
Programme and call	Horizon 2020 Framework Programme for Research and Innovation (2014-2020) NFRP-2019-2020 (Nuclear Fission and Radiation Protection Research)
Coordinator:	Dr. Branislav Hatala
EC Project Officer:	Dr. Cristina Fernandez Ramos
Start date – End date:	01/10/20 – 30/09/2024 i.e. 48 months
Coordinator contact:	+421 905 567 985, branislav.hatala@vuje.sk
Administrative contact:	+420 602 771 784, jakub.heller@evalion.cz
Online contacts (website):	www.safeg.eu

„This project has received funding from the Euratom research and training programme 2019-2020 under grant agreement No 945041".

EXECUTIVE SUMMARY

The SafeG Workshop on Advanced Modelling Techniques was held from July 3rd to 6th at the University of Cambridge as part of the SafeG project's WP5. The event was attended by thirty-five participants from a diverse range of countries, including the Czech Republic, Hungary, Slovakia, the United Kingdom, Germany, Italy, Nigeria, the Philippines, Switzerland, and the USA. Esteemed experts and professors delivered lectures on a wide range of topics, including historical reviews and experience of GFR, GFR design and technology, modelling methods and codes, CFD, thermal hydraulic analysis, and more. In addition to the technical sessions, the workshop also featured a visit to the Sizewell B nuclear power plant and a delightful social dinner event. Participants provided overwhelmingly positive feedback regarding both the content and organisation of the workshop.

This deliverable describes the preparation process, program, and other outcomes. Presentations from the technical lectures are attached to this document.

This document is prepared in compliance with the template provided by the Commission in Annex 1 of the Guidelines on Data Management in Horizon 2020.

CONTENT

1 EVENT DESCRIPTION

The Advanced Modelling Techniques Workshop was organised within SafeG project WP5 at the University of Cambridge, United Kingdom, in 2023. The three and a half days event were targeted at students and young professionals dealing with CFD and other high-fidelity computational tools. The program comprised lectures from GFR modelling and technology experts and a technical tour. The participants were students and young professionals from research and academic institutions involved in the SafeG project and those outside the project. This deliverable briefly describes the preparation and program of the event, the outcomes, and feedback. Apart from this, the purpose of the deliverable is to collect and share presentations from the attached technical lectures.

1.1 Event preparation

The workshop was originally scheduled for the summer of 2022. Due to the COVID restrictions, the first summer school was delayed for one year and held in 2022. Thus, the workshop was organised in 2023 to prevent the overlap. The final dates were from 3rd to 6th July 2023. The preparation activities were launched in March 2023 by the promotion of the event, contacting the speakers and development of the technical programme. To enhance the event promotion, a leaflet was prepared and shared via social media networks, Eventbrite website, emails, printed posters, and SafeG websites (as shown in Figure 1).

Figure 1: GFR Workshop promotional leaflet

More than 35 candidates applied for participation through a registration form. The total capacity of the event, including lecturers, was set to 30. The final number of participants was 35, including 24 students or young professionals and 11 senior participants or lecturers. The participants were from institutions in 10 countries (the Czech Republic, Hungary, Slovakia, the United Kingdom, Germany, Italy, Nigeria, the Philippines, Switzerland, and the USA).

The technical lectures were designed to cover essential topics in GFR development and modelling techniques. A detailed description of the technical program follows in Section 1.2.

1.2 Program description

This section briefly describes the program of the workshop, as shown in Figure 2. The content of lectures is presented in the attached presentation slides.

SafeG Workshop - Advanced Modelling Techniques — UNIVERSITY OF CAMBRIDGE

Programme outline

3rd July 2023		
12:30-13:20	Registration & Lunch, Lecture Room 5	
13:30-14:00	Welcome, Event introduction, Lecture Theatre 6	*E. Shwageraus (UCAM)*
14:00-17:00	Technical session 1, Lecture Theatre 6	
14:00-15:00	A historical review of EU GFR projects	*K. Mikityuk (PSI)*
15:00-15:20	Coffee break, Lecture Room 5	
15:20-16:20	Application of Serpent to modelling of innovative reactors in international projects	*E. Fridman (HZDR)*
16:20-17:00	Q&A + Interaction session	
4th July 2023		
09:00-12:20	Technical session 2, Lecture Theatre 6	
09:00-10:00	Experience and lessons learned from the ALLEGRO TH benchmark	*B. Kvizda (VUJE)*
10:00-10:20	Coffee break, Lecture Room 5	
10:20-11:20	Turbulence in CFD	*G. Mayer (EK)*
11:20-12:20	Use of the deterministic code WIMS to model Gen-IV reactors	*J. Lavarenne (Jacobs)*
12:20-13:50	Lunch, Lecture Room 5	
14:00-15:00	Technical session 2 (continued), Lecture Theatre 6	
14:00-15:00	GFR technology from the modelling perspective	*P. Vacha (UJV)*
15:00-17:00	Cultural visiting: City Tour (Group A) / Botanic Garden (Group B)	
19:00	Event dinner, St Catharine's College	
5th July 2023		
09:00-12:20	Technical session 3, Lecture Theatre 6	
09:00-10:00	Lessons learned from operation of gas-cooled reactors in the UK	*R. Stainsby (Jacobs)*
10:00-10:20	Coffee break, Lecture Room 5	
10:20-11:20	The effect of thermodynamic and transport properties in thermal and hydraulic analysis of gas systems	*V. Dostal (CVUT)*
11:20-12:20	SCONE: a Monte Carlo particle transport code for prototyping of new methods	*P. Cosgrove (UCAM)*
12:20-13:50	Lunch, Lecture Room 5	
14:00-15:30	Technical session 3 (continued), Lecture Theatre 6	
14:00-15:00	Nuclear fuel behaviour during severe accidents: A CFD perspective	*A. Dubey (UCAM)*
15:00-15:30	Q&A + Closing discussion	
15:30-17:00	Cultural visiting: City Tour (Group B) / Botanic Garden (Group A)	
6th July 2023		
08:00-17:00	Technical tour: Sizewell B PWR	

Contact: Jo Boyle jb780@cam.ac.uk / Congjin Ding cd825@cam.ac.uk

Figure 2: Program of the Workshop

The program commenced on Monday July 3rd with a registration and welcome session. A group photo was taken on the first day of the event to capture the excitement and anticipation of all attendees, as shown in Figure 3.

Figure 3: Workshop Group photo in the Department of Engineering

Then, the technical session with the lectures have commenced. **Modelling and Simulation of Advanced Reactors Workshop** talk was given by **Eugene Shwageraus** from UCAM as the event introduction. The nuclear-related research at the University of Cambridge was presented, including its historical achievements and current developments, including research, projects, and education (see Appendix 2.1).

A historical review of EU GFR projects focused on the previous GFR projects and the gained experience talk was given by **Konstantin Mikityuk** from PSI. The selected GFR-related EU projects (2005 –2017) focusing on experiments relevant for validation were reviewed, including FP6 GCFR, FP7 GoFastR, and FP7 ESNII Plus (see Appendix 2.2).

Application of Serpent to modelling of innovative reactors in international projects talk was presented by **Emil Fridman** from HZDR. A few examples of Serpent applications in fast reactor analysis were introduced, including fuel cycle analysis of ESFR multi-batch burnup, Neutronics data for transient analysis of SFRs, dynamic simulations of CEFR control rod drop tests, and mechanical core deformations and CAD models of Phenix reactor core flowering event (see Appendix 2.3).

The lectures encompassed a diverse range of topics, which were presented in an engaging and professional manner. The lecturers facilitated exchanges between the students during the discussion time, resulting in a fruitful and enriching learning experience, as shown in Figure 4 and Figure 5.

Figure 4: Technical session 1

Figure 5: Technical session 2

Lunch and refreshments were conveniently organised in a room adjacent to the lecture theatre, providing ample opportunity for attendees to engage in discussions and network with one another, as shown in Figure 6.

Figure 6: Lunch time

The program on Tuesday 4th July was composed of technical lectures and cultural visits.

Experience and lessons learned from the ALLEGRO TH benchmark lecture was given by **Boris Kvizda** from VUJE. The ALLEGRO design was introduced, along with a benchmark exercise for thermal-hydraulic (TH) calculations. International recommendations and national requirements for nodalisation qualification were discussed, as well as the origins of uncertainties in TH calculations. Tools and methods for qualifying TH models and existing nodalisation codes were also presented (see Appendix 2.4).

Turbulence in CFD talk was given by **Gusztáv Mayer** from EK. Turbulence models, including Reynolds Averaged Navier Stokes (RANS), Large Eddy Simulation (LES), and Direct Numerical Simulation (DNS) were introduced and compared. These models are used to simulate turbulent flows and each has its own advantages and limitations (see Appendix 2.5).

Use of the deterministic code WIMS to model Gen-IV reactors talk was presented by **Jean Lavarenne** from Jacobs. The characteristics of deterministic methods are introduced and compared with Monte Carlo methods. A two-step approach to core modelling is illustrated and case studies using the WIMS code are presented, including modelling of the ESFR SMART and ALLEGRO reactors (see Appendix 2.6).

GFR technology from the modelling perspective presentation was given by **Petr Vácha** from UJV. The designs of GFR and ALLEGRO reactor were outlined. The design and modelling of selected main systems and components, including the core region, main cooling loops, Decay Heat Removal system, and containment, were introduced. Additionally, the modelling of severe accidents in GFRs were presented (see Appendix 2.7).

After the technical session, the cultural visits took place and included a city tour and a trip to the botanical garden, spread over two days. Participants were divided into two groups, each visiting one of the attractions and changing the next day. A photo capturing the moment of the cultural visit is shown in Figure 7.

Figure 7: In the botanical garden

On the evening of the second day, a formal dinner was organised at St Catharine's College as another networking and social event. This provided an excellent opportunity for workshop participants to connect with one another. A photo capturing the atmosphere of the event dinner is shown in Figure 8.

Figure 8: The event dinner at St Catharine's College

The program on Wednesday 5th July also combined both lectures and cultural visits.

Lessons learned from operation of gas-cooled reactors in the UK presentation was given by **Richard Stainsby** form Jacobs. The history of Gas Cooled Reactors in the UK was introduced, including the Windscale Piles, Magnox Reactors, and Advanced Gas Cooled Reactors (AGR). The lessons learned and operational experience from these reactors were summarised. Additionally, the differences between AGRs and GFR are pointed out (see Appendix 2.8).

The effect of thermodynamic and transport properties in thermal and hydraulic analysis of gas systems lecture was presented by **Václav Dostál** from CVUT. The advantages of the Supercritical CO_2 Cycle were introduced and compared with other power cycles. Typical correlations for heat transfer are presented, along with the Decay Heat Removal system and natural circulation in GFR. The geometry and modelling of the ALLEGRO Core Catcher were displayed and discussed (see Appendix 2.9).

SCONE: A Monte Carlo particle transport code for prototyping of new methods was given by **Paul Cosgrove** from UCAM. The features and user experience of the SCONE code were introduced along with several showcases, including thermal radiative transfer, multigroup acceleration of continuous energy Monte Carlo simulations and the random ray method (see Appendix 2.10).

Nuclear fuel behaviour during severe accidents: A CFD perspective talk was presented by **Anuj Dubey** from UCAM. The motion of molten nuclear fuel during an unprotected transient overpower accident was introduced and analysed using CFD modelling and experimental validation. Simulations of severe accidents and the effects of fission gas pressurization were also presented (see Appendix 2.11).

After the lectures concluded, we held a closing discussion and took a group photo in the lecture theatre to commemorate the end of the technical session, as shown in Figure 9.

Figure 9: Group photo in the lecture room

On Thursday July 6th, the final day of the program, participants embarked on a technical tour of the **Sizewell B nuclear power plant**. Located on the Suffolk coast, Sizewell B is the UK's only Pressurised Water Reactor (PWR) and its most modern nuclear power station. The tour provided a unique insight into the plant's technology through its interactive exhibition space. Participants were divided into groups and accompanied by a trained station guide, who provided an introduction and detailed explanation of the technology. A group photo was taken in front of Sizewell B to commemorate the visit, as shown in Figure 10.

Figure 10: Group photo of the technical trip in Sizewell B NPP

After the technical tour, the SafeG Workshop on Advanced Modelling Techniques came to a close. The workshop provided valuable insights and discussions on the latest techniques and methods for modelling nuclear reactors.

1.3 Conclusion and feedbacks

It can be concluded that the 3.5-day workshop was a success, featuring 2.5 days of technical sessions, cultural visits, a social event, and a technical tour. The workshop successfully met its objectives of experience sharing, networking, and disseminating knowledge generated within the SafeG project. Participants provided overwhelmingly positive feedback regarding both the organization and technical content of the workshop.

The lectures, delivered by experts and professors, provided comprehensive coverage of a wide range of topics, including historical reviews and experience of GFR, GFR design and technology, modelling methods and codes, CFD and thermal hydraulic analysis. These sessions facilitated fruitful exchanges between senior experts and young professionals from diverse research backgrounds.

The high-quality program effectively achieved the goals outlined in the work package. The schedule was specifically crafted to balance technical sessions with cultural tours, while the

timing of lectures, coffee breaks, and lunch was intentionally designed to facilitate easy comprehension and focus.

The number of participants exceeded expectations even at the upper bound of our Key Performance Indicator. The highest KPI for this event defined in the project proposal has been achieved (>25 participants is considered “excellent”).

In an effort to further publicise the project and expand our outreach, we shared highlights of the workshop on LinkedIn following its conclusion.

2 APPENDIX – LECTURES PRESENTATIONS

2.1 Modelling and Simulation of Advanced Reactors Workshop

Please see attached pdf document “1-0-Shwageraus”

2.2 A historical review of EU GFR projects

Please see attached pdf document “1-1-Mikityuk”

2.3 Application of Serpent to modelling of innovative reactors in international projects

Please see attached pdf document “1-2-Fridman”

2.4 Experience and lessons learned from the ALLEGRO TH benchmark

Please see attached pdf document “2-1-Kvizda”

2.5 Turbulence in CFD

Please see attached pdf document “2-2-Mayer”

2.6 Use of the deterministic code WIMS to model Gen-IV reactors

Please see attached pdf document “2-3-Lavarenne”

2.7 GFR technology from the modelling perspective

Please see attached pdf document “2-4-Vácha”

2.8 Lessons learned from operation of gas-cooled reactors in the UK

Please see attached pdf document “3-1-Stainsby”

2.9 The effect of thermodynamic and transport properties in thermal and hydraulic analysis of gas systems

Please see attached pdf document “3-2-Dostál”

2.10 SCONE: A Monte Carlo particle transport code for prototyping of new methods

Please see attached pdf document “3-3-Cosgrove”

2.11 Nuclear fuel behaviour during severe accidents: A CFD perspective

Please see attached pdf document “3-4-Dubey”

SafeG

UNIVERSITY OF CAMBRIDGE

Modelling and Simulation of Advanced Reactors Workshop

Eugene Shwageraus

Department of Engineering

University of Cambridge

3-6 July 2023

Agenda

3rd July 2023		
12:30-13:20	Registration & Lunch, Lecture Room 5	
13:30-14:00	Welcome, Event introduction, Lecture Theatre 6	*E. Shwageraus (UCAM)*
14:00-17:00	Technical session 1, Lecture Theatre 6	
14:00-15:00	A historical review of EU GFR projects	*K. Mikityuk (PSI)*
15:00-15:20	Coffee break, Lecture Room 5	
15:20-16:20	Application of Serpent to modelling of innovative reactors in international projects	*E. Fridman (HZDR)*
16:20-17:00	Q&A + Interaction session	
4th July 2023		
09:00-12:20	Technical session 2, Lecture Theatre 6	
09:00-10:00	Experience and lessons learned from the ALLEGRO TH benchmark	*B. Kvizda (VUJE)*
10:00-10:20	Coffee break, Lecture Room 5	
10:20-11:20	Turbulence in CFD	*G. Mayer (EK)*
11:20-12:20	Use of the deterministic code WIMS to model Gen-IV reactors	*J. Lavarenne (Jacobs)*
12:20-13:50	Lunch, Lecture Room 5	
14:00-15:00	Technical session 2 (continued), Lecture Theatre 6	
14:00-15:00	GFR technology from the modelling perspective	*P. Vacha (UJV)*
15:00-17:00	Cultural visiting: City Tour (Group A) / Botanic Garden (Group B)	
19:00	Event dinner, St Catharine's College	

Agenda

5th July 2023		
09:00-12:20	Technical session 3, Lecture Theatre 6	
09:00-10:00	Lessons learned from operation of gas-cooled reactors in the UK	*R. Stainsby (Jacobs)*
10:00-10:20	Coffee break, Lecture Room 5	
10:20-11:20	The effect of thermodynamic and transport properties in thermal and hydraulic analysis of gas systems	*V. Dostal (CVUT)*
11:20-12:20	SCONE: a Monte Carlo particle transport code for prototyping of new methods	*P. Cosgrove (UCAM)*
12:20-13:50	Lunch, Lecture Room 5	
14:00-15:30	Technical session 3 (continued), Lecture Theatre 6	
14:00-15:00	Nuclear fuel behaviour during severe accidents: A CFD perspective	*A. Dubey (UCAM)*
15:00-15:30	Q&A + Closing discussion	
15:30-17:00	Cultural visiting: City Tour (Group B) / Botanic Garden (Group A)	
6th July 2023		
08:00-17:00	Technical tour: Sizewell B PWR	

Cambridge Nuclear History

- William Cavendish donated funds, named after Henry Cavendish discoverer of hydrogen
- J. C. Maxwell first Cavendish Professor of Experimental Physics (1871)
- Lord Rayleigh (1879), argon, Ra number, light scattering
- J. J. Thompson, discovery of electron
- E. Rutherford (1918), atom model, nucleus, proton
- J. Chadwick, neutron (1932)
- William Bragg (1938), x-ray diffraction
- Charles Wilson, Wilson's cloud chamber
- Arthur H. Compton, scattering and absorption of γ-rays, Compton Effect
- John Cockcroft and Ernest Walton particle accelerator
- 30 Nobel Laureates, x-ray diffraction applications, superconductivity
- Oppenheimer (1924-1926), alleged poisoning attempt of Patrick Blackett

Department of Engineering

- Professorship of Natural Experimental Philosophy endowed in 1782
- Morphed into Professorship of Mechanism and Applied Mechanics in 1875
- John Baker theory of plasticity, Backer building opened in 1952
- John A. Inglis, Bertram Hopkinson, James A. Ewing, theory of vibrations
- Frank Whittle, inventor of the jet engine
- Charles W. Oatley, scanning electron microscope
- Harry Ricardo, internal combustion engines, Ricardo PLC
- Ann Dowling, quiet jet engines
- Christopher Hinton, chief engineer of Calder Hall, first chairman of CEGB, led construction of many major nuclear installations in the UK

Nuclear research

- A cross-discipline collaboration:
  - Physics, Engineering, Earth Sciences, Materials Sciences, Chemical Engineering, Economics, Judge Business School
- Coordinates nuclear research and teaching across the University
- Undergraduate modules
- Nuclear Energy MPhil
- Doctoral Training Centre – Nuclear Energy Futures (NEF-CDT)

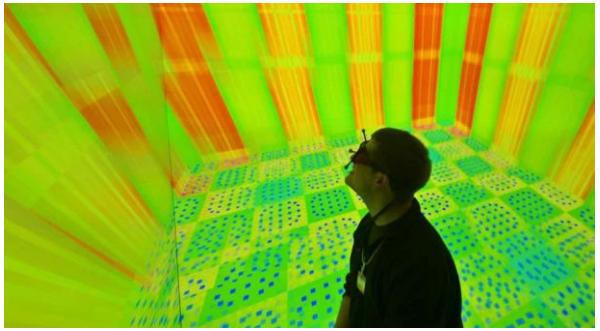

6

MPhil in Nuclear Energy

- **Taught 1 year MPhil** in Nuclear Energy (runs October – August each year)
  - **15 -25 students** from around the world each year
  - **5 core nuclear engineering** modules
  - **Nuclear policy** module
  - **Elective** modules from Engineering, Materials Science, Chemical Engineering, Physics and Judge Business School
  - 4 months project on either:
    - Cambridge University or
    - Industry partner research topic

中广核 CGN
中广核研究院有限公司
China Nuclear Power Technology Research Institute Co.,Ltd.

NDA Nuclear Decommissioning Authority

ROLLS ROYCE

AWE

framatome

urenco The Energy to Succeed

Westinghouse

Research themes

- Advanced reactor design
  - Space propulsion and power
  - Molten Salt-cooled reactors
  - New fuels for LWRs/SMRs
  - Sodium and Gas-cooled Fast Reactors (EU funded projects)
  - Design optimisation methods

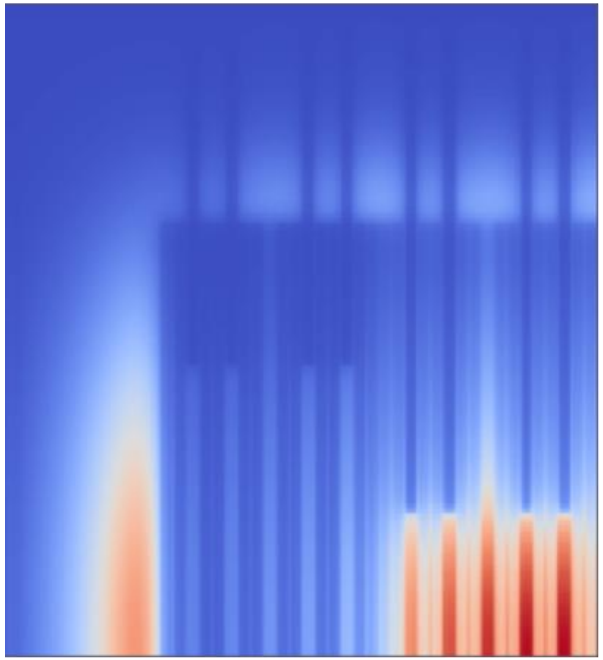

- Modelling methods development
  - Monte Carlo for radiation transport
  - Stochastic Calculator of Neutron Transport Equation (SCONE)
  - Method of Characteristics, Random Rays

MaThRad

MaThRad

- Mathematical Theory of Radiation Transport: Nuclear Technology Frontiers
- £7M, 5-year EPSRC Program Grant
- Translate mathematical advances in probability theory and inverse problems to MC radiation transport
- Reactor analysis, criticality, shielding, medical and space applications
- 26 partners from industry and academia
- 30 postdoc-years, up to 10 PhDs
- Internships and hosting visitors
- Industry workshops and symposia
- UCLH proton treatment team + beam time

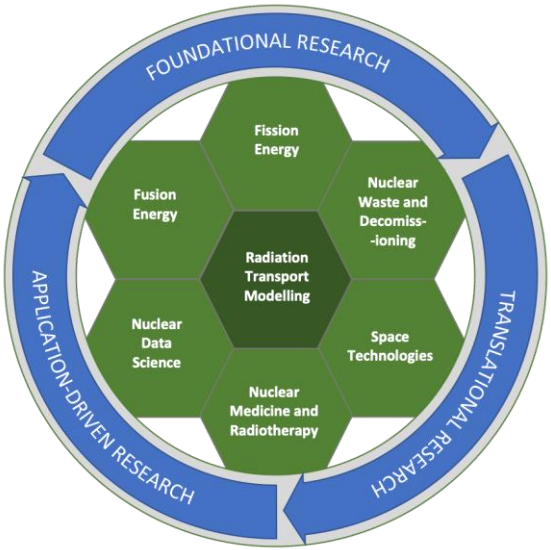

Thank you!

PAUL SCHERRER INSTITUT

PSI

Konstantin Mikityuk :: Advanced Nuclear System Group :: Paul Scherrer Institut

A historical review of EU GFR projects

SafeG Workshop: Advanced Modelling Techniques. University of Cambridge July 3-6, 2023

Outline

Aim: briefly review selected GFR-related EU projects (2005 – 2017) focusing on experiments relevant for validation:

- FP6 GCFR
- FP7 GoFastR
- FP7 ESNII Plus

Generation-IV International Forum: systems

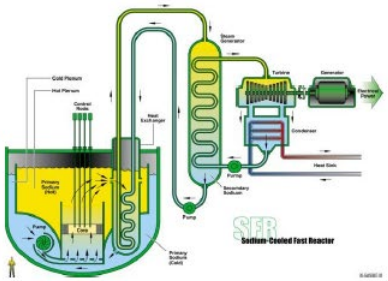

Sodium Fast Reactor

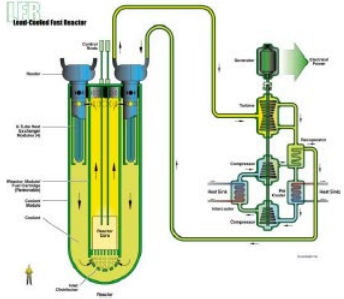

Lead Fast Reactor

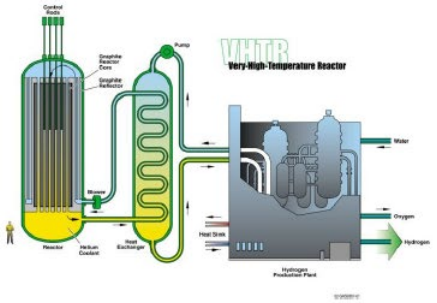

Very High Temperature Reactor

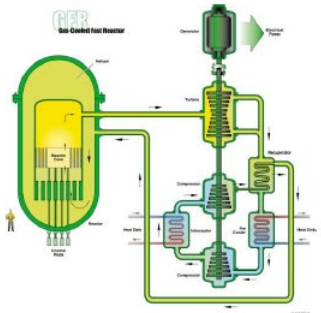

Gas Cooled Fast Reactor

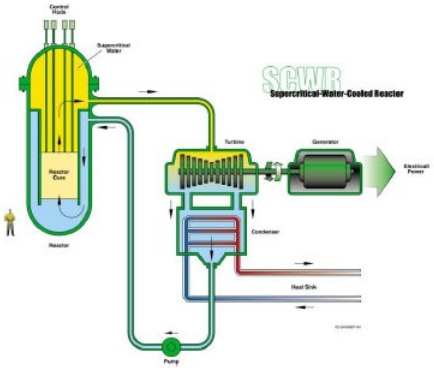

Supercritical Water Cooled Reactor

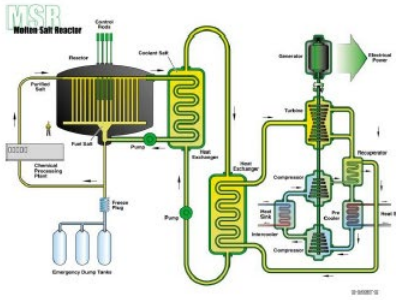

Molten Salt Cooled Reactor

3rd GIF Symposium 2015/ICONE 23 Conference - Makuhari Messe, Japan, May 2015
https://www.gen-4.org/gif/jcms/c_9354/presentations

Generation-IV International Forum: goals

- **Goal 1: Sustainability**
  - Long term fuel supply
  - Minimize waste and long term stewardship burden
- **Goal 2: Safety & Reliability**
  - Very low likelihood and degree of core damage
  - Eliminate need for offsite emergency response
- **Goal 3: Economics**
  - Life cycle cost advantage over other energy sources
  - Financial risk comparable to other energy projects
- **Goal 4: Proliferation Resistance & Physical Protection**
  - Unattractive materials diversion pathway
  - Enhanced physical protection against terrorism

Gen-IV GFR: concept

- No moderator
- Helium coolant
- Both direct and indirect cycle considered (indirect cycle selected)

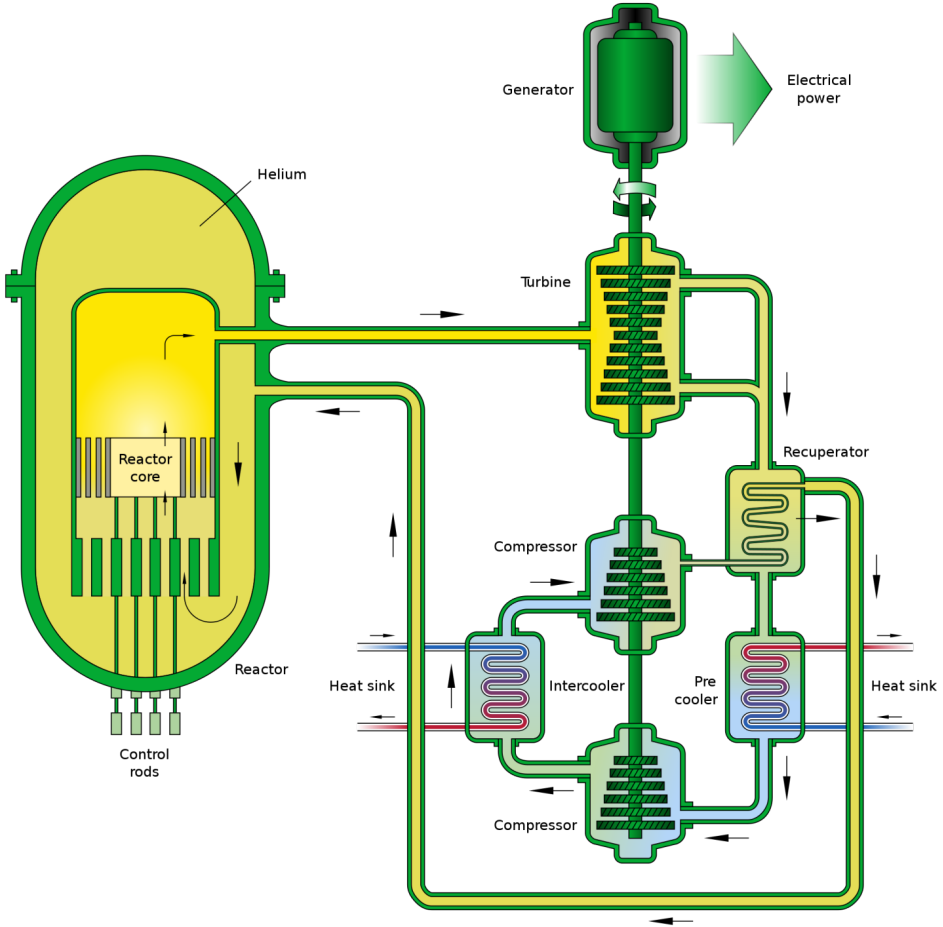

Gen-IV GFR: fact sheet

- **Advantages**
  - Potential for new fissile breeding due to fast neutron spectrum
  - Transparent and inert coolant
  - High efficiency

- **Challenges**
  - Safety demonstration and in particular decay heat removal in case of loss of flow and depressurization accidents
  - High-temperature materials and fuel qualification

- **Designs under development**
  - ALLEGRO 75 MWth
  - GCFR 2400 MWth

- **Reactors under operation**
  - None

Gen-IV GFR: Selected Euratom projects

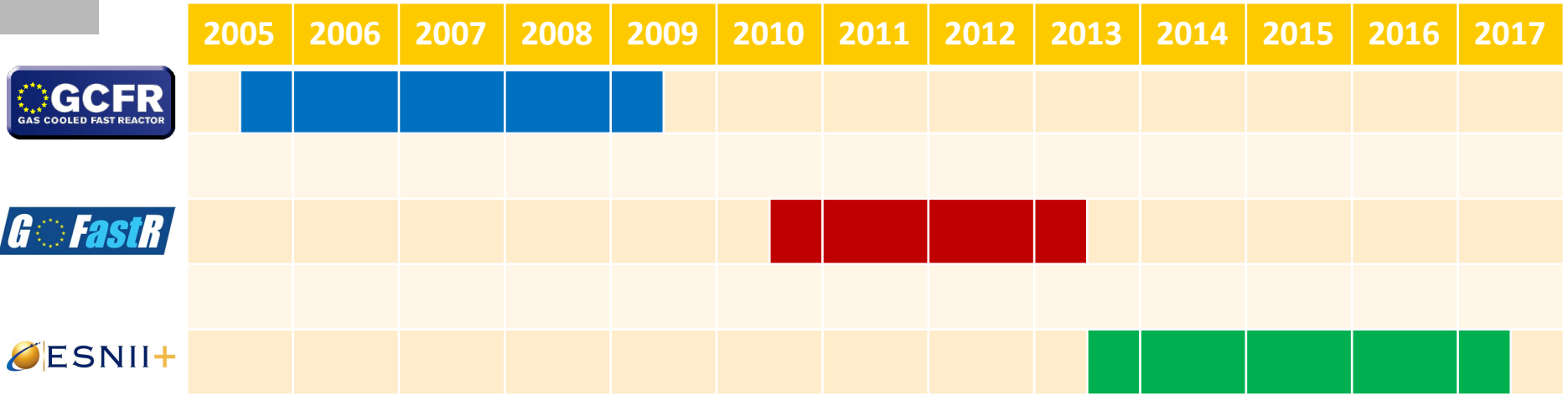

Gas Cooled Fast Reactor

Gas Cooled Fast Reactor

- EU framework: FP6
- Period: March 2005 – February 2009
- Total project cost €3 603 375
- EC contribution €2 000 000
- Participants (10):
  - NNC UK
  - BNFL UK
  - CEA France
  - EA Spain
  - Framatome France
  - ITU and JRC, Europe
  - NRG The Netherlands
  - PSI Switzerland
  - TU Delft The Netherlands
  - Universities Consortium – CIRTEN-UNIPI

Gas Cooled Fast Reactor: objectives

Ambitious long term goals for GFR:

- self-generating cores;
- robust refractory fuel;
- high operating temperature;
- direct conversion with a gas turbine;
- full actinide recycling.

ETDR (Experimental Technology Demonstration Reactor) integrated as milestone to prototype GFR

Specific contributions to the conceptual design decisions and safety demonstration:

- GFR design: decide between direct and indirect cycles and flexibility to burn MAs.
- ETDR design: develop core, protection and safety systems.
- Safety analysis: establish potential risk minimisation measures including passive safety systems as part of a core melt exclusion strategy.

Work Packages

1. GFR: System integration, design and safety

WP1.1 GFR design / integration	CEA, Christian Poette
WP1.3 GFR safety	NNC, Karen Peers

2. ETDR: System integration, design and safety

WP1.2 ETDR design / integration	CEA, Christian Poette
WP1.4 ETDR safety	NNC, Karen Peers

3. Crosscutting R&D challenges

WP1.5 Analysis tools: qualification	PSI, Paul Coddington
WP2.1-6 Fuel materials, fabrication, reprocessing, irradiation	JRC, Joe Somers

4. Project Management

WP3 Interface with other FP6 projects	JRC
WP4 Euratom representation in Gen IV GFR	NNC and JRC
WP5 Coordination	NNC, Colin Mitchell

Main deliverables

WP1.1 GFR design / integration

- GFR first consistent design drawings (direct cycle)
- GFR first consistent design drawings (indirect cycle)
- Thermal cycle optimisation and comparison of the GFR direct and indirect cycle cases
- Actinide Transmutation in GFR
- The direct and indirect cycle concepts for GFR
- GFR mission
- GFR preliminary viability report

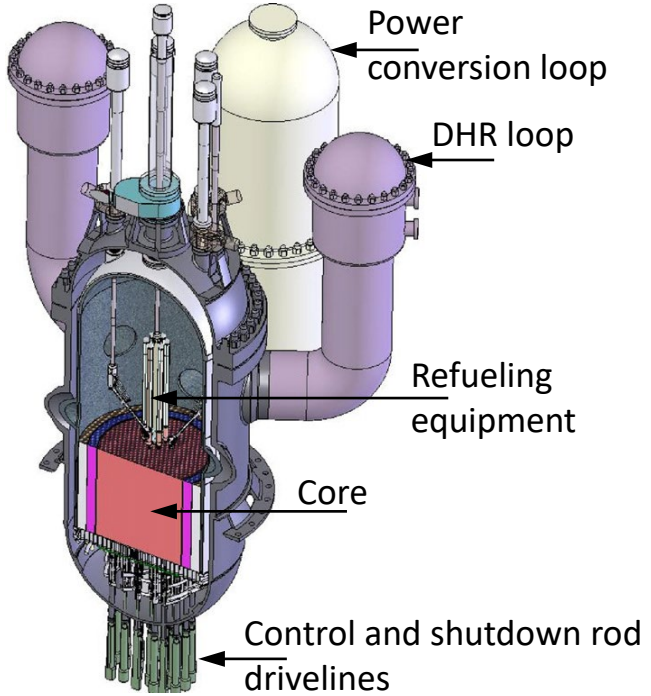

Main deliverables

WP1.2 ETDR design / integration

- Design information and status at start of the project
- ETDR Design option selection
- Detailed physics study of ETDR starting core
- Subassembly design and drawings for ETDR
- Absorber rods and mechanisms for ETDR
- Control and instrumentation for ETDR
- Reflector and shielding for ETDR
- ETDR reference option and alternatives

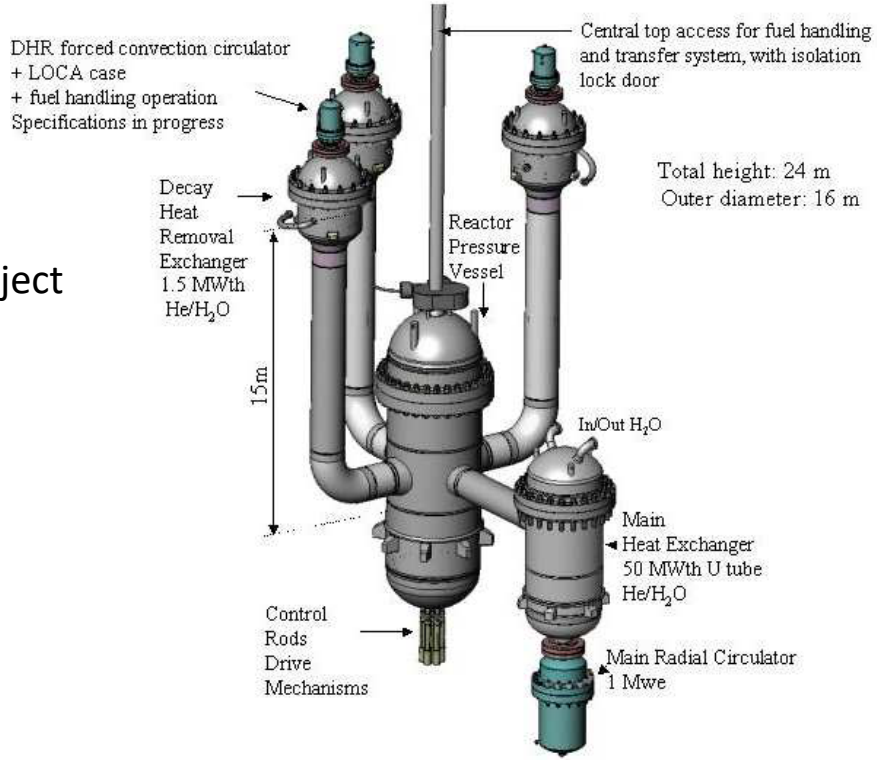

Main deliverables

WP1.3 GFR safety

- GFR safety approach
- Safety assessment of actinide transmutation in GFR
- GFR plant transient analysis reports
- GFR design optimisation for passive safety
- A comparison of safety for direct and indirect cycle GFR concepts

WP1.4 ETDR safety

- ETDR safety options report
- ETDR plant transient analysis reports
- Risk minimisation measures for ETDR
- ETDR preliminary safety report

Spherical guard vessel

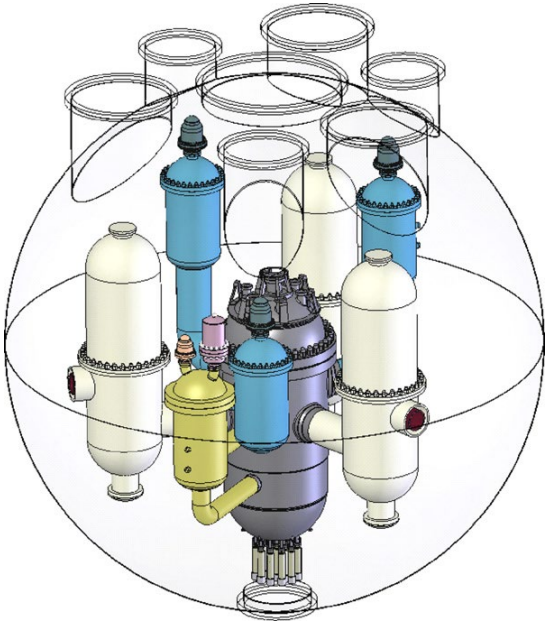

Main deliverables

WP2.1-6 Fuel materials, fabrication, reprocessing, irradiation

- Review of the thermophysical and thermochemical properties of unirradiated candidate materials
- Review of selected and relevant past irradiation programmes
- Review of SiC properties of as a confinement material for fuel
- Review of past fabrication processes and evaluation of innovative developments
- Review of reprocessing options for GFR fuel
- Design and planning of an irradiation experiment

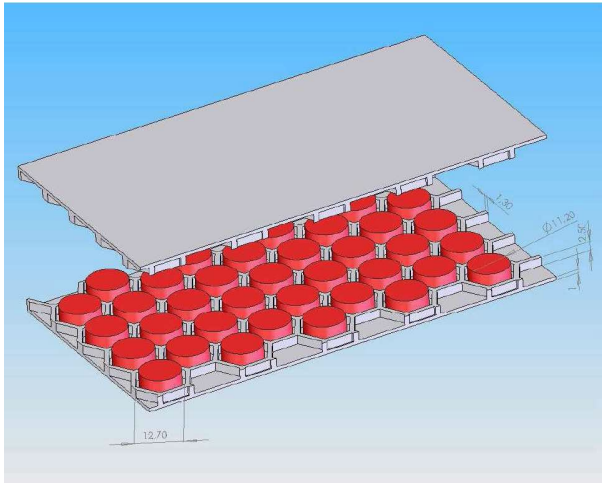

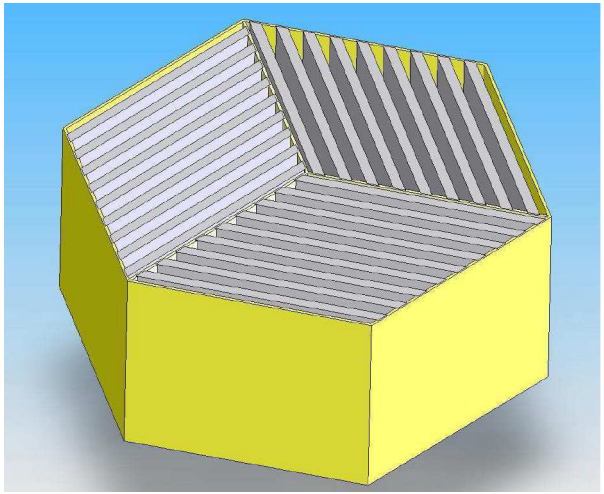

Main deliverables

WP1.5 Analysis tools: qualification

- A list of candidate transient analysis codes for GFR and their validation status
- Benchmark specification for the transient analysis codes
- A benchmark comparison of transient analysis codes
- Transient analysis best practice guide

Bellow more details on

Fuel modeling: P. Petkevich, "Development and Application of an Advanced Fuel Model for the Safety Analysis of the Generation IV Gas-cooled Fast Reactor", EPFL PhD Thesis, https://infoscience.epfl.ch/record/125884

EIR gas loop tests: A. Epiney, "Improvement of the Inherent and Passive Safety Characteristics of Generation IV Gas-cooled Fast Reactor“, EPFL PhD Thesis, http://dx.doi.org/10.5075/epfl-thesis-4792

GCFR-Proteus tests: G. Girardin, "Development of the Control Assembly Pattern and Dynamic Analysis of the Generation IV Large Gas-cooled Fast Reactor (GFR)“, EPFL PhD Thesis, http://dx.doi.org/10.5075/epfl-thesis-4437

GFR fuel modeling approaches

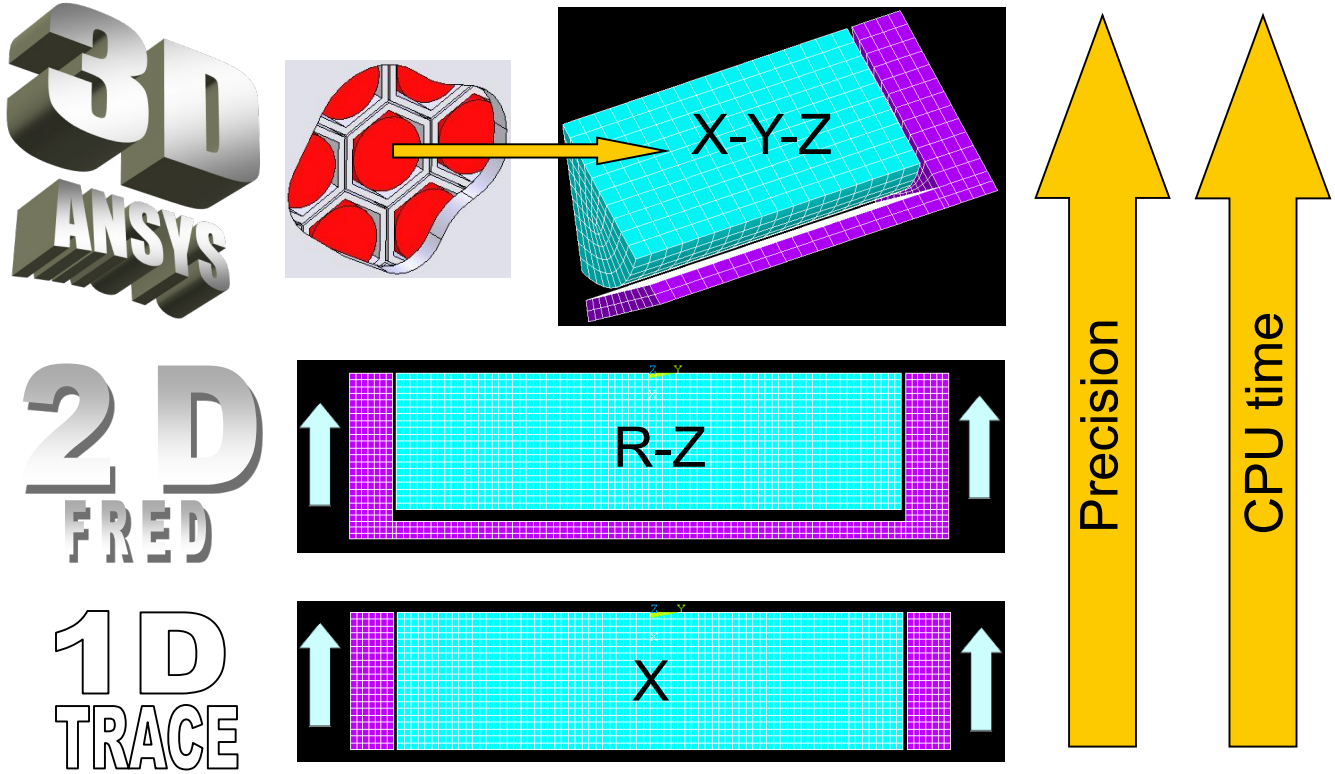

P. Petkevich, EPFL PhD Thesis, https://infoscience.epfl.ch/record/125884

DHR strategies for GFR

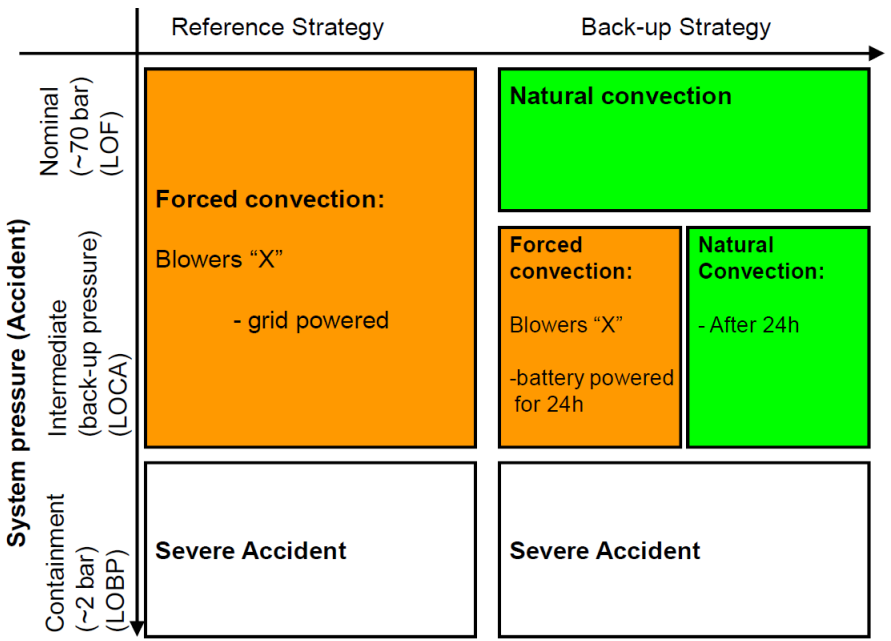

CEA 2006 reference DHR strategy

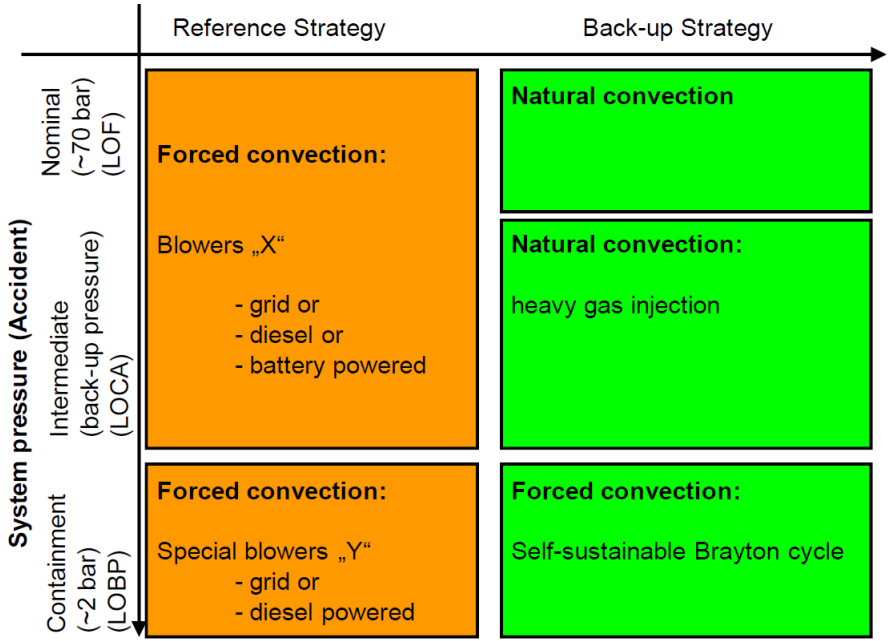

New DHR strategy

A. Epiney, EPFL PhD Thesis, https://infoscience.epfl.ch/record/149808

DHR strategies for GFR

- Guard vessel for backup pressure
- Heavy gas injection in accidents with depressurization
- DHR loops with forced convection

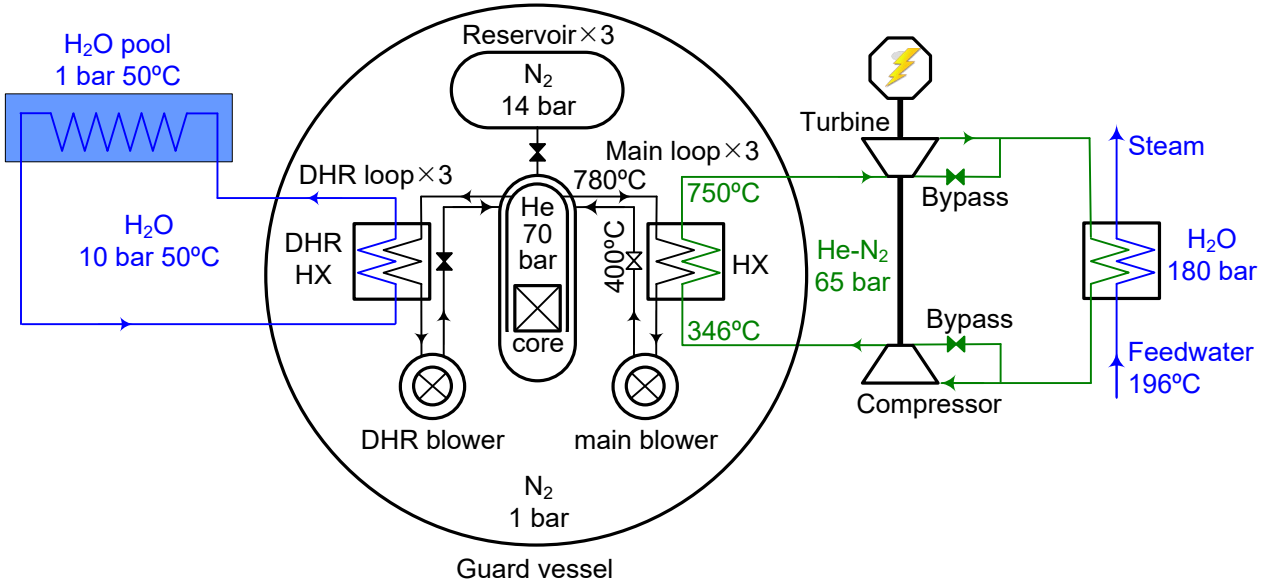

A. Epiney, EPFL PhD Thesis, https://infoscience.epfl.ch/record/149808

DHR strategies for GFR

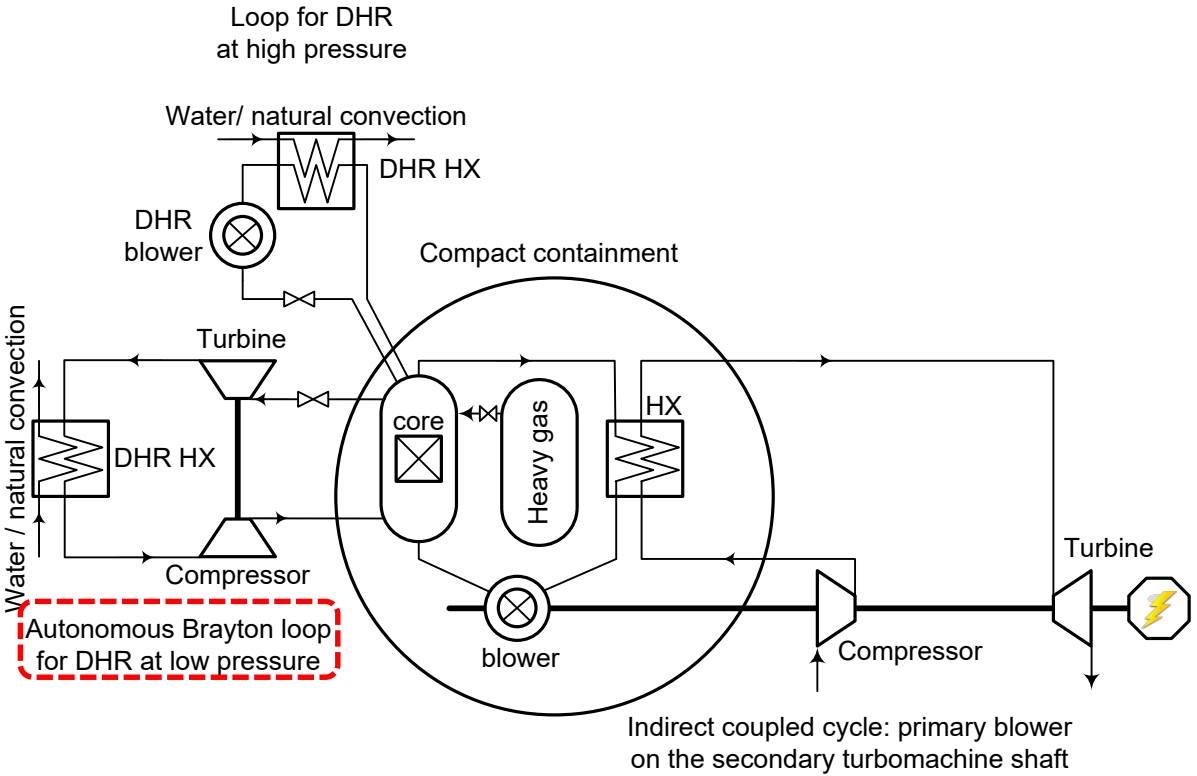

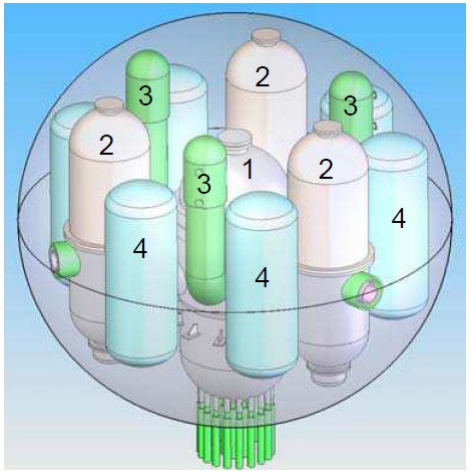

1. Vessel
2. Main HX
3. DHR HX
4. Gas reservoirs

A. Epiney, EPFL PhD Thesis, https://infoscience.epfl.ch/record/149808

DHR strategies for GFR: Bryton cycle

- **Idea**: use of decay heat itself to evacuate it
- As long as there is decay heat to evacuate there is energy to assure the cooling
- Enhance passivity of DHR

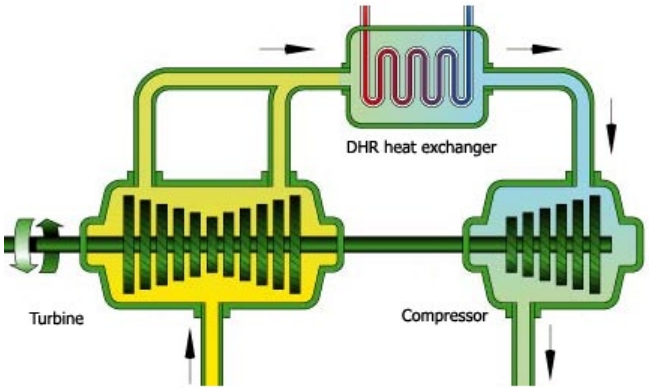

Chosen design point:

- Equilibrium at 2 bar
- 0MW power production
- He mass flow: 32 kg/s
- Press. ratio turb.: 1.0737
- Press. ratio comp.: 1.1135
- W turb./comp.: 4.39 MW
- Turbine stages: 2
- Compressor stages: 4
- Turbine diameter: 1.6 m
- Compressor diameter: 1.8 m
- Turbine blade height: 20 cm
- Compressor blade height: 17 cm

A. Epiney, EPFL PhD Thesis, https://infoscience.epfl.ch/record/149808

EIR gas loop tests: thermal hydraulics

Friction factors and heat transfer investigated in EIR and KfK gas-loop experiments

- GCFR project during late 70s and early 80s
- Gas-loop data for GFR-representative conditions
  - Smooth and artificially roughened surfaces
  - Single rods and rod bundles
  - Heat transfer, friction and spacer losses
  - Different gases: Air, CO_2, He, N
- Knowledge preservation

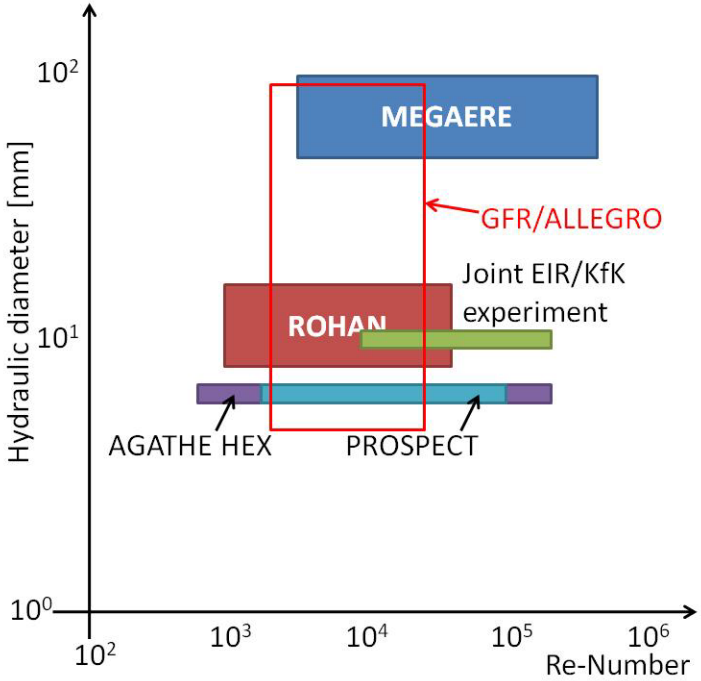

A. Epiney, EPFL PhD Thesis, https://infoscience.epfl.ch/record/149808

EIR gas loop tests: thermal hydraulics

Single channel

- MEGAERE
- ROHAN
- Joint EIR-KfK

Rod-bundle experiments

- PROSPECT
- AGATHE HEX

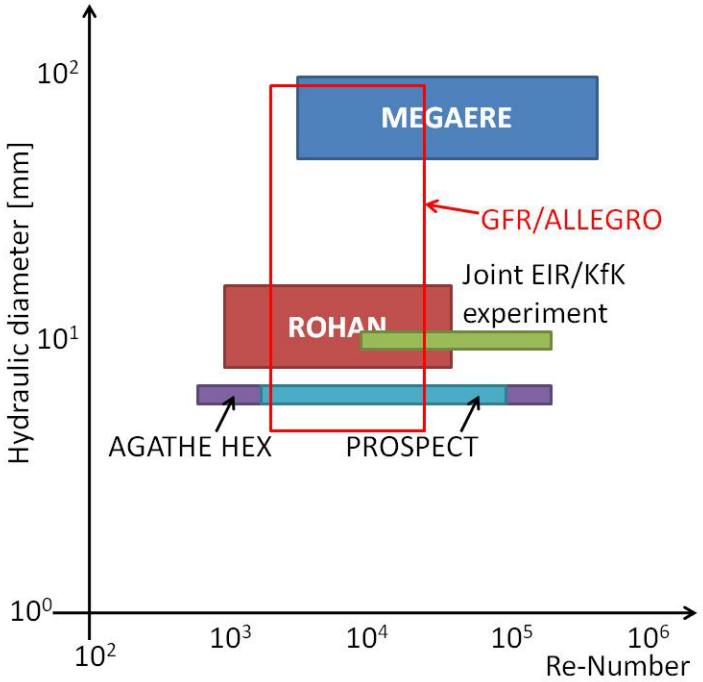

A. Epiney, EPFL PhD Thesis, https://infoscience.epfl.ch/record/149808

EIR gas loop tests: MEGAERE

- Isothermal single-channel open loop for determining empirical constants for turbulent flow modeling
- Test section: ~2 m long tube with smooth walls and diameter of 100 mm
- Inner rods with different diameters from ~ 10 to 50 mm and different roughening patterns
- Measured: pressure drop and velocities

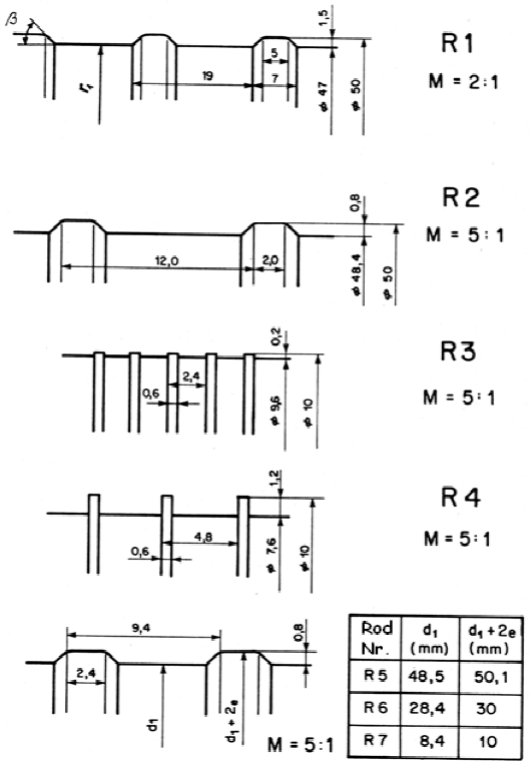

Rod Nr.	d_1 (mm)	$d_1 + 2e$ (mm)
R5	48,5	50,1
R6	28,4	30
R7	8,4	10

Roughening patterns

A. Epiney, EPFL PhD Thesis, https://infoscience.epfl.ch/record/149808

EIR gas loop tests: ROHAN

- Single-channel air loop with annular geometry
- 3 smooth tubes and 30+ different diameters and artificially roughened surfaces tested
- Aim: determine the convective heat transfer under representative GCFR conditions
- Measured: friction factor, Stanton number, inlet, bulk and wall temperatures

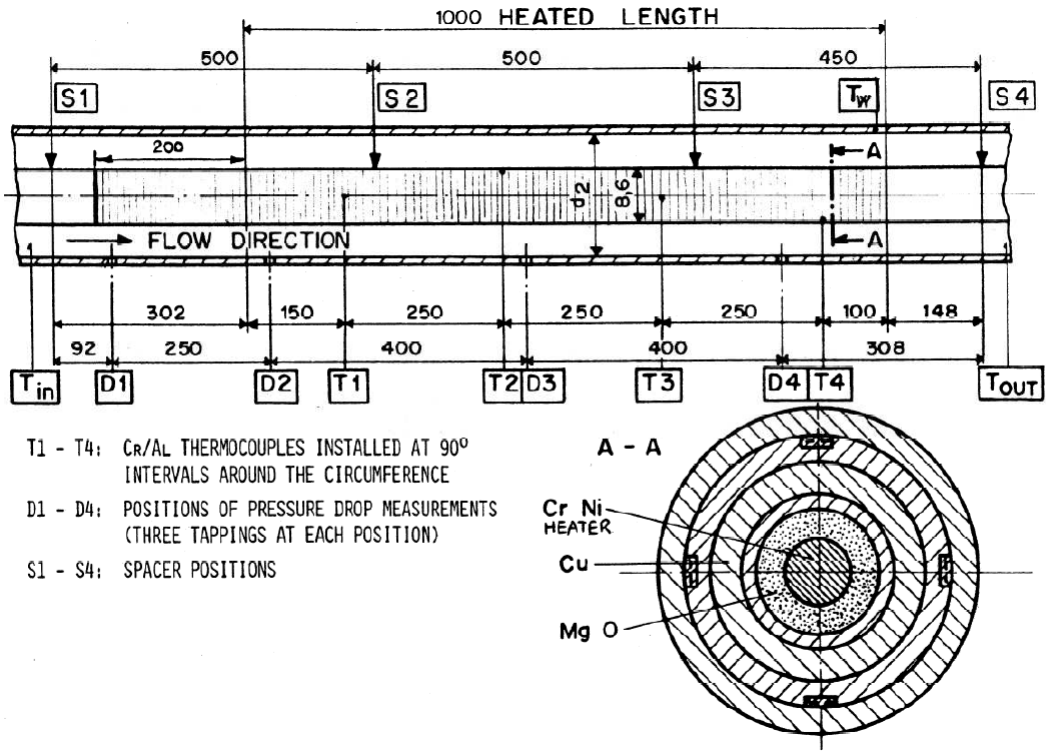

A. Epiney, EPFL PhD Thesis, https://infoscience.epfl.ch/record/149808

EIR gas loop tests: ROHAN analysis with TRACE

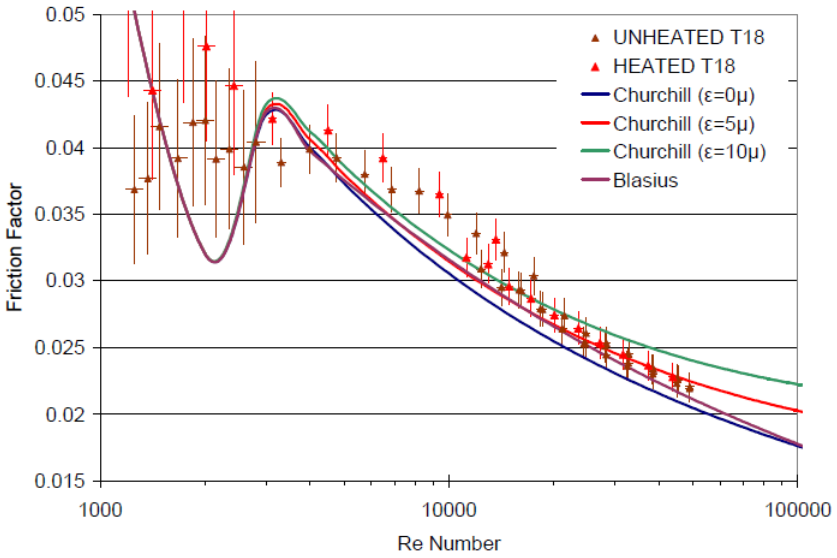

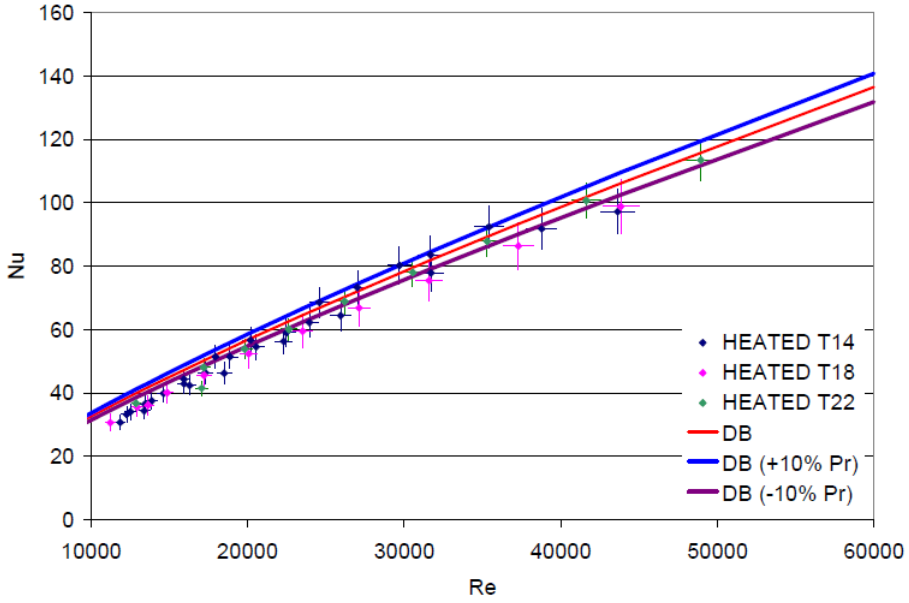

A. Epiney, EPFL PhD Thesis, https://infoscience.epfl.ch/record/149808

EIR gas loop tests: Joint EIR/KfK program

- Single-channel heat transfer and pressure drop experiments with annular geometry
- CO_2, N, He at 1 to 60 bar, 30 to 800 C and heating power of 0 to 1000 kW
- Aim: determine the convective heat transfer under representative GCFR conditions
- Data: friction-factor and Stanton-number plots as a function of Re-number and the bulk-to-wall temperature ratio

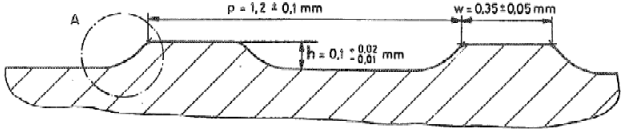

Roughening pattern

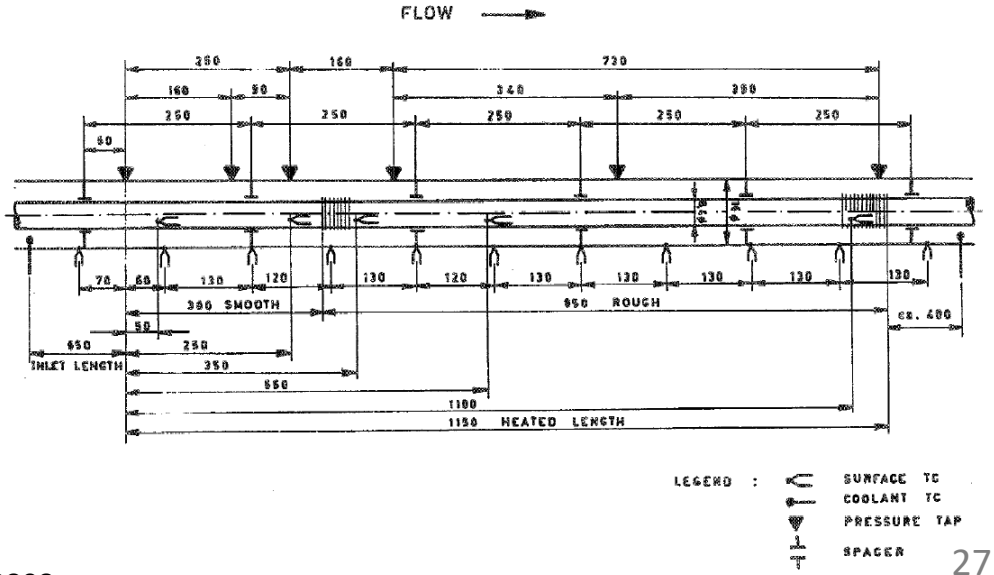

A. Epiney, EPFL PhD Thesis, https://infoscience.epfl.ch/record/149808

EIR gas loop tests: Joint EIR/KfK program

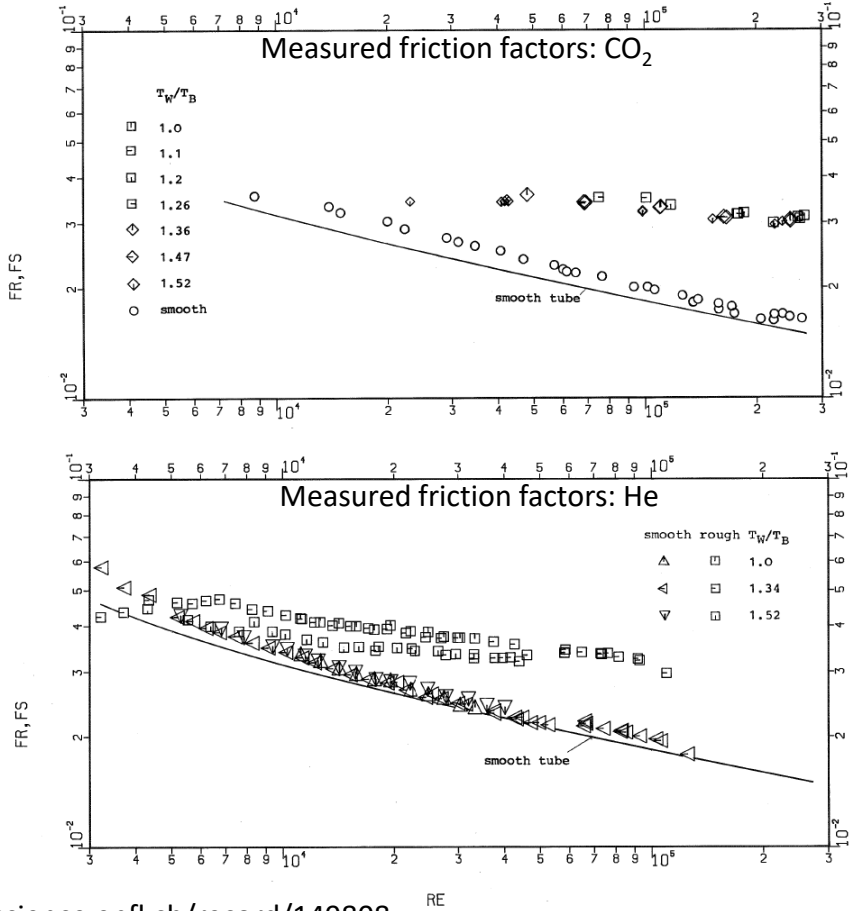

A. Epiney, EPFL PhD Thesis, https://infoscience.epfl.ch/record/149808

EIR gas loop tests: PROSPECT

- Hexagonal 37-rod bundle air test section
- Aim: establish pressure-loss coefficients across grid spacers designed for the GCFR
- Length: 1.45 m, 4 spacers
- Data: pressure difference

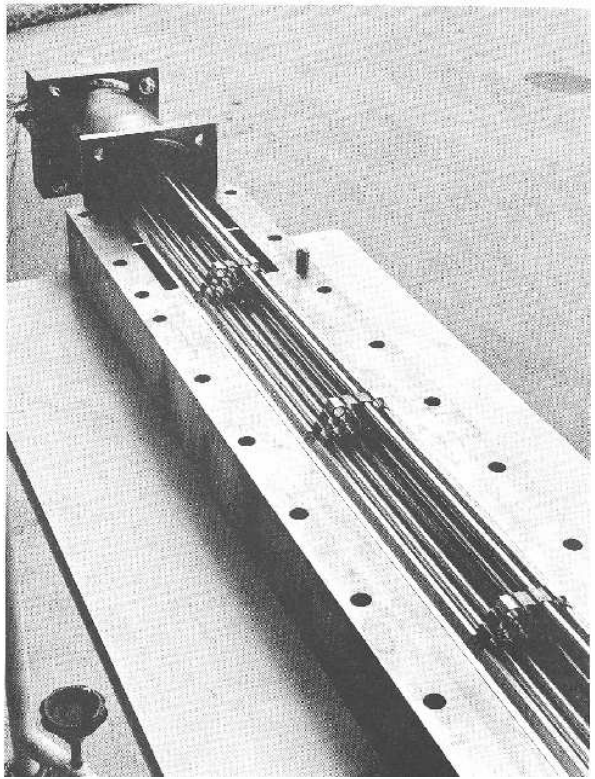

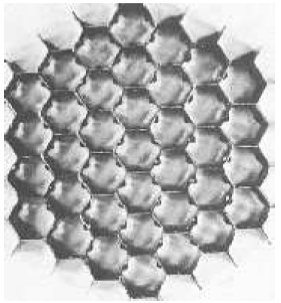

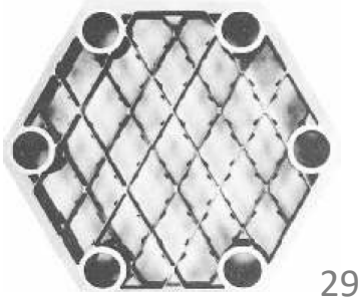

A. Epiney, EPFL PhD Thesis, https://infoscience.epfl.ch/record/149808

EIR gas loop tests: PROSPECT

Dalle-Donne correlation
for pressure losses on the grids

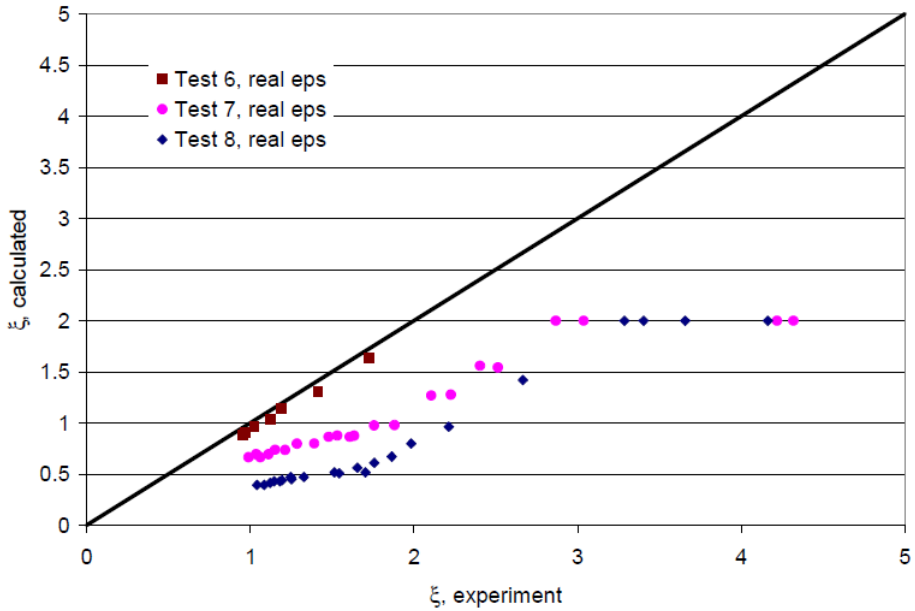

Proposed new correlation

$$\xi_s = C_v \varepsilon^{0.2}$$

$$C_v = 1.104 + \frac{791.8}{\mathrm{Re}^{0.748}} + \frac{3.348 \cdot 10^9}{\mathrm{Re}^{5.652}}$$

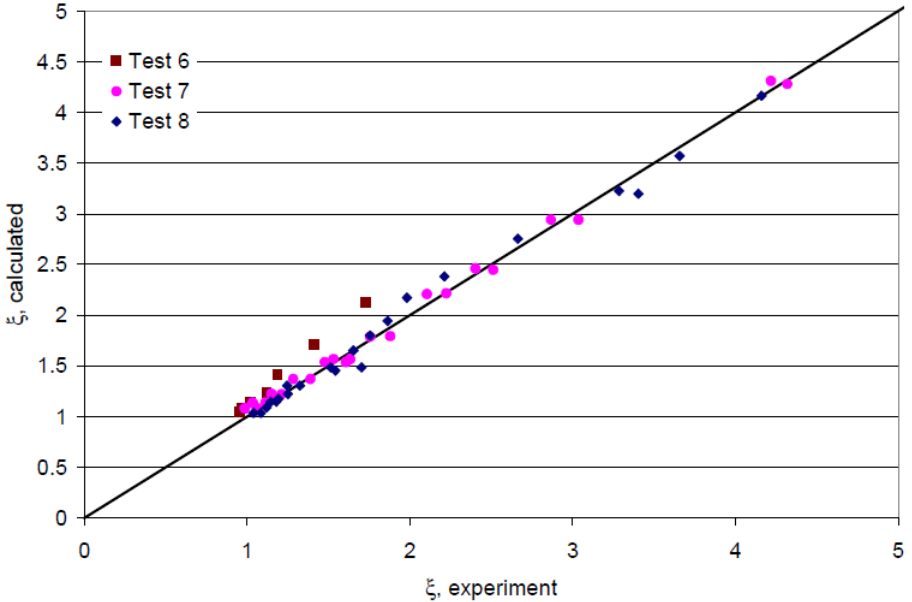

A. Epiney, EPFL PhD Thesis, https://infoscience.epfl.ch/record/149808

EIR gas loop tests: AGATHE HEX

- High-pressure high-temperature loop with CO_2
- Three different hexagonal rod bundles with rods roughened in the upper part with the same pattern as in PROSPECT
- Aim: establish pressure-loss coefficients across grid spacers designed for the GCFR
- Data: axial profiles of pressure and temperature

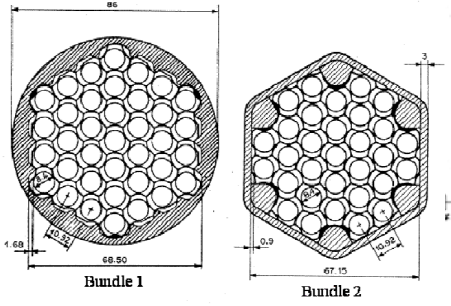

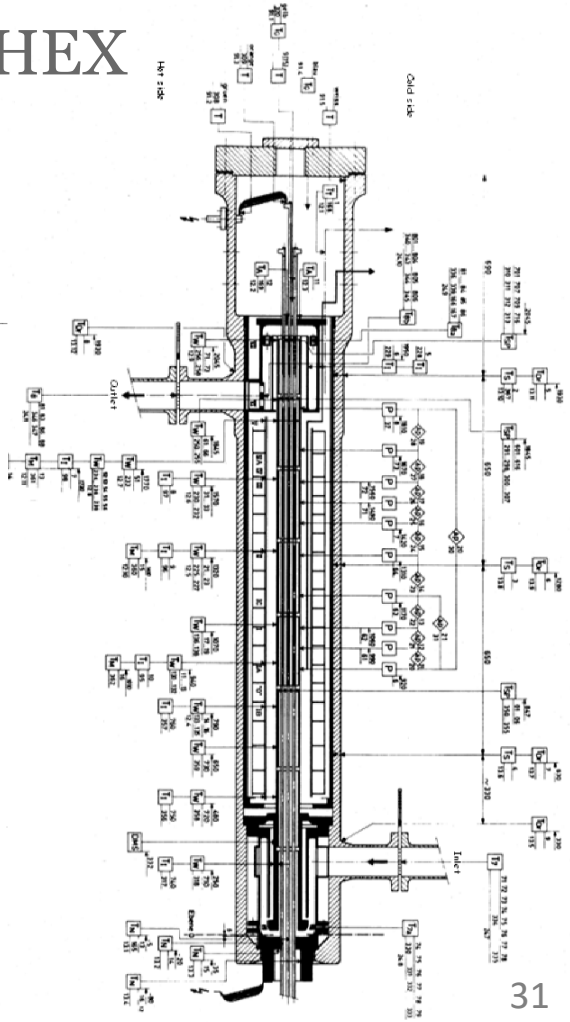

A. Epiney, EPFL PhD Thesis, https://infoscience.epfl.ch/record/149808

EIR gas loop tests: AGATHE HEX analysis

Cigarini and Dalle-Donne correlation for pressure losses on the grids

Cladding temperature

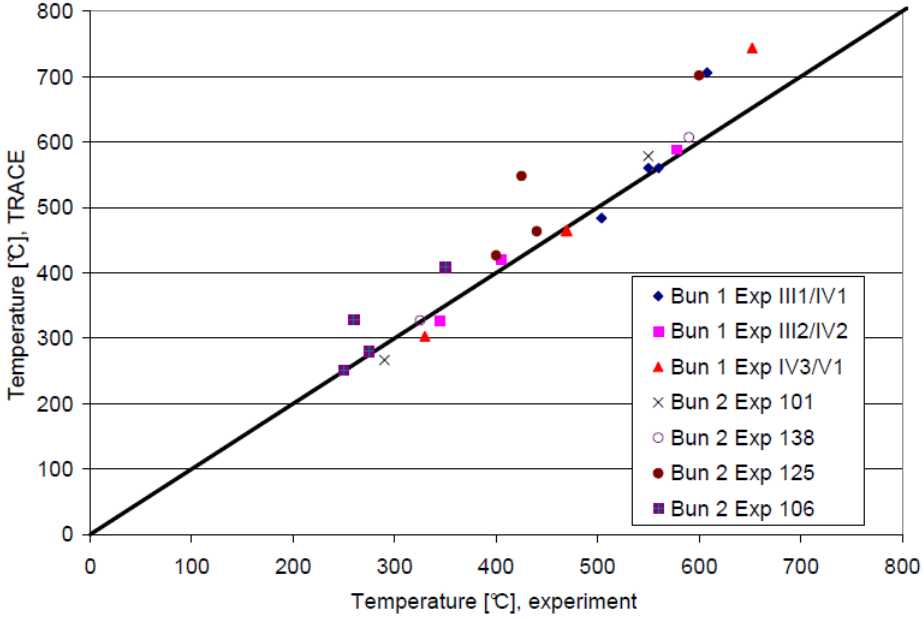

Bundle pressure drop

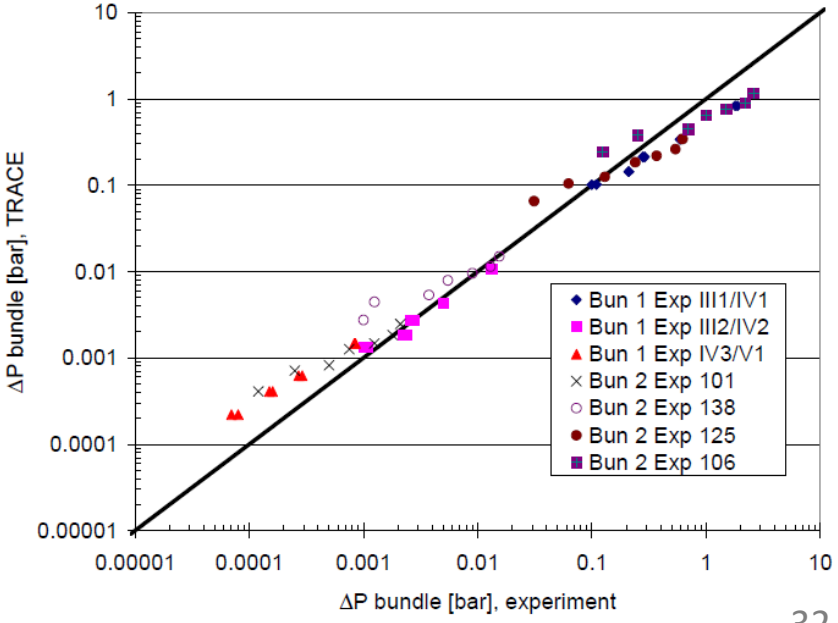

A. Epiney, EPFL PhD Thesis, https://infoscience.epfl.ch/record/149808

GCFR-Proteus: neutronics

- GCFR-Proteus integral tests carried out during the 1970's at the PROTEUS critical facility of EIR, now PSI, Switzerland
- Aim: to study physics characteristics of gas-cooled fast reactors and to provide a validation base for available neutronics tools developed mainly for SFRs
- Fuel: $(U,Pu)O_2$ with 15% Pu

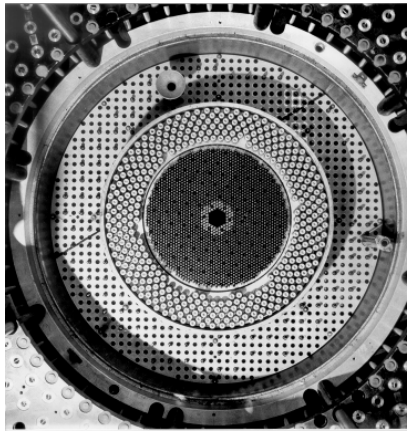

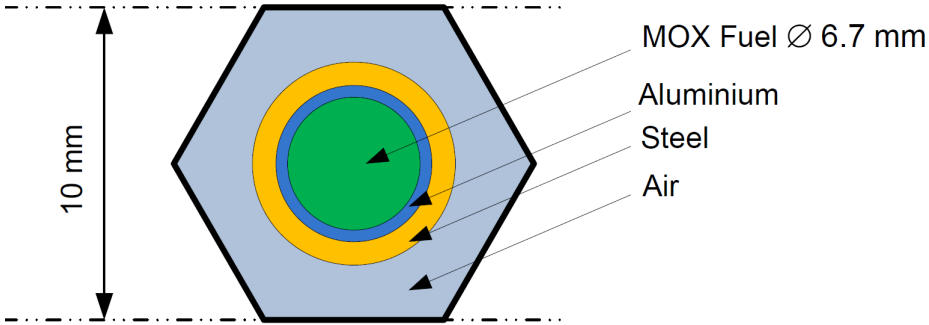

G. Girardin, EPFL PhD Thesis, https://infoscience.epfl.ch/record/136746

GCFR-Proteus: multi-zone zero-power facility

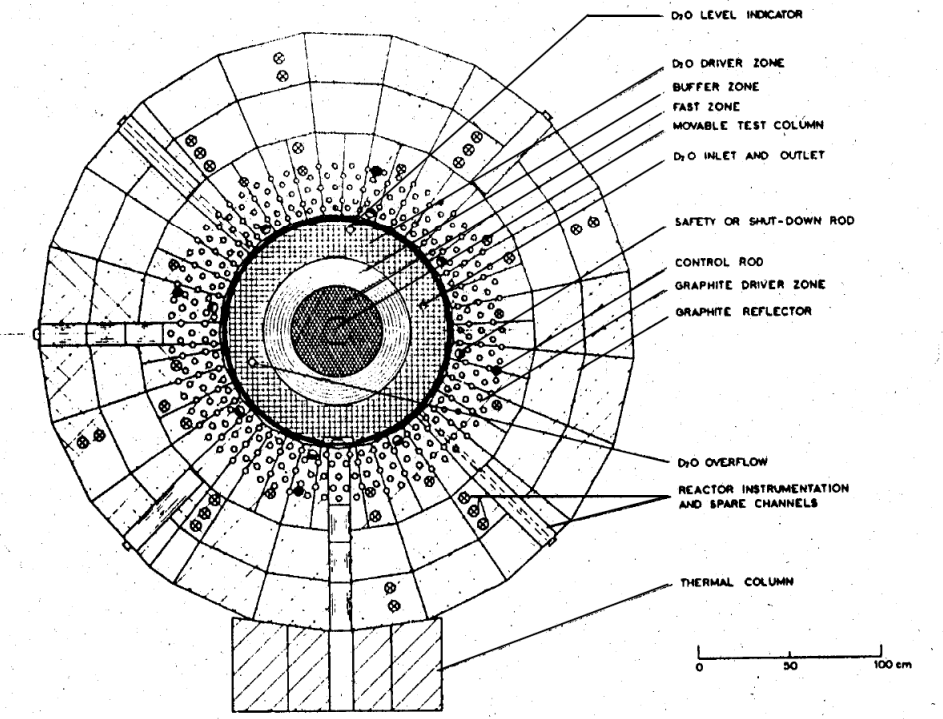

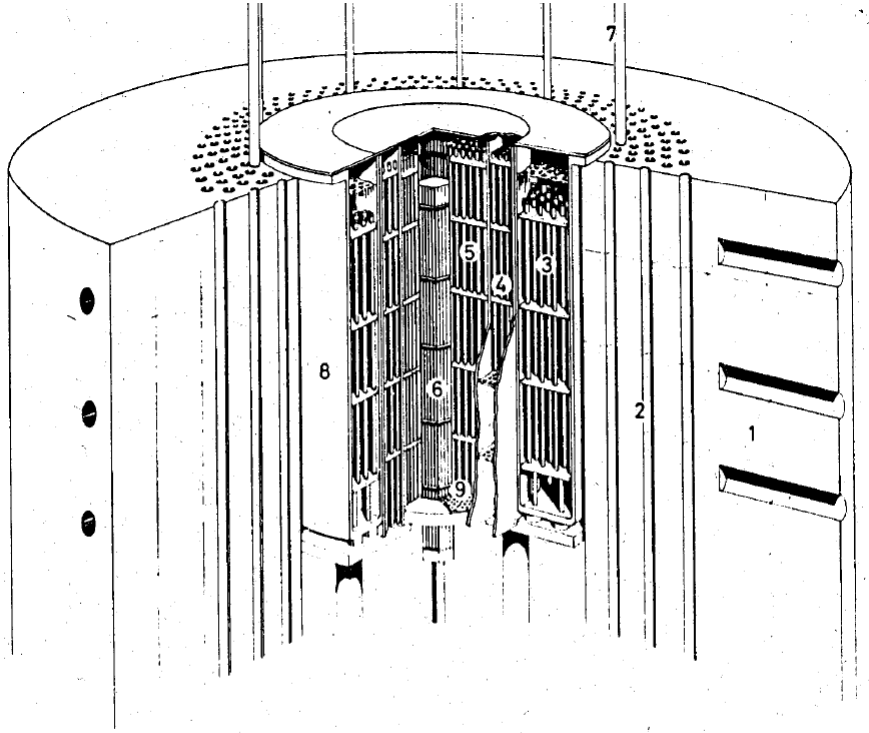

G. Girardin, EPFL PhD Thesis, https://infoscience.epfl.ch/record/136746

GCFR-Proteus: neutron spectra

Spectra comparison for different systems: GCFR-PROTEUS, GFR, SFR and ETDR

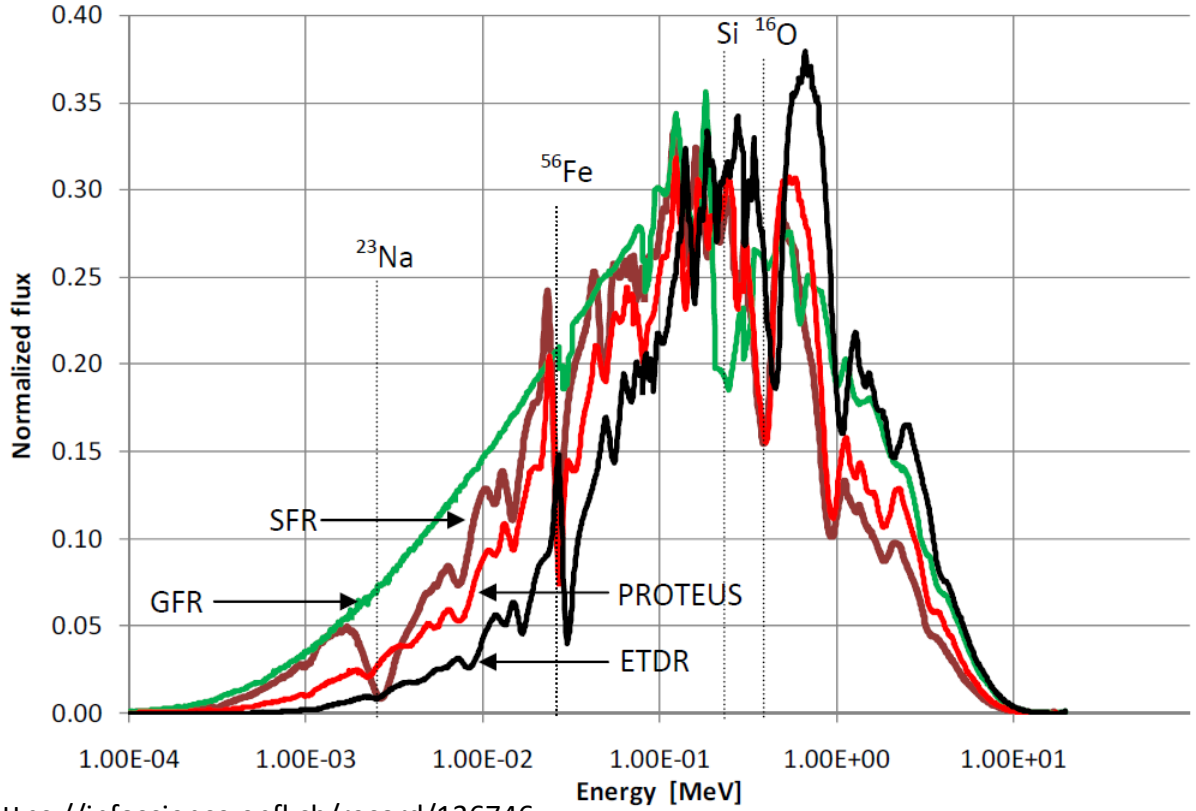

G. Girardin, EPFL PhD Thesis, https://infoscience.epfl.ch/record/136746

GCFR-Proteus: data

Measured (unadjusted) reaction rate ratios, correction factors, the propagated 1σ experimental uncertainty

Ratio	Experimental value	Correction factor*	1σ, %
C8/F9	0.13270 ± 1.1 %	0.994 ± 0.5 %	1.2
F8/F9	0.03111 ± 1.3 %	0.974 ± 0.5 %	1.4
F5/F9	1.0100 ± 1.4 %	1.004 ± 0.5 %	1.5
C2/F9	0.2000 ± 1.3 %	1.022 ± 0.5 %	1.4
F2/F9	8.061E-03 ± 2.0 %	0.979 ± 0.5 %	2.1
F3/F9	1.5190 ± 1.3 %	1.027 ± 0.5 %	1.4
(n,2n)2/C2	6.840E-03 ± 2.5 %	0.973 ± 0.5 %	2.6
C7/F9	0.8260 ± 2.3 %	1.020 ± 1 %	2.5
F7/F9	0.2270 ± 1.8 %	0.975 ± 1 %	2.1

*Correction factor is reaction rate for whole multi-zone PROTEUS configuration divided by reaction rate single-zone critical cell calculations for reference lattice (fundamental mode)

G. Girardin, EPFL PhD Thesis, https://infoscience.epfl.ch/record/136746

European Gas Cooled Fast Reactor

European Gas Cooled Fast Reactor

- EU framework: FP7
- Period: March 2010 – February 2013
- Total project cost €5 430 276
- EC contribution €3 000 000
- Participants (22):
  - AMEC UK
  - AREVA France
  - CEA France
  - CIRTEN Italy
  - EA Spain
  - KIT-G Germany
  - Imperial UK
  - IRSN France
  - JRC-ITU Europe
  - NRG Netherlands
  - PSI Switzerland
  - Rolls-Royce UK
  - TUD Netherlands
  - TÜV Germany
  - SRS Italy
  - BME Hungary
  - ENEA Italy
  - Ansaldo Nucleare Italy
  - AEKI Hungary
  - FZJ Germany
  - RC-Rez Czech Republic
  - NNLL UK

European Gas Cooled Fast Reactor: objectives

- To assess main challenges to viability of GFR system
- To develop new GFR fuel concept
- To design and assess new all-ceramic core
- To assess performance of shutdown, decay heat removal and guard containment systems
- To carry out probabilistic safety assessments for the first time for Gen IV GFR system
- To start severe accident studies in order to assess progression of accidents leading core melt
- To assess provision for and design of potential “core-catcher” structures

Work Packages

1. GFR: System integration, design and safety

WP1.1 GFR conceptual design	CEA, Christian Poette
WP1.3 GFR safety studies	PSI and AMEC, K. Mikityuk and K. Peers

2. ALLEGRO: System integration, design and safety

WP1.2 ALLEGRO conceptual design	CEA, Christian Poette
WP1.4 ALLEGRO safety studies	PSI & AMEC, K. Mikityuk and K. Peers

3. Education and training

WP6 Education and training	TUD, Jan Leen Kloosterman

4. Crosscutting R&D challenges

WP1.5 Methods development and qualification	PSI, Konstantin Mikityuk
WP2 Fuel and other core materials	NRG & JRC-ITU, Joe Somers
WP7 Generic Safety Studies	IRSN, Daniel Blanc

5. Project Management

WP3 Links with other Euratom activities	AMEC
WP4 Euratom representation within Gen IV	AMEC
WP5 Coordination	AMEC, Richard Stainsby

Main deliverables

WP1.1 GFR design / integration

- Reference 2400 MWth core definition
- GFR penetration in a nuclear park
- Technologies for BOP components
- Technologies for DHR components
- CFD investigation of ceramic pin core
- GFR core transmutation capabilities
- Power conversion system
- Heat exchanger technology
- Alternative power conversion cycles
- GFR core characterizations
- Alternative pressure boundary systems
- Gen IV GFR viability report

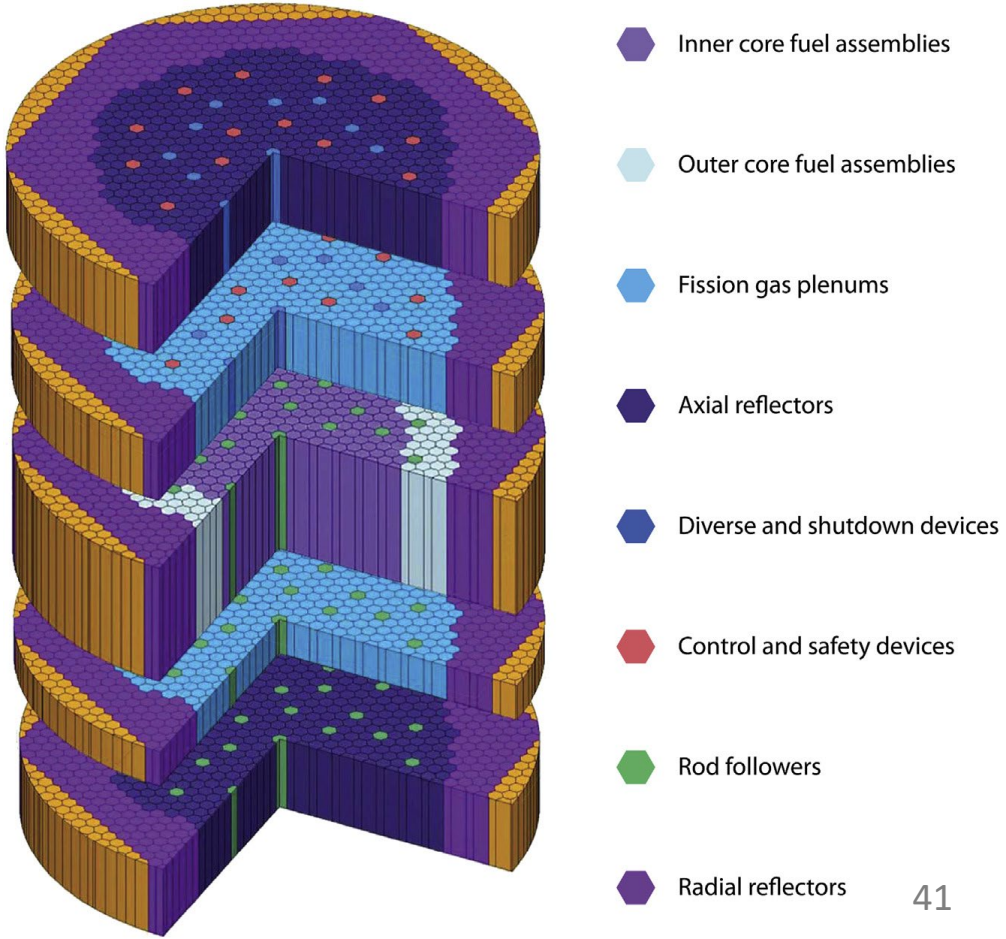

Main deliverables

WP1.2 ALLEGRO conceptual design

- ALLEGRO 75 MW cores definition (MOX + ceramic cores)
- Reference ALLEGRO system definition
- Basis key components of ALLEGRO and of their applicability to a GFR power reactor
- MOX and ceramic core designs (neutronics, CFD studies of SAs and minor actinide burning)
- Design of experimental SAs loaded in MOX core (including minor actinide burning)
- MOX fuel pin performance analysis
- Third level shutdown system
- Neutron and biological shielding
- ALLEGRO viability
- Final report on ALLEGRO, mission, design and safety

Main deliverables

WP1.3 GFR safety studies

- GFR Safety Approach
- GFR Probabilistic Safety Approach
- GFR Reliability Analysis Methodology
- GFR Severe Accident Model Development
- GFR Risk Minimisation Studies
- GFR Transient analysis
- GFR Severe Accident Management Solutions
- GFR Severe Accident Analysis

Main deliverables

WP1.4 ALLEGRO safety studies

ALLEGRO Safety Approach and Risk Minimisation Studies

ALLEGRO Severe Accident Model Development

ALLEGRO reliability study of key systems and events

ALLEGRO transient analysis

ALLEGRO Severe Accident Management Solutions

ALLEGRO Severe Accident Analysis

Main deliverables

WP1.5 Methods development and qualification

- HE-FUS3 benchmark specifications
- HE-FUS3 benchmark results
- L-STAR benchmark specifications
- L-STAR benchmark results
- Evaluation of uncertainties for GFR and ALLEGRO cores
- Evaluation of uncertainties for GFR and ALLEGRO cores

WP2 Fuel and other core materials

- Workhorse fuel concepts
- Ceramic fuel design for ALLEGRO 1st core test assembly
- Material alternatives
- Irradiation test preparation

GCFR-2400: fuel

(U-Pu)C fuel pellet

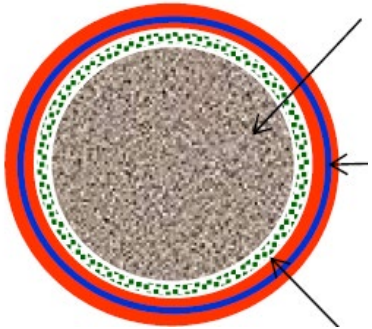

Sandwich cladding Ø~9 mm:
— inner SiC/SiC layer
— middle metalic liner
— outer SiC/SiC layer

Buffer bond:
— high-porosity C-based braid

CEA manufactured “Sandwich” cladding

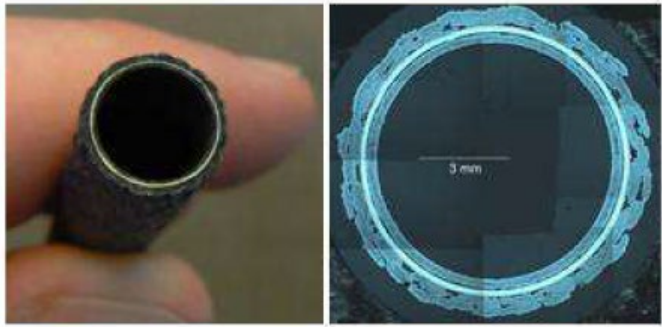

M. Zabiégo, et al. “Overview of CEA's R&D on GFR fuel element design: from challenges to solutions”, FR’13 conference proceedings

HEFUS-3 helium loop: objective

EBBTF is facility integrating a lead lithium and a helium loop, helium cooled lithium lead to test helium cooled lithium lead breeder blanket concept for ITER.

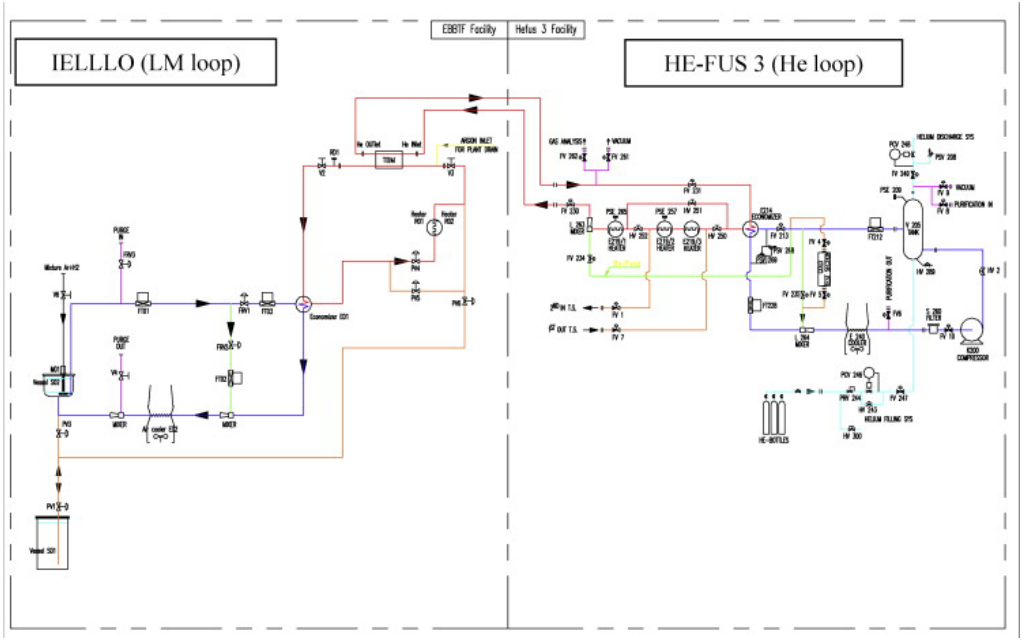

HEFUS-3 helium loop: scheme

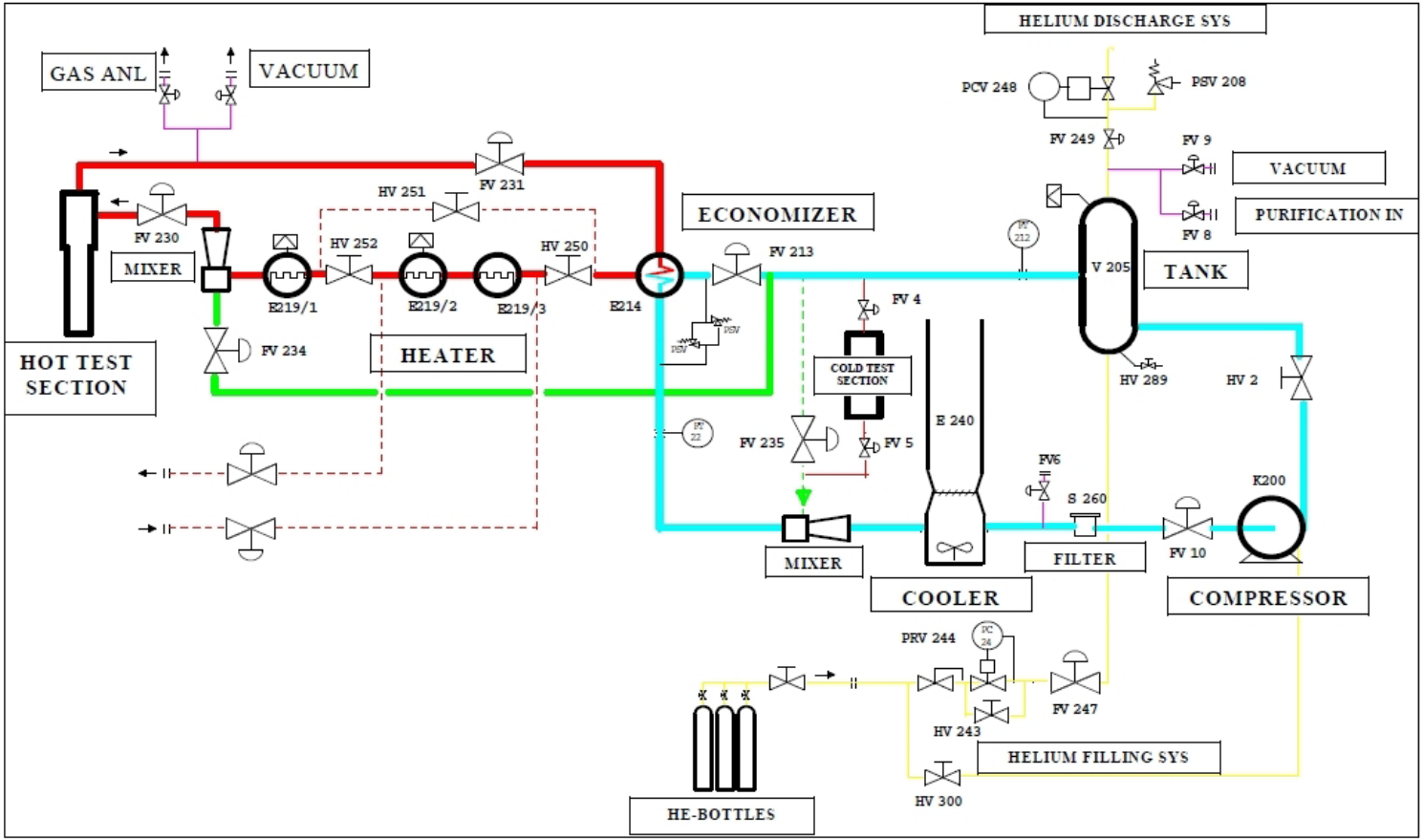

HEFUS-3 helium loop: TRACE model

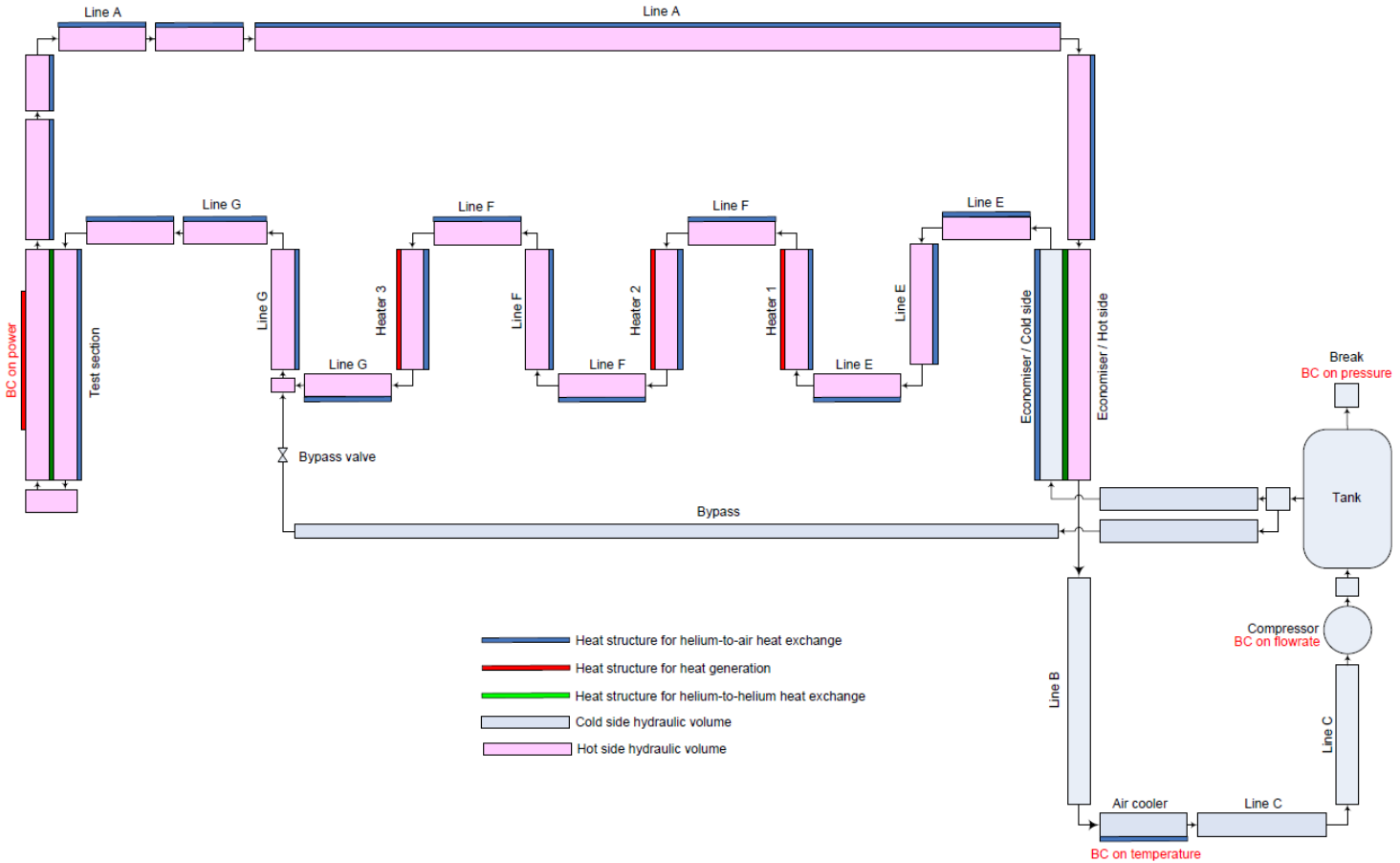

HEFUS-3 helium loop: Steady state 1

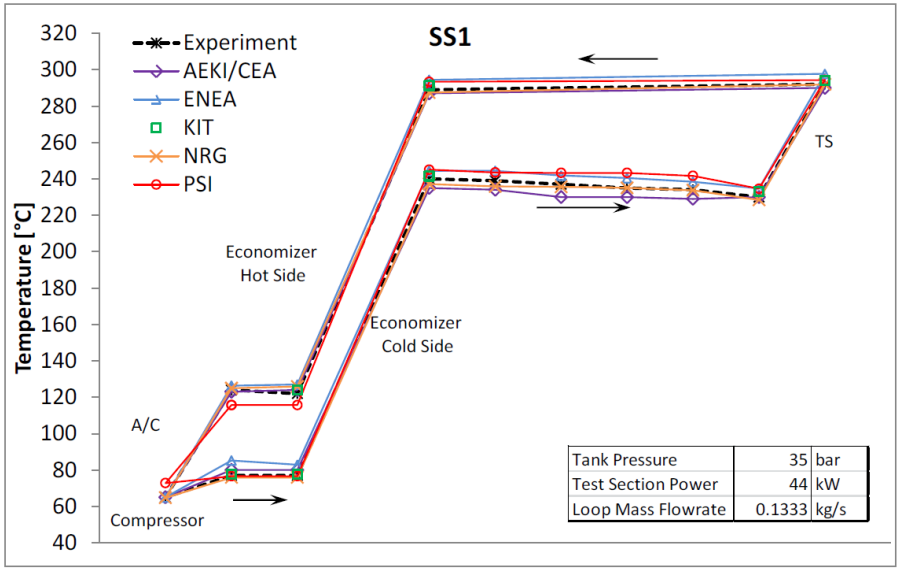

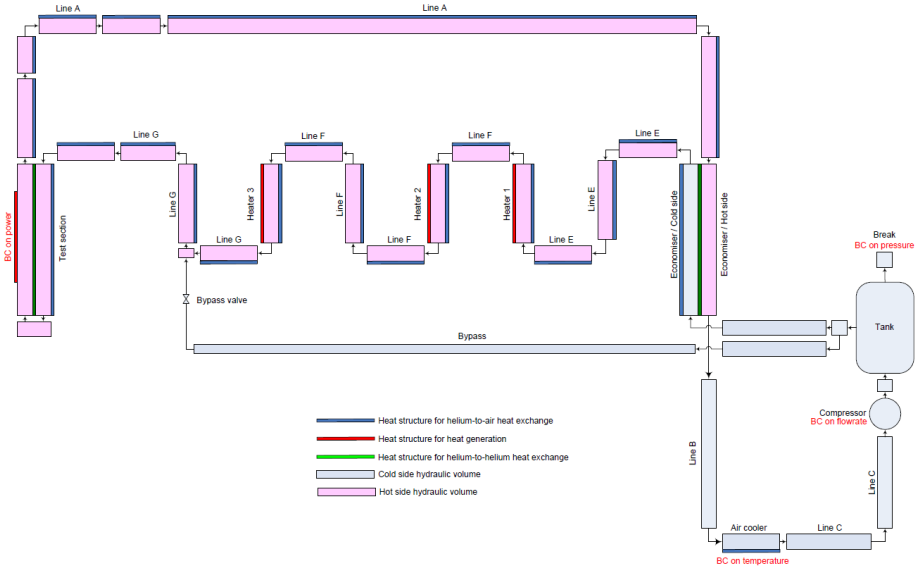

HEFUS-3 helium loop: Steady state 2

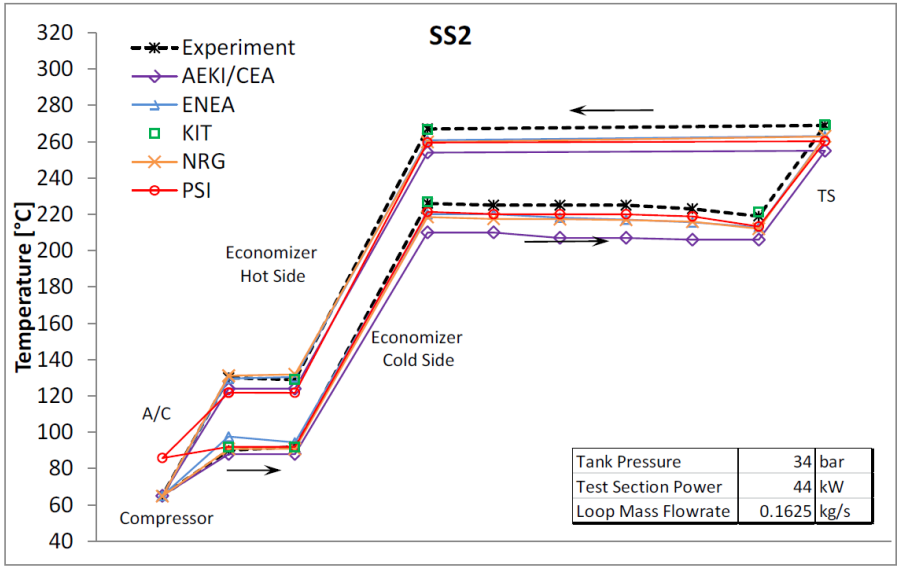

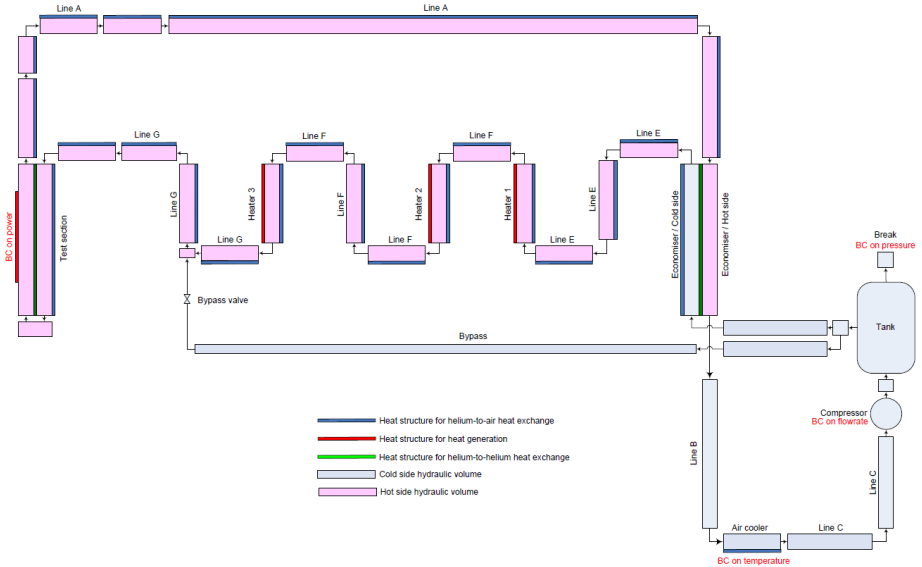

HEFUS-3 helium loop: Steady state 3

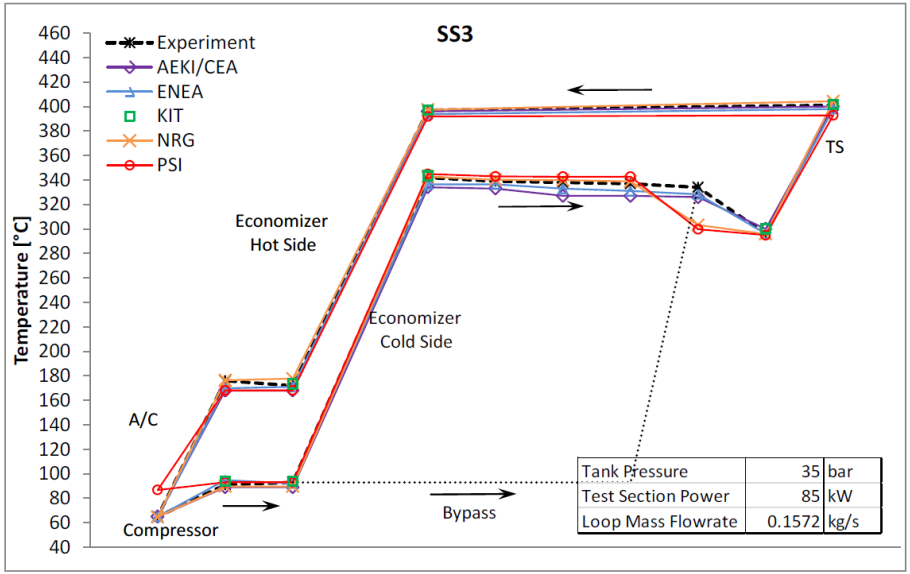

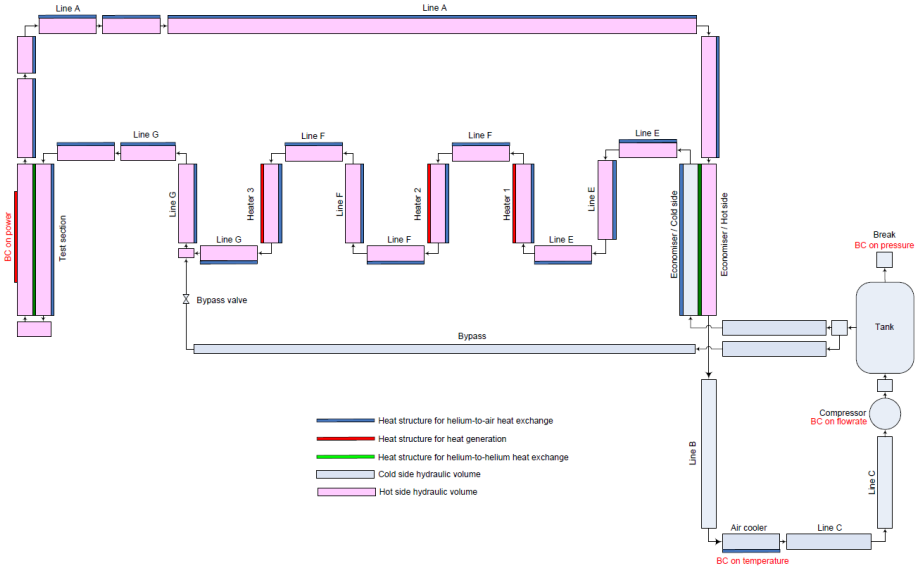

HEFUS-3 helium loop: Steady state 4

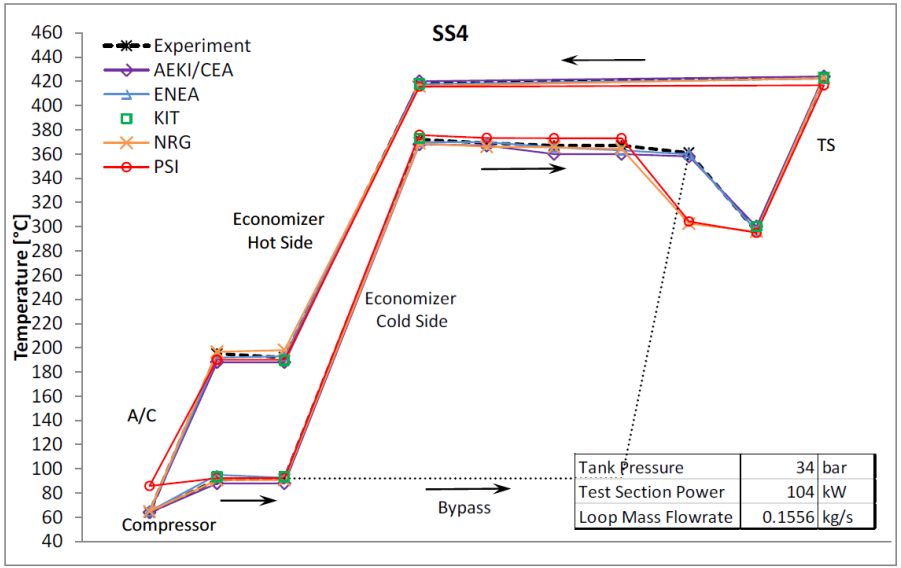

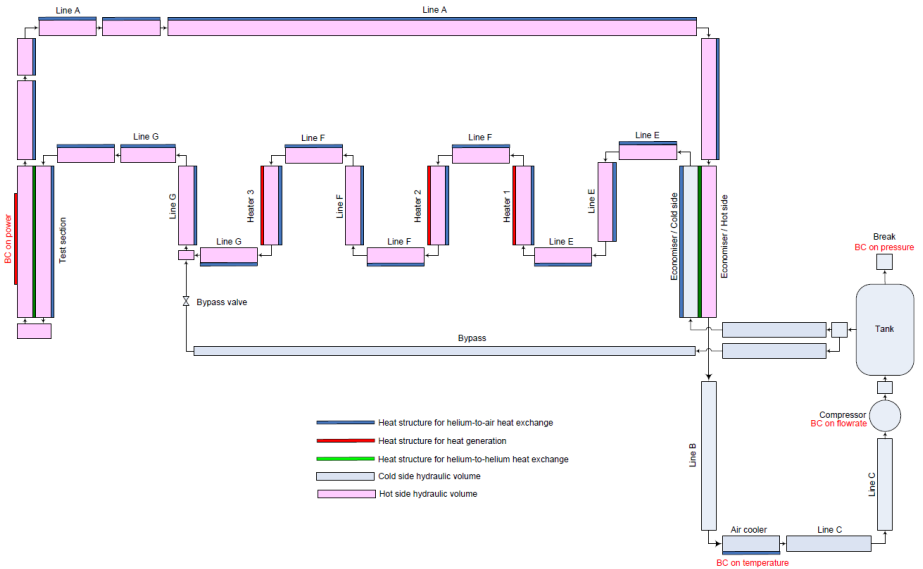

HEFUS-3 helium loop: Steady state 5

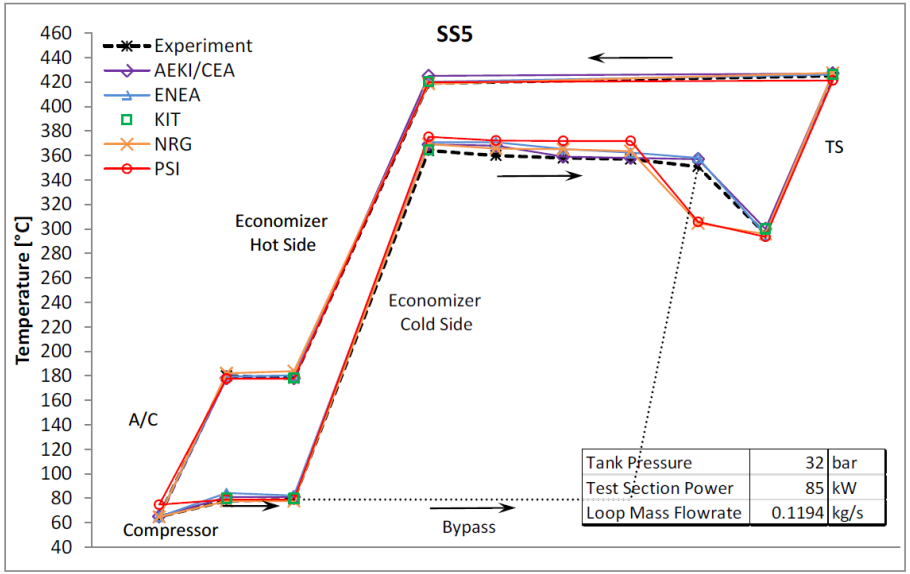

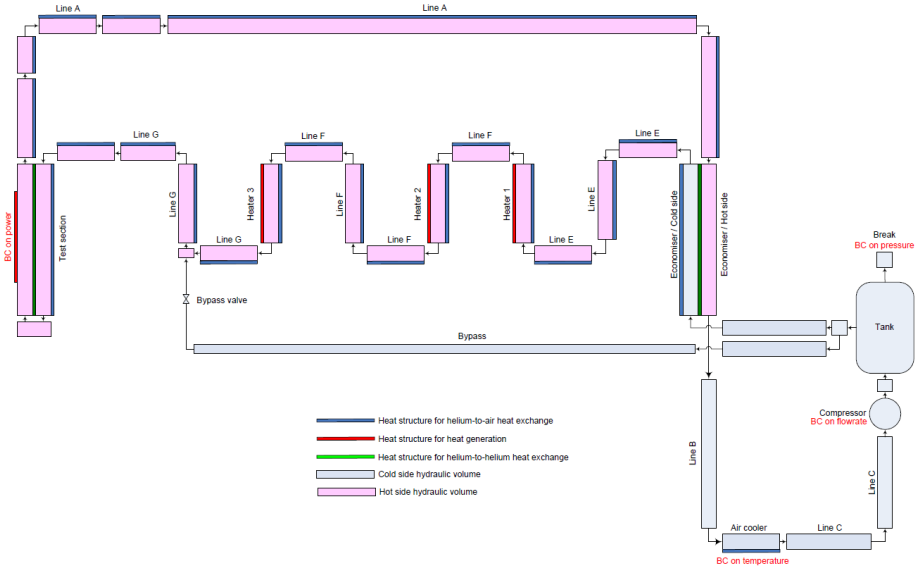

HEFUS-3 helium loop: Steady state 6

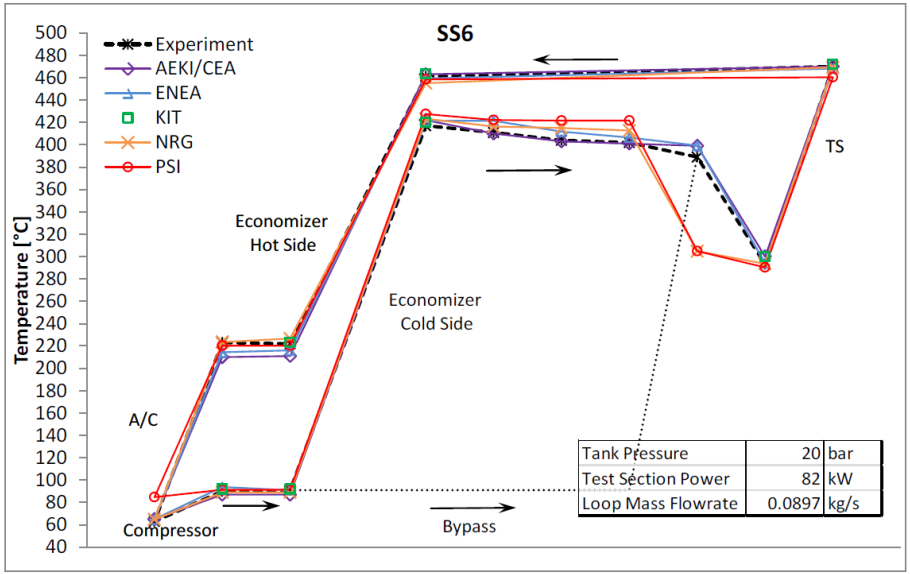

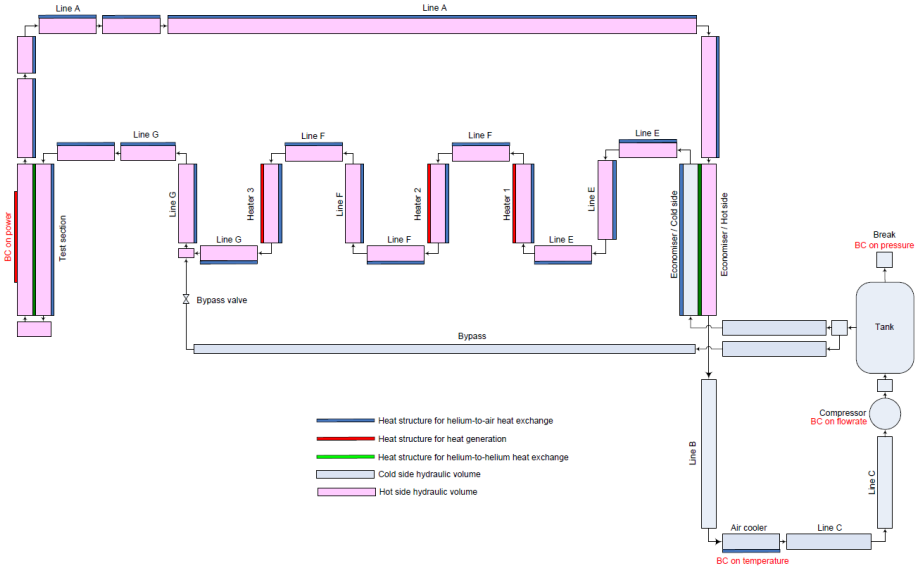

HEFUS-3 helium loop: Steady state 7

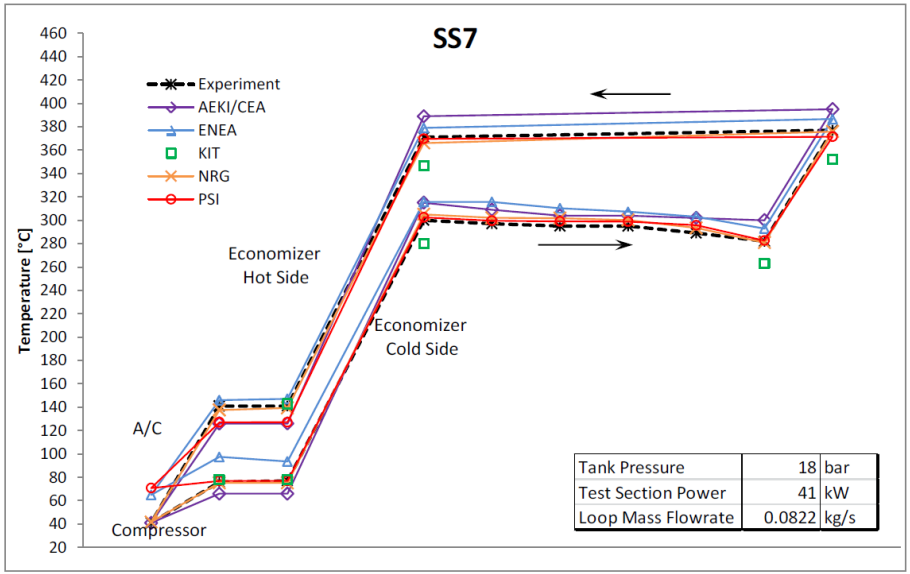

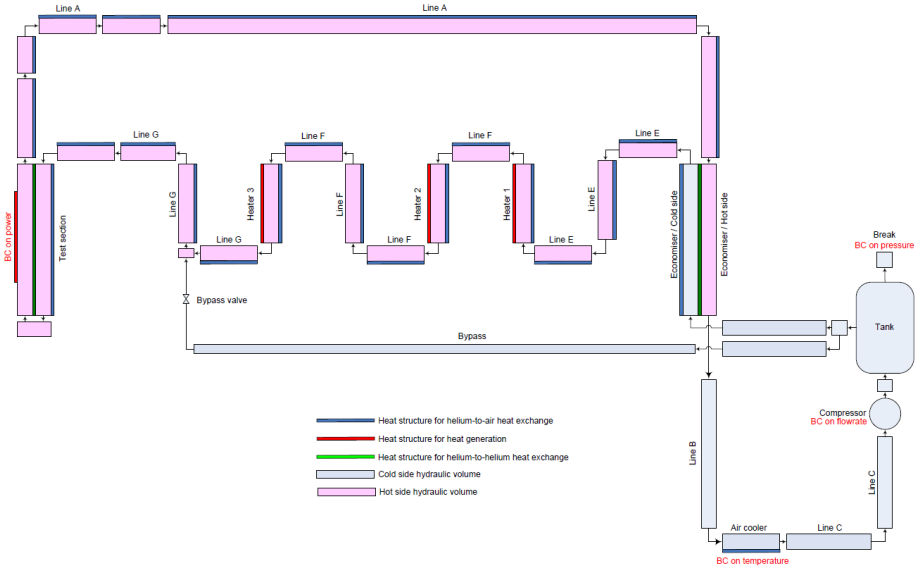

HEFUS-3 helium loop: transients

LOFA1: Compressor slowdown

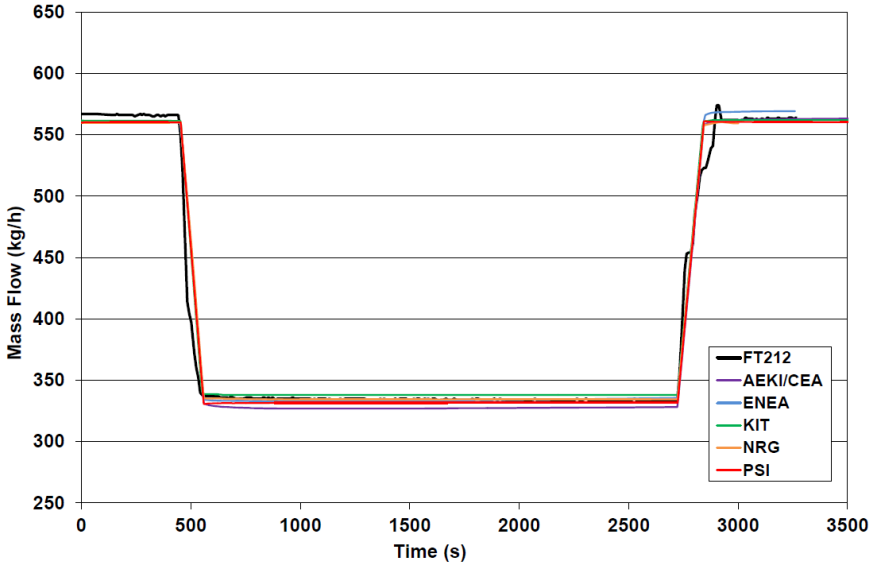

Loop mass flowrate

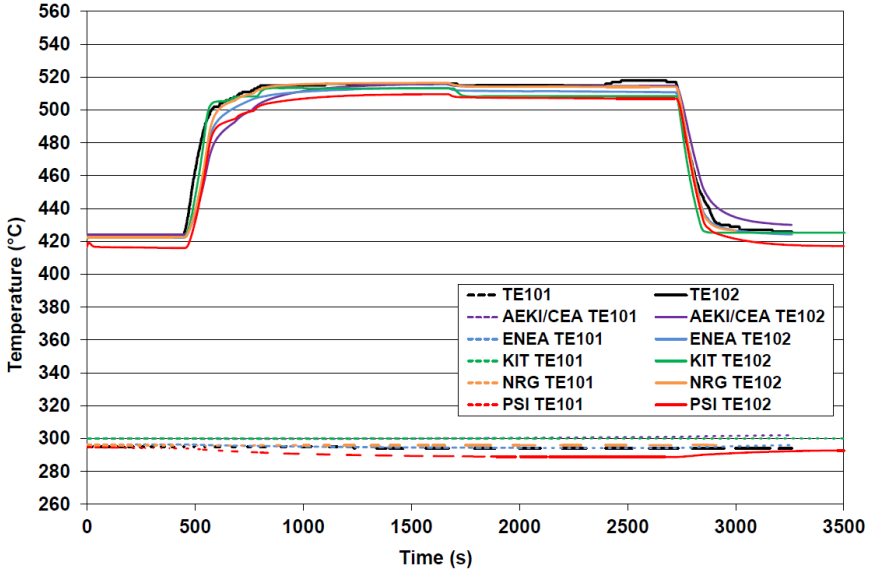

Helium temperatures at test section inlet and outlet

HEFUS-3 helium loop: transients

LOFA2: Bypass valve opening

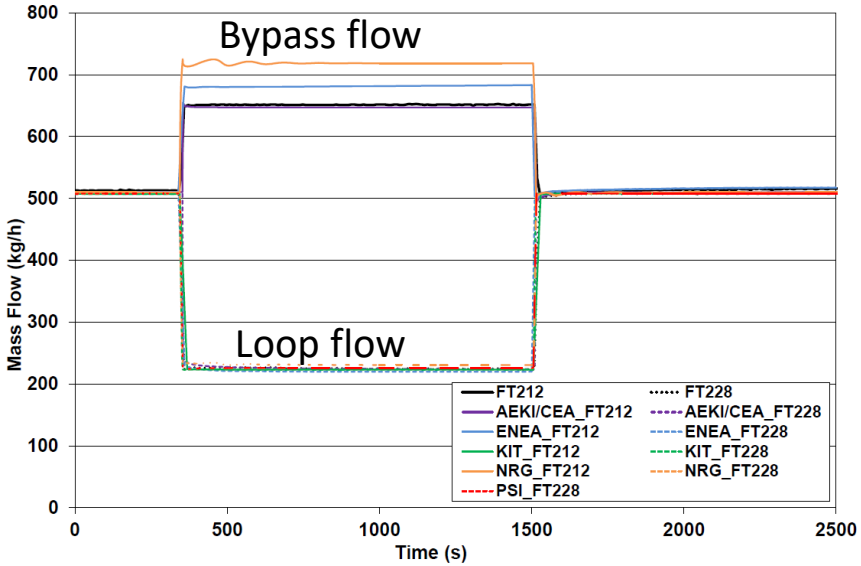

Loop mass flowrate

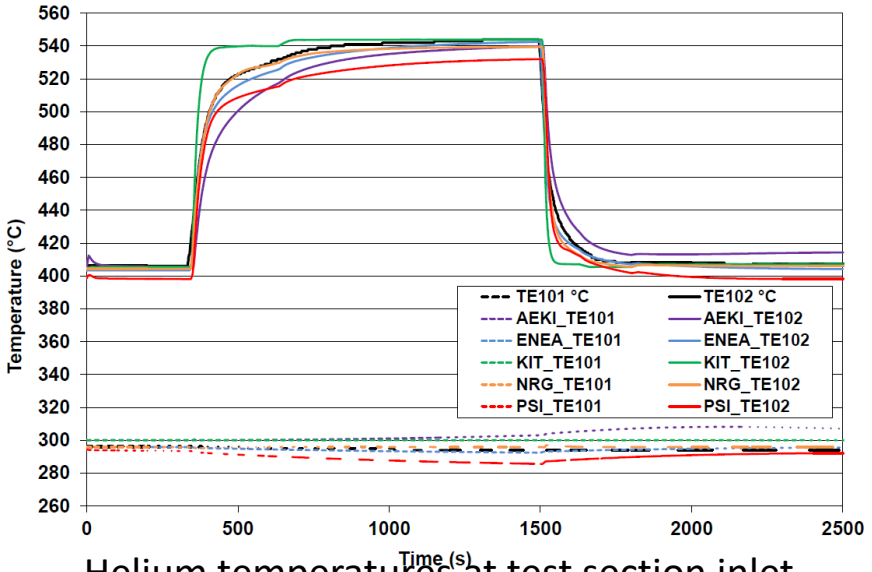

Helium temperatures at test section inlet and outlet

L-STAR air loop: objectives

L-STAR is an air loop at KIT

The main objectives of the project are:

- to study the influence of the walls on the flow structures and the effects of different wall topologies
- to establish a database for the improvement and qualification of computational fluid dynamics (CFD) codes, to simulate turbulent flows in the vicinity of textured surfaces
- to provide friction and heat transfer correlations suitable for system codes
- to contribute to the technology development of gas loops (particle removal, transient behaviour and control, spacer geometries, fatigue and wear)

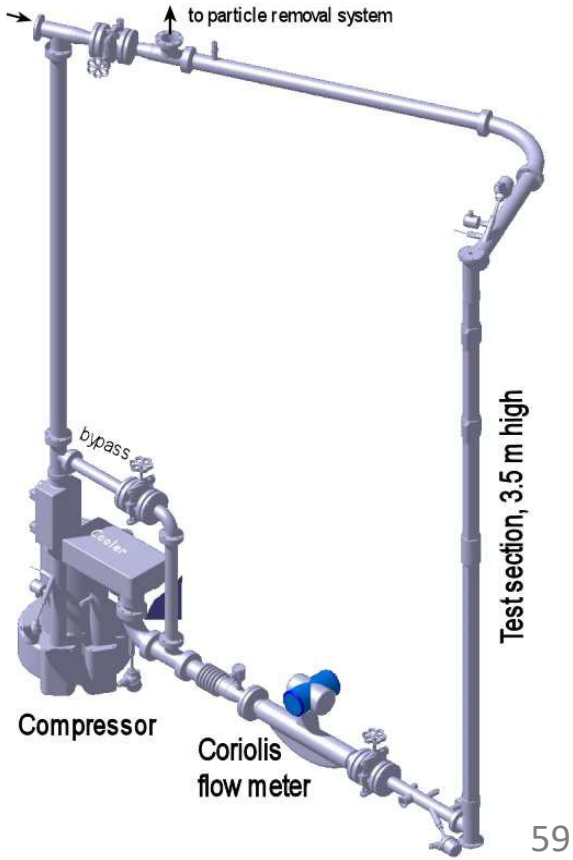

L-STAR air loop: schematics

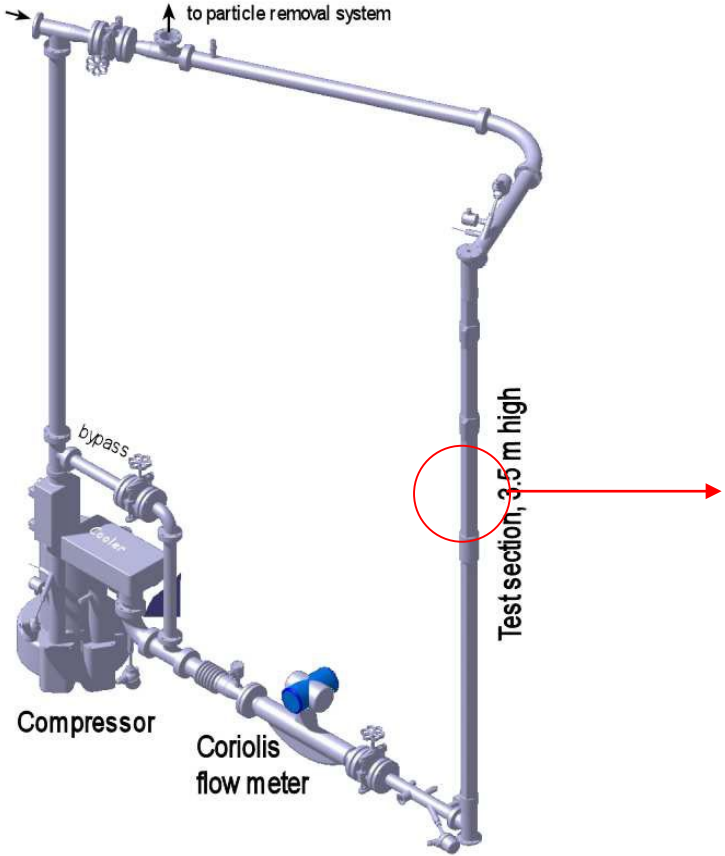

Flow domain of the L-STAR/SL 67/35/2500 test section
d_w=35mm, h_{hex}=33.65mm, r_{hex}=6.5mm
A_c=3027.4mm^2
S_w=334.2mm

optical windows (blue) and LDA profile trajectories (green, dashed) are indicated.

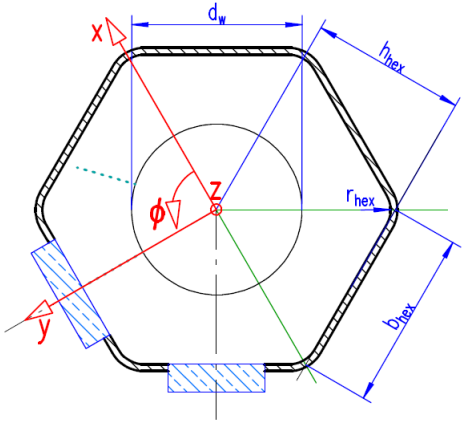

L-STAR air loop: test section

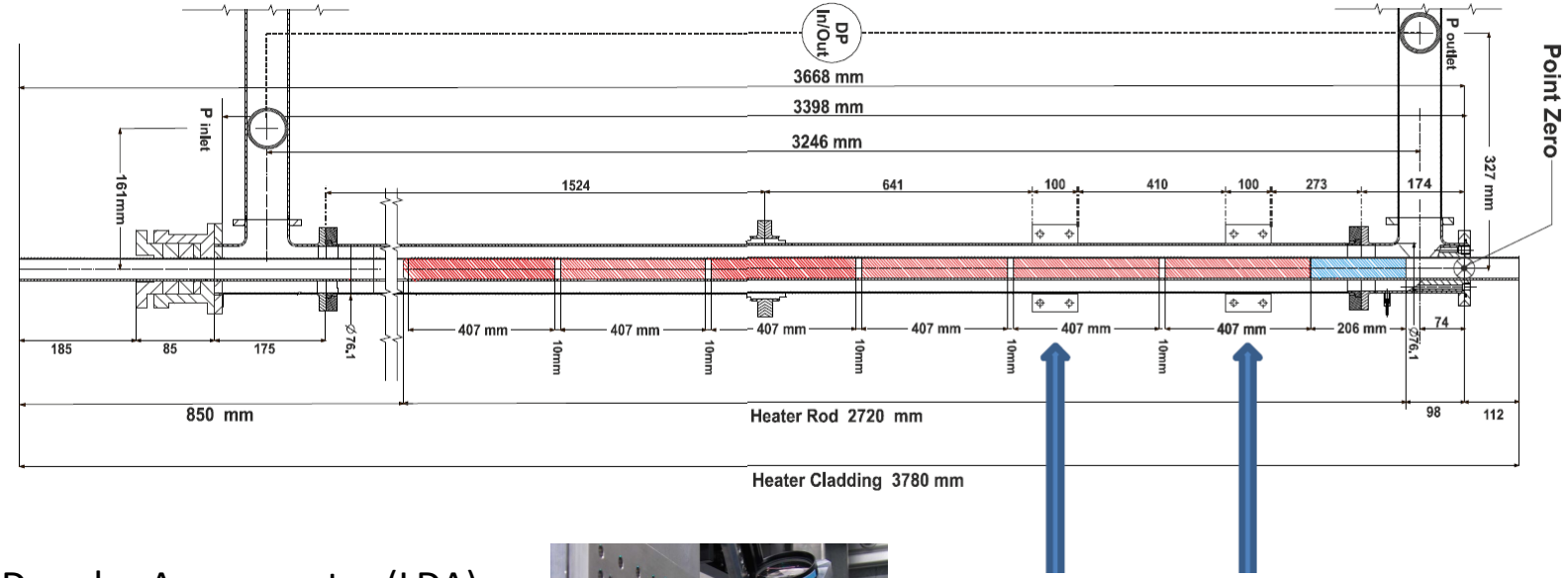

LDA windows

Laser-Doppler Anemometry (LDA)
Profile sensor at L-STAR/SL testsection

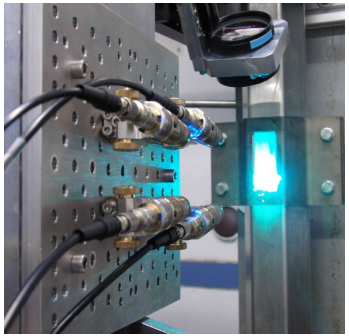

L-STAR air loop: example of meshing

KIT CFX 14.0 mesh details from the heater rod and hexcan area

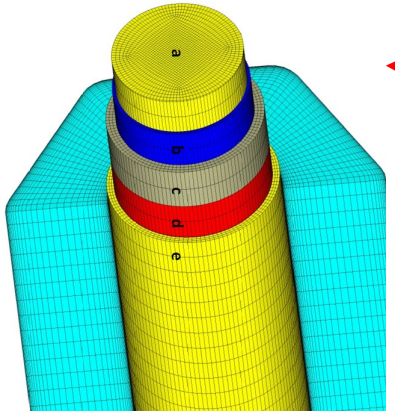

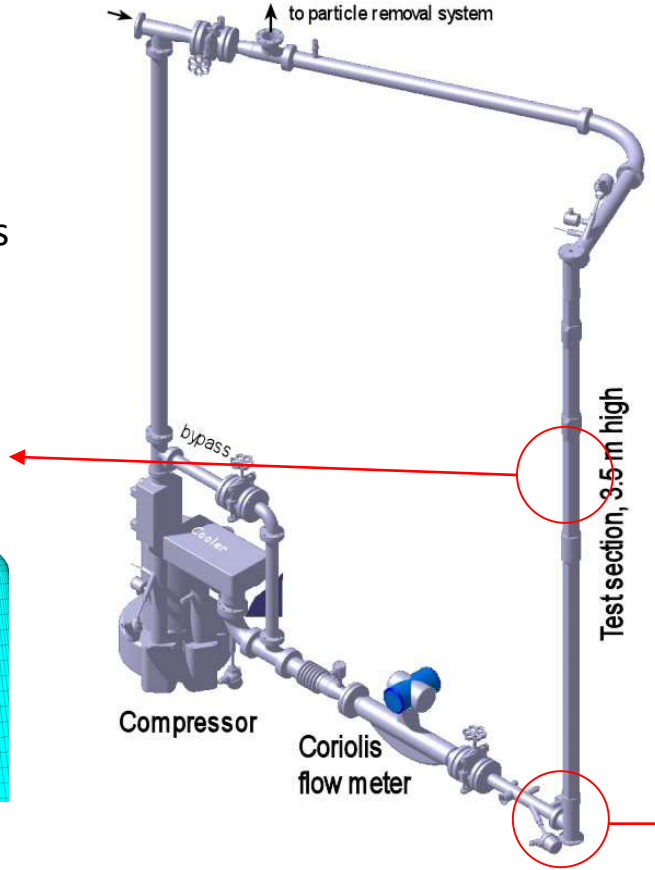

KIT CFX 14.0 mesh details at the inlet bend

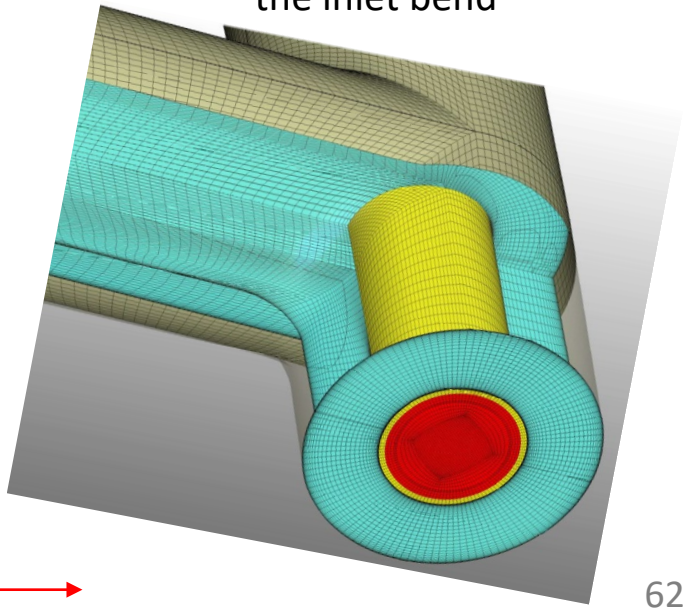

L-STAR air loop: results

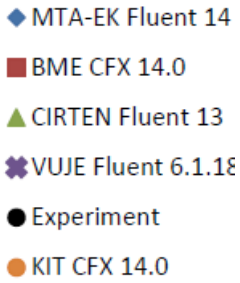

12.6 kg/s and 508 W

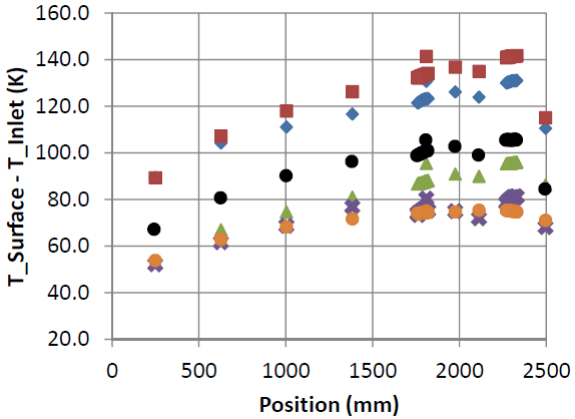

25.3 kg/s and 1016 W

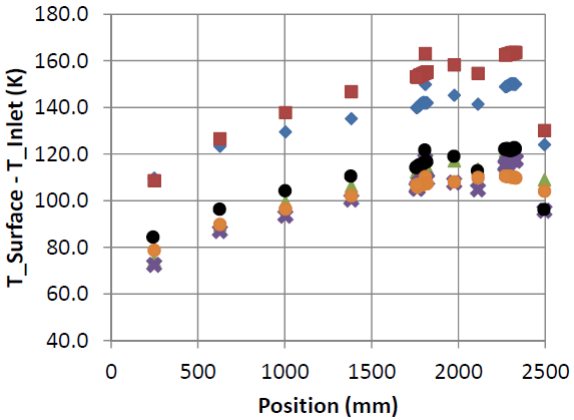

37.9 kg/s and 1523 W

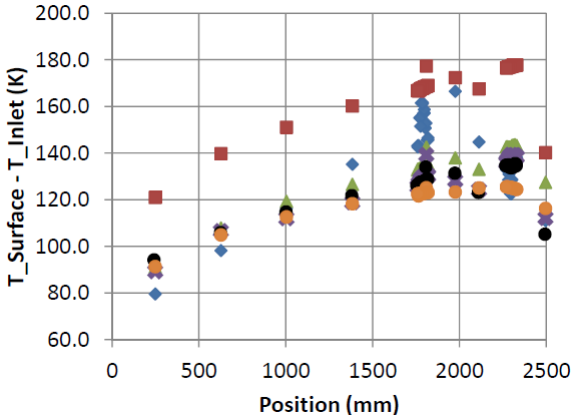

L-STAR air loop: results

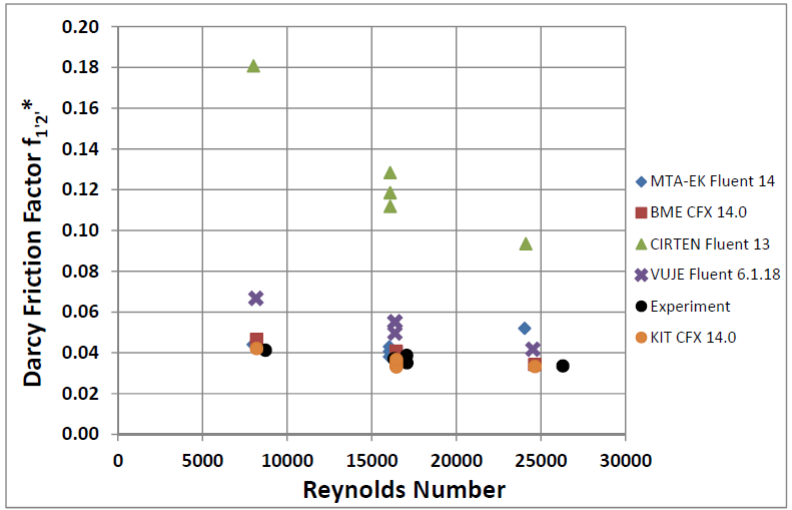

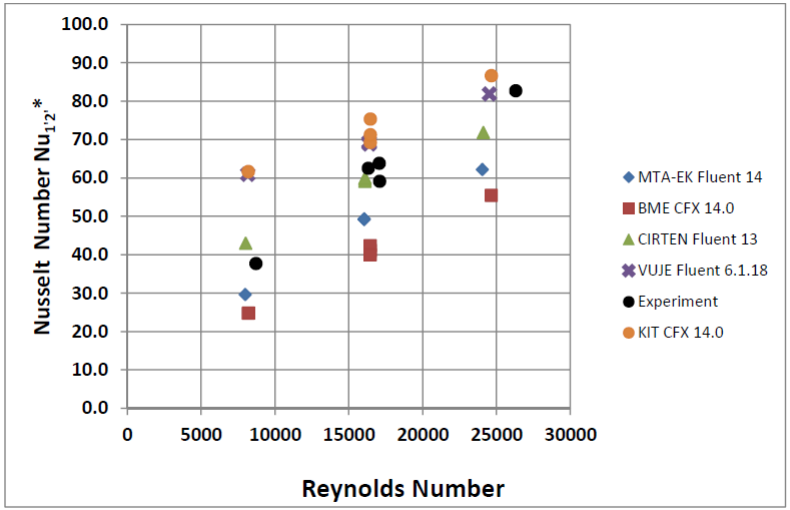

Preparing ESNII for HORIZON 2020

Preparing ESNII for HORIZON 2020

- EU framework: FP7
- Period: September 2013 – August 2017
- Total project cost €10 362 135
- EC contribution €6 455 000
- Participants (35):
  - CEA France
  - AMEC UK
  - ANSALDO Italy
  - AREVA France
  - CIEMAT Spain
  - CIRTEN Italy
  - EDF France
  - EA Spain
  - ENEA Italy
  - GRS Germany
  - HZDR Germany
  - INR Romania
  - JRC Belgium
  - KIT Germany
  - KTH Sweden
  - LGI France
  - MTA EK Hungary
  - NCBJ Poland
  - NNL United Kingdom
  - NRG The Netherlands
  - NUMERIA Italy
  - NUVIA France
  - PSI Switzerland
  - RSE Italy
  - SCK-CEN Belgium
  - SINTEC Italy
  - TE Belgium
  - TU DELFT The Netherlands
  - UJV Řež Czech Republic
  - UPM Spain
  - UPV Spain
  - VUJE Slovakia
  - IPUL Latvia
  - Chalmers Sweden
  - UNIRM Italy

Preparing ESNII for HORIZON 2020: objectives

- The aim of this cross-cutting project is to develop a broad strategic approach to advanced fission systems* in Europe in support of the European Sustainable Industrial Initiative (ESNII)
- The project aims to prepare ESNII structuration and deployment strategy, to ensure efficient European coordinated research on Reactor Safety for the next generation of nuclear installations.

*ASTRID prototype (sodium), the demonstrators ALFRED (lead) and ALLEGRO (gas), a fast neutron spectrum multipurpose irradiation facility (MYRRHA)

ESNII+ Work Packages

1. Structuring ESNII

WP1 Structuring ESNII for HORIZON 2020	NNL, Richard Sainsby
WP2 Strategic Roadmapping	SCK-CEN, Peter Baeten
WP3 Support to facilities development	MTA-EK, Zoltan Hozer
WP4 Industrial perspectives	ANSALDO, Michele Frignani

2. Education and training

WP5 Training and dissemination	CEA, Christian Latge

3. Joint research on crosscutting R&D challenges

WP6 Core Safety	PSI, Konstantin Mikityuk
WP7 Fuel Safety	CEA, Nathalie Chauvin
WP8 Seismic Studies	ENEA, Massimo Forni
WP9 Instrumentation for safety	SCK-CEN, Marc Schyns

4. Project Management

WP10 Coordination and support	CEA, Alfredo Vasile

Main GFR-related deliverables

- ALLEGRO core safety parameters and influence of model uncertainties on transients
- ALLEGRO core specification
- R&D needs for ALLEGRO core safety

R&D needs for ALLEGRO core safety

System design:

- Clad melt is not acceptable for unprotected transients being originally DBC2 events like main blower failure or inadvertent control rod withdrawal.
- The only solution is a new core design with decreased power density or/and reactor power.

Testing and qualification

- ALLEGRO will be test bed to develop and qualify the high-temperature, high-power density fuel required for a commercial-scale high-temperature GFR

Modeling

V&V

Summary

Three European projects reviewed with a focus on GFR-related experimental data

- **GCFR**:
  - EIR gas loop tests: data for validating correlations in particular for artificial roughness
  - GCFR-Proteus: data for neutroncis codes validation
- **GoFastR**:
  - HEFUS-3 helium loop: data for system thermal-hydraulics codes validation
  - L-STAR air loop: data for CFD codes validation
- **ESNII Plus**:
  - Important conclusion on the need to reduce ALLEGRO power

PAUL SCHERRER INSTITUT

Wir schaffen Wissen – heute für morgen

Thank you for your attention.

72

Modeling of innovative reactors with Serpent

Examples from international projects

E. Fridman

HELMHOLTZ ZENTRUM
DRESDEN ROSSENDORF

Quick intro: what's special about Serpent?

- First Monte Carlo code especially developed for reactor physics applications
- Started gaining popularity around 2010
- Constantly growing user's community
- One of the main reactor physics tools nowadays

Example: Serpent “share” in SFR-related EU project

CP-ESFR
(2009 – 2013)

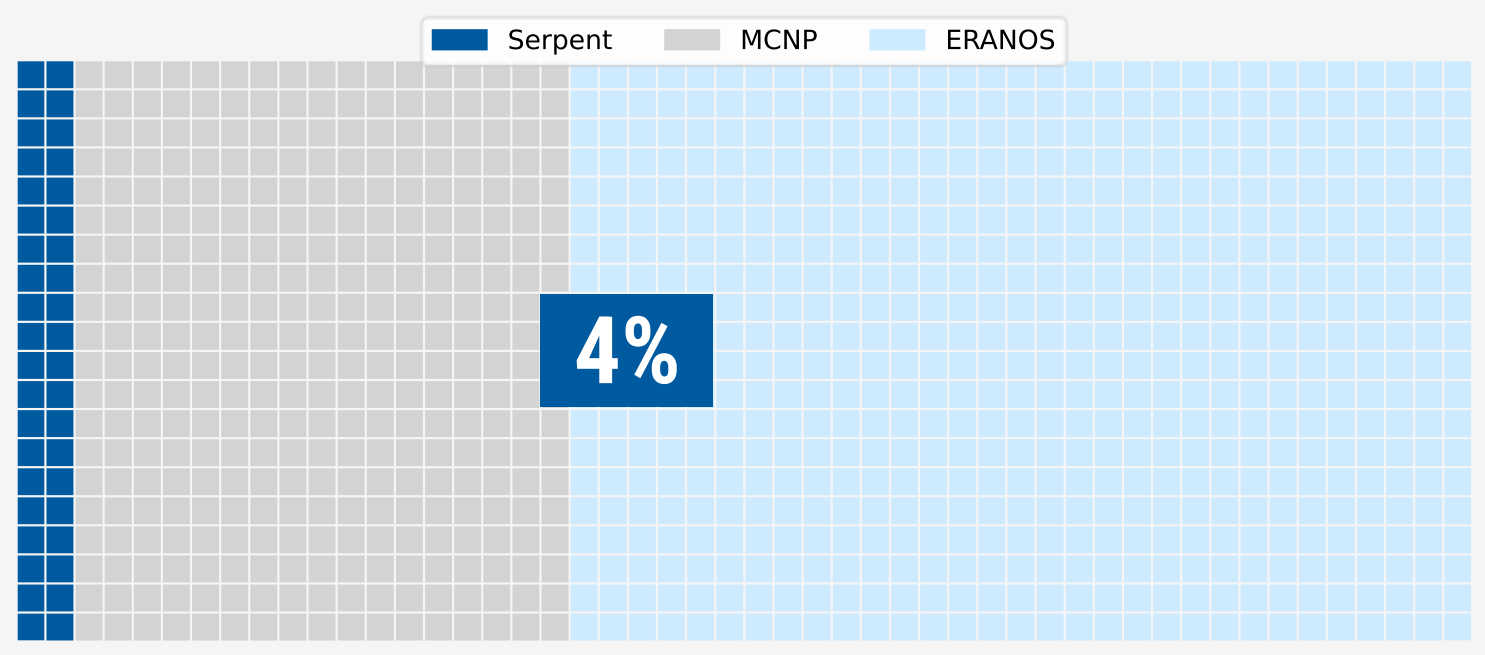

Example: Serpent “share” in SFR-related EU project

CP-ESFR (2009 – 2013) → ESNII+ (2013 – 2017)

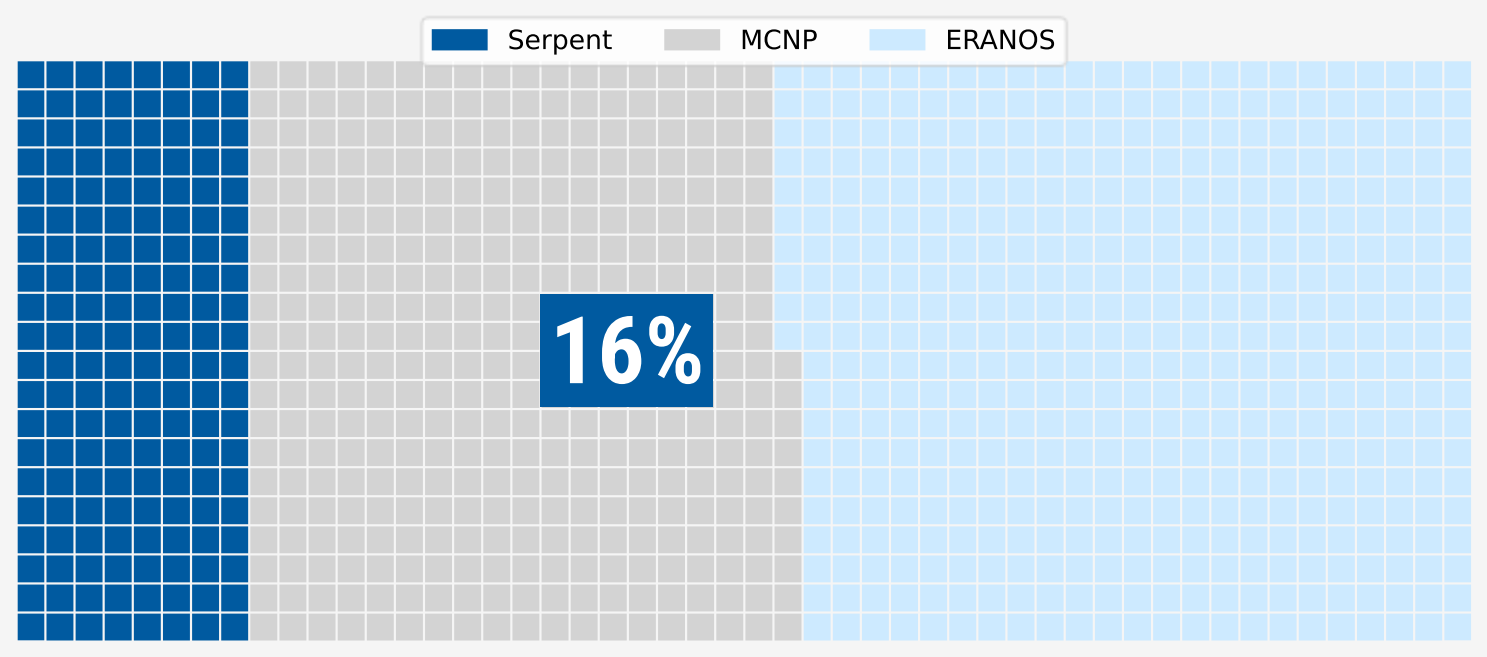

Example: Serpent “share” in SFR-related EU project

CP-ESFR (2009 – 2013) → ESNII+ (2013 – 2017) → ESFR-SMART (2017 – 2022)

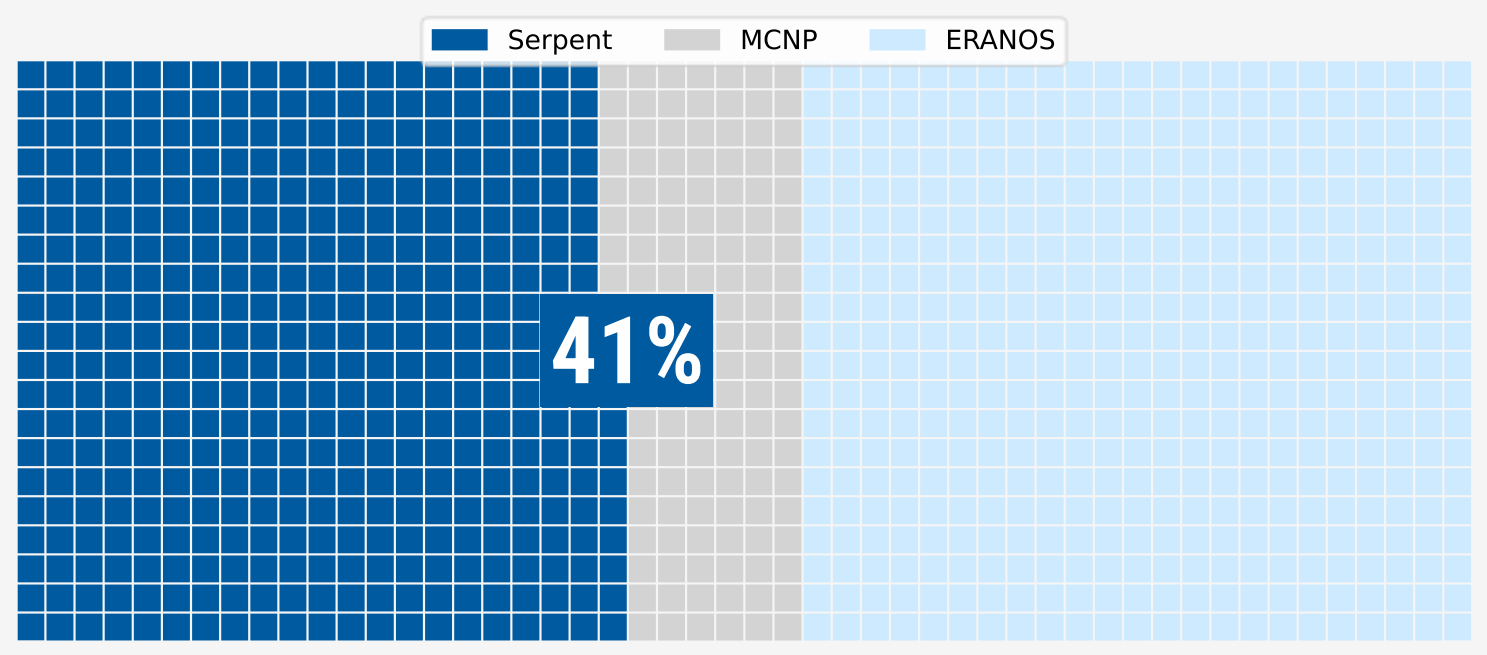

Example: Serpent “share” in SFR-related EU project

CP-ESFR (2009 – 2013) → ESNII+ (2013 – 2017) → ESFR-SMART (2017 – 2022) → ESFR-SIMPLE (2022 – 2026)

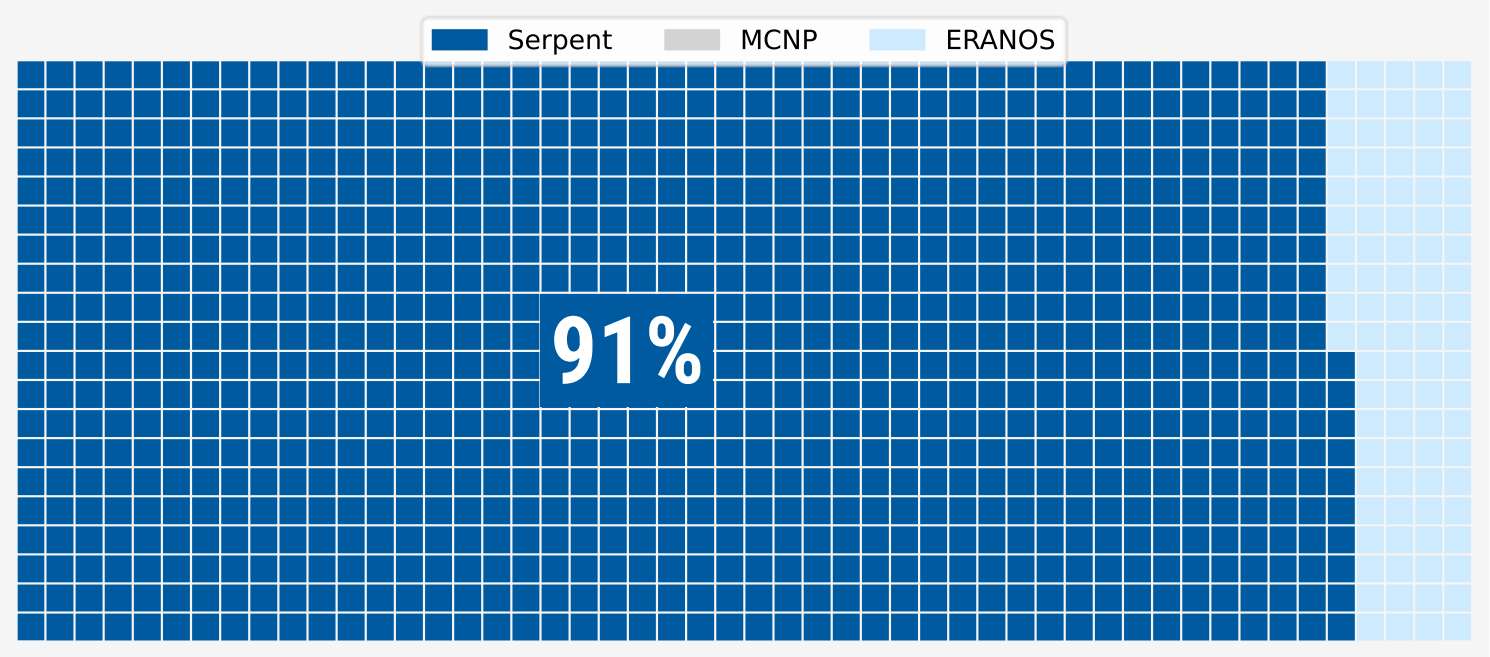

Application examples in this presentation

Fuel cycle analysis

ESFR multi-batch burnup

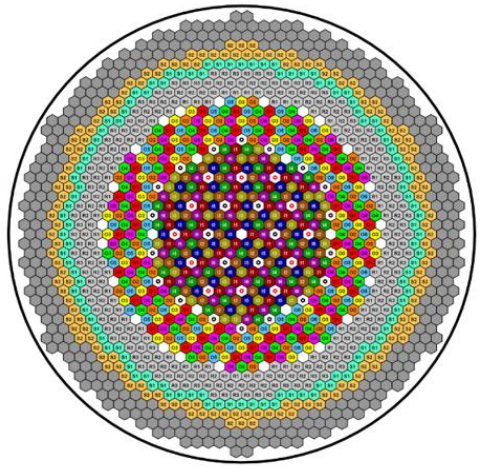

HZDR 8

Neutronics data for transient analysis of SFRs

Superphénix start-up tests

FFTF loss of flow test

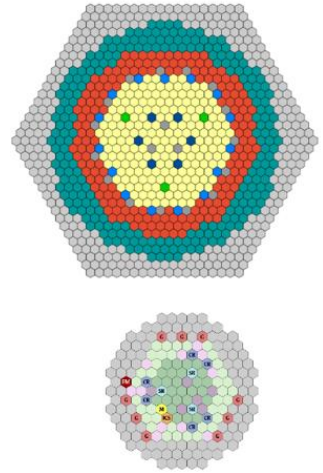

HZDR 13

Dynamic simulations

CEFR control rod drop tests

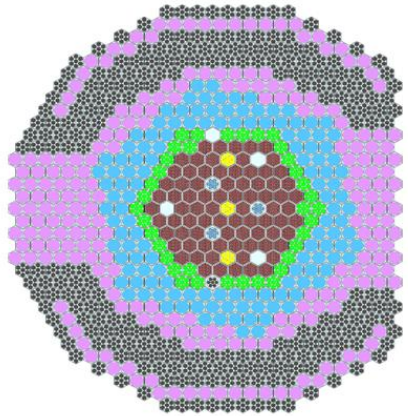

HZDR 33

Mechanical core deformations and CAD models

Phénix flowering

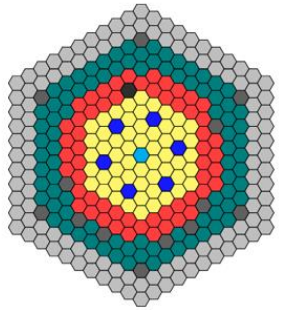

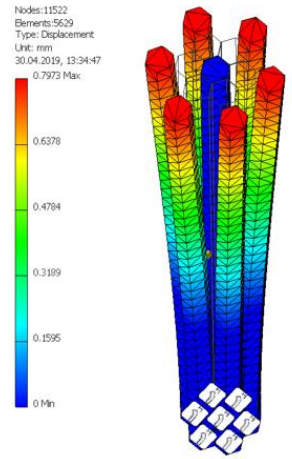

HZDR 39

Fuel cycle analysis

ESFR multi-batch burnup

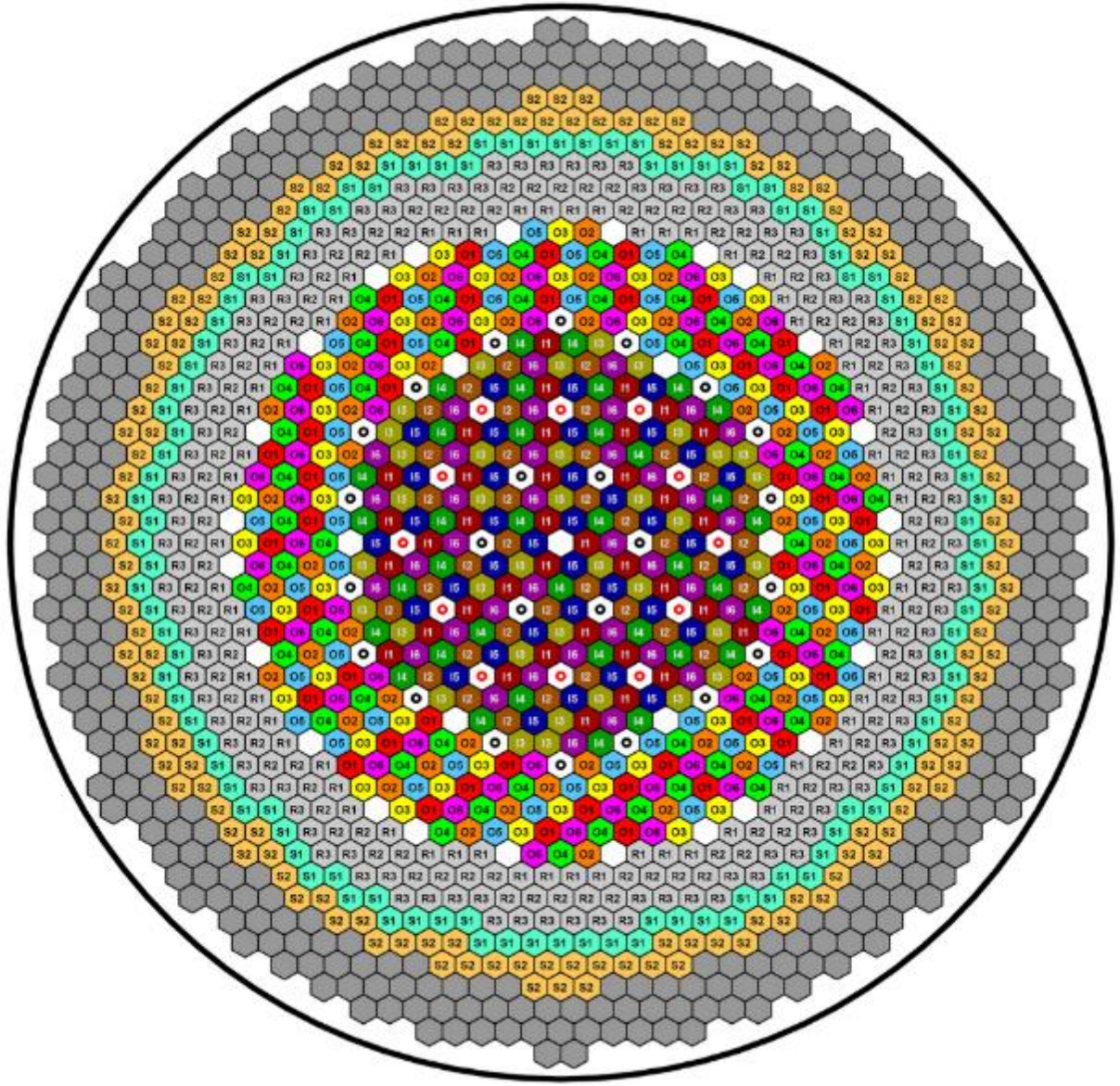

ESFR overview

- Pool-type SFR
- 3600 MWth
- 216 inner + 288 outer MOX fuel SAs
- 6-batch symmetric reloading scheme
- 1-year fuel cycle length
- 6-year in-core residence time

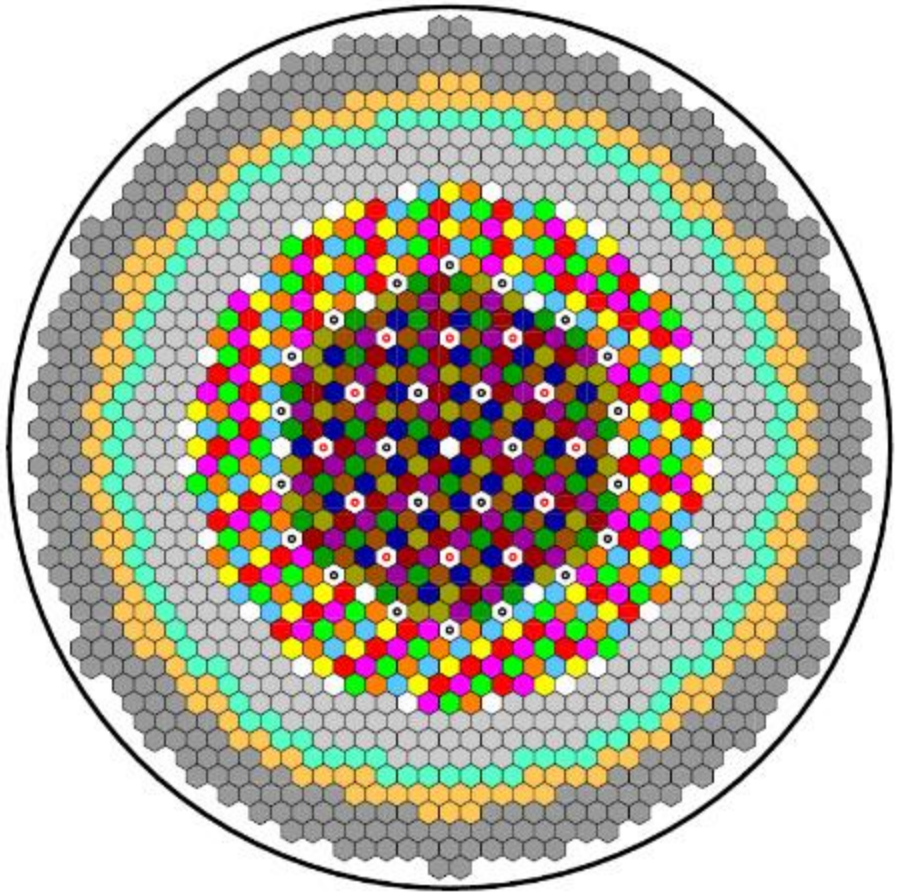

IF: 6 batches × 36 = 216 SAs

OF: 6 batches × 48 = 288 SAs

Multi-batch burnup calculations
Towards equilibrium core

- EOEC core is used for accident analysis
- Established after 18 successive fuel cycles
- 1/6th of the core is reloaded every cycle
- Axial zoning via **automated depletion zone division**
  - 8 axial burnable regions in IF
  - 6 axial burnable regions in OF
  - No need to re-define geometry
- New cycles via **restart option**

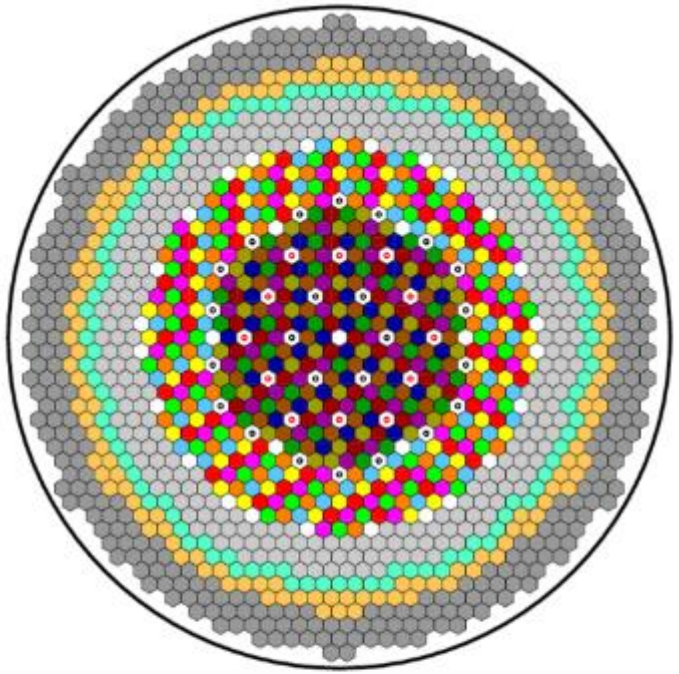

IF: 6 batches × 36 = 216 SAs

OF: 6 batches × 48 = 288 SAs

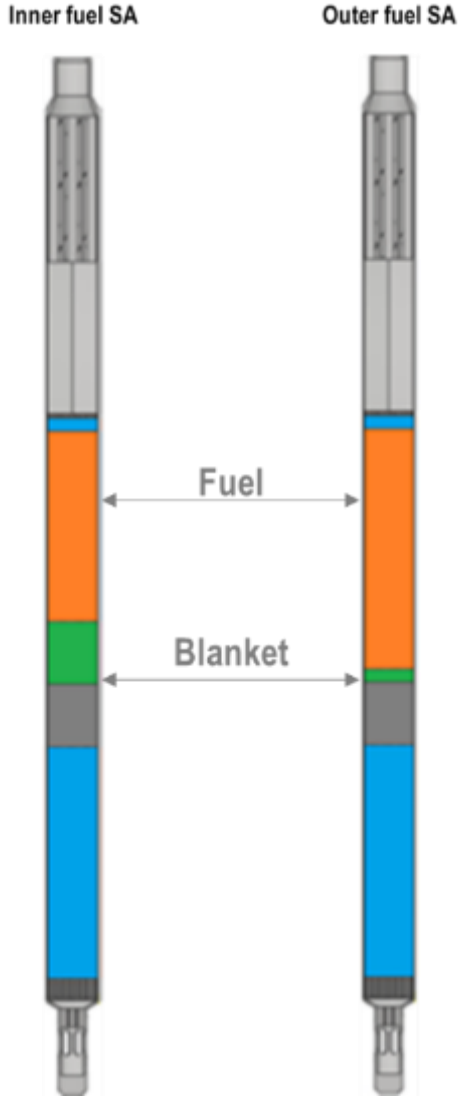

Multi-batch burnup calculations

Cycle-wise core reactivity

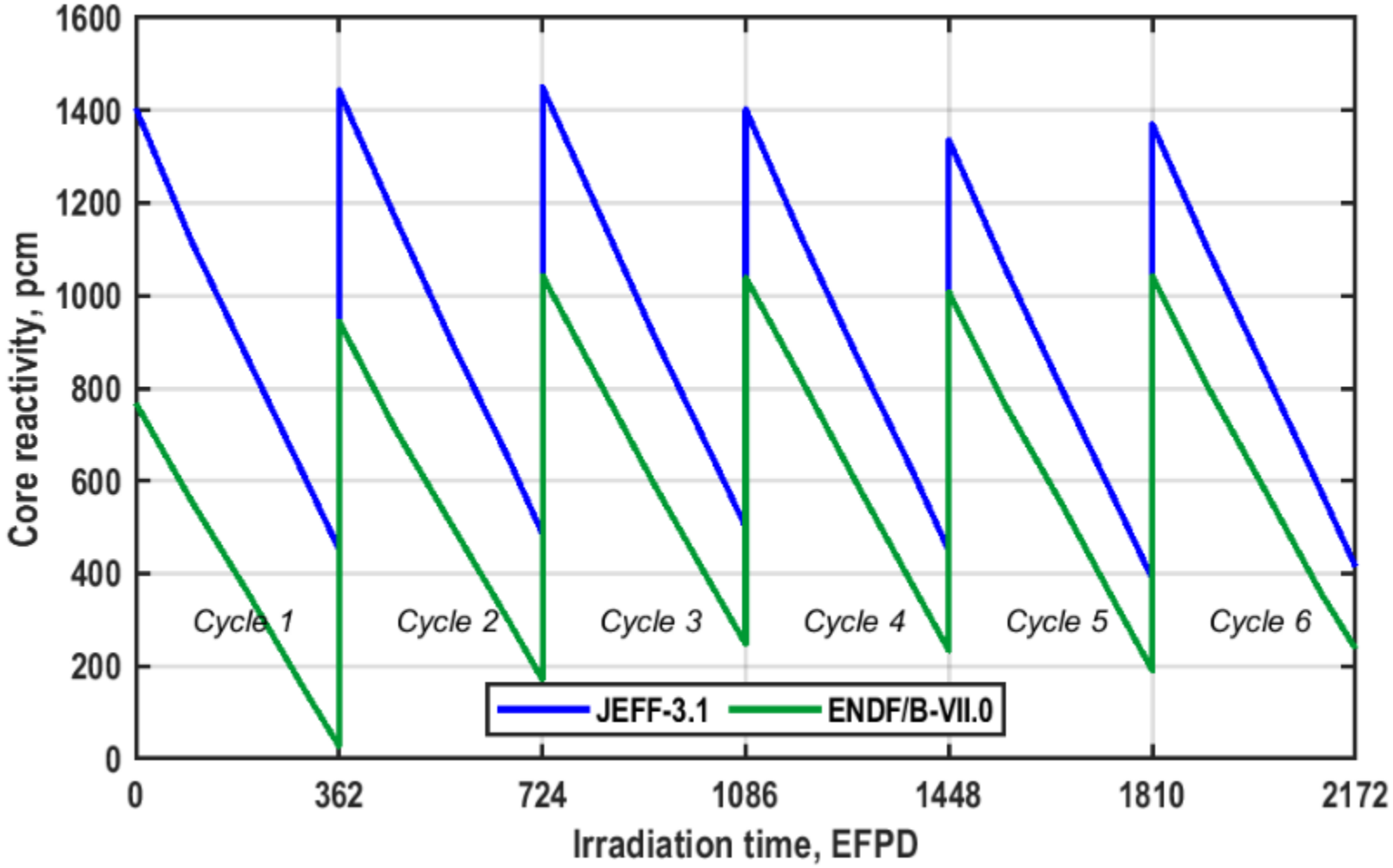

Multi-batch burnup calculations
Breeding performance

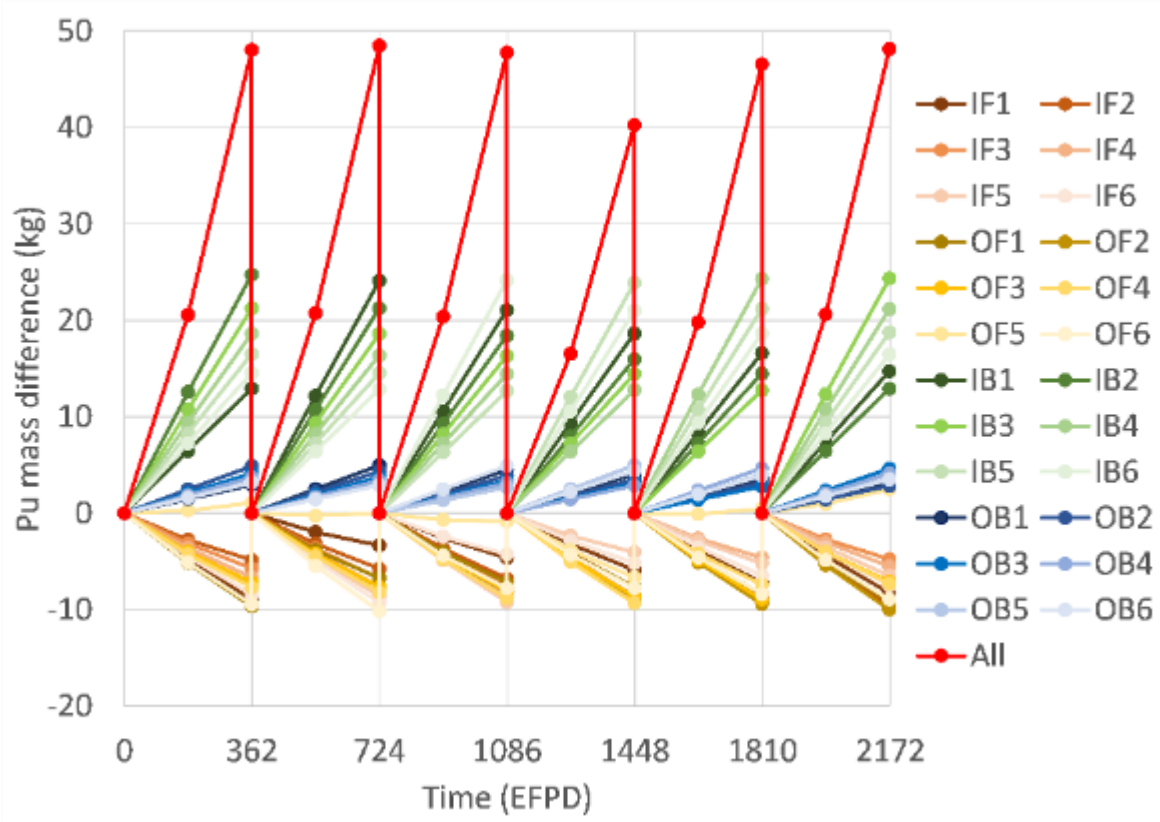

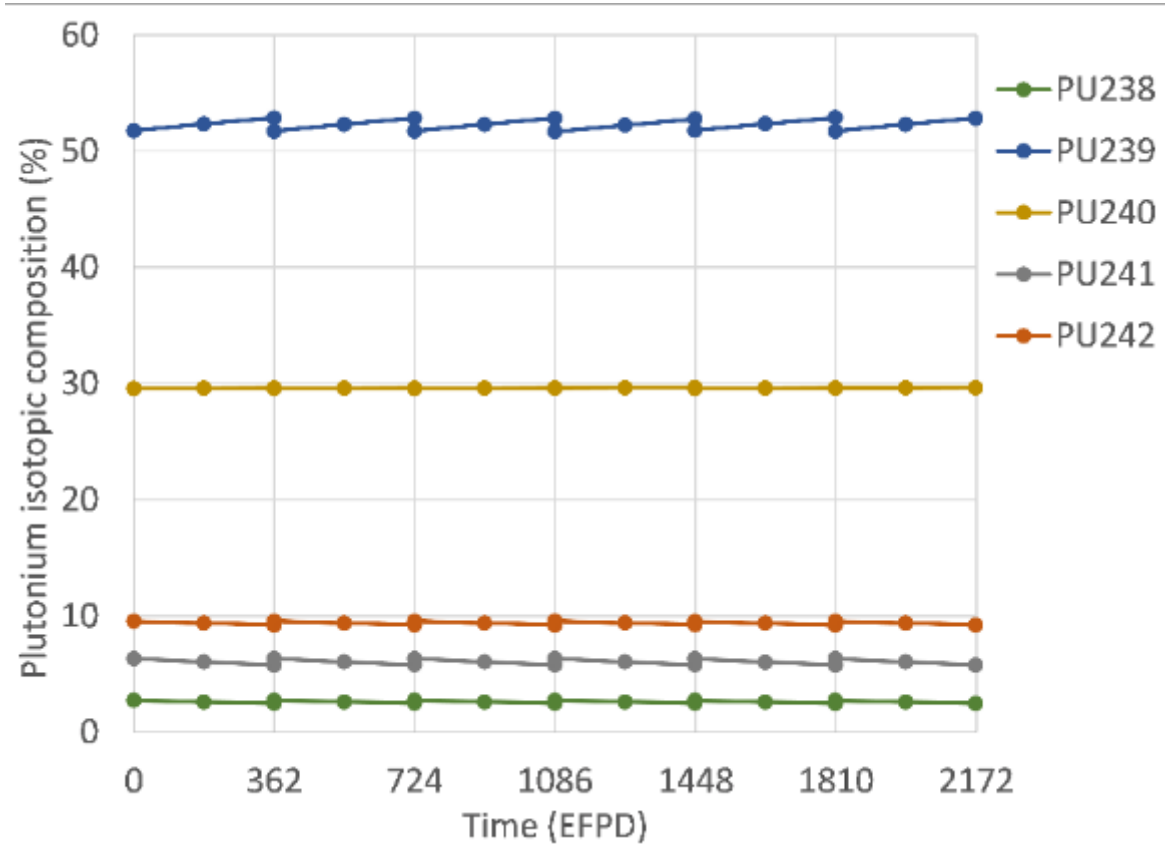

Neutronics data
for transient analysis of SFRs

Superphénix start-up tests

FFTF loss of flow test

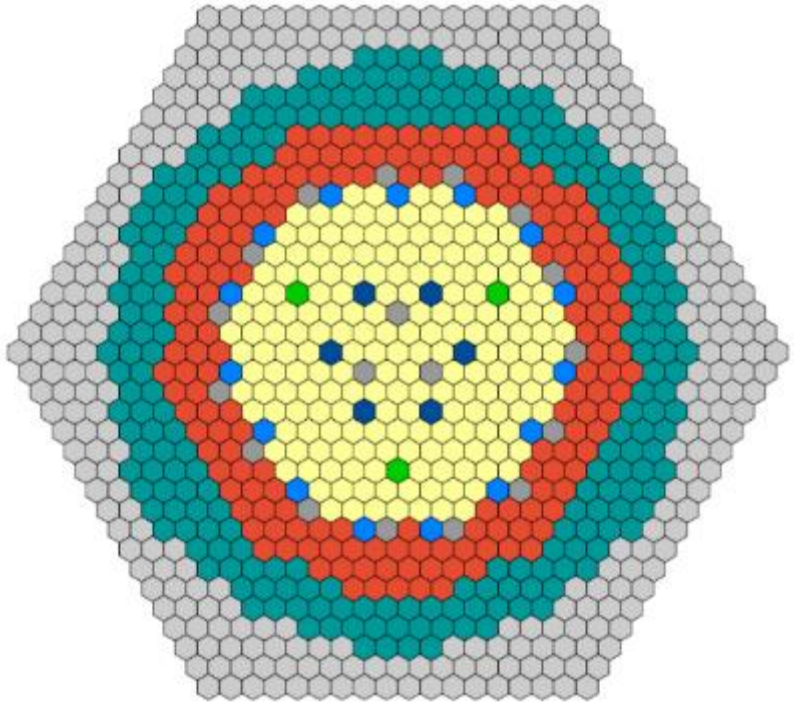

Transient analysis options

0D point kinetics
+ system TH

3D spatial kinetics
+ system TH

Transient analysis options

0D point kinetics
+ system TH

Examples:
TRACE
ATHLET

3D spatial kinetics
+ system TH

Examples:
PARCS/TRACE
DYN3D/ATHLET

What neutronics data is needed?

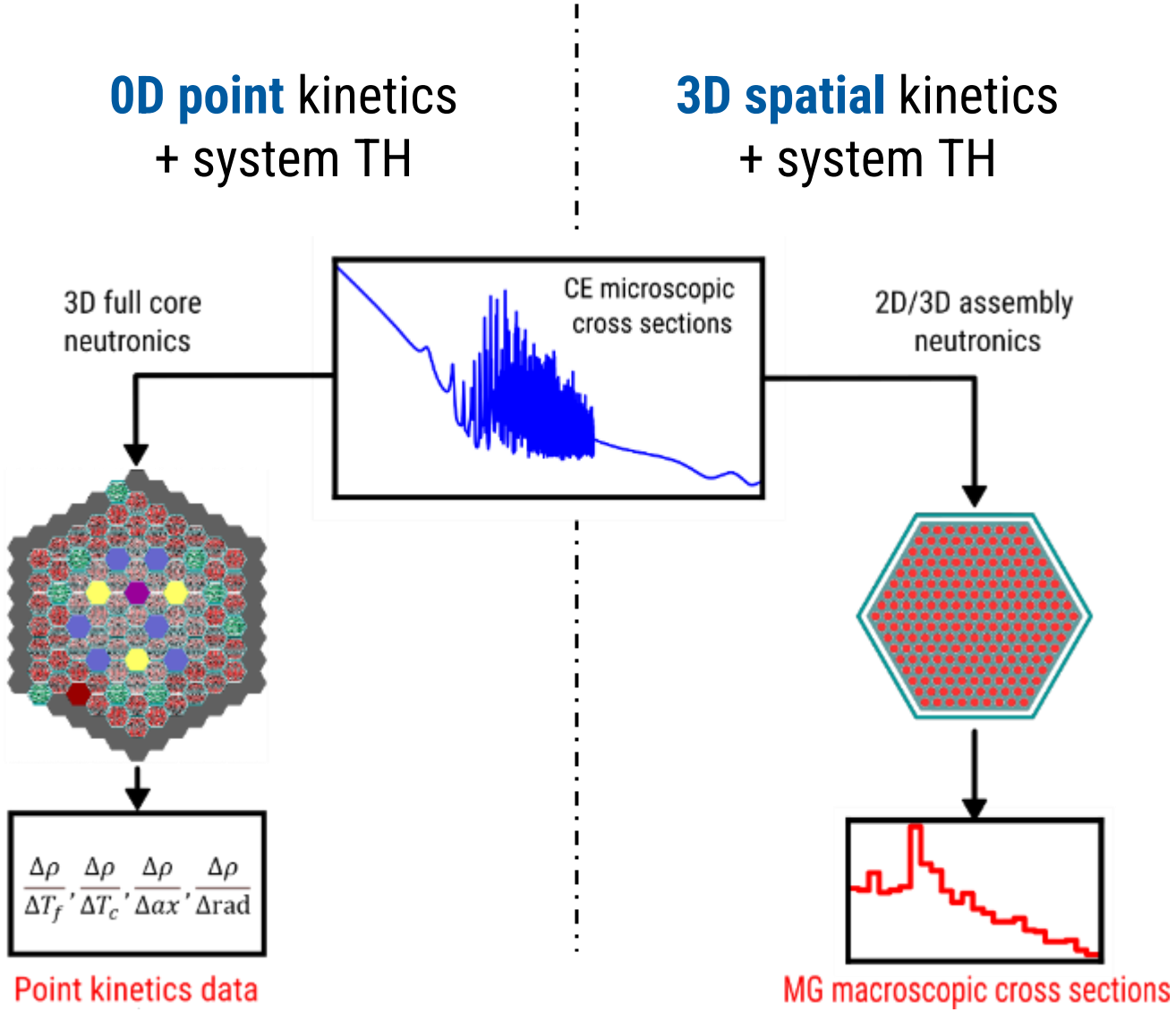

Superphénix start-up tests

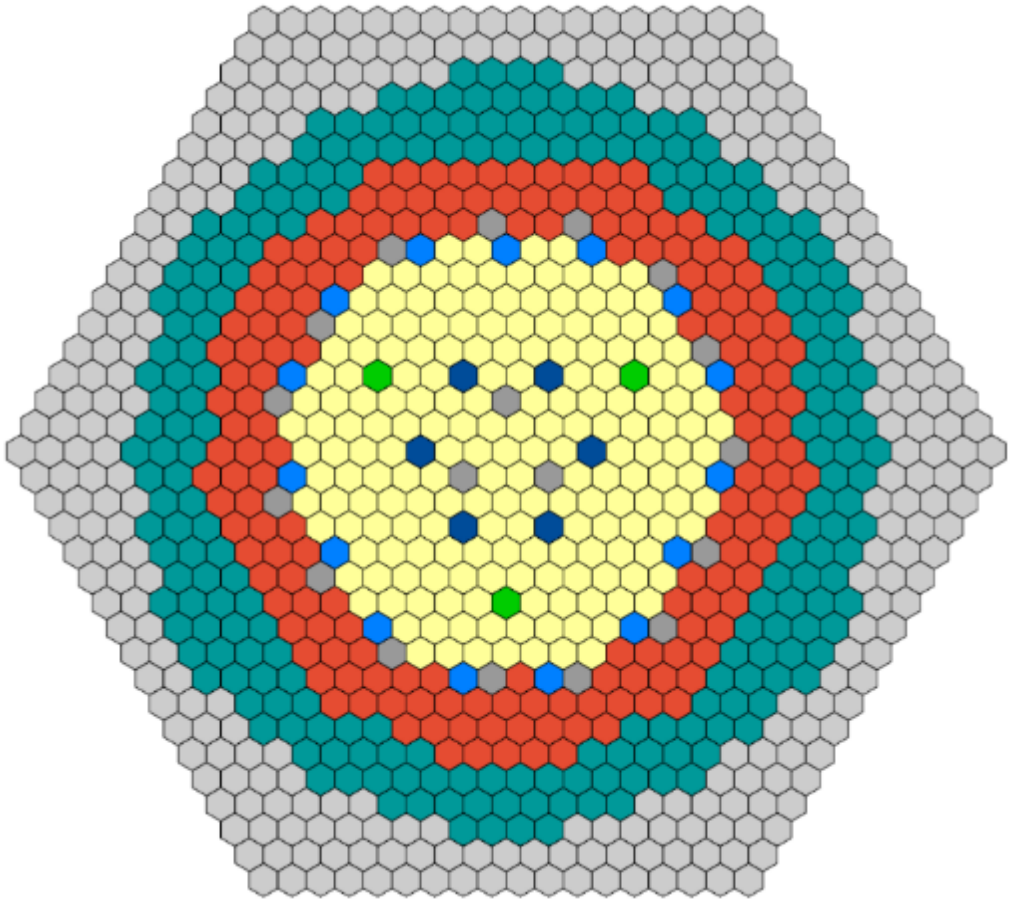

Superphénix reactor

- Largest ever operated Fast Reactor
- Pool-type SFR
- 3000 MWth
- MOX fuel
- 190 inner fuel SA (16% Pu)
- 168 outer fuel SA (20% Pu)
- 225 blanket SA (depleted UO2)

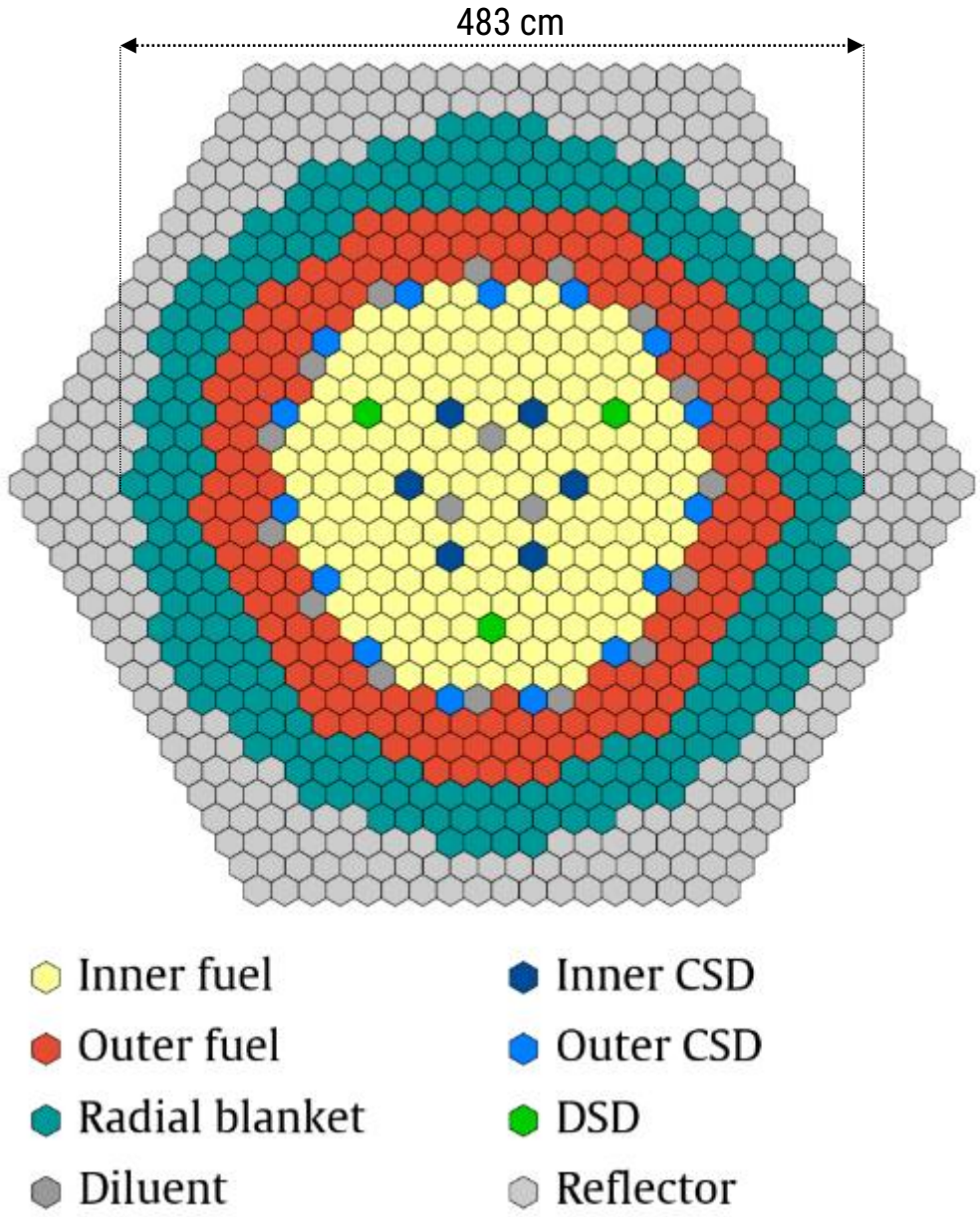

Superphénix star-up tests

- New benchmark defined during the ESFR-SMART project
- Based on the start-up experiments
- Static neutronics and transients

#	Test name	Description
1	MOFC1	−50 pcm reactivity insertion at 692 MW_{th}
2	MOFC2	+10% secondary mass flow rate increase at 633MW_{th}
3	MOFC3	−10% primary mass flow rate reduction at 663MW_{th}
4	Reactivity step (RS)	−74 pcm stepwise reactivity insertion at 1542 MW_{th}
5	Primary flow step (PFS)	−10% primary mass flow rate reduction at 1415 MW_{th}
6	Self-stabilization test (SST)	+30 pcm reactivity insertion at hot zero power
MOFC = Measurement of Feedback Coefficient		

Superphénix star-up tests

- New benchmark de
- Based on the start-
- Static neutronics a

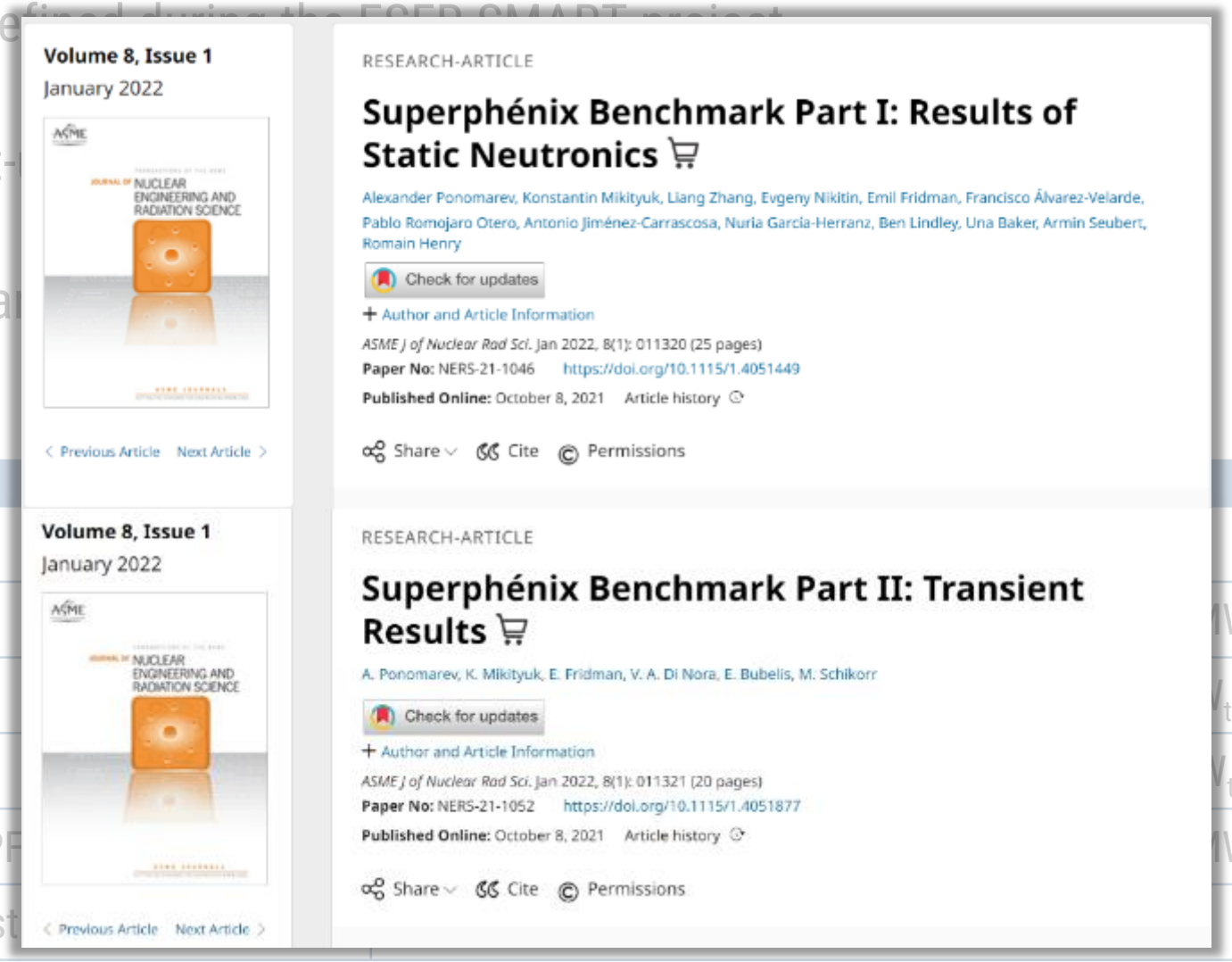

#	Test name	
1	MOFC1	
2	MOFC2	MW_{th}
3	MOFC3	MW_{th}
4	Reactivity step (RS)	MW_{th}
5	Primary flow step (PF	MW_{th}
6	Self-stabilization test	

MOFC = Measurement of Feedback Coefficient

Superphénix star-up tests
Effects to consider

- Standard dependencies
  - Fuel Doppler
  - Coolant temperature + density
- In-core expansions
  - Radial fuel and wrapper expansion
  - Radial diagrid expansion
  - Axial fuel expansion
- Ex-core expansions
  - Strongback expansion
  - Control rod drive line expansion
  - Vessel expansion

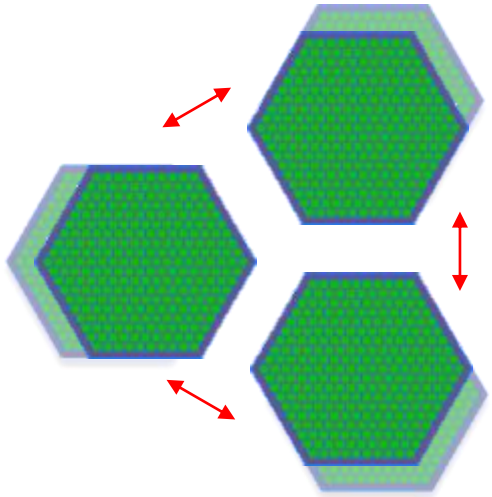

Diagrid radial expansion

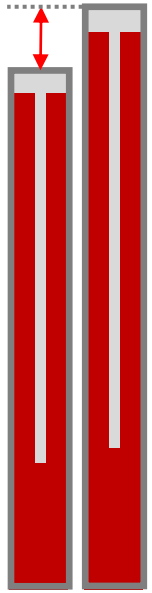

Fuel axial expansion

CRDL expansion

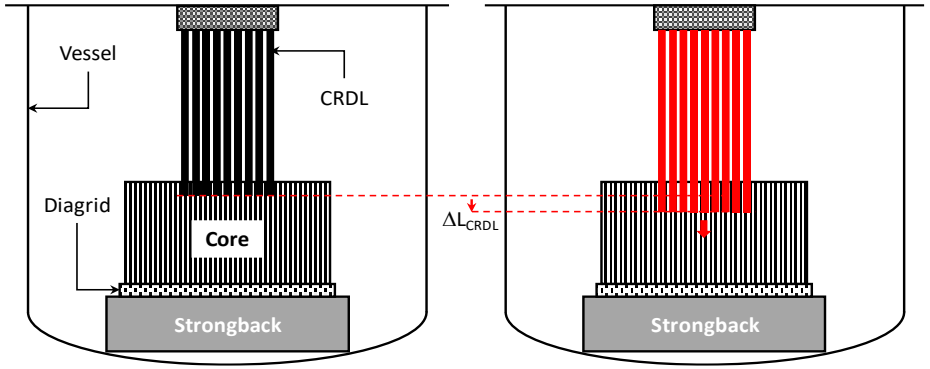

Strongback expansion

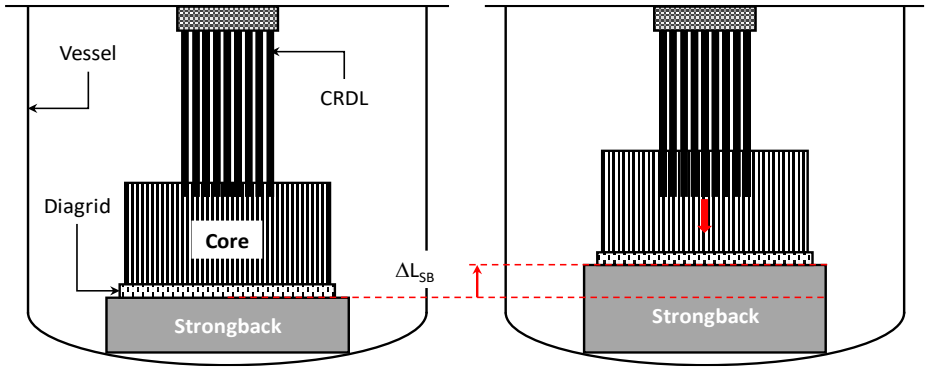

Vessel expansion

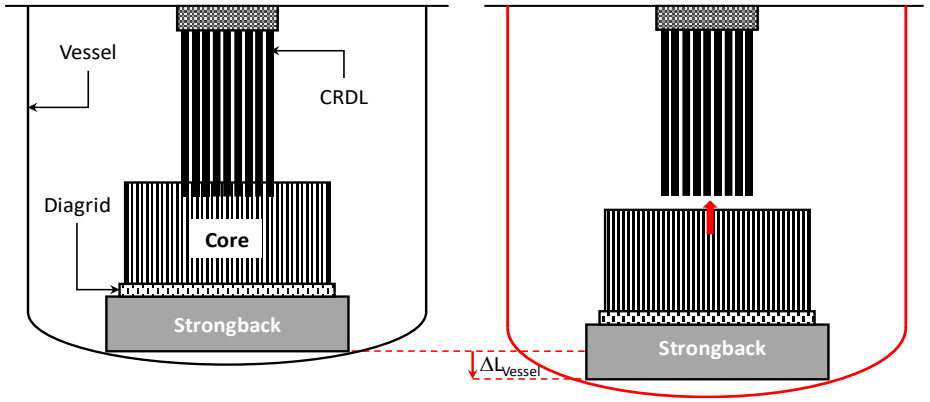

Superphénix star-up tests
Transient analysis with Serpent/DYN3D/ATHLET

- Serpent : Cross-sections and kinetics data
- DYN3D: 3D spatial kinetics
- ATHLET: system thermal-hydraulics (TH)

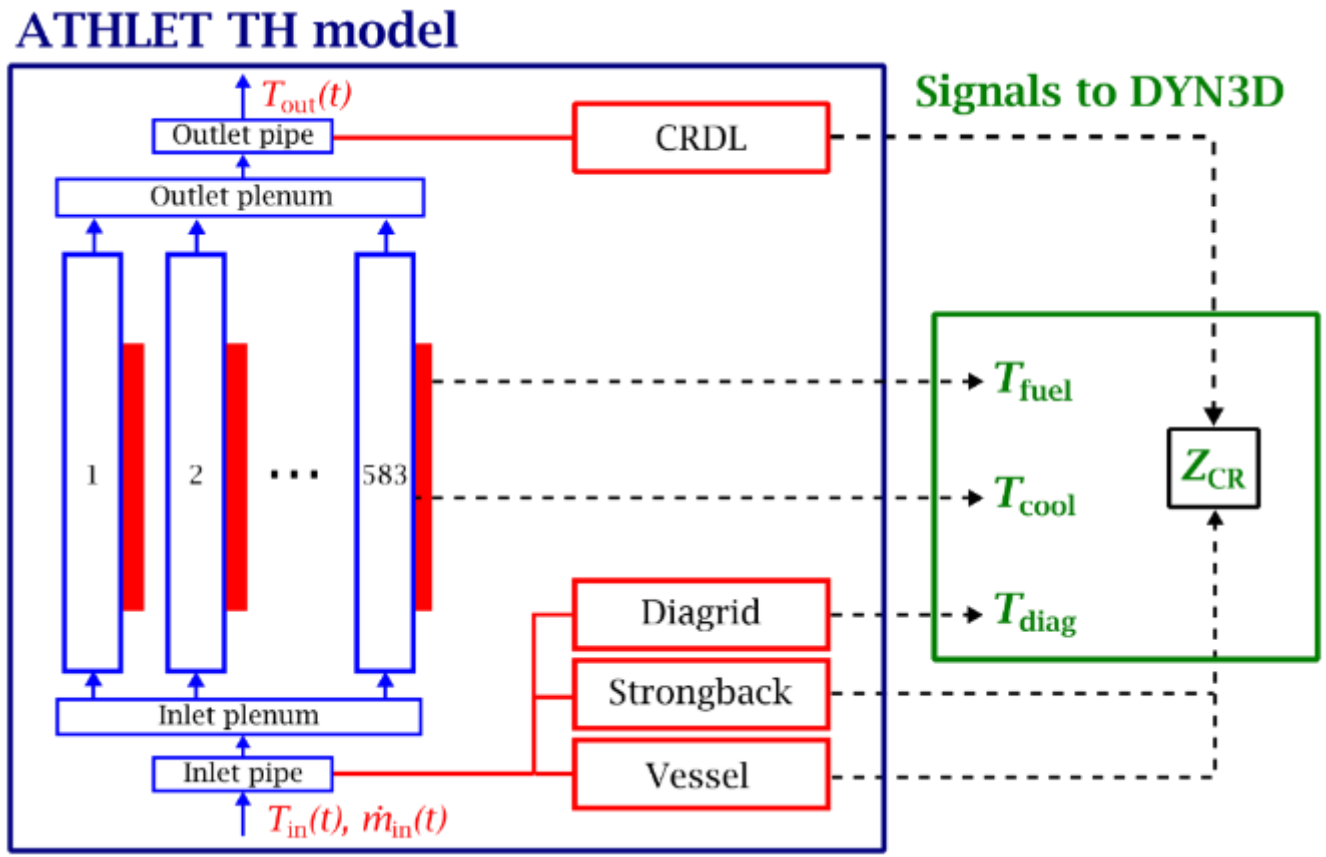

Superphénix star-up tests

Representative results: MOFC1

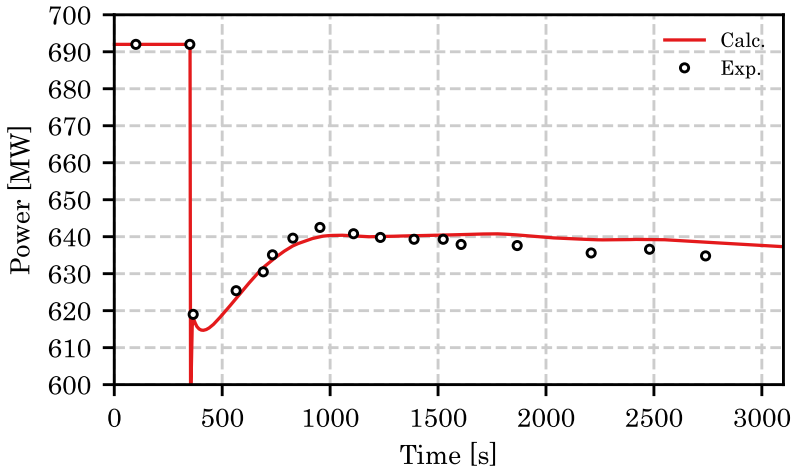

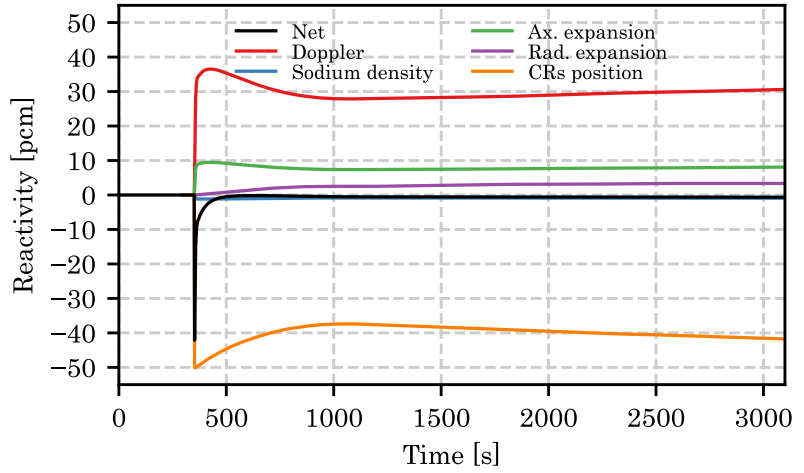

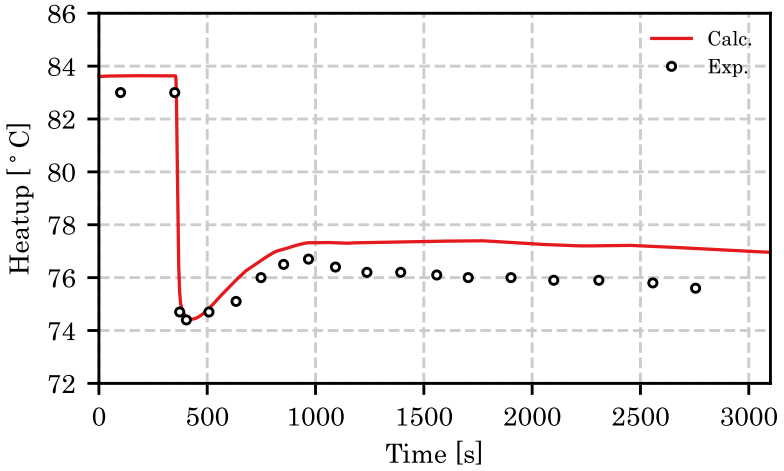

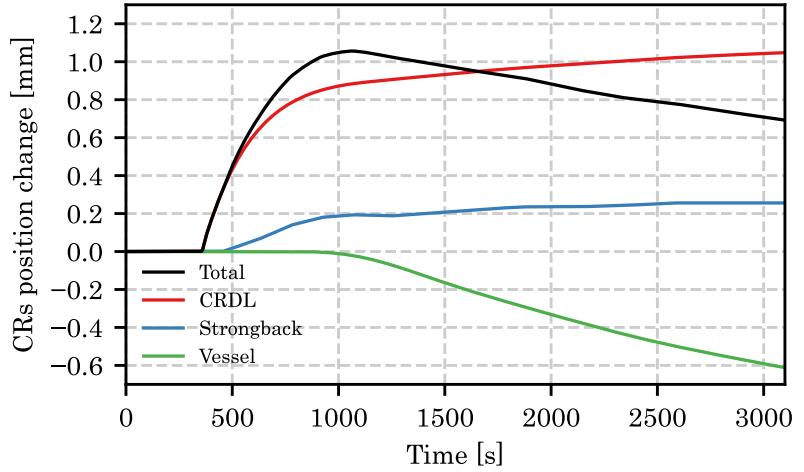

Superphénix star-up tests
Representative results: MOFC2

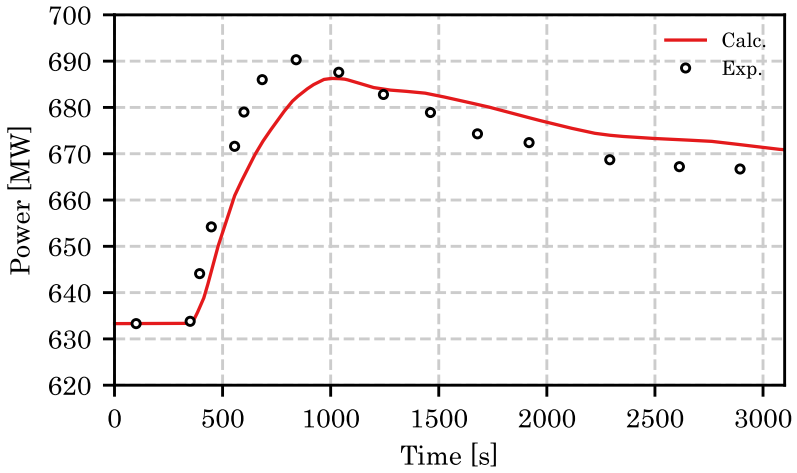

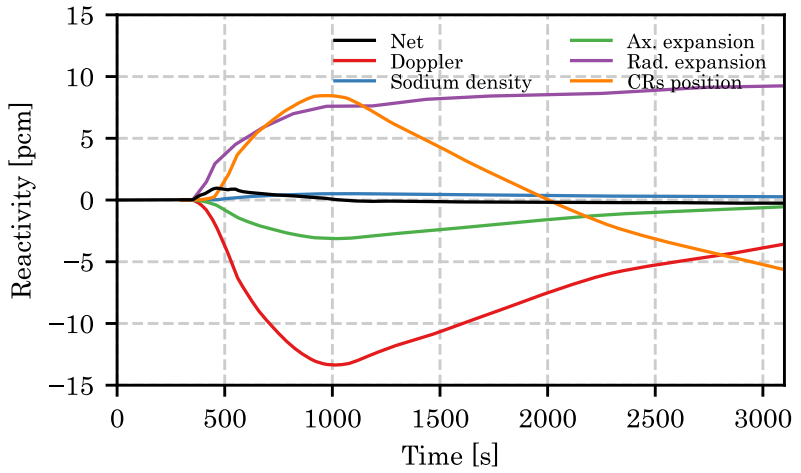

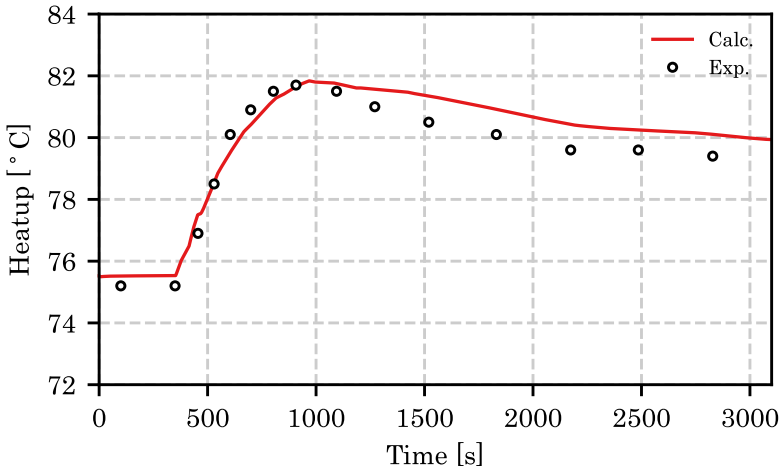

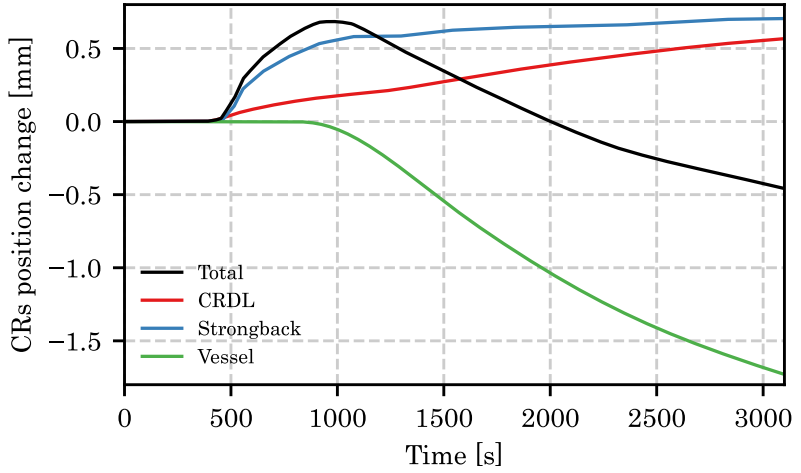

Superphénix star-up tests

Representative results: RC (reactivity step)

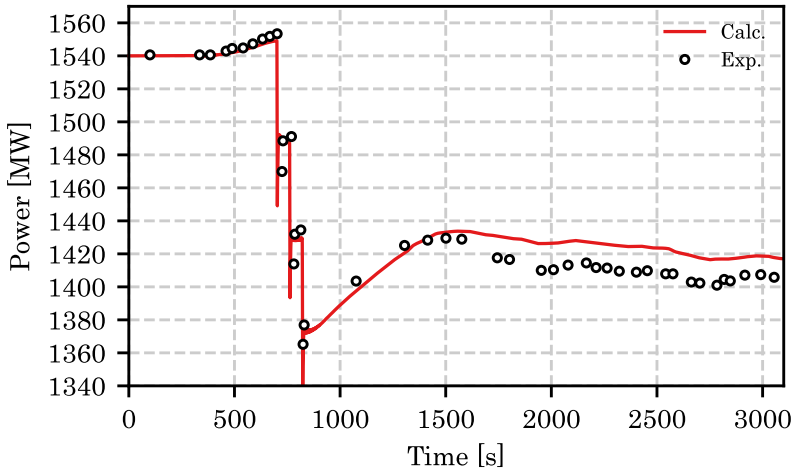

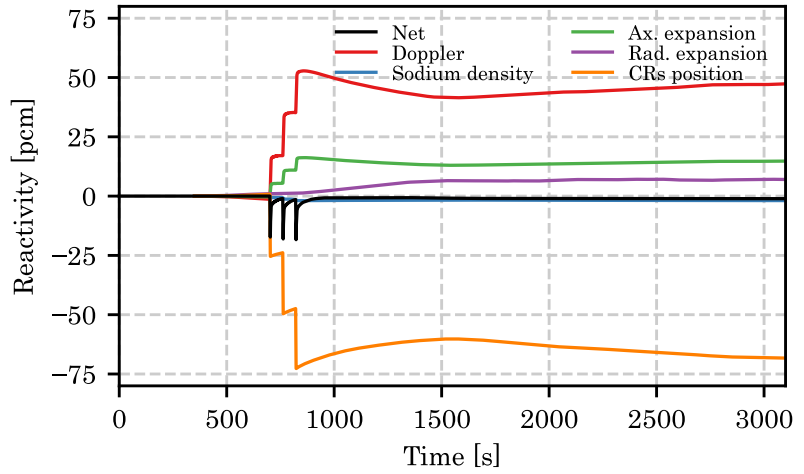

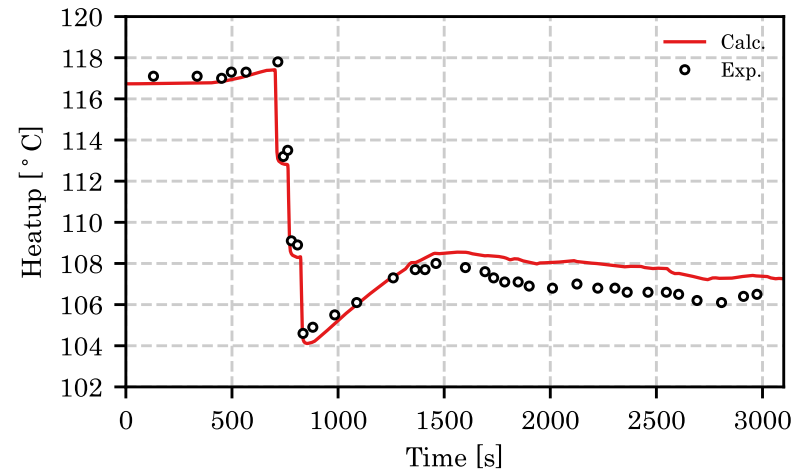

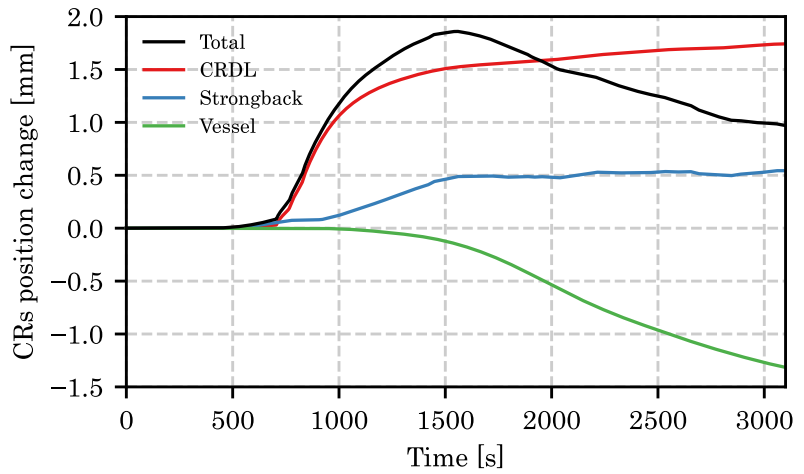

FFTF loss of flow test

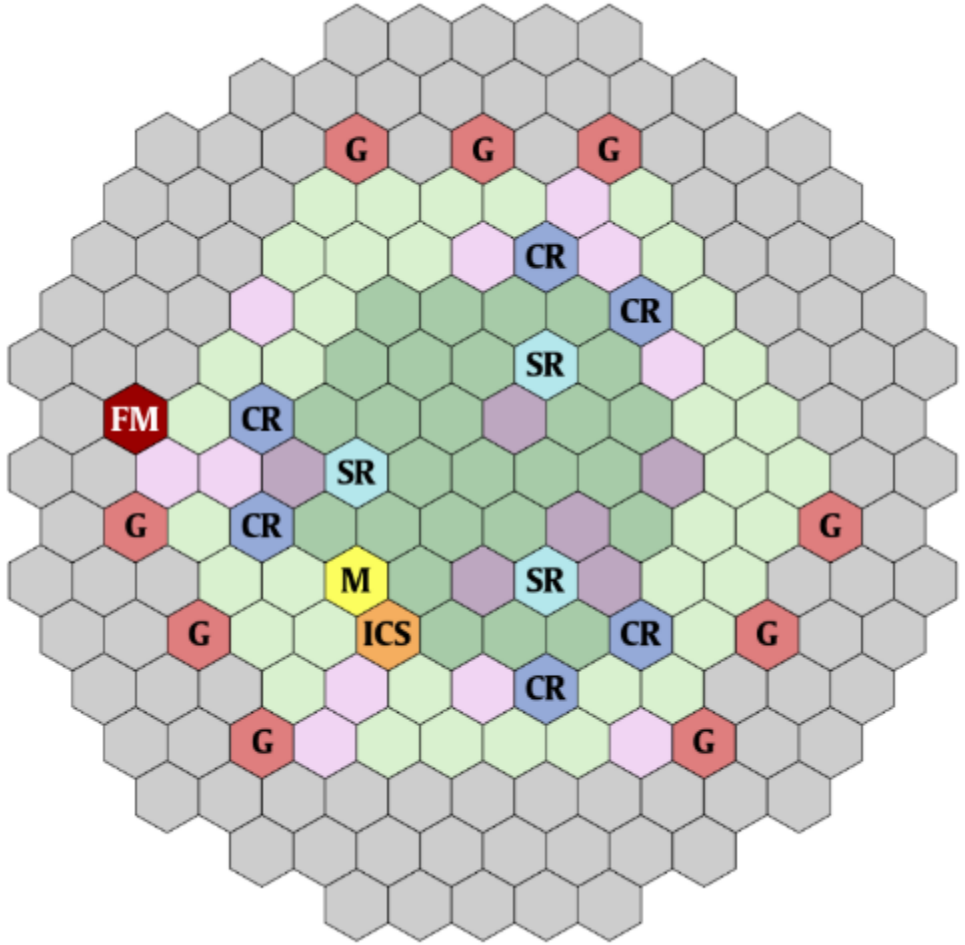

FFTF = Fast Flux Test Facility

- Loop-type SFR
- 400 MWth
- MOX fuel
- 80 fuel SA
- Testing of advanced fuels and materials

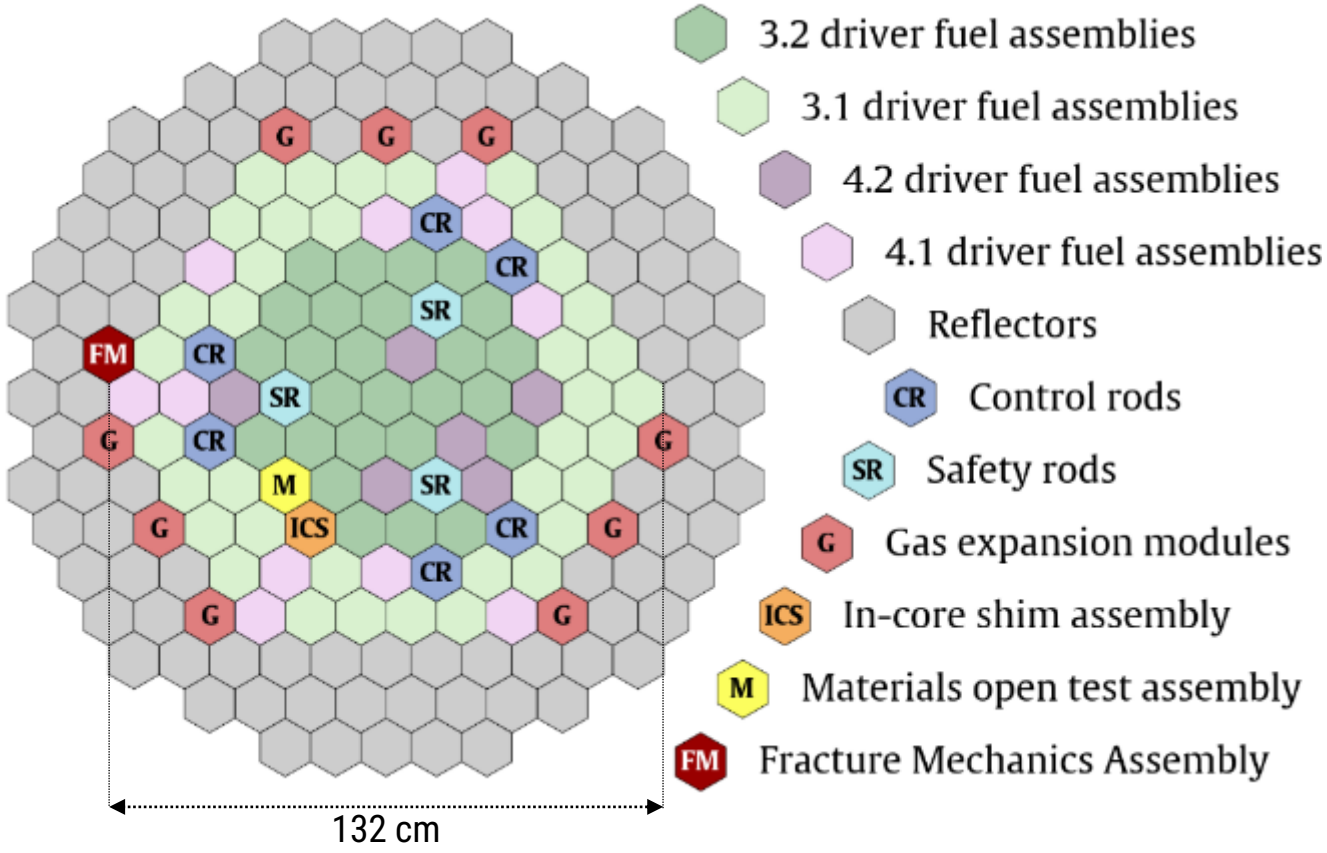

- Operated by Pacific Northwest National Laboratory (1980 – 1983)

FFTF unique safety features

GEMs – gas expansion modules

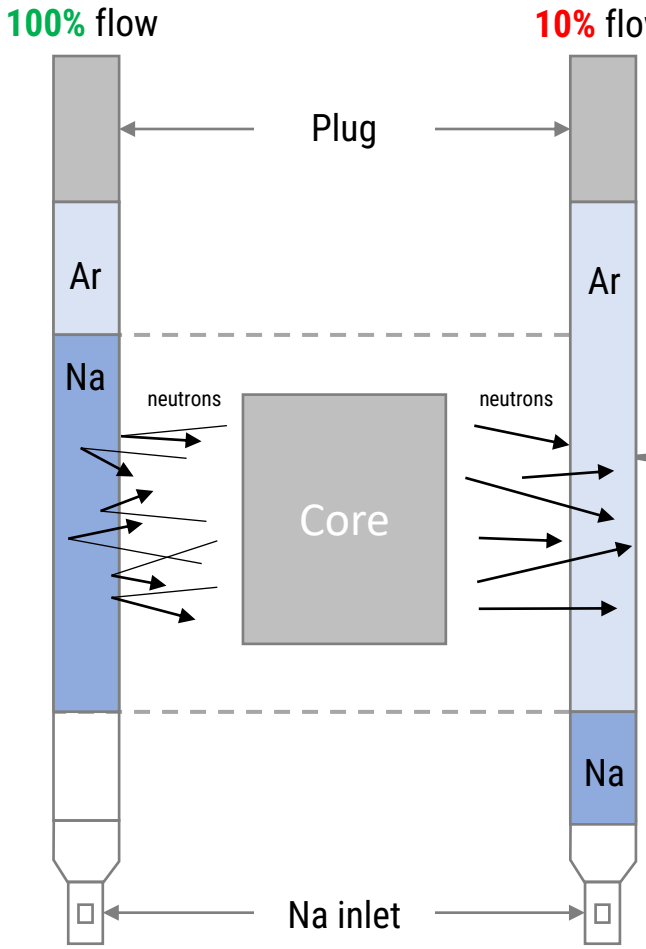

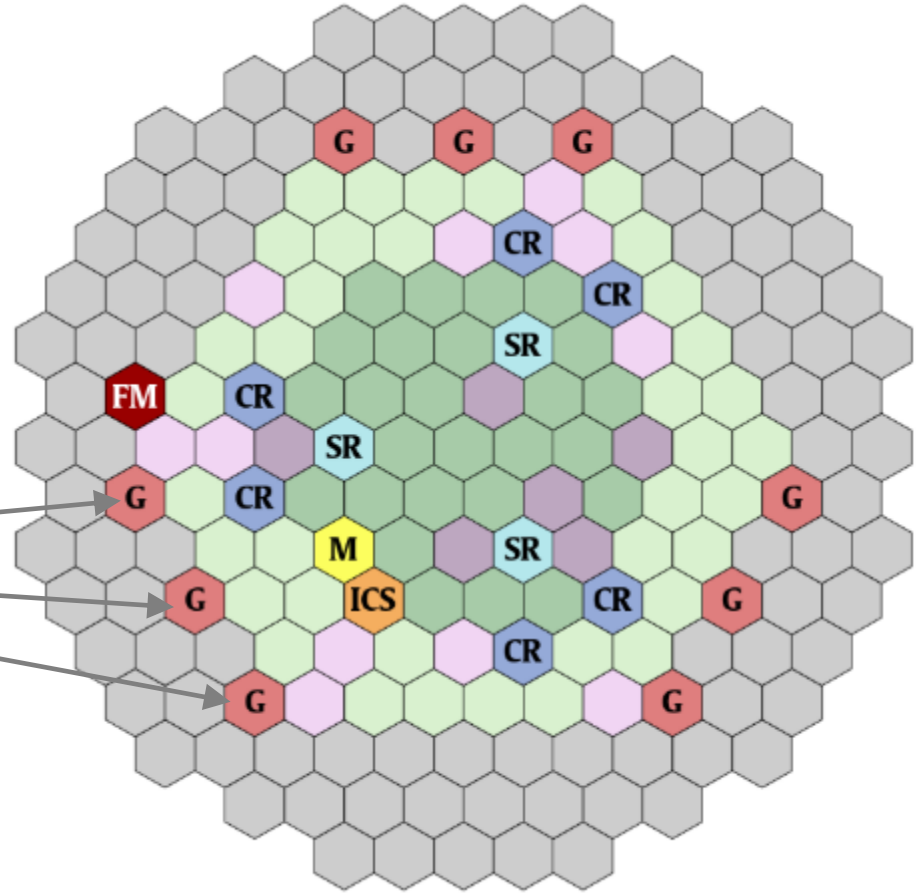

FFTF unique safety features

Core restraint system with limited free-bow

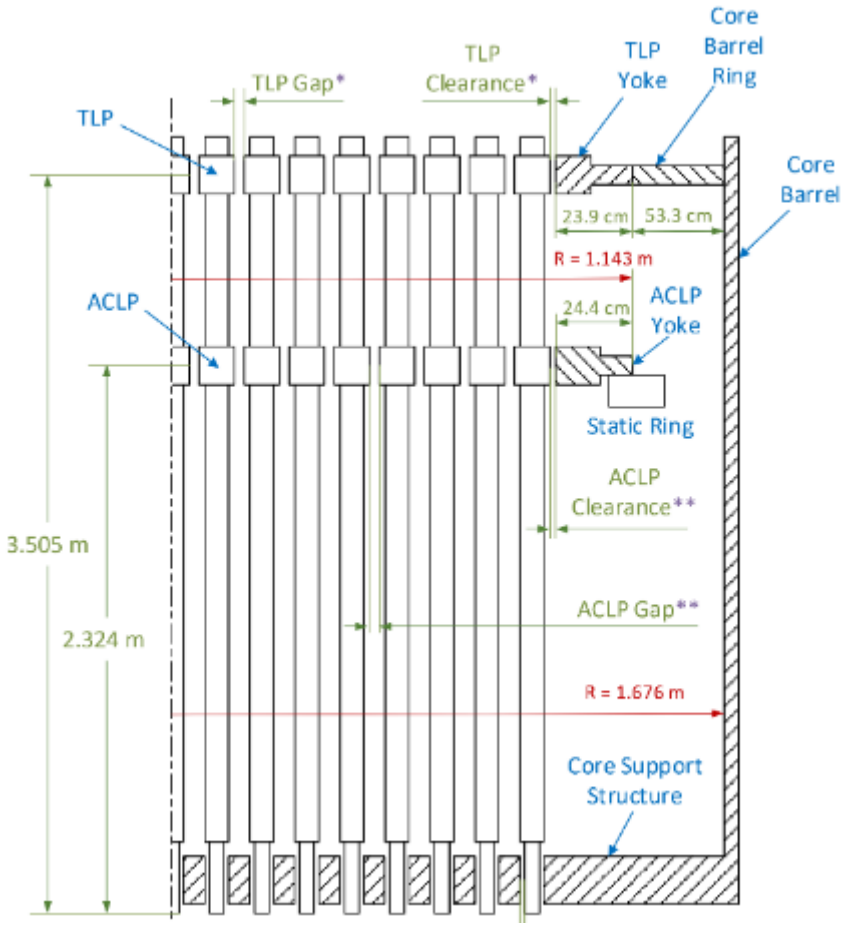

FFTF LOFWOS tests

- LOFWOS = Loss of Flow without SCRAM
- Total 13 conducted LOFWOS tests
- Demonstrating passive safety features + potential survival of severe accidents
- LOFWOS Test #13 = pump trip at 50% power without SCRAM
- LOFWOS Test #13 data was shared with IAEA by PNNL and ANL

IAEA
International Atomic Energy Agency
Atoms for Peace

IAEA CRP on Analysis of FFTF LOFWOS Test (2018 – 2022)

FFTF LOFWOS tests
Effects to consider

- Standard dependencies
  - Fuel Doppler
  - Coolant temperature + density
- In-core expansions
  - Radial fuel and wrapper expansion
  - Radial diagrid expansion
  - Axial fuel expansion
- Ex-core expansions
  - Strongback expansion
  - Control rod drive line expansion
  - Vessel expansion
- **GEM reactivity**

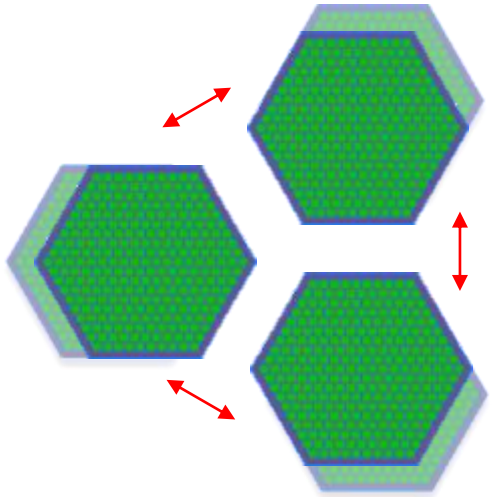

Diagrid radial expansion

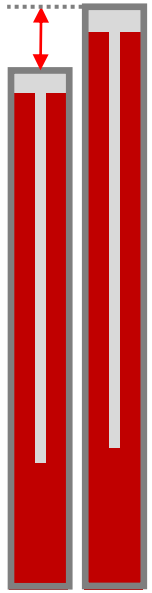

Fuel axial expansion

CRDL expansion

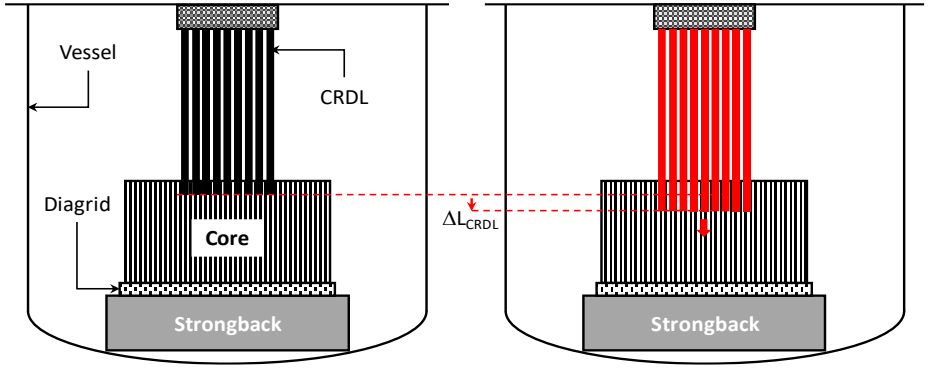

Strongback expansion

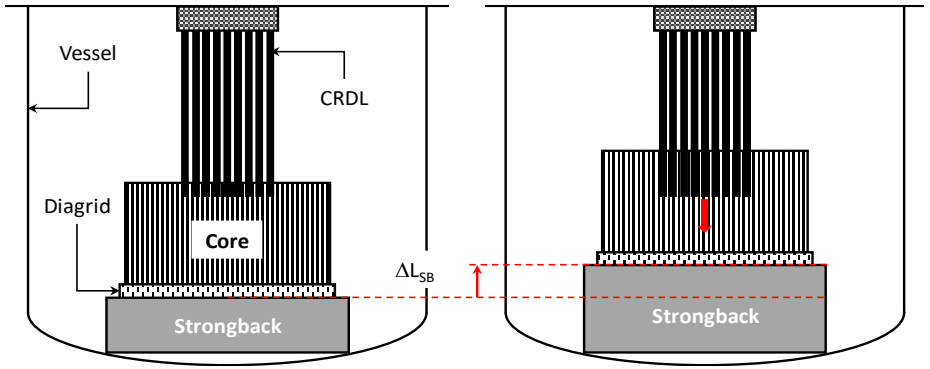

Vessel expansion

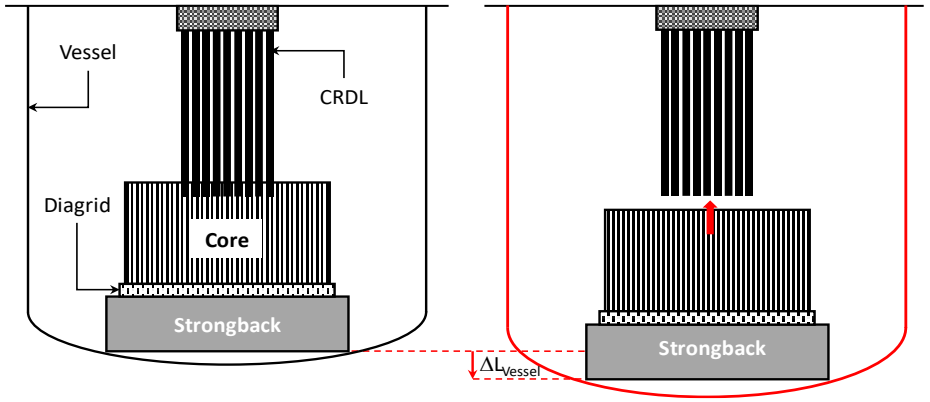

FFTF loss of flow test:
ATHLET and DYN3D/ATHLET vs. experiment

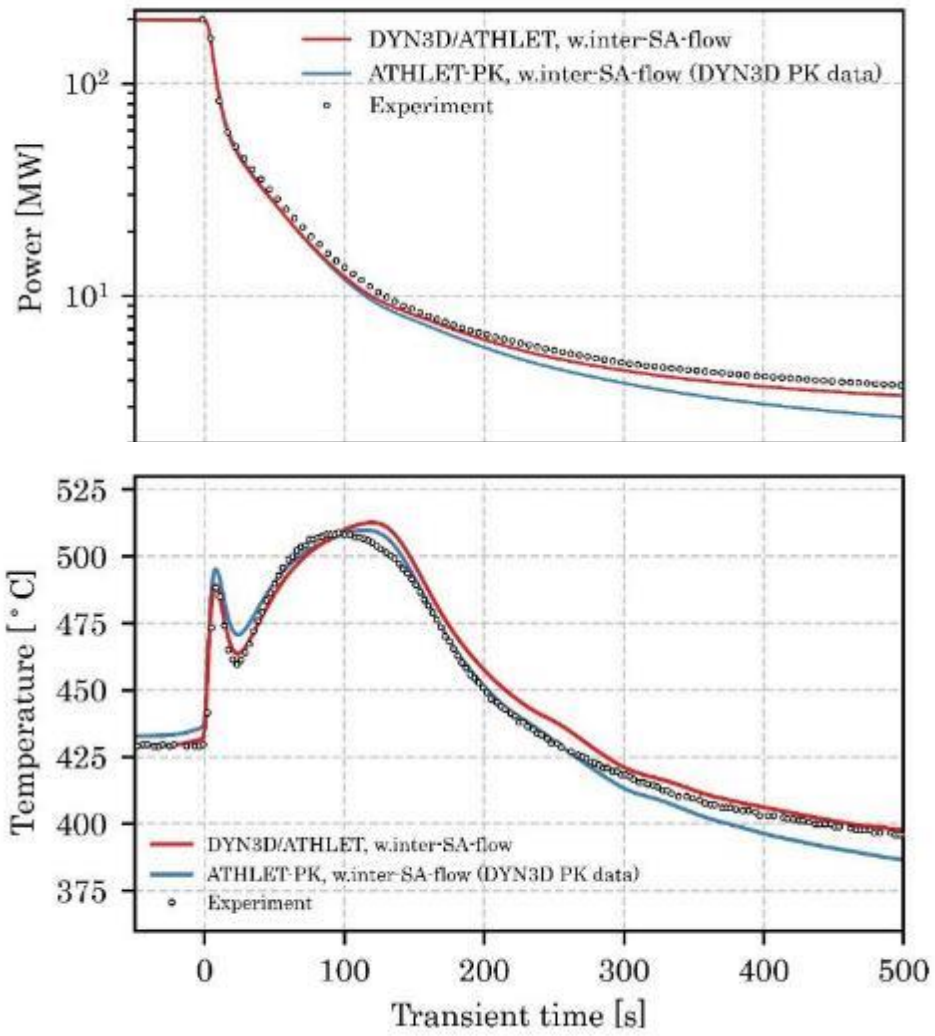

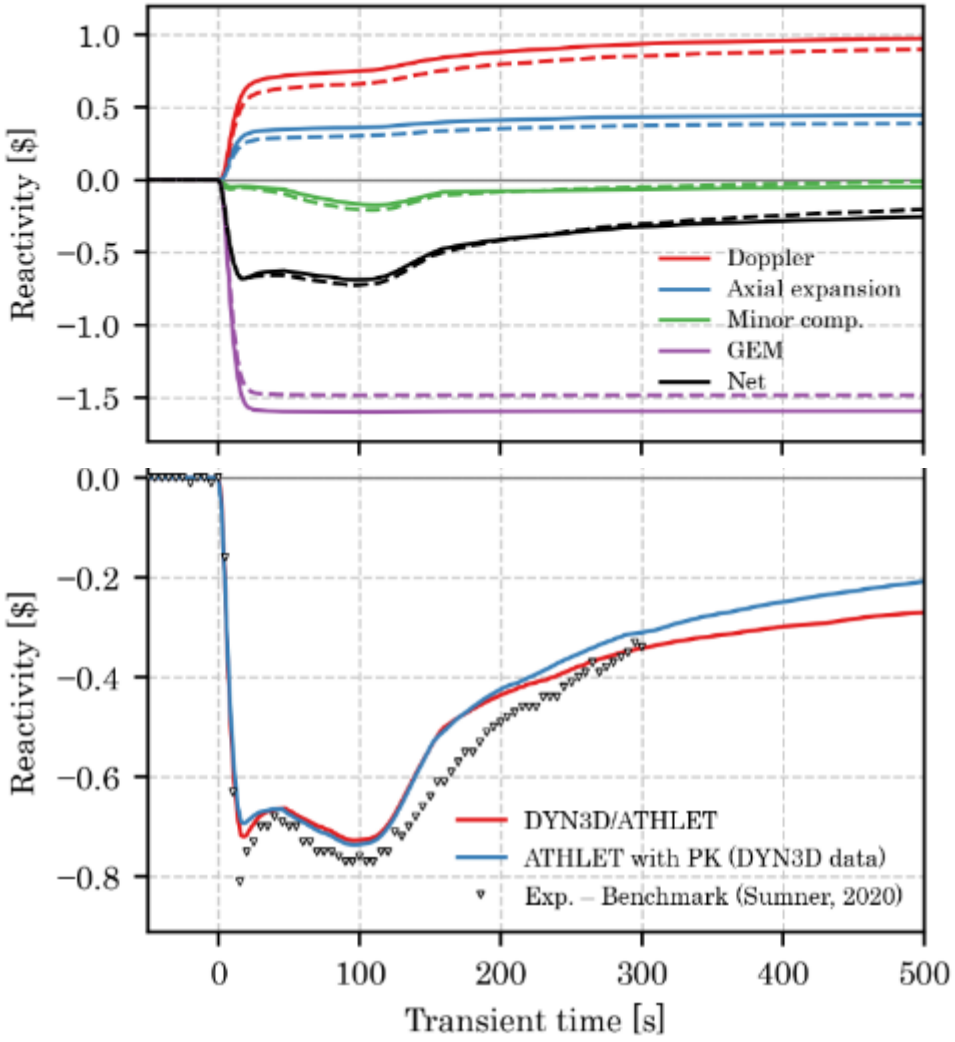

Dynamic simulations

CEFR control rod drop tests

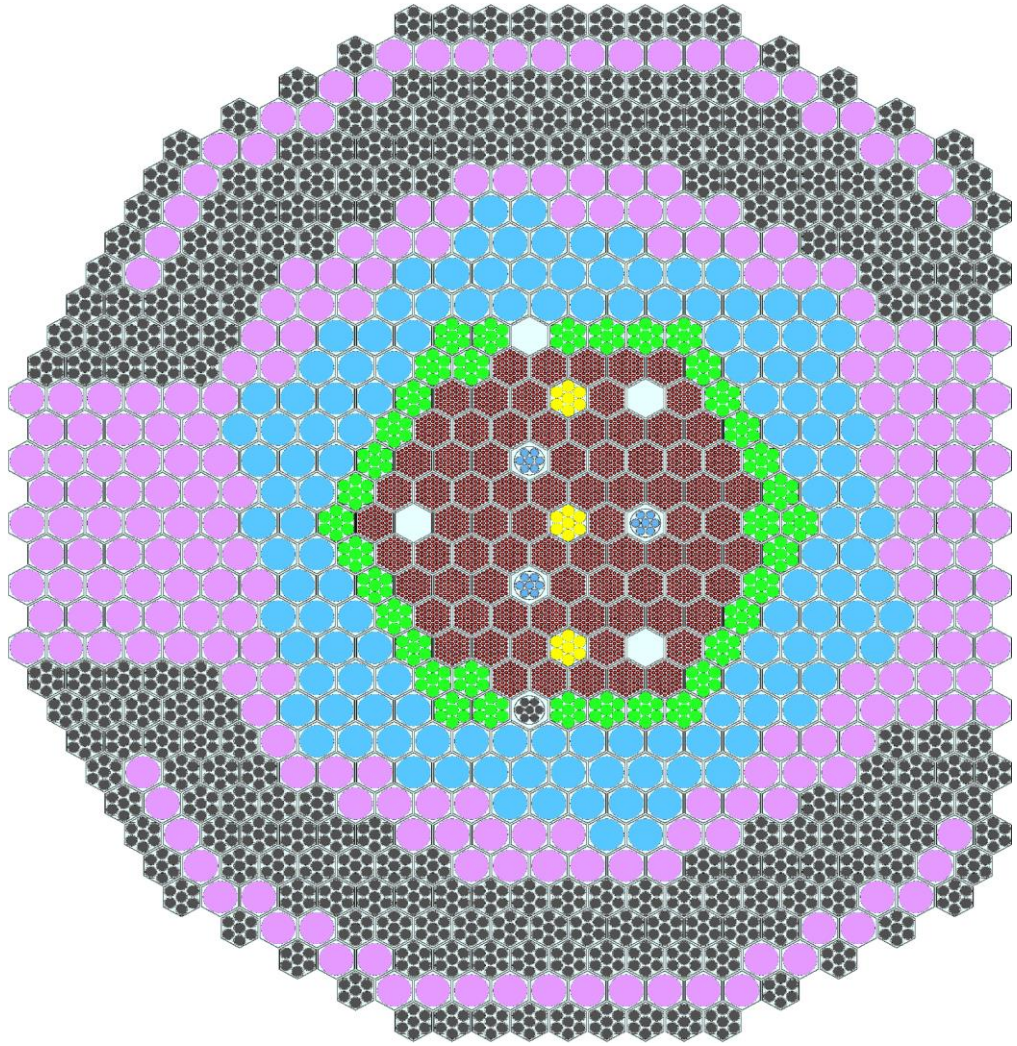

CEFR - China Experimental Fast Reactor

- Pool-type SFR
- 65MWth
- 64.4 wt% enriched UO2 fuel
- 79 fuel SA
- First SFR operated in China

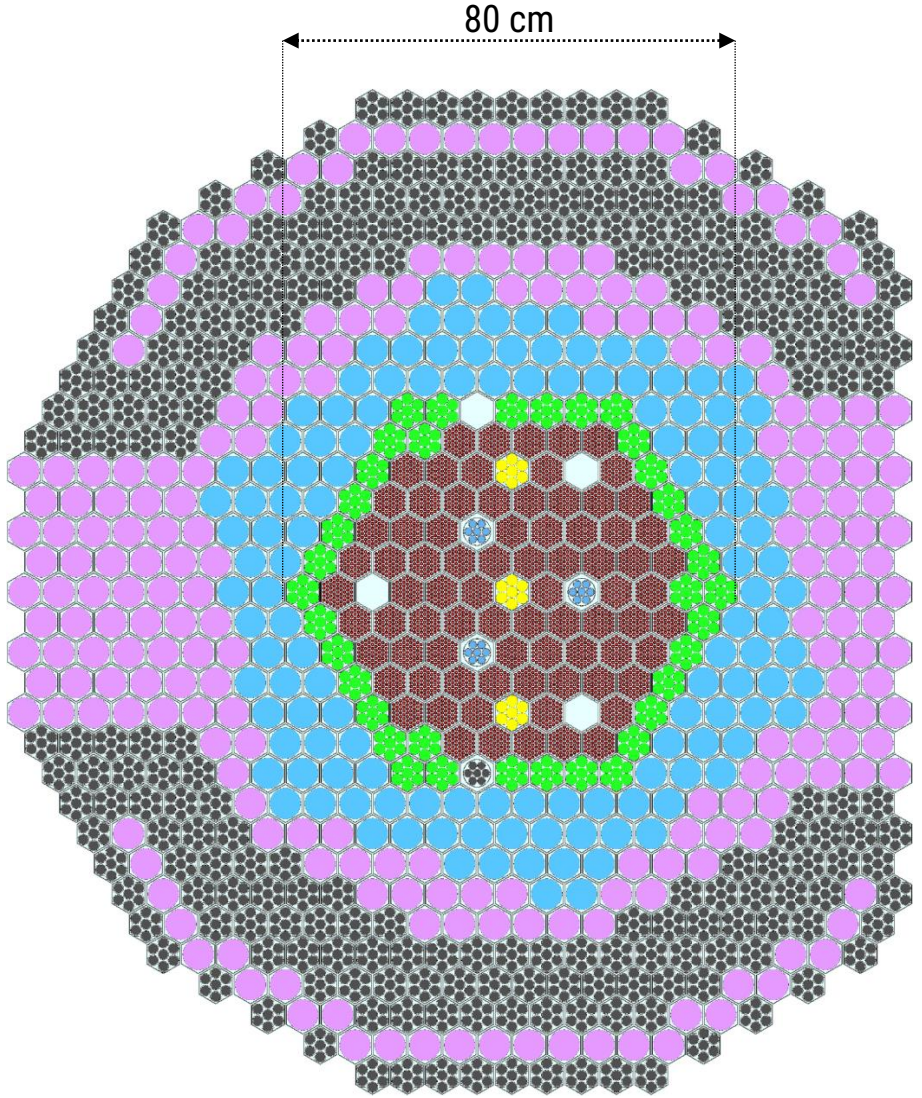

IAEA
International Atomic Energy Agency
Atoms for Peace

IAEA CRP on Neutronics Benchmark of CEFR Start-Up Tests (2018 – 2024)

CEFR control rods worth via rod drop tests

- Part of the physical start-up tests performed in 2010
- Isothermal CZP conditions at 245°C
- Real-time reactivity calculations based on the source range detector data
- CEFR CRs: 2 fine control + 3 shim + 3 safety

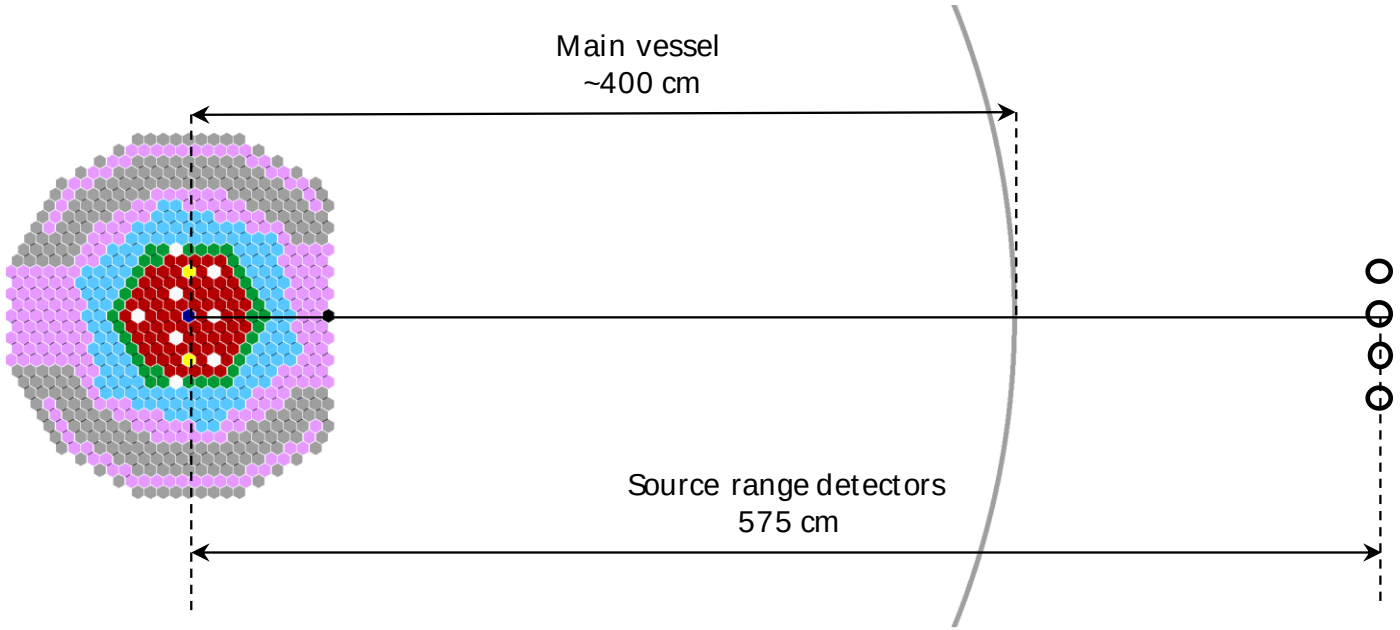

Transient modeling of the CR drop with Serpent

- Stage 1: Static simulation to get a source of neutrons and precursors
- Stage 2: Dynamic simulation of the CR drop process
- Step-wise CR position update via time-dependent geometry transformation
- CRW estimation using dynamic reactivity
  - Inverse point kinetics (IPK)
  - Instant neutron balance (NB)

Transient modeling of the CR drop with Serpent

- Stage 1: Static simulation to get a source of neutrons and precursors
- Stage 2: Dynamic simulation of the CR drop process
- Step-wise CR position update via time-dependent geometry transformation
- CRW estimation using dynamic reactivity
  - Inverse point kinetics (IPK)
  - Instant neutron balance (NB)

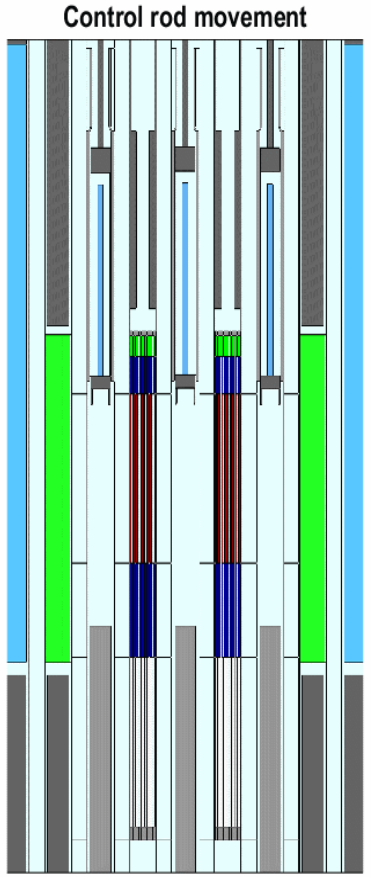

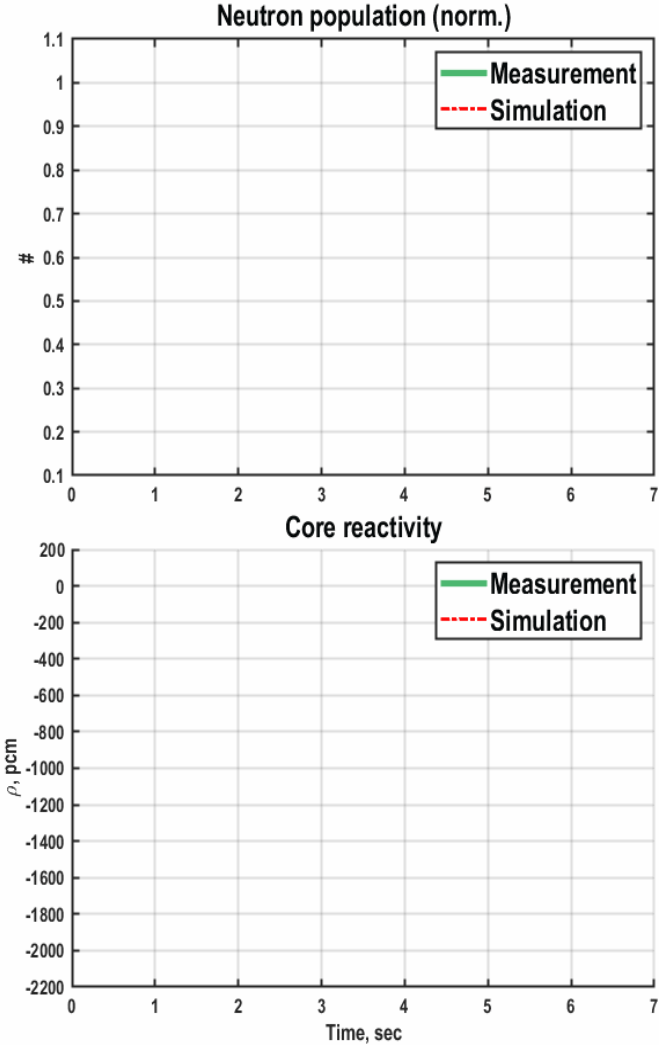

Simulation vs. experiment (SH2 drop) – time to scale!

Neutron population and reactivity: Safety rods

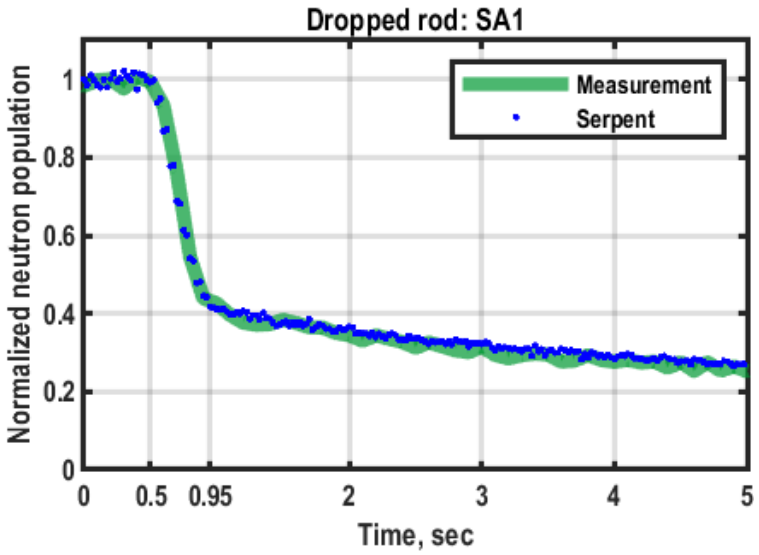

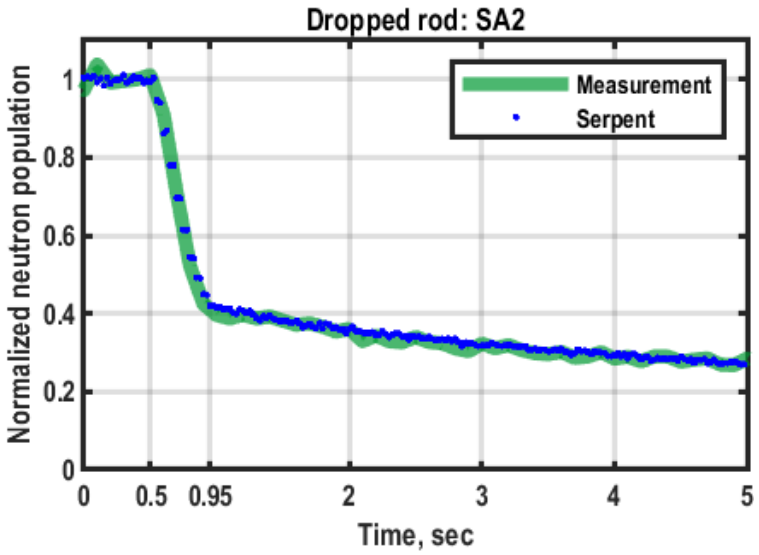

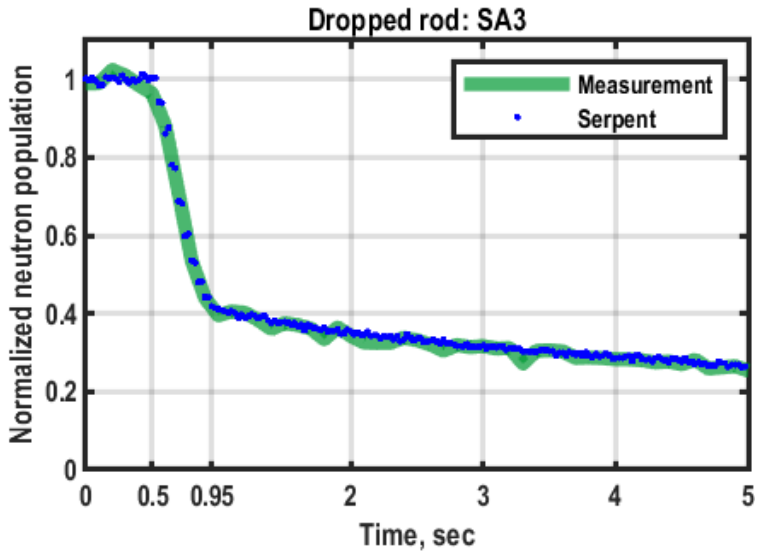

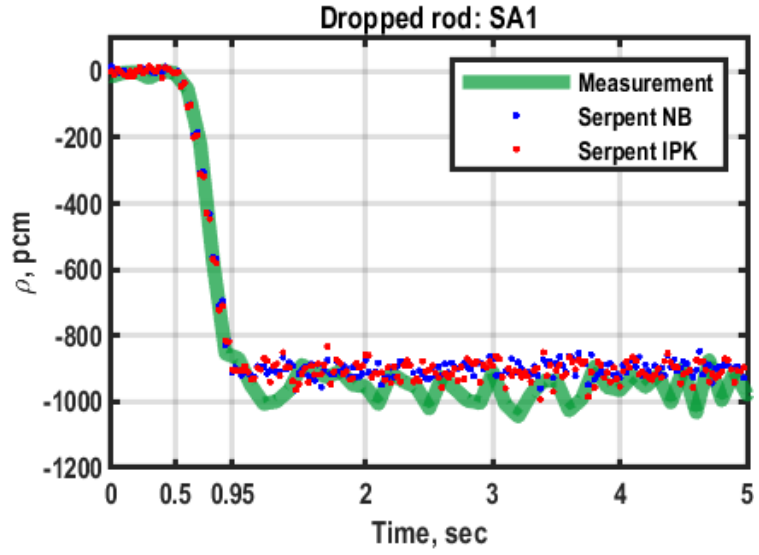

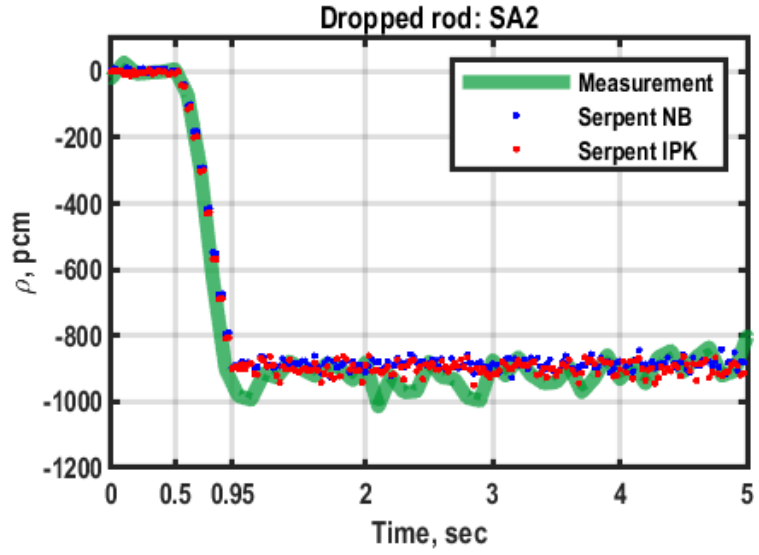

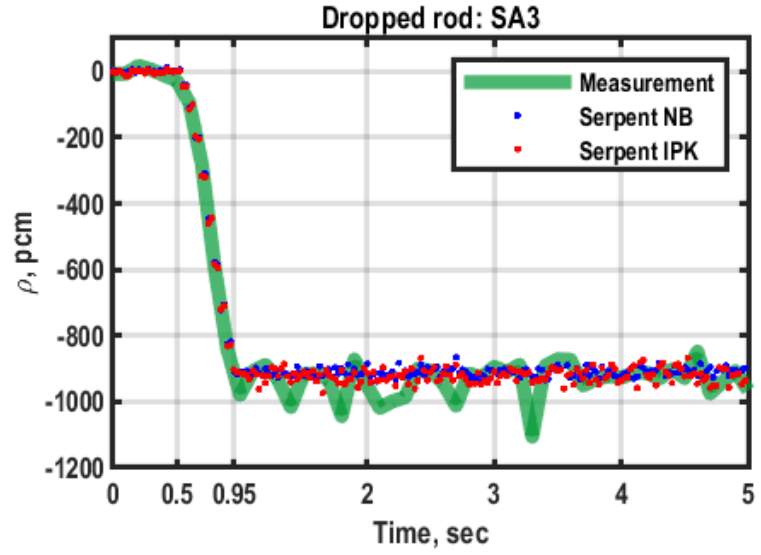

Mechanical core deformations and CAD models

Phénix flowering

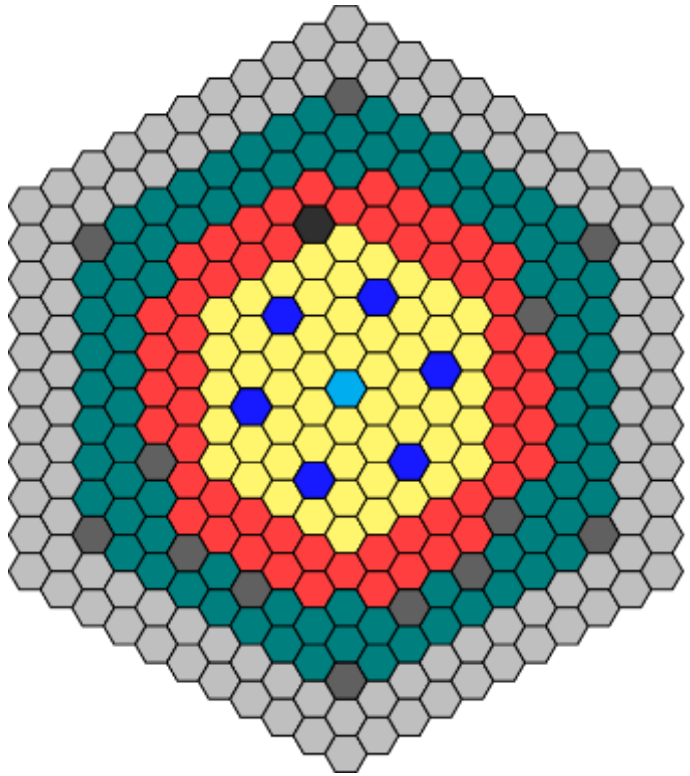

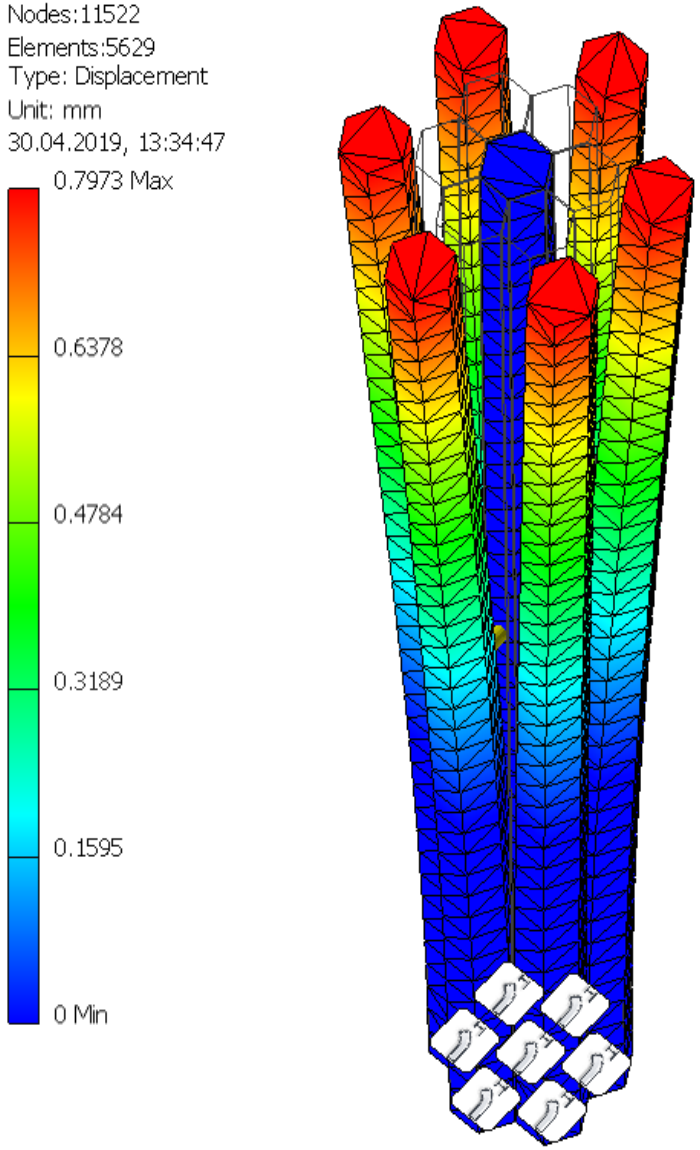

Phenix “flowering” tests

- Mechanical tests at the Phenix EOL core
- Identify potential reasons for “AURN”:
  - “Arrêt d’Urgence par Réactivité Negative”
  - 4 reactivity events at Phenix
- Step-wise core deformations
- Induced by a special “flowering” device
- Reactivity effects measured for every step

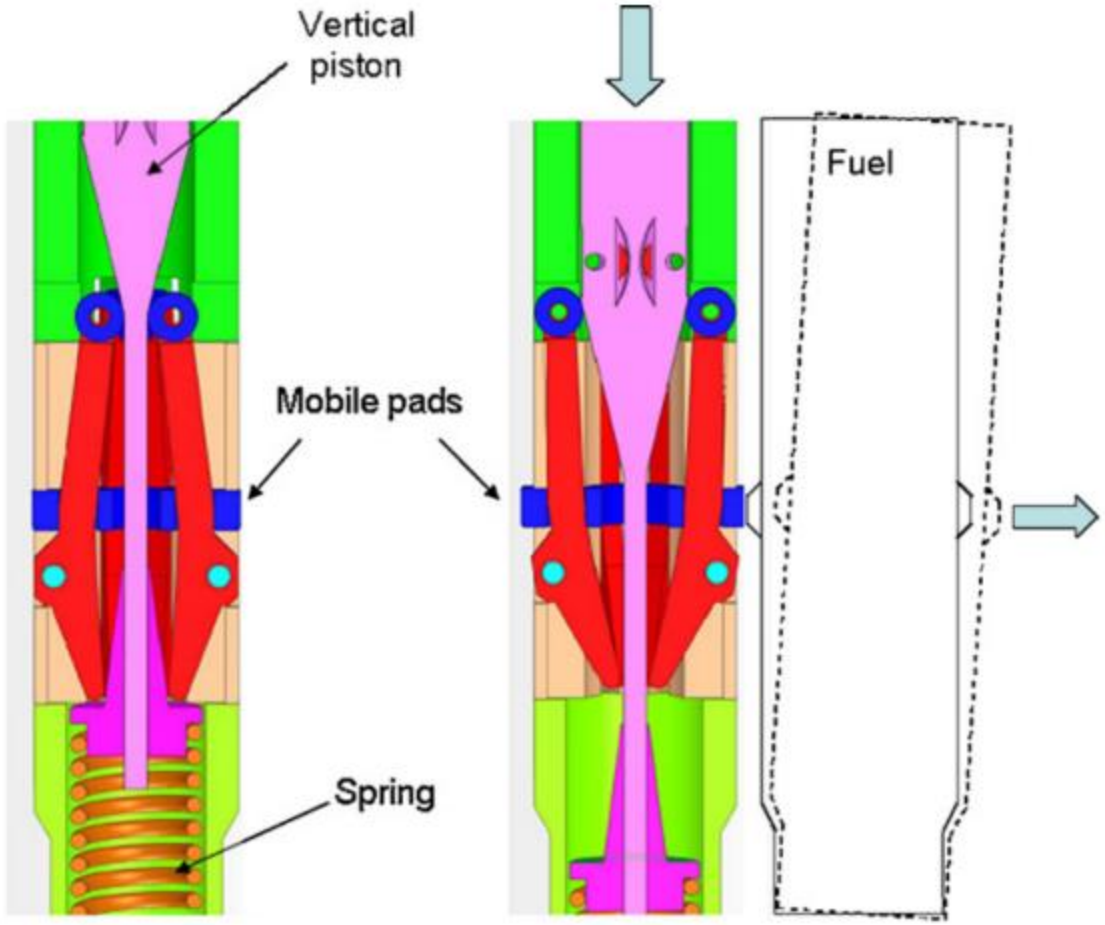

Modeling Phenix “flowering” tests
PSI methodology

- Finite element solver + Serpent

CAD model → Finite Element Analysis

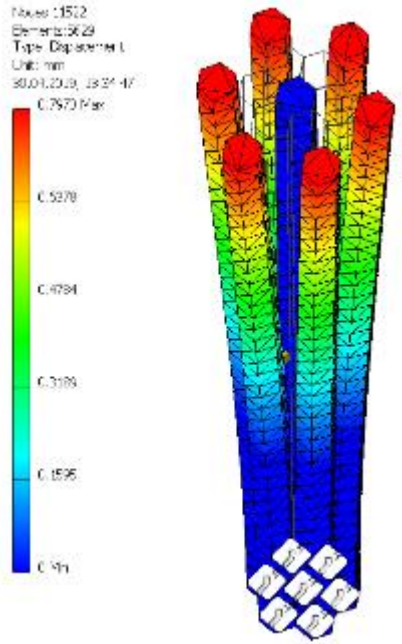

Modeling Phenix “flowering” tests
PSI methodology

- Finite element solver + Serpent

CAD model → Finite Element Analysis → Deformed geometry snapshots

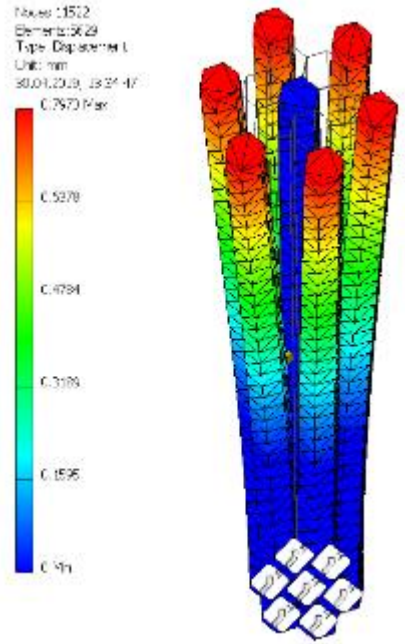

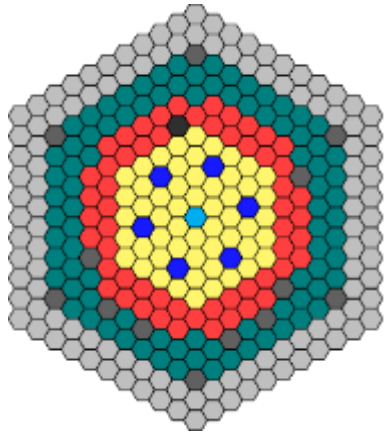

Modeling Phenix “flowering” tests
PSI methodology

- Finite element solver + Serpent

CAD model → Finite Element Analysis → Direct **Serpent** simulation → Reactivity effects

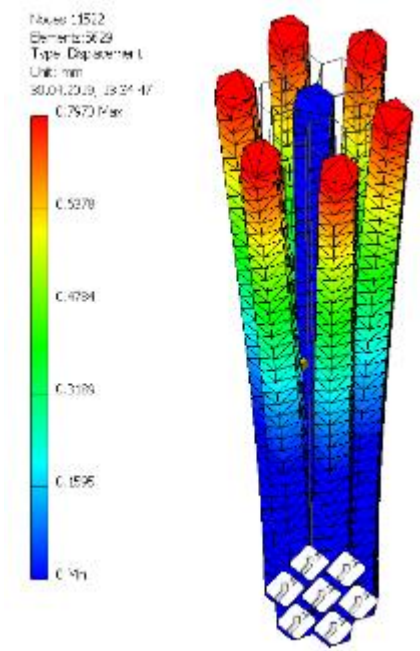

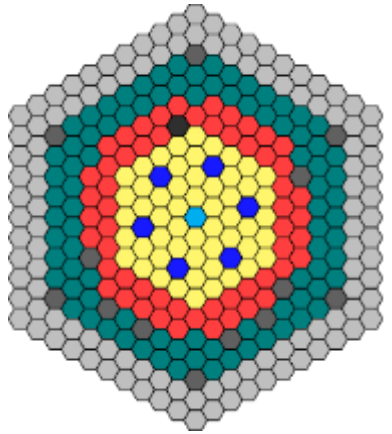

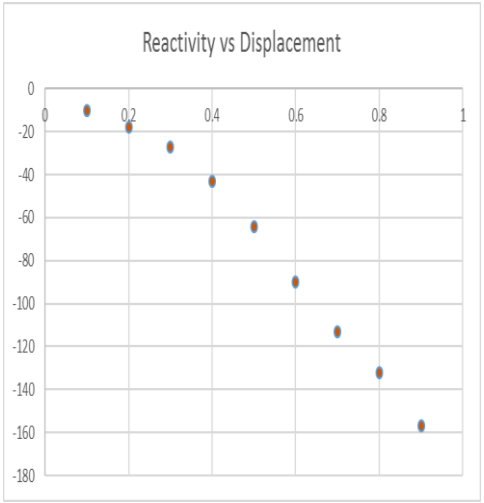

Modeling Phenix “flowering” tests
HZDR methodology

- Serpent + nodal diffusion

Deformed geometry snapshots

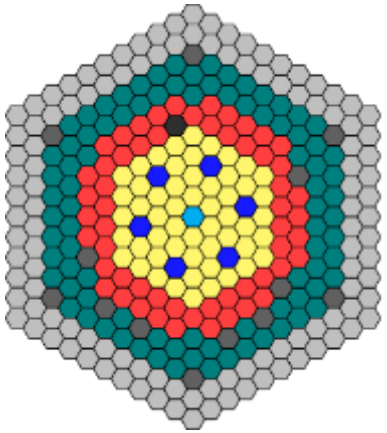

Few-group XS with **Serpent**

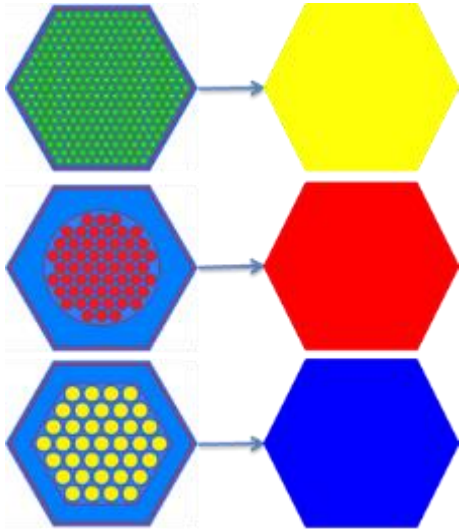

Diffusion calculations with **DYN3D**

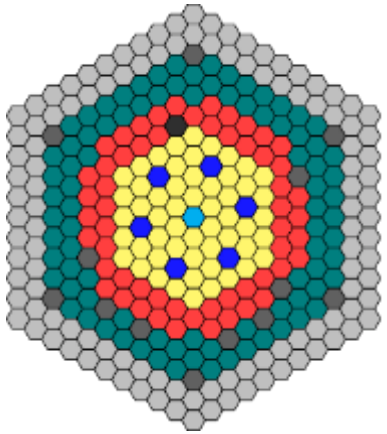

Reactivity effects

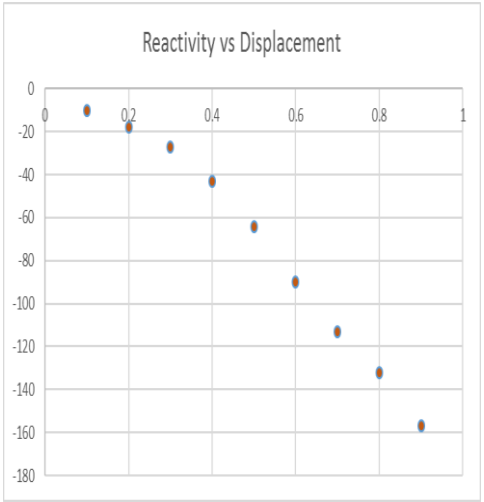

Modeling Phenix “flowering” tests
Application example

- Core deformations due to pressure waves
- Load duration = 30 msec
- Full simulation time = 210 msec
- Geometry snapshot at 15 time points

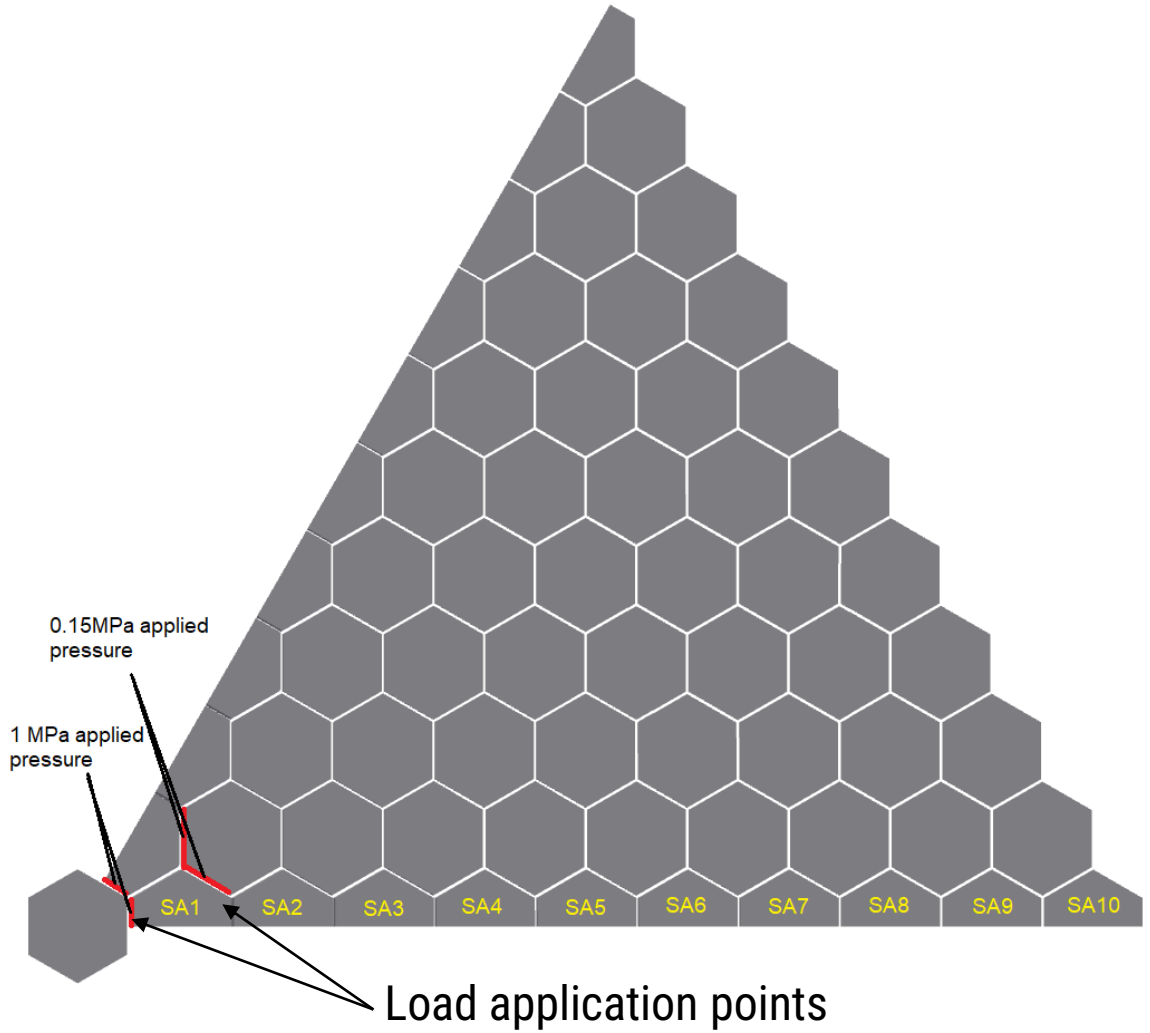

Modeling Phenix “flowering” tests

Selected snapshots of Phenix core geometry

- Averaged change of inter-assembly gap (red – expansion, blue – compaction)

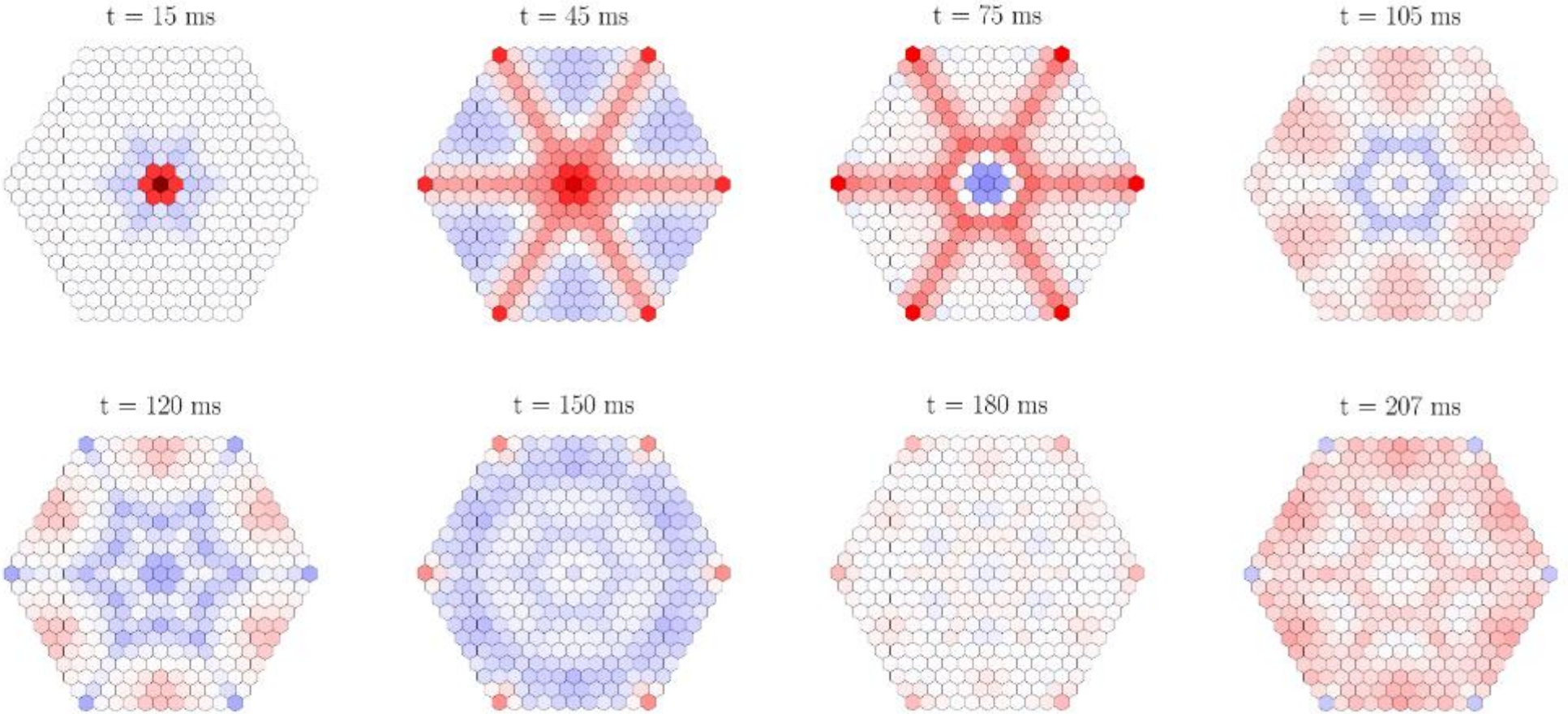

Modeling Phenix “flowering” tests
Serpent and DYN3D solutions

- Detailed CAD models for deformed geometries
- Static neutronic calculations for 14 geometry snapshots

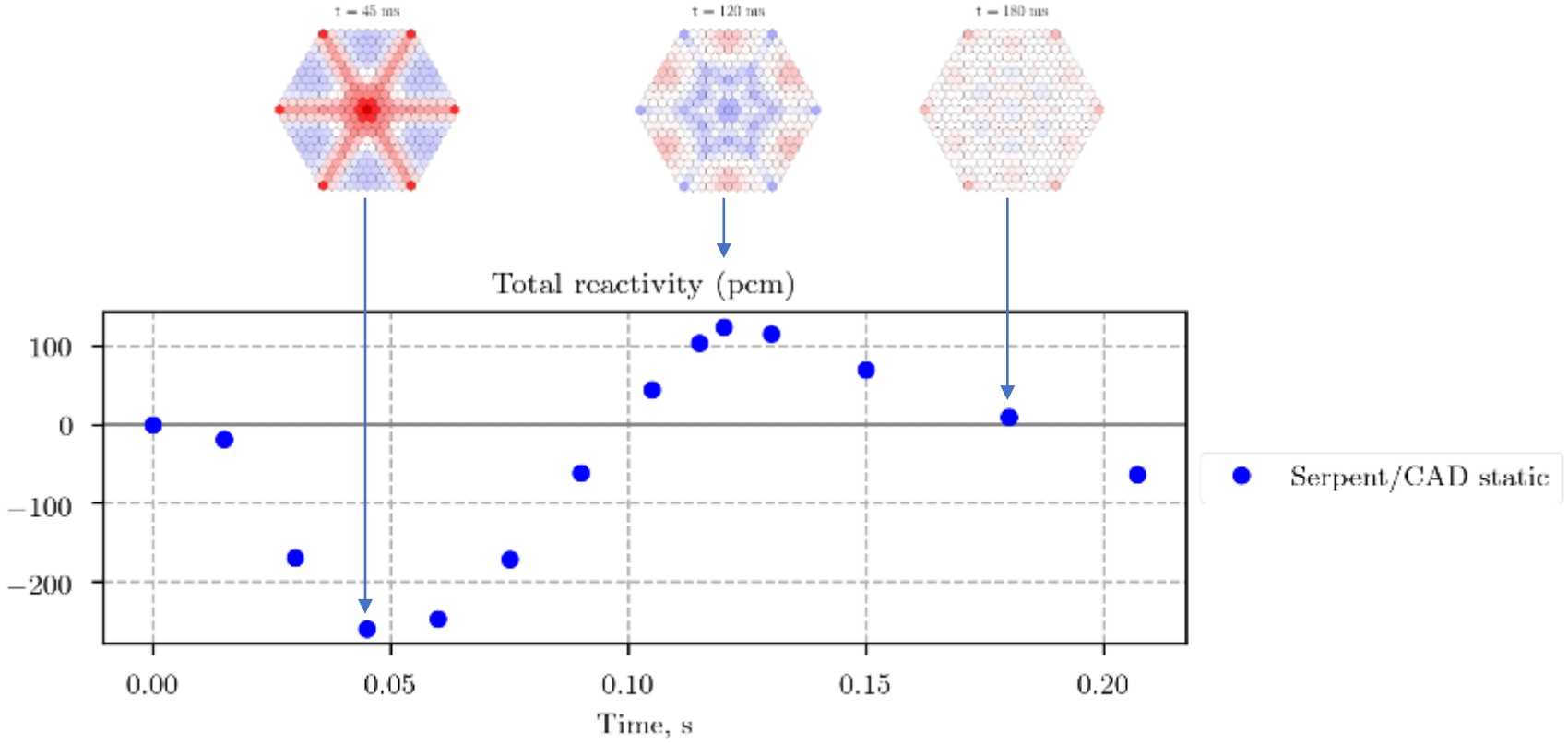

Modeling Phenix “flowering” tests
Serpent and DYN3D solutions

- Few group XS with Serpent
- Numerical mesh remains regular and fixed (use of Coordinate Transformation Method)

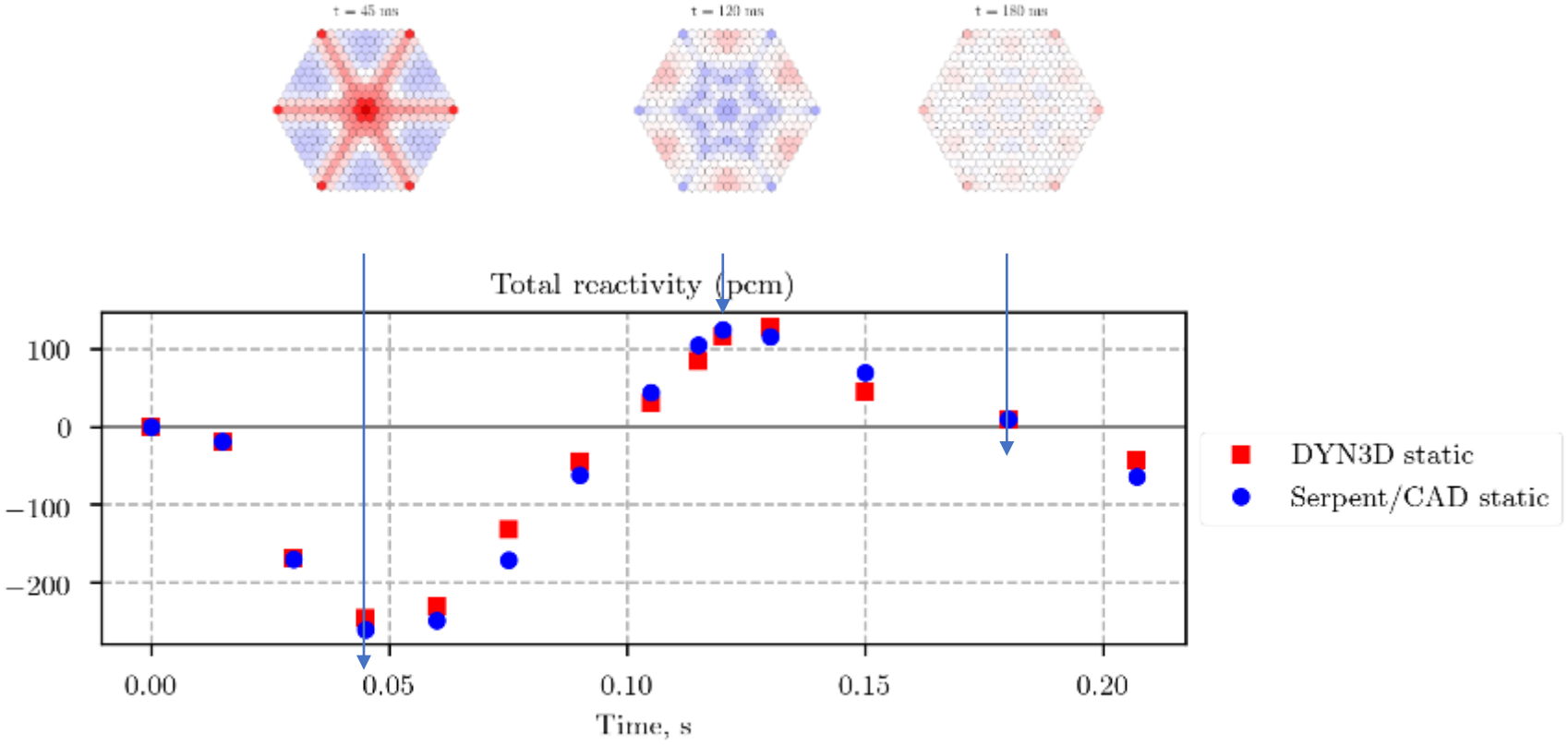

Summary

- A few examples of Serpent applications in fast reactor analysis
- Serpent expansion into fields dominated by deterministic codes
- However, deterministic codes are still relevant

Announcement: OECD/NEA Serpent-2 bootcamp for beginners

- 3.5 day training course
- Date: 14-17 November 2023
- Place: NEA Headquarters in Paris
- Course fee: 700 EUR
- Registration deadline: 13 October 2023

NEA
NUCLEAR ENERGY AGENCY

https://www.oecd-nea.org/jcms/pl_82693/serpent-2-bootcamp-for-beginners

Lessons learned from the ALLEGRO TH benchmark

Workshop - Advanced Modelling Techniques, St Catharine's College, Cambridge

Boris Kvizda
VUJE a.s., Trnava
Slovakia

SafeG
SAFETY OF GFR THROUGH INNOVATIVE MATERIALS, TECHNOLOGIES AND PROCESSES

This project has received funding from the Euratom H2020 programme NFRP-2019-2020-06 under grant agreement No 945041.

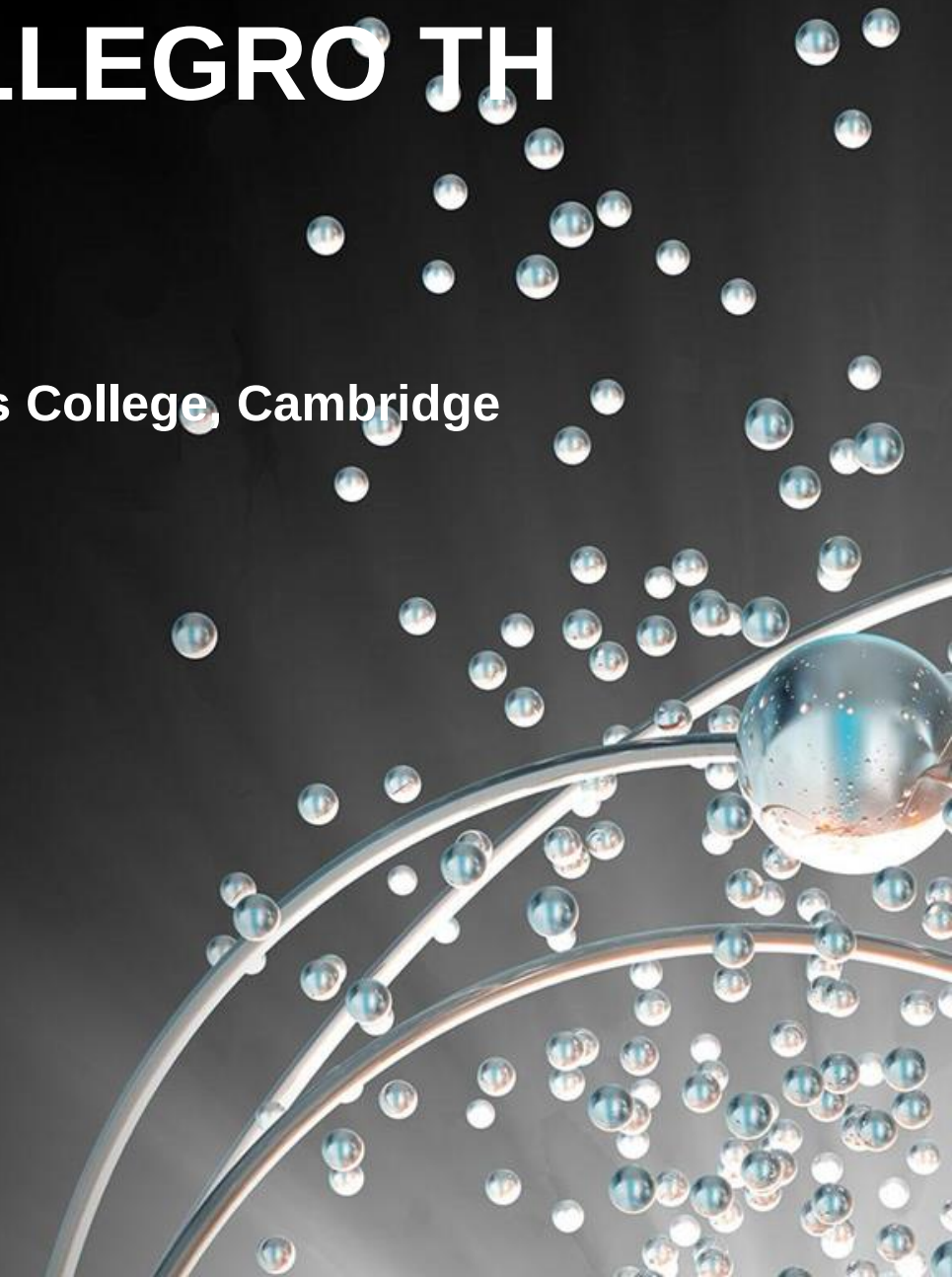

Content

- *ALLEGRO design and its options*
- *VINCO project TH benchmark exercise (identified distortions among the models)*
- *International recommendations and national requirements on nodalization qualification*
- *Origins of uncertainties in TH calculations*
- *Tools and methods to qualify the nodalization*
- *Fast Fourier Transformation Based Method (FFTBM)*
- *Role of Kv-Scaled calculations in nodalization qualification*
- *Conclusions*

ALLEGRO 75 MW

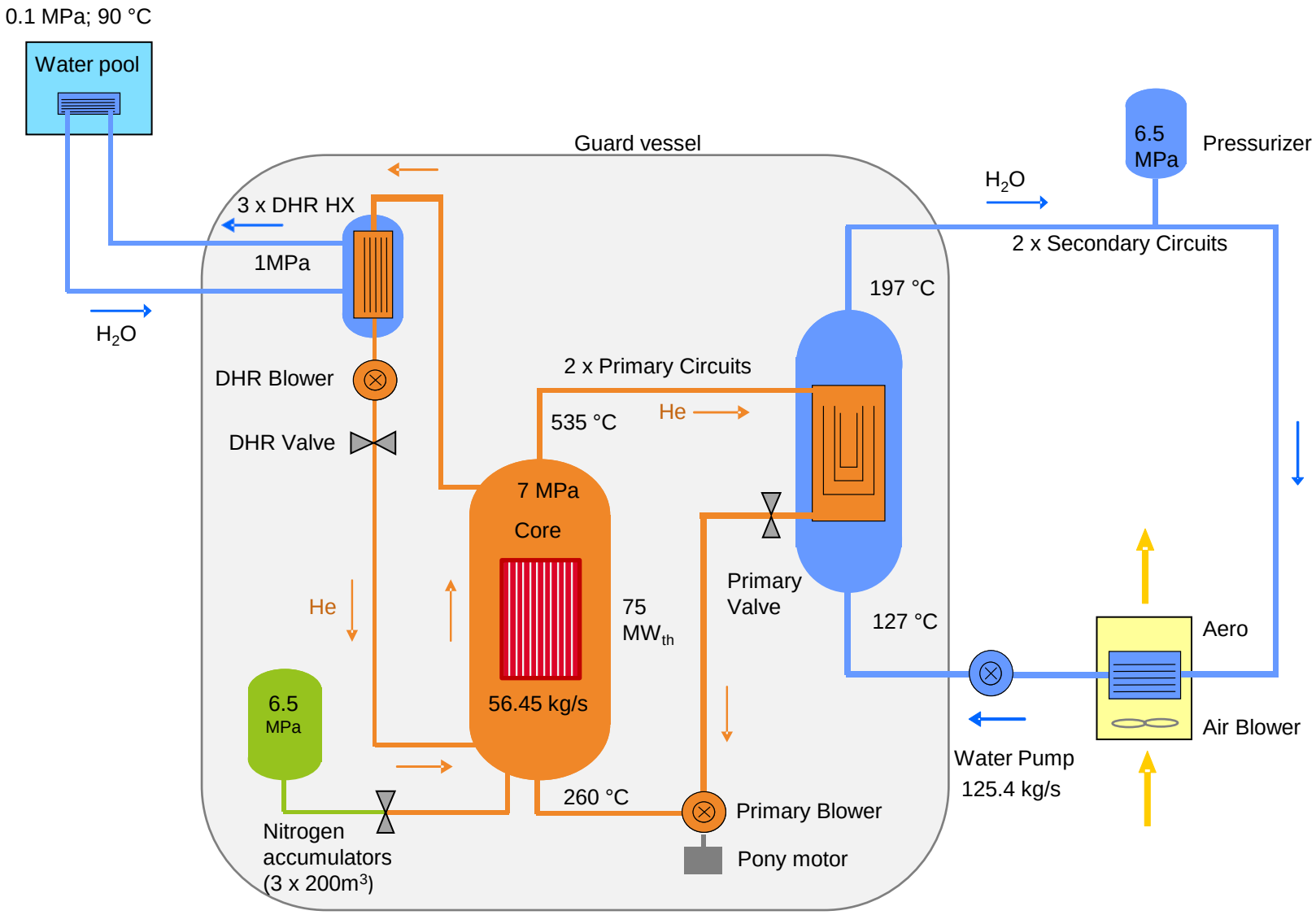

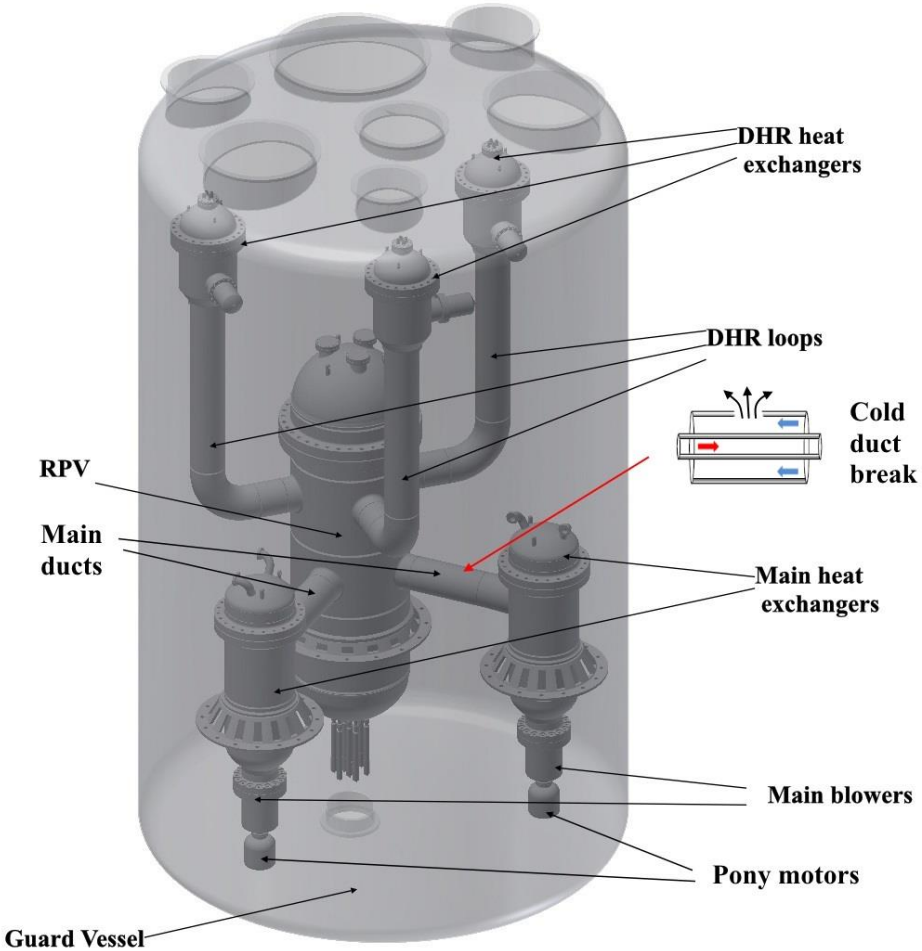

ALLEGRO 75 MW MOX core – main characteristics

Parameter	Value	Unit	Notes
Nominal power (thermal)	75	MW	Reduced power has been considered in the range of 30 – 75 MW
Nominal power (electrical)	0	MW	
Power density	100	MW/m^3	Reduced power density has been investigated in the range of 50 – 75 MW/m^3
Fuel	MOX / SS cladding		Start-up core. MOX core optimization has been performed
	UOX / SS cladding		UOX for the start-up core has been investigated
	UPuC/ SiCSifC cladding		Long term refractory core
Type of fuel assembly	Hexagonal wrapper and wired fuel rods		
Number of fuel rods per assembly	169		
Number of fuel assemblies	81		
Number of experimental fuel assemblies	6		
Number of control and shutdown rods	10		
Primary circuit coolant	Helium		
Secondary circuit coolant	Water		Gas-gas option is being investigated
Tertiary circuit coolant	Air		Atmosphere
Primary pressure	70	bar	
Core inlet/outlet temperatures	260/516	°C	Should be upgraded for full core refractory fuel
Number of primary loops	2		Third primary loop is being investigated
Number of secondary loops	2		
Number of DHR loops	3		Directly connected to the primary vessel
DHR circuits coolant	Helium		Fully Passive solution without DHR blower has been investigated
DHR intermediate circuits coolant	Water		
DHR heat sink	Water pool		
Number of accumulators	3		Filled with Nitrogen, Additional helium injection system has been investigated.

ALLEGRO TH benchmark - phases

- Phase 0: Selection of the GFR technology to be used for TH benchmarking
- Phase I: Database for TH analyses (collection of relevant data)
- Phase II: TH benchmark specification (scenarios, I&B cond. etc.)
- Phase II: TH models development (codes, engineering handbook)
- Phase IV: Steady state calculations
  - blind
  - qualification procedure (criteria of acceptability)
  - identification of model distortions
  - model modification until criteria of acceptability are met
- Phase V: On transient calculations
  - blind
  - Qualitative and Quantitative assessment
  - identification of model distortions
  - model modification

ALLEGRO TH benchmark – codes and models

Company / Institute	Country	Code
VUJE, a.s.	Slovakia	RELAP3D 4.3.4 CATHARE2 v2.5_3 mod6.1 (SERPENT, DYN-3D, HELIOS)
ÚJV Řež, a.s.	Czech Republic	MELCOR 2.1
MTA EK	Hungary	CATHARE2 v2.5_3 mod6.1
NCBJ	Poland	CATHARE2 v2.5_3 mod6.1

ALLEGRO TH benchmark – RELAP5-3D nodalization

(VUJE)

Reactor Pressure Vessel, Primary system, Guard vessel

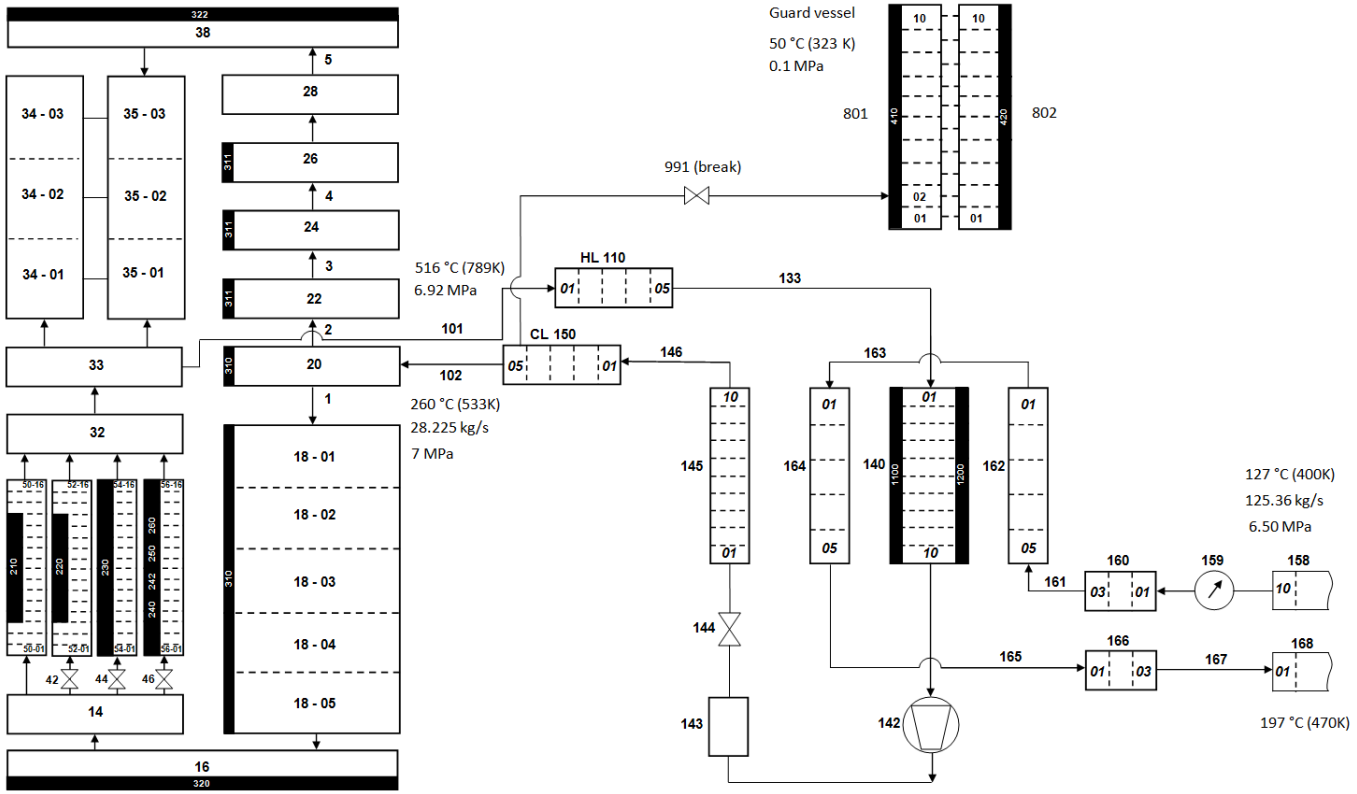

Secondary system + Air cooler

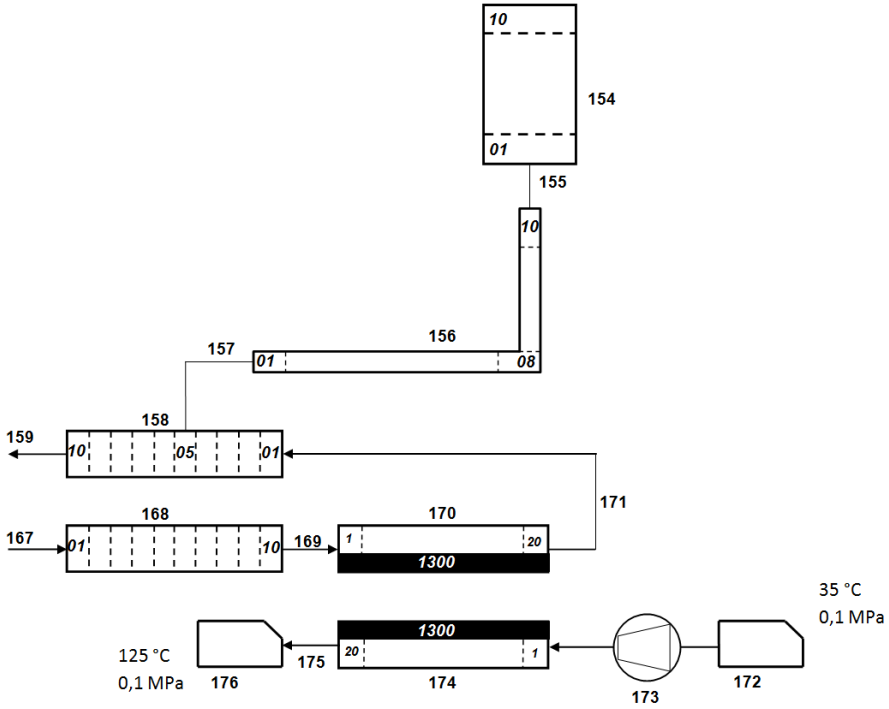

ALLEGRO TH benchmark – RELAP5-3D nodalization

(VUJE)

Decay Heat Removal system (Loop No.1)

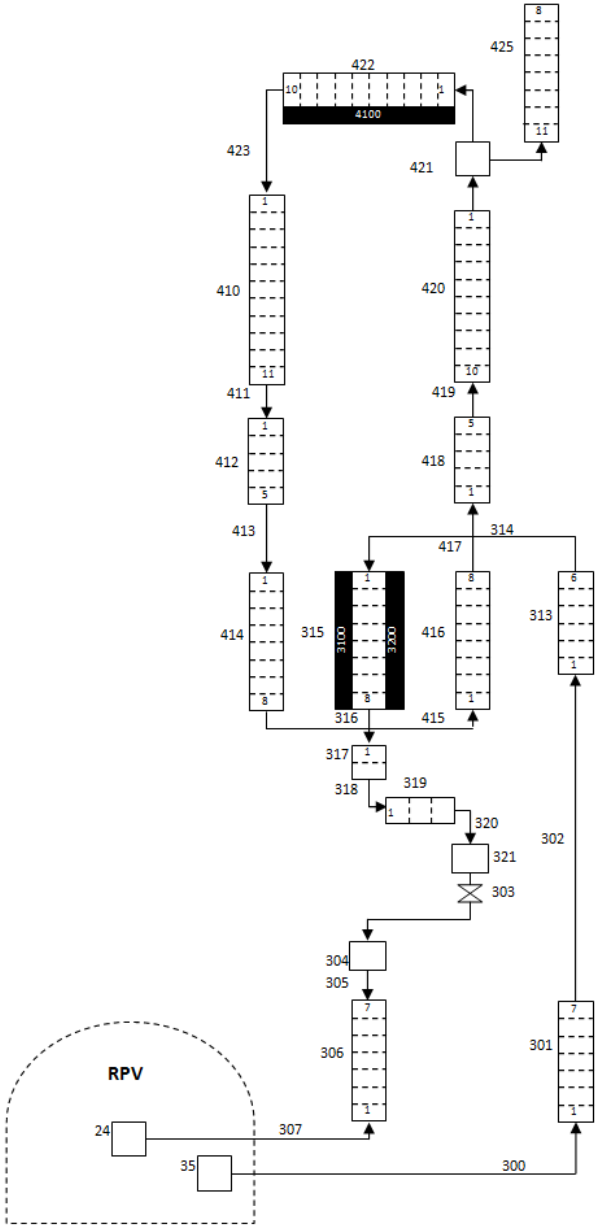

ALLEGRO TH benchmark – reaching steady state

Calculated ALLEGRO steady state conditions.

Contributor					VUJE			VUJE			MTA-EK			NCBJ			UJV		
Code					RELAP5-3D			CATHARE			CATHARE			CATHARE			MELCOR		
Parameter	Unit	Ref. value	Accu. [%]	Ac. Err. [%]	Value	Err.	Judg.	Value	Err.	Judg.	Value	Err.	Judg.	Value	Err.	Judg.	Value	Err.	Judg.
Core power	MWt	75.0	0.5	2.0	75.0	0.00	E	75.0	0.00	E	75.00	0.00	E	75.00	0.00	E	75.00	0.00	E
Core inlet pressure	MPa	7.00	0.5	0.1	7.00	0.00	E	7.00	0.00	E	7.02	0.00	E	7.00	0.00	E	7.01	0.00	E
Core inlet temp.	°C	260.00	0.5	0.5	261.78	0.18	E	259.27	0.00	E	260.50	0.00	E	260.21	0.00	E	259.10	0.00	E
Core outlet temp. (mean)	°C	516.00	0.5	0.5	515.91	0.00	E	515.07	0.00	E	516.30	0.00	E	516.04	0.00	E	519.60	0.00	E
Total system flow	kg/s	56.45	1.0	2.0	56.39	0.00	E	56.46	0.00	E	56.45	0.00	E	56.45	0.00	E	56.79	0.00	E
Mean channel flow	kg/s	0.662	1.0	2.0	0.660	0.00	E	0.662	0.00	E	0.660	0.00	E	0.660	0.00	E	0.654	0.00	E
Hot channel flow	kg/s	–	–	–	0.758	–	–	0.756	–	–	0.753	–	–	0.759	–	–	0.721	–	–
Total core bypass flow	kg/s	2.823	1.0	10.0	2.816	0.00	E	2.823	0.00	E	2.820	0.00	E	2.830	0.00	E	2.822	0.00	E
Main blower velocity	rpm	3919.0	0.5	1.0	3919.0	0.00	E	3885.1	0.37	E	3885.1	0.00	E	3918.3	0.00	E	N.A.	N.A	N.A
MHX water flow (mean)	kg/s	125.36	1.0	2.0	125.10	0.00	E	125.53	0.00	E	125.12	0.00	E	125.36	0.00	E	127.50	0.70	E
MHX inlet water temp. (mean)	°C	127.1	0.5	0.5	126.6	0.00	E	127.9	0.00	E	127.1	0.00	E	128.1	0.31	E	127.1	0.00	E
MHX temp. rise (mean)	°C	197.0	0.5	0.5	196.1	0.00	E	197.6	0.00	E	197.0	0.00	E	197.0	0.00	E	195.1	0.00	E
MHX outlet pressure (mean)	MPa	6.50	0.5	0.1	6.49	0.00	E	6.50	0.00	E	6.49	0.00	E	6.50	0.00	E	6.50	0.00	E
Guard vessel initial pressure	MPa	0.1	0.5	0.1	0.1	0.00	E	0.1	0.00	E	0.1	0.00	E	0.1	0.00	E	0.1	0.00	E
Guard vessel initial temperature	°C	50.0	0.5	0.5	50.0	0.00	E	50.0	0.00	E	50.0	0.00	E	50.0	0.00	E	50.0	0.00	E
DHR pressure (water side)	MPa	1.00	0.5	0.1	1.00	0.00	E	1.00	0.00	E	1.00	0.00	E	1.00	0.00	E	1.00	0.00	E
Maximum cladding temp.	°C	–	–	–	578.0	–	–	580.3	–	–	577.4	–	–	573.9	–	–	625.0	–	–
Maximum fuel temperature	°C	–	–	–	1047.8	–	–	981.6	–	–	969.9	–	–	973.2	–	–	839.3	–	–
Volume																			
He volume in RPV	m^3	112.62	0.0	1.0	112.62	0.00	E	112.62	0.00	E	112.62	0.00	E	112.91	0.26	E	111.95	0.59	E
He volume in the primary system (with DHR loops)	m^3	178.95	0.0	1.0	178.70	0.14	E	178.97	0.01	E	178.95	0.00	E	179.37	0.22	E	178.41	0.30	E
Guard vessel free volume	m^3	2600.0	0.0	1.0	2600.0	0.00	E	2600.0	0.00	E	2598.0	0.08	E	2600.0	0.00	E	2600.0	0.00	E
H2O volume in secondary system	m^3	27.852	0.0	2.0	27.908	0.20	E	28.178	1.17	E	27.834	0.06	E	27.840	0.04	E	27.960	0.39	E
H2O volume in single DHR system	m^3	2.098	0.0	2.0	2.090	0.36	E	2.082	0.74	E	2.090	0.22	E	2.100	0.18	E	2.101	0.16	E
Pressure drop/rise																			
Core	kPa	84.00	0.5	10.0	84.30	0.00	E	84.82	0.47	E	81.44	2.56	E	83.28	0.34	E	81.50	2.49	E
MHX (He side)	kPa	20.00	0.5	10.0	20.20	0.50	E	16.39	17.64	U	21.49	6.92	E	19.88	0.09	E	15.94	19.90	U
MHX (H_2O side)	kPa	11.61	0.5	10.0	12.00	2.84	E	28.50	143.8	U	11.00	4.78	E	11.61	0.00	E	11.10	3.91	E
Air HX (H_2O side)	kPa	124.21	0.5	10.0	126.70	1.50	E	108.10	12.5	U	117.00	5.33	E	124.13	0.00	E	120.40	2.58	E
Main blower	kPa	104.00	0.5	10.0	104.93	0.39	E	102.84	0.62	E	102.93	0.53	E	103.16	0.29	E	97.89	5.40	E
Water pump	kPa	141.61	0.5	10.0	142.80	0.34	E	141.90	0.00	E	158.00	11.02	U	141.51	0.00	E	135.30	3.98	E
Heat exchange area																			
MHX (H_2O side)	m^2	121.02	0.0	10.0	137.25	13.41	U	128.70	6.35	E	127.55	5.40	E	121.00	0.02	E	134.56	11.19	U
Air HX (H_2O side)	m^2	596.99	0.0	10.0	596.99	0.00	E	596.99	0.00	E	596.98	0.00	E	596.98	0.00	E	596.98	0.00	E
Air HX (air side)	m^2	16134.5	0.0	10.0	2158.4	86.62	U	15065.0	6.63	E	14058.0	12.87	U	16134.5	0.00	E	16753.7	3.84	E
DHR HX (He side)	m^2	80.14	0.0	10.0	80.14	0.00	E	78.40	2.16	E	78.41	2.15	E	80.14	0.00	E	80.14	0.00	E
DHR HX (H_2O side)	m^2	161.20	0.0	10.0	161.20	0.00	E	161.20	0.00	E	161.20	0.00	E	161.20	0.00	E	161.20	0.00	E
Fuel pins (cladding)	m^2	242.25	0.0	0.1	242.25	0.00	R	242.30	0.00	E	242.25	0.00	E	242.25	0.00	E	242.25	0.00	E
Mass																			
Fuel assemblies	kg	1500.0	0.0	14.0	1500.0	0.00	E	1500.0	0.00	E	1500.0	0.00	E	1500.0	0.00	E	1501.8	0.12	E
Radial reflector assemblies	kg	33430.0	0.0	14.0	33431.7	0.01	E	33429.5	0.00	E	33430.0	0.00	E	33430.0	0.00	E	33485.0	0.16	E
Radial shielding assemblies	kg	12900.0	0.0	14.0	12933.9	0.13	E	12945.9	0.03	E	12950.0	0.00	E	12900.0	0.00	E	13007.5	0.44	E

ALLEGRO TH benchmark – selection of initiating events

Scenarios to cover both depressurized and pressurized conditions have been selected.

Exercise #1: 3 inch LOCA on the cold duct
Exercise #2: Total station blackout, 1 DHR available

ALLEGRO TH benchmark – distortions among the models identified

Identification of the key model distortions.

N.	Distortion	Participant/code	Effect
1.	Core decay heat profile after scram. The NCBJ, VUJE, MTA EK CATHARE2 model uses the same decay heat. The VUJE RELAP5-3D underestimates and UJV MELCOR overestimates decay heat profile with respect to CATHARE2 models.	All	Different power generation after scram has substantial effect on the core heat removal under natural convection (e.g. SBO) according to findings of the Best Estimate Plus Uncertainty study (Batki et al., 2018) carried out in cooperation between VUJE and MTA EK.
2.	Heat conductivity in the gap between fuel pellet and cladding.	All	Differences of the initial fuel temperature.
3.	Underestimation of pressure rise of main blowers.	VUJE/CATHARE2 UJV/MELCOR	If main blower pressure rise is underestimated and user keeps correct core pressure drop it leads to underestimation of MHX pressure drop. This affects flow distribution in primary system influencing core heat-up and cool-down phase during LOCA.
4.	MHX (water side) pressure drop overestimation. U-tubes are represented by single vertical channel 3 m long instead of two vertical channels.	MTA EK/CATHARE2 VUJE/CATHARE2NCBJ/ CATHARE2	Hydrostatic pressure of water column does not allow decreasing MHX total pressure loss to less than 30 kPa. MTA EK (NCBJ) shows MHX pressure drop omitting hydrostatic pressure in Tab.2. VUJE assumes MHX pressure drop as purely hydrostatic. Consequently, VUJE does not assume friction losses in MHX tubes and on the contrary MTA EK does. This has effect on flow distribution during secondary system LOCA and Loss Of Flow Accident (LOFA) transients.
5.	Pressure rise of the secondary system water pump.	MTA EK/CATHARE2	Consequence of item 4 is overestimation of water pump pressure rise in MTA EK (NCBJ) and underestimation of MHX friction losses in VUJE model. This has effect on flow distribution during secondary system LOCA and LOFA transients.
6.	Pressure loss of water-to-air heat exchanger (water side)	VUJE/CATHARE2	Minor effect on flow distribution inside secondary system during secondary system LOCA and LOFA.
7.	Water to air heat exchanger model (air side). RELAP5-3D model uses default heat transfer code correlation and heat transfer coefficient is adjusted by multiplication factor to keep energy balance in steady state. CATHARE2 models rely on user defined heat transfer correlation proposed by CEA.MELCOR model uses default heat transfer code correlation.	All	Different approaches to model aluminum fins in the models affects ultimate heat sink efficiency during LOCA transient.
8.	Point kinetic model not used.	UJV/MELCOR	Effect on the core power before the scram.

International recommendations on V&V (IAEA)

Hierarchy of IAEA safety standards

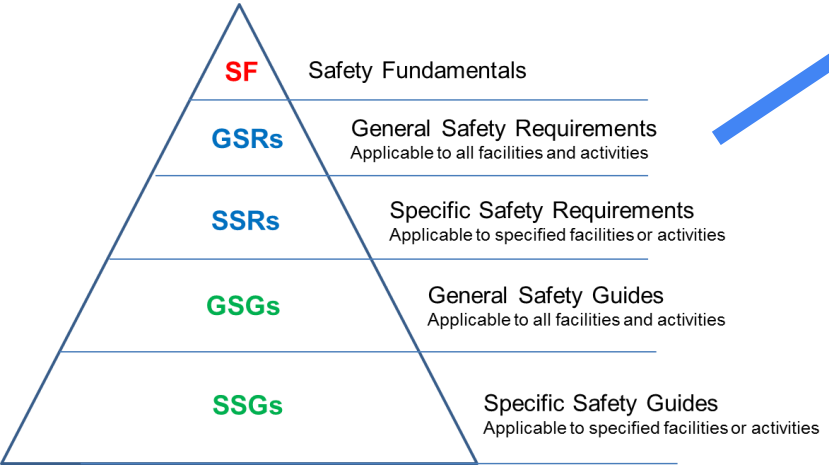

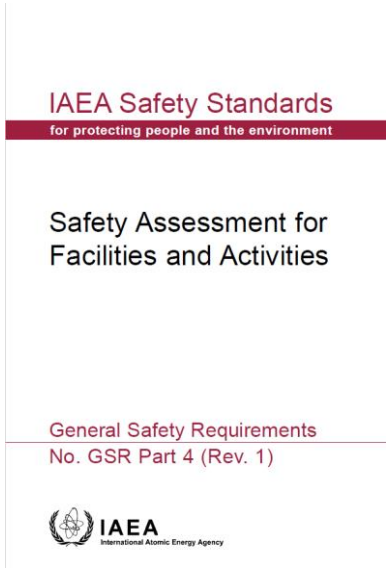

IAEA, Safety Assessment for Facilities and Activities, IAEA Safety Standards Series **No. GSR Part 4 (Rev.1).** Vienna: IAEA, 2016, 26-27. ISBN 978-92-0-109115-4.

Requirement 18 of GSR Part 4 (Rev. 1)

Any calculation methods and computer codes used in the safety analysis shall undergo verification and validation.

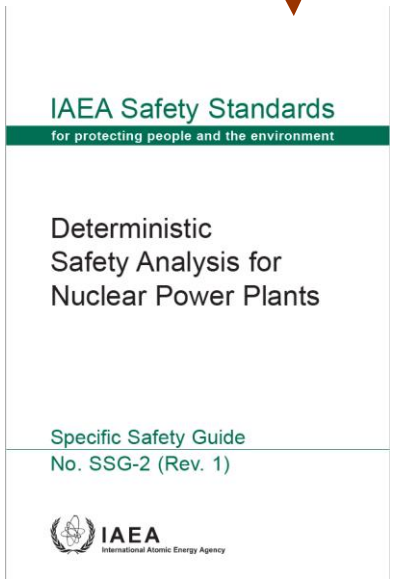

IAEA, Deterministic Safety Analysis for Nuclear Power Plants, IAEA Safety Standards Series **No. SSG-2 (Rev.1)**. Vienna: IAEA, July 2019. ISBN 978–92–0–102119–9

International recommendations on V&V (IAEA)

IAEA Safety Standards

for protecting people and the environment

Deterministic Safety Analysis for Nuclear Power Plants

Specific Safety Guide

No. SSG-2 (Rev. 1)

IAEA International Atomic Energy Agency

International recommendations on V&V (IAEA)

5. USE OF COMPUTER CODES FOR DETERMINISTIC SAFETY ANALYSIS

BASIC RULES FOR THE SELECTION AND USE OF COMPUTER CODES

- Selection of the proper computer code (phenomena)
- Accuracy of the computer code
- Predictions shall be compared with experiments, plant data, other codes, numerical benchmarks if available
- User qualification (training, experience, guidance …)
- Nodalization qualification (comprehensive procedure)

National requirements on V&V in Slovakia (ÚJD SR)

Requirements for assuring of software quality for safety analyses.

BN 1/2019, Požiadavky na zabezpečenie kvality softvéru pre analýzy bezpečnosti (4. vydanie – revidované a doplnené), EDÍCIA Bezpečnosť jadrových zariadení, ISBN 978-80-89706-25-9, Bratislava, apríl 2019

Origin of uncertainties 1/2

- Code equations are approximate
- Presence of different fields of the same phase. Only one velocity per phase is considered.
- Geometry averaging at a cross section scale. (Different velocity vectors in the model and reality)
- Geometry averaging at a volume scale. (Different velocity vectors in the model and reality)
- Presence of large or small vortex or eddy in reality not covered in the TH model. (e.g. natural circulation in the DHR ducts or in the RPV upper plenum)
- The 2nd law of thermodynamics is not necessarily fulfilled by codes.
- The numerical solution is approximate. Approximate equations are solved by approximate numerical methods. The degree of approximation is not necessarily documented.
- Use of empirical correlations:
  - validity not fully documented
  - usage outside of validation range
  - approximately implemented in the code
  - reference database affected by scatter and errors
- Material and fluid properties approximate
- The computer HW/SW platform and source code compiler effect

Origin of uncertainties 2/2

- Nodalization effect. Partly connected with user effect, however there are other factors as: code manual guidance, rather large number of required input values that cannot be covered by the available documentation and expertise.
- Initial and boundary conditions (unknown, approximate, large uncertainty)
- Severe physical model deficiencies, which are unknown to the code user.
- User effect (!)

Origin of uncertainties – user effect

ALLEGRO code-to-code TH benchmark
3 inch LOCA

- Guard vessel internal wall model was not properly modelled in VUJE_R5

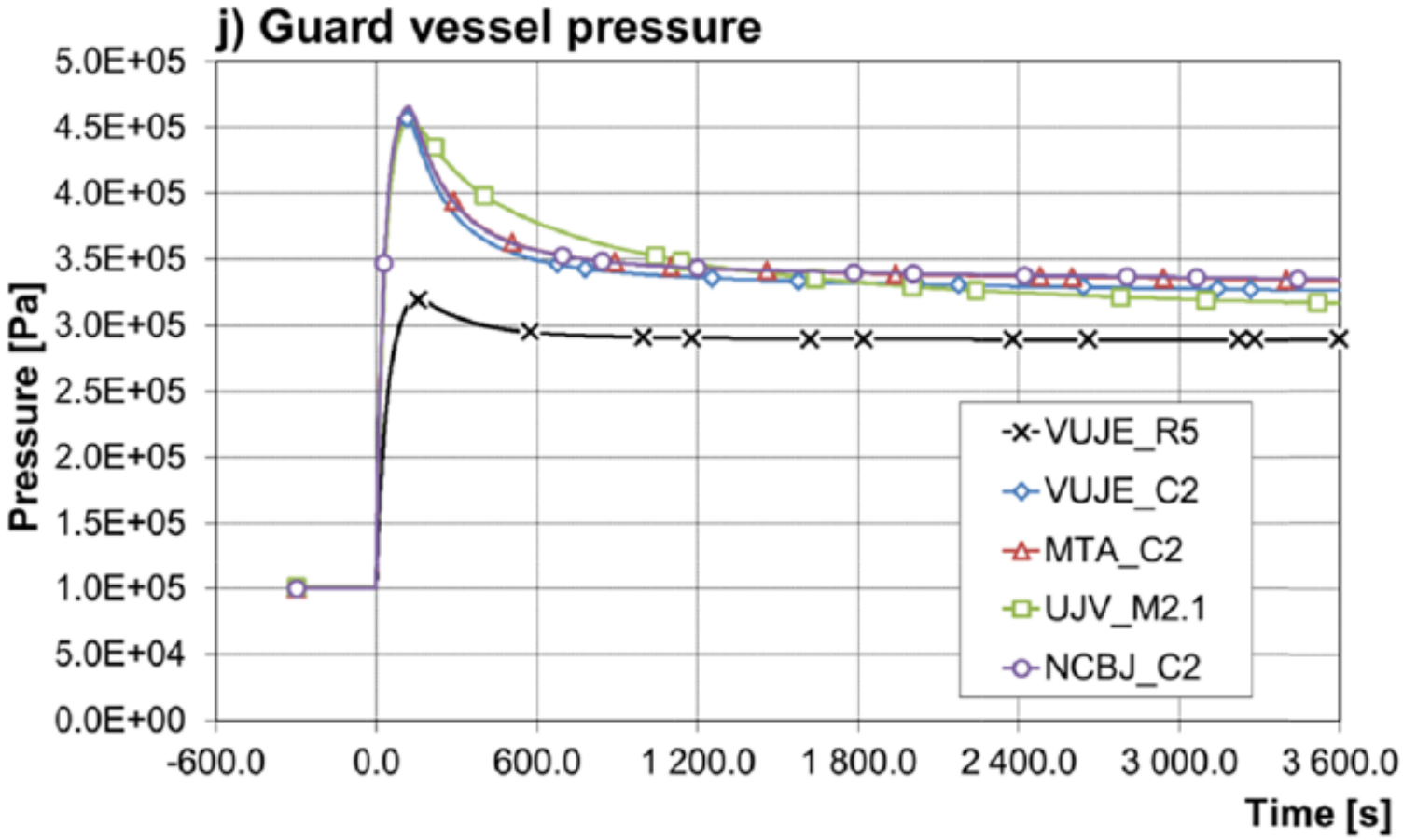

Origin of uncertainties – code correlations, user effect

ALLEGRO code-to-code TH benchmark
3 inch LOCA

- Heat transfer correlations in MHX model

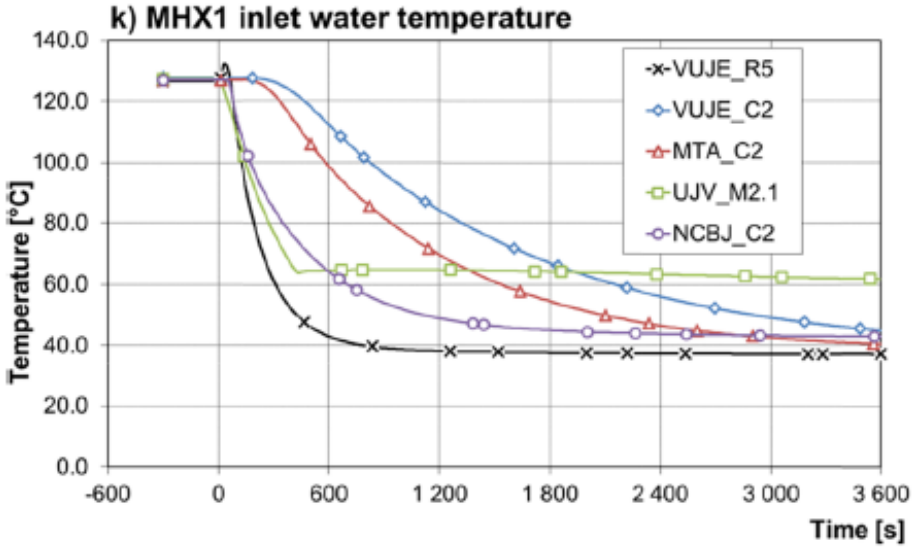

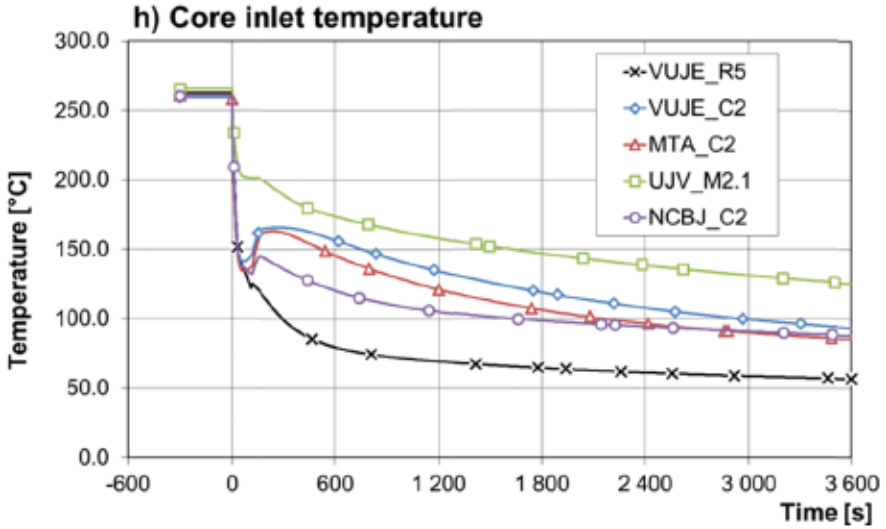

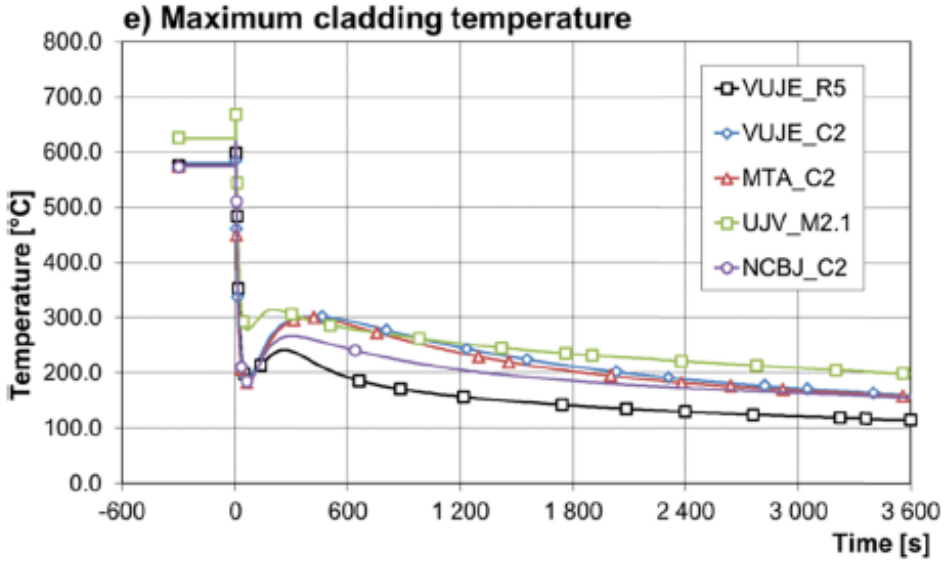

Origin of uncertainties – user effect, inconsistent IBC

ALLEGRO code-to-code TH benchmark
3 inch LOCA

- Control rod insertion delay missing (VUJE, MTA)
- Reactivity coefficients diff. (C2, R5)
- Point kinetic model missing (M2.1)

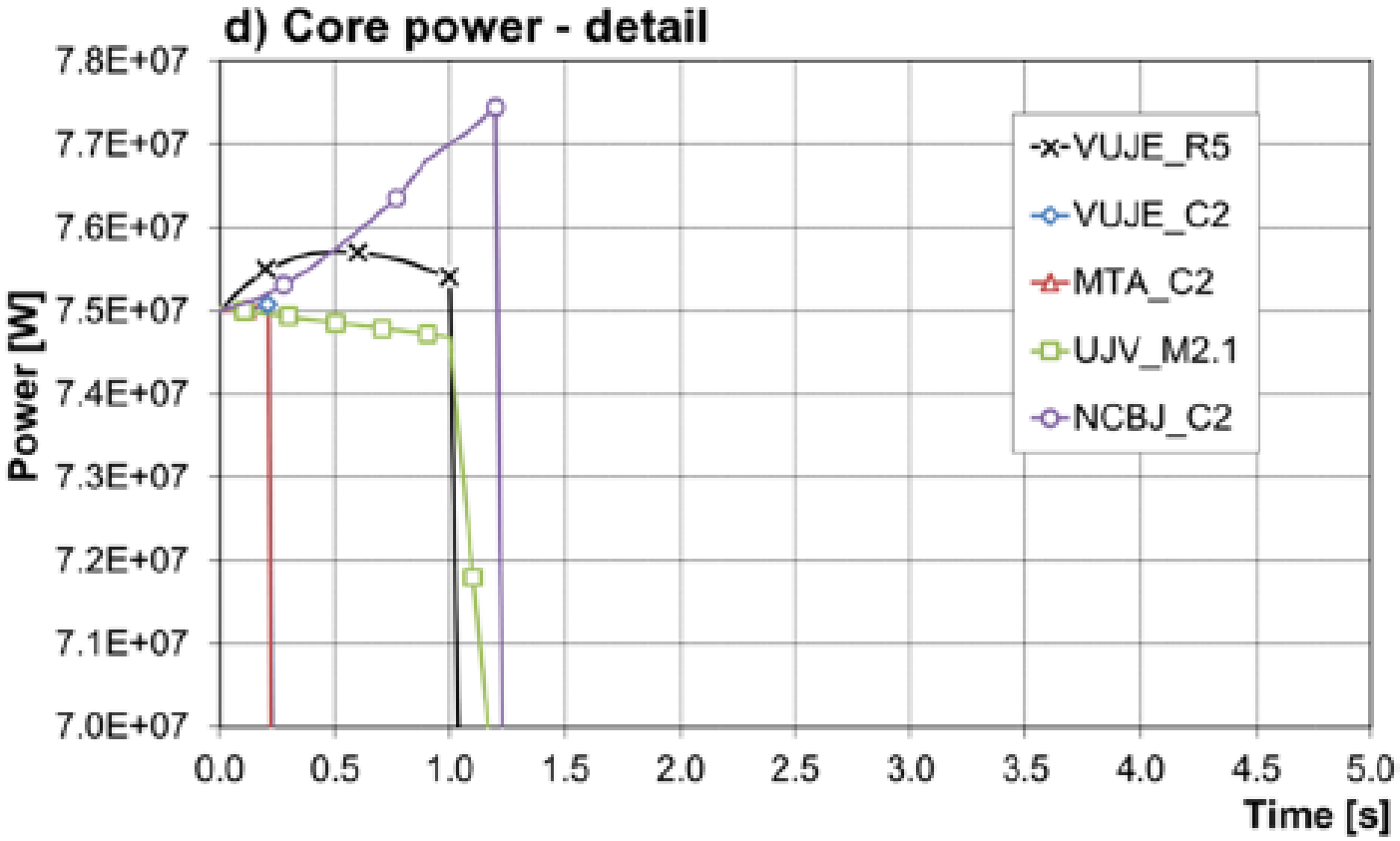

Origin of uncertainties – user effect, inconsistent IBC

ALLEGRO code-to-code TH benchmark
3 inch LOCA

- Gap conductivity (initial temperature difference)
- Discrepancy in radial heat transfer model.

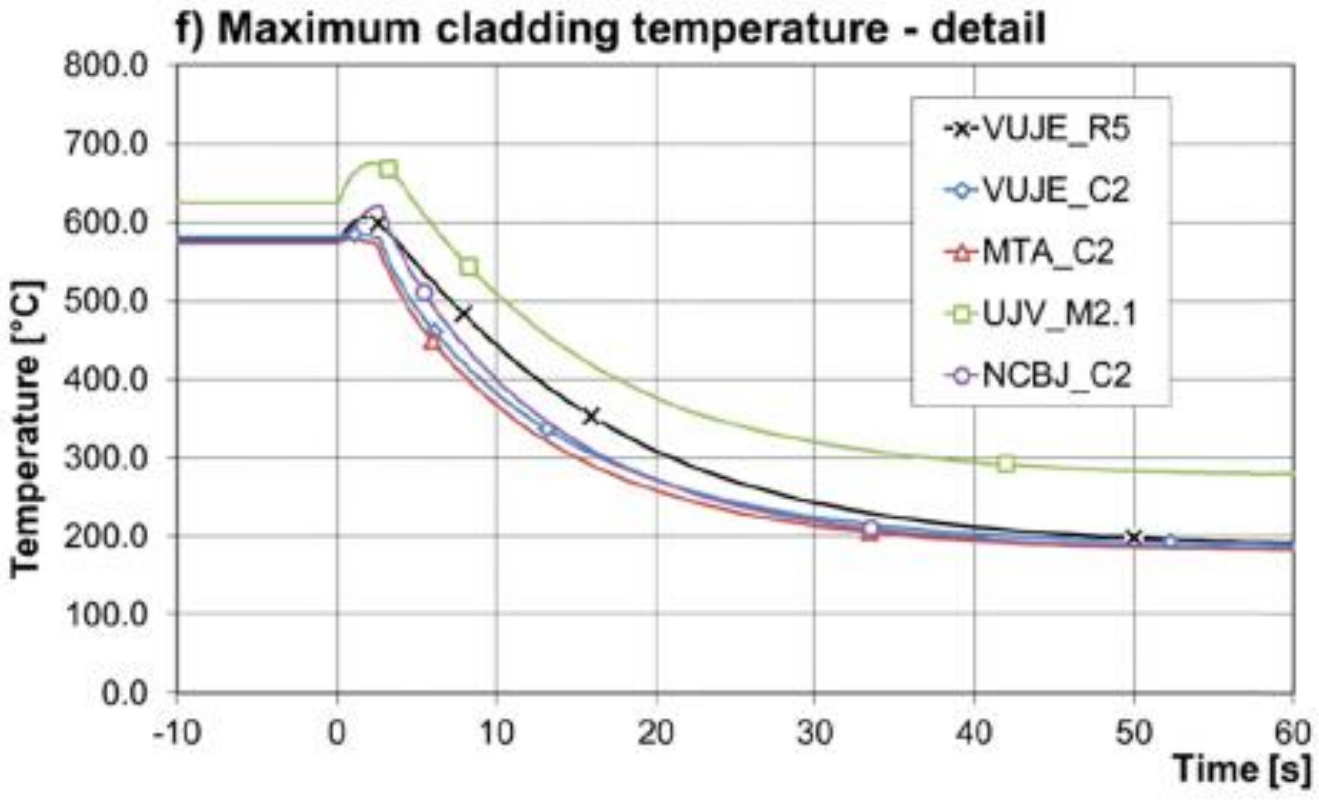

Origin of uncertainties – imperfect code model

ALLEGRO code-to-code TH benchmark
Total station blackout, 1 DHR

Main blower inertia and friction (effect on natural circulation onset, effect on forced convection)

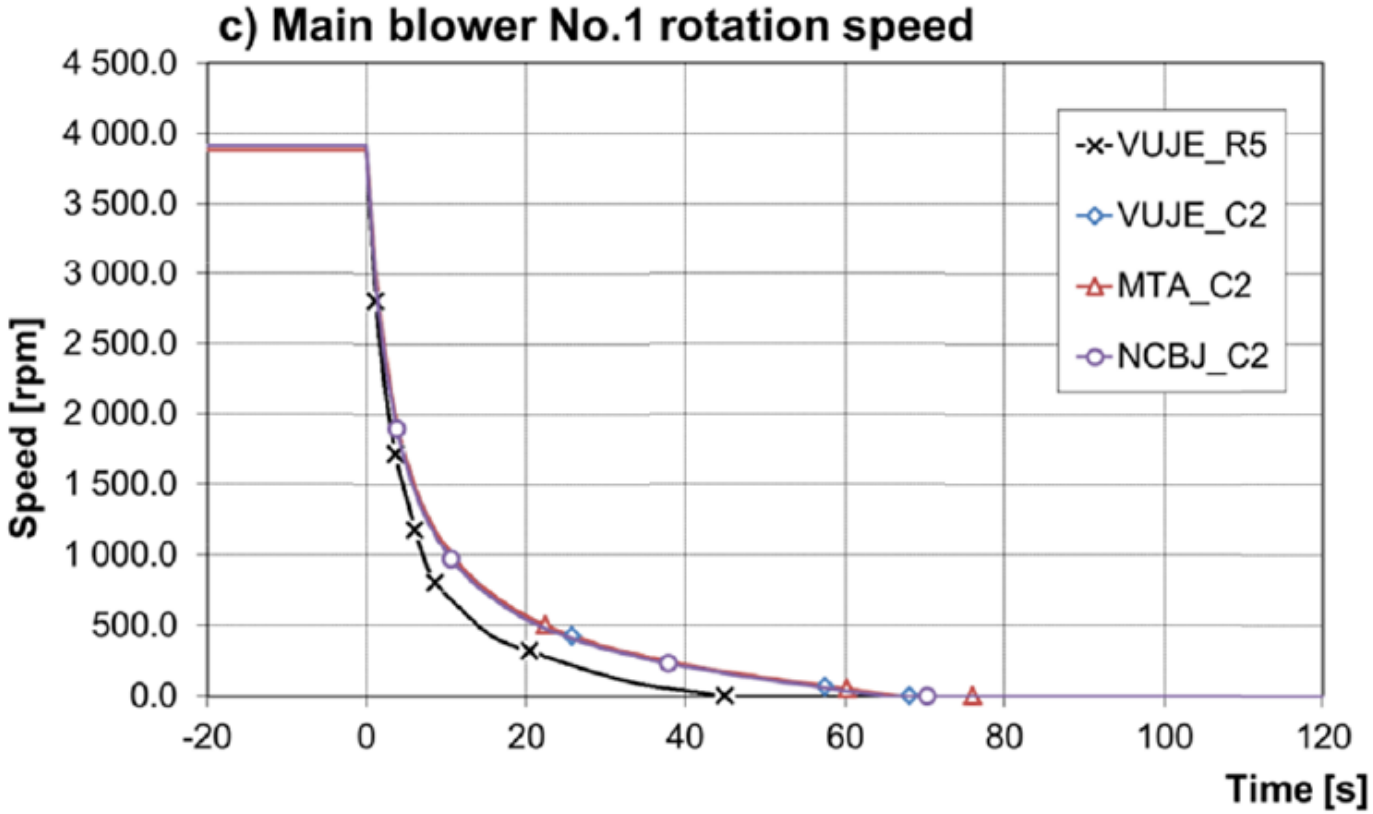

Origin of uncertainties – user effect, imperfect knowledge of IBC

ALLEGRO code-to-code TH benchmark
Total station blackout, 1 DHR

Flow resistance in DHR loop

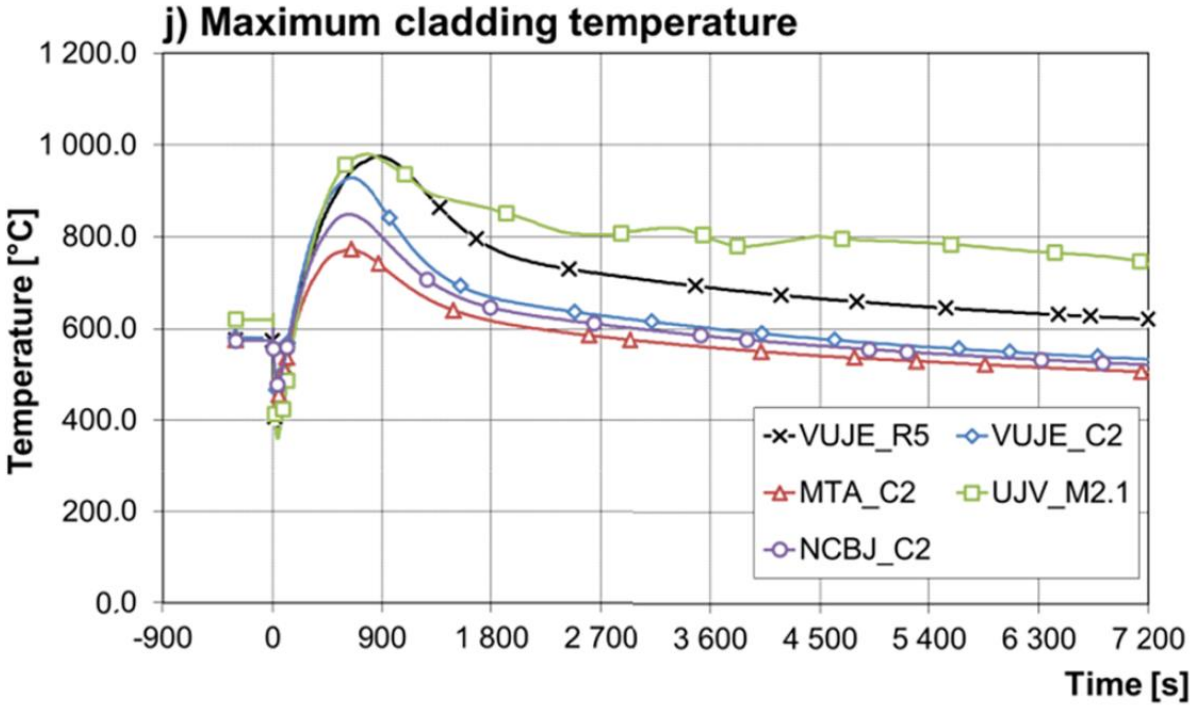

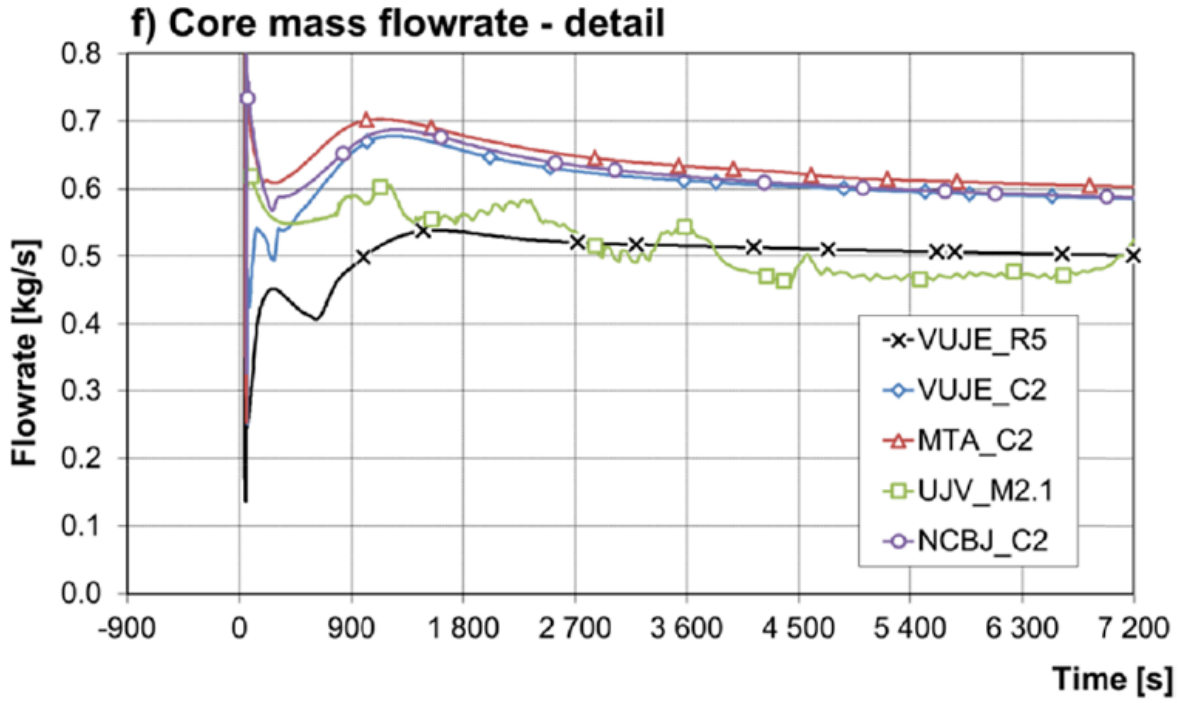

Origin of uncertainties – user effect

EVO loop benchmark
Loss of load transient

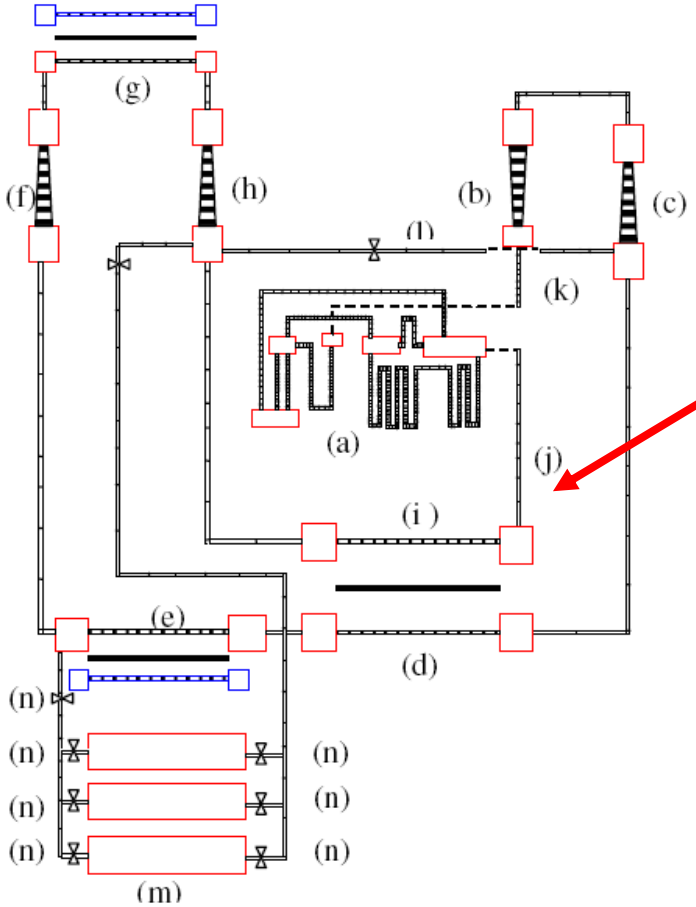

Figure 3: *Schematic of CATHARE nodalization. (a) burner, (b) high pressure turbine, (c) low pressure turbine, (d) recuperator hot side, (e) precooler, (f) low pressure compressor, (g) intercooler, (h) high pressure compressor, (i) recuperator cold side, (j) colduct, (k) hotduct, (l) by-pass line, (m) helium storage tanks, (n) Tanks isolation valves.*

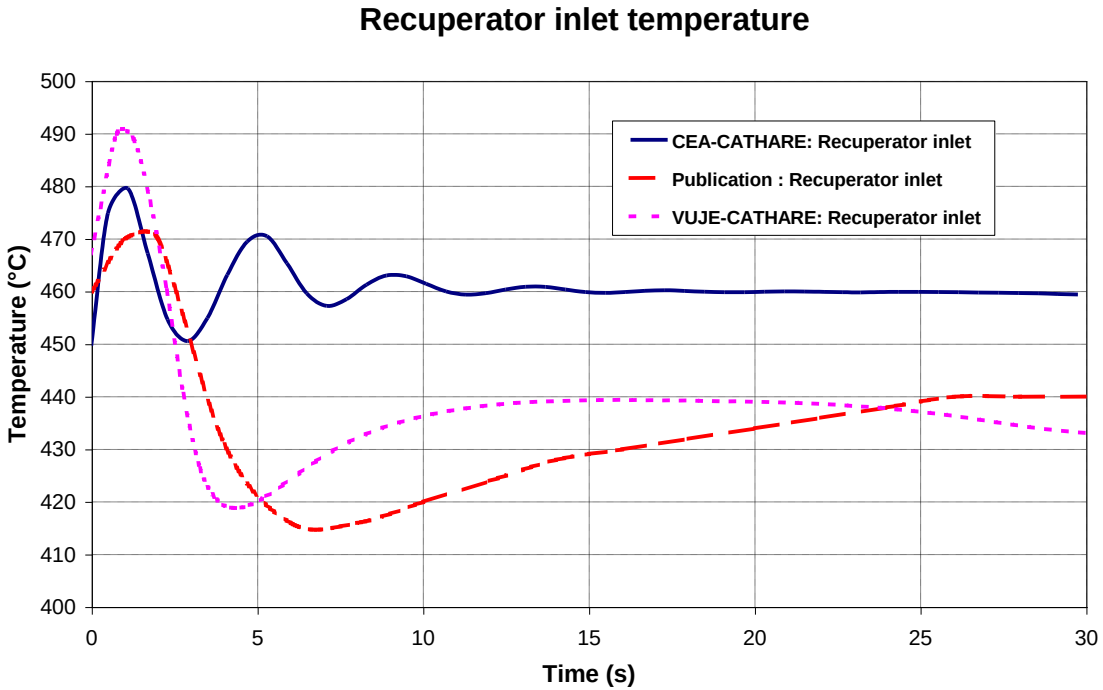

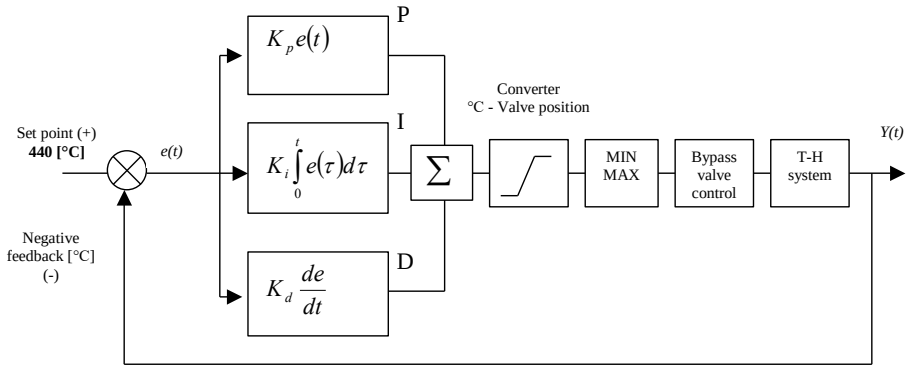

Corrections made

- Initial conditions of PID settings
- Negative feedback correction
- Converter added
- Time step control during the transient (equidistant)
- Tuning of PID constants by Ziegler-Nichols method

Origin of uncertainties – imperfect knowledge of IBC

EVO loop benchmark
Load following transient

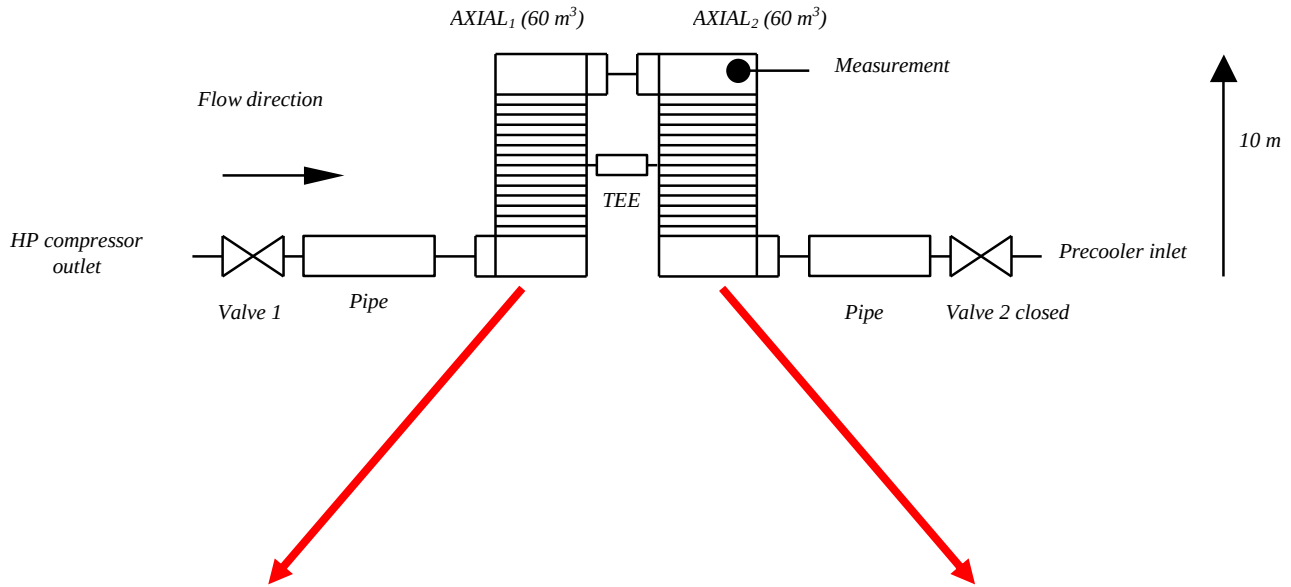

Temperature in Tank 1

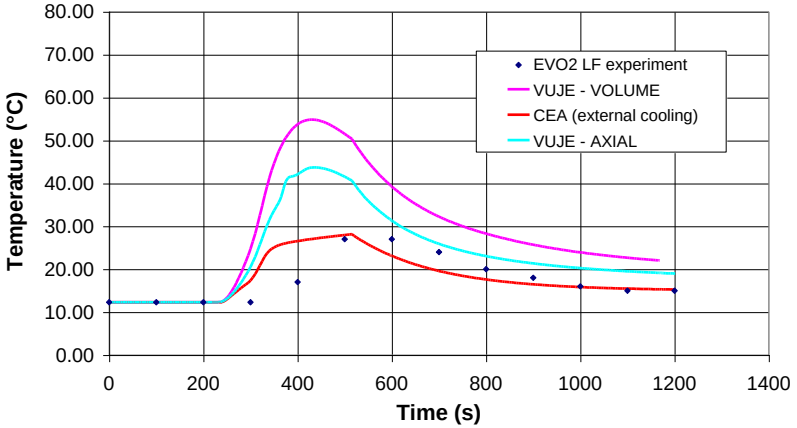

Temperature in Tank 2

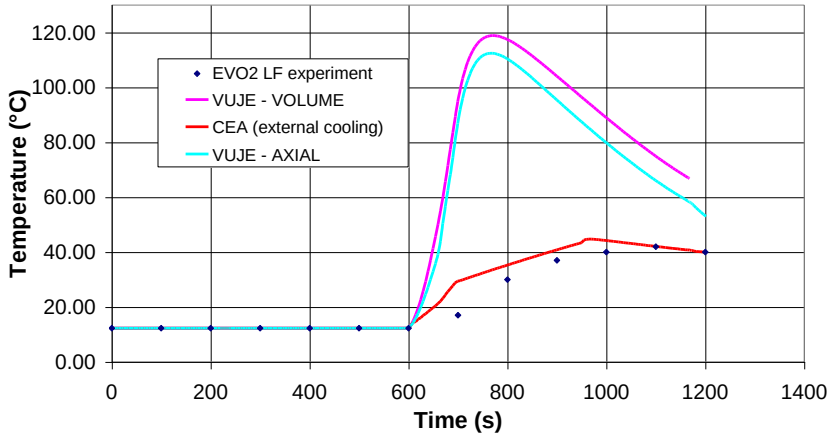

Tools and methods to qualify TH models (codes)

IAEA-TECDOC-1332

Safety margins of operating reactors

Analysis of uncertainties and implications for decision making

INTERNATIONAL ATOMIC ENERGY AGENCY IAEA

January 2003

Concept of Safety margins of operating NPPs

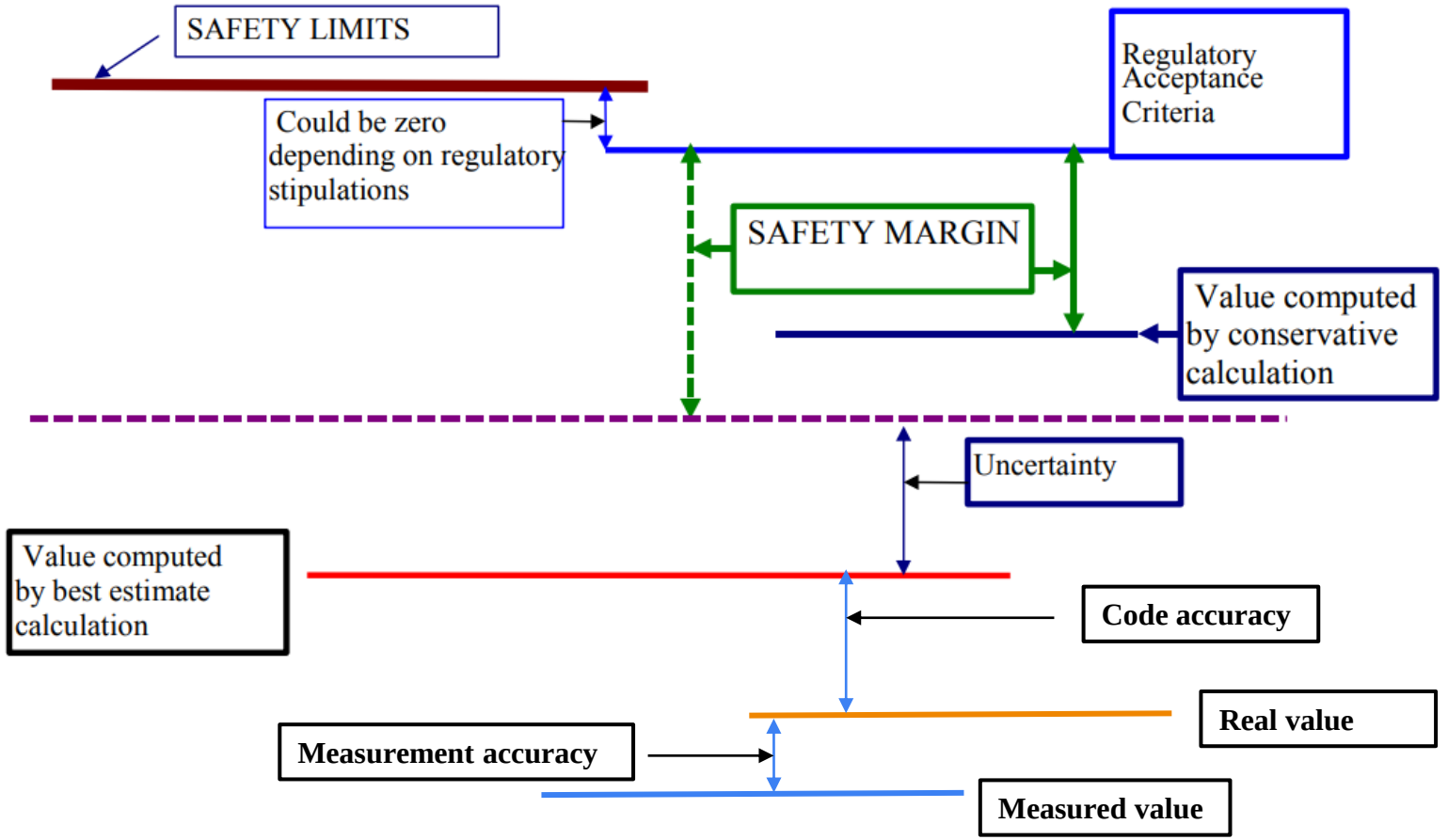

Tools and methods to qualify TH models (codes)

SafeG

Accuracy

Known error between a code prediction and the real experimental value obtained from NPP measurement, Integral Test Facility (ITF), Separate Effect Test Facility (SETF), full scale NPP. It is a measure of error that characterize the comparison. Experimental data are needed!

Uncertainty

Unknown error related to the prediction of a e.g. Nuclear Power Plant (NPP) transient or Integral Test Facility (ITF) scenario. It is a measure of the error that characterizes the prediction.

Tools and methods to qualify existing nodalization (codes)

Fast Fourier Transformation Based Method (FFTBM)

We have both experiment and calculation data of the same facility (!)

What is needed

Nodalization to be qualified ITF (NPP)
Experimental data ITF (NPP)
TH code simulation data ITF (NPP)

Comprehensive ITF (NPP) database
Comprehensive engineering hand book for ITF (NPP) nodalization

Tools and methods to qualify existing nodalization (codes)

SafeG

Fast Fourier Transformation Based Method (FFTBM)

1. Steady state qualification

1.1 Steady state calculation

1.2 Verification of the TH model (e.g. height vs. volume curve, dP vs length curve, demonstration of IBC compliance with thresholds of acceptability, independent check of the nodalization by experienced user …)

Initial conditions for PMK SPE-4 (experiment and calculation results)

No	Quantity	Unit	EXP	CALC	Measur. Error	Acc. Error	Err.
1	Pressure UPL	MPa	12.33	12.38	± 0.05 MPa	0.1 %	0 %
2	Loop flow	kg/s	4.91	4.89	±0.06 kg/s	2 %	0 %
3	Core inlet temp	K	540.10	540.08	± 1.0 K	0.5 %	0 %
4	Core power	kW	665.12	665.14	±3.0 kW	2 %	0 %
5	PRZ level	m	1.58	1.58	± 0.02 m	0.05 m	0 %

Tools and methods to qualify existing nodalization (codes)

Fast Fourier Transformation Based Method (FFTBM)

1. Steady state qualification (volume vs height curve)

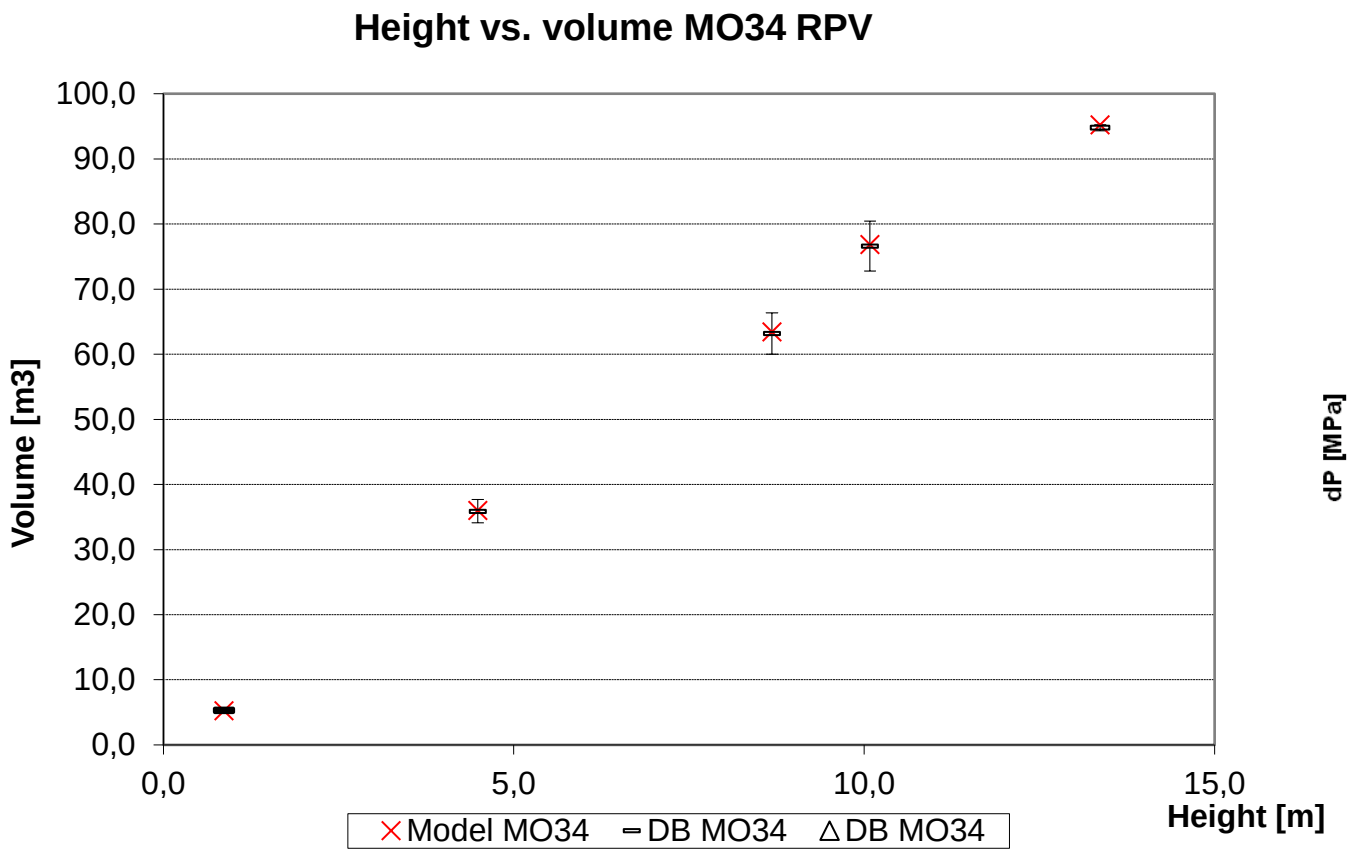

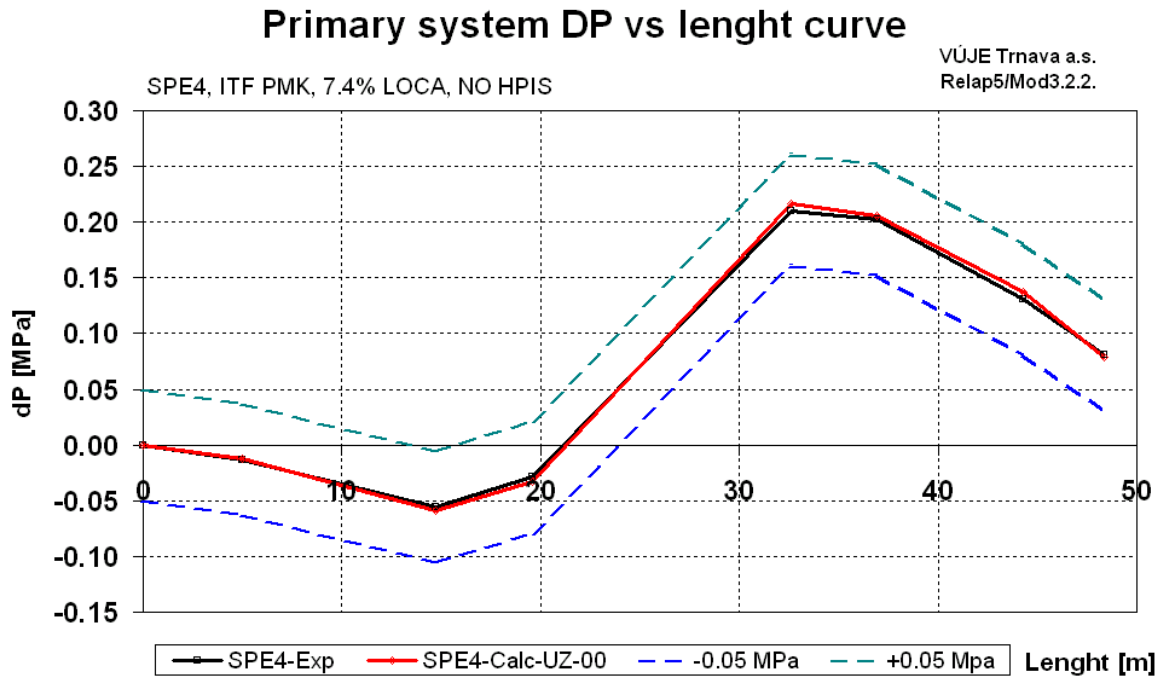

Tools and methods to qualify existing nodalization (codes)

Fast Fourier Transformation Based Method (FFTBM)

2. On-transient qualification (qualitative evaluation)

2.1 Transient calculation

- Subdivision into phenomenological windows (Ph.W.)

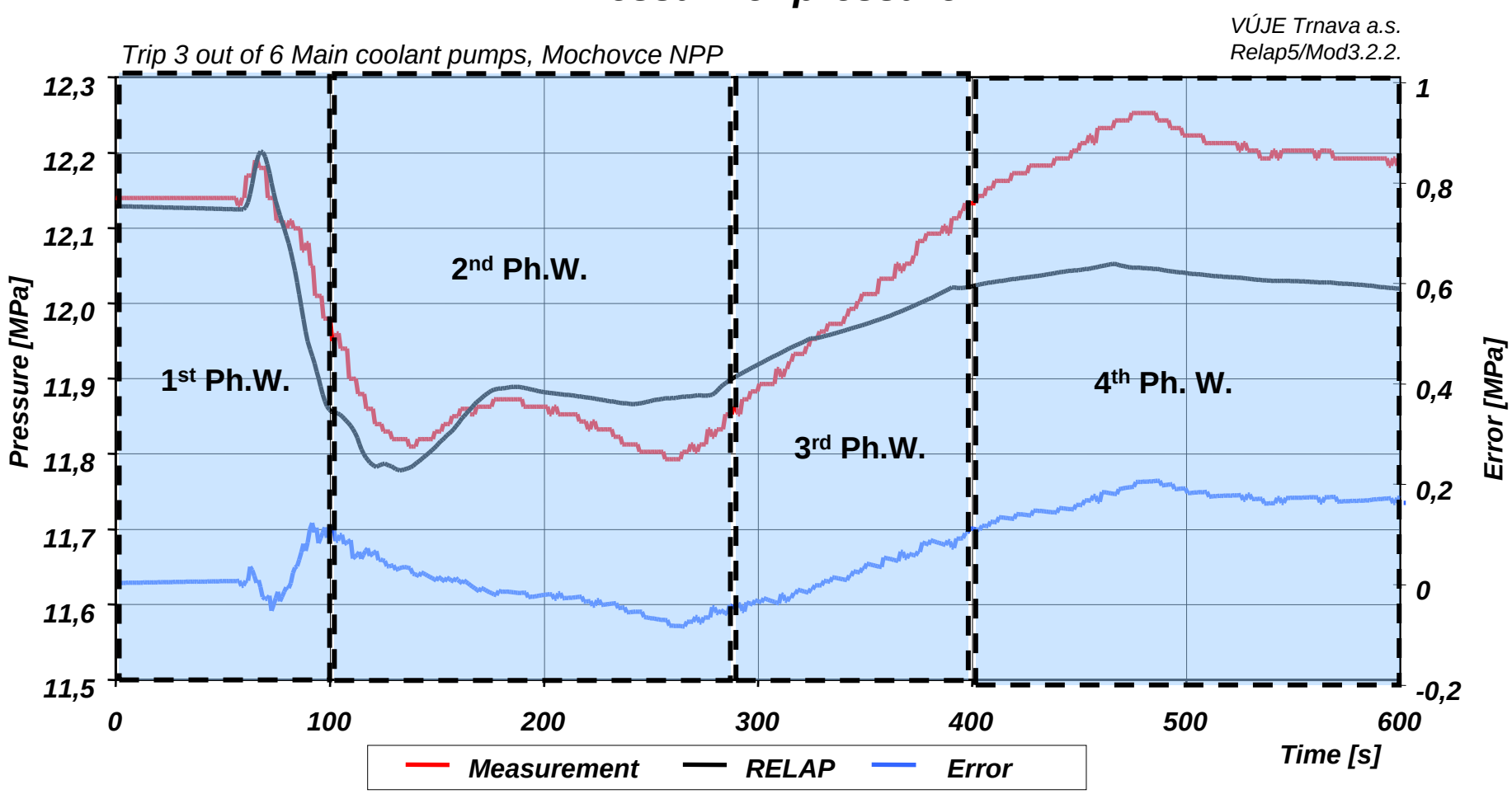

Tools and methods to qualify existing nodalization (codes)

Fast Fourier Transformation Based Method (FFTBM)

2. On-transient qualification (qualitative evaluation)

2.1 Transient calculation

Trip 3 out of 6 Main coolant pumps, Mochovce NPP

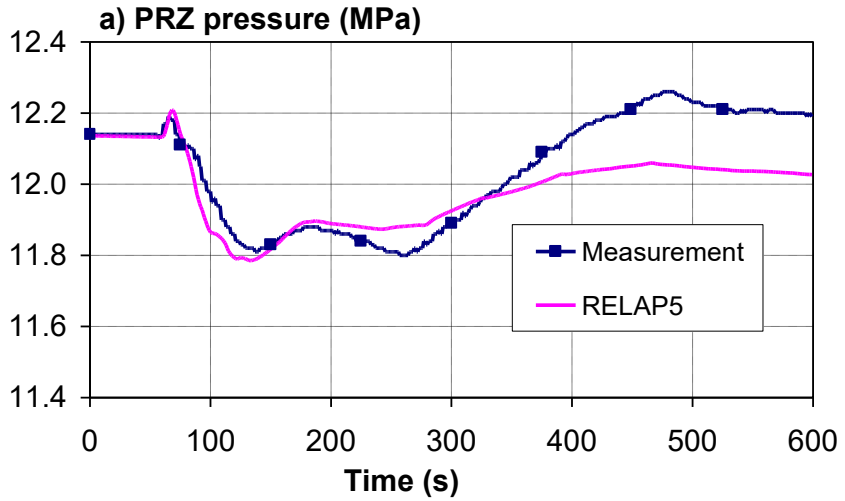

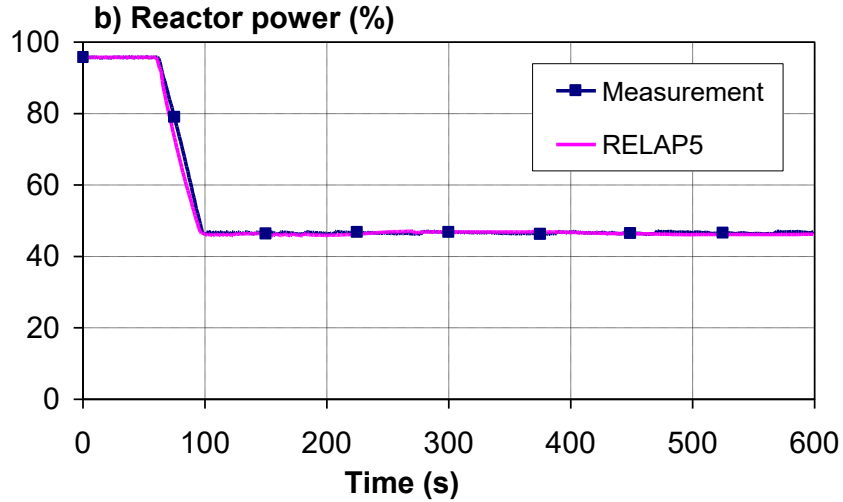

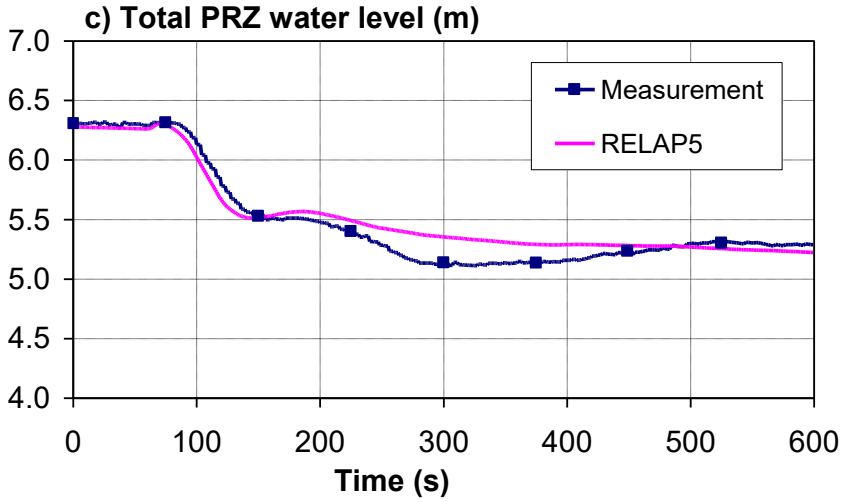

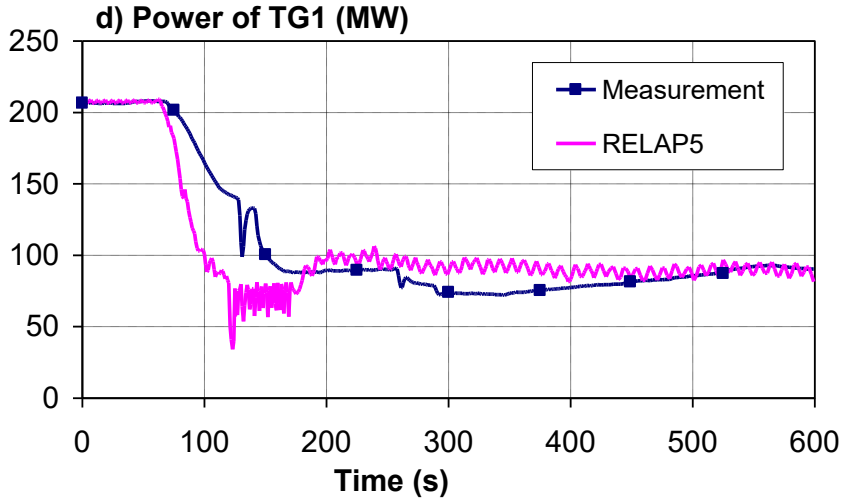

Fast Fourier Transformation Based Method (FFTBM)

2. On-transient qualification
(qualitative evaluation)

2.1 Transient calculation

- Specification of the key phenomena typical for the transient

- Identification of the Relevant TH Aspects (RTA)

- Selection of the parameters characterizing RTA

- Selection of at least 20 independent values characterizing the process

- Subjective judgement based on the visual observation

Excellent	*(E)*	*- code predicts the parameter qualitatively and quantitatively*
Reasonable	*(R)*	*- code predicts the parameter qualitatively but not quantitatively*
Minimal	*(M)*	*- code does not predict the parameter but reason is understood*
Unqualified	*(U)*	*- code does not predict the parameter at all*

Tools and methods to qualify existing nodalization (codes)

SafeG

Fast Fourier Transformation Based Method (FFTBM)

2. On-transient qualification (qualitative evaluation)

2.1 Transient calculation

Trip 3 out of 6 Main coolant pumps, Mochovce NPP

Description of event	Measurement		RELAP5/Mod 3.2.2		Type of RTA (judgement)
	Time (s)	Value	Time (s)	Value	
Beginning of calculation (measurement)	0.0	–	0.0	–	TSE (E)
Total core power decreasing (60–100 s)					
MCP in loops 1, 3, 5 shut downed	60.0	–	60.0	–	TSE (E)
ARM controller starts to decrease power	60.0	–	60.0	–	TSE (E)
MCP in loops 2, 4, 6 in operation	–	Available	–	Available	N.A.
Reactor power reaches 47%	98.0	–	96.0	–	TSE (E)
1. and 2. group of PRZ heaters switched on	All the time	–	All the time	–	TSE (E)
Primary pressure stabilised (100–279 s)					
Minimum PRZ pressure (MPa)	138.0	11.80	132.0	11.79	TSE (E) SVP (E)
Minimum MSH (secondary) pressure (MPa)	120.0	4.24	120.0	4.23	TSE (E) SVP (E)
PRZ level decreasing; level at 279 s (m)		5.153		5.378	SVP (R)
SG no. 1 FW stopped	160.0	–	185.0		TSE (R)
SG no. 3 FW stopped	160.0	–	196.0		TSE (R)
SG no. 5 FW stopped	160.0	–	209.0		TSE (R)
SG nos. 2, 4, 6 FW		Available		Available	N.A.
Primary pressure recovering (279–391 s)					
PRZ heater group no. 5	279.0	Actuated	319.0	Actuated	TSE (M)
SG nos. 1, 3, 5 FW recovered	–	–	381.0	–	TSE (M)
PRZ pressure start recovering (MPa)	260.0	11.80	280.0	11.89	TSE (R) SVP (R)
Primary pressure restoration (391–599 s)					
Maximum primary pressure (MPa)	484.0	12.26	467.0	12.06	TSE (R) SVP (R)
PRZ pressure at 599 s (MPa)	–	12.2	–	12.0	SVP (R)
PRZ level at 599 s (m)	–	5.29	–	5.24	SVP (E)

Tools and methods to qualify existing nodalization (codes)

SafeG

Fast Fourier Transformation Based Method (FFTBM)

2. On-transient qualification (qualitative evaluation)

2.1 Transient calculation

Trip 3 out of 6 Main coolant pumps, Mochovce NPP

Phenomenological windows			*I.*	*II.*	*III.*	*IV.*
ID	*Variable*	*Description of variable*	*Power decreasing*	*PRZ pressure stabilisation*	*PRZ pressure recovering*	*PRZ pressure restoration*
1	*PRZP*	*PRZ pressure*	*E*	*E*	*R*	*R*
2	*MCPDP1*	*Pressure variation on MCP No. 1*	*E*	*R*	*R*	*R*
3	*MCPDP2*	*Pressure variation on MCP No. 2*	*E*	*R*	*R*	*R*
4	*RPWER*	*Reactor power*	*E*	*E*	*E*	*E*
5	*POWTG1*	*Power of TG1*	*R*	*E*	*E*	*E*
6	*POWTG2*	*Power of TG1*	*E*	*E*	*E*	*E*
7	*TLEVPRZ*	*Total PRZ water level (from bottom)*	*E*	*E*	*R*	*E*
8	*PSG1*	*Pressure in SG No. 1*	*E*	*R*	*R*	*R*
9	*PSG2*	*Pressure in SG No. 2*	*R*	*R*	*R*	*R*
10	*STMFSG1*	*Steam flow from SG No. 1*	*E*	*R*	*R*	*R*
11	*STMFSG2*	*Steam flow from SG No. 2*	*E*	*R*	*R*	*R*
12	*FWSG1*	*Feed water of SG No. 1*	*E*	*E*	*R*	*R*
13	*FWSG2*	*Feed water of SG No. 2*	*R*	*R*	*R*	*R*
14	*TMPCL1*	*Cold leg temperature No. 1*	*E*	*R*	*R*	*R*
15	*TMPCL2*	*Cold leg temperature No. 2*	*R*	*R*	*R*	*R*
16	*TMPHL1*	*Hot leg temperature No. 1*	*E*	*E*	*E*	*E*
17	*TMPHL2*	*Hot leg temperature No. 2*	*R*	*R*	*R*	*R*
18	*LEVSG1*	*Total water level of SG No. 1*	*R*	*R*	*R*	*R*
19	*LEVSG2*	*Total water level of SG No. 2*	*E*	*E*	*E*	*E*

Excellent (E), Reasonable(R), Minimal(M), Unqualified (U)

Tools and methods to qualify existing nodalization (codes)

Fast Fourier Transformation Based Method (FFTBM)

2. On-transient qualification (quantitative evaluation)

Fourier theory: Any periodic waveform (signal) can be expressed by means of an infinite sum of sinusoids at the frequencies , amplitudes and phases.

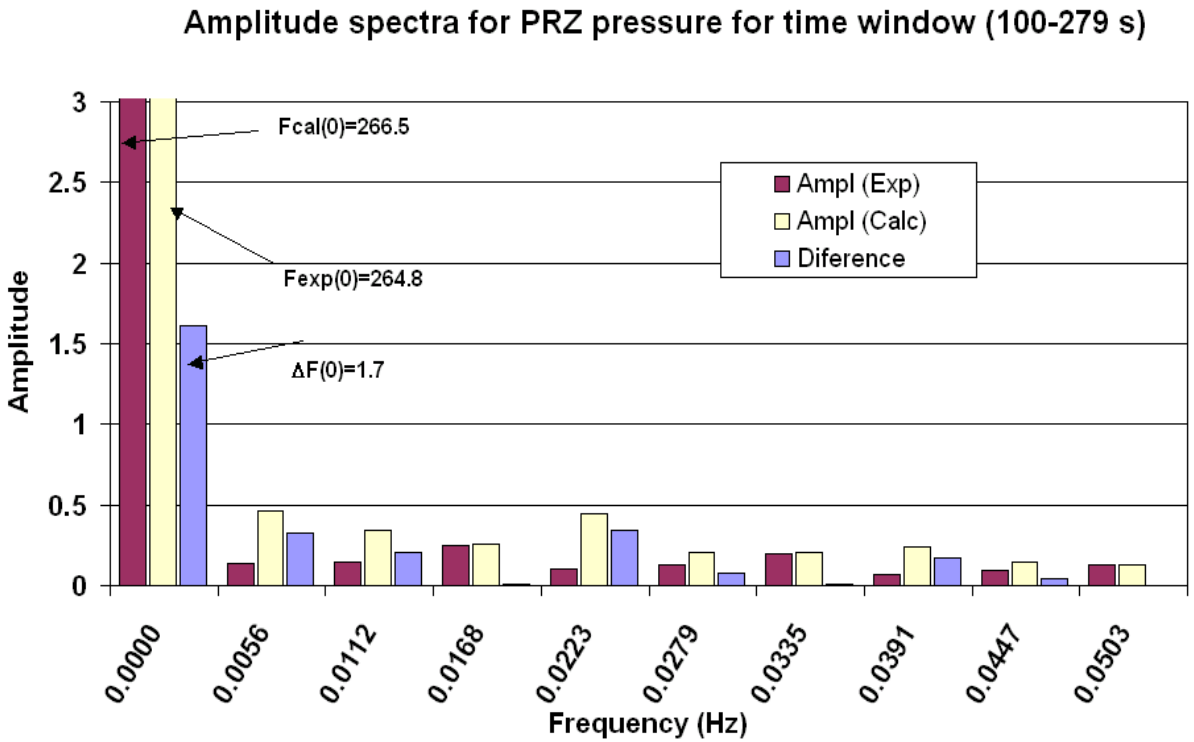

$$x(t) = \sum_{n=0}^{\infty} A_n \cos(2\pi f_0 nt + \phi_n)$$

A_n- amplitude

f – frequency

ϕ - phase

Tools and methods to qualify existing nodalization (codes)

Fast Fourier Transformation Based Method (FFTBM)

2. On-transient qualification (quantitative evaluation)

$$\Delta F(t) = F_{calc}(t) - F_{\exp}(t)$$

$$AA = \frac{\sum_{n=0}^{2^m} \left| \widetilde{\Delta F}(f_n) \right|}{\sum_{n=0}^{2^m} \left| \widetilde{F}_{\exp}(f_n) \right|}$$

$$WF = \frac{\sum_{n=0}^{2^m} \left| \widetilde{\Delta F}(f_n) \right| f_n}{\sum_{n=0}^{2^m} \left| \widetilde{\Delta F}(f_n) \right|}$$

Basic idea of the FFTBM is to quantify the discrepancy with single values.

The most significant information is given by Average Accuracy (AA), relative magnitude of the discrepancy between the calculation and the experimental variable time history.

The Weighted Frequency (WF) characterizes the kind of an error. Generally in TH transients, better accuracy is represented by low AA values at high WF values.

Fast Fourier Transformation Based Method (FFTBM)

2. On-transient qualification (quantitative evaluation)

The overall picture of the accuracy is obtained by defining average performance indexes total weighted average amplitude AA_{tot} and total weighted frequency WF_{tot}

	w_{exp}	w_{saf}	w_{norm}
Pressure drops	0.7	0.7	0.5
Mass inventories	0.8	0.9	0.9
Flowrates	0.5	0.8	0.5
Primary pressure	1.0	1.0	1.0
Secondary pressure	1.0	0.6	1.1
Fluid temperatures	0.8	0.8	2.4
Clad temperatures	0.9	1.0	1.2
Collapsed levels	0.8	0.9	0.6
Core power	0.8	0.8	0.5

w_{exp} - *contribution related to experimental accuracy*

w_{saf} - *contribution expressing the safety relevance of the addressed parameter*

w_{norm} – *normalization with respect to the AA value calculated for the primary pressure*

$$\mathrm{WF}_{\mathrm{tot}} = \sum_{i=1}^{N_{\mathrm{var}}} (\mathrm{WF})_{\mathrm{i}} \cdot (w_{\mathrm{f}})_{\mathrm{i}} \qquad \mathrm{AA}_{\mathrm{tot}} = \sum_{i=1}^{N_{\mathrm{var}}} (\mathrm{AA})_{\mathrm{i}} \cdot (w_{\mathrm{f}})_{\mathrm{i}}$$

$$\cdot (w_{\mathrm{f}})_{\mathrm{i}} = \frac{(w_{\exp})_i \cdot (w_{saf})_i \cdot (w_{norm})_i}{\sum_{i=1}^{N\,\mathrm{var}} (w_{\exp})_i \cdot (w_{saf})_i \cdot (w_{norm})_i}$$

Tools and methods to qualify existing nodalization (codes)

SafeG

Fast Fourier Transformation Based Method (FFTBM)

2. On-transient qualification (quantitative evaluation)

Variables	Time interval 60–100 s			Time interval 60–279 s			Time interval 60–391 s			Time interval 60–599 s		
	AA	WF	VA	AA	WF	VA	AA	WF	VA	AA	WF	VA
1. PRZ pressure	0.02	0.94	0.03	0.02	0.14	0.03	0.02	0.12	0.03	0.04	0.12	0.07
2. Pressure variation on MCP1	0.14	0.49	0.05	0.16	0.17	0.06	0.17	0.14	0.07	0.17	0.16	0.07
3. Pressure variation on MCP2	0.10	0.69	0.04	0.10	0.20	0.04	0.10	0.15	0.04	0.11	0.18	0.04
4. Reactor power	0.05	0.09	0.03	0.06	0.09	0.03	0.07	0.08	0.03	0.07	0.09	0.03
5. Power of TG1	0.63	0.86	0.32	0.43	0.12	0.22	0.44	0.10	0.22	0.46	0.11	0.23
6. Power of TG2	0.09	0.68	0.04	0.19	0.15	0.10	0.21	0.12	0.10	0.26	0.13	0.13
7. Total PRZ water level	0.04	0.73	0.03	0.08	0.19	0.05	0.07	0.10	0.05	0.06	0.08	0.04
8. Pressure in SG1	0.03	0.51	0.03	0.04	0.13	0.04	0.04	0.11	0.04	0.04	0.10	0.04
9. Pressure in SG2	0.05	0.50	0.05	0.05	0.09	0.06	0.05	0.07	0.06	0.06	0.08	0.06
10. Steam flow from SG1	0.16	0.40	0.05	0.27	0.14	0.08	0.29	0.11	0.09	0.30	0.12	0.09
11. Steam flow from SG2	0.13	0.75	0.04	0.42	0.14	0.13	0.43	0.12	0.14	0.45	0.12	0.14
12. Feedwater flow of SG1	0.44	0.57	0.14	0.27	0.09	0.08	0.27	0.07	0.09	0.28	0.07	0.09
13. Feedwater flow of SG2	0.56	0.88	0.18	0.37	0.11	0.12	0.38	0.08	0.12	0.41	0.09	0.13
14. Cold leg temperature no. 1	0.01	0.66	0.04	0.02	0.06	0.06	0.02	0.04	0.06	0.02	0.05	0.06
15. Cold leg temperature no. 2	0.01	0.23	0.03	0.01	0.04	0.03	0.01	0.04	0.03	0.01	0.04	0.04
16. Hot leg temperature no. 1	0.01	0.33	0.02	0.06	0.10	0.14	0.06	0.08	0.14	0.06	0.09	0.14
17. Hot leg temperature no. 2	0.02	0.41	0.04	0.03	0.09	0.07	0.03	0.07	0.07	0.03	0.07	0.07
18. Total water level of SG1	0.34	0.94	0.23	0.24	0.11	0.16	0.23	0.07	0.16	0.28	0.11	0.19
19. Total water level of SG2	0.04	0.86	0.02	0.08	0.09	0.05	0.08	0.08	0.05	0.08	0.08	0.05
Total	0.07	0.54	N.A.	0.08	0.10	N.A.	0.08	0.08	N.A.	0.09	0.08	N.A.

Fast Fourier Transformation Based Method (FFTBM)

2. On-transient qualification (quantitative evaluation)

The most suitable factor for the definition of an acceptability criterion is the total average amplitude AA_{tot}

$$AA_{tot} < K$$

K is acceptability factor valid for the whole transient. The Lower the AA_{tot} is achieved the more accurate is the calculation.

$AA_{tot} \leq 0.3$	*very good code predictions,*
$0.3 < AA_{tot} \leq 0.5$	*good code predictions,*
$0.5 < AA_{tot} \leq 0.7$	*poor code predictions,*
$AA_{tot} > 0.7$	*very poor code predictions.*

Acceptability limit for primary pressure

$AA \leq 0.1$

Andrej Prošek, Boris Kvizda: Quantitative assessment of MCP trip transient in a VVER, Nuclear Engineering and Design 227 (2004) 85-96.

Tools and methods to qualify existing nodalization (codes)

Kv-scaled calculation

We have experiment data of the scaled down facility S-ALLEGRO (or e.g. PMK-2) and calculation data of the full size facility ALLEGRO (or e.g. VVER 440 NPP)

What is needed ?

Nodalization to be qualified NPP
Experimental data from ITF
TH code simulation data NPP

Comprehensive ITF, NPP database
Comprehensive engineering hand book of NPP nodalization

Tools and methods to qualify existing nodalization (codes)

Kv-scaled evaluation

- *Demonstration of the capability of the NPP nodalization to reproduce the relevant thermal hydraulic phenomena expected in TH calculation.*
- *Addressing the 'scaling' issue in the overall application*
- *To prove there are no new phenomena with respect to relevant experiment performed on relevant ITF*

Steps

1. Steady state qualification level

- *Transfer IBC from experiment to NPP calculation, scaling factor considered, for IBC and imposed sequence of main events.*
- *Identification of scaling distortions to explain differences in between NPP model prediction and ITF measured transient*

2. On-transient qualification level (NPP calculation vs. Experiment)

- *Comparison of resulting sequence of main events*
- *Qualitative evaluation of accuracy based on visual observation*
- *Identification and comparison of Relevant Thermal-hydraulic Aspects (RTA)*

Tools and methods to qualify existing nodalization (codes)

Kv-scaled evaluation (PRISE, rupture of 10 SG tubes)

NPP nodalization to be qualified : Mochovce NPP unit 3 (Slovakia), RELAP5 mod 3.2.2 beta

Experiment: PHV-12, PMK-2 test facility (Hungary)

Steady state qualification level

IBC adjusted and compared considering scaling factor(s)

No.	Parameter	Meas. point	PMK (PHV-12) Test	Direct scaling	Kv-scaled MO34 calc.	Note
1.	Primary pressure UPL	PR21	12.81 MPa	12.81 Mpa	12.81 Mpa	1)
2.	SG pressure	PR81	4.4 Mpa	4.4 Mpa	4.4 Mpa	1) 2)
3.	Core exit flow	FL-52	4.3 kg/s	8895.9 kg/s	8761.1 kg/s	3)
4.	Core power	PW01	664.2 kW	1374.9 MW	1374.9 MW	4)
5.	Core inlet temperature	TE63	540.5 K	540.5 K	536.7 K	5)
6.	Core outlet temperature	TE22	567.3 K	567.3 K	567.3 K	5)
7.	PRZR level	LE71	8.78 m (0.98 m)	3.71 m	3.73 m	6)
8.	PRZR level (volume equivalent)	-	1.79123×10^{-3} m^3	15.80 m^3	15.94 m^3	6)
9.	PRZR spray flow	-	0,0024 kg/s	4,97 kg/s	4.97 kg/s	7)
10.	PRZR spray temperature	-	293 K (19.85 °C)	293 K (19.85 °C)	293 K (19.85 °C)	
11.	SG level	LE81	8.82 m (2.49 m)	2.49 m	2.105 m	8)
12.	Total FW flow	FL81	0.36 kg/s	745.2 kg/s (124.2 kg/s per SG)	750.7 kg/s (125.1 kg/s per SG)	9)
13.	FW inlet temperature	TE81	485.0 K	485.0 K	494.4 K	10)

Notes

1) PMK-2 is full pressure facility

2) SG pressure in MO34 model in the table is the average value from all 6 SGs.

3) Initial reactor flow rate was scaled according to ratio 1:2070

4) Core power was scaled according to ratio 1:2070

5) Inlet and outlet core initial temperature is affected by the different core dP and difference in nominal primary system flow rate

6) PRZR height in PMK-2 is not scaled and due to this the initial PRZR water volume was kept by ratio 1:2070

7) PRZR spray flow rate was kept according to ratio 1:2070. The spray valve orifice was also kept. Differences in depressurization are expected due to lack of data with respect to spray system effectiveness

8) Nominal collapsed level in all 6 SG in MO34 model was assumed. SG water volume in PMK-2 is not scaled. The scaled liquid volume in PMK-2 SG secondary side is about 3 times larger than in MO34 NPP. Differences due to greater fluid inertia are expected.

9) Nominal FW flow rate to each SG 125 kg/s in MO34 model was kept.

10) SG FW temperature in MO34 is greater due to distortions in secondary system model. The fluid has more energy accumulated in MO34 model

Tools and methods to qualify existing nodalization (codes)

Kv-scaled evaluation (PRISE, rupture of 10 SG tubes)

Steady state qualification level

Imposed sequence of main events

¤	Parameter/Event¤	PMK·(PHV-12)·Test¤	MO34¤	Note¤	¤
1.→	Break·starts·to·open¤	0.0·s¤	0.0·s¤	¤	¤
2.	Break·opened¤	0.2·s¤	0.2·s¤	¤	¤
3.	HA·isolated¤	900.0·s¤	900.0·s¤	¤	¤
4.	FW·isolation¤	0.0·s¤	0.0·s¤	¤	¤
5.	Steam·line·isolation¤	0.0·s¤	0.0·s¤	¤	¤
6.	MCP(s)·trip¤	0.0·s¤	0.0·s¤	Real· RCP· NPP· coast· down¤	¤
7.	Scram¤	0.0·s¤	0.0·s¤	¤	¤
8.	Turbine·trip¤	0.0·s¤	0.0·s¤	¤	¤
9.	·PRZ·heaters·tripped¤	0.0·s¤	0.0·s¤	¤	¤
10.	HPIS·initial·pressure¤	<·9.3·MPa¤	<·9.3·MPa¤	¤	¤
11.	HPIS·actuation·delay¤	17.0·s¤	17.0·s¤	¤	¤
12.	HPIS·stopped¤	-¤	-¤	¤	¤
13.	HPIS·restart¤	-¤	-¤	¤	¤
14.	PRZR·spray·initiation¤	1000.0·s¤	1000.0·s¤	¤	¤
15.	Secondary·bleed··SDV-A¤	2196.0·s¤	2200.0·s¤	¤	¤
16.	End·of·transient¤	7000.0·s¤	7000.0·s¤	¤	¤

Tools and methods to qualify existing nodalization (codes)

Kv-scaled evaluation (PRISE, rupture of 10 SG tubes)

Steady state qualification level

Identification of scaling distortions

¤	Parameter¤	PMK-2·ITF¤	Mochovce¶ NPP¤	Note¤	¤
1.	– Number·of·SG¤	1¤	6¤	¤	¤
2.	– SG· heat· transfer· area/· nominal·core·power¤	8.179e-5·m²/W¤	1.826e-6· m²/W¤	Bigger·effect·of·SG··is·expected·in·PMK¤	¤
3.	– Number·of·fuel·rods/core· power¤	2.706e-5·W-1¤	2.859e-5·W-1¤	¤	¤
4.	– Heat·transfer·area·in·the· core·/·PS·mass¤	1.59e-2·m²/kg¤	1.69e-m²/kg¤	HTA_{PMK}=1.35795·m²¶ HTA_{NPP}=2809.7·m²¤	¤
5.	– Average·linear·power¤	14.0·kW/m¤	14.0·kW/m¤	¤	¤
6.	– Maximum·linear·power¤	14.0·kW/m¤	32.5·kW/m¤	PMK·uniform·power·distribution¤	¤
7.	– Primary/secondary· side· mass¤	0.255¤	0.854¤	SG· secondary· side· volume· in· PMK· is· not· scaled¶ Larger· fluid· inertia· in· PMK· SG· SS· is· expected.¤	¤
8.	– Scaling· factor· of· heat· transfer· area· of· passive· structures¤	1/√2070=2.20e-2¶ instead·of·¶ 1/2070=4.83e-4¤	1.0¤	The·ITF·is·volume·and·full·height·scaled.¶ The· scaling· value· reported· for· PMK· is· roughly·estimated.¤	¤

Tools and methods to qualify existing nodalization (codes)

Kv-scaled evaluation (PRISE, rupture of 10 SG tubes)

On transient qualification level
Resulting sequence of main events comparison

¤	Event¤	PMK-2(PHV-12)¤	MO34¤
1. → ¤	Opening·of·the·break¤	0.0¤	0.0¤
2. → ¤	Scram¤	0.0¤	0.0¤
3. → ¤	MCP·trip¤	0.0¤	0.0¤
4. → ¤	Isolation·of·the·secondary·side¤	0.0¤	0.0¤
5. → ¤	PRZR·empty¤	~·80.0¤	80.0¤
6. → ¤	Blowdown·in·saturated·conditions¤	82.0¤	65.0¤
7. → ¤	HPIS·start·at·9.3·MPa¤	83.01¤	65.1¤
8. → ¤	RCP·stopped¤	~·150.0¤	215.0·–·230.0¤
9. → ¤	HA·to·DC·actuated¤	135.0¤	240.0¤
10.→¤	HA·to·UP·actuated¤	175.0¤	256.0¤
11.→¤	Maximum·break·flow·rate¤	6.0¶ (scaled·328.3·kg/s)¤	1.5¶ (239.0·kg/s)¤
12.→¤	HA·to·DC·termination¤	900.0¤	900.0¤
13.→¤	HA·to·UP·termination¤	900.0¤	900.0¤

Tools and methods to qualify existing nodalization (codes)

Kv-scaled evaluation (PRISE, rupture of 10 SG tubes)

On transient qualification level
Visual observation

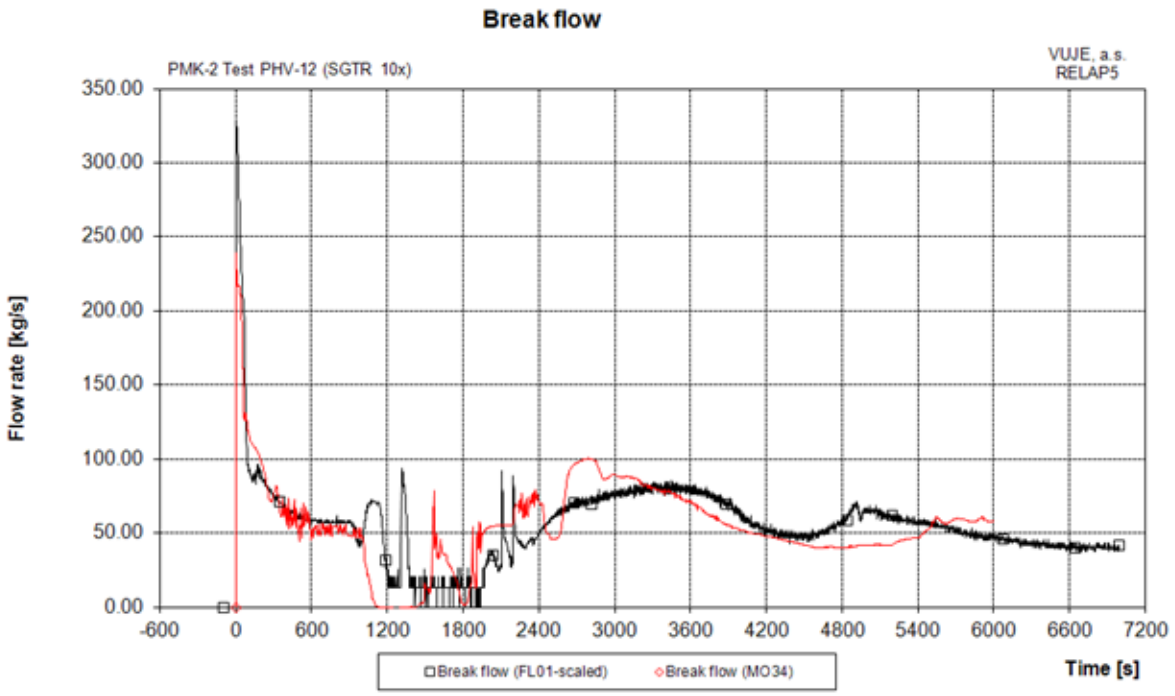

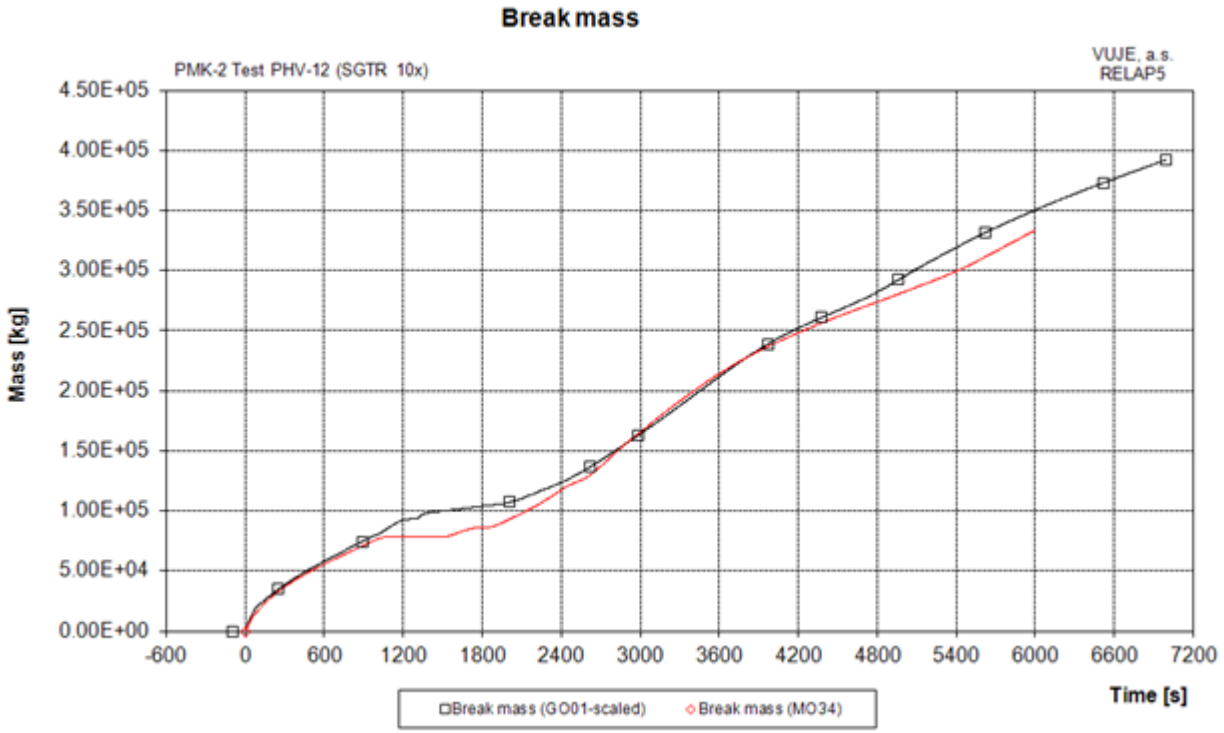

Tools and methods to qualify existing nodalization (codes)

Kv-scaled evaluation (PRISE, rupture of 10 SG tubes)

On transient qualification level
Visual observation

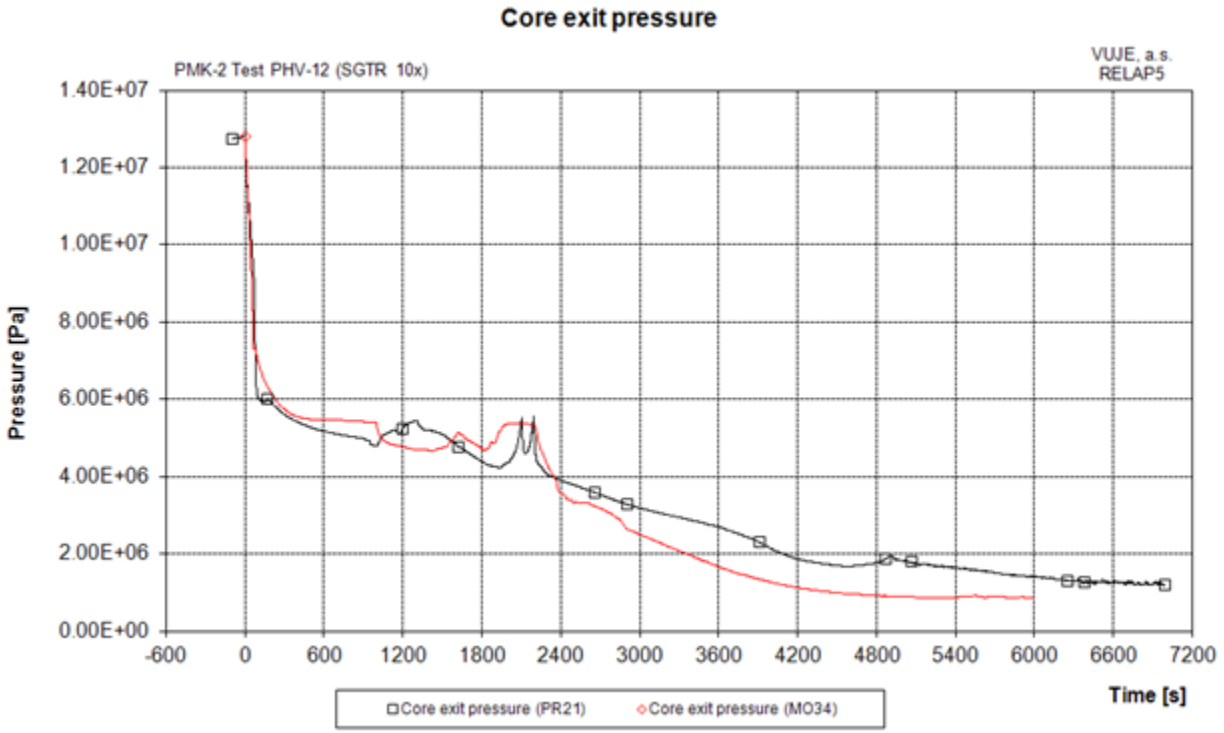

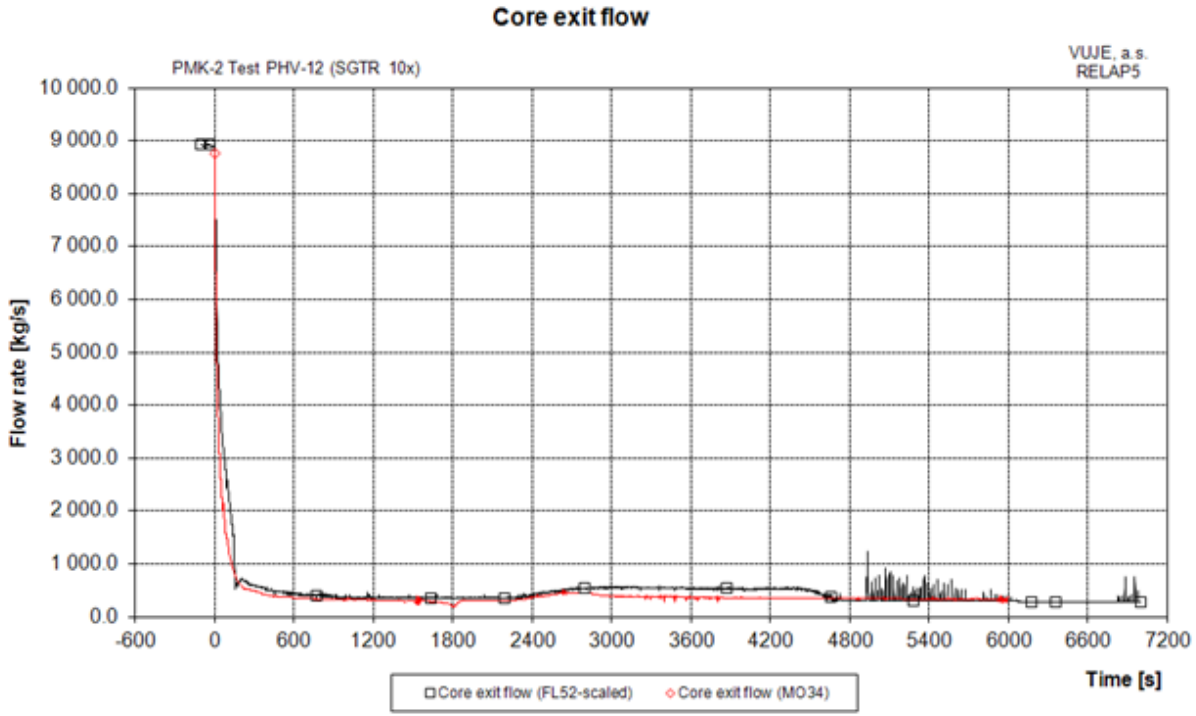

Tools and methods to qualify existing nodalization (codes)

Kv-scaled evaluation (PRISE, rupture of 10 SG tubes)

On transient qualification level
Visual observation

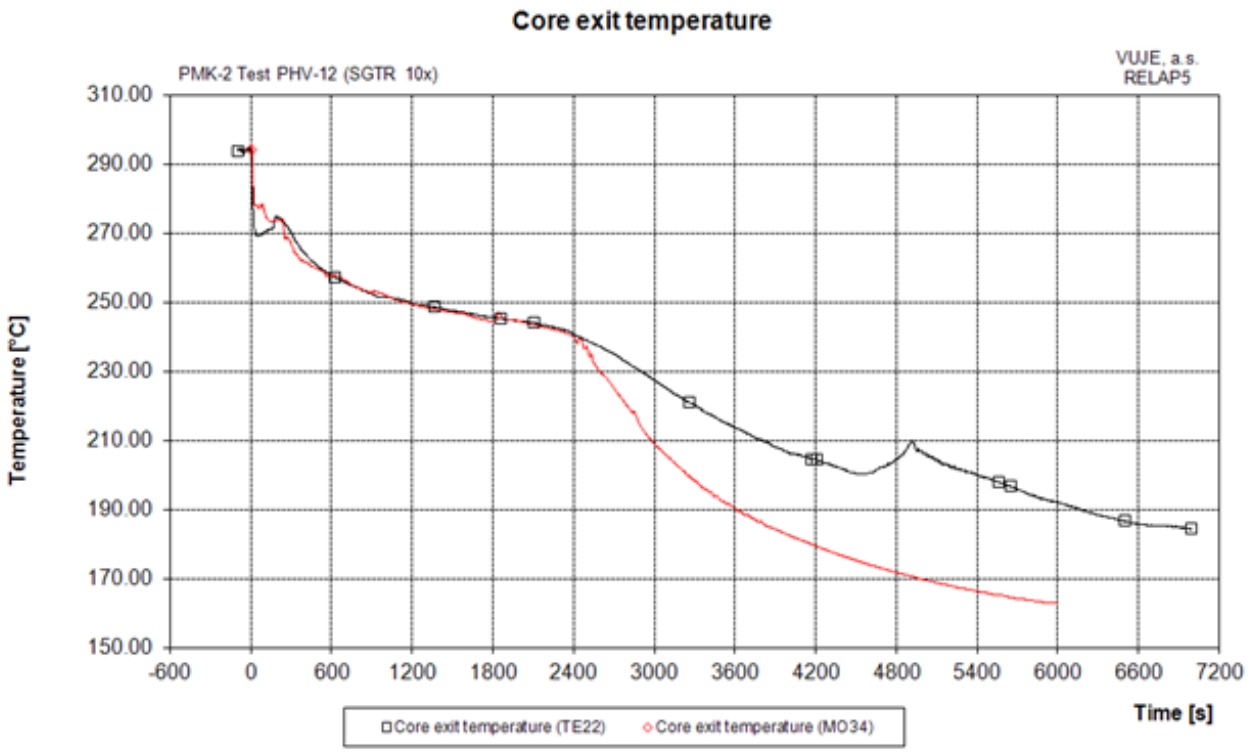

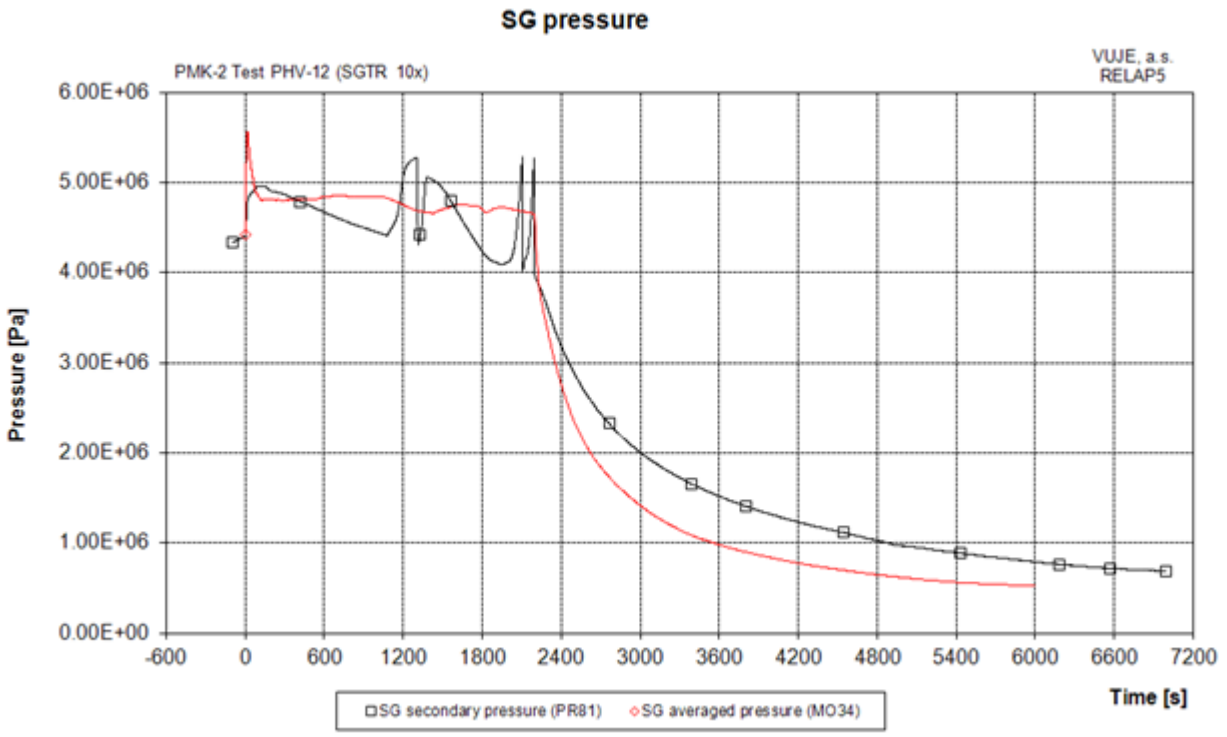

Tools and methods to qualify existing nodalization (codes)

Kv-scaled evaluation (PRISE, rupture of 10 SG tubes)

On transient qualification level
Relevant Thermal-hydraulic Aspects

1) Secondary pressure response in PMK-2 is not so quick. This is due to the fact that scaled **PMK-2 coolant volume in SG is about 3 times greater than in NPP** (scaling distortion) and greater SG initial level in PHV-13 test. Therefore more energy from leaking coolant has to be added in PMK-2 SG coolant volume to obtain comparable pressure response.

2) **PMK-2 has approximately 3 times more coolant accumulated in SG secondary side compared to NPP SGs.** This results to greater fluid inertia in PMK-2 facility. The result is that energy accumulated in the PMK 2 SG is greater which results to less secondary side pressure decrease and more coolant release to atmosphere.

		Unit	PMK-2 (PHV-12)	MO34	Judg.
RTA: Pressurizer empting					
TSE	Emptying time (PRZ_L < 0.02m)	s	~80.	80.0	E
TSE	Scram time	s	0.0	0.0	E
IPA	Integrated volumetric flow from PRZ surge line (0. s – emptying)	m^3	7.63285x10^{-3} (Scaled 15.8)	15.94	E
RTA: Pressurizer spray intervention					
TSE	Spray flow initiation time	s	1000.0	1000.0	E
IPA	Integrated volumetric flow from PC to PRZ (Since spray start to reaching maximum)	m^3	32.2	40.7	R
TSE	Time of reaching maximum PRZ volume	s	1900.0	1428.0	R
TSE	Start of PRZ level recovery	s	1270.0	920.0	R
RTA: Steam generator secondary side behavior					
TSE	SG FW isolation SL isolation SG SDV-A first opening/closure	s s s	0.0 0.0 -	0.0 0.0 11.0/944.0	E E M[1]
SVP	Core exit pressure at 23 s when all SG SDV-As are fully opened obtained in NPP Kv-scaled calculation	MPa	11.36	11.16	E
SVP	SG outlet pressure at 23 s when all SG SDV-As are fully opened obtained in NPP Kv-scaled calculation	MPa	4.81	5.5	R[1]
SVP	Difference between PS and SG SS pressure at 20 s	MPa	6.68	5.85	R
SVP	SG pressure - → peak SG pressure after SS isolation - → time of peak SG pressure - → time when PS pressure equals SS pressure - → SG pressure when first HA starts injection	 MPa s s MPa	 4.96 96.0 1210. 4.95	 5.69 21.0 1080.0 ~4.8 (SG1-6)	 R[1] M[1] R R
SVP	SG level - → at 500 s - → at the end of the process	 m m	 2.65 2.82	 1.91 (SG1) 2.11 (SG2-6) 2.26 (SG1) 2.64 (SG2-6)	 M[2] R

Conclusions

- *ALLEGRO design is still under development*
- *Necessity to qualify the TH models (both ALLEGRO and S-ALLEGRO) used in ALLEGRO design*
- *There are known and widely used methods to be in use for nodalization qualification (e.g. FFTBM or Kv-Scaling calculations)*
- *The code-to-code benchmark is useful but it has got limitations.*

Sources worth to study:

A. *Petruzzi, F. D'Auria, "Thermal-Hydraulic System Codes in Nuclear Reactor Safety and Qualifications Procedures," Science and Technology of Nuclear Installations, 2008, pp. 1-16 (2008). https://doi.org/10.1155/2008/460795*

B. *F. D'Auria, G. M. Galassi, "Scaling in nuclear reactor system thermal-hydraulics," Nuclear Engineering and Design, 240, pp. 3267-3293 (2010). https://doi.org/10.1016/j.nucengdes.2010.06.010*

C. *Andrej Prošek, Boris Kvizda "Quantitative assessment of MCP trip transient in a VVER" Nuclear Engineering and Design, 227, pp. 58-96 (2004), https://doi.org/10.1016/j.nucengdes.2003.07.005*

D. *Boris Kvizda, Alessandro Petruzzi, Qualification and Uncertainty Evaluation of a Best Estimate Loca Study of the Mochovce NPP by RELAP5/3.2-Gamma and CIAU, https://doi.org/10.1115/ICONE14-89203*

Thank you for your attention!

Turbulence in CFD

Gusztáv Mayer, Centre for Energy Research

Advanced modelling techniques workshop
3rd – 6th July 2023, Cambridge

SafeG
SAFETY OF GFR THROUGH INNOVATIVE MATERIALS, TECHNOLOGIES AND PROCESSES

This project has received funding from the Euratom H2020 programme NFRP-2019-2020-06 under grant agreement No 945041.

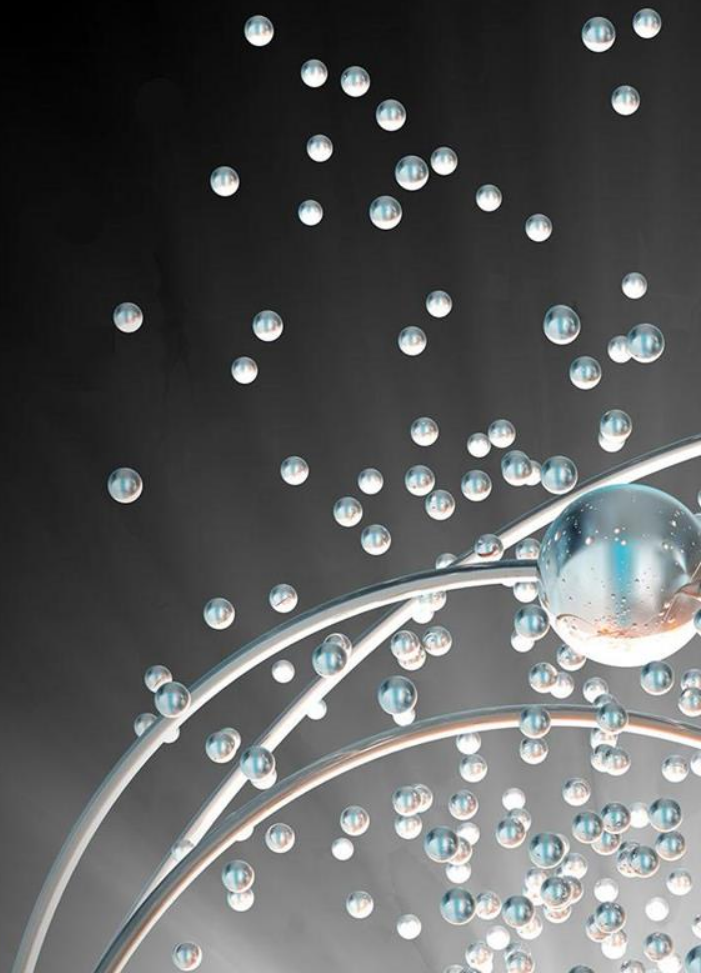

Bottom Up Approach – DNS, LES, RANS

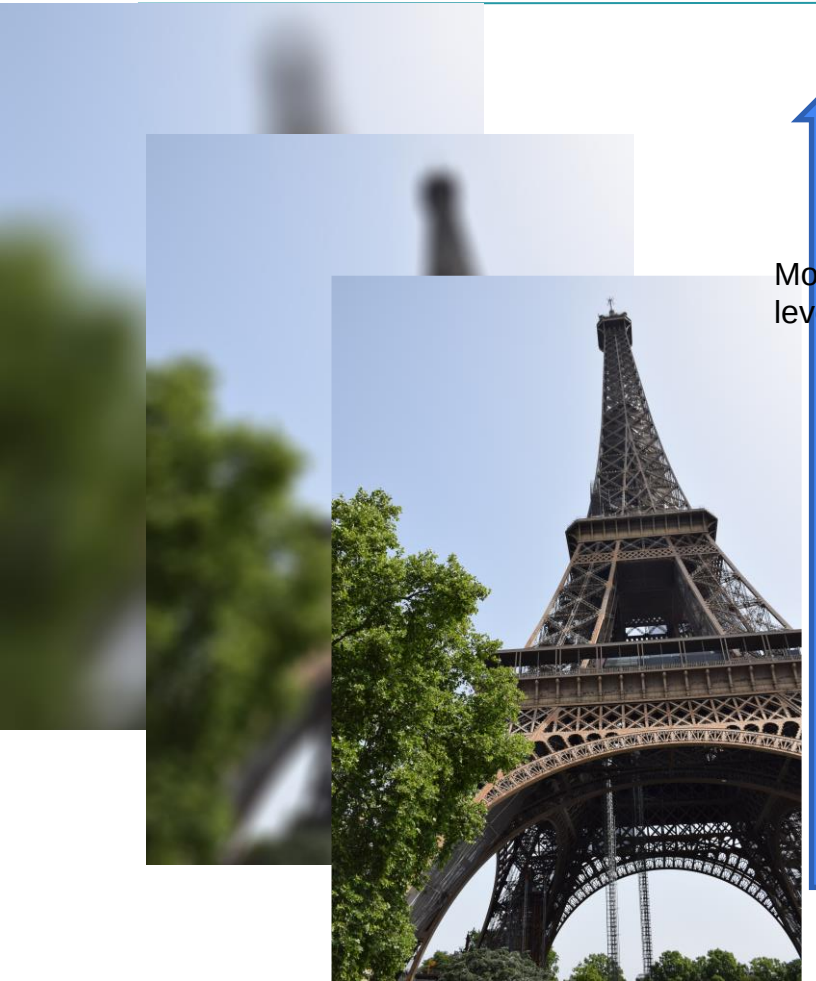

Modeling level

3. RANS

Reynolds Averaged Navier Stokes

2. LES

Large Eddy Simulation

1. DNS

Direct Numerical Simulation $Re^{9/4}$

High computational cost

1.
DNS – Direct Numerical Simulation

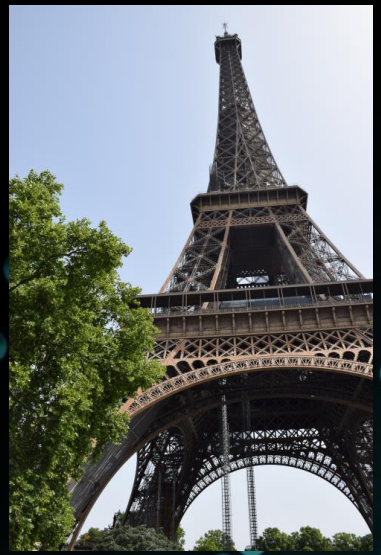

Incompressible Navier Stokes equations

SafeG

- Continuum model
- Density, viscosity constant
- Newtonian fluid, $\tau = \mu \frac{du}{dy}$, $\tau_{ij} = \mu \left(\frac{\partial u_i}{\partial y_j} + \frac{\partial u_j}{\partial y_i} \right)$, isotropic

$$\nabla \cdot \boldsymbol{u} = 0$$

Conservation of mass

$$\frac{d}{dt}(m\boldsymbol{v}) = \mathbf{F}$$

Newton's second law

$$\frac{D\boldsymbol{u}}{Dt} = \frac{\partial \boldsymbol{u}}{\partial t} + (\boldsymbol{u} \cdot \nabla)\boldsymbol{u} = -\frac{1}{\rho}\nabla p + \nu \nabla^2 \boldsymbol{u} + \boldsymbol{g}$$

Conservation of momentum

Incompressible Navier Stokes equations

SafeG

$$\frac{\partial u_x}{\partial x}+\frac{\partial u_y}{\partial y}+\frac{\partial u_z}{\partial z}=0$$

$$\frac{\partial u_x}{\partial t}+u_x\frac{\partial u_x}{\partial x}+u_y\frac{\partial u_x}{\partial y}+u_y\frac{\partial u_x}{\partial z}=-\frac{1}{\rho}\frac{\partial p}{\partial x}+\nu\left(\frac{\partial^2 u_x}{\partial x^2}+\frac{\partial^2 u_x}{\partial y^2}+\frac{\partial^2 u_x}{\partial z^2}\right)+g_x$$

$$\frac{\partial u_y}{\partial t}+u_x\frac{\partial u_y}{\partial x}+u_y\frac{\partial u_y}{\partial y}+u_z\frac{\partial u_y}{\partial z}=-\frac{1}{\rho}\frac{\partial p}{\partial y}+\nu\left(\frac{\partial^2 u_y}{\partial x^2}+\frac{\partial^2 u_y}{\partial y^2}+\frac{\partial^2 u_y}{\partial z^2}\right)+g_y$$

$$\frac{\partial u_z}{\partial t}+u_x\frac{\partial u_z}{\partial x}+u_y\frac{\partial u_z}{\partial y}+u_z\frac{\partial u_z}{\partial z}=-\frac{1}{\rho}\frac{\partial p}{\partial z}+\nu\left(\frac{\partial^2 u_z}{\partial x^2}+\frac{\partial^2 u_z}{\partial y^2}+\frac{\partial^2 u_z}{\partial z^2}\right)+g_z$$

Unknowns: u_x, u_y, u_z, p

$\rho = const, \nu = const$

Energy equation is neglected

DNS

Star Wars (George Lucas)

The Good

Obi-Wan Kenobi
(Source: Wikipedia)

Darth Vader/
Anakin Skywalker
(Source: Wikipedia)

The Bad

Sheev Palpatine
Darth Sidious / The Emperor
(Source: Wikipedia)

Incompressible Navier Stokes equations

SafeG

$$\frac{\partial \boldsymbol{u}}{\partial t} + (\boldsymbol{u} \cdot \nabla)\boldsymbol{u} = -\frac{1}{\rho}\nabla p + \nu \nabla^2 \boldsymbol{u} + \boldsymbol{g}$$

The Bad

Sheev Palpatine
Darth Sidious / The Emperor
(Source: Wikipedia)

The Good

Obi-Wan Kenobi
(Source: Wikipedia)

Dimensionless form of N-S equations

$$[St]\frac{\partial \boldsymbol{u}^\star}{\partial t^\star} + (\boldsymbol{u}^\star \cdot \nabla^\star)\boldsymbol{u}^\star = -[Eu]\nabla^\star p^\star + \left[\frac{1}{Re}\right]\nabla^{\star 2}\boldsymbol{u}^\star + \left[\frac{1}{Fr^2}\right]\boldsymbol{g}^\star$$

$St = \frac{fL}{U}$,
Strouhal number

$Eu = \frac{P - P_\infty}{P_0 - P_\infty}$,
Euler number

$Fr = \frac{U}{\sqrt{gL}}$,
Froude number

$Re = \frac{UL}{\nu} = \frac{\rho UL}{\mu}$

Darth Vader/ Anakin Skywalker (Source: Wikipedia)

Turbulent energy cascade

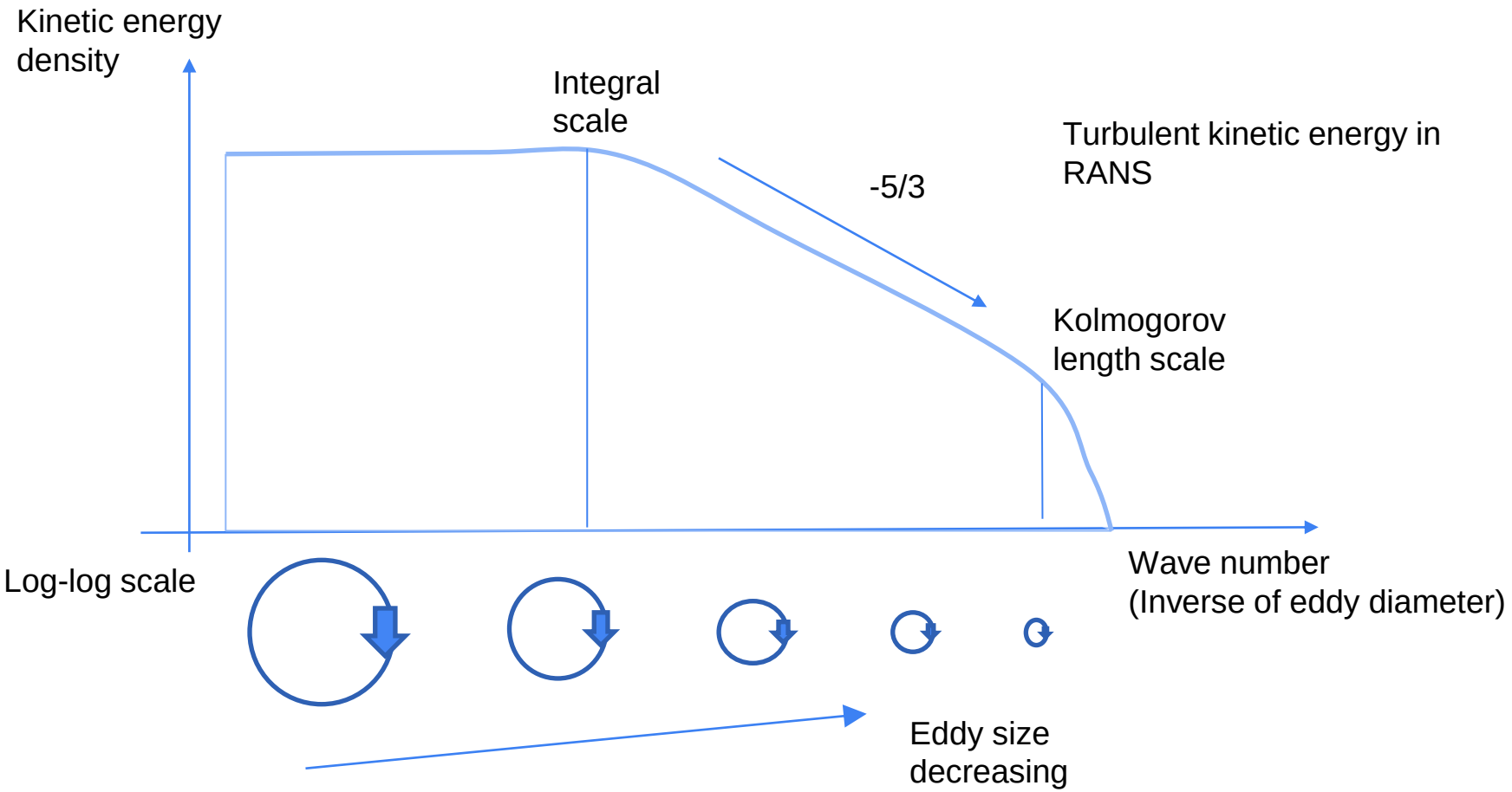

Lattice Boltzmann Method

- PhD – self-developed LBM code
- A very simple method for solving the incompressible Navier-Stokes Equations
- Fast and effective for DNS
- The following slides were created using this method

Lattice types:

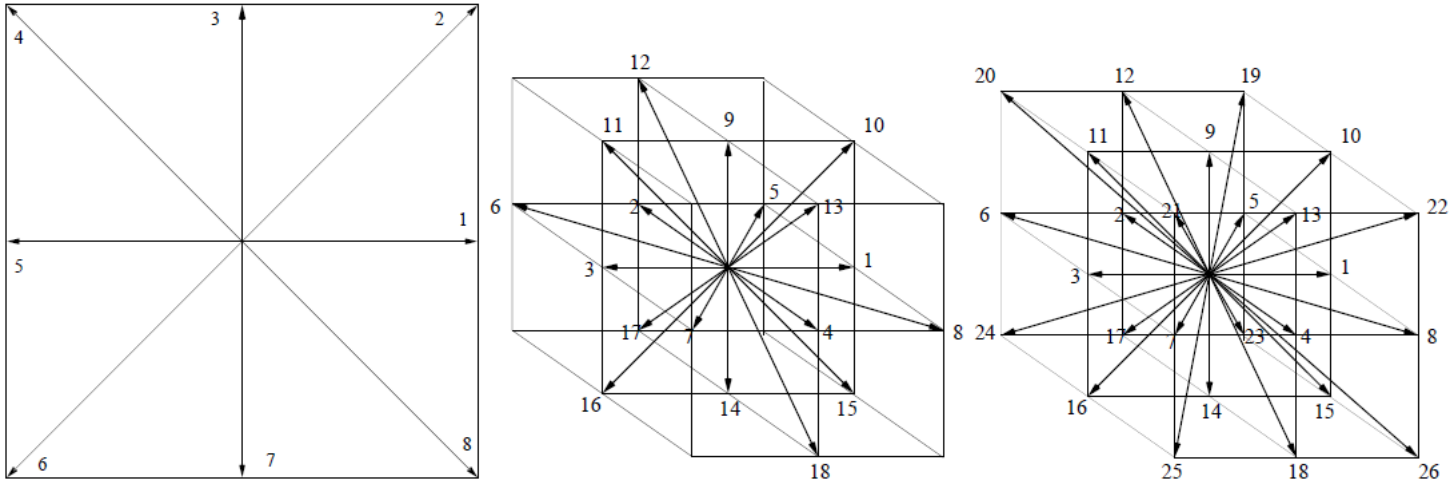

Testing of a CFD code (laminar)

Flow between parallel plates
There is analytic solution

$$u_x(y) = \frac{1}{2\nu}\frac{\Delta p}{\Delta x}\left[\left(\frac{a}{2}\right)^2 - y^2\right]$$

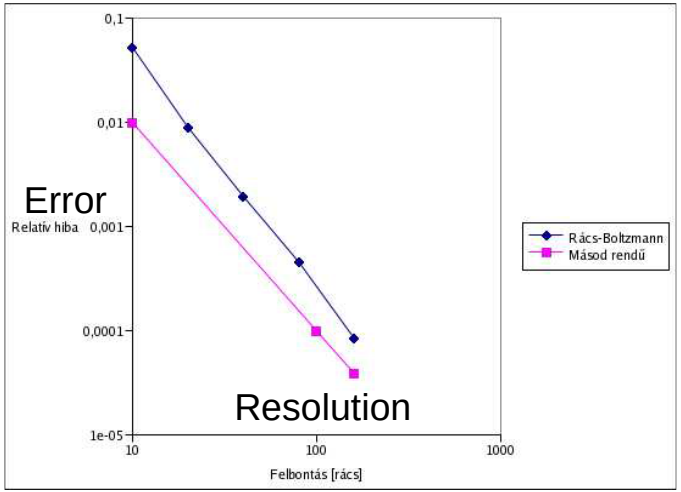

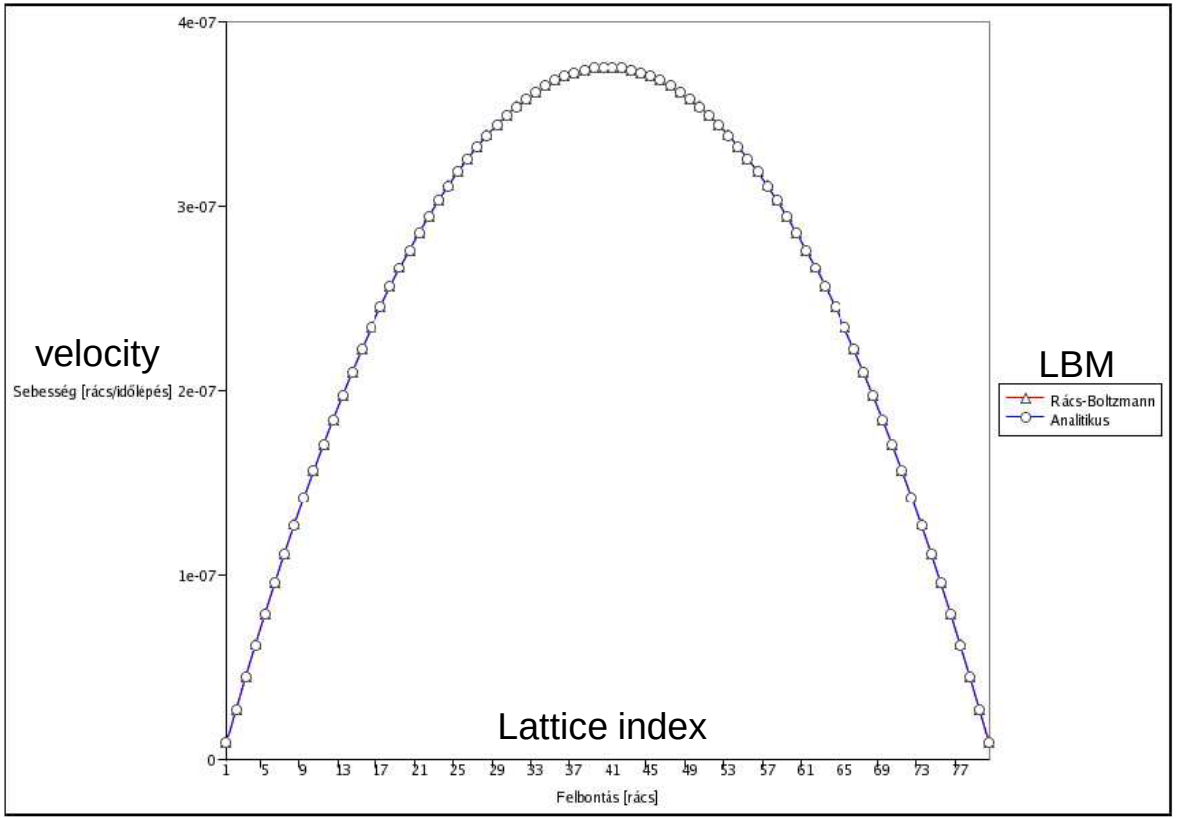

Testing of a CFD code (turbulent)

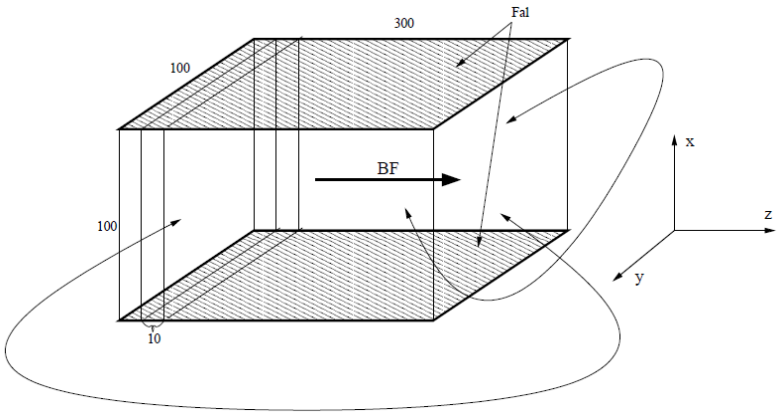

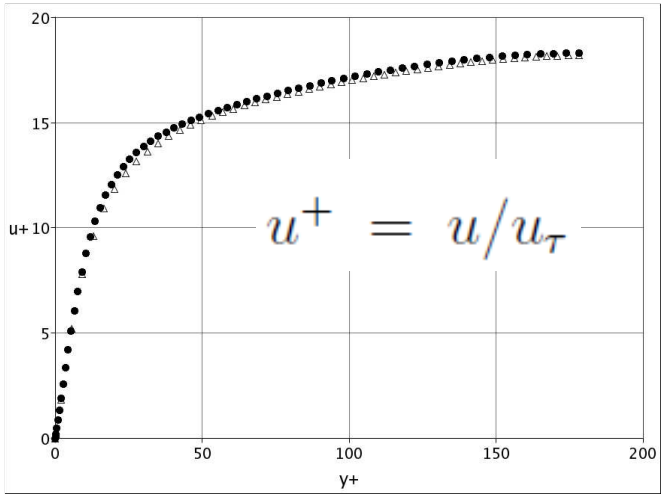

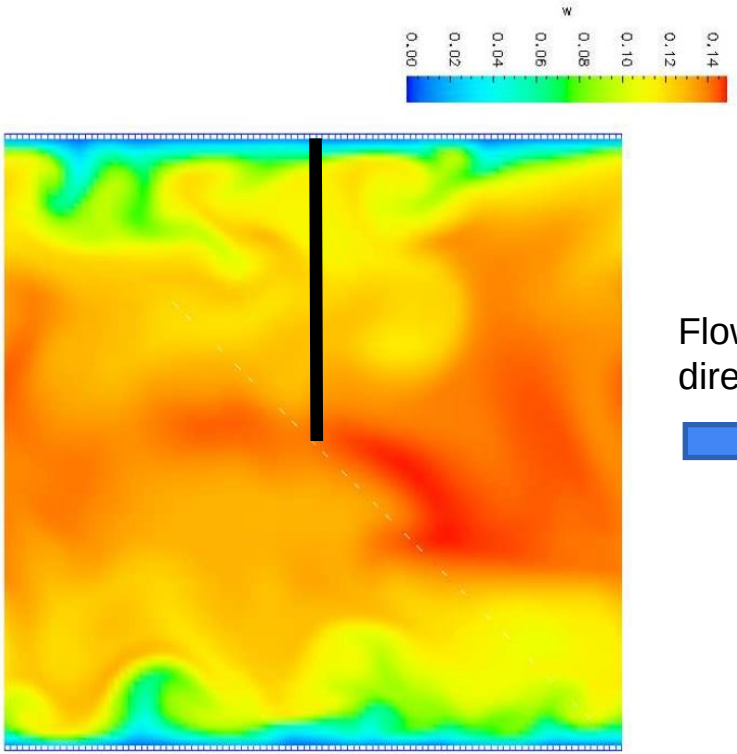

Flow direction

Δ G. Mayer, PhD dissertation, 2009

● D. Moser, J. Kim, és N. N. Mansour. Direct numerical simulation of turbulent channel flow up to Re_tau=590. *Phys. Fluids*, 11(4):943, 1999.

Testing of a CFD code (turbulent)

SafeG

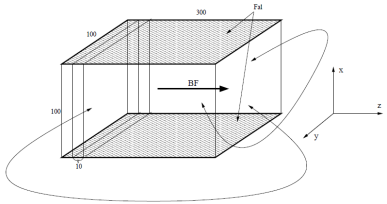

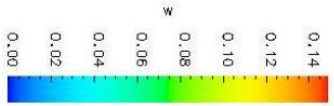

Reynolds stresses

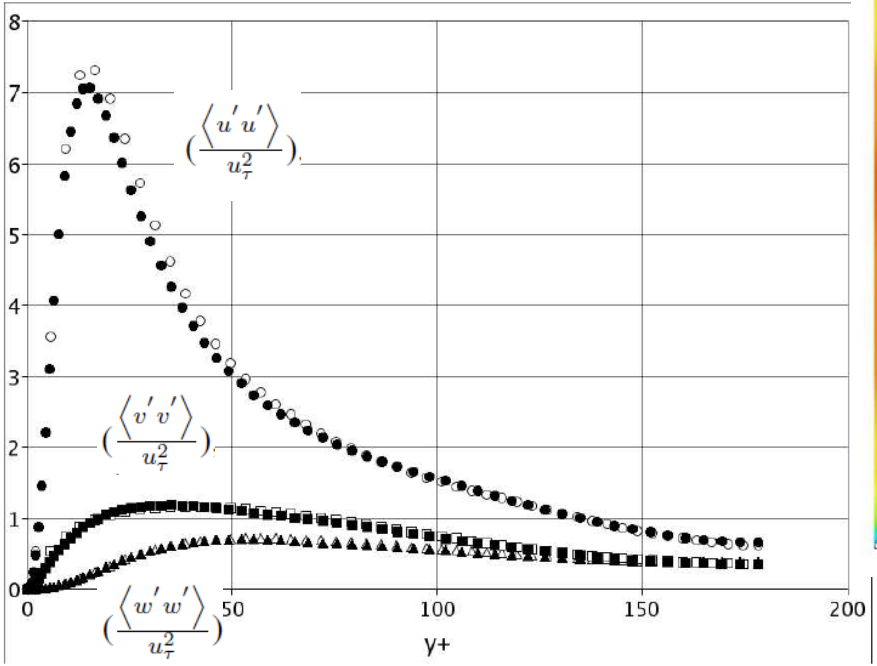

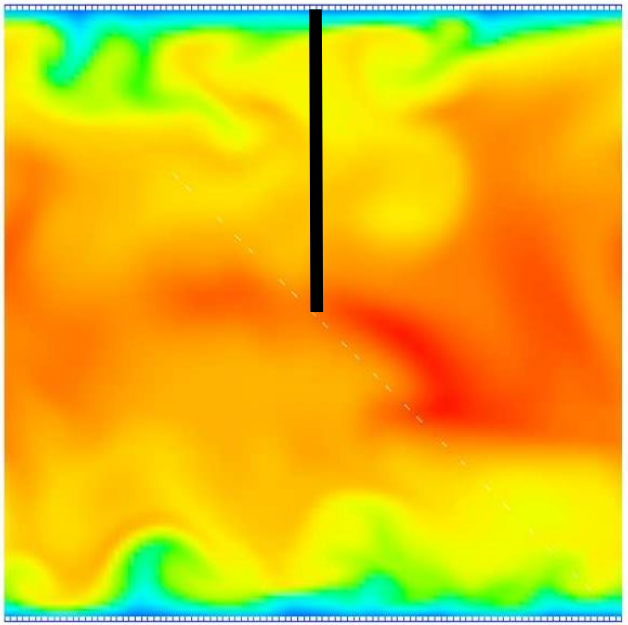

Flow direction

Testing of a CFD code (turbulent)

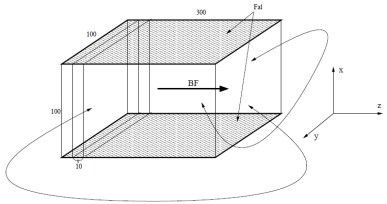

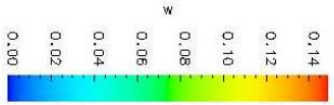

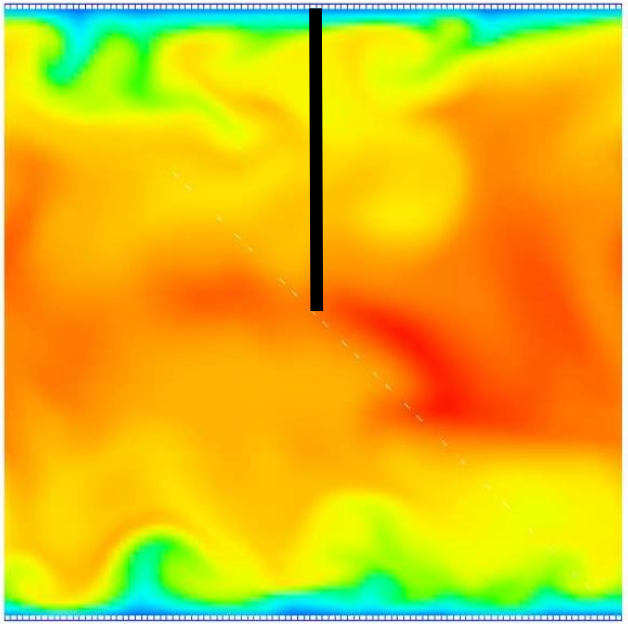

Flow direction

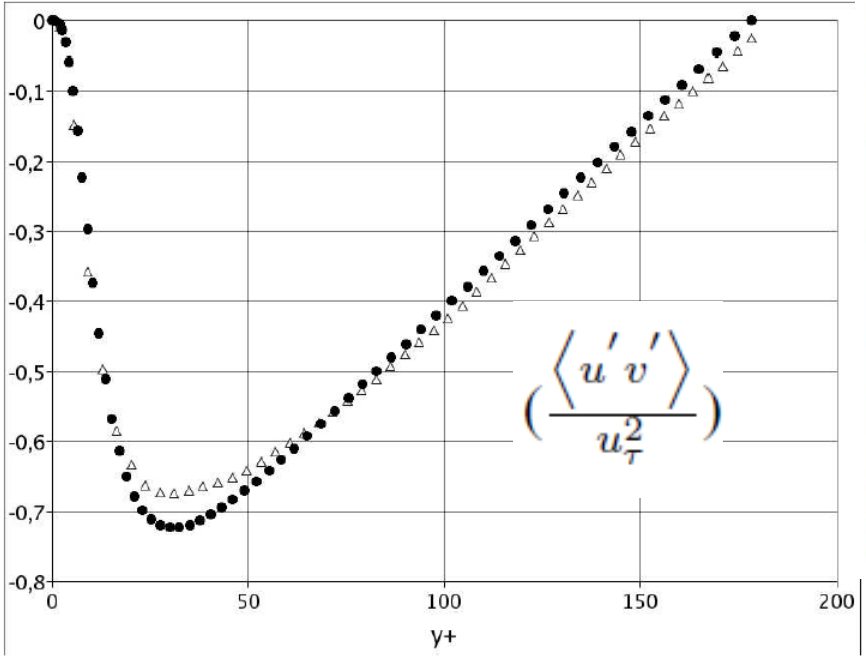

Reynolds stresses

Δ G. Mayer, PhD dissertation, 2009

● D. Moser, J. Kim, és N. N. Mansour. Direct numerical simulation of turbulent channel flow up to Re_tau=590. *Phys. Fluids*, 11(4):943, 1999.

Flow past a cylinder, Re=3.6

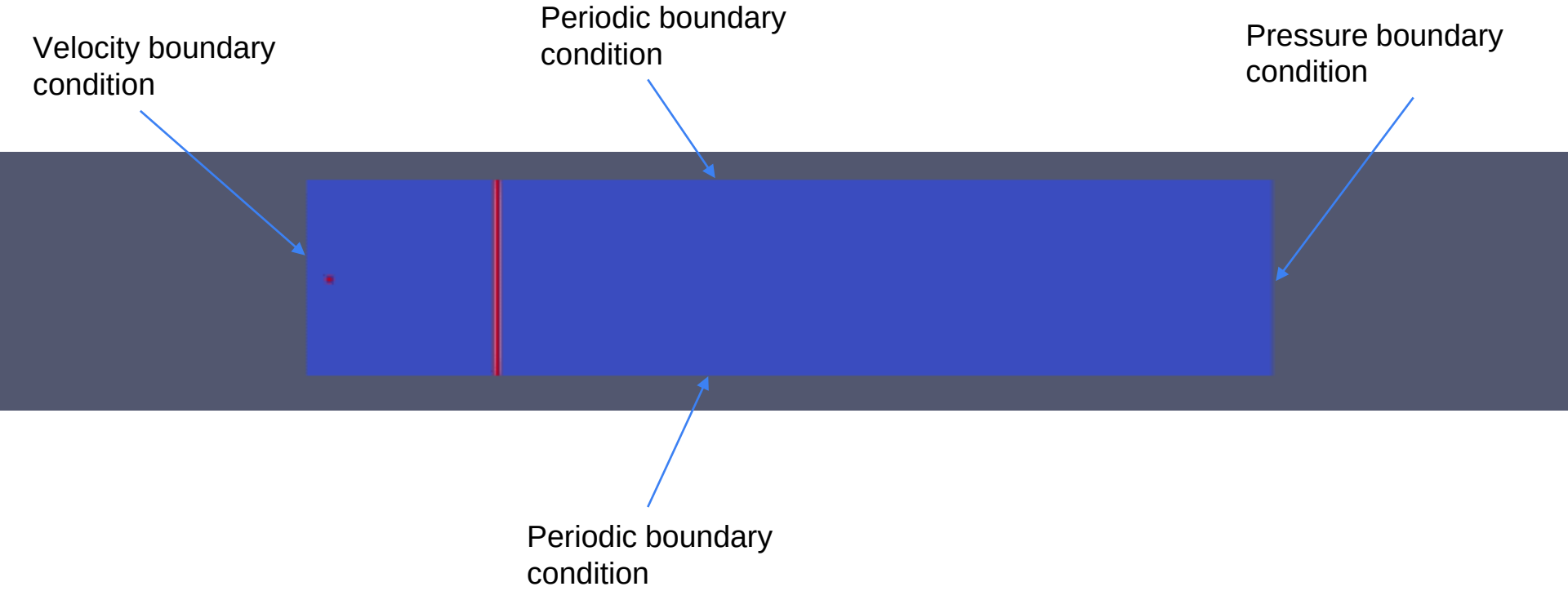

Flow past a cylinder, Re=22.5

Flow past a cylinder, Re=45

Critical Reynolds number ~ 40-75, Uriel Frisch, Turbulence The Lagacy of A. N. Kolmogorov

Flow past a cylinder, Re=600

SafeG

Karman Vortex Street ☺ ~~☺~~ ?????? ☹

Perturbation is needed!!!

Flow past a cylinder, Re=300

SafeG

Karman Vortex Street ☺

With velocity perturbation

Flow past a cylinder, Re=600

SafeG

Karman Vortex Street ☺

With velocity perturbation

2.
LES – Large Eddy Simulation

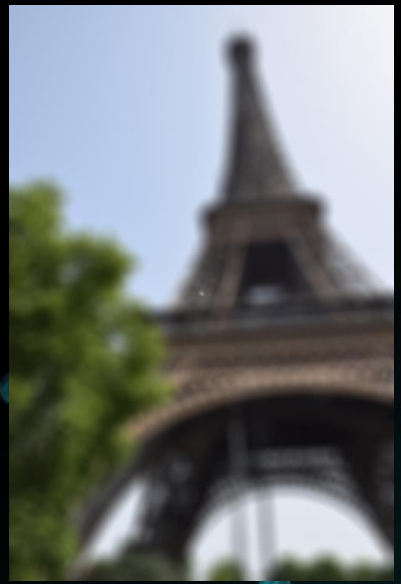

Turbulent energy cascade

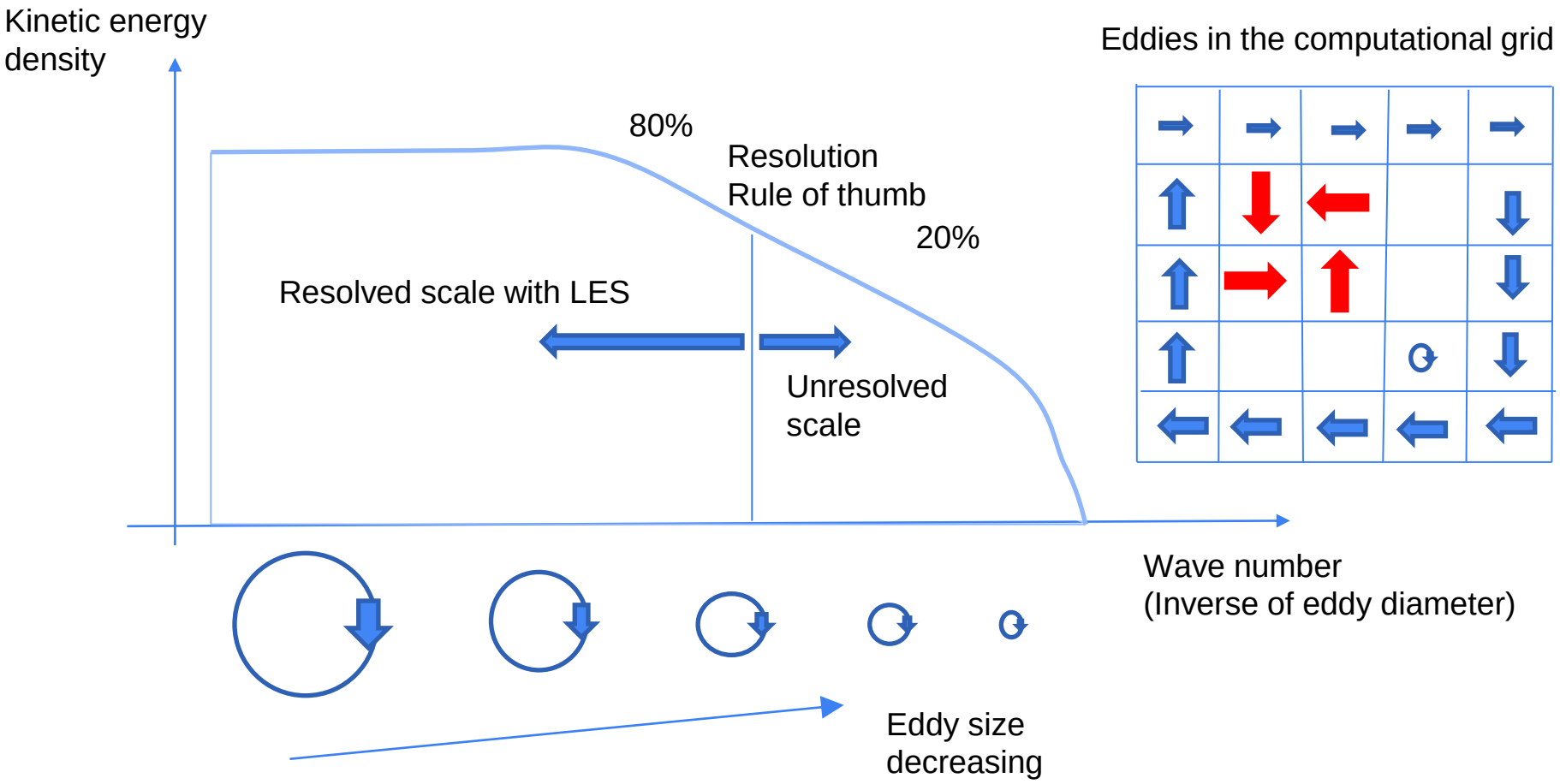

Space filtering of Navier Stokes equations

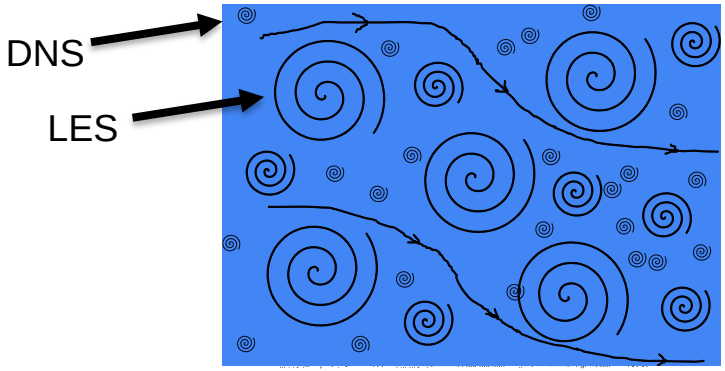

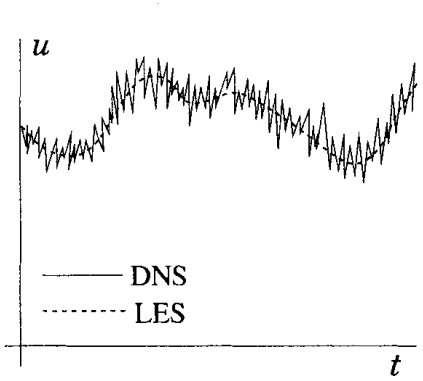

$$\nabla \cdot \boldsymbol{u} = 0$$

$$\frac{\partial \boldsymbol{u}}{\partial t} + (\boldsymbol{u} \cdot \nabla)\boldsymbol{u} = -\frac{1}{\rho}\nabla p + \nu \nabla^2 \boldsymbol{u} + \boldsymbol{g}$$

$$\overline{u}_i(x) = \int G(x, x')\, u_i(x')\, \mathrm{d}x'$$

Ferziger, Peric, Computational Methods for Fluid dynamics, 3rd edition, 2002

Space filtering of LES

DNS

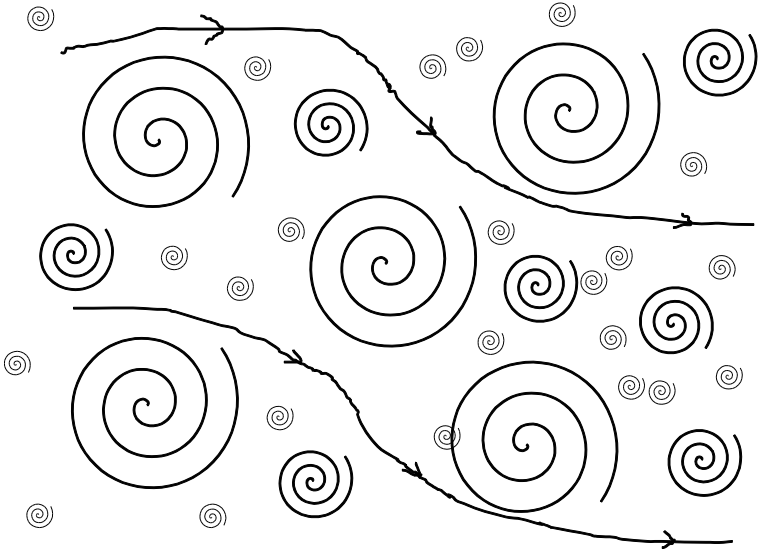

LES

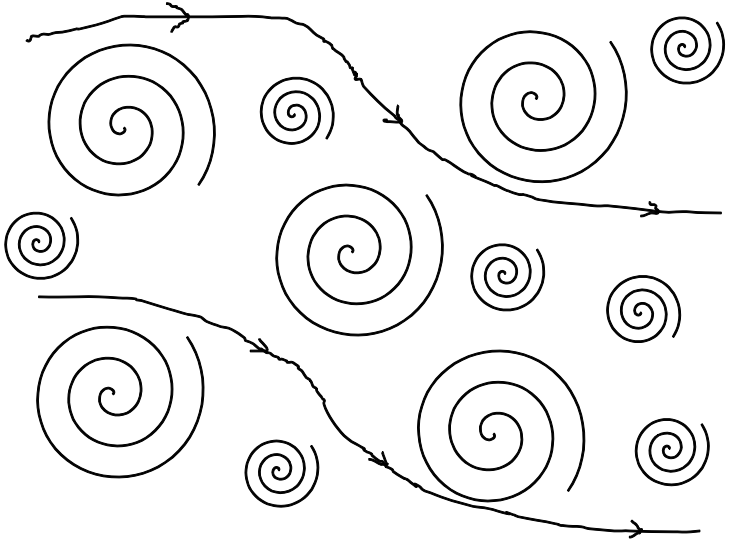

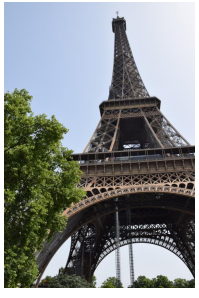

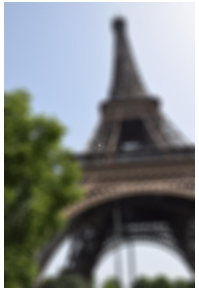

Space filtering of Navier Stokes equations

SafeG

$$\overline{u}_i(x) = \int G(x, x')\, u_i(x')\, \mathrm{d}x'$$

$$\frac{\partial(\rho\overline{u}_i)}{\partial x_i} = 0\ .$$

$$\frac{\partial(\rho\overline{u}_i)}{\partial t} + \frac{\partial(\rho\overline{u_i u_j})}{\partial x_j} = -\frac{\partial \overline{p}}{\partial x_i} + \frac{\partial}{\partial x_j}\left[\mu\left(\frac{\partial \overline{u}_i}{\partial x_j} + \frac{\partial \overline{u}_j}{\partial x_i}\right)\right]$$

$$\overline{u_i u_j} \neq \overline{u}_i \overline{u}_j$$

$$\tau_{ij}^{\mathrm{s}} = -\rho\left(\overline{u_i u_j} - \overline{u}_i \overline{u}_j\right)$$ Subgrid-scale Reynolds stress

$$\tau_{ij}^{\mathrm{s}} - \frac{1}{3}\tau_{kk}^{\mathrm{s}}\delta_{ij} = \mu_{\mathrm{t}}\left(\frac{\partial \overline{u}_i}{\partial x_j} + \frac{\partial \overline{u}_j}{\partial x_i}\right) = 2\mu_{\mathrm{t}}\overline{S}_{ij} \qquad \mu_{\mathrm{t}} = C_{\mathrm{S}}^2 \rho \Delta^2 |\overline{S}|$$

Flow in a bare rod bundle

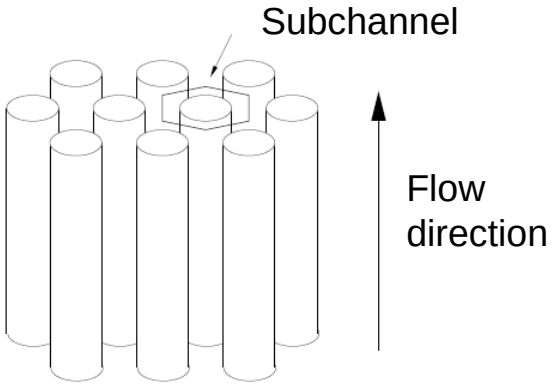

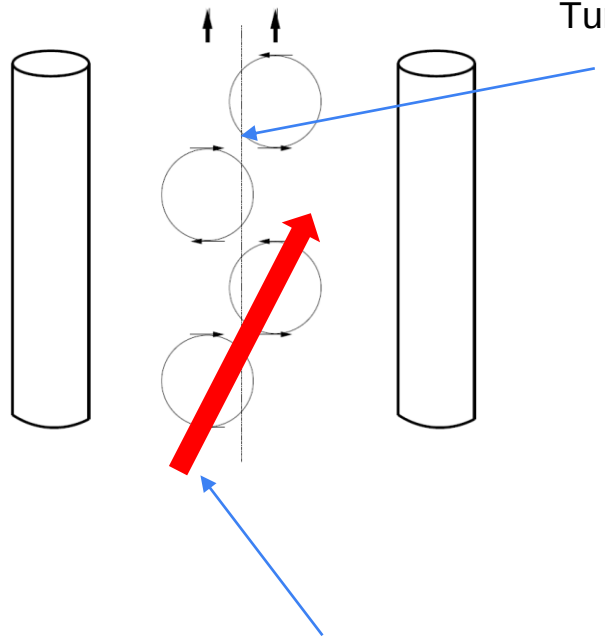

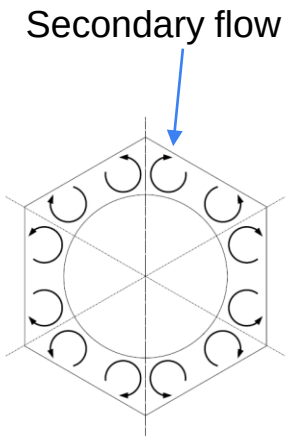

Flow in a bare rod bundle (LES)

Axial velocity component

Re=13915

Time average

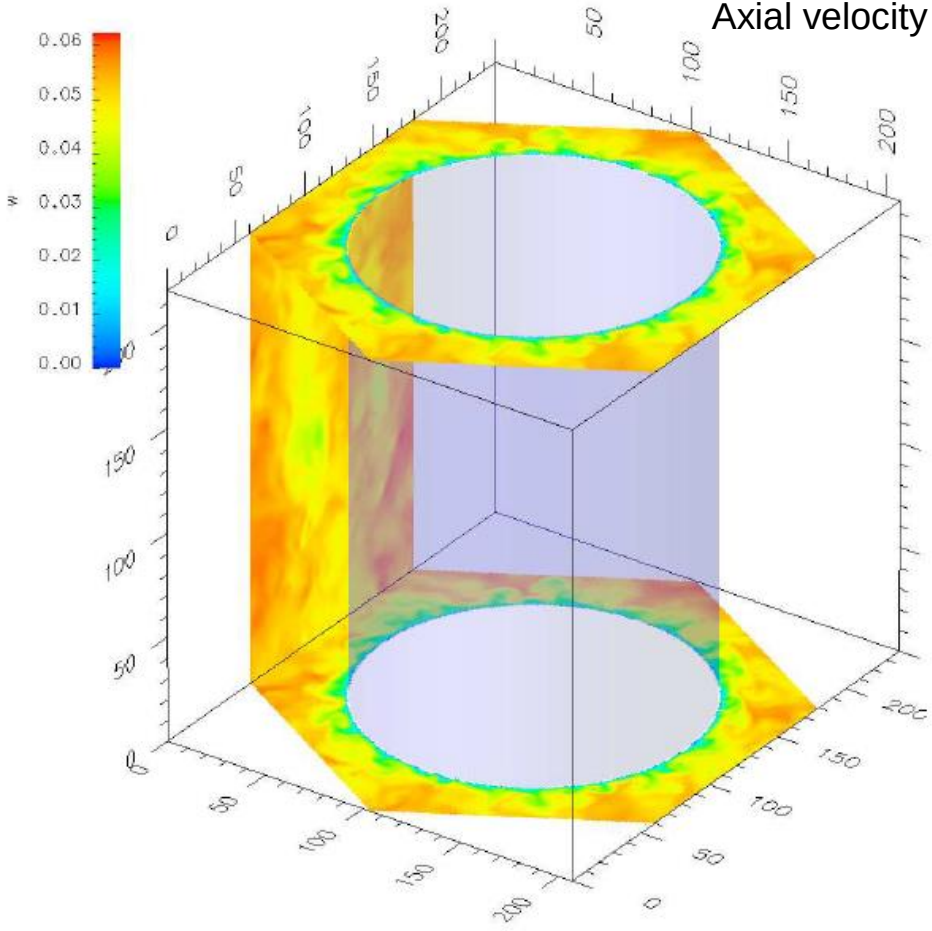

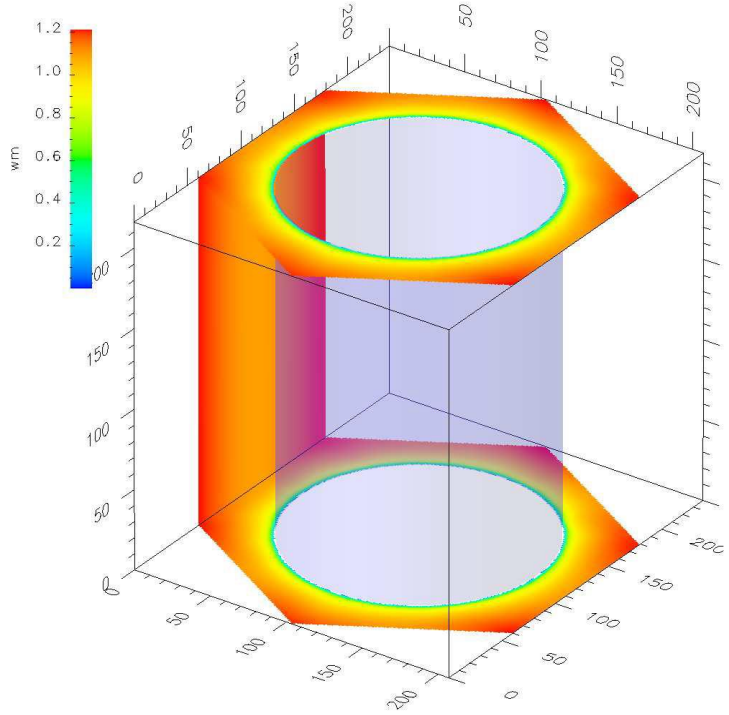

Flow in a bare rod bundle (LES)

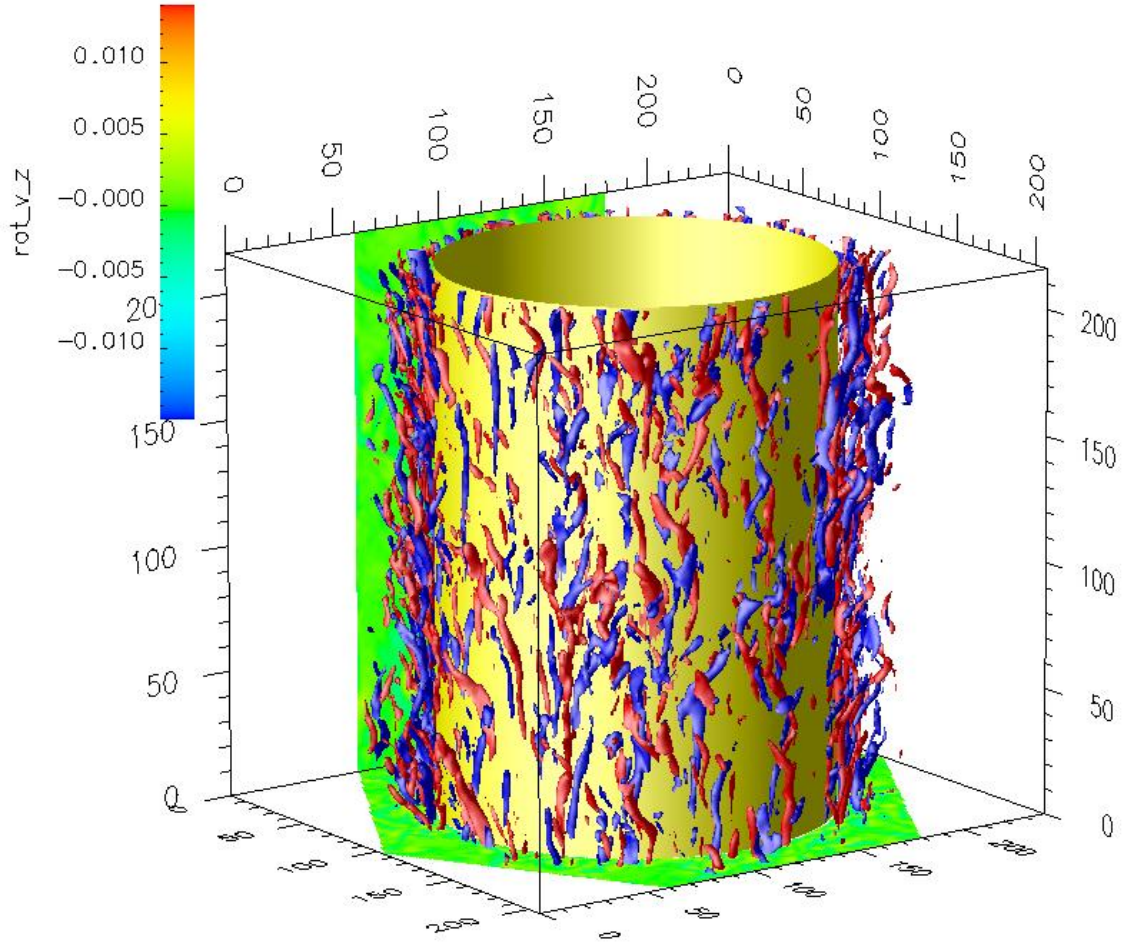

Vorticity – axial direction

Time evolution of axial velocities, DNS and LES

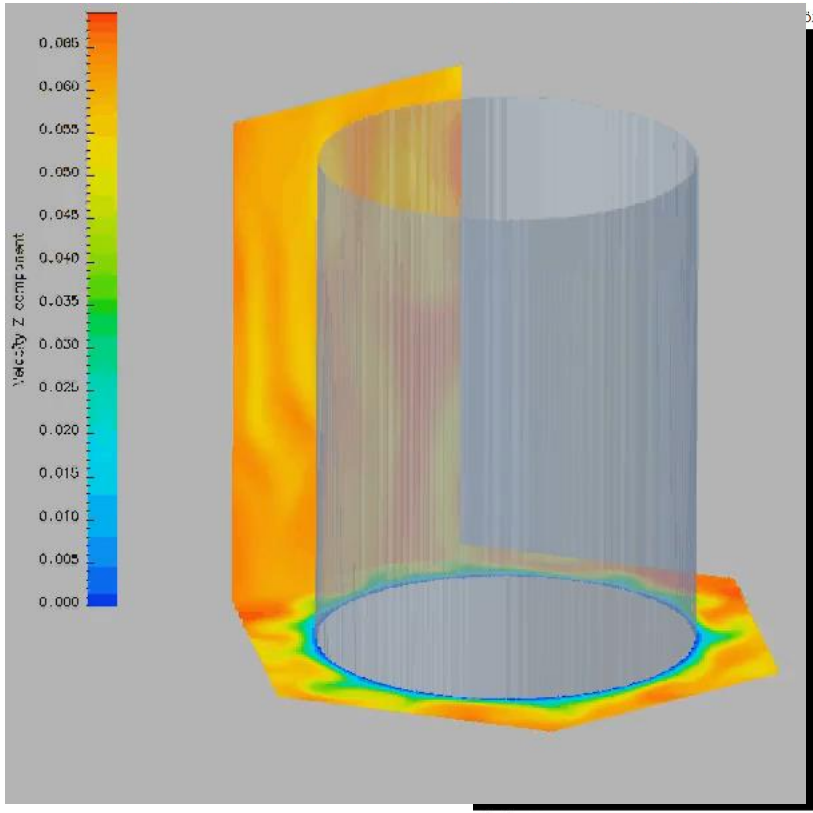

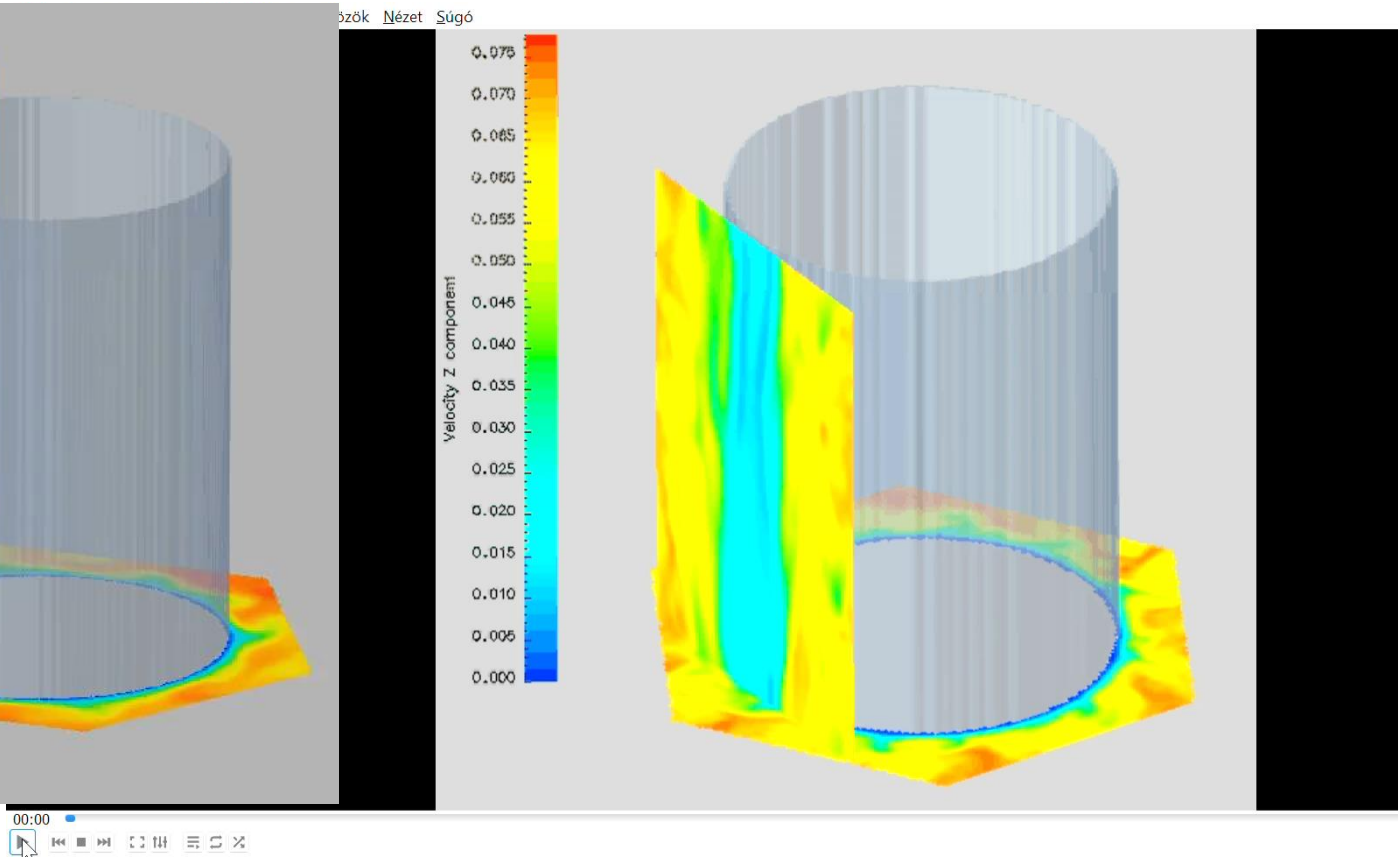

Re=3680

Re=13915

Flow in a bare rod bundle

Lateral time averaged velocity vectors

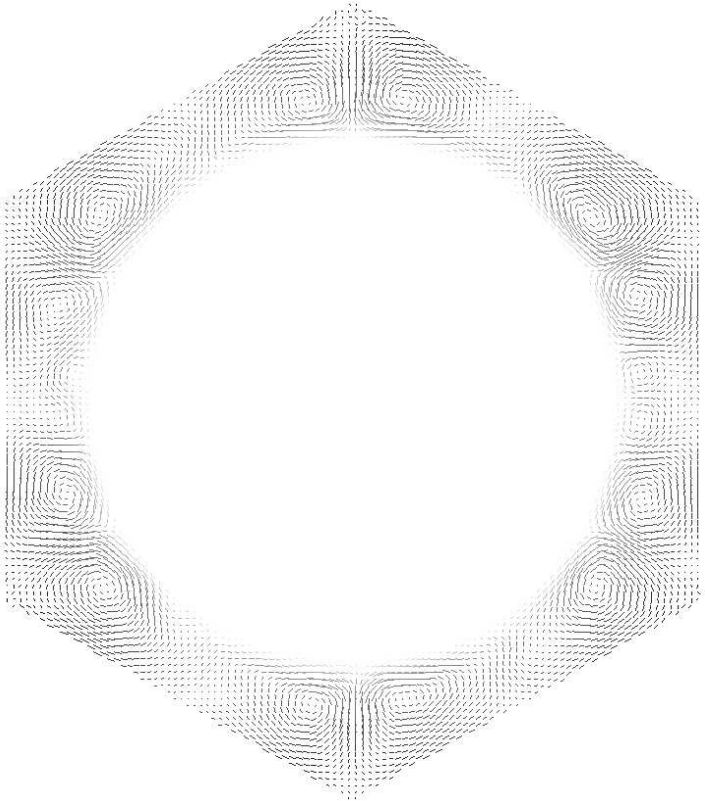

$$\overline{w'w'} \neq \overline{v'v'},$$

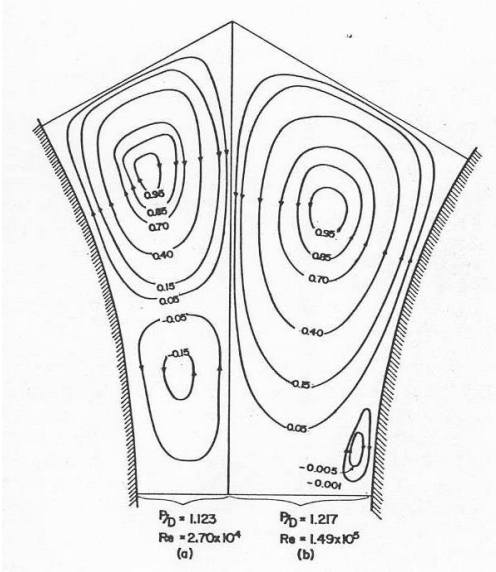

P. Carajilescov és N. E. Todreas. Experimental and analytical study of axial turbulent flows in an interior subchannel of a bare rod bundle. *Jounal of Heat Transfer*, page 262, 1976.

Flow in a bare rod bundle

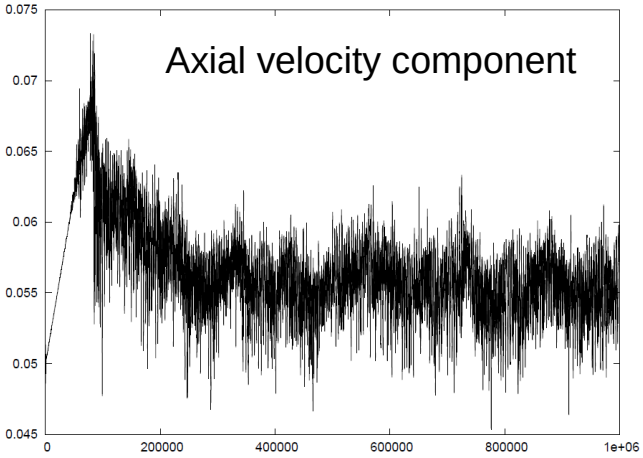

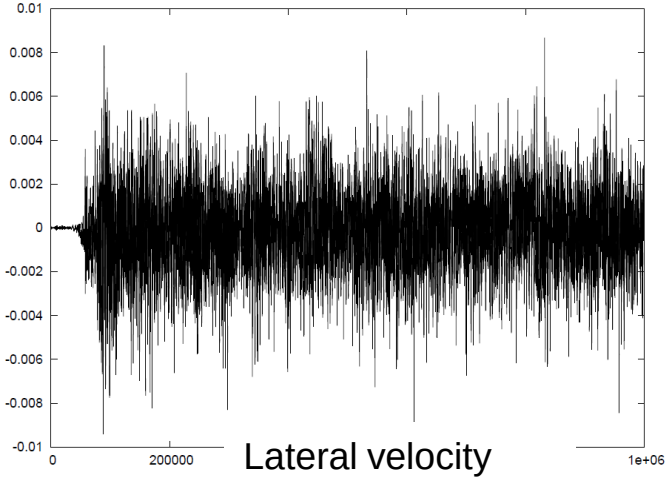

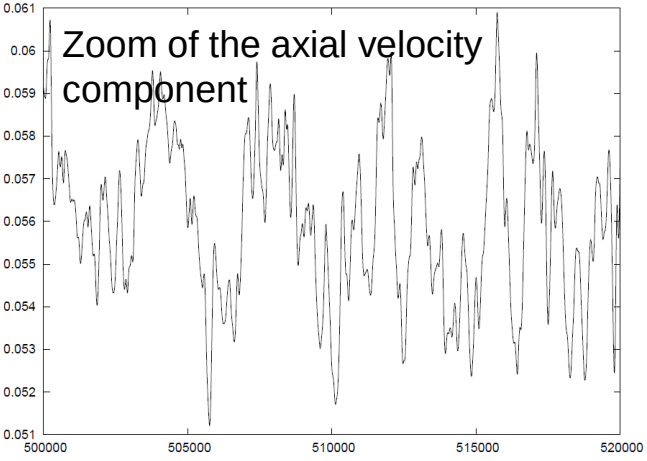

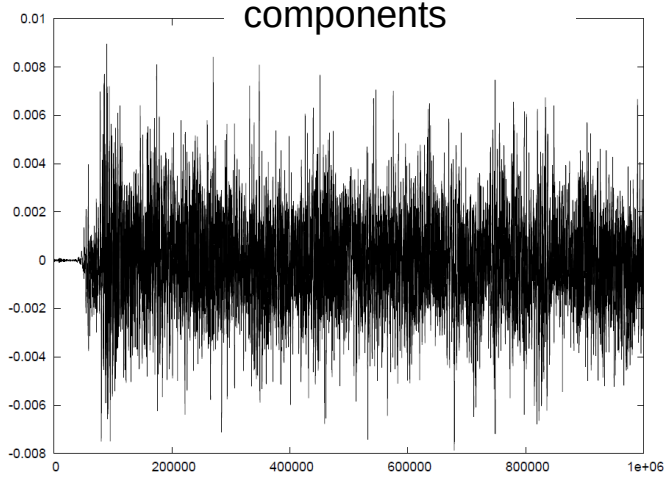

X axis: time step

3.
RANS – Reynolds Averaged Navier-Stokes Simulation

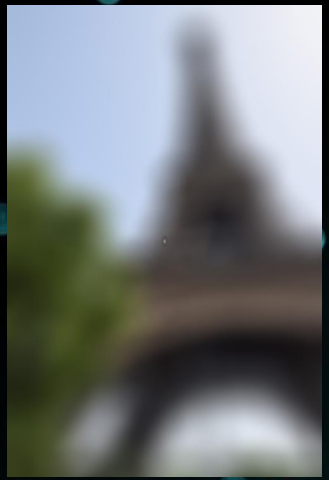

Reynolds Averaged N-S equations (RANS)

SafeG

$$\nabla \cdot \boldsymbol{u} = 0$$

$$\frac{\partial \boldsymbol{u}}{\partial t} + (\boldsymbol{u} \cdot \nabla)\boldsymbol{u} = -\frac{1}{\rho}\nabla p + \nu \nabla^2 \boldsymbol{u}$$

$$\boldsymbol{u}(\boldsymbol{x}, t) = \bar{\boldsymbol{u}}(\boldsymbol{x}) + \boldsymbol{u}'(\boldsymbol{x}, t)$$

$$p(\boldsymbol{x}, t) = \bar{p}(\boldsymbol{x}) + p'(\boldsymbol{x}, t)$$

$$\bar{\boldsymbol{u}} = \lim_{T \to \infty} \frac{1}{T} \int_0^T \boldsymbol{u}(\boldsymbol{x}, t) dt$$

$$\overline{\boldsymbol{u}'} = 0 \qquad \overline{\boldsymbol{u}'\boldsymbol{u}'} \neq 0$$

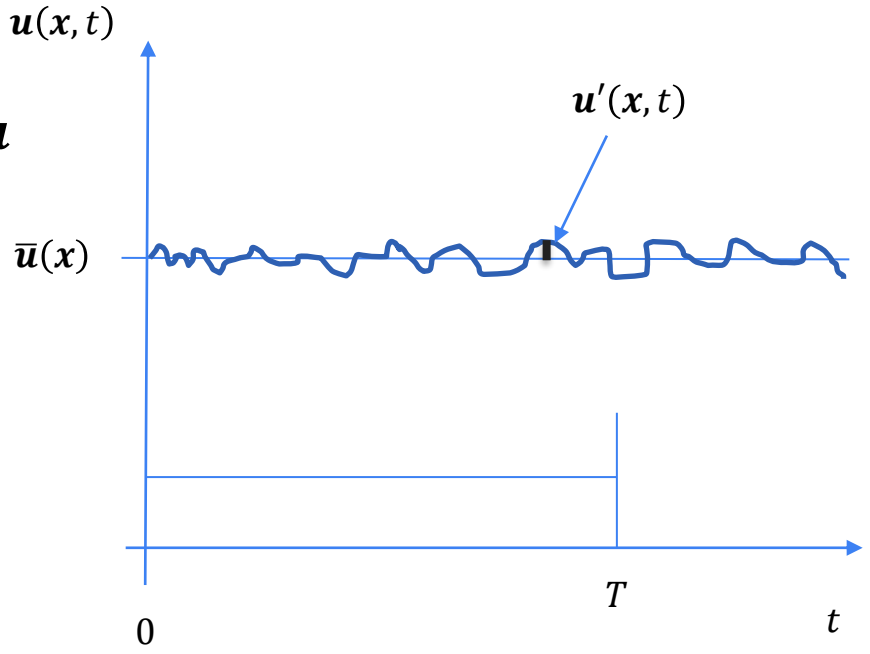

Reynolds Averaged N-S equations (RANS)

$$\frac{\partial \bar{v}_i}{\partial x_i} = 0$$

$$\rho \frac{\partial \bar{v}_i \bar{v}_j}{\partial x_j} = -\frac{\partial \bar{p}}{\partial x_i} + \frac{\partial}{\partial x_j}\left(\mu \frac{\partial \bar{v}_i}{\partial x_j} - \rho \overline{v_i' v_j'}\right)$$

$$\overline{v_1' v_2'} = \overline{v_2' v_1'}$$

The Reynods stress tensor is symmetric

Closure problem. Unknowns: p, v_x, v_y, v_z, + 6 Reynolds stresses

Lars Davidson, Fluid mechanics, turbulent flow and turbulence modeling, 2023

Time filtering of RANS

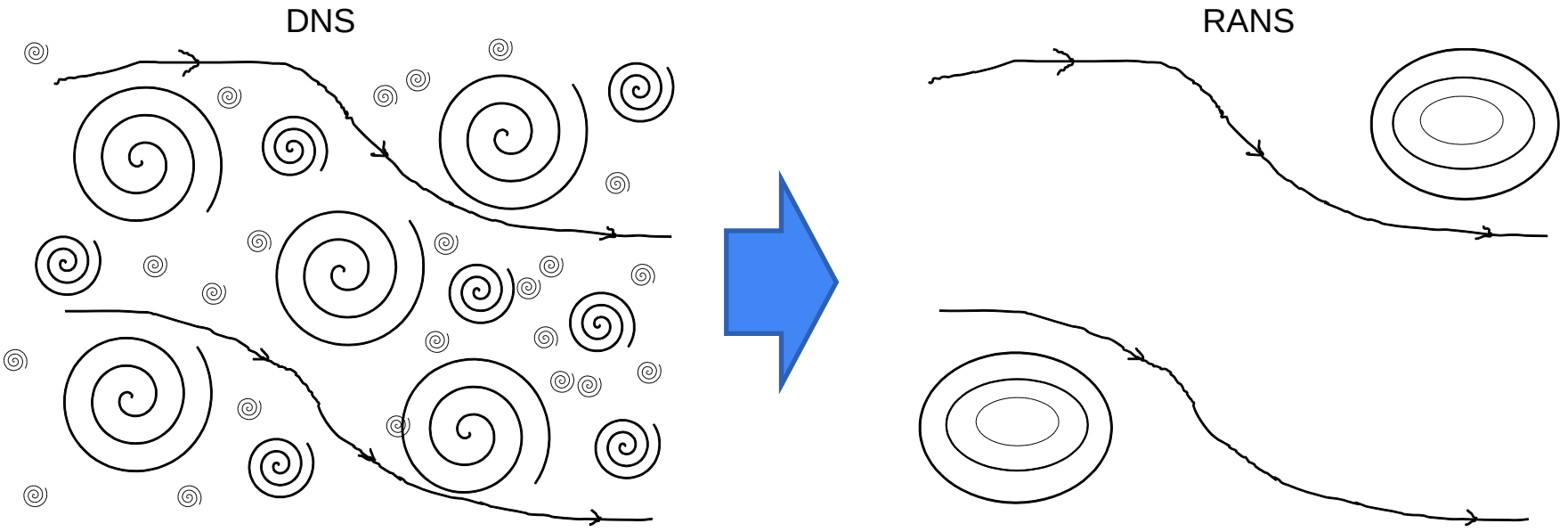

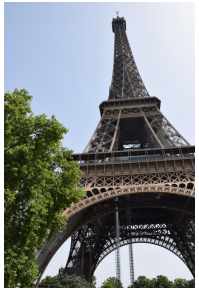

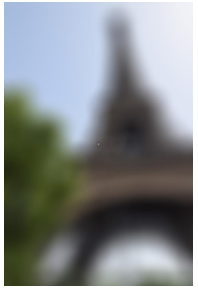

Energy spectrum

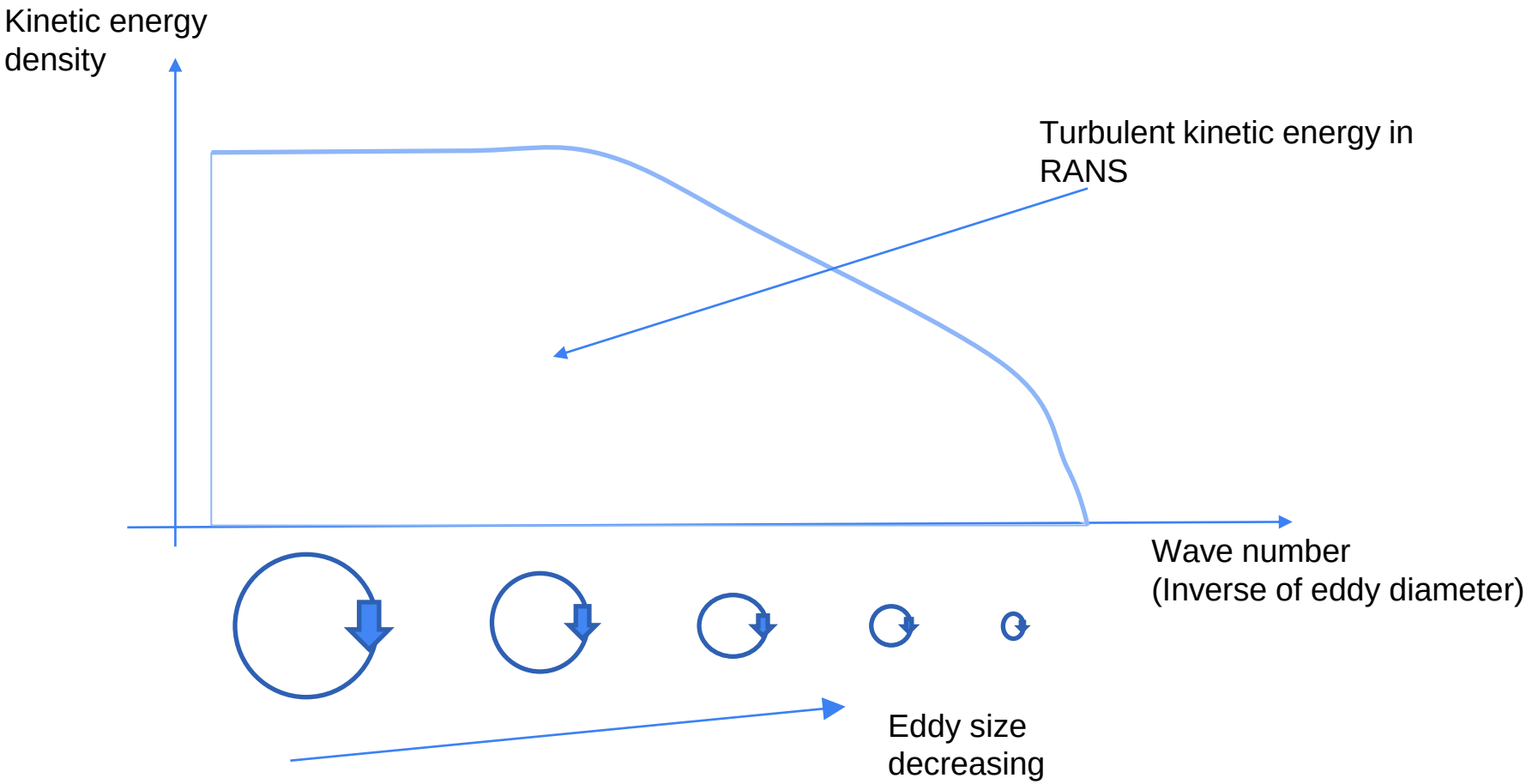

Importance of wall function

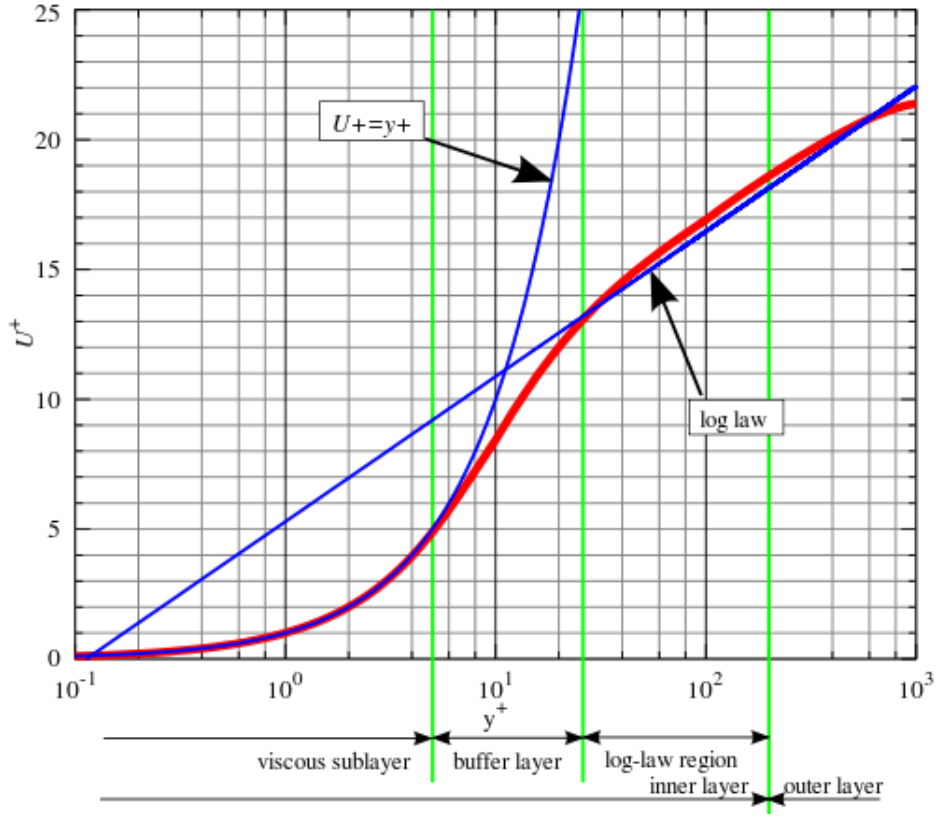

Source: Wikipedia

$$u^+ = \frac{1}{\kappa} \ln y^+ + C^+$$

$$y^+ = \frac{y\, u_\tau}{\nu} \qquad u^+ = \frac{u}{u_\tau}$$

$$u_\tau = \sqrt{\frac{\tau_w}{\rho}}$$

The first cell centre should avoid the buffer layer

Final Remarks

Two-dimensional turbulence

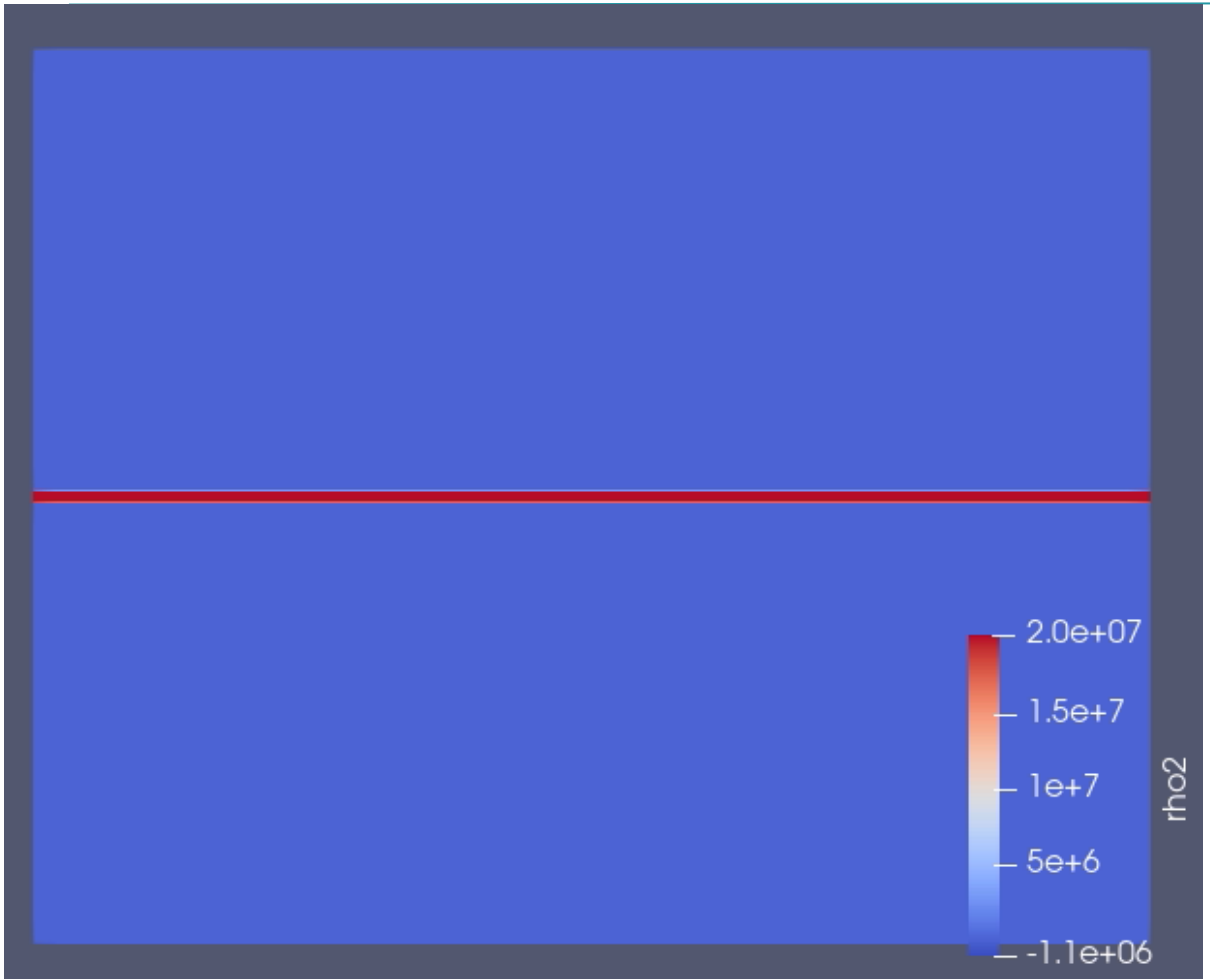

Initial velocity

Shear layer

Initial velocity

Werner Heisenberg:

"When I meet God, I am going to ask him two questions: Why relativity? And why turbulence? I really believe he will have an answer for the first."

Millennium Prize Problems:

The Clay Institute has pledged a US$ 1 million prize for solving:

Navier–Stokes existence and smoothness problem

Conclusion 1 (Simplified characterisation!!!)

SafeG

DNS

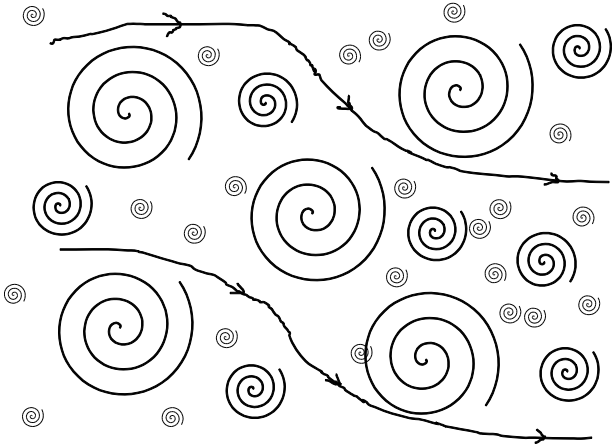

LES

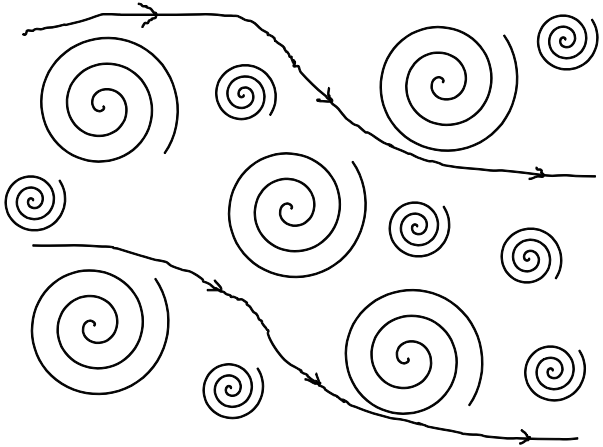

RANS

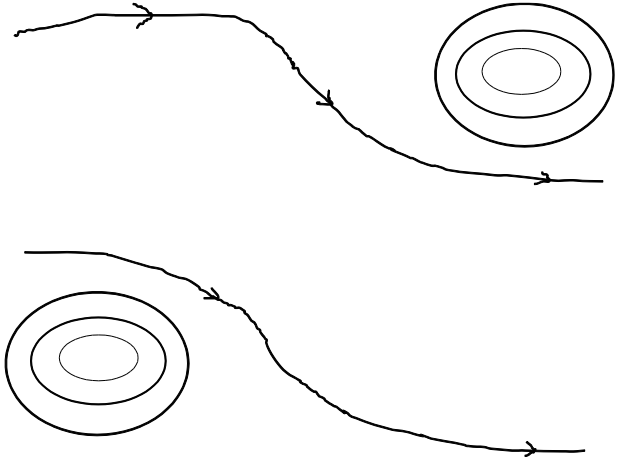

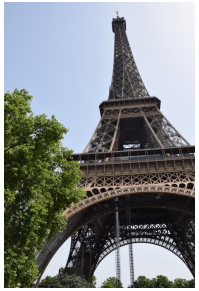

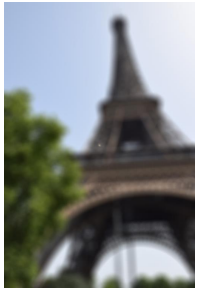

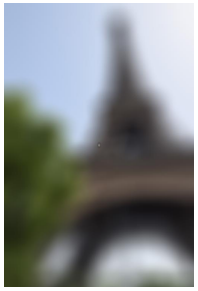

Conclusion 2

SafeG

Use the Bottom Up Approach when you think about CFD

Nuclear Energy Agency (NEA) - Best Practice Guidelines for the Use of CFD in Nuclear Reactor Safety Applications – Revision (oecd-nea.org)

Thank you for your attention!

Is this cavity flow turbulent?

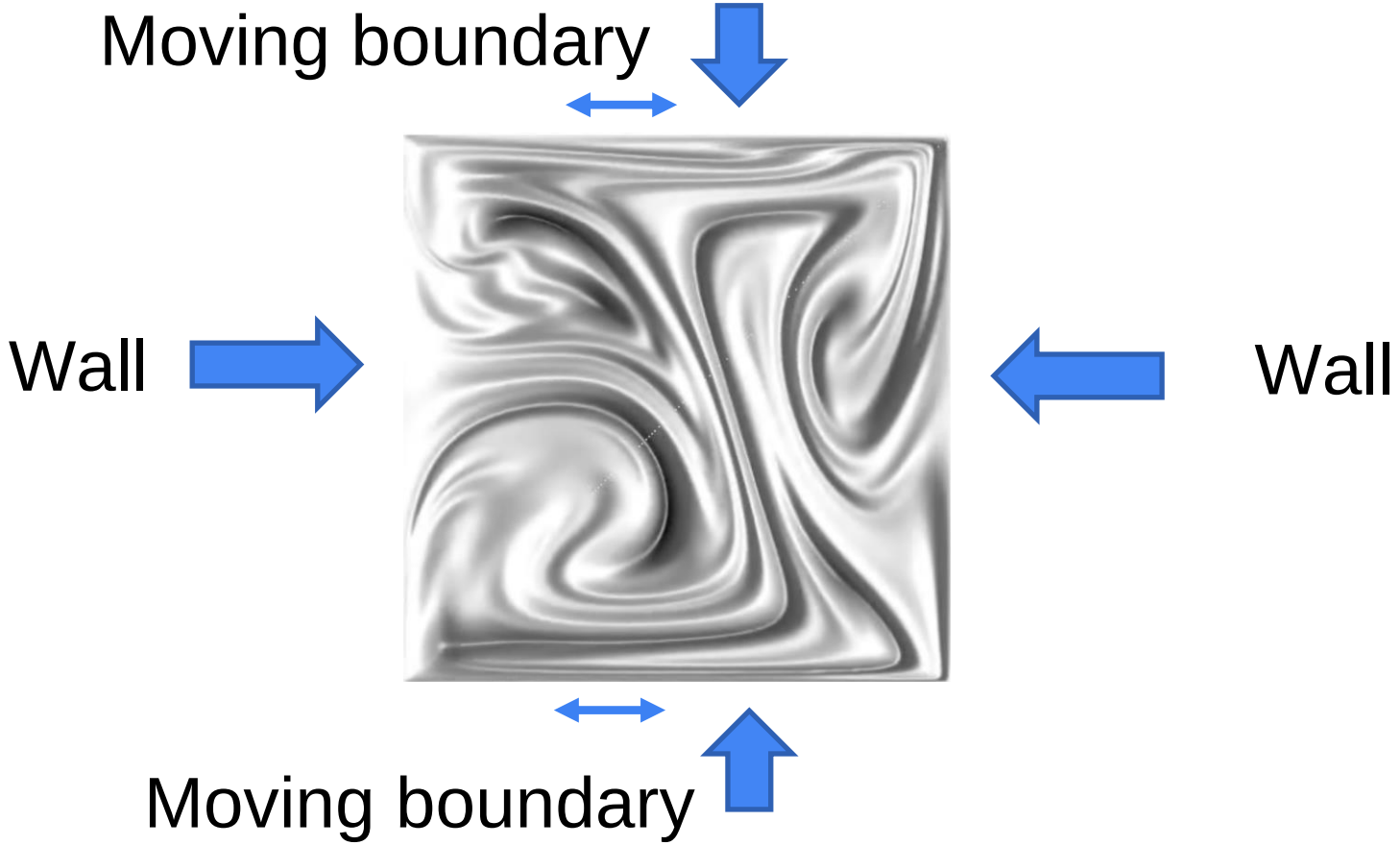

Cavity flow

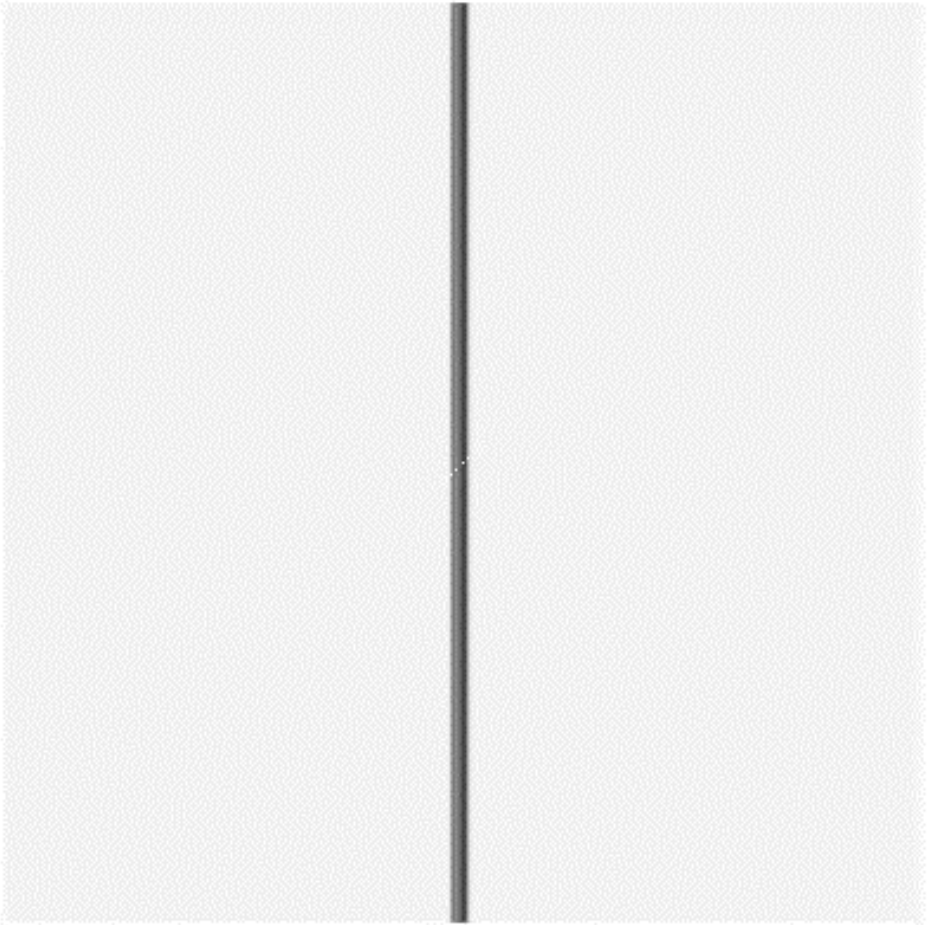

Stretching and folding

Jacobs Challenging today. Reinventing tomorrow.

Use of the deterministic code WIMS® to model Gen-IV Fast Reactors

SAFEG Summer School
04/07/2023

Jean Lavarenne

Content

- Deterministic v Monte-Carlo
- Deterministic method
- Overview of the 2-step approach to core modelling
- Modelling ESFR-SMART and ALLEGRO using WIMS

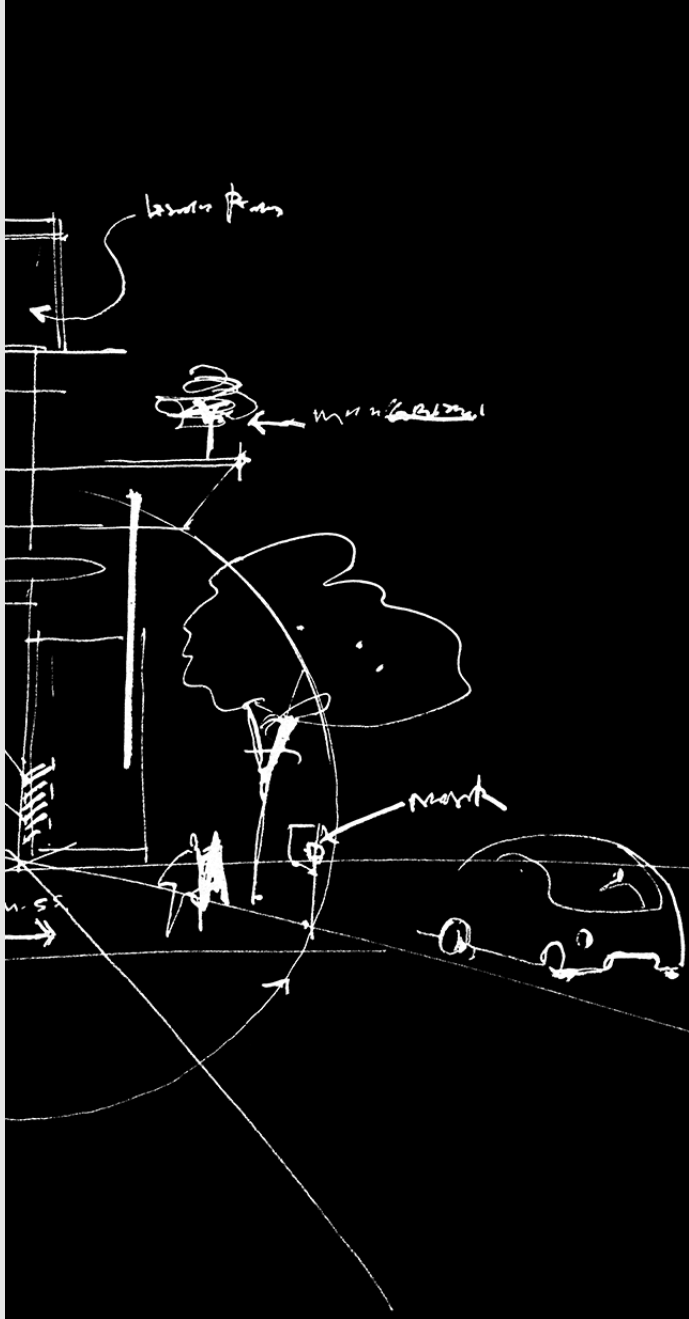

Deterministic v Monte-Carlo

Deterministic v Monte-Carlo (1)

- Monte-Carlo method
  - Follow large population of neutrons around with random selection of events & consequences
  - Use the real physics – cross-sections for absorption, scattering, fission in continuous energy
  - Real geometry, no mesh
  - Very accurate (if done properly) but long run times
- Deterministic method
  - Solve transport equation numerically
    - Simplify problem using assumptions
    - Energy and spatial discretization
    - Solve numerically the equation at each point of the spatial mesh, in every energy group
  - Faster than Monte-Carlo but introduce approximations

Deterministic v Monte-Carlo (2)

- Computers are getting faster and faster… Why bother with deterministic codes?
- Fair point… and ultimately we probably will use Monte-Carlo for everything
- BUT:
  - Designing a core requires optimizing many parameters from safety (limit power peaking, shut down margin), to operational (cycle length, power output)
  - This requires you to run thousands and thousands of flux calculations & cross-section generations
  - Many core iterations from interacting with other disciplines – fault studies, chemistry, structural integrity etc.
  - You need a code that spits out results in seconds/minutes
- Designing cores is thus much easier/less time-consuming using deterministic codes
- Monte-Carlo model used to validate the deterministic model and provide confidence in the results

Deterministic Method

The dreaded transport equation (1)

- $N(E, \boldsymbol{r}, \boldsymbol{\Omega}, t).dV.d\boldsymbol{\Omega}.dE$ = Number of neutrons in volume dV around $\boldsymbol{r}$, with energy between E and $E+dE$, travelling in a direction between $\boldsymbol{\Omega}$ and $\boldsymbol{\Omega} + d\boldsymbol{\Omega}$, at time t

- $\Psi(E, \boldsymbol{r}, \boldsymbol{\Omega}, t)$ = Angular flux = $N(E, \boldsymbol{r}, \boldsymbol{\Omega}, t) \times v$ where v is the neutron velocity

- Balance equation of neutrons in volume around $\boldsymbol{r}$, with energy between E and $E+dE$, travelling in a direction between $\boldsymbol{\Omega}$ and $d\boldsymbol{\Omega}$ at time t:

$$\frac{\partial N(E,\boldsymbol{r},\boldsymbol{\Omega},t)}{\partial t} = \frac{1}{v}\frac{\partial \Psi(E,\boldsymbol{r},\boldsymbol{\Omega},t)}{\partial t} = \text{neutrons gained in } dV - \text{neutrons lost}$$

The dreaded transport equation (2)

- Loss terms:
  - Neutrons escaping volume dV
  - Neutrons captured or scattered: $\Sigma_T(E, \boldsymbol{r}, t) \times \Psi(E, \boldsymbol{r}, \ \boldsymbol{\Omega}, t)$ – where Σ_T = total cross-section
- Gain terms:
  - Neutrons entering volume dV
  - Neutrons scattering from energy E' and angle $\boldsymbol{\Omega}'$ to energy E and angle $\boldsymbol{\Omega}$: $\Sigma_S(E' \rightarrow E, \boldsymbol{\Omega}' \rightarrow \boldsymbol{\Omega}, \boldsymbol{r}, t) \times \Psi(E', \boldsymbol{r}, \ \boldsymbol{\Omega}', t)$
  - Neutrons produced through fission, from a neutron with energy E' and angle $\boldsymbol{\Omega}'$: $\frac{\chi_P(E)}{4\pi} \times \nu(E') \times \Sigma_F(E', \boldsymbol{r}, t) \times \Psi(E', \boldsymbol{r}, \boldsymbol{\Omega}', t)$ where:
    - $\chi_P(E)$: probability function of energy E for neutrons produced by fission
    - $\nu(E')$: average number of neutrons produced per fission
  - Other production: $\frac{Q(E,\boldsymbol{r},t)}{4\pi}$

The dreaded transport equation (3)

- Putting things together:
  - Neutrons entering volume dV − Neutrons escaping volume $dV = -\boldsymbol{\Omega}.\nabla\,\Psi(E,\boldsymbol{r},\ \boldsymbol{\Omega},t)$
  - Integrate fission and scattering terms over all energies E' and all angles $\boldsymbol{\Omega}'$

$$\frac{1}{v}\frac{\partial\Psi(E,\boldsymbol{r},\ \boldsymbol{\Omega},t)}{\partial t} + \boldsymbol{\Omega}.\nabla\,\Psi(E,\boldsymbol{r},\boldsymbol{\Omega},t) + \Sigma_T(E,\boldsymbol{r},t)\times\Psi(E,\boldsymbol{r},\boldsymbol{\Omega},t)$$
$$= \int_0^\infty dE' \int_{4\pi} \boldsymbol{d\Omega}'\Sigma_S(E'\to E,\boldsymbol{\Omega}'\to\boldsymbol{\Omega},\boldsymbol{r},t)\times\Psi(E',\boldsymbol{r},\boldsymbol{\Omega}',t) +$$
$$\frac{\chi_P(E)}{4\pi}\int_0^\infty dE' \int_{4\pi} \boldsymbol{d\Omega}'\nu(E')\times\Sigma_F(E',\boldsymbol{r},t)\times\Psi(E',\boldsymbol{r},\boldsymbol{\Omega}',t) + \frac{Q(E,\boldsymbol{r},t)}{4\pi}$$

The dreaded transport equation (4)

- Putting things together:
  - Neutrons entering volume dV − Neutrons escaping volume $dV = -\boldsymbol{\Omega}.\nabla\,\Psi(E,\boldsymbol{r},\ \boldsymbol{\Omega},t)$
  - Integrate fission and scattering terms over all energies E' and all angles $\boldsymbol{\Omega}'$

$$\frac{1}{v}\frac{\partial\Psi(E,\boldsymbol{r},\ \boldsymbol{\Omega},t)}{\partial t} + \boldsymbol{\Omega}.\nabla\,\Psi(E,\boldsymbol{r},\boldsymbol{\Omega},t) + \Sigma_T(E,\boldsymbol{r},t)\times\Psi(E,\boldsymbol{r},\boldsymbol{\Omega},t)$$
$$= \int_0^\infty dE' \int_{4\pi} \boldsymbol{d\Omega}'\Sigma_S(E'\to E,\boldsymbol{\Omega}'\to\boldsymbol{\Omega},\boldsymbol{r},t)\times\Psi(E',\boldsymbol{r},\boldsymbol{\Omega}',t) +$$
$$\frac{\chi_P(E)}{4\pi}\int_0^\infty dE' \int_{4\pi} \boldsymbol{d\Omega}'\nu(E')\times\Sigma_F(E',\boldsymbol{r},t)\times\Psi(E',\boldsymbol{r},\boldsymbol{\Omega}',t) + \frac{Q(E,\boldsymbol{r},t)}{4\pi}$$

Deterministic method

- The aim is to solve the transport equation numerically
- Different mathematical methods can be used
- No time to go through them, but always involve making assumptions to simplify the problem
- Key is to have a grasp of the assumptions made and when they start breaking down
- Examples of methods: Method of Characteristics (MoC), Collision probability, Spherical Harmonics (P_N), Diffusion, SP_3, Discrete Ordinate (S_N)

Deterministic method

- Discretization of the variables: energy, position (sometimes angle & time)
- Solving the equation at each point of the spatial mesh and in each energy group
- The user chooses the discretization
- Compromise between speed and accuracy

2-step approach in deterministic codes (1)

- Fine resolution at the assembly level for generating cross-sections
  - Explicit, heterogeneous geometry
  - Fine spatial mesh – a few subdivision per pincell
  - Fine energy group – Over a thousand groups
  - Flux solved using MoC, Collision probability in an infinite medium
  - Flux calculation provides: macroscopic cross-sections, reaction rates etc.

- Homogenization and condensation
  - Create an homogenized medium made of fuel, coolant, cladding, with one set of cross-sections in the region
  - Condensing flux and cross-section to a smaller number of groups

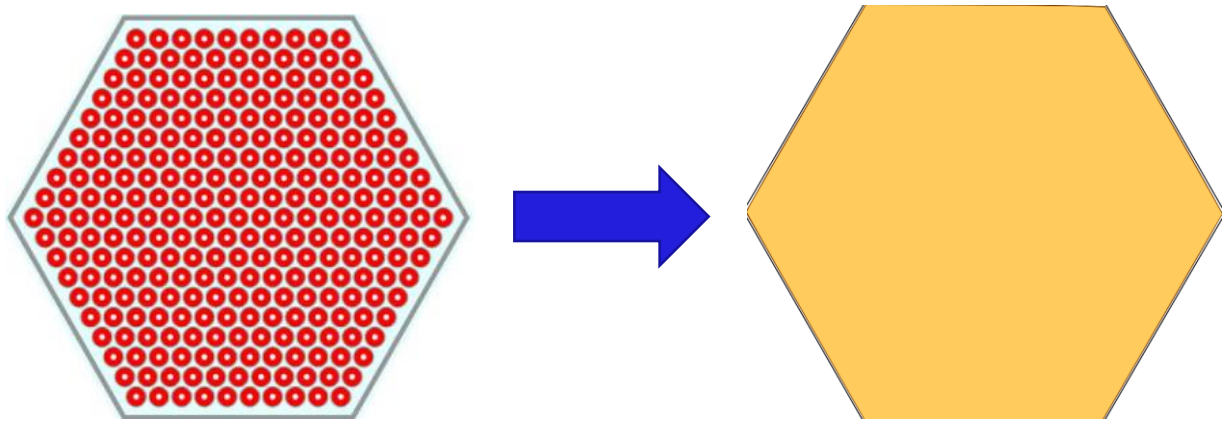

2-step approach in deterministic codes (2)

- Whole core calculations
  - Homogenized assemblies
  - Coarser spatial mesh – a few subdivisions per assembly
  - Fewer energy groups
  - Flux calculated using diffusion, SP_3, S_N or MoC

- Options to do:
  - Thermal-hydraulics coupling – important for reactivity feedback in Sodium/lead cooled reactors, for transients in GFRs
  - Burn-up

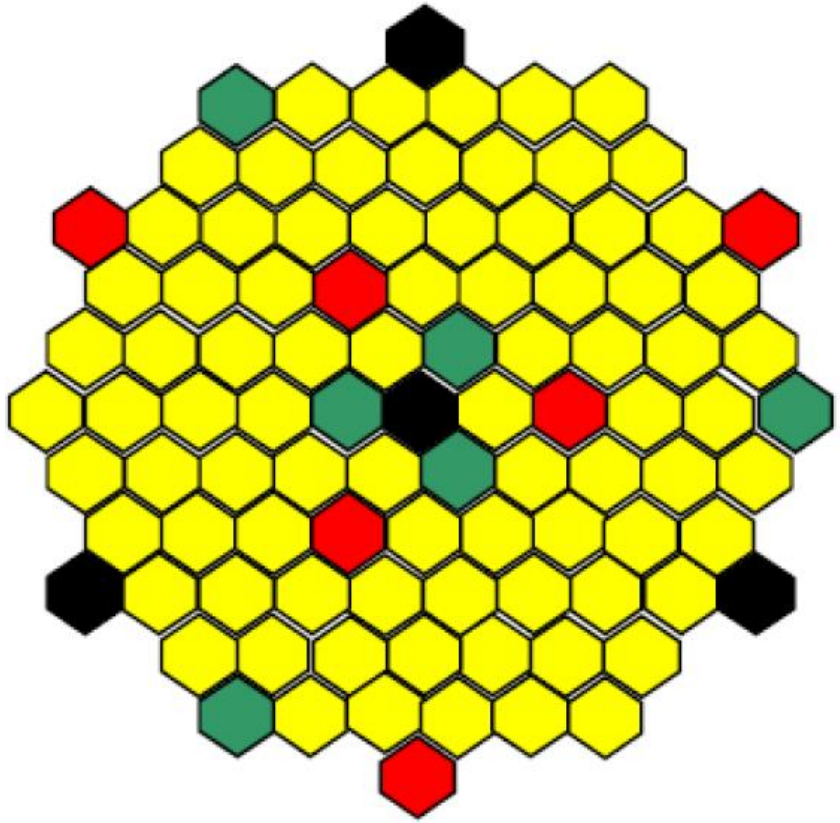

Case studies – ESFR and Allegro

ALLEGRO Core description

- Helium-cooled fast reactor
- 75 MWth.
- 81 assemblies, 169 pins per assembly.
- MOX with 23.3% Pu.
- 86cm active core height.

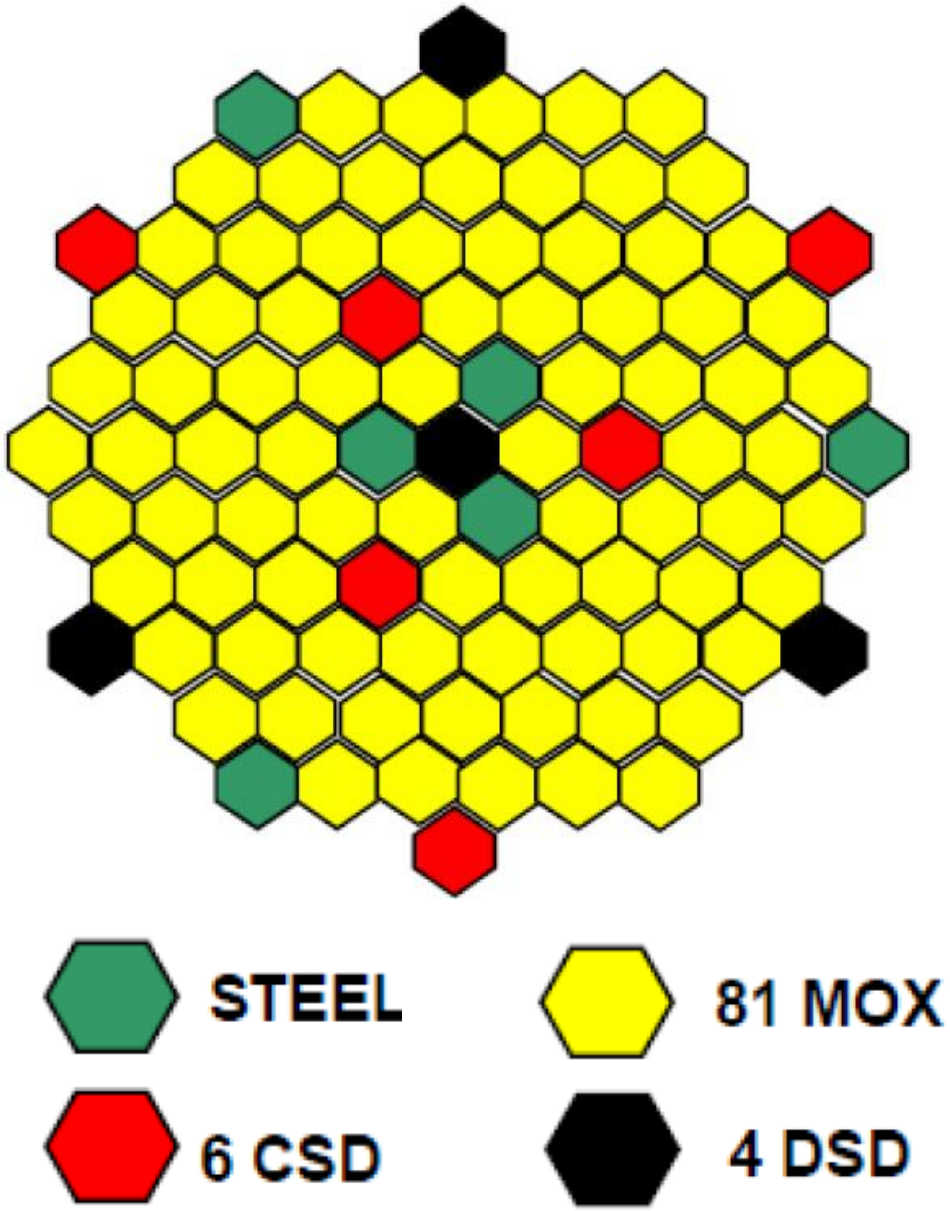

ESFR-SMART Core description

- Sodium-cooled fast reactor.
- 3600 MWth.
- 504 assemblies, 271 pins per assembly.
- MOX with 17.99% Pu.
- 1-meter active core height.

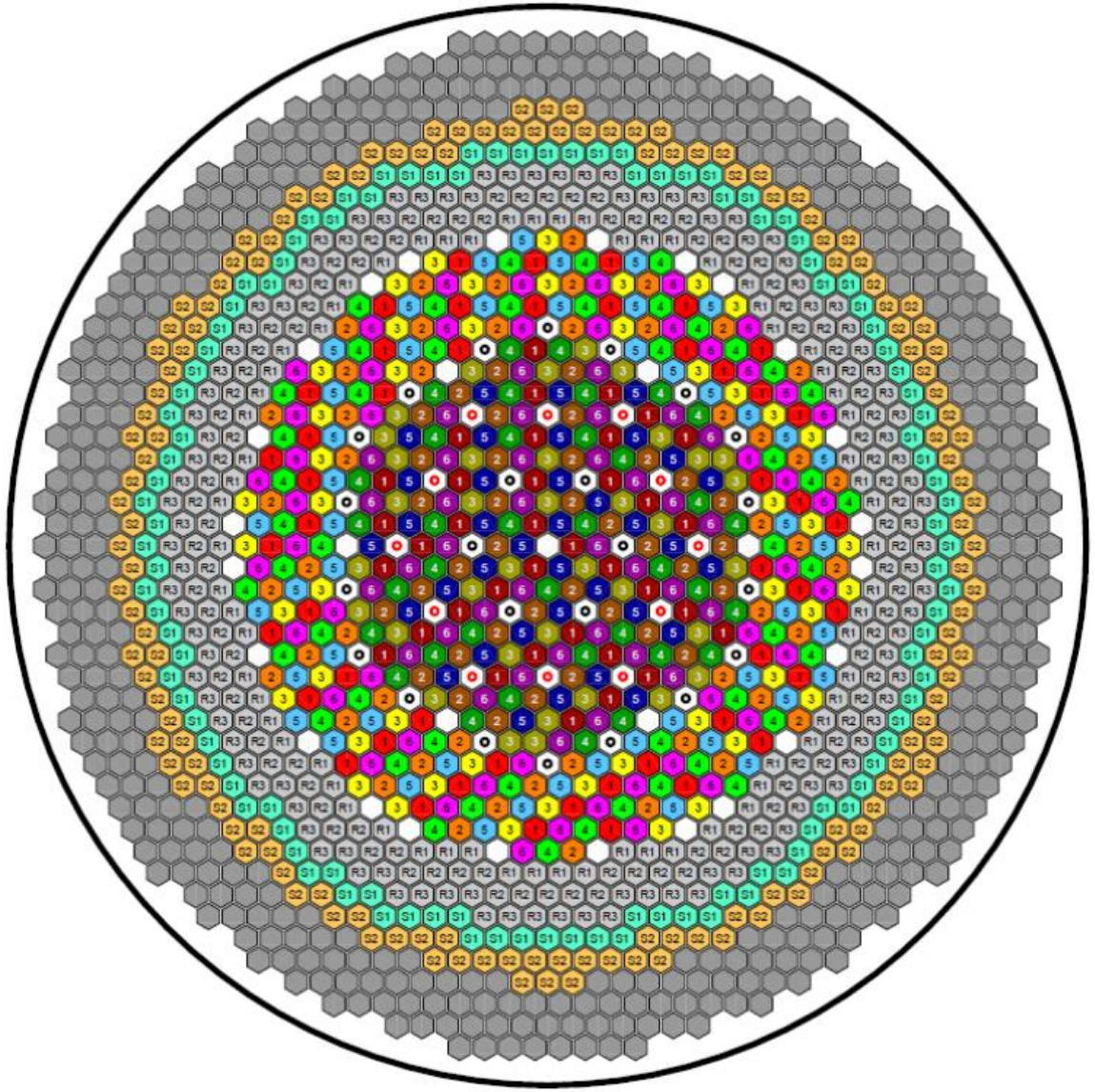

WIMS deterministic code

- WIMS is a deterministic code developed by ANSWERS® (part of Jacobs) in the UK
- ECCO fine-energy (1968) groups capability for cross-section generation
- Lattice calculation using Method of Characteristics or Collision probability
- Super-homogenization capability for generating cross-sections in control rods
- Whole core solver MERLIN with Diffusion, SP_3, S_N,Group Monte-Carlo
- 1D thermal-hydraulics solver ARTHUR

Assembly calculation

- While the two reactors are very different the calculation approach is the same
- Collision probability calculation using ECCO libraries of fine energy (1968) groups, then condensed into 172
- Lattice calculation done with reflective boundary conditions
- Flux solved using the Method of Characteristics in 172 groups
- Calculations repeated for different fuel temperatures/coolant densities etc.
- This allows to interpolate macroscopic cross-sections between different state points (useful when using thermal feedback)

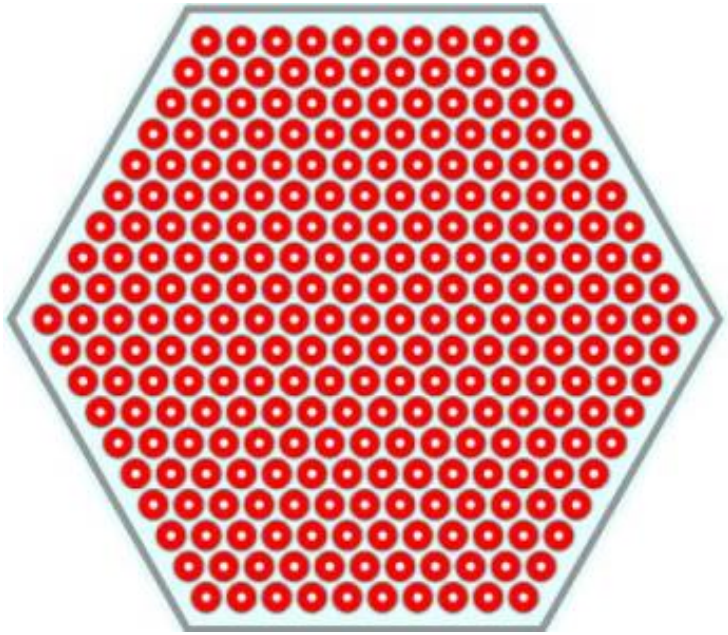

ESFR hexagonal fuel assembly

Treatment for non-multiplicative media

- Any medium where fission does not occur (control rod, reflector, shielding, etc.
- We need to understand how neutrons coming from nearby fuel assemblies behave there (scatter, get absorbed, get back to fuel assemblies)
- A simple assembly calculation is not possible because a source of neutron is needed
- Two routes:
  - A slab calculation: flux calculation of a homogenized slab representing the non-multiplicative assembly next to a fuel assembly
  - A supercell calculation: non-multiplicative assembly explicitly modelled next to a fuel assembly

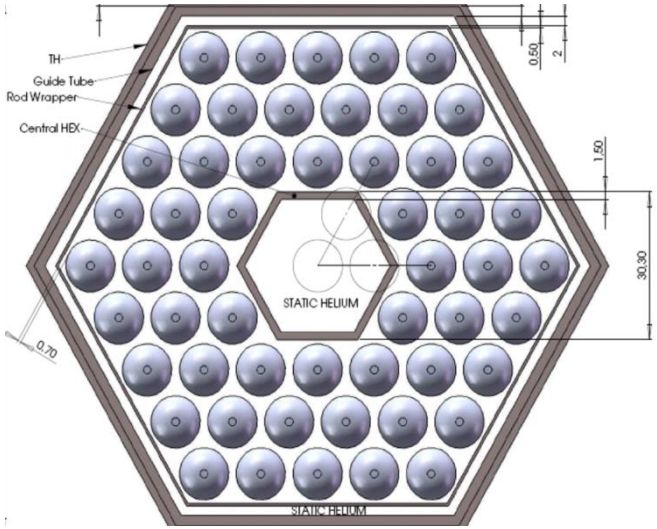

ALLEGRO control rod

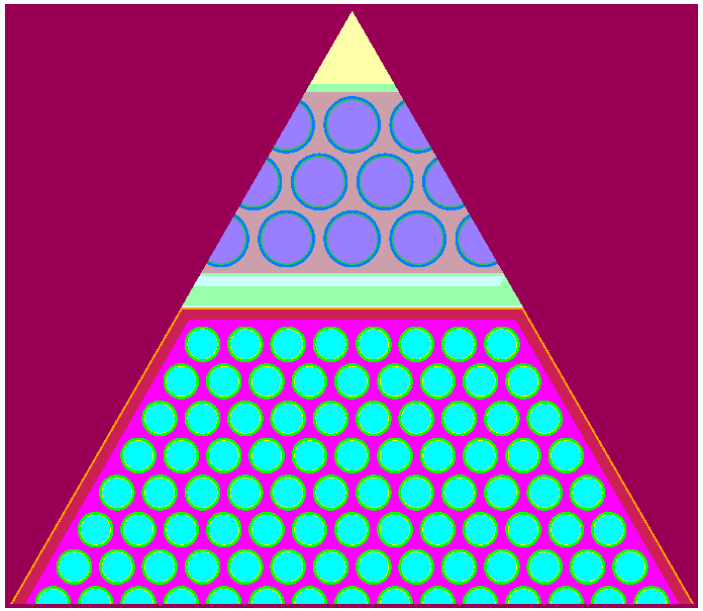
ALLEGRO control rod supercell

Homogenization

- Calculate a set of homogenized equivalent cross-sections based on the heterogeneous ones

- Two methods used:
  - flux x volume weighting method – suitable for assemblies in which the flux is relatively constant
  - Superhomogenization (SPH): iterative procedure for regions with strong absorbers

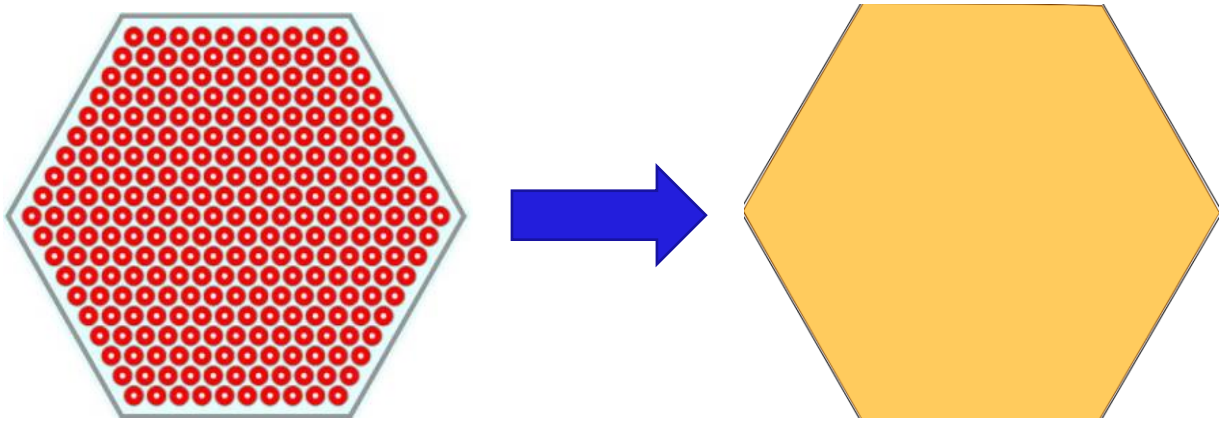

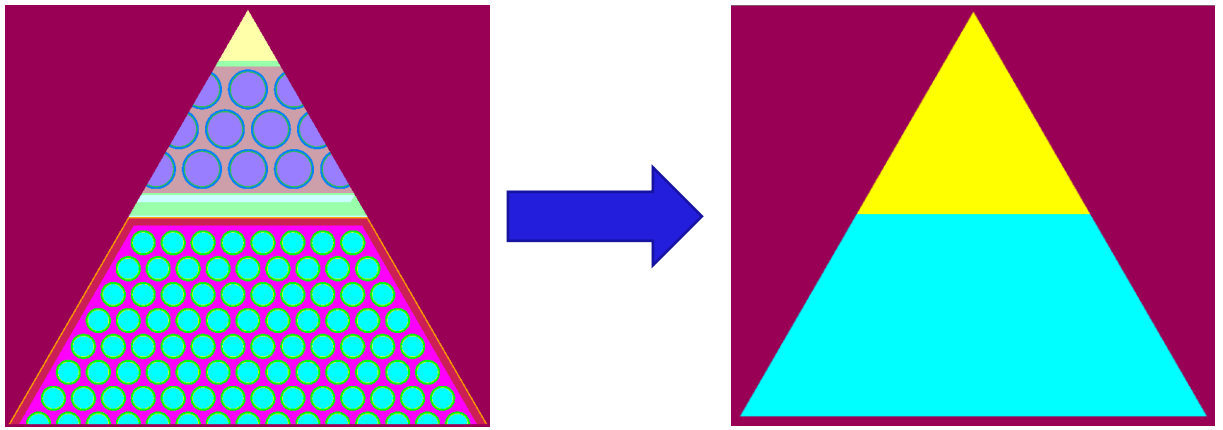

Energy Group Condensation

- Assembly calculations to prepare cross-sections done in 172 energy groups

- Whole core calculation is done in 33 groups

=> Condensing flux and cross sections from 172 to 33 groups

- R-Z calculation of the core performed using SP_3 that provides a condensing spectrum

- This helps to improve accuracy, in particular regarding leakage.

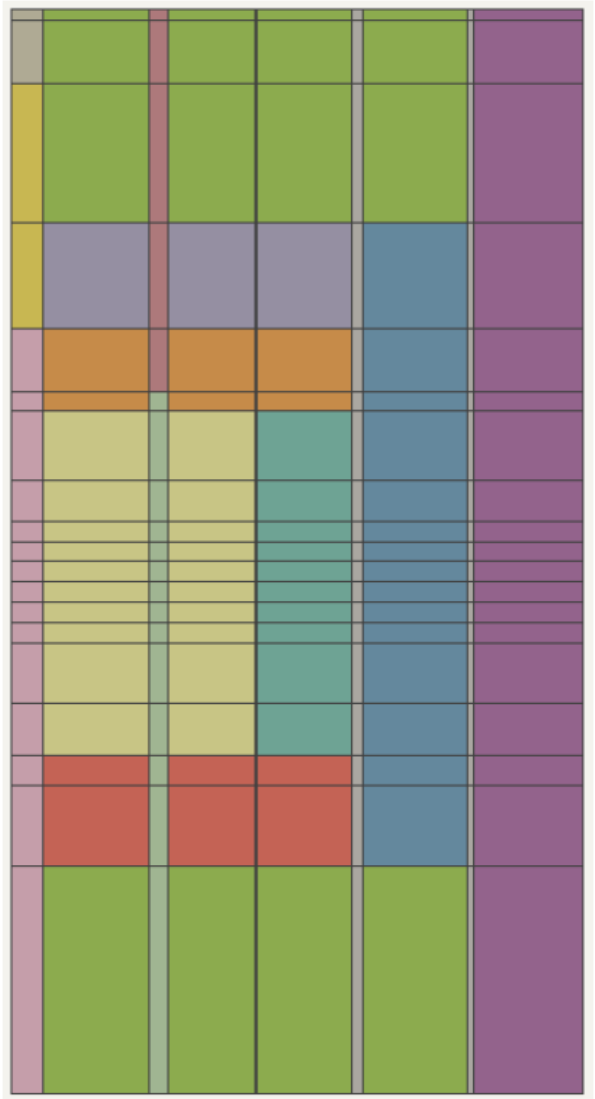

ALLEGRO RZ model

Whole core calculation

- Giant 3D puzzle, putting the homogenized lattices in the right places

- Flux calculation performed in MERLIN with diffusion or SP_3 solvers

- Frequent calculations are:
  - Rods in, rods out cases
  - Burn-up: Flux used to change the composition of the core over time
  - Thermal-hydraulic feedback (see next slide)
  - Reactivity coefficient calculations e.g. fuel temperature, coolant void (in LMFRs)

Thermal feedback in whole core calculation

- In WIMS this is done by the ARTHUR module
- ARTHUR is a 1D thermal hydraulics solver
- It requires TH correlations and properties for fuel, and coolant tabulated on temperature (e.g. thermal conductivity, coolant viscosity, etc.)
- Iterations are made between MERLIN and ARTHUR until the results have converged

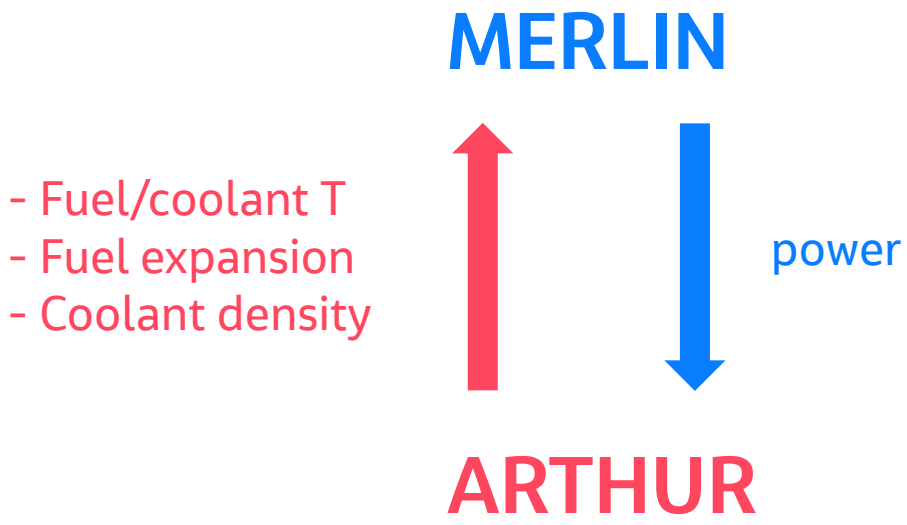

Difference between LWR and Fast reactor modelling

Same approach used for LWRs apart from the following:

- ECCO very fine energy groups used – more groups at fast energies are needed to capture fast fission events + scatter from structural materials
- LWRs usually use square assemblies (apart from VVER)
- Control rod sub assemblies instead of control rods inside fuel assemblies for PWRs
- No branch calculations needed for burn-up in fast reactors as cross-sections (resonance self-shielding) changes very little with burn-up in fast reactors

Results and analysis

The good… ESFR-SMART

- Excellent agreement between Monte-Carlo & WIMS SP_3
  - Rod worth calculation (performing flux calculations at various rod insertions), max error of 100 pcm
  - Assembly powers : Root mean square difference of 0.7%

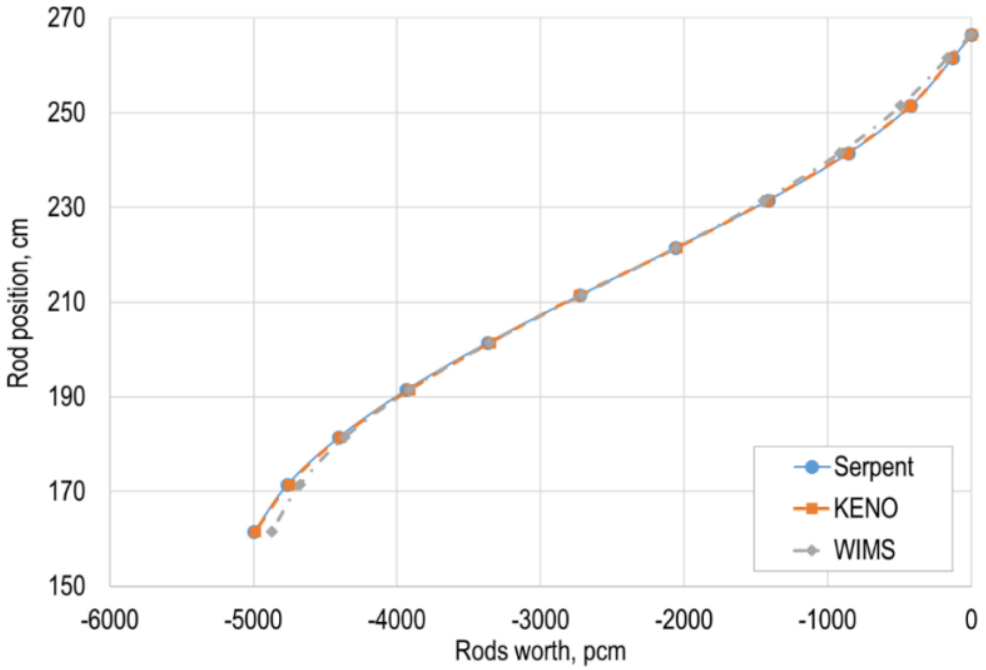

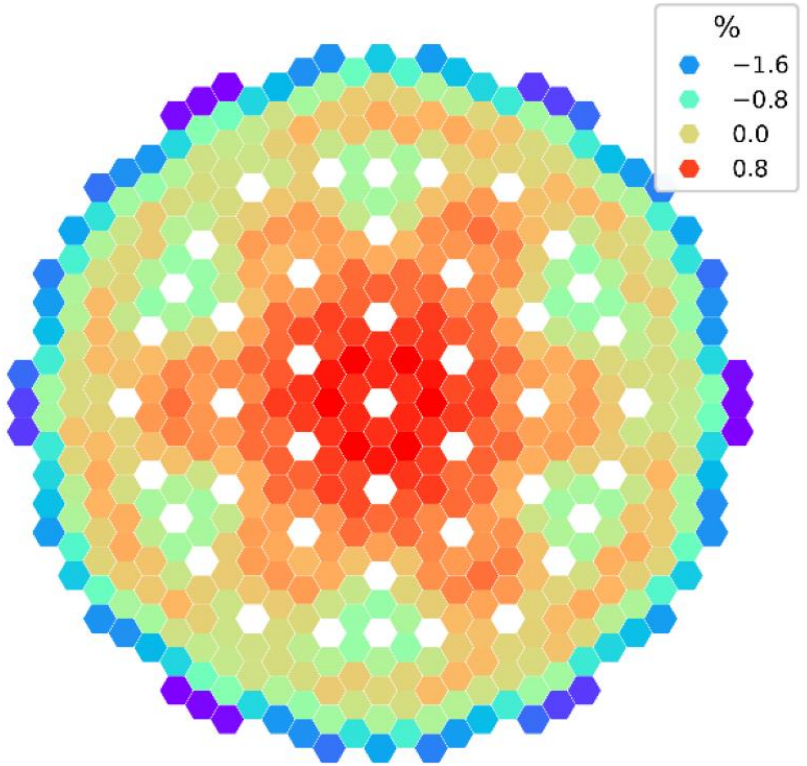

WIMS v SERPENT
RMS: 0.7%

Export Control Rating: Not Controlled – No License Required

The… not so good… ALLEGRO

- Same method, fast reactor but…

- Fresh core, all rods out case

	Δk-effective (pcm) v SERPENT
WIMS SP_3 (slab reflectors)	-1350
WIMS diffusion (slab reflectors)	-2300

The… not so good… ALLEGRO

- Same method, fast reactor but…

- Fresh core, all rods out case

	Δk-effective (pcm) v SERPENT
WIMS SP_3 (slab reflectors)	-1350
WIMS diffusion (slab reflectors)	-2300
WIMS SP_3 (supercell reflectors)	-1350
WIMS diffusion (supercell reflectors)	-2300

=> Still a major discrepancy between Monte-Carlo and Deterministic SP_3 or diffusion

- What's going wrong and can we do better?

Alternatives and impact on performance

- SP_3 and diffusion struggle with very heterogeneous core, and with estimating leakage in small fast reactors, and this becomes a real issue here for ALLEGRO

- How about group Monte-Carlo: Δk-effective v SERPENT = - 30 pcm

- Produce better results, but large impact on performance

	Runtime	# core
WIMS Diffusion	2 min 3 sec	1
WIMS SP_3	3 min 49 sec	1
WIMS- Group MC	2 hours	1
SERPENT	1.5-3.5 hours	12

Conclusion

- Very short introduction to deterministic codes
- Simplify the transport equation using assumptions and solve numerically
- 2-step approach to whole core modelling with:
  - High fidelity at assembly level to produce cross sections
  - Lower fidelity at the core level
- It can produce very good results at a fraction of the computational cost of Monte-Carlo
- BUT: Beware of each method limitation, highlighted here is the inaccurate leakage & flux shape prediction by SP_3 and diffusion in a small & very heterogeneous reactor

Thanks for your attention,

Any questions?

Bibliography

- ESFR-SMART core description and results taken from:
  - ESFR-SMART core burnup calculation on radially infinite lattice with Monte-Carlo Code https://zenodo.org/record/3324565#.XSbpTOgzY2w
  - Fast Reactor Multiphysics and Uncertainty propagation within WIMS https://zenodo.org/record/4260387#.X6kLvWhKg2w

- ALLEGRO core description taken from:
  - https://www.gen-4.org/gif/upload/docs/application/pdf/2019-03/geniv_template-_dr._ladislav_belovsky_final_3-20-19.pdf

GFR TECHNOLOGY FROM THE MODELLING PERSPECTIVE

PETR VÁCHA ON BEHALF OF THE V4G4 COE AND SAFEG CONSORTIUM

ADVANCED MODELLING TECHNIQUES WORKSHOP, 4.7.2023, CAMBRIDGE, UK

SafeG

SAFETY OF GFR THROUGH INNOVATIVE MATERIALS, TECHNOLOGIES AND PROCESSES

This project has received funding from the Euratom H2020 programme NFRP-2019-2020-06 under grant agreement No 945041.

Outline

- **GFR**
- **ALLEGRO reactor design overview**
- **Design and modelling of selected main systems/components:**
  - The core region
  - Main cooling loops
  - Decay Heat Removal system
  - Containment
- **Severe accidents**
  - Modelling of severe accidents in GFR
  - SA prevention and mitigation measures

GFR- GAS-COOLED FAST REACTOR

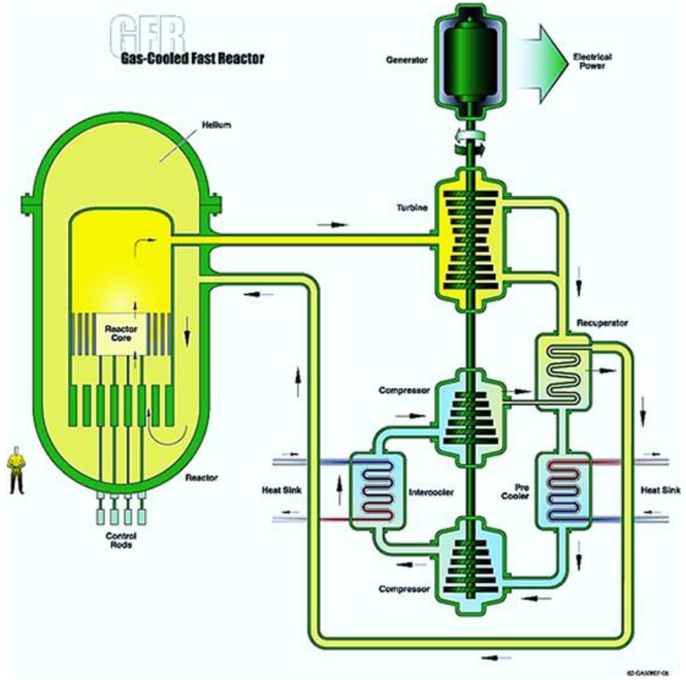

Source: www.gen-4.org

- **Combination of FAST and HIGH-TEMPERATURE reactor**
  - Closed fuel cycle
  - Waste minimalization
  - High-potential heat production, electricity production with high efficiency
- **Main features:**

+ High core outlet temperature (>850 °C)
+ Good neutronic safety (for a fast reactor)
+ Transparent, chemically inert coolant
+ Very effective breeder or burner
-Less effective cooling (than water, molten metals or salts)
- Extreme demands on material properties

- **Challenges:**
  - Core cooling during LOCA
  - Fuel handling at elevated pressure in the primary circuit

HISTORY OF GFR

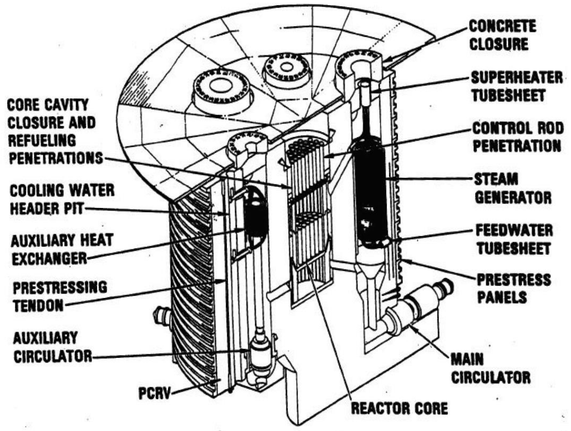

70‘s - Concept GCFR 300 MWth
General Atomics

- **Surprisingly rich:**
  - Dates back to the 60‘s – first wave of fast reactor development
  - Concepts developed in Europe, USA, USSR, Japan
  - Never built – too ambitious and demanding on materials and technologies of the era + success in SFR development

- **Modern Era**
  - GFR as one of the GIF technologies for the 21st century
  - R&D Focused in Europe, USA and Japan
  - ETDR -> ALLEGRO
  - EM^2 -> FMR

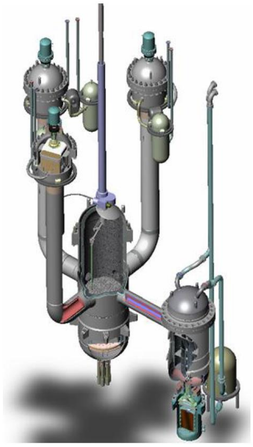

2002 – ETDR, CEA

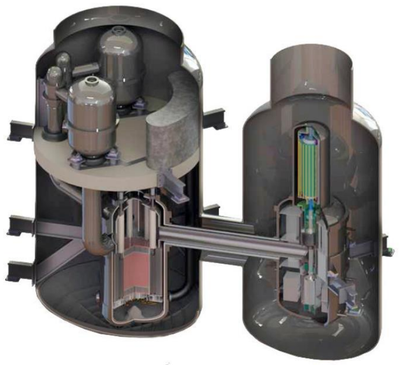

2009 – EM^2, GA

HISTORY – GAS-COOLED REACTORS

- **Gas-cooled reactors with moderator:**
  - Rich history of commercial operation (since the end of 50‘s)
  - MAGNOX and AGR in Great Britain
  - Helium-cooled reactors in Germany, USA, Japan, China
  - In total – more than 500 reactor-years of experience
  - Still under operation and new builds commissioned
  - Biggest drawback – very low power density (~ 4-10 MW/m^3)

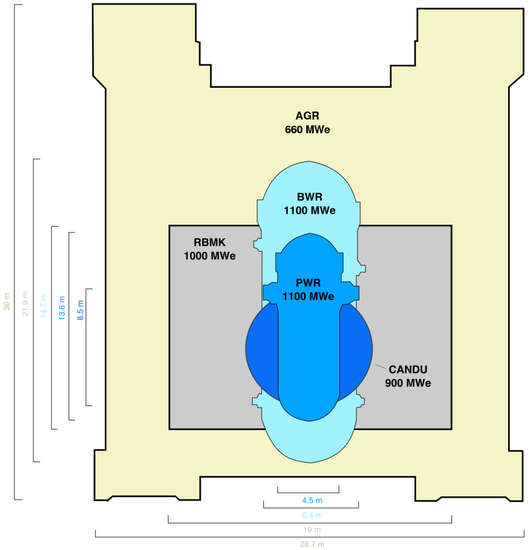

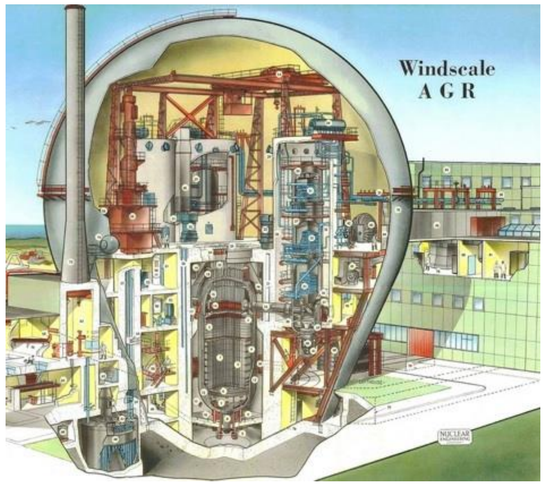

1965 – AGR, theengineer.co.uk

1985 – THTR 300, thtr.de

2022 – HTR-PM, world-energy.org

FAST REACTOR COOLANTS COMPARISON

Property (unit)	**Helium** (550°C / 70bar)	**Sodium** (550°C / 1bar)	**Lead** (550°C / 1bar)
Density (kg/m^3)	4.217	820	10 300
Specific heat capacity (kJ/kg.K)	5.19	1.25	0.14
Thermal conductivity (W/m.K)	0.310	67	20.2
Dynamic viscosity (Pa.s)	3.1e^{-5}	2.2e^{-4}	1.6e^{-4}
Melting point (°C)	-272	97.5	327
Boiling point (°C)	-269	883	1775

FAST REACTOR COOLANTS COMPARISON - HELIUM

Property (unit)	**Helium** (550°C / 70bar)	**Sodium** (550°C / 1bar)	**Lead** (550°C / 1bar)
Density (kg/m^3)	4.217	820	10 300
Specific heat capacity (kJ/kg.K)	5.19	1.25	0.14
Thermal conductivity (W/m.K)	0.310	67	20.2
Dynamic viscosity (Pa.s)	3.1e^{-5}	2.2e^{-4}	1.6e^{-4}
Melting point (°C)	-272	97.5	327
Boiling point (°C)	-269	883	1775

Helium as a nuclear reactor coolant

- Advantages: transparent, inert, no phase change, excellent specific properties
- Disadvantages: extremely low density
- Conclusions: need for either very high thermal capacity of the core combined with low power density (HTR), or keeping a steady coolant flow through the core at all times (GFR)

ALLEGRO – DESIGN OVERVIEW

- **Two consecutive core configurations**
  - Driver core – MOX/UO2 pin-type fuel in steel cladding, experimental positions for fuel qualification
  - Refractory core – (U,Pu)C pin-type fuel in SiC-SiCf cladding <- GFR reference fuel
- **Target core outlet temperature 850°C**
- **Power density up to 100 MW/m3**
- **Focus on fully passive safety to meet GENIV objectives**

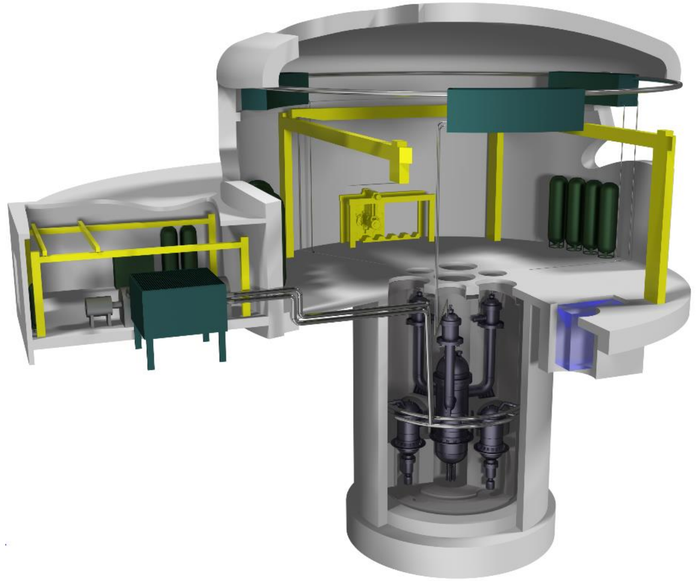

ALLEGRO main characteristics	
Nominal Power (thermal)	75 MW
Driver core fuel/cladding	MOX(UO2) / 15-15ti Steel
Experimental fuel/cladding	UPuC / Sic-Sicf
Fuel enrichment	35% (MOX) / 19.5% (UO2)
Power density	100 MWth/m3
Primary coolant	He
Primary pressure	7 MPa
Driver core in/out temperature	260°C / 530°C
Experimental fuel in/out T	400°C / 850°C

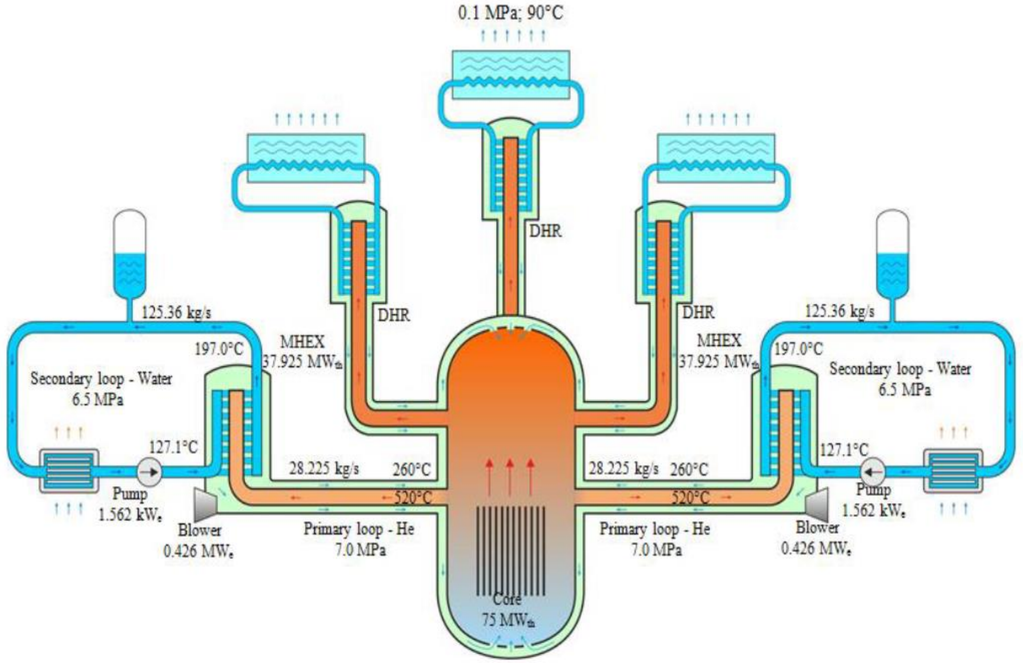

ALLEGRO – PRIMARY CIRCUIT LAYOUT

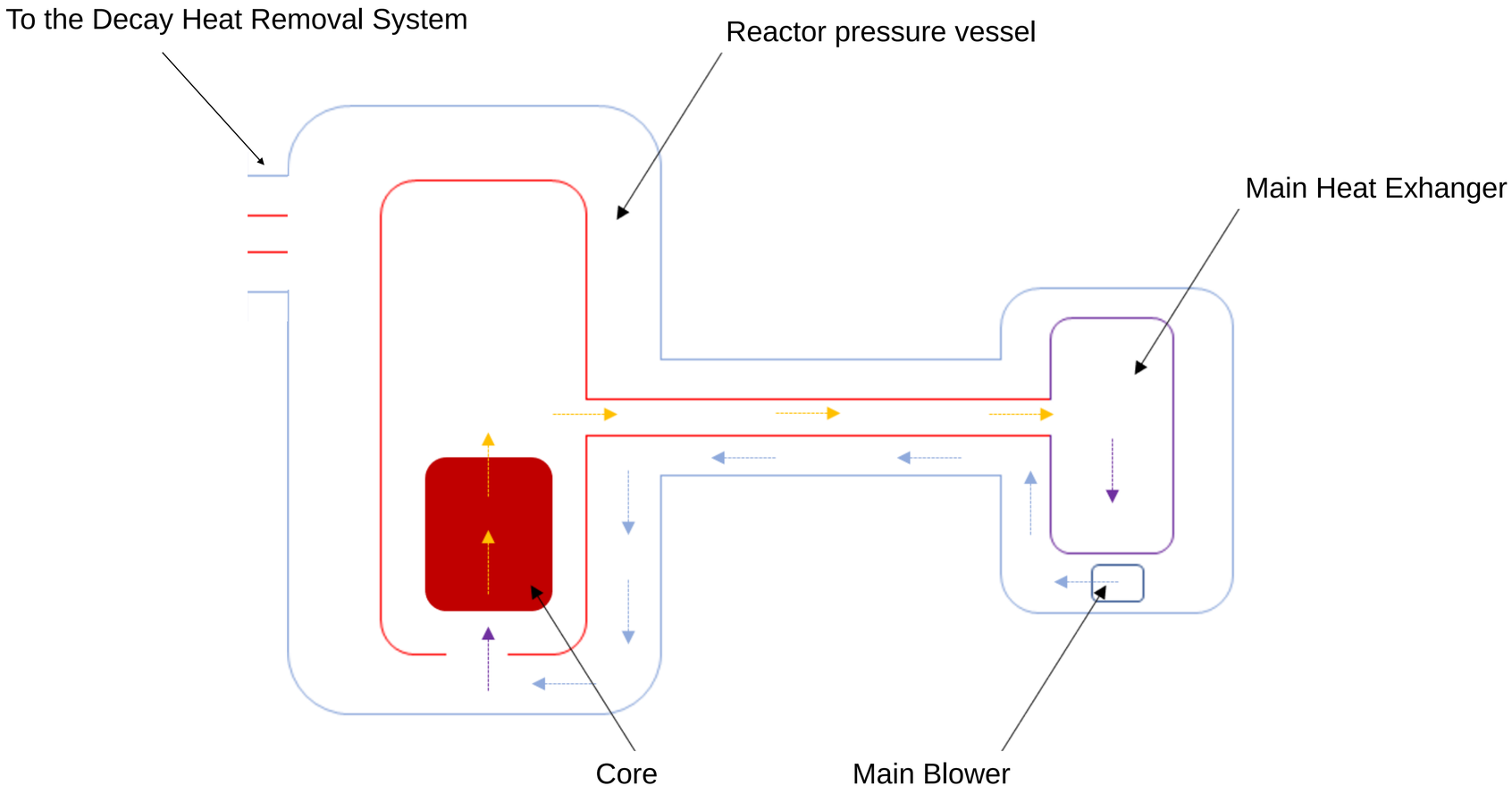

ALLEGRO – DRIVER CORE (MOX)

- MOX (25 % 239Pu enrichment) fuel
- Pin type, stainless steel cladding
- Fuel derived from Phénix reactor
- Wire-spaced fuel pins
- Control and shutdown SAs contain B4C in steel wrapper tubes
- Cladding and wrapper tubes made from AIM1 steel
- Experimental positions filled with steel dummies

Number of sub-assemblies	CEA 2009 First core
Experiment	6
Fuel	81
Control	6
Shutdown	4

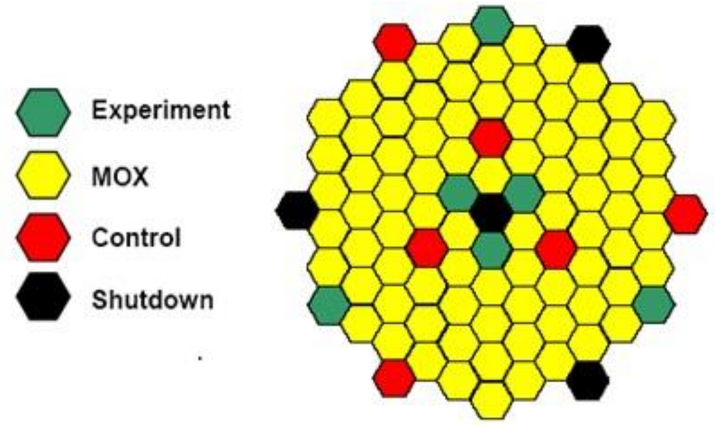

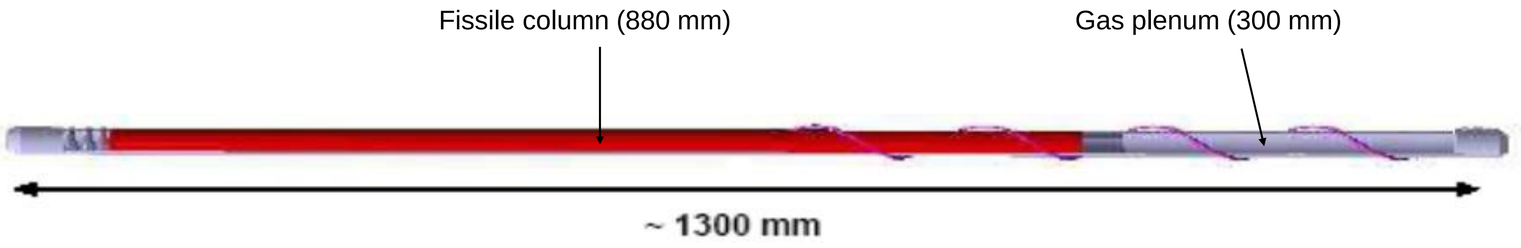

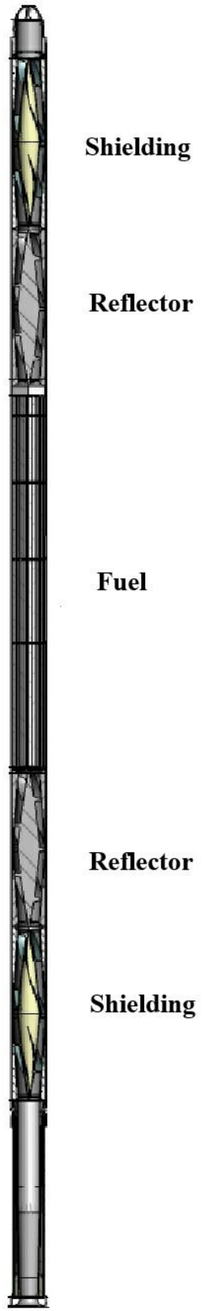

ALLEGRO – DRIVER CORE (MOX) – CFD ANALYSIS

- **No symmetry – very large mesh**
- **Total height of the domain: 3 854 mm**
- **Modelled in 3 steps:**
  - The inlet area up to the pin-bundle entry area
  - 1/20 of the fuel column
  - 2/20 of the fuel column

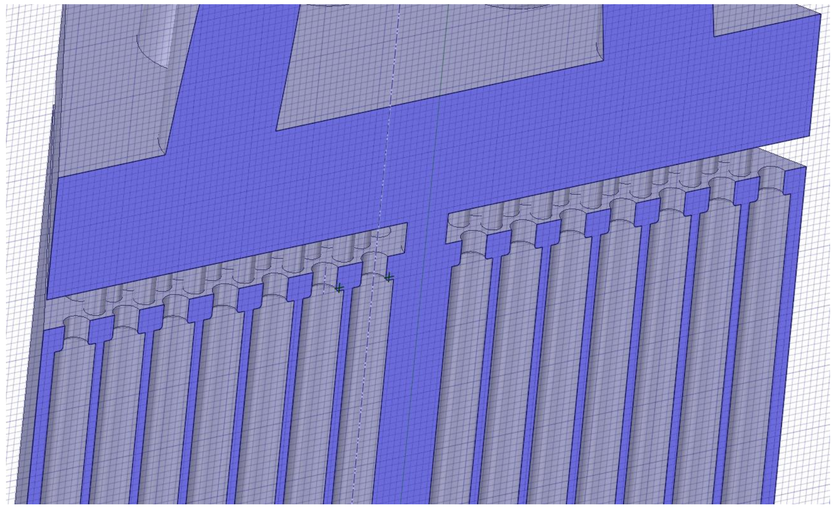

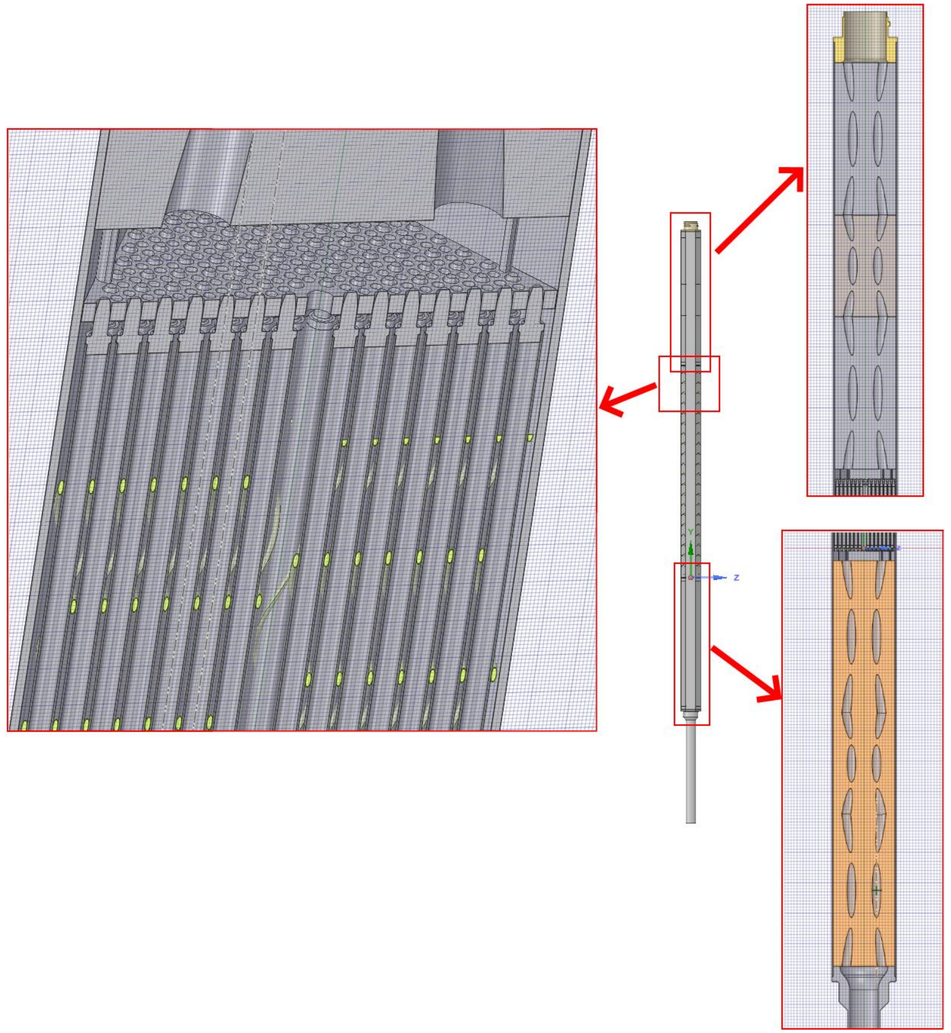

CFD ANALYSIS RESULTS

- **Problem: the un-even outlet velocity in one block adds up through the domain and causes significant differences in outlet temperature**

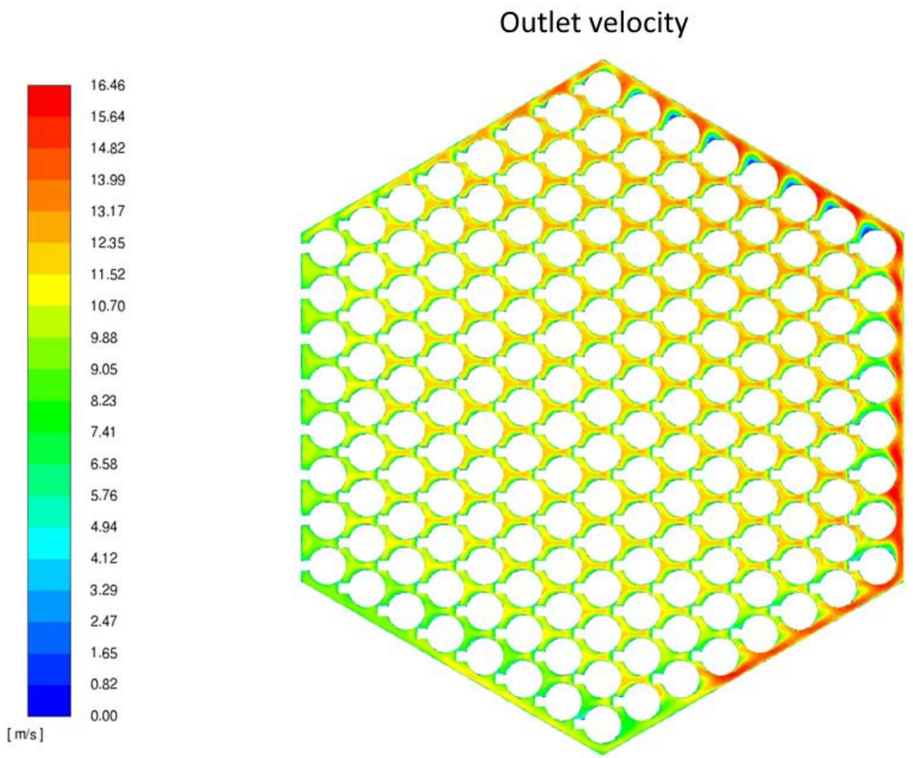

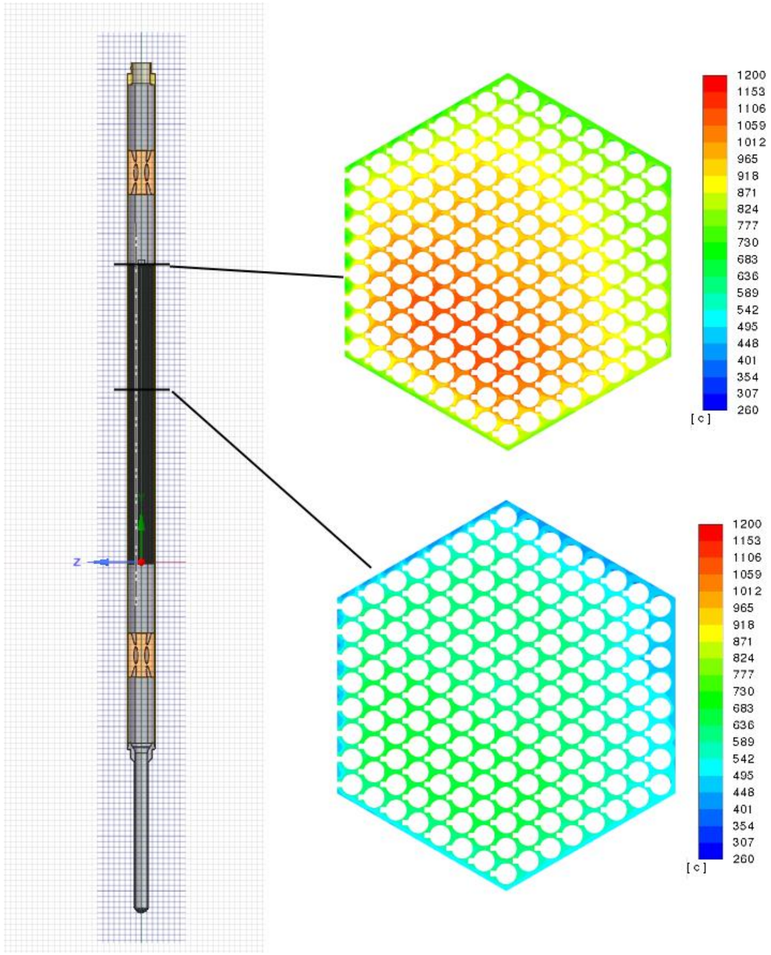

ALLEGRO – FUEL WITH SPACER GRIDS

Annals of Nuclear Energy 164 (2021) 108628

Contents lists available at ScienceDirect

Annals of Nuclear Energy

journal homepage: www.elsevier.com/locate/anucene

CFD modelling of mixing vane spacer grids for ALLEGRO relevant gas cooled reactor fuel geometry

Gergely Imre Orosz *, Attila Aszódi

Institute of Nuclear Techniques, Budapest University of Technology and Economics, Műegyetem rkp. 9, H-1111 Budapest, Hungary

- **Refractory core – spacer grid design**
  - Good mixing from the start
  - By using mixing vanes, the velocity/temperature profile is further equalized

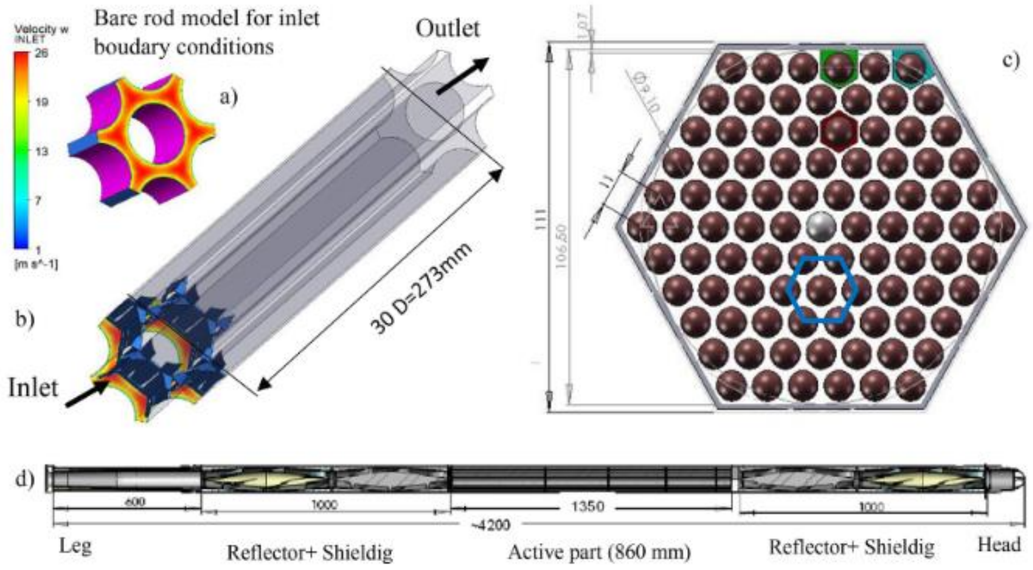

Fig. 2. ALLEGRO ceramic assembly and the geometry of the model.

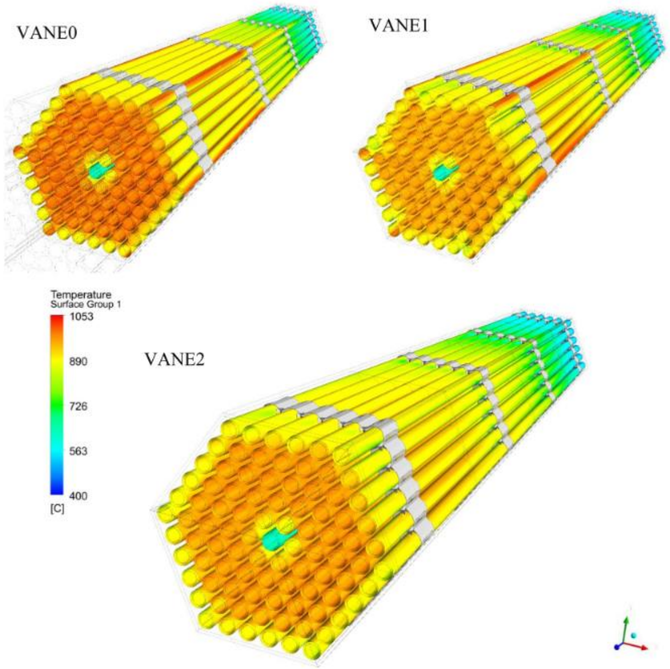

Fig. 32. Rod outer wall surface temperature distributions.

ALLEGRO – PRIMARY CIRCUIT

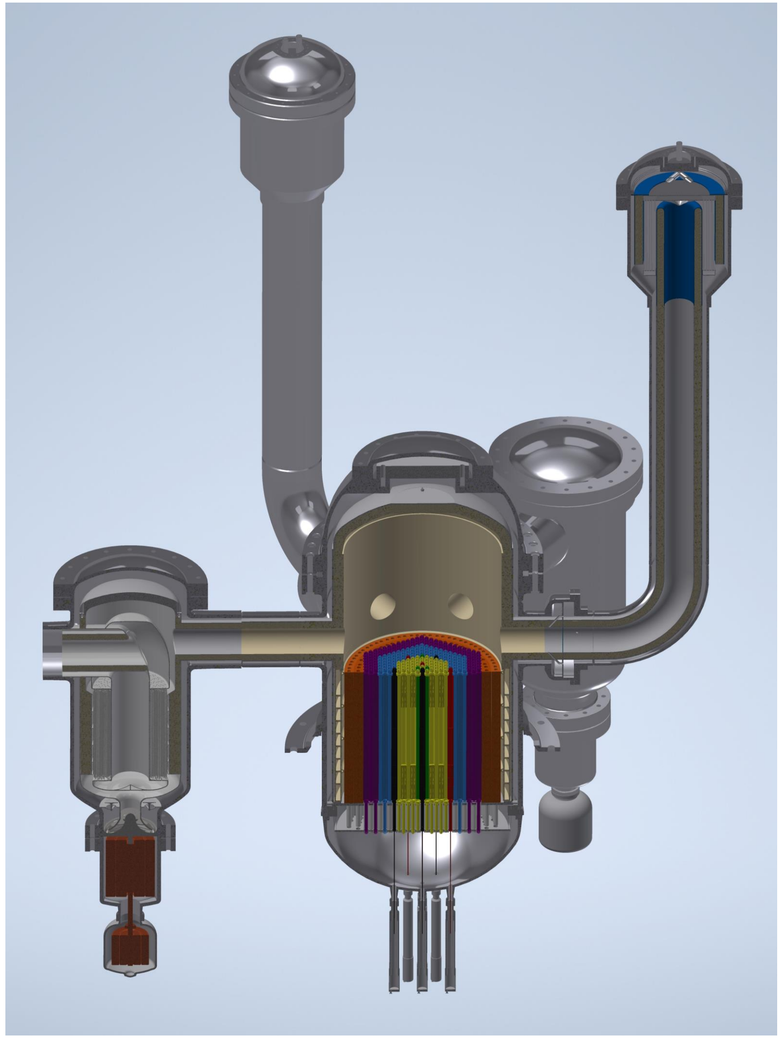

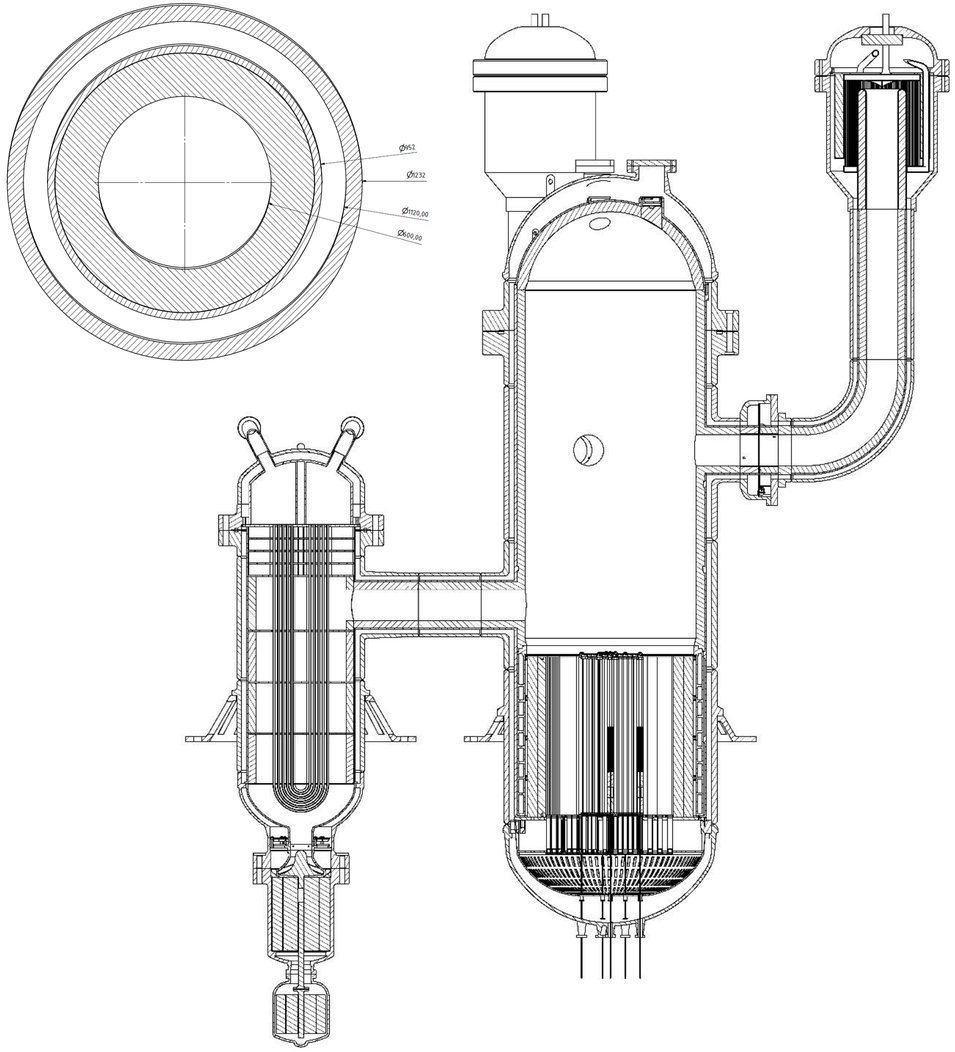

MAIN DUCT DESIGN – CROSS SECTION

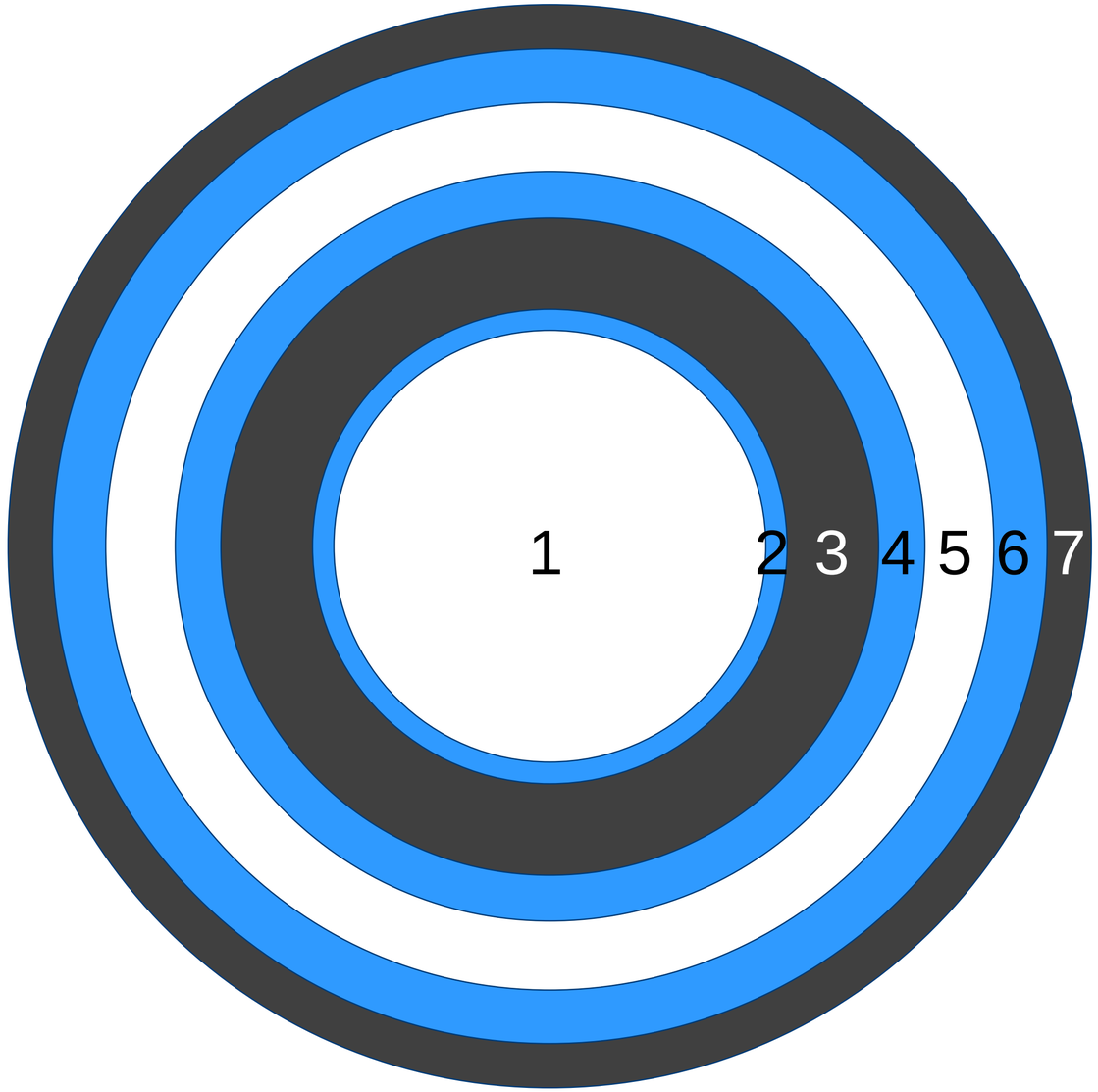

Helium

Metal

Insulation

1 - Hot duct medium (He)
2 - Hot duct liner
3 - Hot duct insulation
4 - Hot duct structural part
5 - Cold duct medium (He)
6 - Cold duct structural part
7 - Cold duct insulation

MAIN HEAT EXCHANGER DESIGN OVERVIEW

- **344 helical tubes**
  - Helium/helium helical shell-and-tube
  - DN16, 2 mm wall thickness
  - Total area 248 m2
  - Average length 11.5m
  - Average inclination 10°
  - Tubes made from INCONEL 617
- **Relatively compact desing**
  - Coaxial duct on both sides
  - Can be upscaled by lowering the inclination and adding more rows

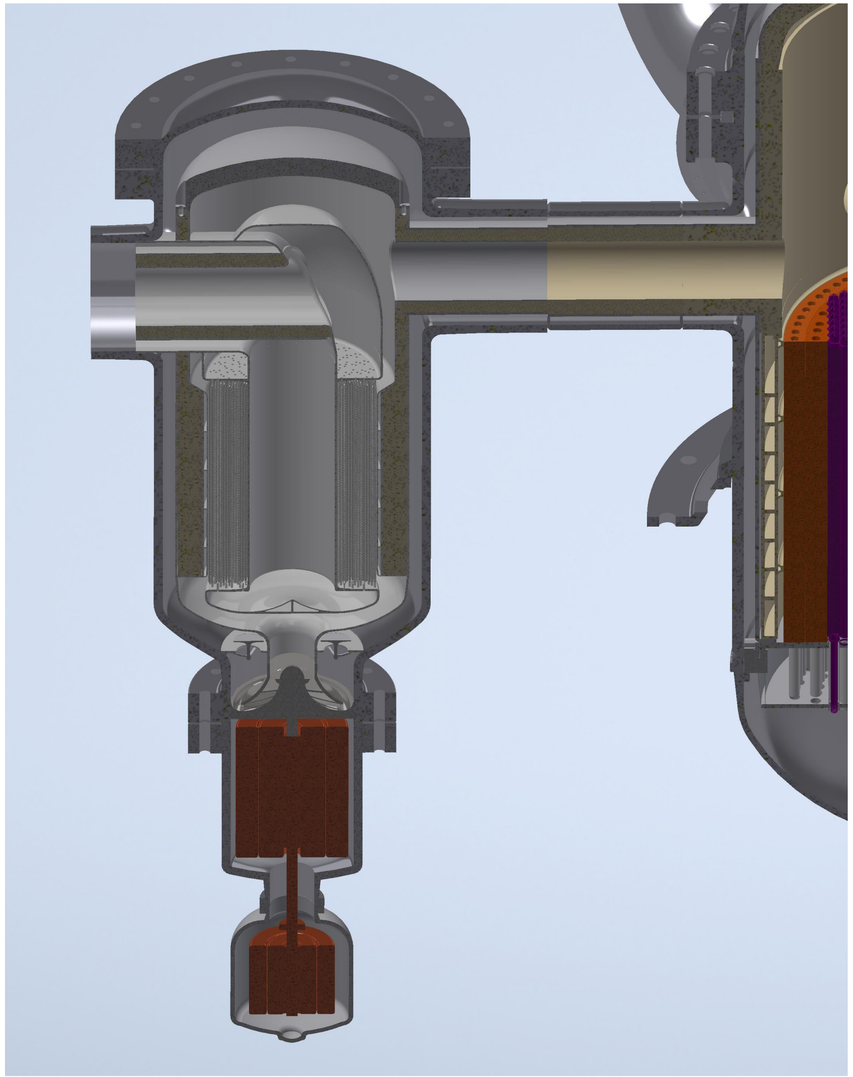

GAS-GAS HX HEAT TRANSFER COEFFICIENT

Nuclear Engineering and Design 251 (2012) 374–380

Contents lists available at SciVerse ScienceDirect

Nuclear Engineering and Design

journal homepage: www.elsevier.com/locate/nucengdes

Analysis of the influence of different heat transfer correlations for HTR helical coil tube bundle steam generators with the system code TRACE

Markus Esch[a,b,*], Antonio Hurtado[a], Dietrich Knoche[b], Wolfgang Tietsch[b]

[a] Technische Universität Dresden, George-Bähr-Str. 3b, 01069 Dresden, Germany
[b] Westinghouse Electric Germany GmbH, Dudenstraße 44, 68167 Mannheim, Germany

- **Complicated shape -> hard to find Nu number corelation**

The first Nusselt number correlation is a Grimison's equation applied to the THTR SG geometry. In Table 4 this correlation is refered to as V1:

$$Nu_{V1} = 0.271 \cdot (f_a \cdot Re)^{0.624} \cdot Pr^{1/3} \quad (4)$$

The second equation was the outcome of the steam generator exchange program for the heavy water gas cooled reactor (HWGCR) EL-4 in Brenellis, France (correlation V2):

$$Nu_{V2} = 0.0917 \cdot (f_a \cdot Re)^{0.725} \cdot Pr^{1/3} \quad (5)$$

The third and fourth equations were worked out by further helical coil tube bundle steam generator experiments (correlation V3):

$$Nu_{V3} = 0.16 \cdot (f_a \cdot Re)^{0.682} \cdot Pr^{1/3} \quad (6)$$

and correlation V4:

$$Nu_{V4} = 0.1135 \cdot (f_a \cdot Re)^{0.714} \cdot Pr^{1/3} \quad (7)$$

The fifth correlation applies to helix bundles coiled in the same direction (V5):

$$Nu_{V5} = 0.238 \cdot (f_a \cdot Re)^{0.634} \cdot Pr^{1/3} \quad (8)$$

And the sixth equation is for helix bundles coiled in the opposite direction (correlation V6):

$$Nu_{V6} = 0.1286 \cdot (f_a \cdot Re)^{0.692} \cdot Pr^{1/3} \quad (9)$$

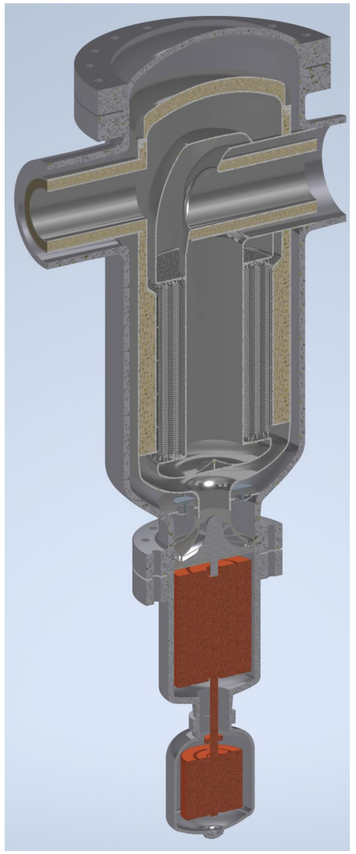

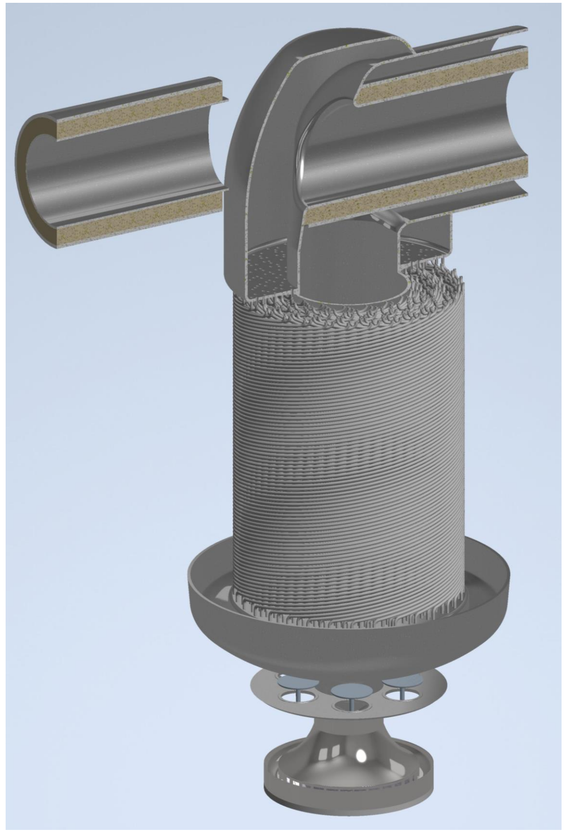

MAIN LOOP ISOLATION VALVES

- **Fully passive design**
  - Open with overpressure created by the main blower
  - When the blower is tripped, after the force drops under a certain limit, it closes automatically
  - Simple and (hopefully) reliable design – under investigation

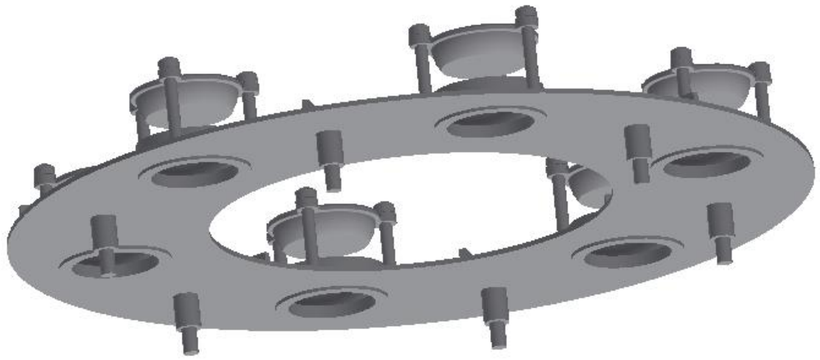

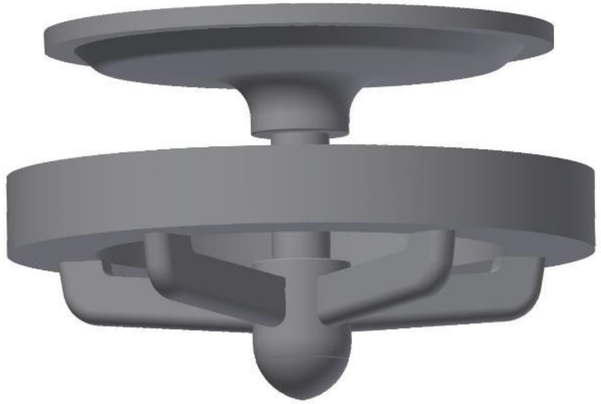

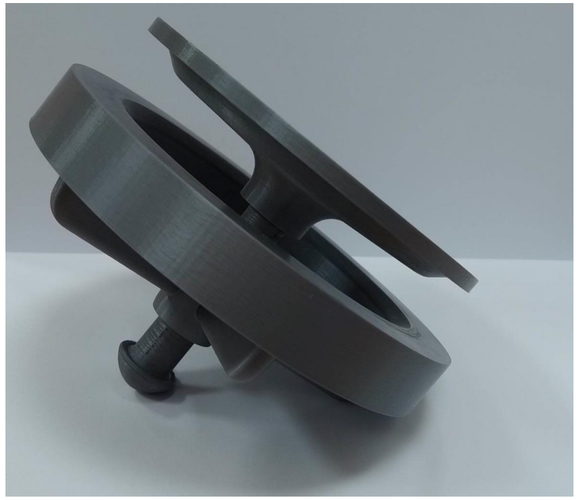

ISOLATION VALVE FUNCTION ANALYSIS

Valve closure on start-up

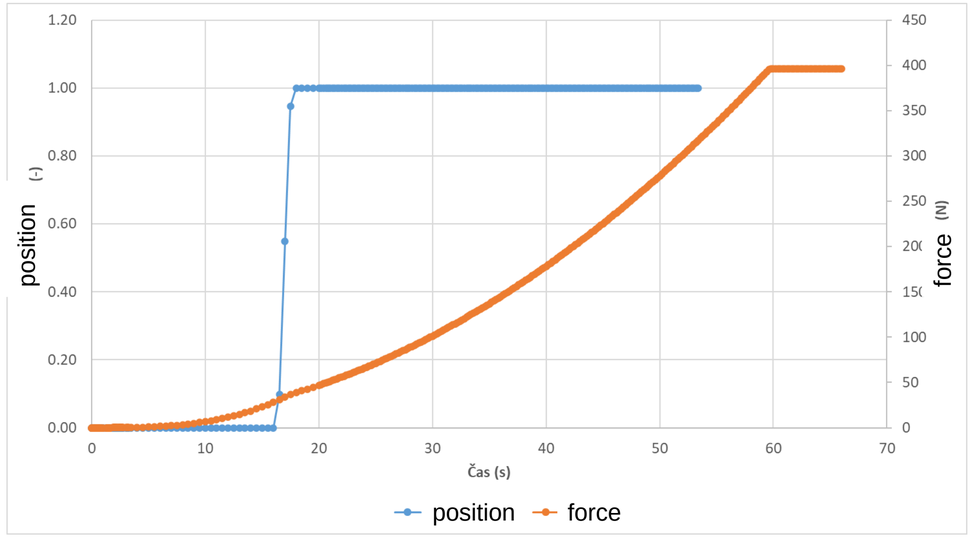

Detailed view

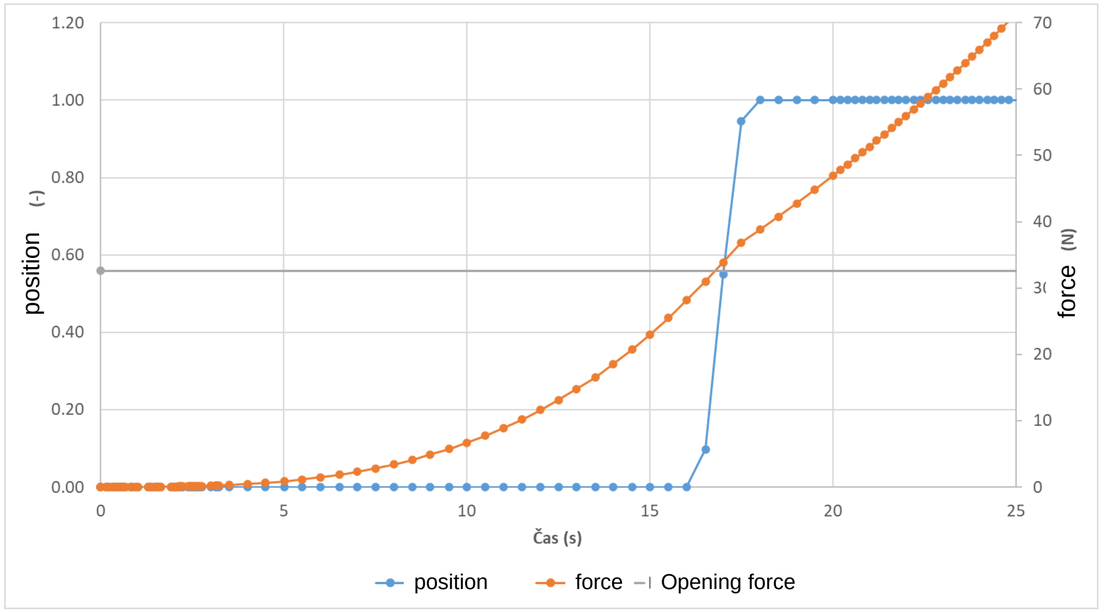

TESTING THE FUNCTION AND RELIABILITY

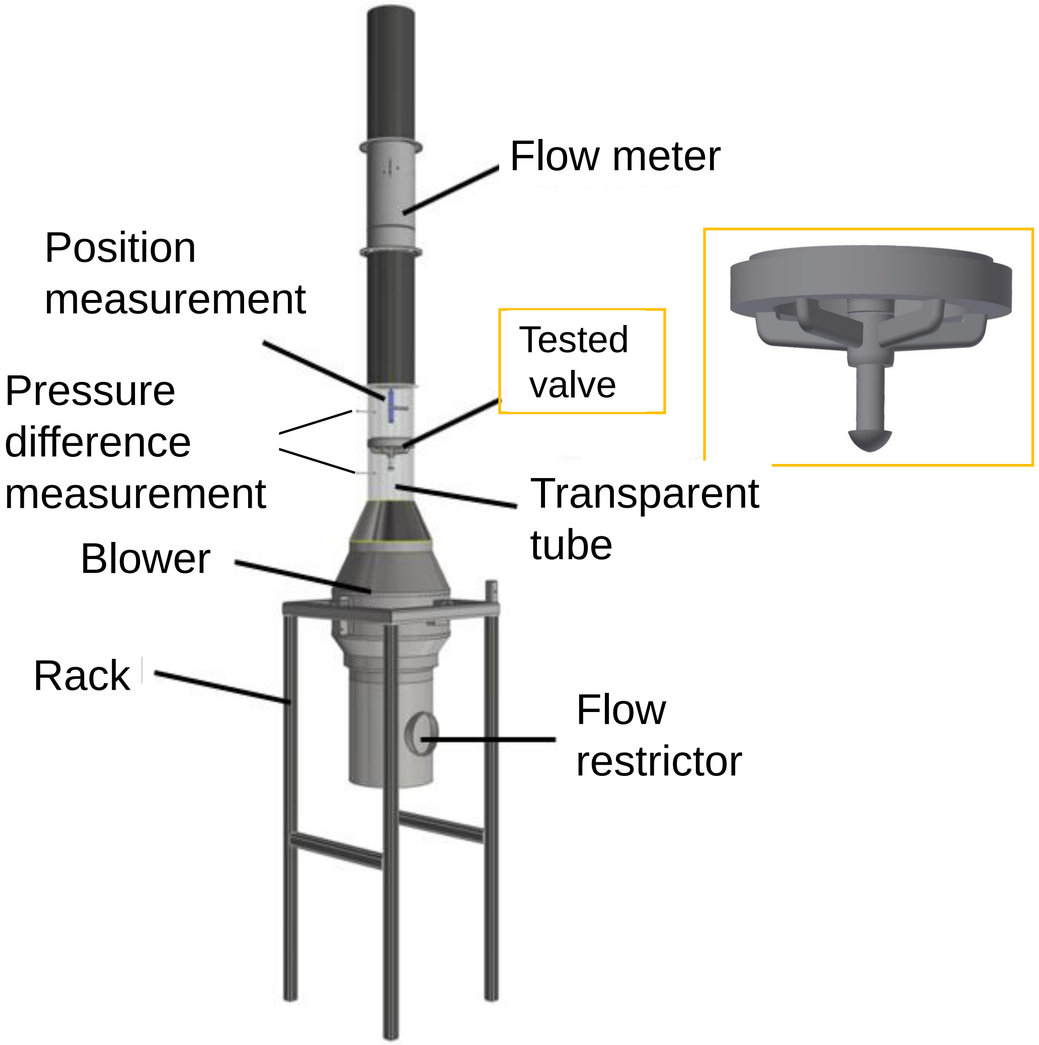

DECAY HEAT REMOVAL (DHR) SYSTEM

- **Dedicated cooling loops**
- **Key safety system in pressurized transients**
- **Ensuring uninterupted coolant flow through the core**
- **Three main parts**
  - Heat Exchanger (Helium / water shell-and-tube)
  - Connecting coaxial duct
  - Preconditioning device

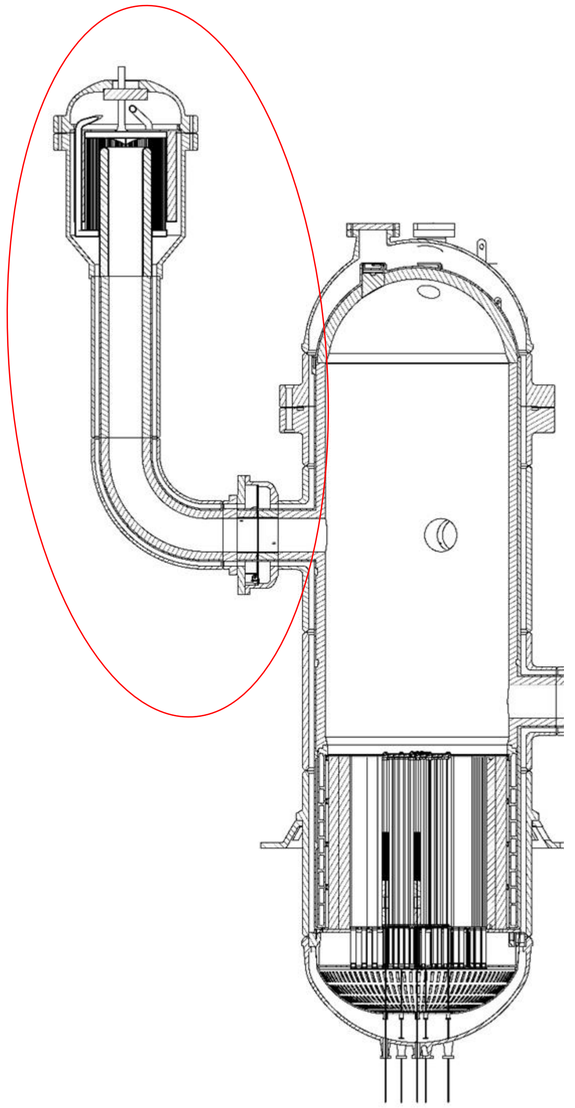

IMPROVING PERFORMANCE IN NATURAL CONVECTION

- **Natural cirulation in closed systems is dependant on:**
  - Elevation of cooler above the heater
  - Density difference of hot and cold medium
  - Proper geometry of the circuit

$$\Delta p_{driving} = (\rho_{cold} - \rho_{hot}).h.g$$

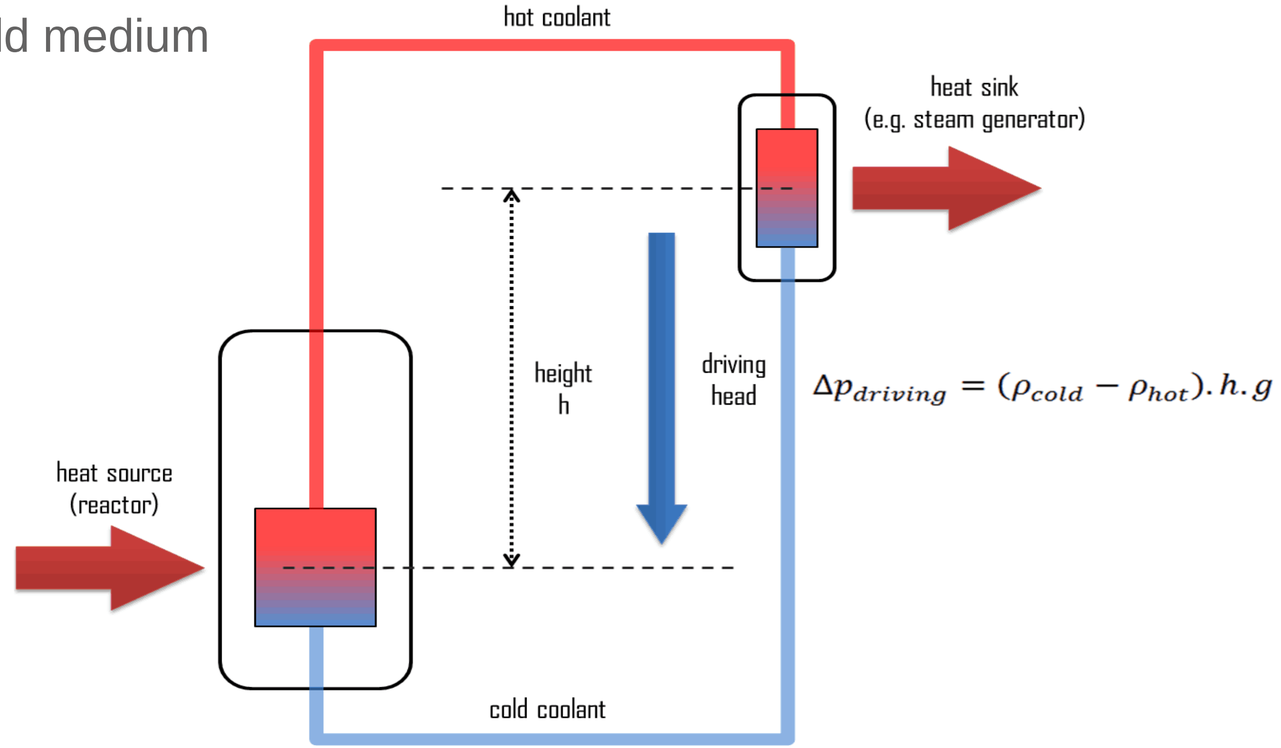

NATURAL CONVECTION (2)

$$\Delta p_{driving} = (\rho_{cold} - \rho_{hot}).h.g$$

- The equation suggest, that the driving force is linear function of height difference
- However, with decreased driving force, the temperature of hot medium will rise – if we keep the temperature of the cold medium the same (as in ALLEGRO DHR systém), the difference of densities rises
- Lowering of the hydraulic ressistance of the circuit has positive effect without regards to the above-mentioned facts (in ALLEGRO where friction losses are generally low)

EFFECT OF DHR SYSTEM ELEVATIONS – SIMPLIFIED STUDY

- Simplified model – detailed core, but only 1 DHR loop (no main loops)
- Initial and boundary conditions:
  - DHR MX secondary side – water, fixed at 1MPa, 160°C
  - Power equal to decay power of ALLEGRO
  - Initial core inlet/outlet temperature 260°C/530°C
  - Initial flow velocity 0 m/s
  - Initial pressure in the system 1 MPa or 7MPa
- 8 different elevations of the DHR system (5,7,10,13,15,17,20,30 meters)
- All calculations done for both initial pressures
- 16 cases in total

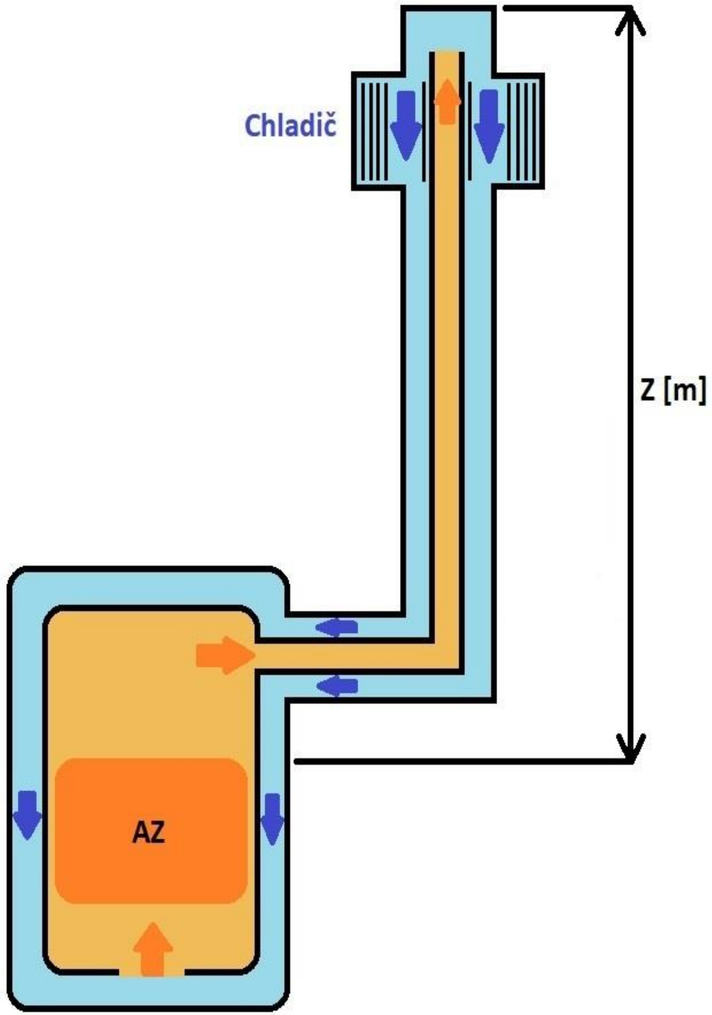

EFFECT OF DHR SYSTEM ELEVATIONS – SIMPLIFIED STUDY RESULTS – MAXIMUM CLAD T AT 7MPA

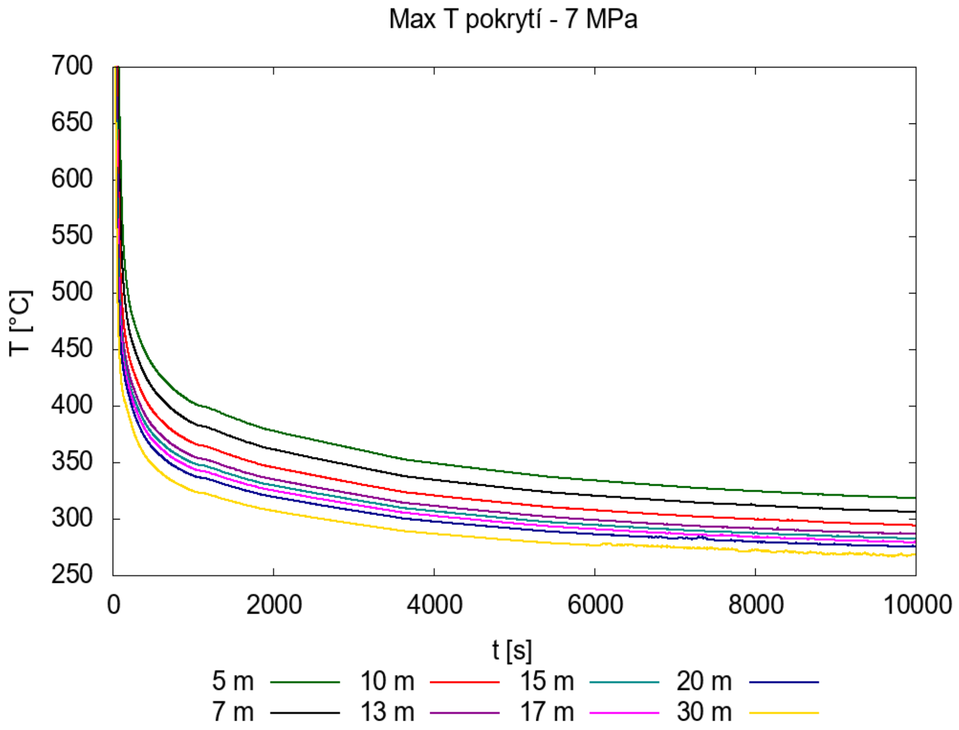

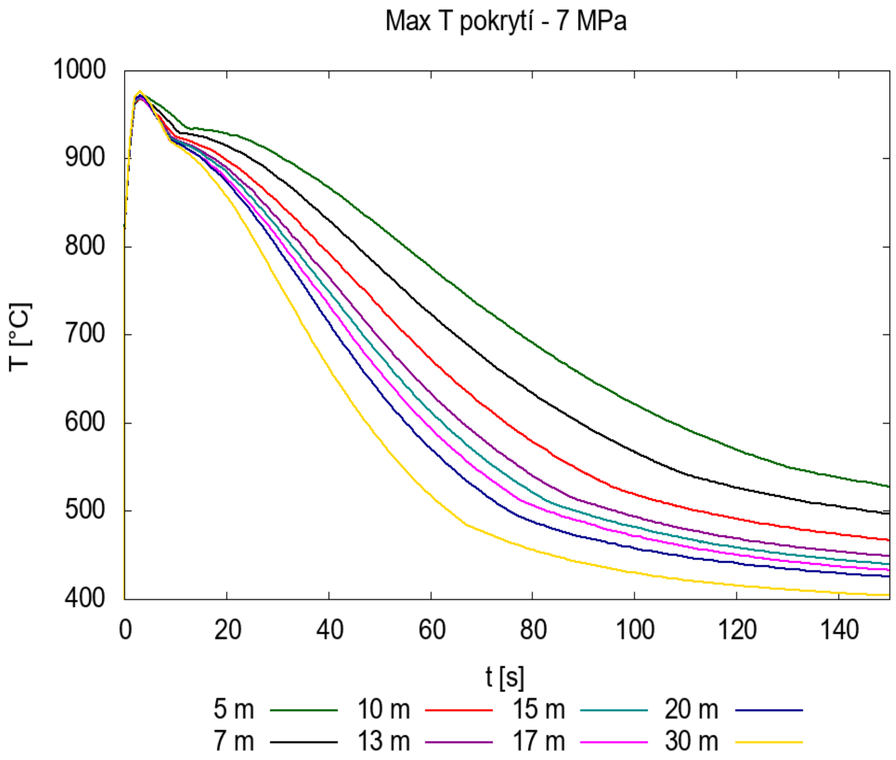

EFFECT OF DHR SYSTEM ELEVATIONS – SIMPLIFIED STUDY RESULTS – DRIVING PRESSURE AT 7MPA

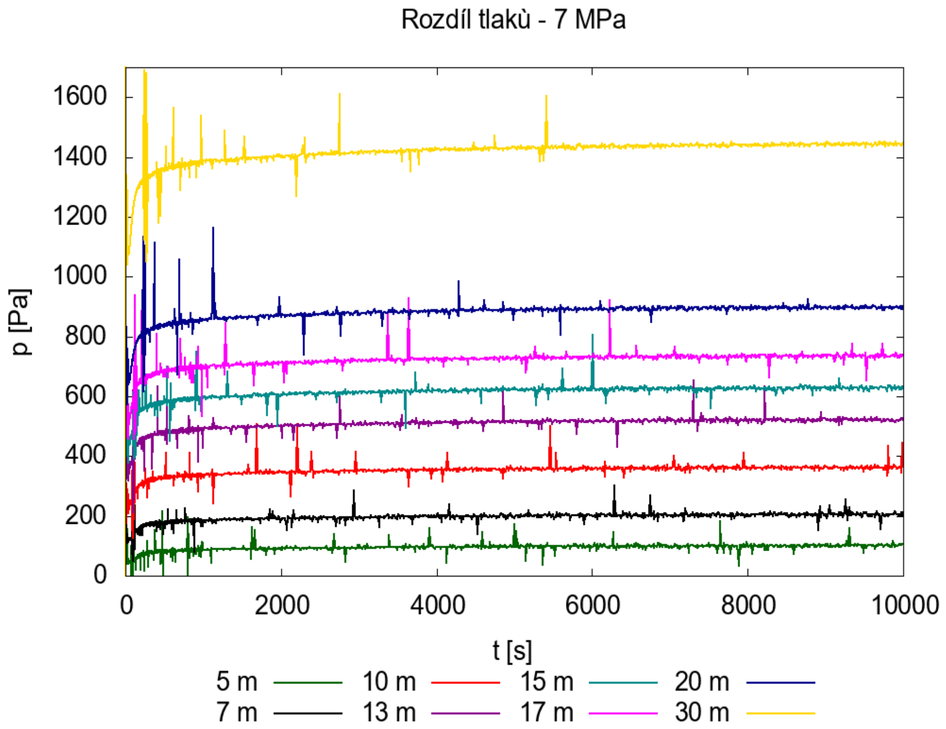

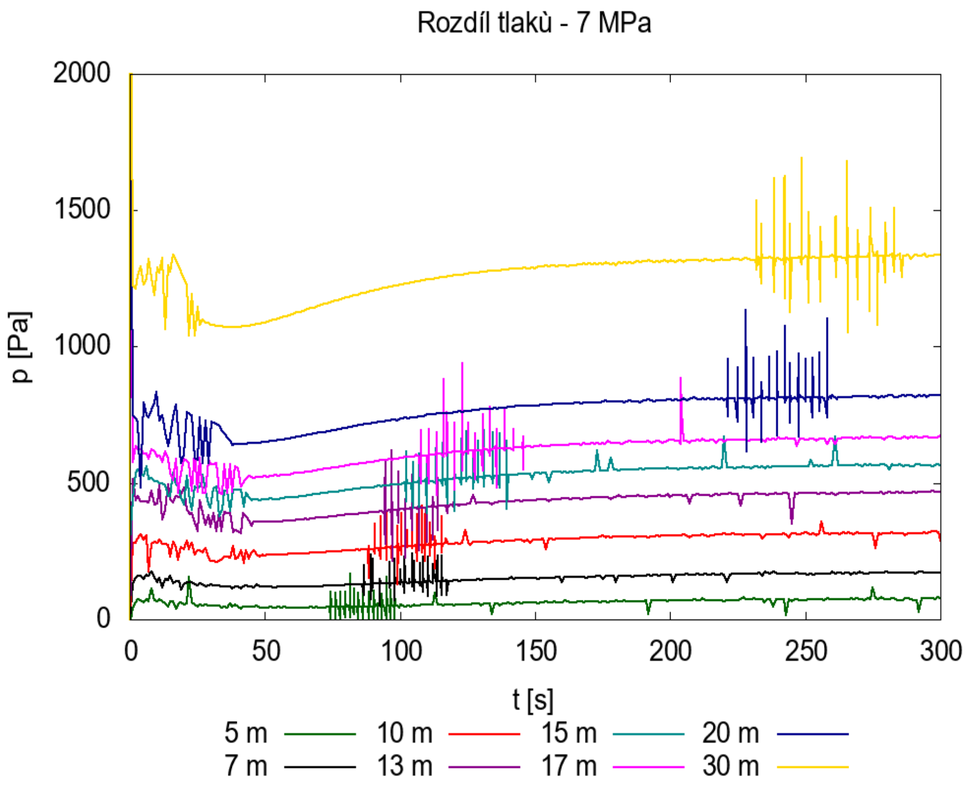

EFFECT OF DHR SYSTEM ELEVATIONS – SIMPLIFIED STUDY RESULTS – DENSITY DIFFERENCE AT 7MPA

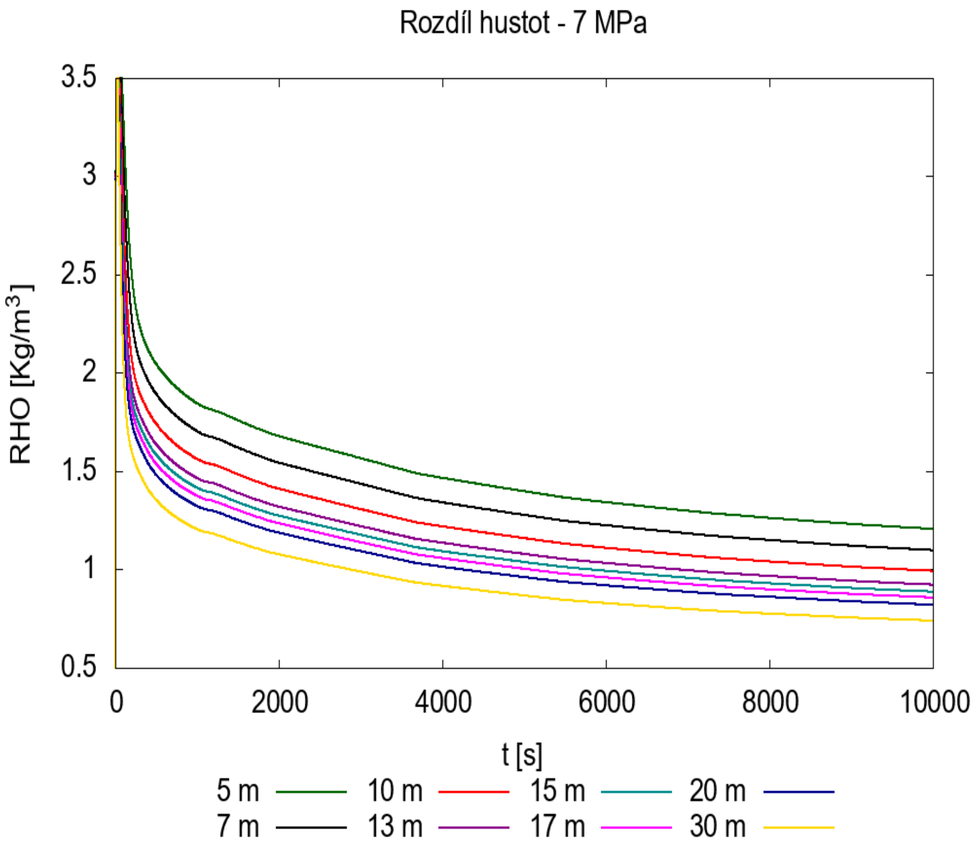

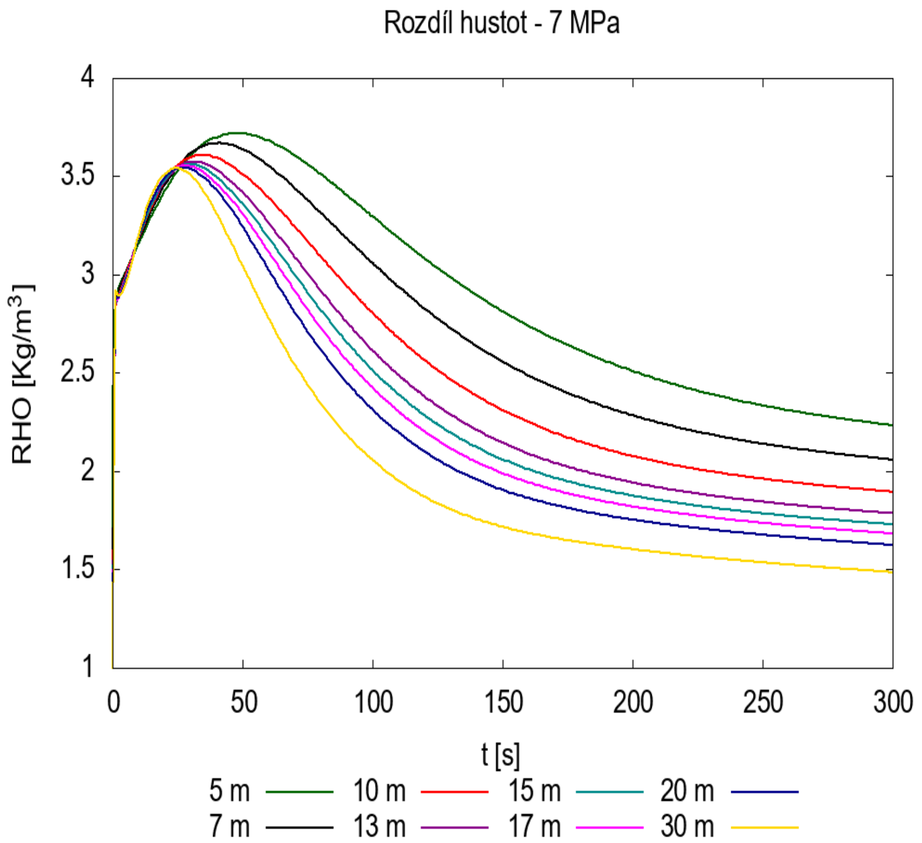

EFFECT OF DHR SYSTEM ELEVATIONS AND PRESSURE RESISTANCE

- Full MELCOR ALLEGRO model
- 2 basic scenarios:
  - SBO
  - LOCA 75mm + SBO, 3x200m3 N2 accumulators available
- For each scenario: Case with 1 DHR loop available (A) and 3 DHR loops available(B)
- For each case – three levels of pressure drop coefficient of the DHR blower (see the table)
- For each case – DHR system at standard elevation, -5m and +5m.
- 36 cases in total (2*18)

DHR Elevation		A1	A3	A5	B1	B3	B5
10m	DHR loops	1	1	1	3	3	3
	ξ blower	72	18	0	72	18	0
15m	DHR loops	1	1	1	3	3	3
	ξ blower	72	18	0	72	18	0
20m	DHR loops	1	1	1	3	3	3
	ξ blower	72	18	0	72	18	0

LOCA+SBO RESULTS – MAX. CLADDING TEMPERATURE – SCENARIOS A (1DHR LOOP)

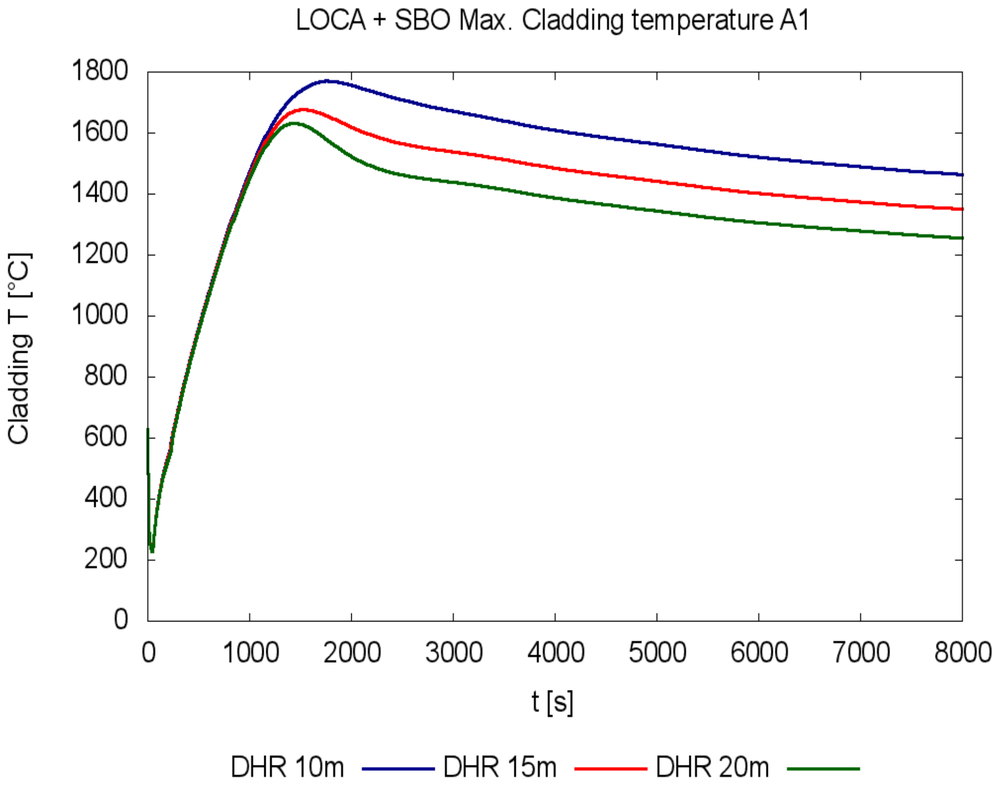

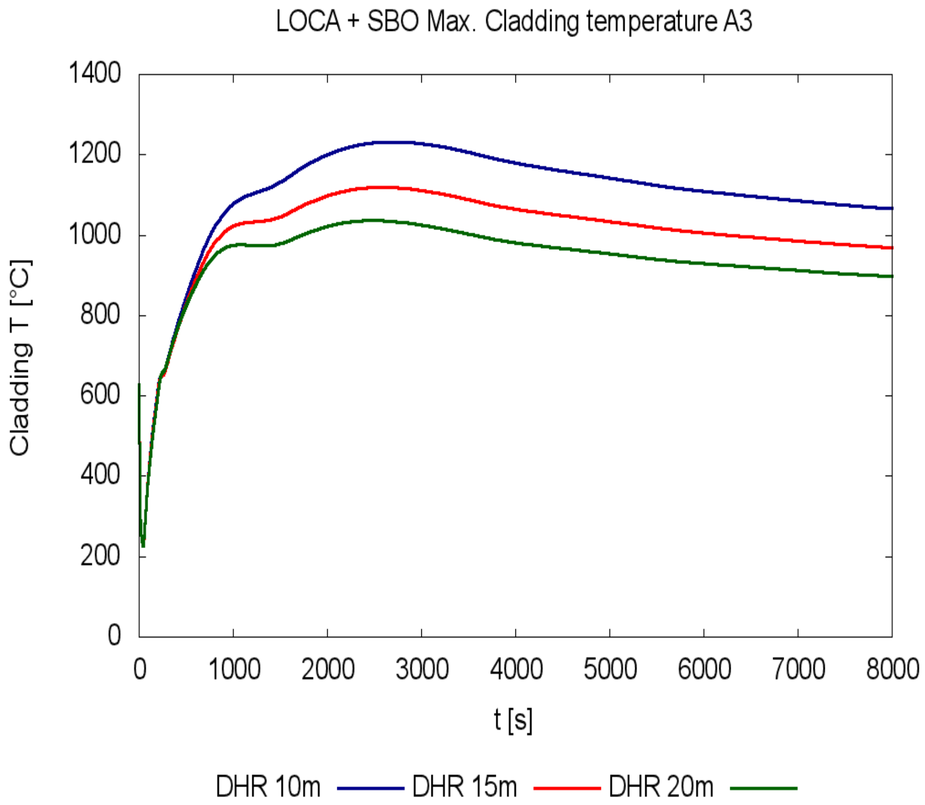

LEGACY DHR HX DESIGN

- **U-Tubes**
  - Problems with natural convection in the cooling (water) circuit
  - Good coping with thermal expansion
  - Poor compactness

- **Cold and hot water plenum**
  - Very complicated design
  - High pressure loss coef.
  - Would be challenging to manufacture
  - Possible problems with leak-tightness

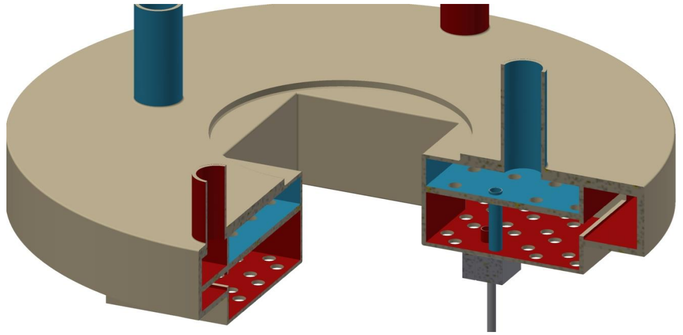

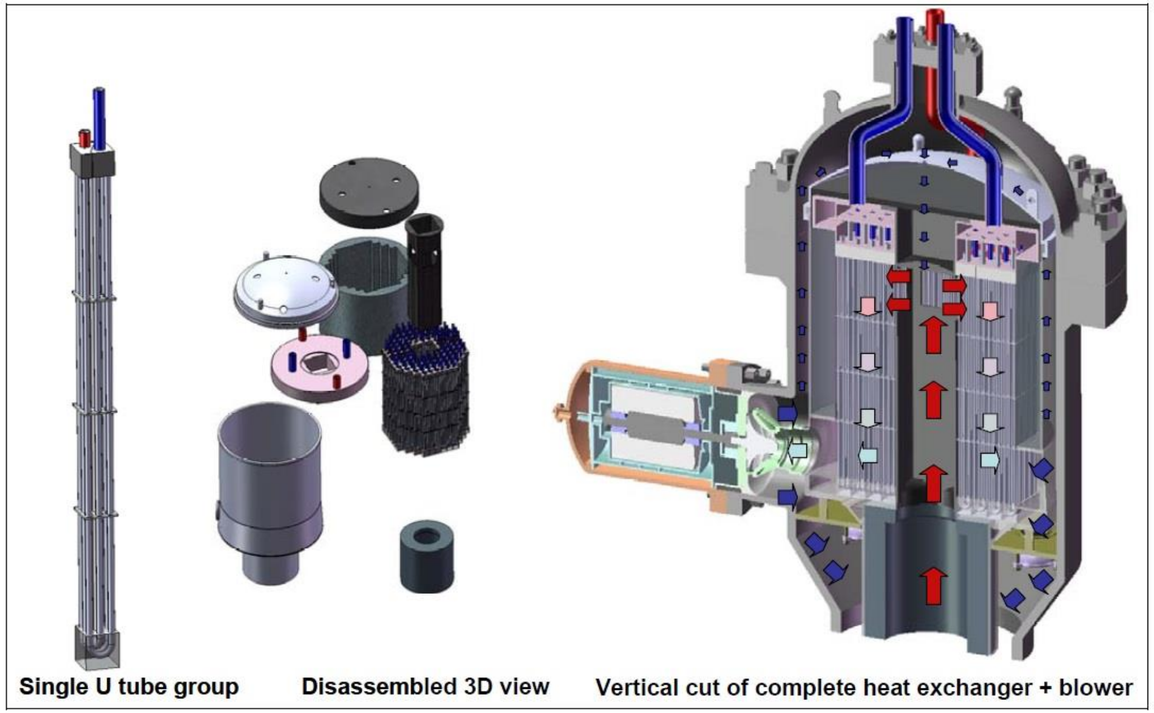

NEW DHR HX DESIGN

- **No blower**
  - Very low pressure loss coeff due to simplified design
- **Straight tubes**
  - Ideal for natural convection in the cooling (water) circuit
  - Potential problems with thermal expansion
  - Better compactness
- **Cold and hot water plenum**
  - Simplified design
  - Separated plenums
  - Easy to manufacture and more reliable
  - No problems with higher pressure in the water circuit if needed

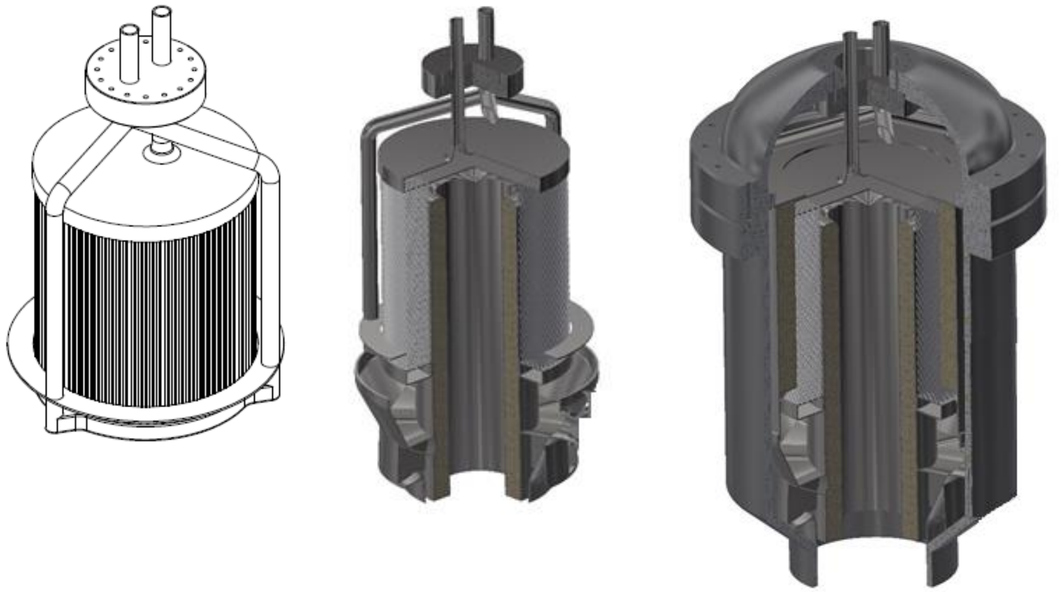

PRECONDITIONING DEVICE

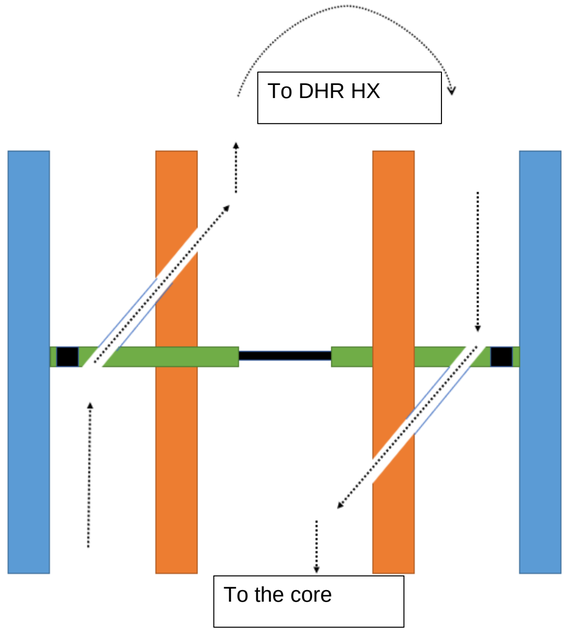

System in the pre-conditioning settings

Closed valves
Hot duct walls
Cold duct walls
Plate
Coolant flow

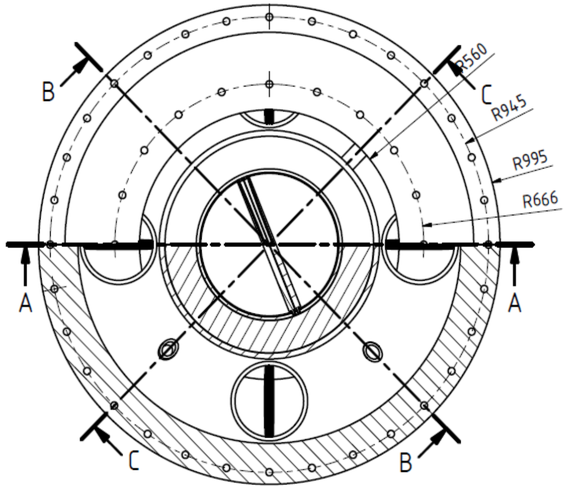

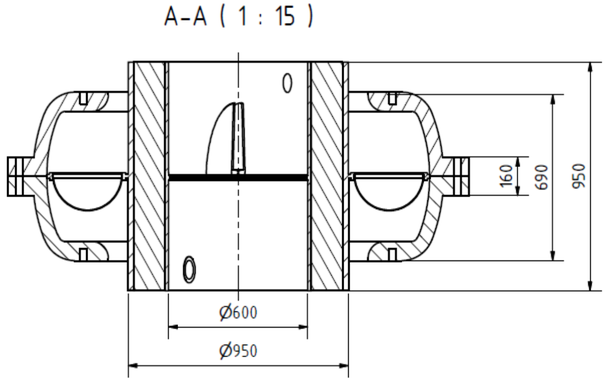

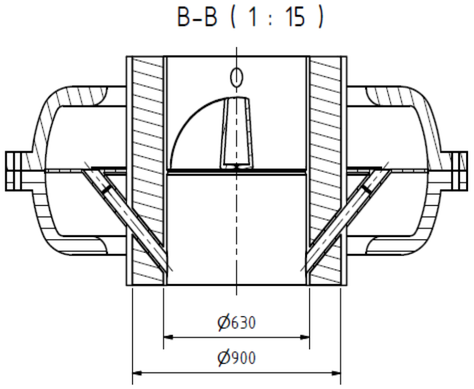

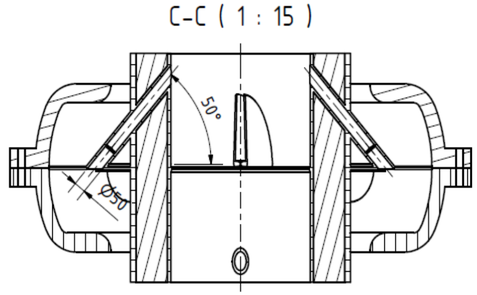

Decay heat removal system – new design

- **Dedicated system:**
  - Fully passive, based on natural convection
  - Severely reduced hydraulic resistance
  - Continuously pre-conditioned during normal reactor operation with a small controlled primary coolant flow
  - Key safety systems in LOFA
  - 2 x 100 % loops
  - Patented in the Czech Republic, international patent pending

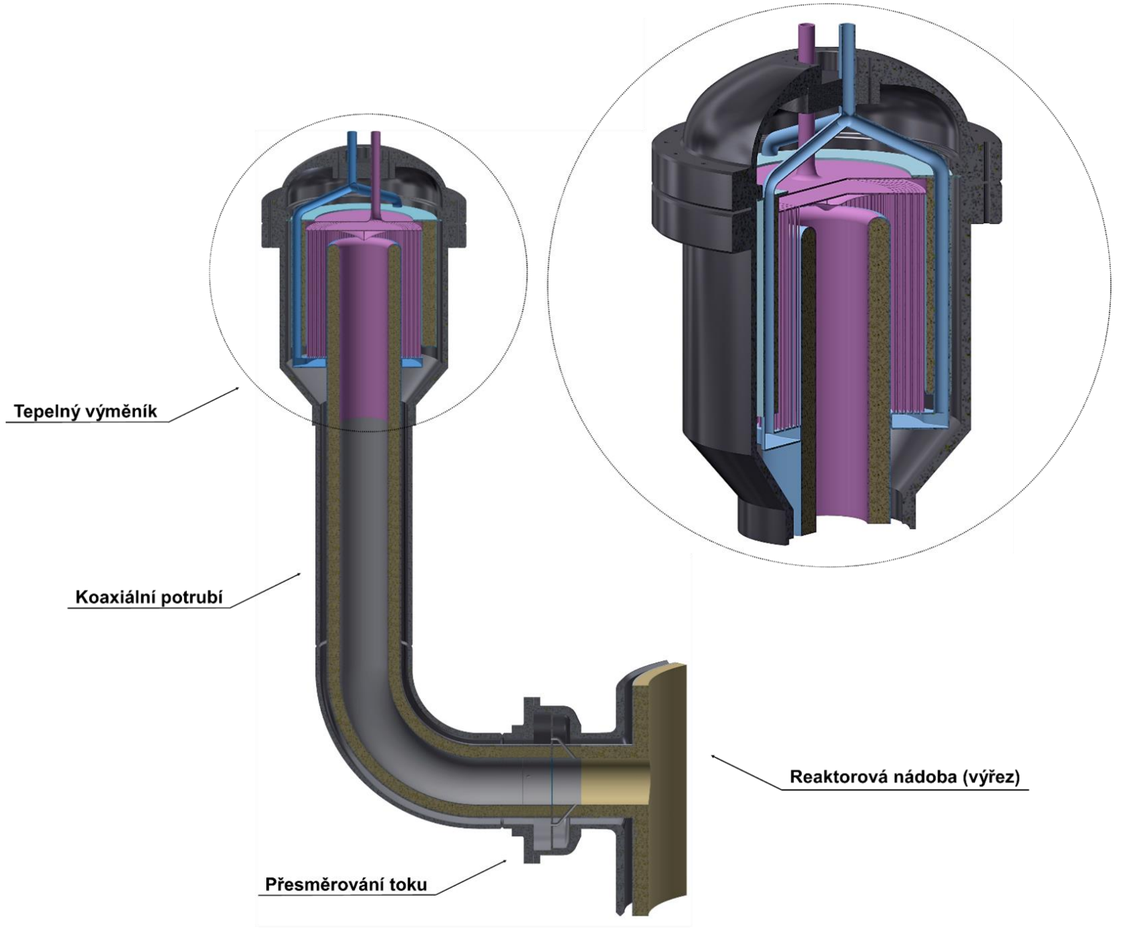

CFD MODELLING OF THE PRECONDITIONING DEVICE

- **Goal of the CFD study:**
  - Small leakage through the largest valve
  - Simulation of real operation
  - To find how much compromised the device become with small leakages in the device

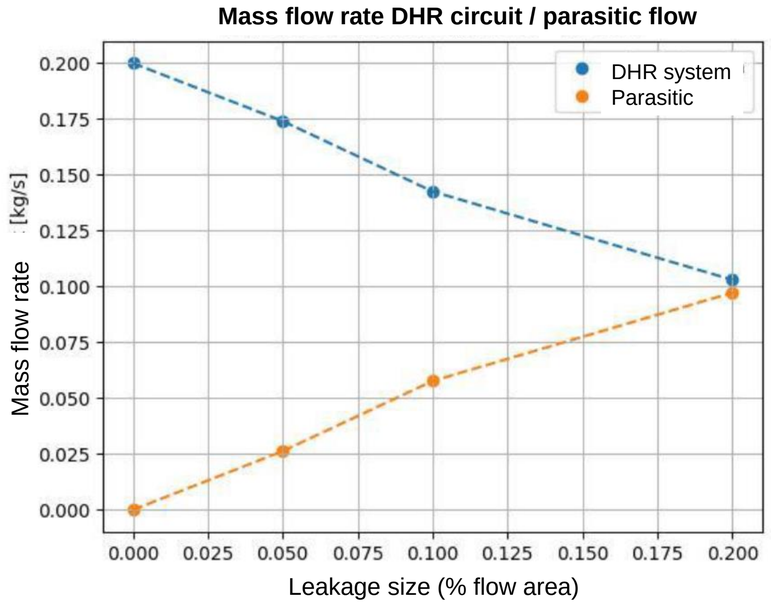

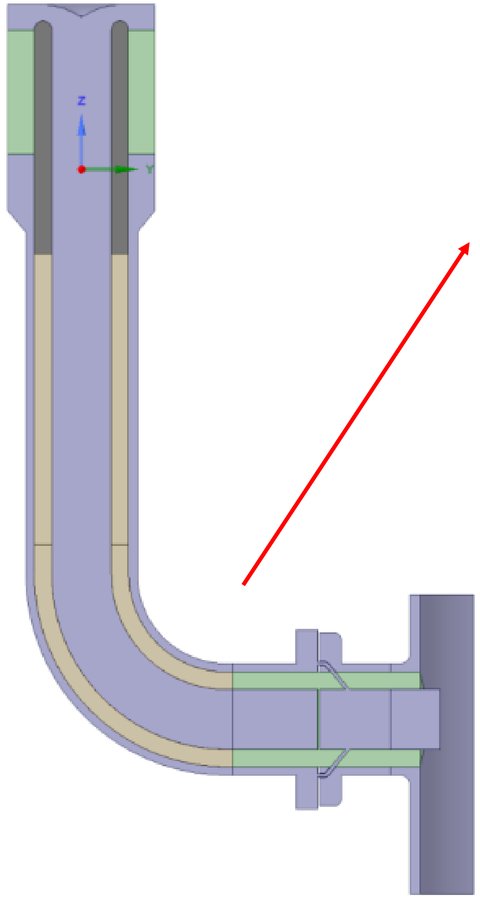

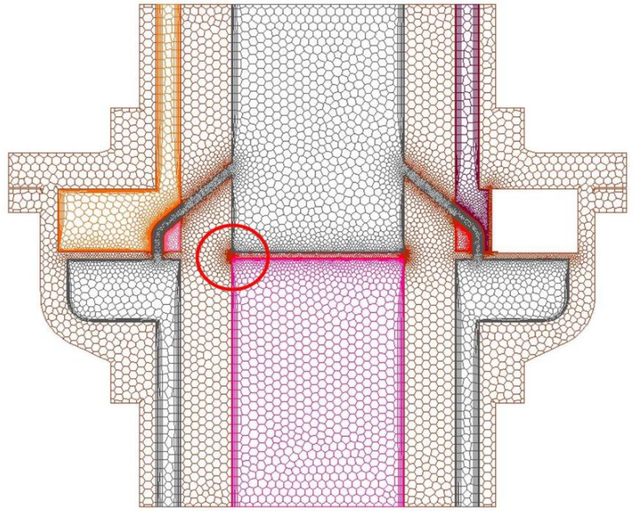

SEVERE ACCIDENTS IN GFRS

- **SA phenomenology**
  - Quite different from other fast-reactor types. Not as high risk of a CDA (core disruptive accident), the accident progression more like in PWRs, but faster
  - Reactivity-induced accidents remain the limiting events, however, their effect is usually more local (no coolant boiling and induced problems)
  - Corium relocation to the lower plenum, RPV failure and ex-vessel phase is usually possible – another difference from liquid metal-cooled fast reactors
  - Various computer codes can be used – MELCOR as the integral one, SIMMER for detailed core degradation simulation

TYPICAL SEVERE ACCIDENT PROGRESSION IN GFR

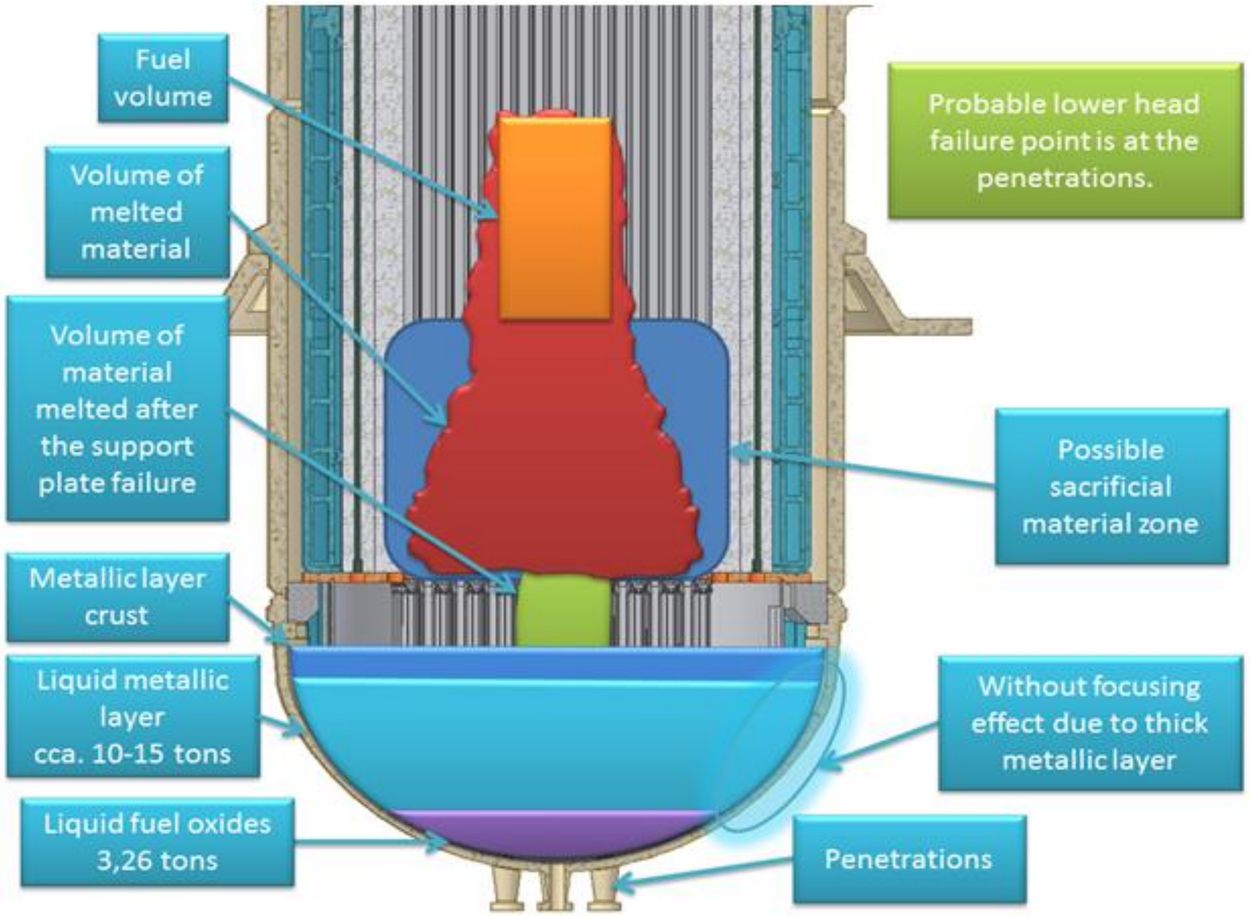

MELCOR SIMULATION RESULTS EXAMPLE

SBO + SB-LOCA + Failure of gas injection, in the driver core configuration

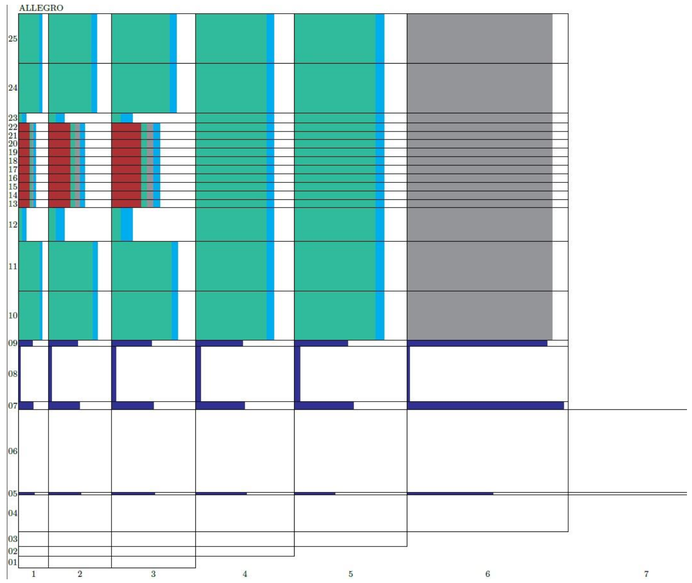

Normal operation

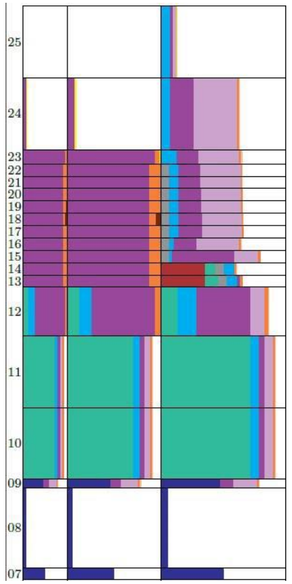

a) t = 4 h

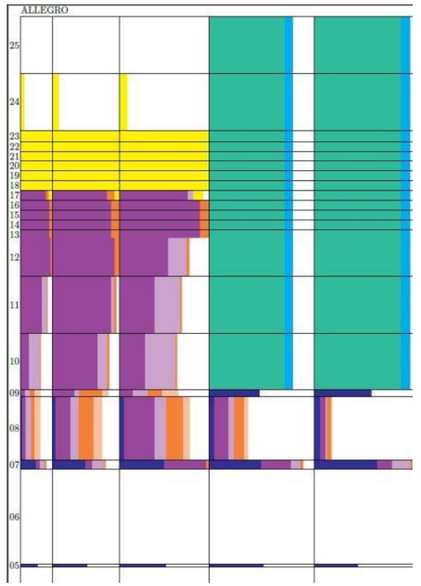

b) t = 18 h

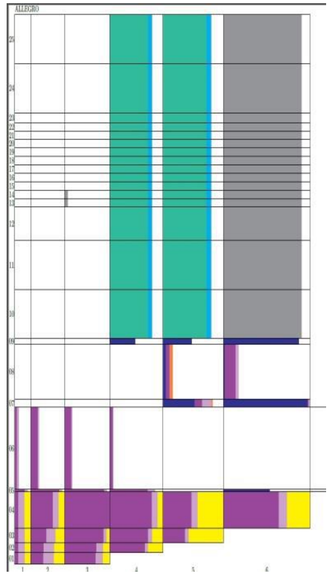

c) t = 23 h

Fuel | constr. mater. | cladding | shield. | support plate | helium | debris | melt

Thanks for the attention!

Petr.Vacha@ujv.cz

ÚJV Řež, a. s.
Hlavní 130, Řež
250 68 Husinec, Czech Republic

e-mail: sales@ujv.cz
www.ujv.cz

Skupina ÚJV
LIDÉ I INOVACE I TECHNOLOGIE

Jacobs

Challenging today.
Reinventing tomorrow.

UK Gas Reactors Operational Feedback

Richard Stainsby

So why do we need nuclear power ?

UK Gas-cooled Reactors

- Due to the UK's pioneering position in reactor technology the licensing standards had to evolve to match the evolution of reactor technology.
- In the earliest days a regulator did not exist.
- The Windscale Pile 1 fire in 1957 led to the creation of first an internal regulator (the Safeguards Group) and then to a truly independent regulatory body.

- There have been two previous generations of gas cooled reactors:
  - Windscale Piles – air-cooled (plus small experimental air-cooled reactors at Harwell)
  - Magnox Reactors – CO_2 cooled
  - Advanced Gas-cooled Reactors (AGR) - CO_2 cooled

- Plus one He-cooled experimental High Temperature Reactor (HTR) - Dragon

A Brief and Inconcise History of UK Gas Cooled Reactor Families

- 1947, Windscale Piles, UK - Military plutonium production
- Atmospheric air cooled, graphite moderated reactors
- Low temperature
- Open cycle
- Natural uranium metal fuel in aluminium cladding.

Lorna Arnold OBE, 1915 - 2014

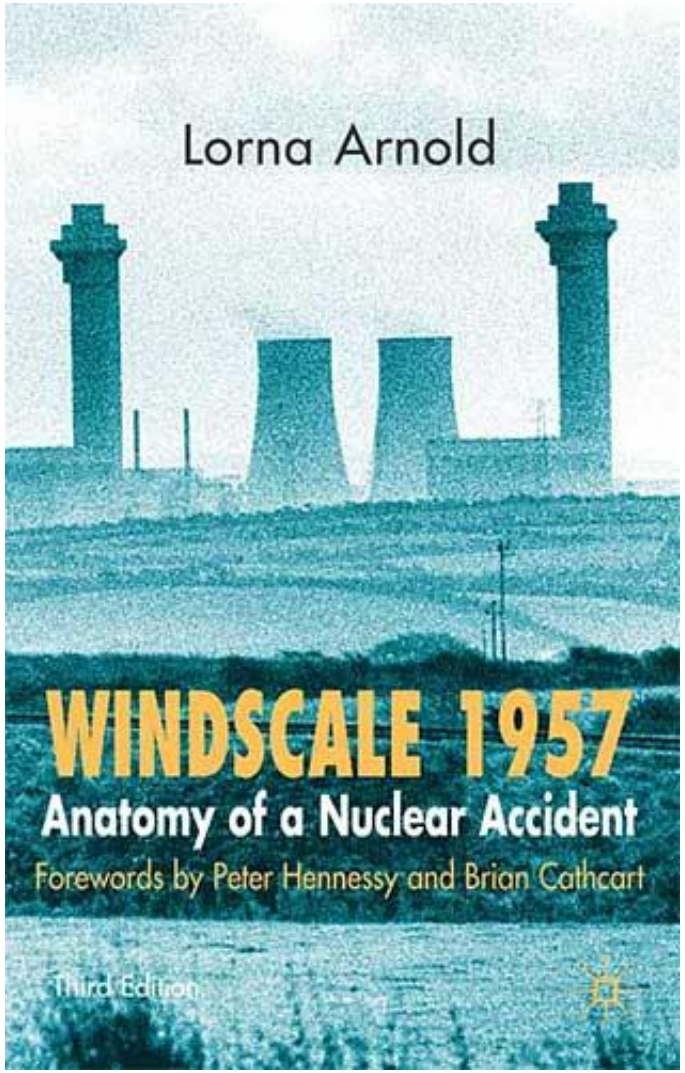

Windscale Air-Cooled Plutonium Production Piles

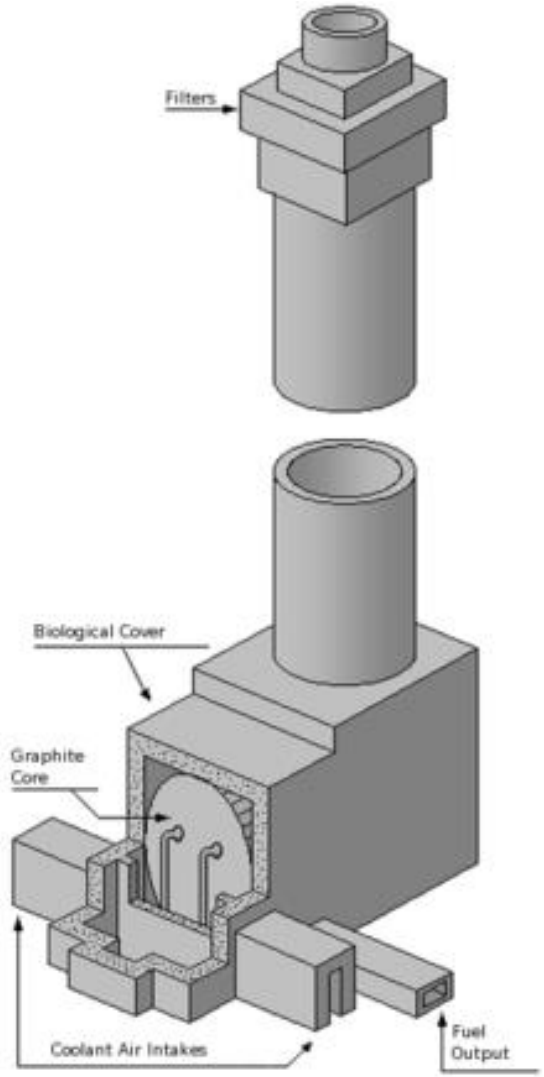

Windscale Piles

Description:

- Air cooled core – the atmosphere is the primary circuit
- Containment:
  - 1st barrier (incomplete), natural uranium metal fuel rod
  - 2nd barrier, aluminium cladding of the fuel elements
  - 3rd barrier (incomplete), filters in the chimney stacks
- Reactivity Control (two systems)
  - Control rods inserted and driven from the sides of the core
  - Shutdown rods, inserted from the top of the core and gravity-driven
- Cooling:
  - Massive electrically driven blowers assisted by chimneys
  - Natural convection driven by the chimneys for long-term decay heat removal

Windscale Piles – Lessons Learned

- Wigner Growth in graphite was known about at the time of the Windscale piles but Wigner Energy was not:
  - Wigner Energy was discovered when energy spontaneously released itself during operation in an uncontrolled manner.
  - Regular periodic anneals of the core were carried out thereafter to allow controlled release of the Wigner Energy.
    - Annealing was carried out by deliberately overheating the core to trigger the release.
    - Initiating temperature needed to release energy was increasing with time.
    - Rate of graphite oxidation at any temperature was increasing with time – sodium contamination from salt-laden sea air.
    - The two curves crossed in 1957 ….
- Don't cool reactor cores with atmospheric air.
- Operate at high enough temperatures so that neutron induced damage in the graphite is self-annealing.

Carbon dioxide cooled – Magnox reactors, 1953 - 2014

- Closed cycle with carbon dioxide gas
- Pressurised coolant to reduce pumping power
- Natural uranium metal fuel
- Magnesium alloy low-absorption cladding
- Higher temperatures with lower oxidation rate than for air
- Temperature high enough for commercial electricity generation
- Steel pressure vessel
- No recognisable containment building (for early plants)
- World's first commercial nuclear power station to export power to a distribution grid
- Generation-I technology

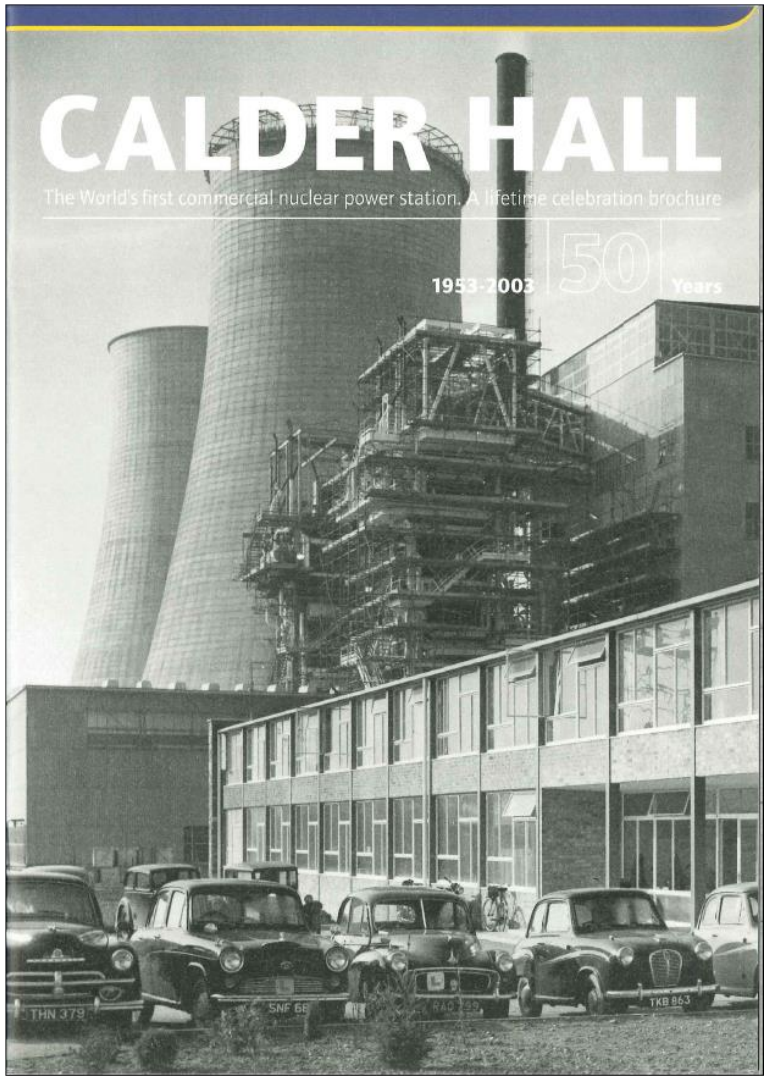

Calder Hall Nuclear Power Station (Magnox) (2 of 4 reactors shown)

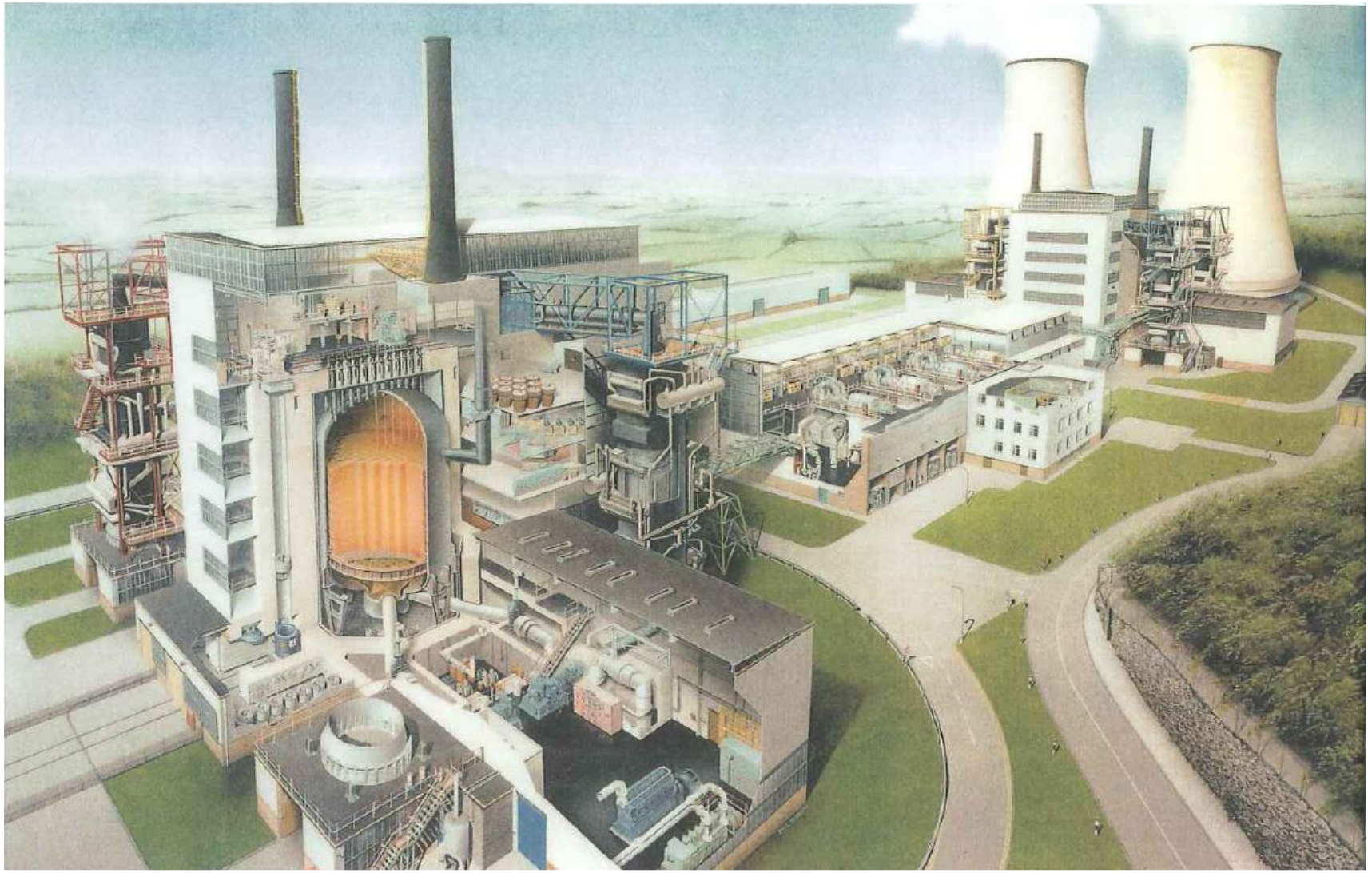

Early MAGNOX reactors

Description:

- Pressurised CO_2 cooled core in a closed primary circuit
- Containment:
  - 1st barrier (incomplete), natural uranium metal fuel rod
  - 2nd barrier, Magnox cladding of the fuel elements
  - 3rd barrier, carbon steel primary circuit boundary
- Reactivity Control (two systems)
  - Control rods inserted from the top of the core
  - Shutdown rods, inserted from the top of the core and gravity-driven
- Cooling:
  - Electrically driven gas circulators
  - Boilers used for normal and decay heat removal
  - Back up electrical supplies, low voltage systems and feedwater systems
- The containment system of later Magnox reactors resembles that of the AGR

Magnox Reactors – Lessons Learned

- Gas-cooling is a viable means of generating electricity using nuclear reactors on a commercial basis.
- Magnox reactors were the first in the world to be connected to a national grid providing reliable baseload generation.
- Extensive use of carbon steel in the construction of the pressure vessels and the garter core restraint system in early reactor led to severe corrosion issues.
- Embrittlement of the RPVs was found to be an issue in some reactors.
- All Magnox reactors exceeded their design lives by considerable margins.
- Fuel generally performed well, but to low burn-up.
  - Produced very high-quality plutonium that fuelled the UK fast reactor programme
- Spent fuel degraded quickly when stored in water – needed to be dismantled and reprocessed quickly.

Carbon dioxide cooled – Advanced gas cooled reactors (AGRs) (late 1960s onwards)

- Generation II technology
- Enriched uranium
- Stainless steel-clad uranium-oxide ceramic fuel
- Pre- (and post) stressed concrete pressure vessel with integral gas circulators, boilers and decay heat removal boilers
- Gas-tight (but lightweight) upper reactor building
- Coolant outlet temperature up to 650^{o}C
- Good quality superheated (and reheated) steam (comparable to quality from a highly optimised coal plant)
- High thermal efficiency – 42%

AGR 37-pin fuel element

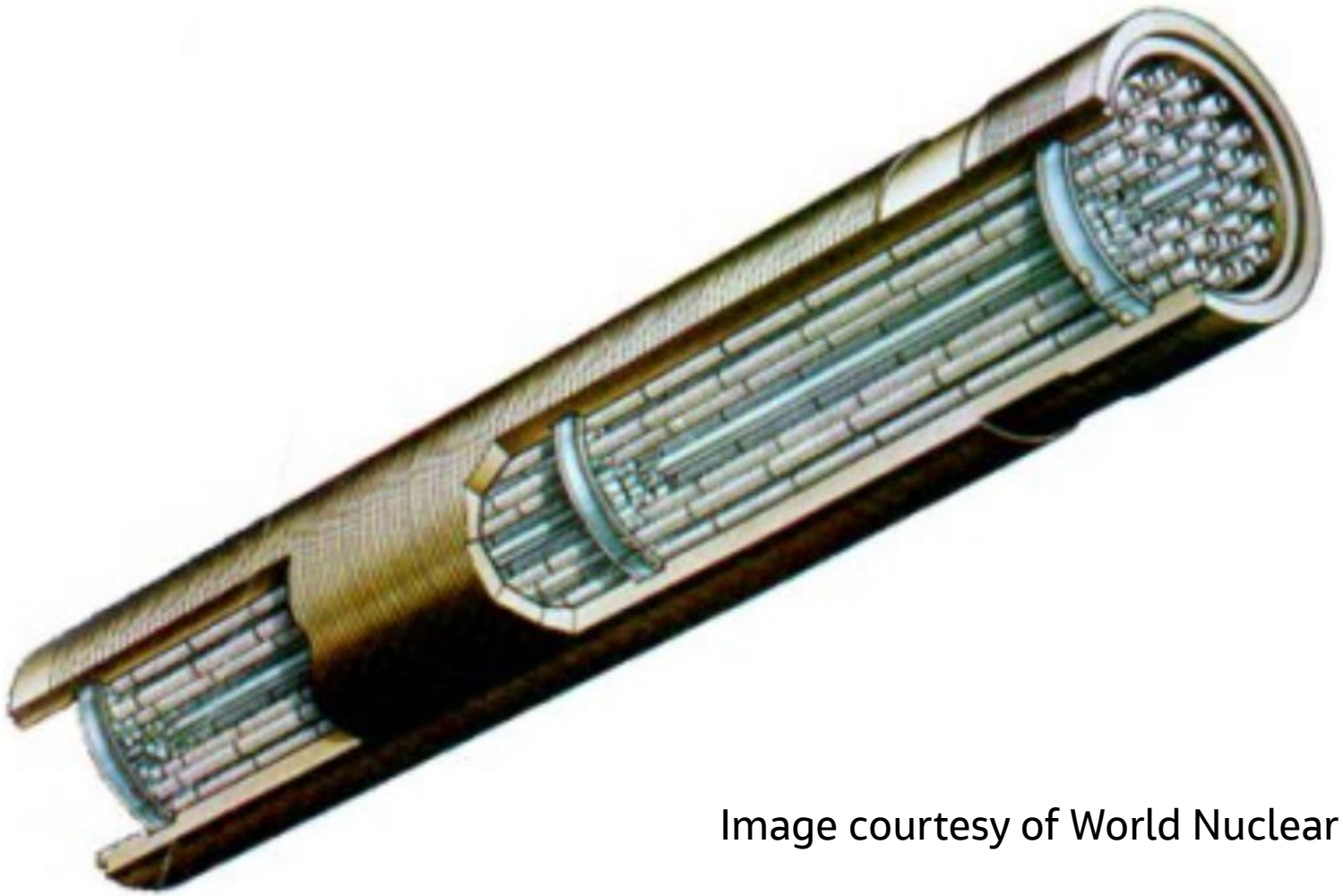

Image courtesy of World Nuclear Association

Modified Pin Surfaces for Gas-Cooled Reactors

- Transverse ribs
  - Increased turbulence and disruption of the boundary layer
- Multi-start helical ribs
  - As above but with additional circumferential mixing
- Axial fins
  - Only gives increased surface area – not actually used in AGRs as it introduced to much steel with enhancing heat transfer as much as ribs.

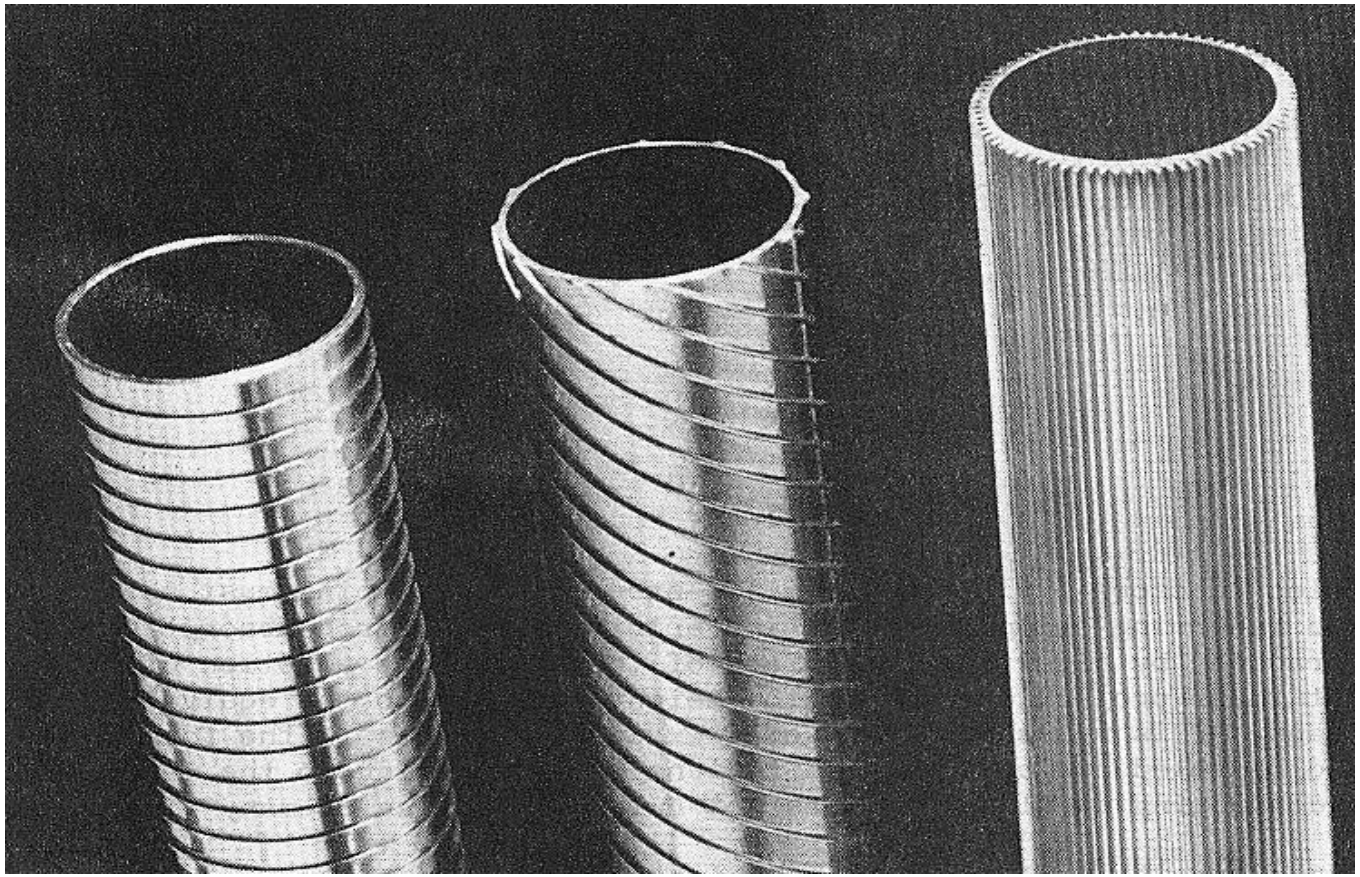

Heat transfer Enhancement for Modified Surfaces

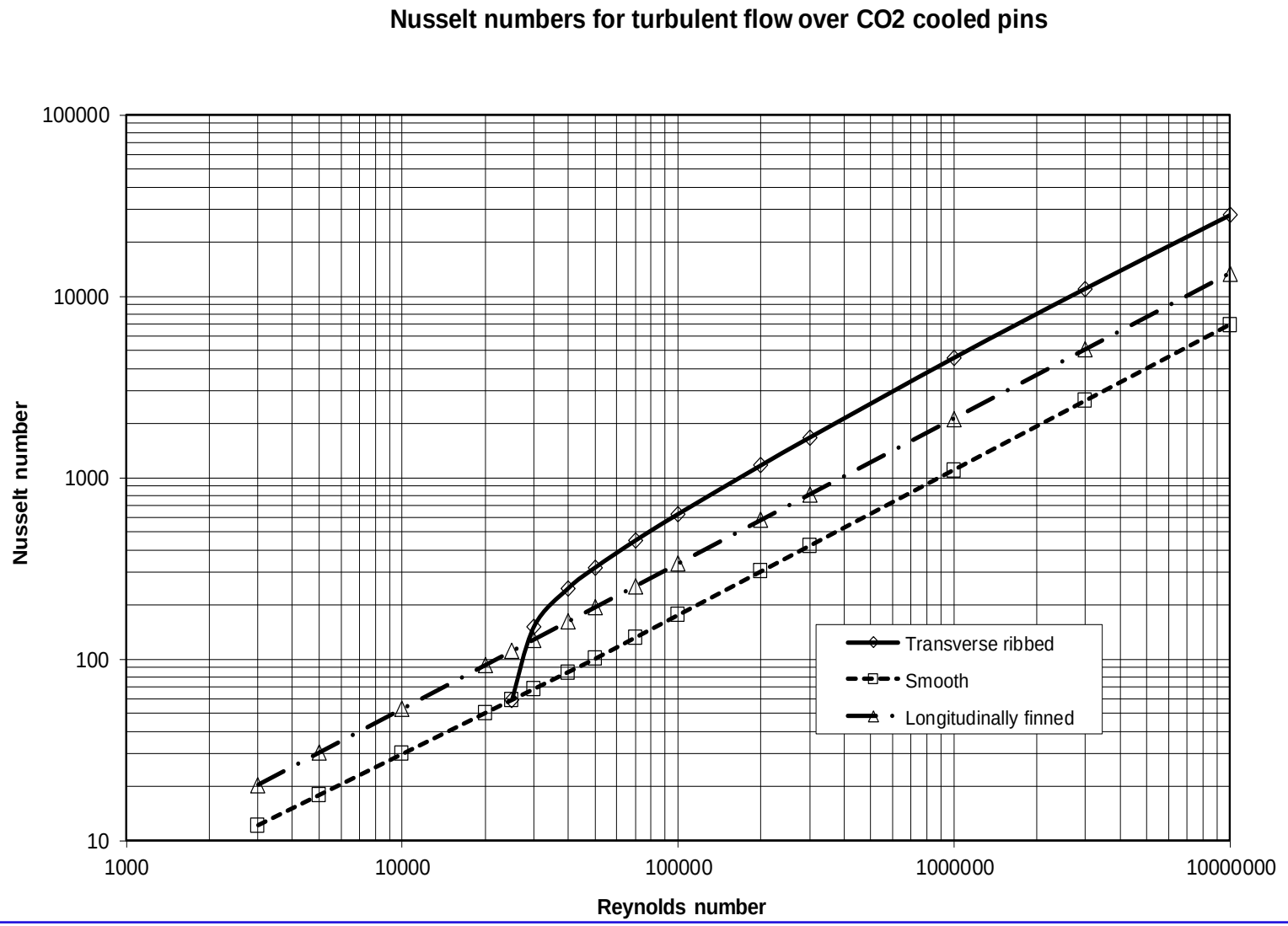

Torness AGR Nuclear Power Station

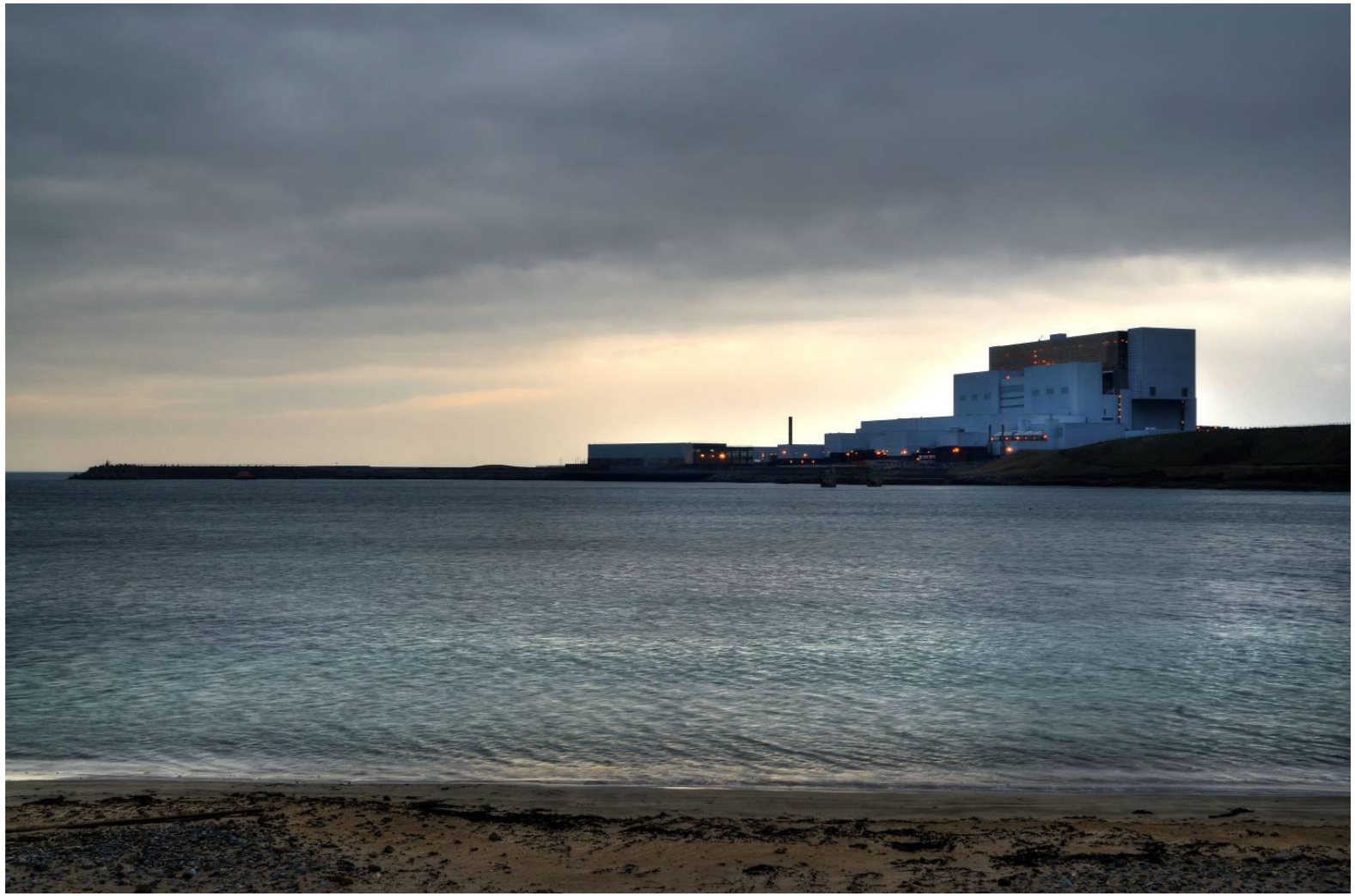

Cut-away view of an AGR reactor building

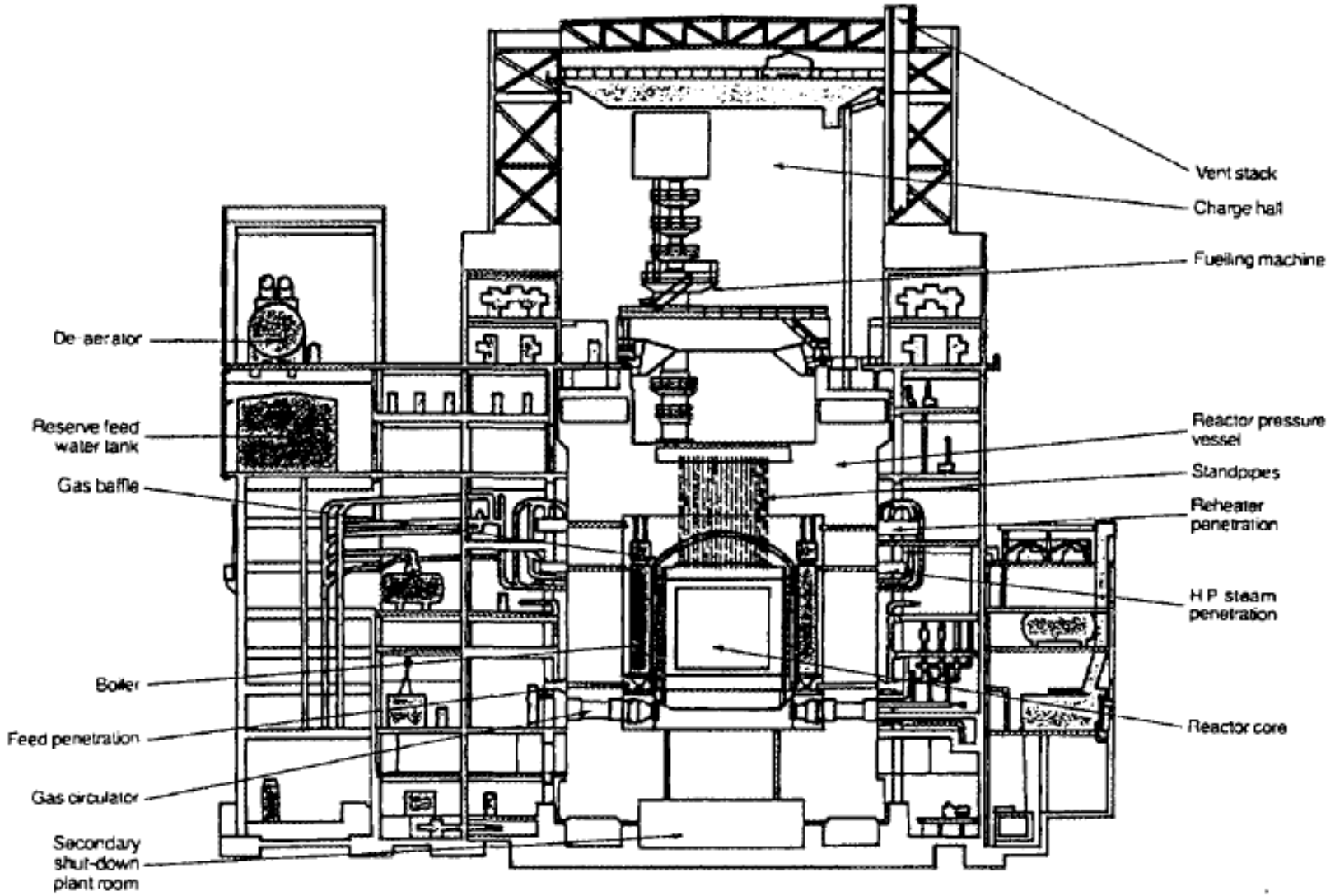

Location of the UK's 7 twin AGR NPPs

Architecture of a carbon dioxide cooled AGR

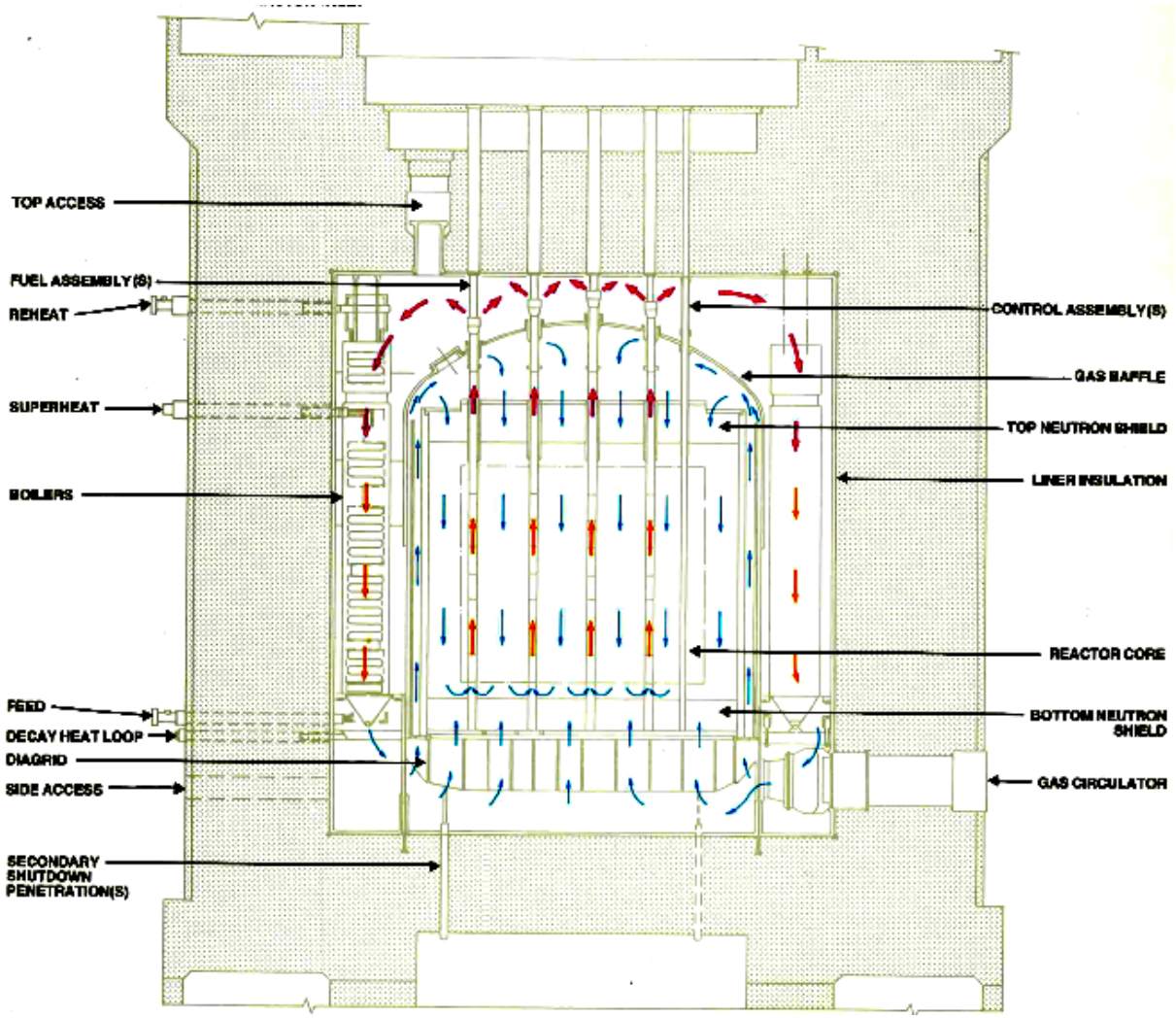

AGR Core Under Construction

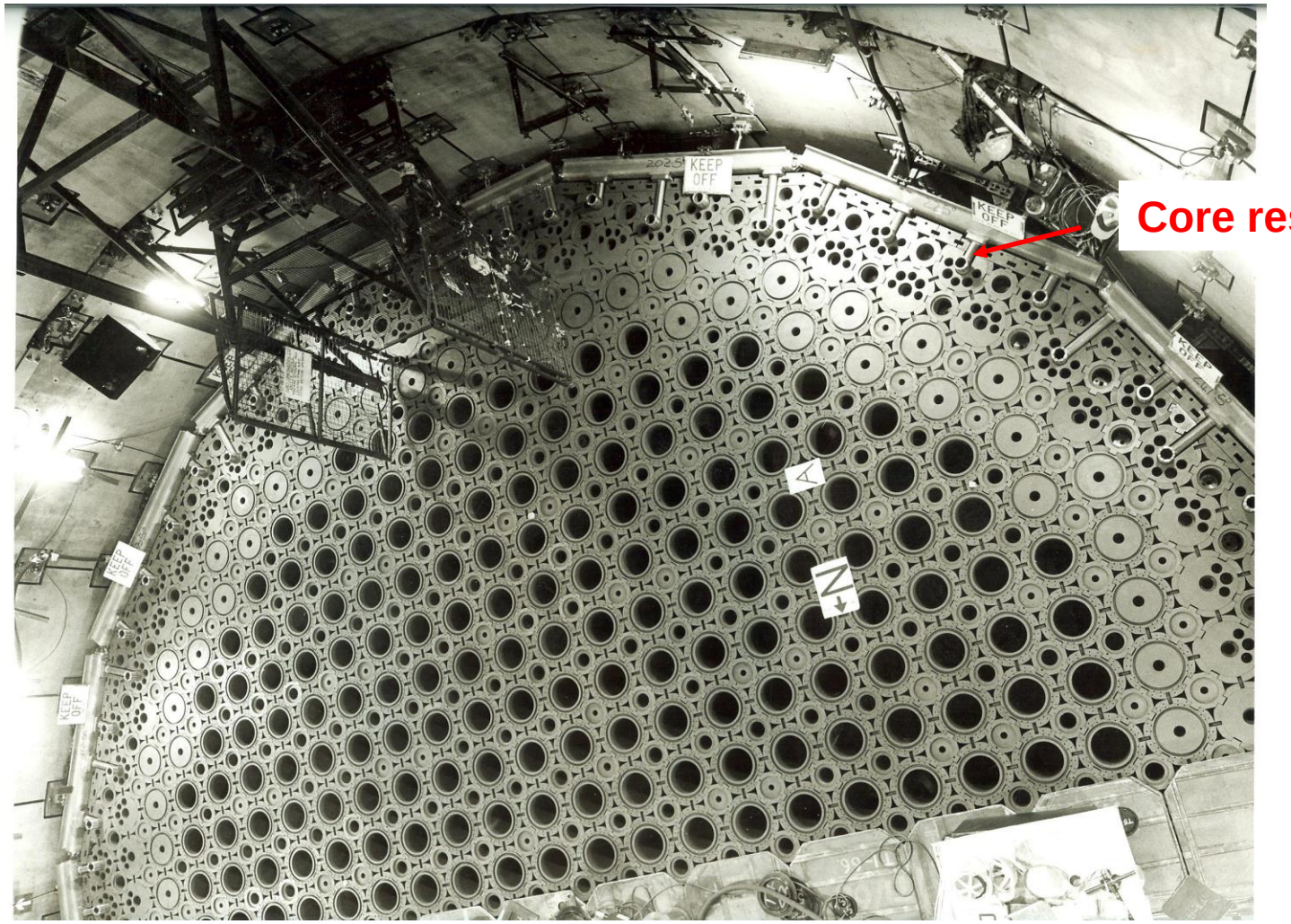

Core restraint system

Accommodation of Dimensional Change – the Keying System

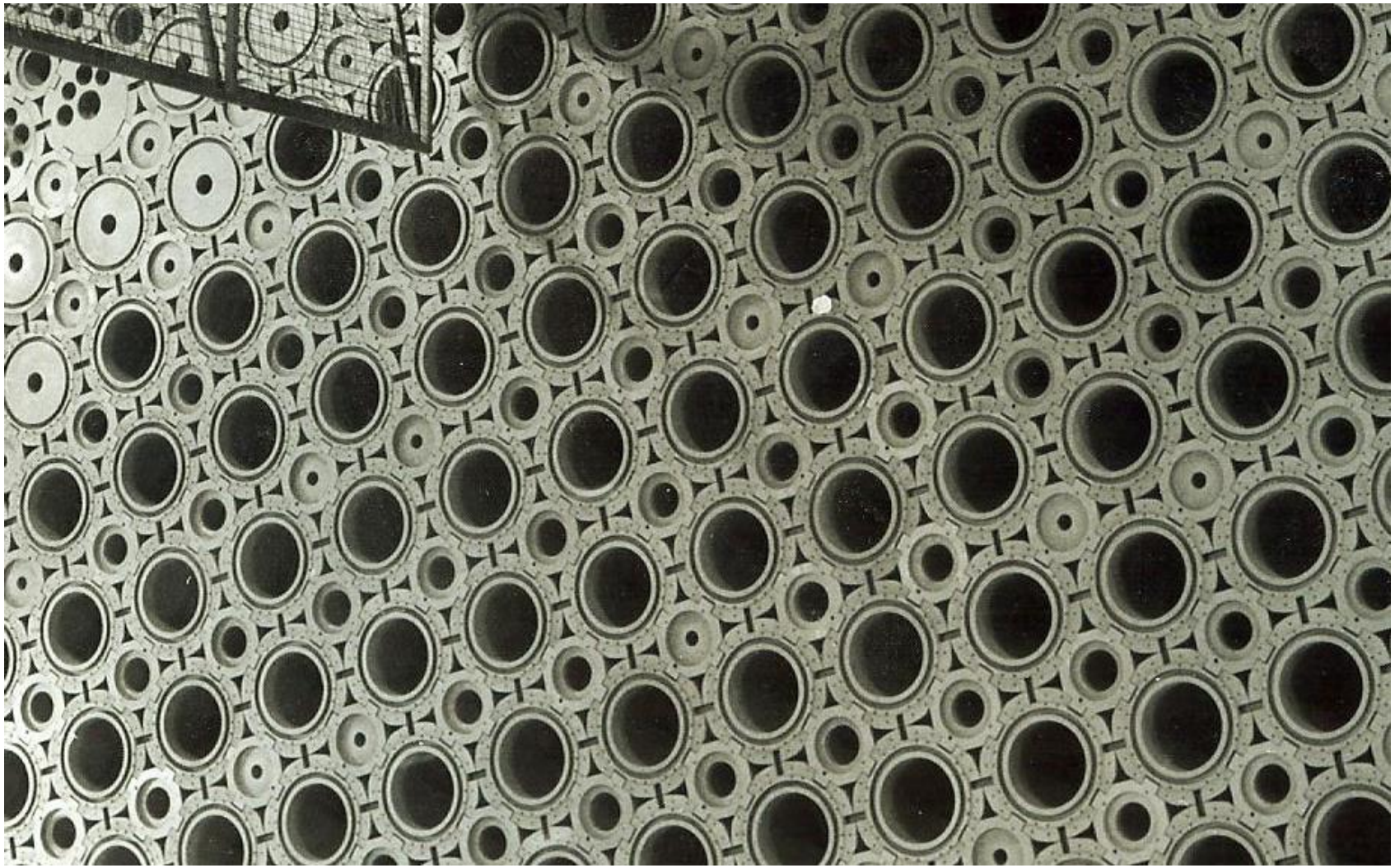

Advanced Gas-cooled Reactors (AGR)

Description:

- Pressurised CO_2 cooled core in a closed primary circuit
- Containment:
  - 1st barrier (incomplete), uranium dioxide ceramic fuel pellets
  - 2nd barrier, Stainless steel cladding of the fuel elements
  - 3rd barrier, Primary circuit boundary fully enclosed in a steel-lined pre- (and post-) stressed concrete pressure vessel.
  - 4th barrier, gas-tight reactor building
- Reactivity Control (two systems)
  - Control rods and Shutdown rods inserted from the top of the core
  - Tertiary shutdown by either boron bead injection or nitrogen injection
- Cooling:
  - Electrically driven variable geometry gas circulators
  - Boilers used for normal and post-trip heat removal
  - Decay heat boilers for long term decay heat removal
  - Back up electrical supplies, low voltage systems and feedwater systems

Containment

- Incredibility of failure is declared for the bulk structure of the pressure vessel and for its penetrations to eliminate the rapid depressurisation case.
- Small breach loss of coolant is still possible and the large reactor building is capable of containing escaped gas.
- There is no phase change of coolant so the level of pressurisation of the reactor building is predictable.
- … As such, there is no heavy containment building as in the case of a PWR.
- Primary circuit and building can be blown-down through filters to protect the structures
- Design basis faults:
  - Hot gas release – leakage of coolant from the primary circuit – main hazard is loss of coolant pressure and impingement on structures and instrumentation systems
  - Steam release – leakage of steam from the secondary circuit – main hazards are blast loading and overpressure of the reactor building and impingement on sensitive equipment

Heat removal

- Normal heat removal requires gas circulators, the feed system, turbine and condenser to be operational.
- Immediate post trip cooling can be by venting steam or by diverting steam to the condenser.

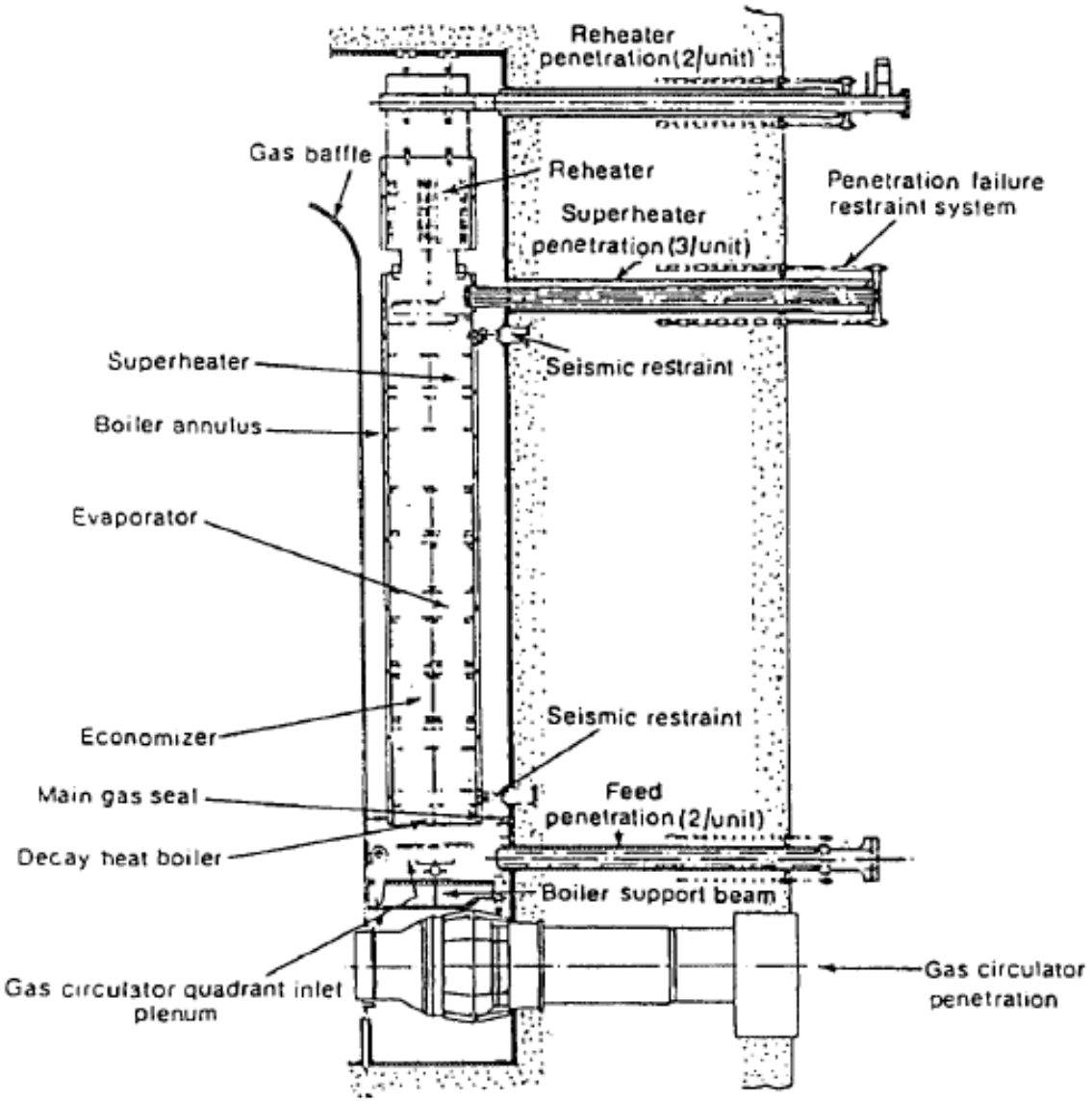

Decay Heat Removal

- Low power density and large thermal inertia of the graphite core provide long grace times.
- Pressurised decay heat removal can occur by either forced or natural convection of the primary coolant.
- Rate of depressurisation is limited by the reactor pressure vessel design.
- Depressurised decay heat removal requires the circulators to be operable (at 3000 rev/min)
- Back up water supplies, power supplies and feedwater pumping capacity are provided to cope with all of the loss of cooling faults within the design basis

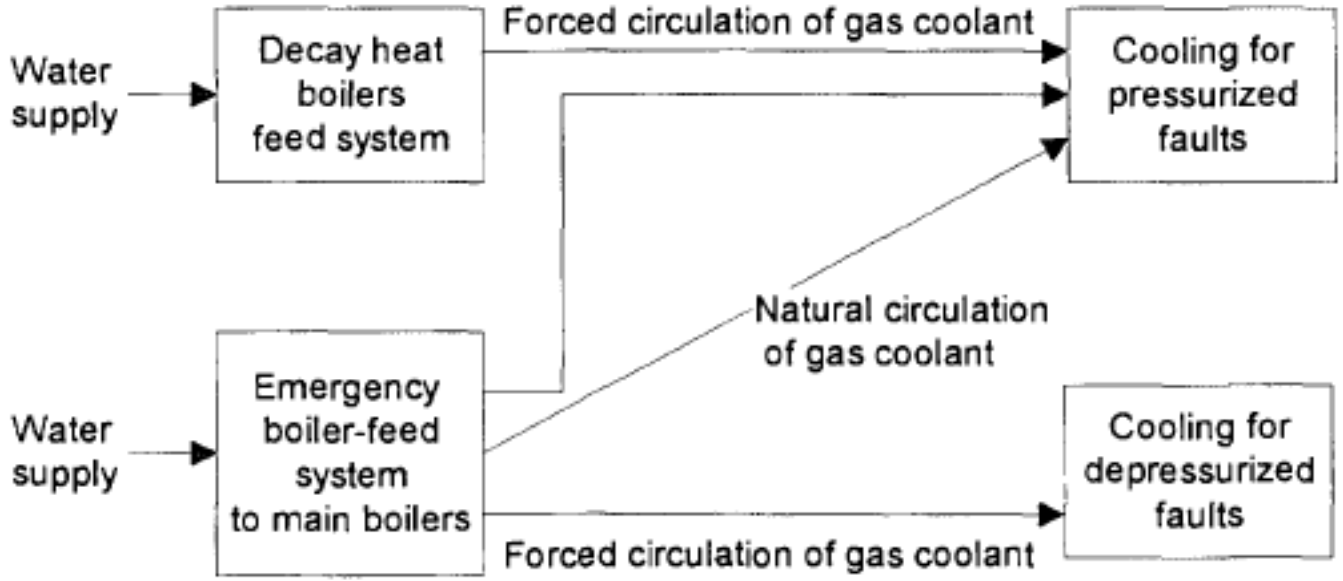

Operational Experience

- Fuel Stringer problems
  - Oscillation of the fuel stringer during on-load refuelling
  - Refuelling at 30% power is permitted for some reactors
- Boiler tube failures leading to water/steam ingress into the graphite core
- Boiler closure unit restraint faults (reactors with “pod” boilers)
- Boiler spine cracking (reactors with pod boilers)
- Graphite weight loss leading to loss of moderation (and loss of strength)
- Graphite cracking
  - Key-way root cracking – result of turn-around phenomenon in irradiated graphite.
- No accidental depressurisation events
- Some circulator failures – mechanical and electrical (latter after boiler tube failure)
- All reactors have exceeded their design lives – oldest by almost a factor of 2.

EDF Energy Stations Today

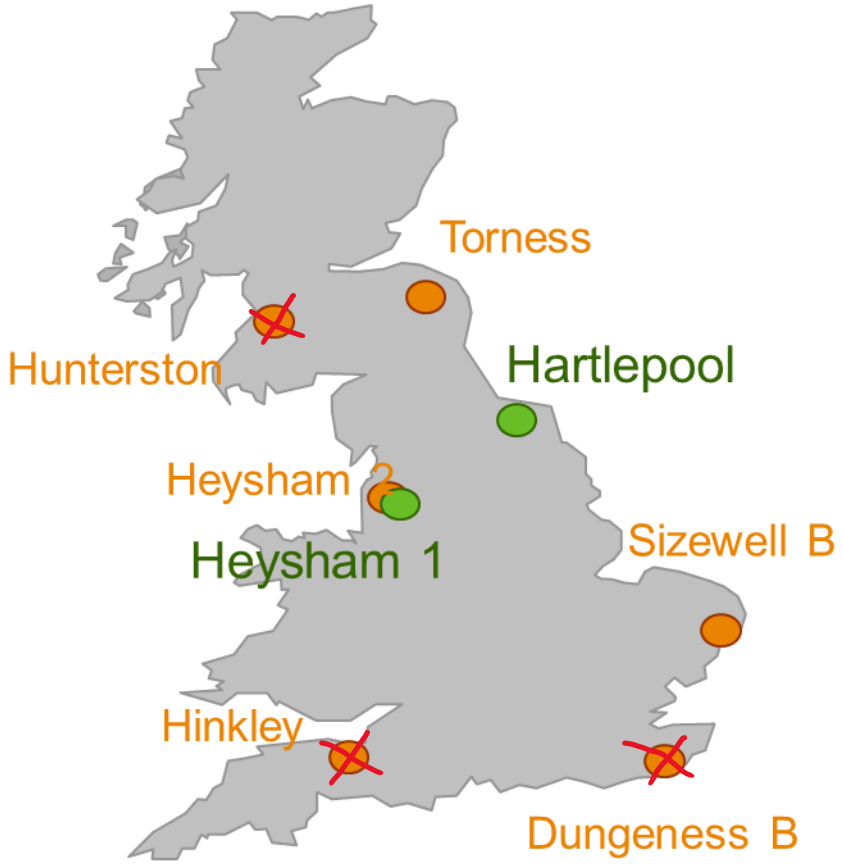

Hartlepool / Heysham 1 Boiler Closure Unit (BCU) repairs

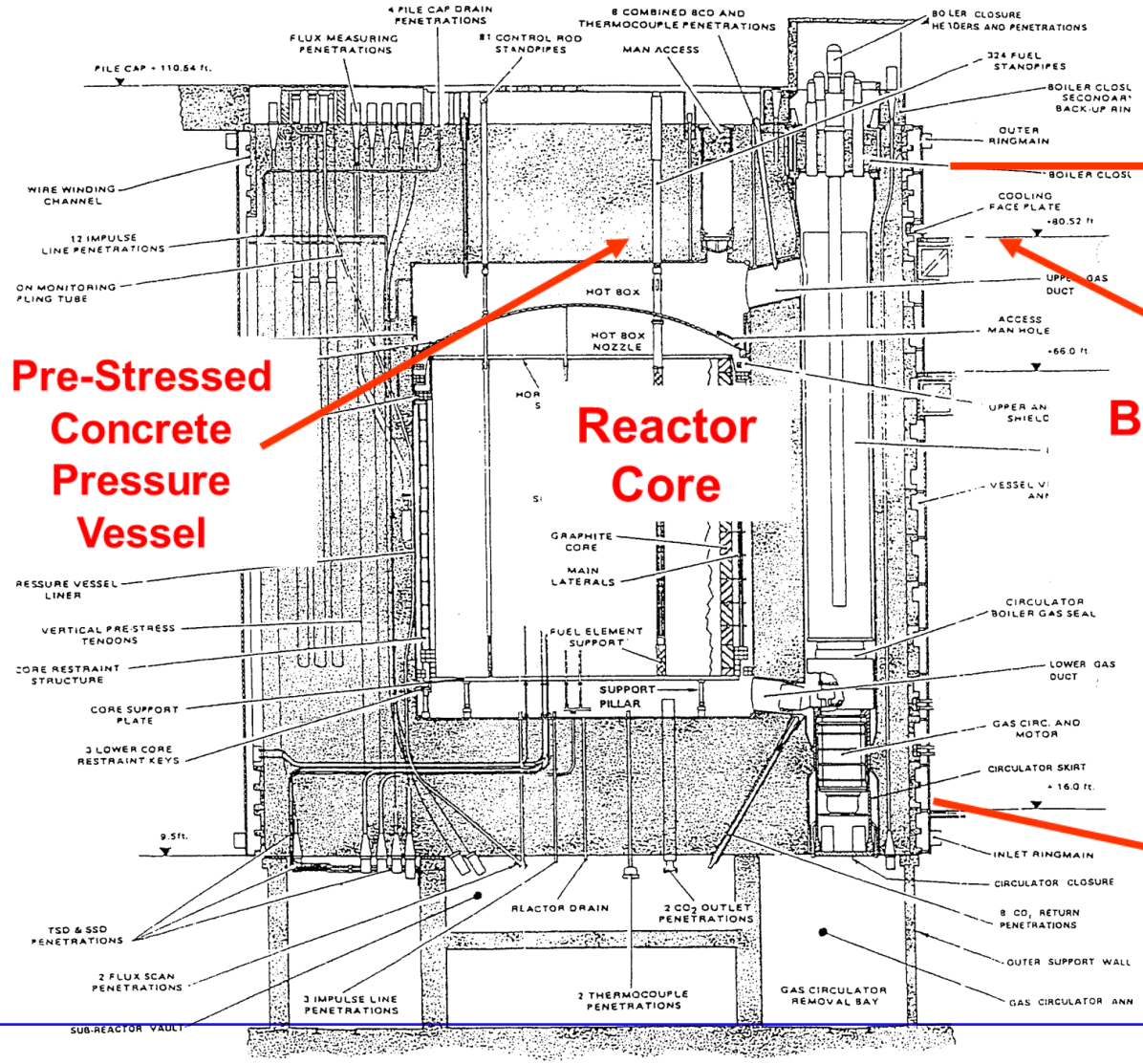

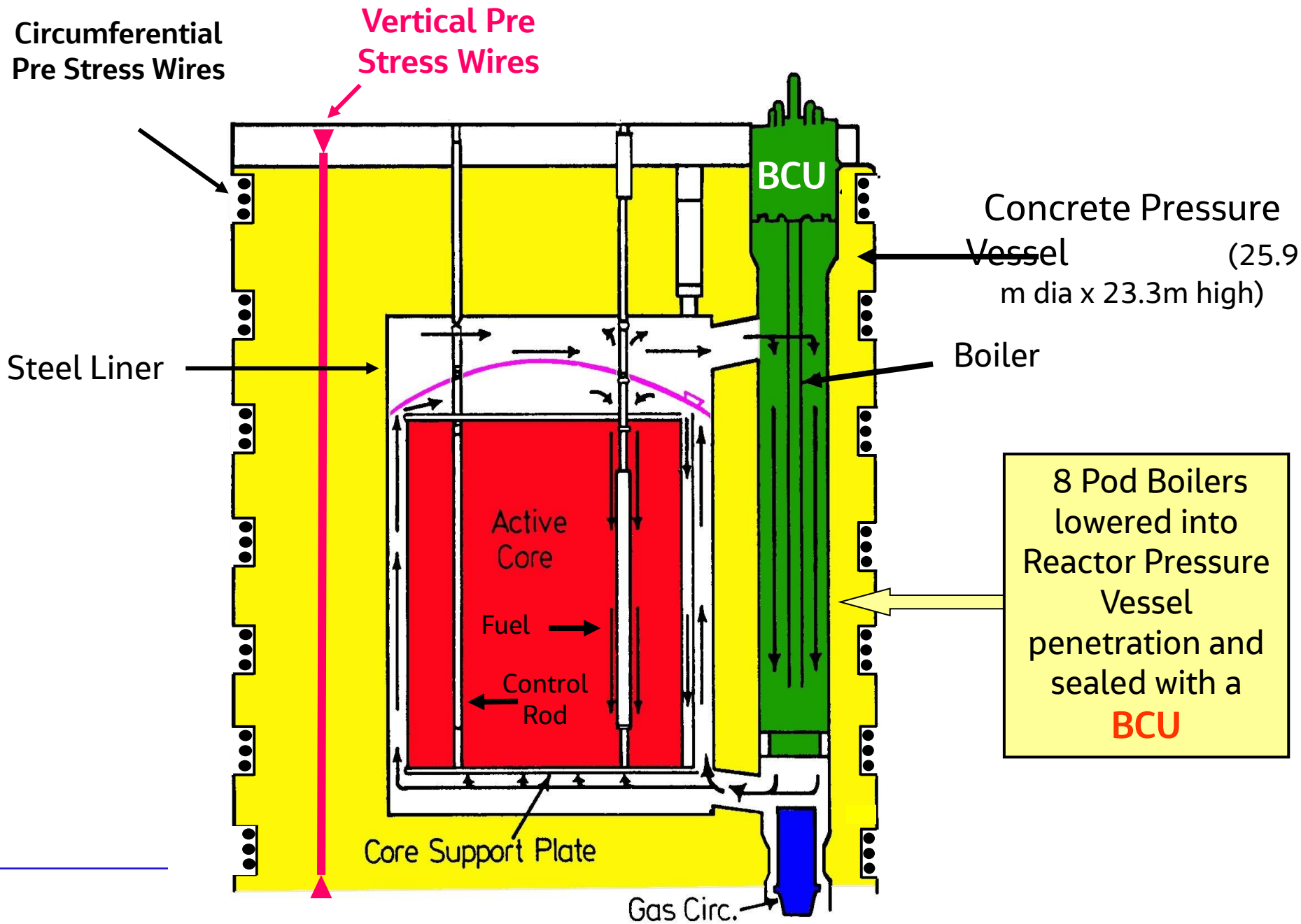

Original Installation

- Photograph taken during construction

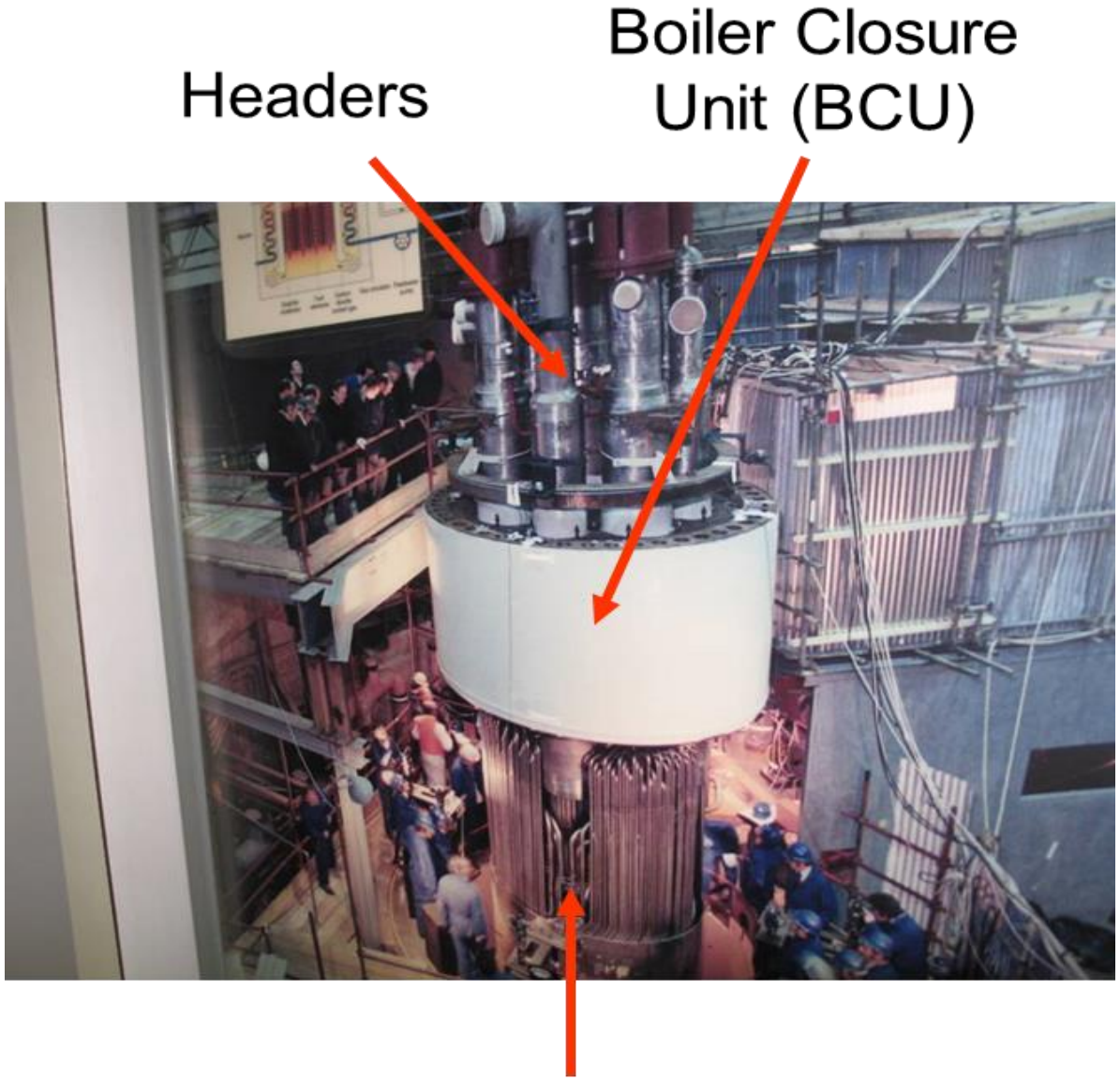

Pre-stress wires

Frictional Restraint

Friction restraint and ESR

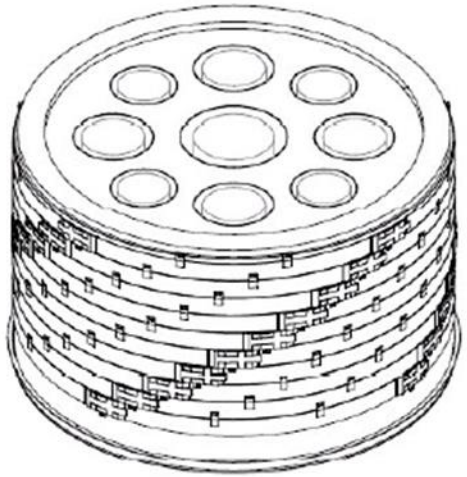

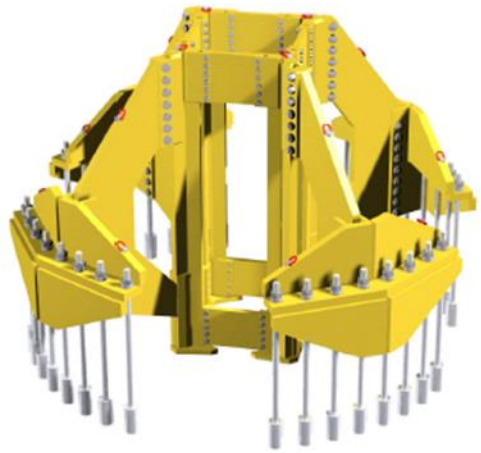

It was a busy workplace!

In respect of safety, how does an AGR differ from GFR?

- Core power density
  - Low power density in an AGR ~ 5 MW/m^3
- Core thermal inertia much larger owing to graphite moderator
- Steel-lined pre-(and post-) stressed concrete pressure vessel with integral primary circuit makes depressurisation a rare event and rapid depressurisation impossible
- Higher density coolant
- Like GFR, natural convection is adequate to remove decay heat in pressurised conditions
- But external power is required to remove decay heat to prevent fuel damage in depressurised conditions.

The future of gas-cooled reactors ?

Image used under license

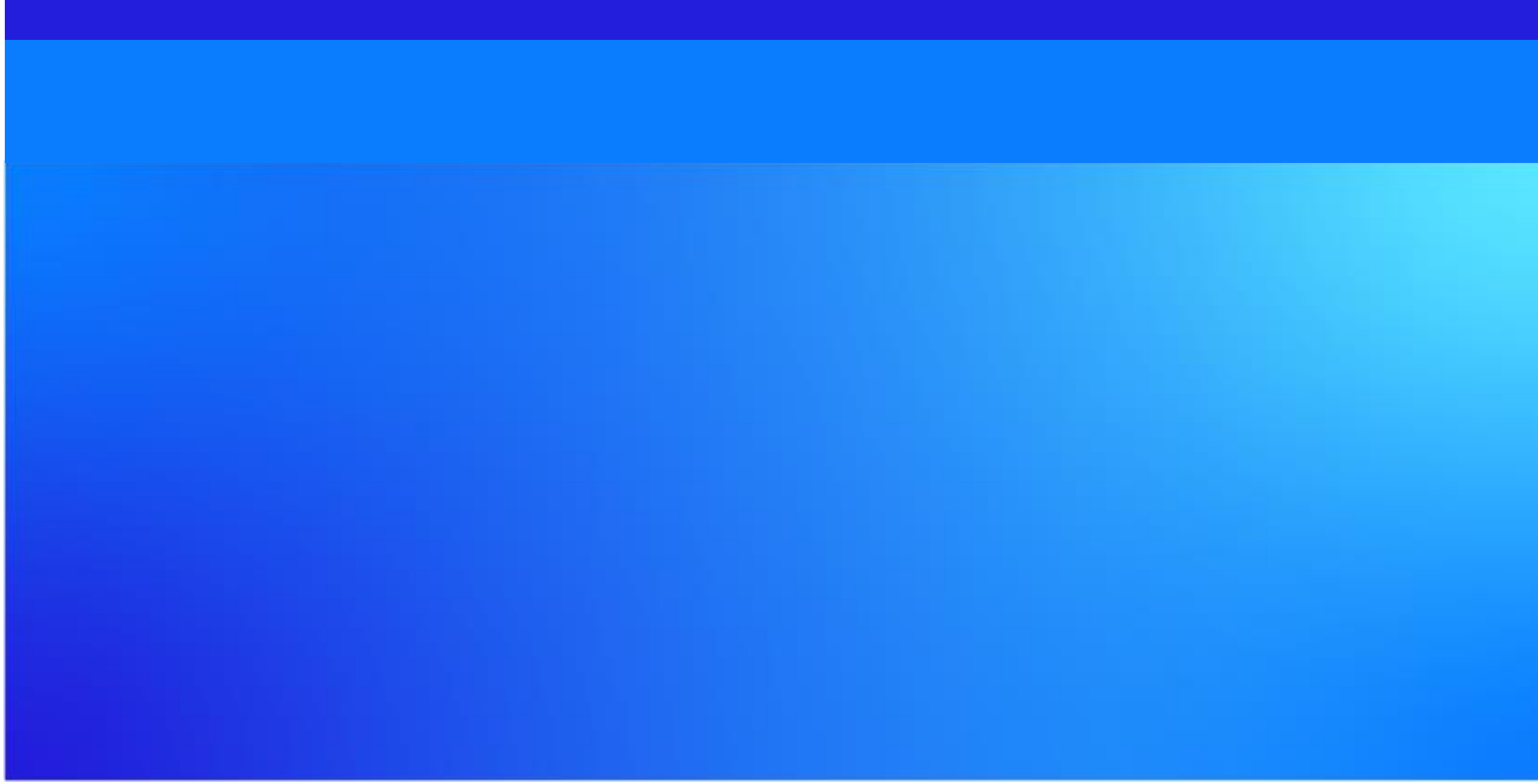

Jacobs

Challenging today.
Reinventing tomorrow.

The effect of Thermodynamic and Transport Properties in Thermal and Hydraulic Analysis of Gas Systems

doc. Ing. Václav Dostál, Sc.D.

FAKULTA STROJNÍ ČVUT V PRAZE

Ústav energetiky

Outline

The effect of Thermodynamic and Transport Properties in Thermal and Hydraulic Analysis of Gas Systems

- Effect on efficiency
- Temperature profiles in the heat exchanger
- Heat transfer correlations
- Cooler analysis
- Decay heat removal system and natural circulation (MIT GFR)
- Core catcher (ÚJV, CTU in Prague)

GFR Research at MIT (2005-2008)

- Optimized, Competitive Supercritical-CO2 Cycle GFR for Gen IV Service
- 2005-2008
- NUCLEAR ENERGY RESEARCH INITIATIVE (NERI)
- Project (Grant No. DE-FC07-05ID14671)
- Project No. 05-044

Closed Gas Cycles

- **Helium (and ideal gas) Brayton cycles require core outlet temperatures around 900 ^{o}C in order to achieve attractive efficiencies (~ 45 – 48%).**
- **The high temperature environment is challenging to structural materials.**
- **Hence, supercritical cycles operating with technically familiar and more benign gases are of considerable interest.**
- **CO_2 is selected because of:**
  - **the moderate value of its critical pressure,**
  - **its stability and relative inertness (for the temperature range of interest),**
  - **sufficient knowledge of its thermodynamic properties,**
  - **non-toxicity,**
  - **abundance**
  - **and low cost.**

Supercritical Cycles - What are they?

- Thermodynamic cycles that take advantage of the changes of properties around the critical point.
- ? supercritical, transcritical, hypercritical ?
- 2 major types
  - supercritical steam cycle - heating above critical pressure increases temperature of heat addition
  - supercritical CO_2 cycle - compression near the critical point reduces compressor work (i.e. reduction of temperature of heat rejection)

Advantages of Supercritical CO_2 Cycle

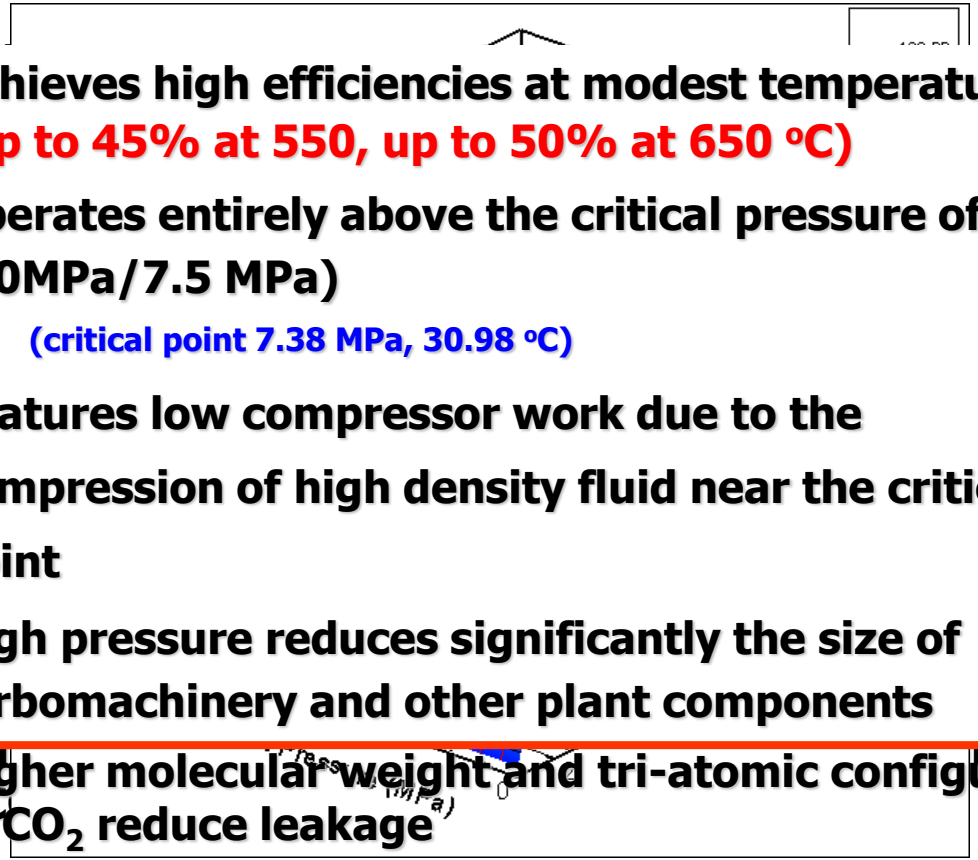

- Achieves high efficiencies at modest temperatures (up to 45% at 550, up to 50% at 650 °C)
- Operates entirely above the critical pressure of CO_2 (20MPa/7.5 MPa)
  - (critical point 7.38 MPa, 30.98 °C)
- Features low compressor work due to the compression of high density fluid near the critical point
- High pressure reduces significantly the size of turbomachinery and other plant components
- Higher molecular weight and tri-atomic configuration of CO_2 reduce leakage

Comparison with Other Advanced Power Cycles

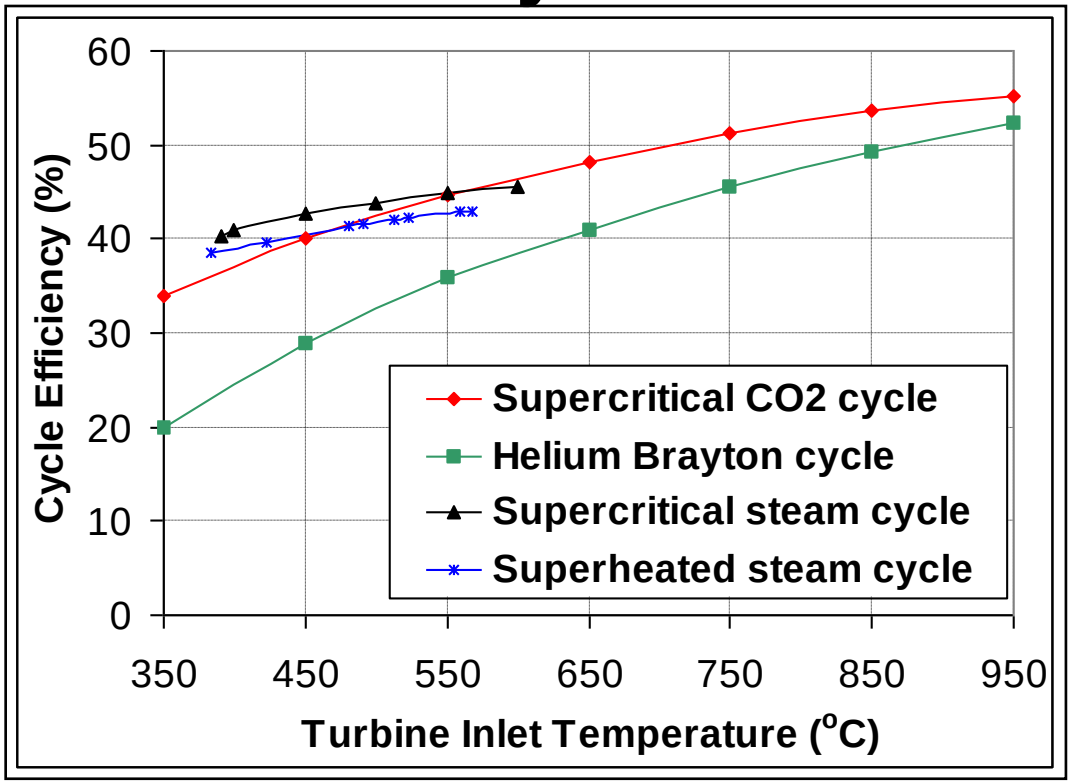

Respecting Real Gas Properties

- If the critical point of the working fluid is close to the temperature range at which the cycle operates the real gas properties must be used
- Some gas cycles take advantage of operation close to the critical point
- Abrupt property changes, especially that of specific heat, causes difficulties in cycle design (for example pinch-point in recuperator).
- Recompression and parallel expansion cycle layouts are then necessary

Changes of Specific Heat Close to the Critical Point

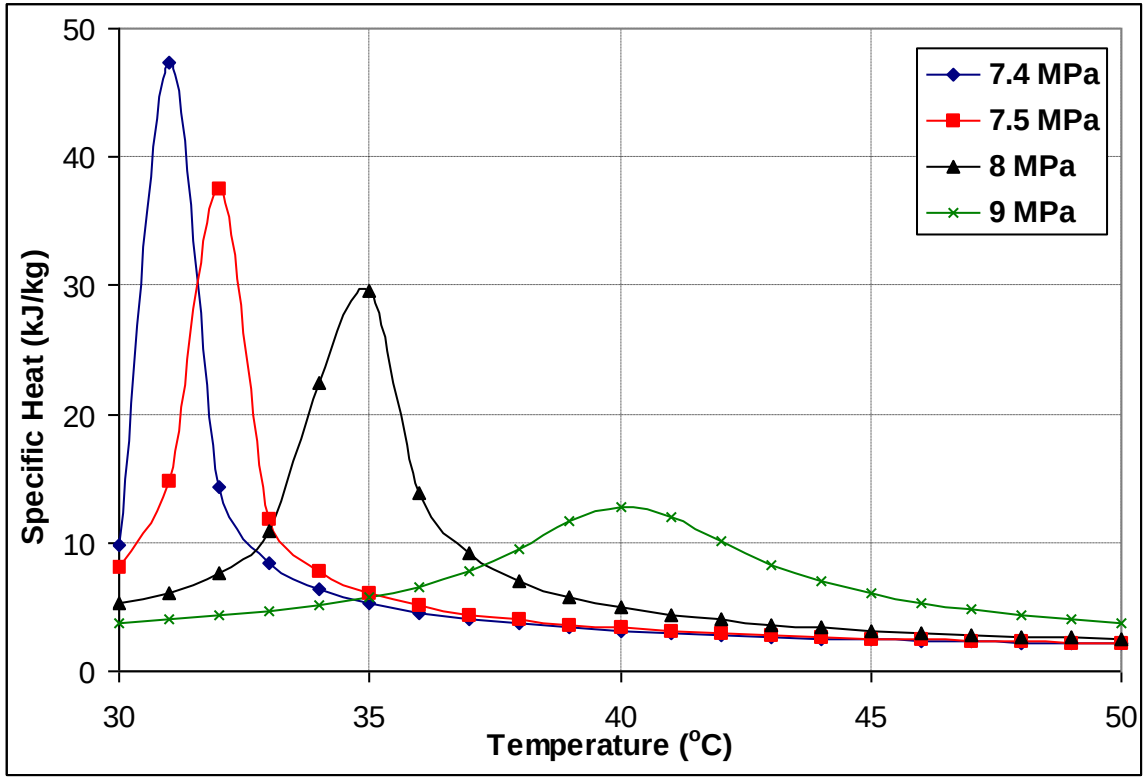

Pinch-point in Recuperator

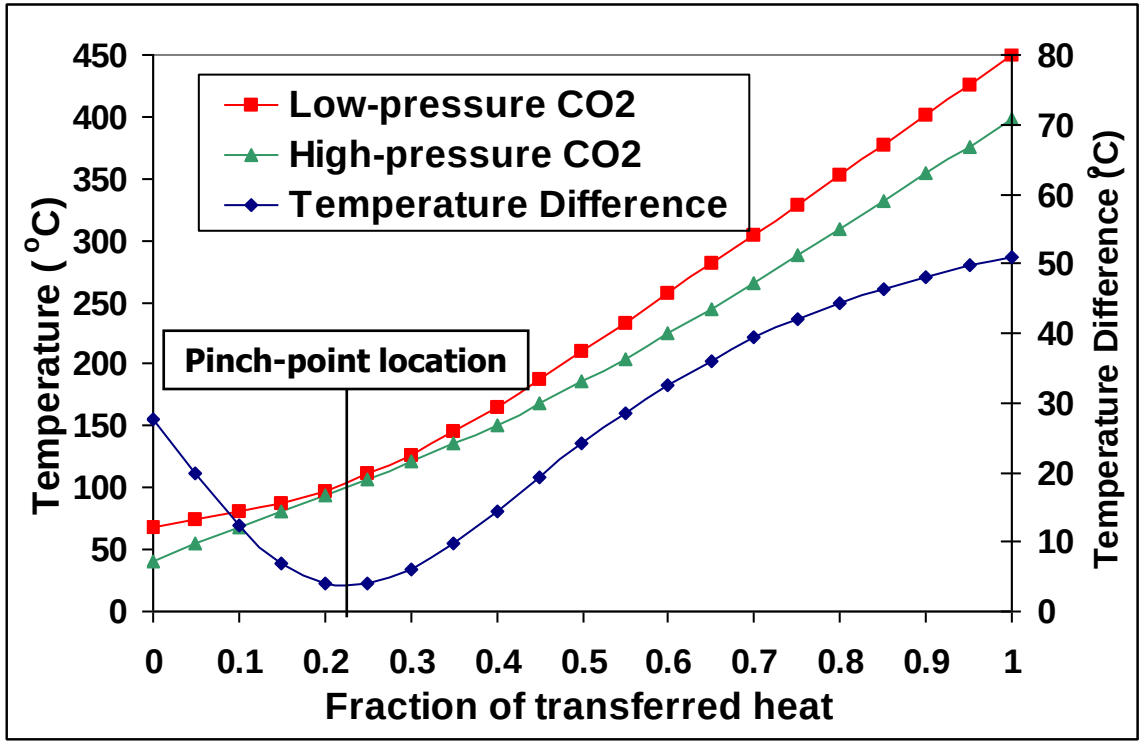

Heat Transfer Correlations

- Gas coolants are in general less effective heat transfer medium.
- This leads to higher temperature gradients close to the wall.
- Pressure drop requirements may lead to transitional or laminar flows.
- What are the typical requirements on the heat transfer correlations?
- Typical correlations:
  - Dittus Boelter
  - Sider Tate
  - Gnielinski

Typical Correlations

Correlation: Dittus-Boelter

$$Nu_{Dh} = 0.023\, Re_{Dh}^{0.8}\, Pr^{0.4}$$

where:
Dh is the hydraulic diameter [m]
Re is the Reynolds number [-]
Pr is the Prandtl number [-]
Nu is the Nusselt number [-]

Validity:

$$0.6 \leq Pr \leq 160$$

$$Re_{Dh} > 10000$$

$$\frac{L}{D} > 10$$

Correlation: Sieder-Tate

$$Nu_{Dh} = 0.027\, Re_{Dh}^{4/5} Pr^{1/3} \left(\frac{\mu}{\mu_s}\right)^{0.14}$$

where:
Dh is the hydraulic diameter [m]
Re is the Reynolds number [-]
Pr is the Prandtl number [-]
Nu is the Nusselt number [-]

Validity:

$$0.7 \leq Pr \leq 16700$$

$$Re_{Dh} > 10000$$

$$\frac{L}{D} > 10$$

Correlation: Gnielinski

$$Nu_{Dh} = \frac{(f/8)(Re_{Dh} - 1000)Pr}{1 + 12.7(f/8)^{1/2}(Pr^{2/3} - 1)}$$

where:
Dh is the hydraulic diameter [m]
Re is the Reynolds number [-]
Pr is the Prandtl number [-]
Nu is the Nusselt number [-]
f is the Darcy friction factor [-]

Validity:

$$0.5 \leq Pr \leq 2000$$

$$3000 \leq Re_{Dh} \leq 5\ x\ 10^6$$

$$\frac{1}{\sqrt{f}} = -4log\left(\frac{\varepsilon}{3.7D} + \frac{1.255}{Re\sqrt{f}}\right)$$

$$\frac{1}{\sqrt{f_D}} = -2log\left(\frac{\varepsilon}{3.7D} + \frac{2.51}{Re\sqrt{f_D}}\right)$$

$$f = \left(\frac{1}{1.8\, logRe - 1.5}\right)^2$$

Requirements on Cooling Water

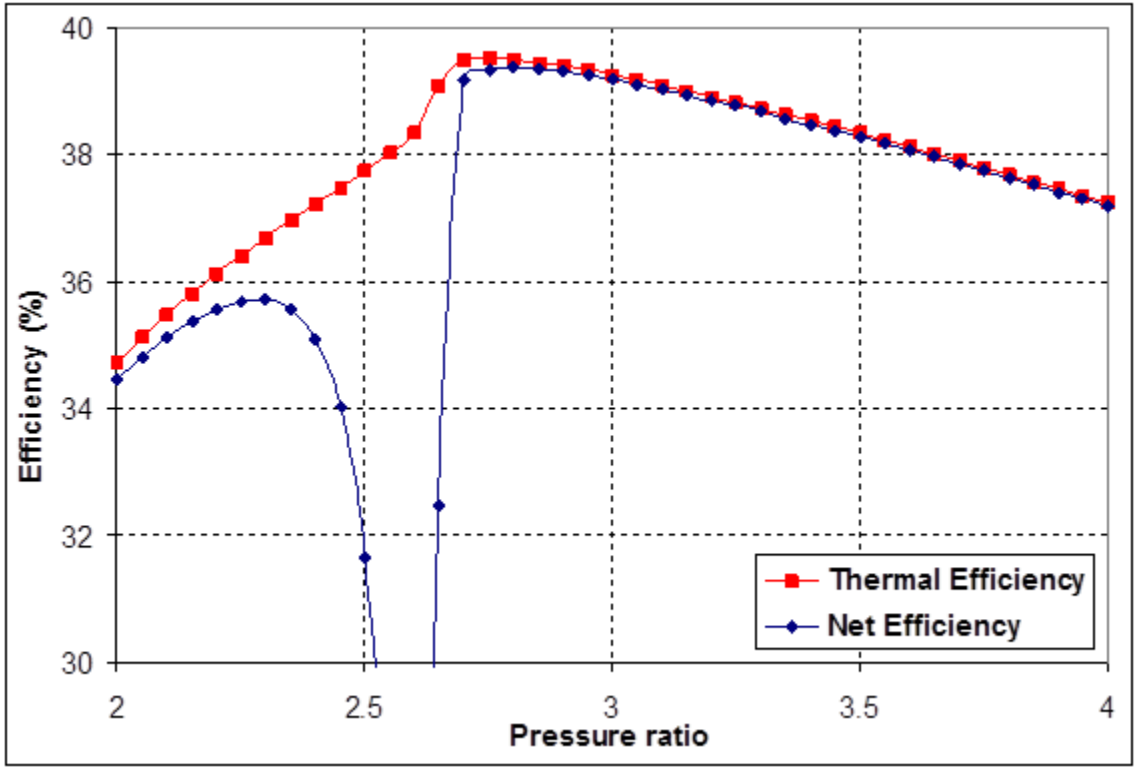

Changes of Specific Heat Close to the Critical Point

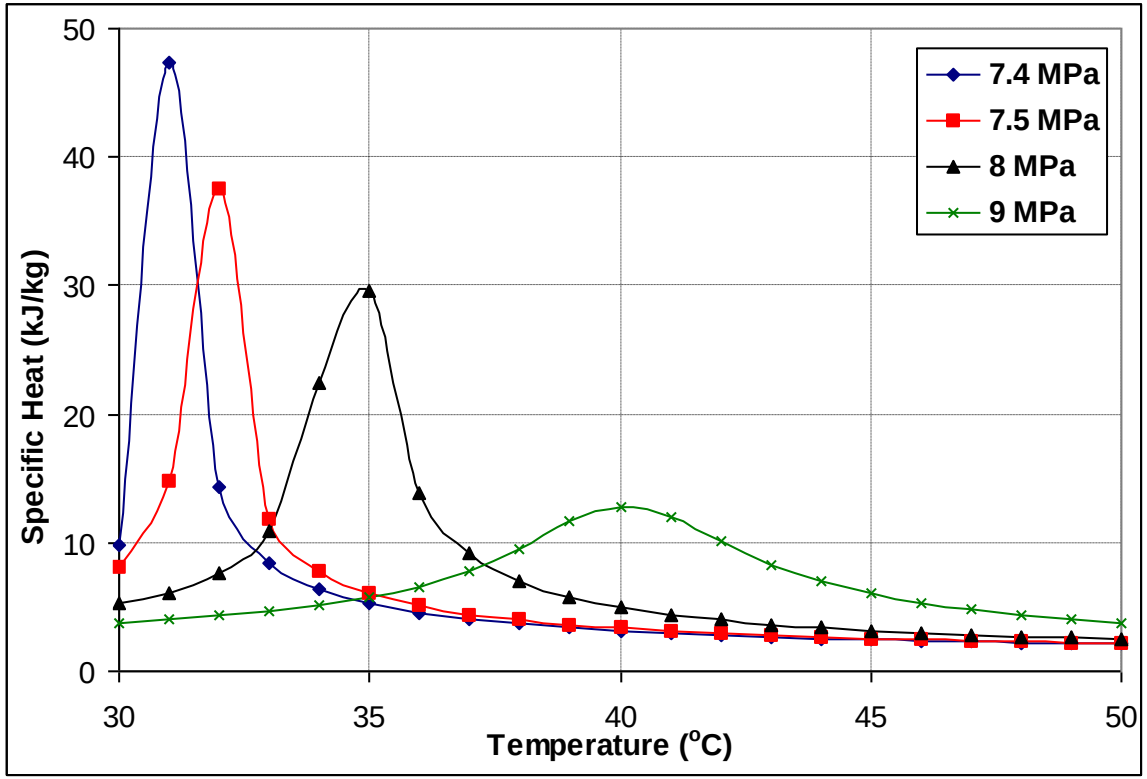

Cooler Analysis

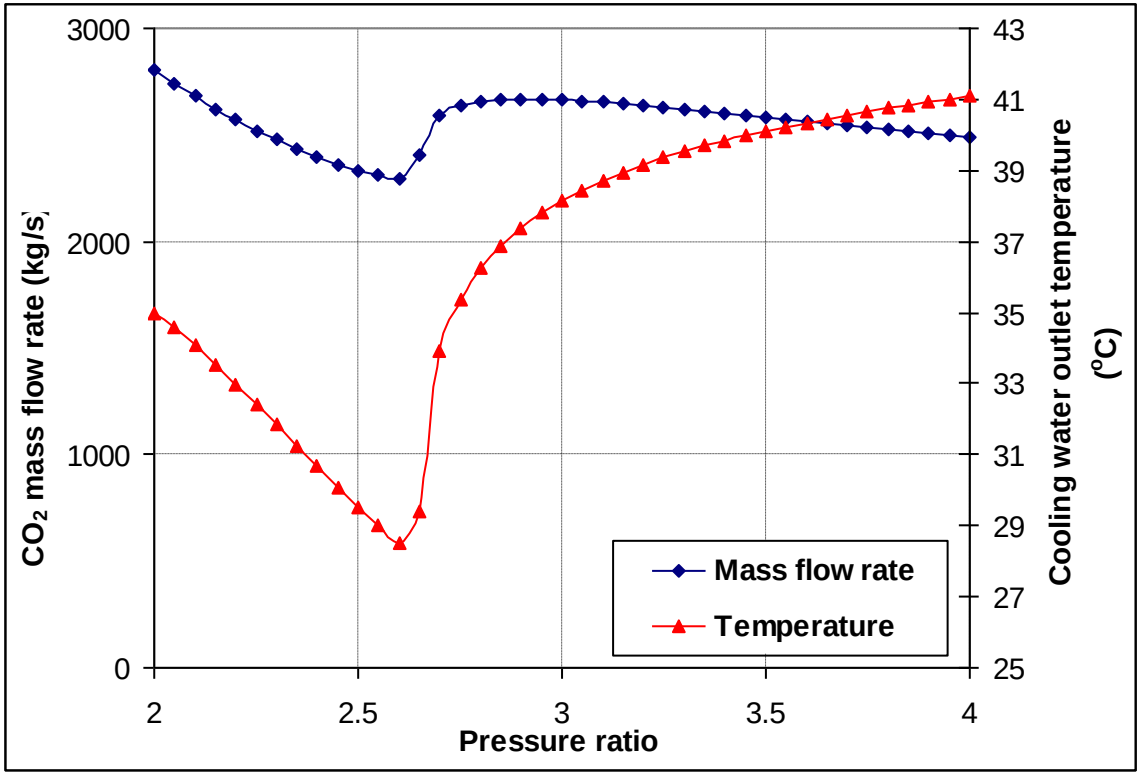

Requirement on Pumping Power

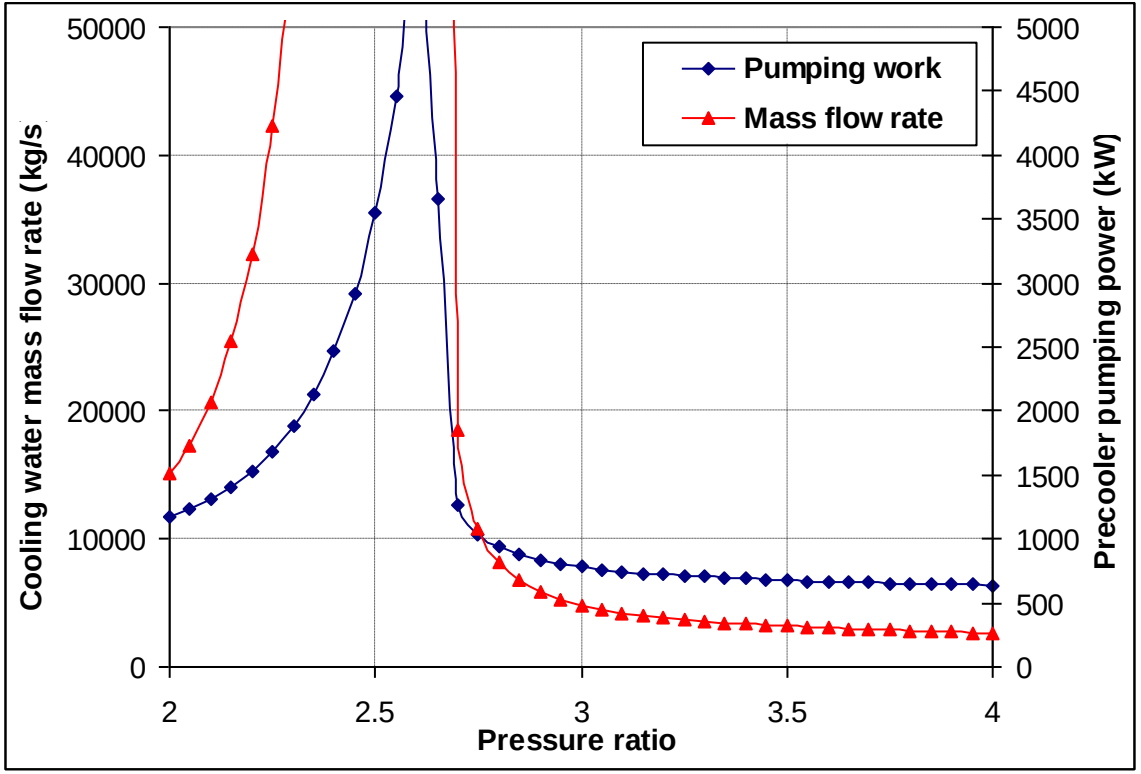

GFR Decay Heat Removal

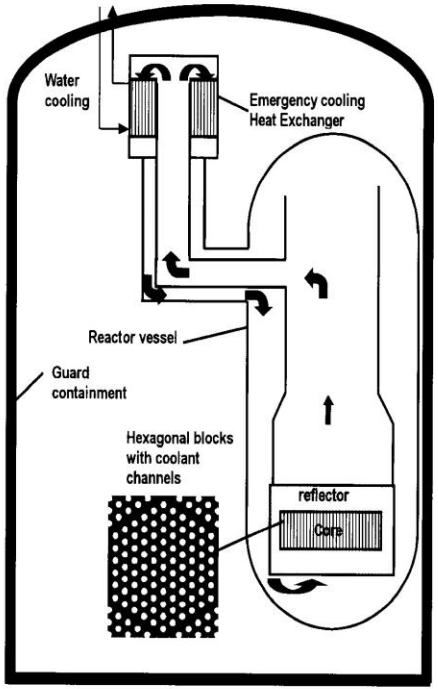

GFR DHRS Analysis

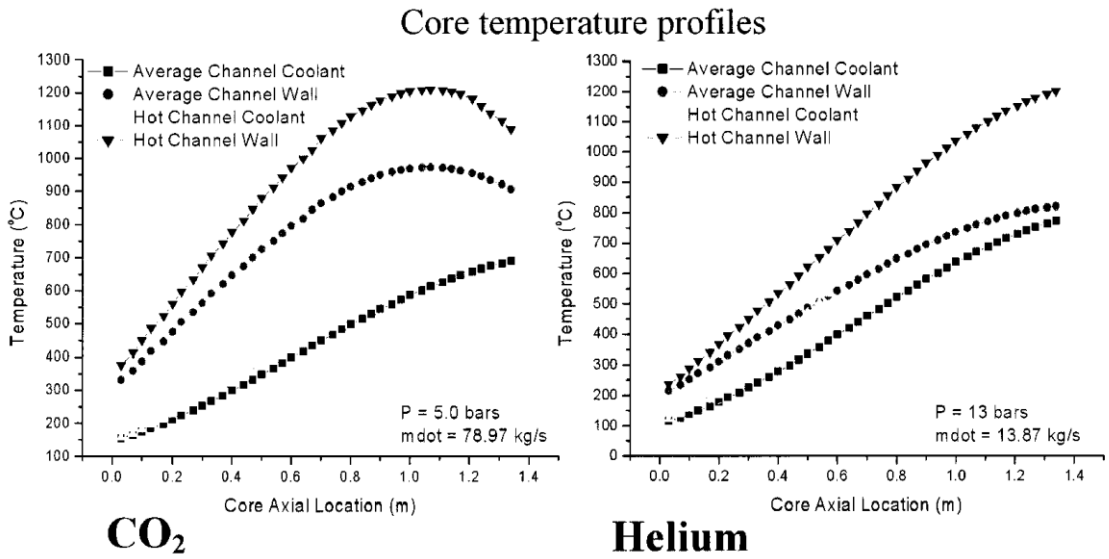

Post LOCA temperature profiles for CO_2 and helium-cooled 600 MWth cores

Gas Pressure Drop

- Moody diagram from Idelchik

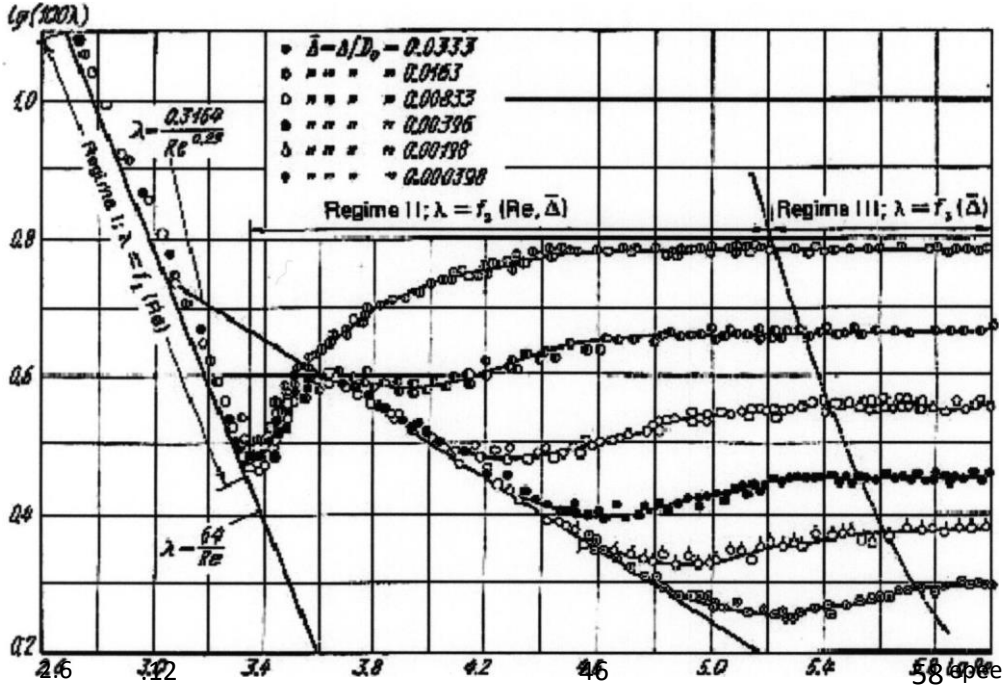

Transition Reynolds Number Lines

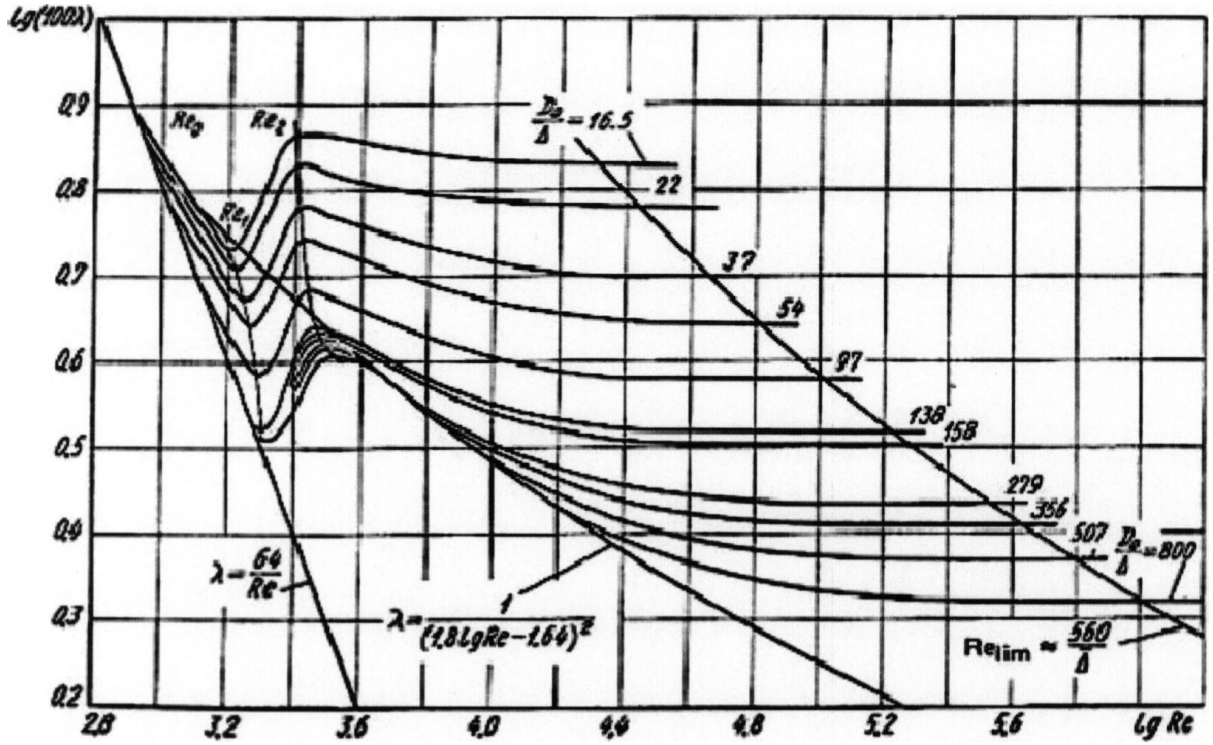

Buoyancy Altered Friction Factor

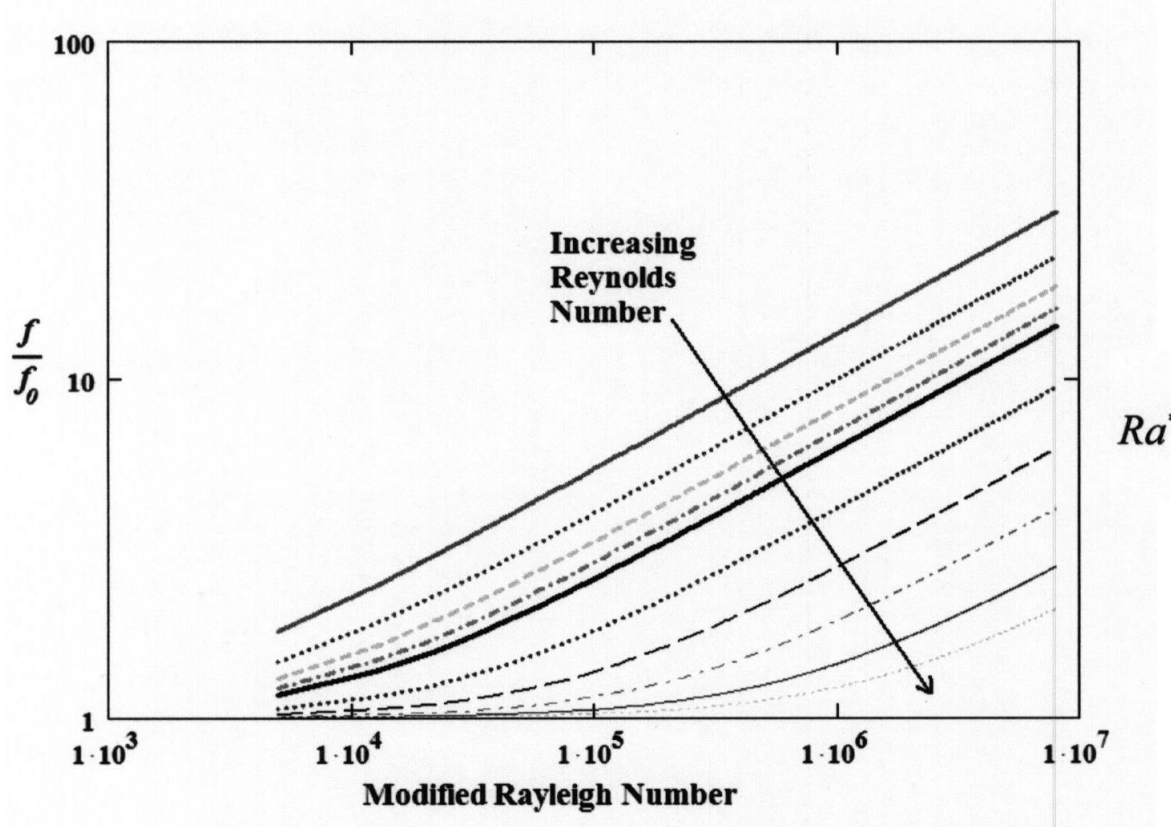

$$\mathrm{Ra} = \mathrm{GrPr}.$$

$$Ra^* = \frac{g\beta \,\mathrm{Pr}\, D^4 (dT_b / dL)}{\nu^2}$$

Buoyancy Altered Friction Factor

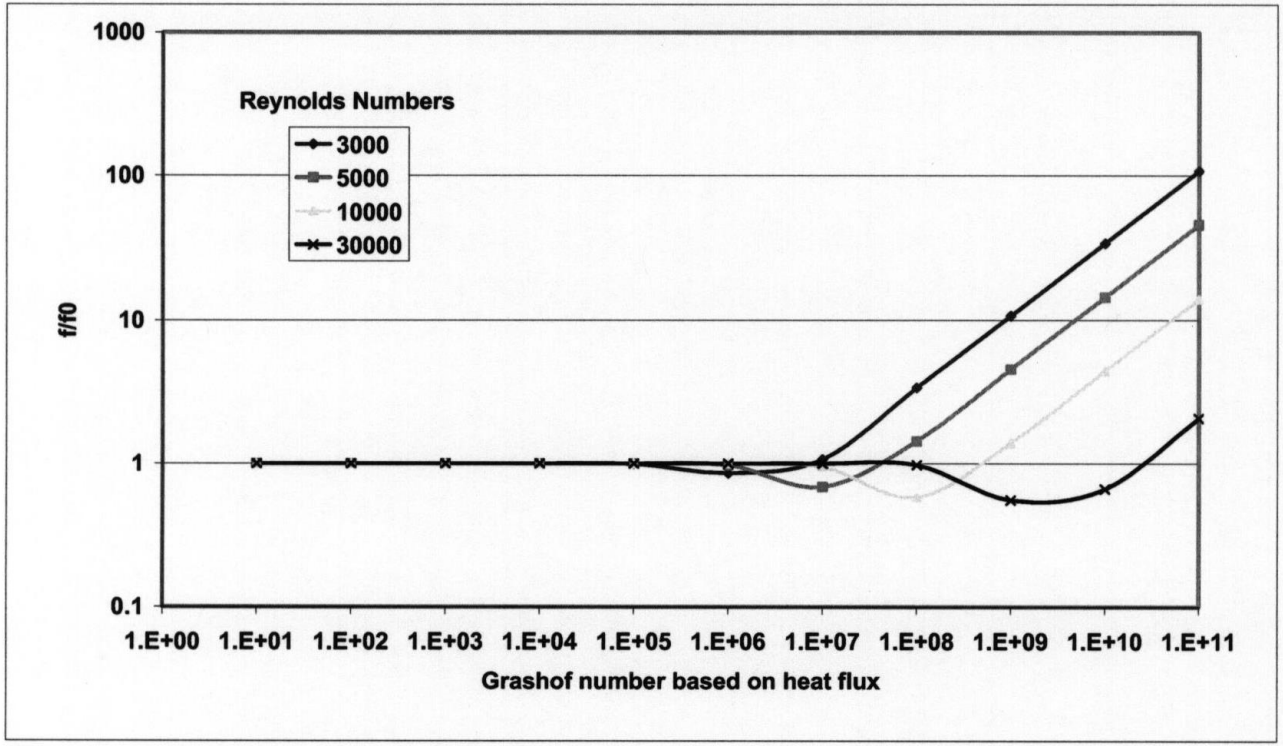

Single Phase Convection Flow Regime Map for Vertical Pipes

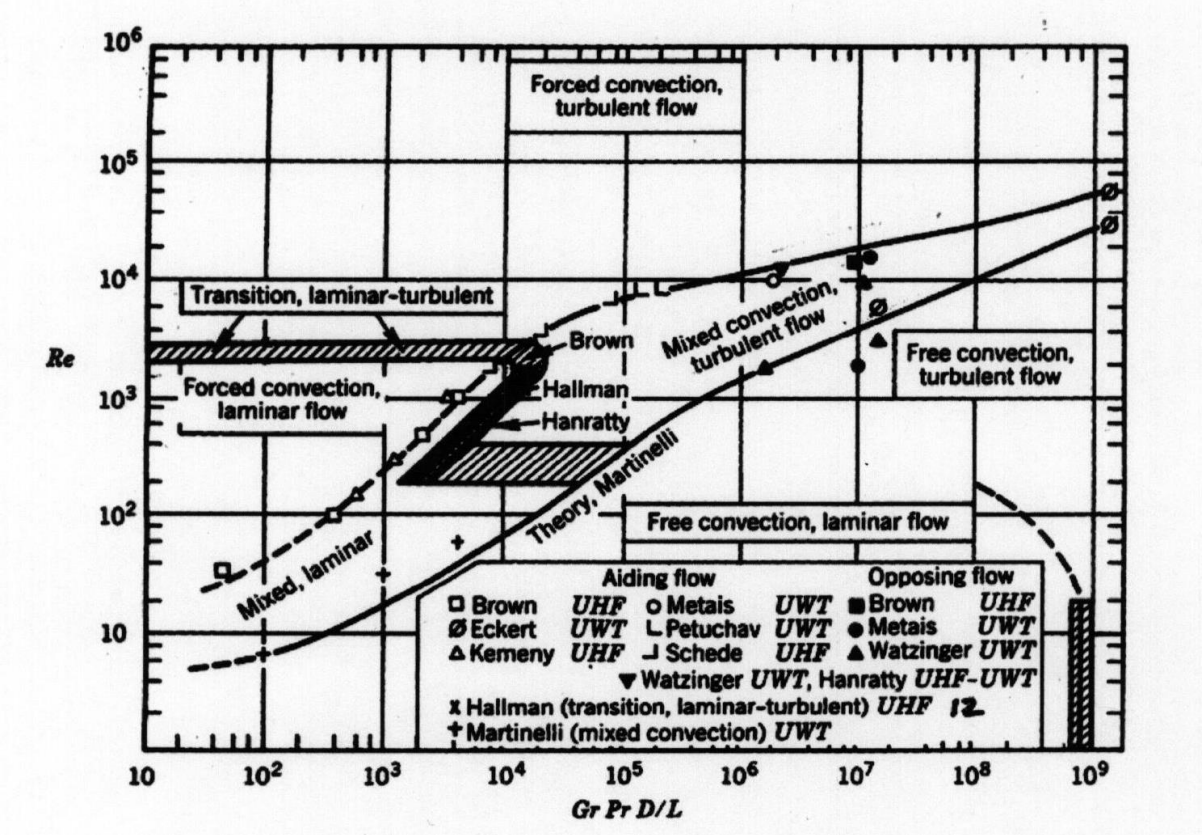

Flow Regime Map for Gas System

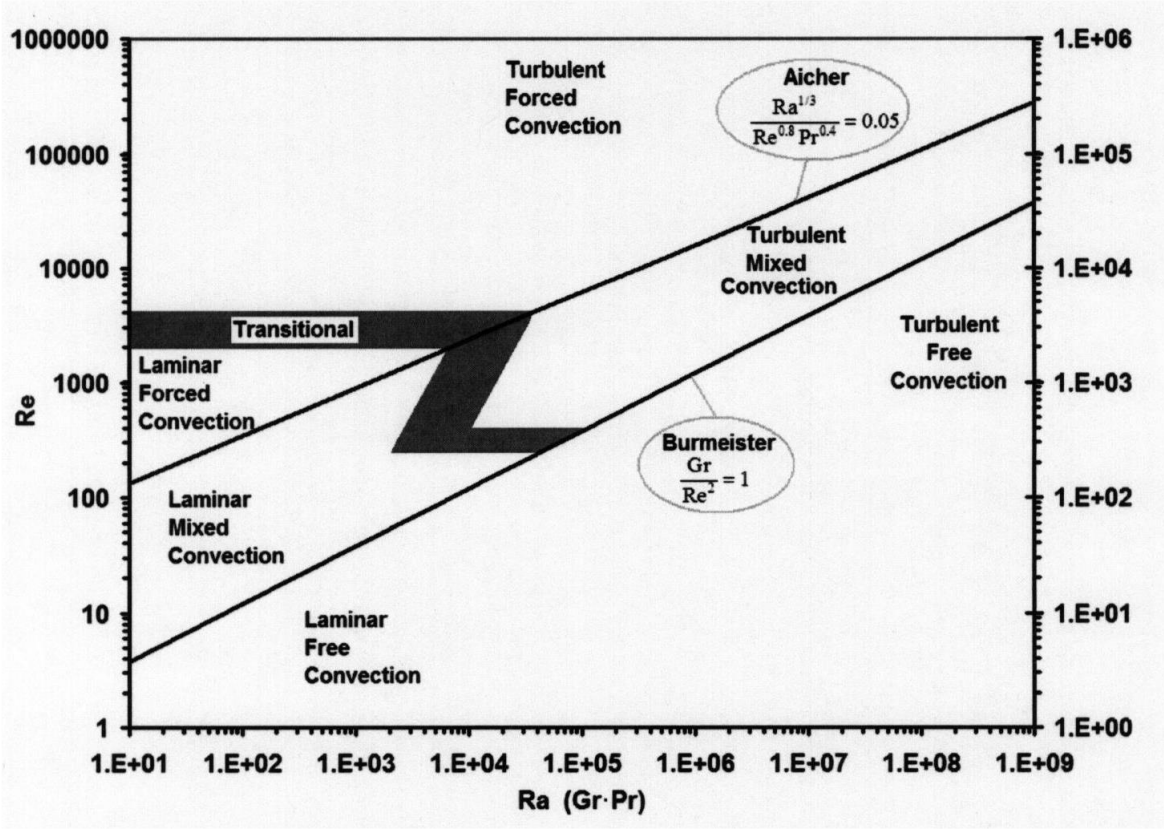

Heat Transfer for Opposing Turbulent Mixed Convection

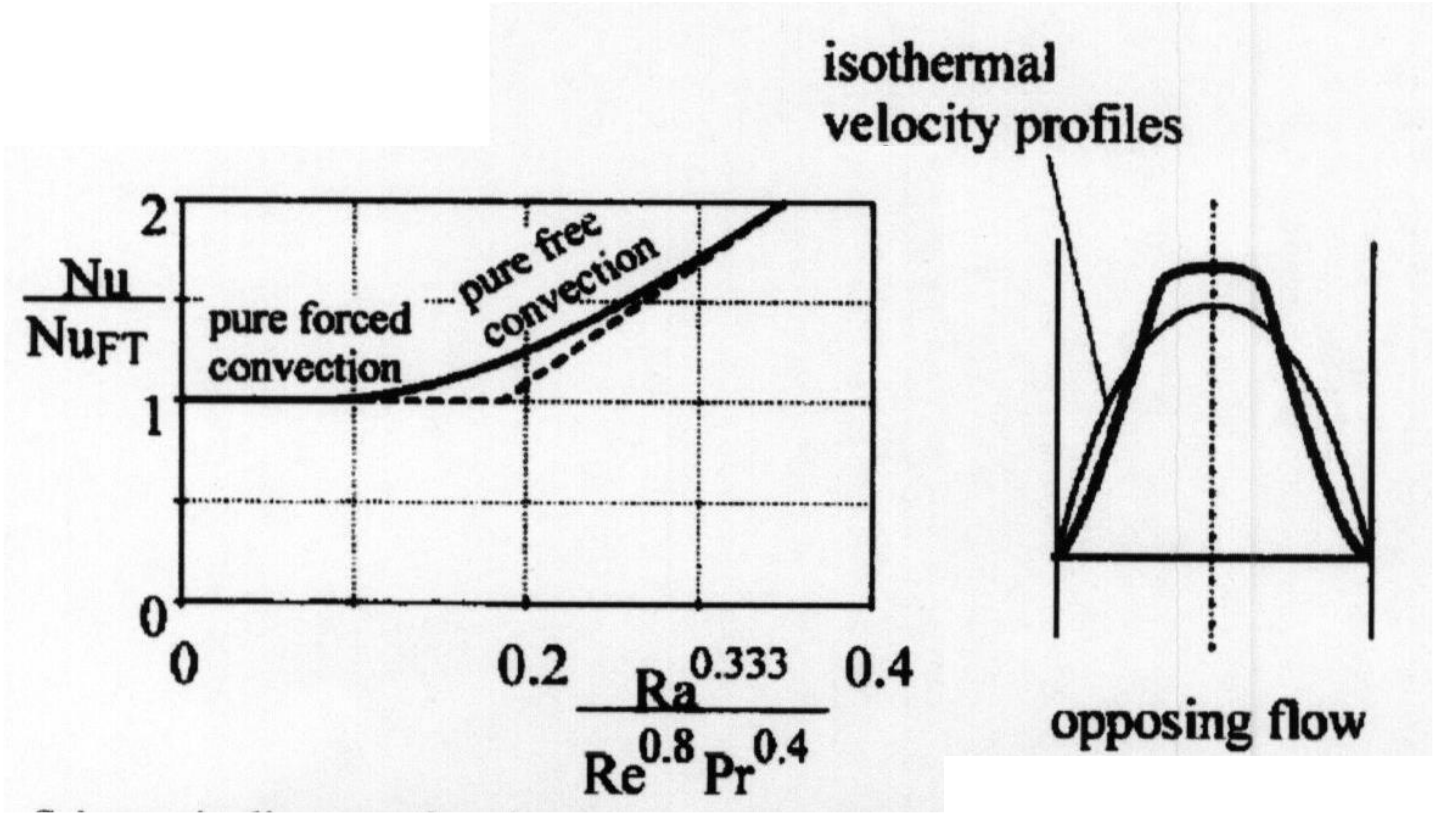

Heat Transfer for Aiding Turbulent Mixed Convection

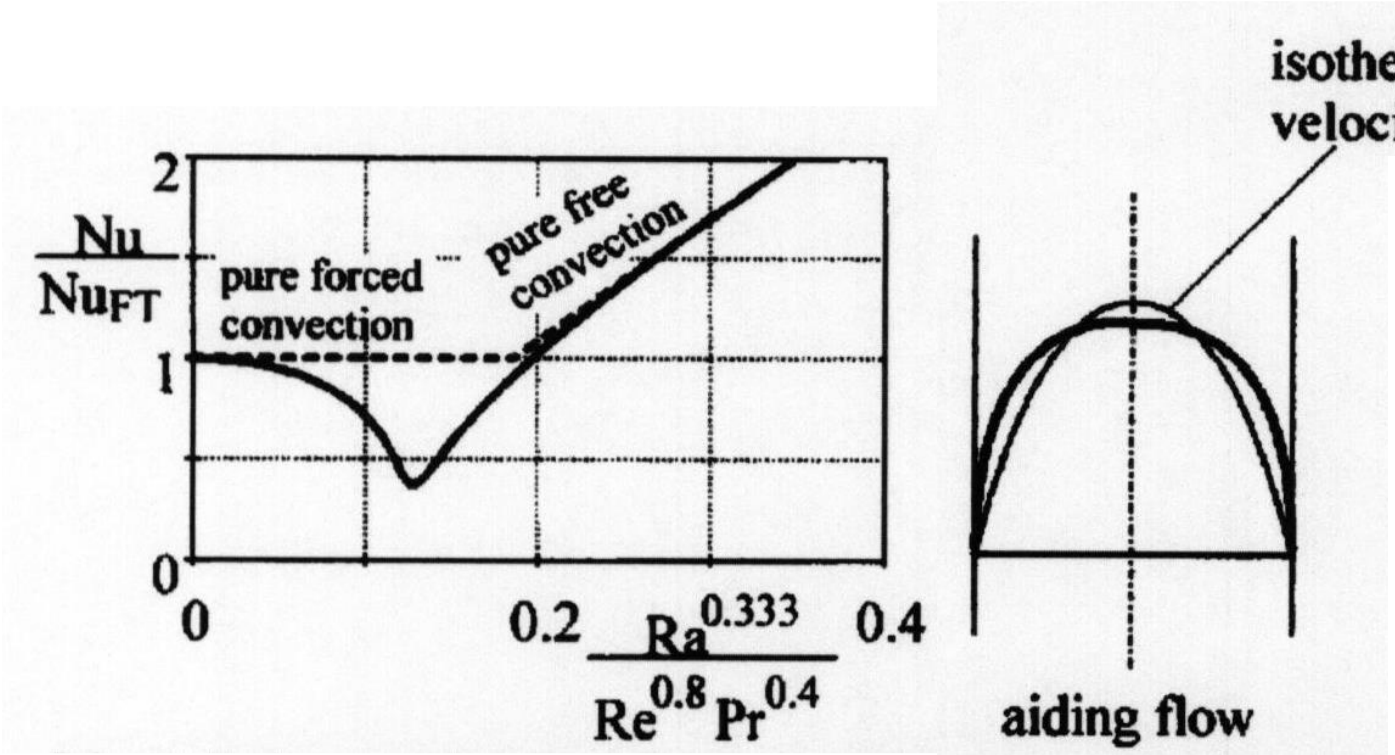

Heat Transfer for Laminar Mixed Convection

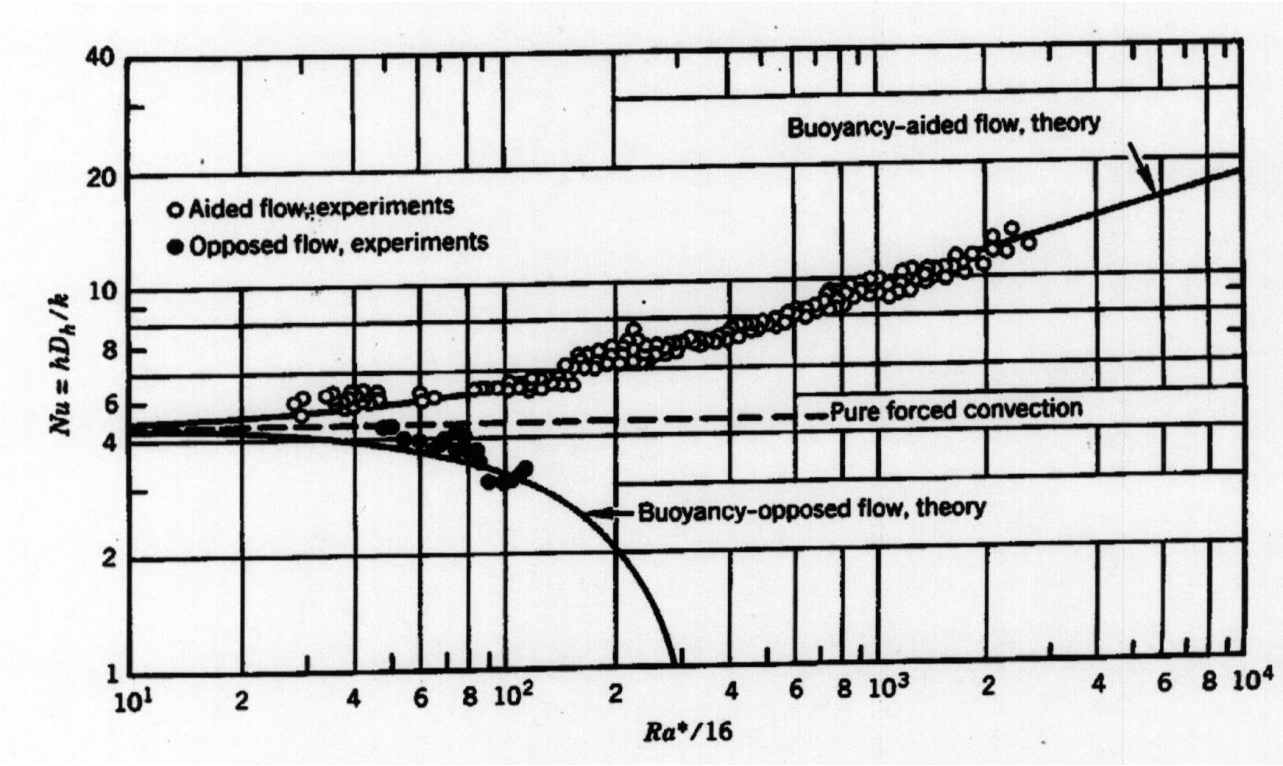

Question

- What correlation package is used in your favourite code?

ALLEGRO Core Catcher Geometry

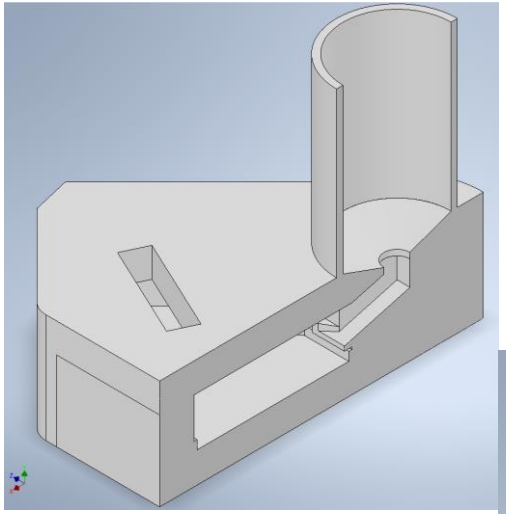

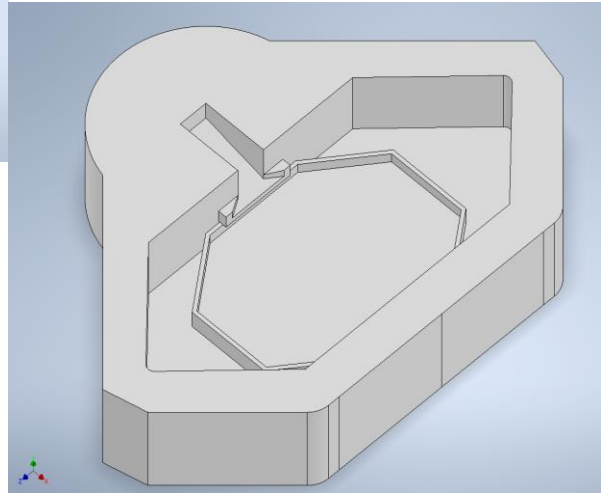

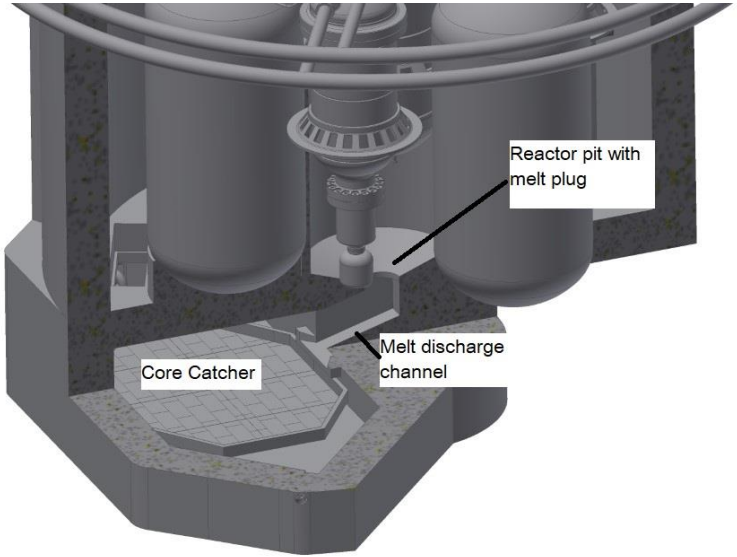

Core Catcher Modelling

- Complex severe accident scenario with a core melt down
- Subsequent simulations using
  - Integral code MELCOR
  - Mechanistic code CORQUENCH
  - CFD program ANSYS Fluent
- Simulation of corium properties for modeling of ALLEGRO core catcher behavior and main properties

CFD - Mesh

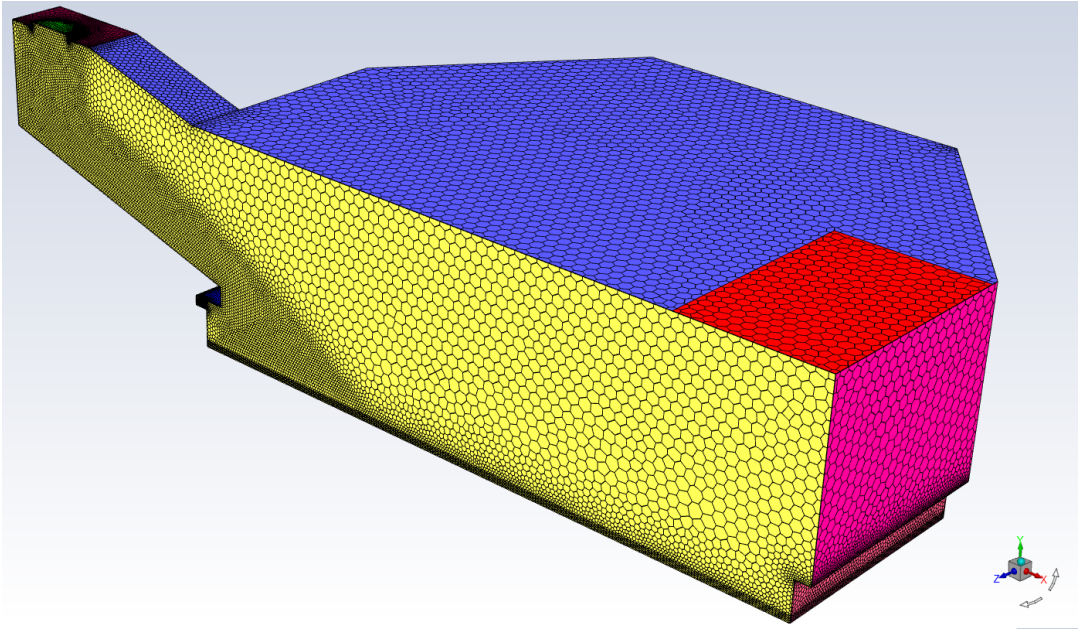

CFD – Corium Spreading

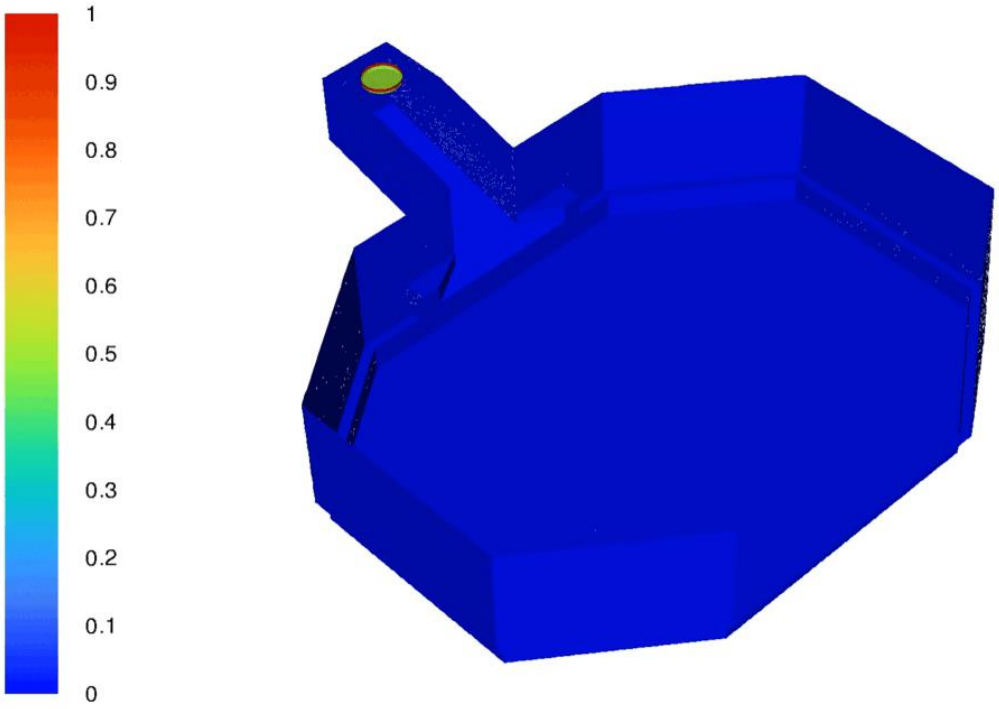

CFD – VOF vs Eulerian model

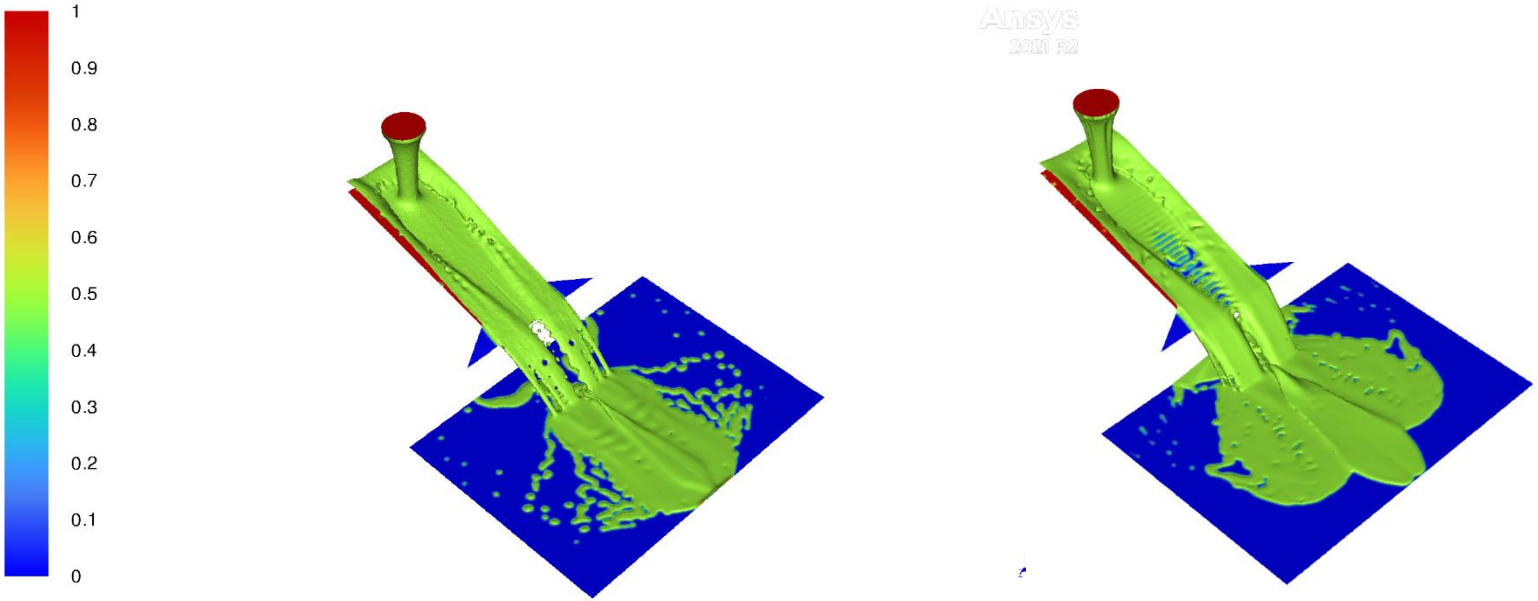

Conclusion

- Real thermodynamic and transport properties have a strong effect on simulation of gas systems.
- The intrinsic behavior of gas systems lead to high temperature gradients and mixed flow issues.
- Correlation precision is much less in these phenomena and they are often not integrated into the calcualtion codes.
- Obtaining the real properties may prove very difficult as well as subsequently obtainning precise correlations and models.

Thank you for your attention

UNIVERSITY OF CAMBRIDGE

SCONE: a Monte Carlo particle transport code for prototyping of new methods

Presented: Paul Cosgrove

Developed: Nuclear Energy Research Group (largely Mikolaj Kowalski)

Department of Engineering, University of Cambridge

SafeG workshop **5 July 2023**

Contents

- What/why is SCONE
- What SCONE can do
- User experiences
- Showcase:
  - Thermal radiative transfer
  - Multigroup acceleration of continuous energy MC
  - The random ray method

What is SCONE

Stochastic
Calculator
Of
Neutron Transport
Equation

- Particle transport Monte Carlo code for nuclear engineering applications
- Target audience → research students
- Designed for modification: Object-Oriented, well-defined abstractions
- Use: Teaching, Prototyping of New Algorithms
- Prioritise modifiability over performance

History and features

- Written in Fortran 2008:
  - Easy to learn & read without sacrificing performance
  - Informative compiler errors, easy-to-read standard
  - Reasonably well supported
- Automated testing:
  - Unit and integration tests with pfUnit framework
- Strict style guide
- Open-source: the only open-source reactor physics code in the UK
- Accessible at:
  github.com/CambridgeNuclear/SCONE

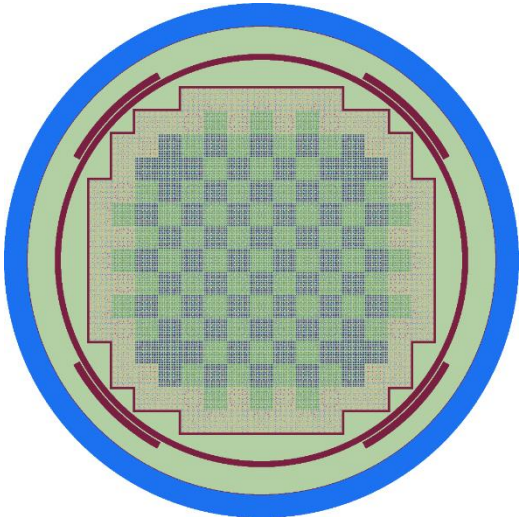

Current features

- Standard Monte Carlo capabilities:
  - Transport with continuous energy and multi-group data
  - OpenMP parallelism
  - K-eigenvalue and fixed source
  - Full neutron physics (unresolved resonance and S(α,β))
  - Standard CSG representation – also mesh geometries
  - Standard and home-grown algorithmic acceleration techniques
- *Most* of photon transport
  - Photoelectric, pair production, Rayleigh + Compton
  - Final fixes on electron handling underway

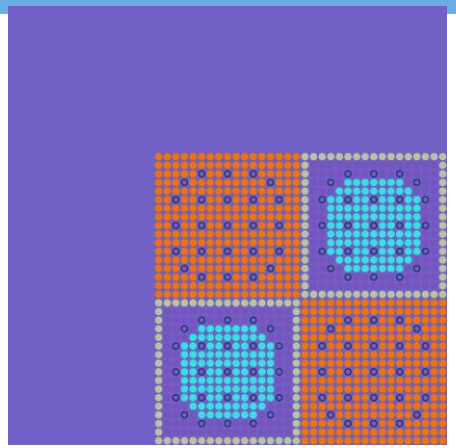

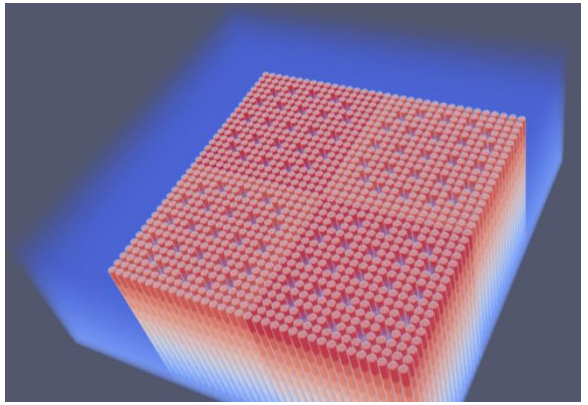

Validation

Successfully tested on standard MCNP criticality benchmarks: compared to MCNP and/or Serpent reference results

Works on fast, thermal, uranium, plutonium, water, deuterium…

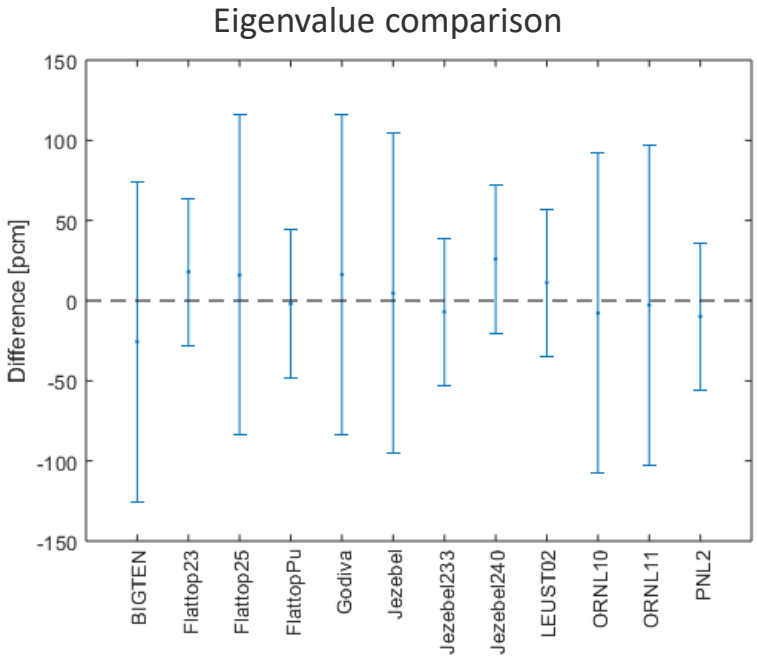

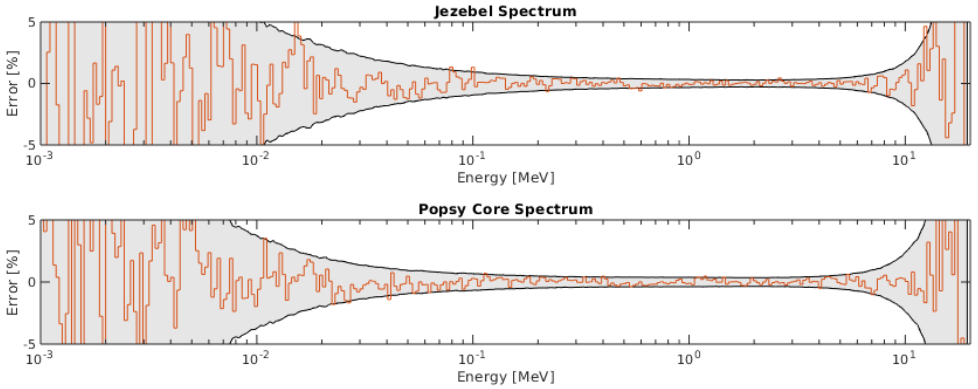

Mosteller (2008). "ENDF/B-VII.0, ENDF/B-VI, JEFF-3.1, and JENDL-3.3 results for the MCNP criticality validation suite and other criticality benchmarks", PHYSOR.

Master projects

Experience with SCONE Masters projects

- Successful completion in short time (3 to 6m)
- Meaningful contribution to the development
- Positive feedback from the students ☺
- ‘Hook’ to fish people to join reactor physics community

Lessons learned:

- Students tend to stay quiet: can spend a lot of time struggling with problems easy to correct if they ask for help
- Necessary to enforce good style

Previous projects:

- Photon transport
- Unstructured meshes
- Alpha eigenvalue
- Photon-neutron coupling
- Implicit Monte Carlo
- Low population systems
- DBRC + OTF Doppler

Ongoing projects:

- CMFD acceleration
- Dynamic Monte Carlo

Proposed projects:

- HFR geometry modelling
- Power deposition models

‘Not so greats’: New user experience

Small (and) Cambridge-based user base

- Guide for compilation may be confusing, examples are sparse
- Within lab a minor problem
- **Externalise Q&A process. Github discussions!**

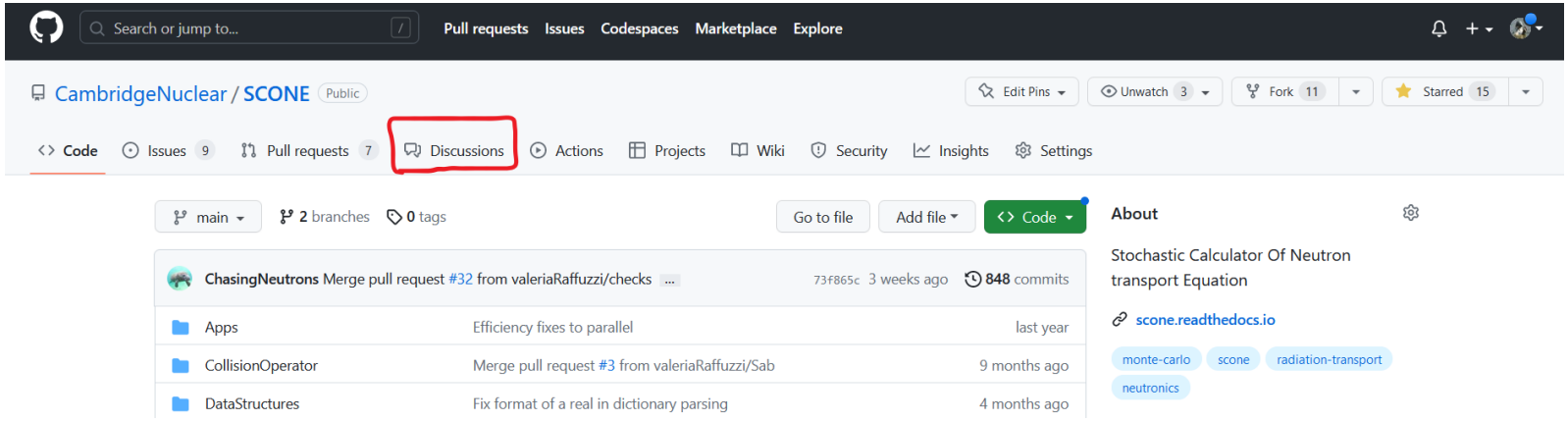

Work on generating user manual from in-source documentation comments is ongoing.

- Parsing and object-documentation association is working (using FORD)
- Next week: work on Sphinx domain and manual-generation will begin

‘Not so greats’: New user experience

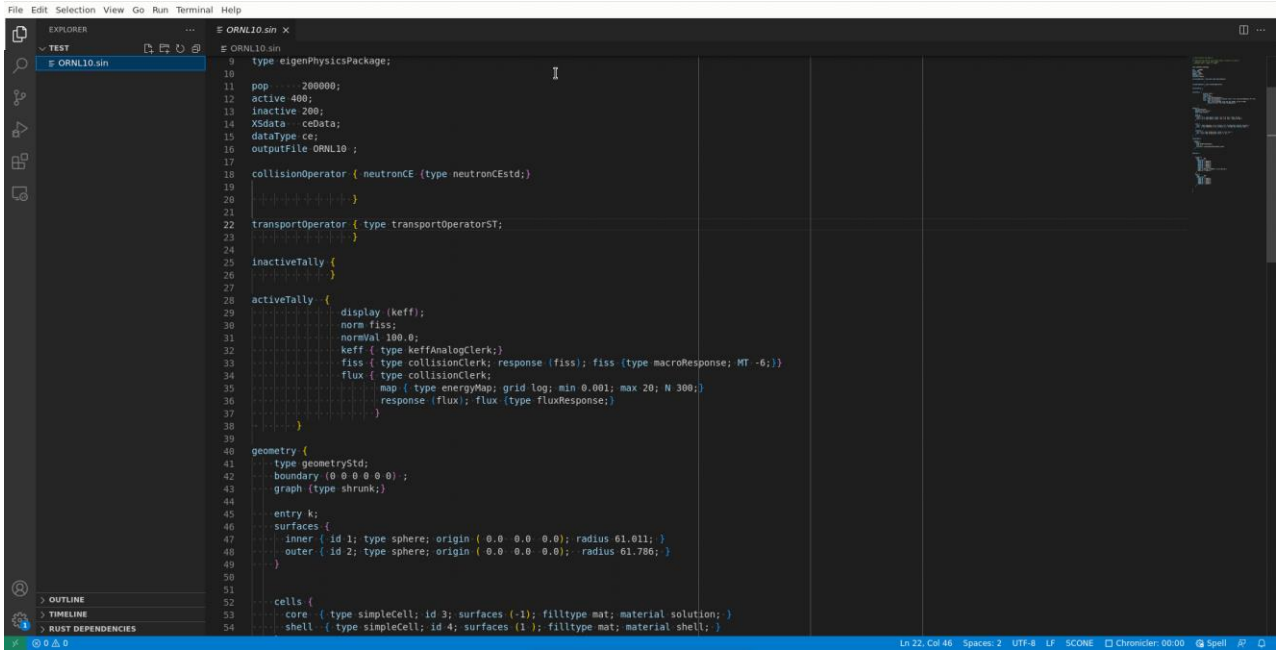

https://github.com/CambridgeNuclear/vscode-scone

Some low hanging fruits:

- VSCode integration: Syntax highlighting (including invalid syntax), folding etc.
- We will use VSCode Language Server Protocol for context-sensitive help

‘Not so greats’: Dependency Management

Manual setup of dependencies can be time-consuming. Also deviates from modern day standards:

- Make LAPACK & BLAS dependency optional
- Use FetchContent (or CPM) to get rest of dependencies automatically with CMake:
  - Downloads dependencies on configure step. Compiles on build.
  - Will increase first compilation time (no effect on recompilation)
  - Requires internet access

Work ongoing:

- ❑ Switching to pFUnit 4 (supports FetchContent build)
- ❑ `Modernisation’ of Cmake configuration

Showcase 1: thermal radiative transfer

Sometimes known as ‘implicit Monte Carlo’

Non-linear due to temperature dependence of emission rate and ‘opacities’ (cross sections)

Mostly the same mechanics as regular MC

Differences:

- Time evolution
- Material internal energy tallies
- Cross section updates

$$\frac{1}{c}\frac{\partial I}{\partial t} + \boldsymbol{\omega}\cdot\nabla I + \sigma_{\mathrm{t}} I = \sigma_{\mathrm{a}} B(T) + \frac{\sigma_{\mathrm{s}}}{4\pi}\int_{4\pi} I \,\mathrm{d}\boldsymbol{\omega}' \,,$$

$$\frac{\partial u_m}{\partial t} = c\sigma_{\mathrm{a}}\left(\int_{4\pi} I \,\mathrm{d}\boldsymbol{\omega}' - 4\pi B(T)\right) \,.$$

$$B(T) = aT^4/4\pi$$

Showcase 1: thermal radiative transfer

SCONE simulation of the Marshak wave benchmark with ‘Courant-like’ teleportation error at dimensionless time = 500

Source of particles at left boundary, propagates through cold medium over time

Due to material discretization and uniform sampling of photons within material, possible for energy wave to propagate unphysically quickly

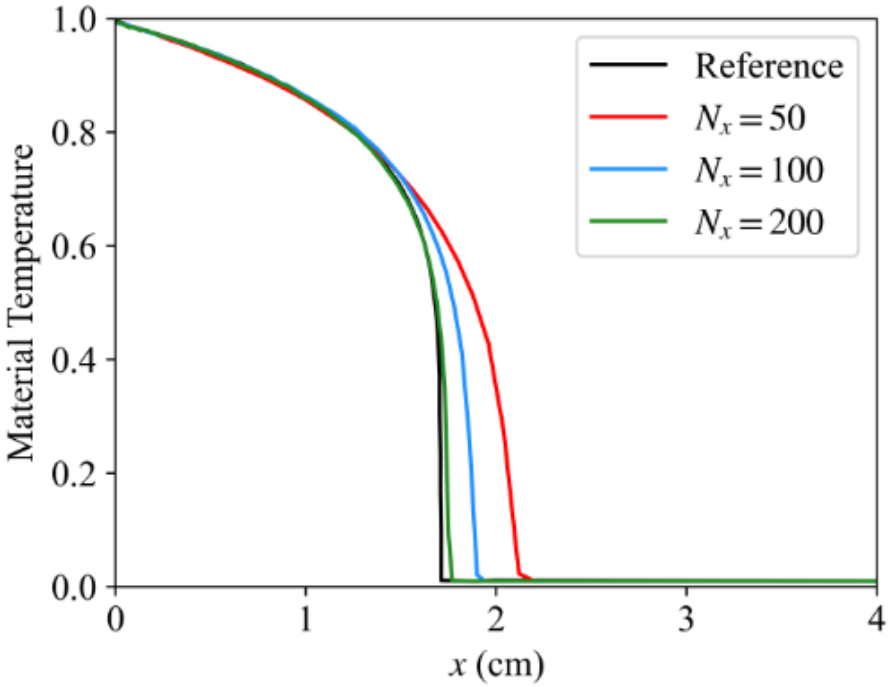

Showcase 1: thermal radiative transfer

In IMC, delta tracking is rarely used…. Why?

Opacities/XSs are temperature dependent in a nasty way. Often $\sigma \propto \frac{1}{T^n}$

Results in very poor delta tracking efficiencies: cold regions have much higher cross sections than hot regions (where photons are!)

Solution: throw a coarse grid over the problem, perform delta tracking within a coarse mesh element while checking distances to the boundaries of the mesh element

More benefit in problems which suffer from teleportation effect

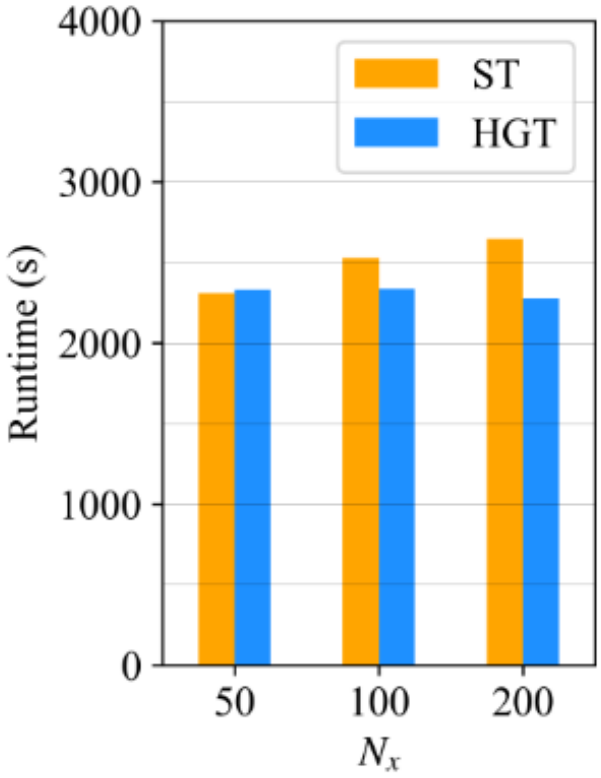

ST = (standard) surface tracking
HGT = hybrid grid tracking

Showcase 2: multigroup convergence acceleration

“Continuous” energy: use of point-wise cross sections

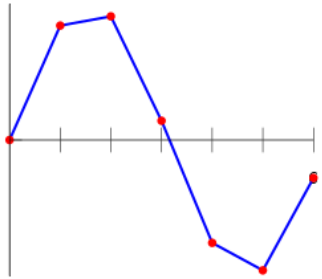

very fine energy grid with linear-linear interpolation

- Resonances are fully represented: self-shielding is automatically taken into account
- High fidelity but very time consuming

Multi-group cross sections

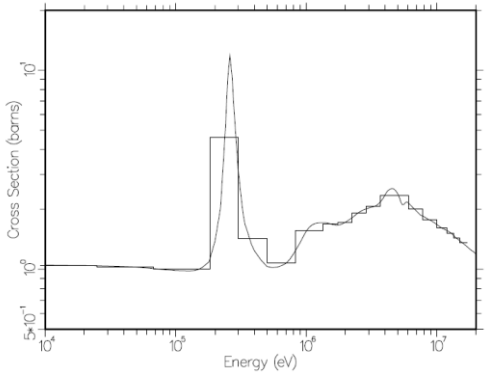

- Same cross section representation as for deterministic methods
- Introduces some approximations: low fidelity method
- Up to 5 times faster than CE

Showcase 2: multigroup convergence acceleration

- Monte Carlo needs inactive and active cycles

- The simulation takes long to converge in problems with a high dominance ratio

- Calculation route:
  - Calculate MG cross sections on-the-fly during few CE cycles
  - Switch to multi-group cross sections for the rest of the inactive cycles
  - Switch back to continuous energy for all the active cycles (to maintain full fidelity)

Showcase 2: multigroup convergence acceleration

- Speed-up convergence by a factor of 4
- Memory usage doesn't grow substantially
- Final results are generally unaffected

Burnt PWR assembly test case

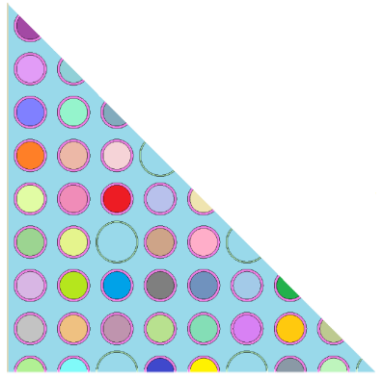

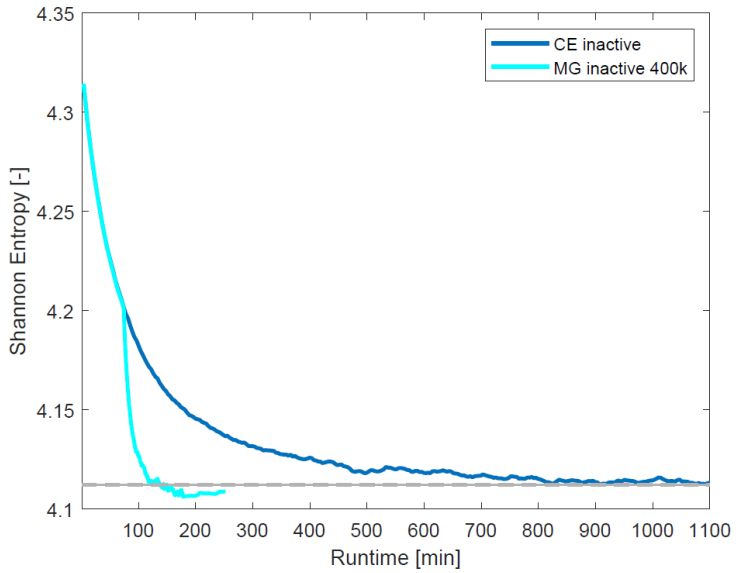

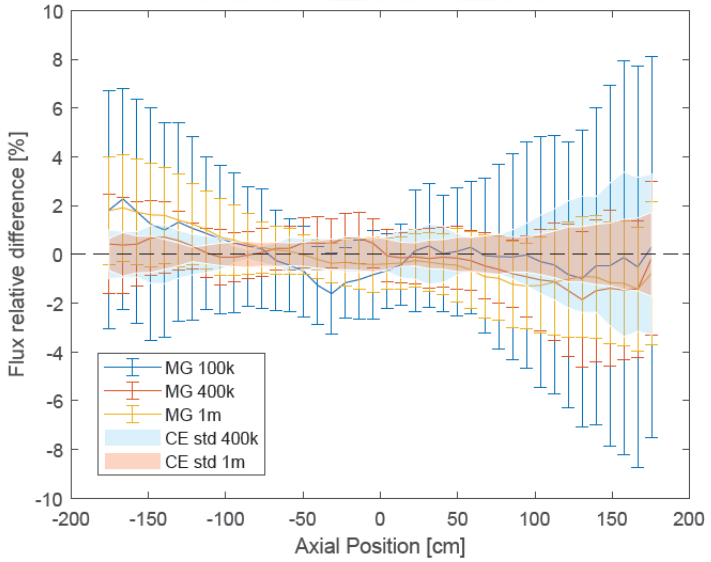

Showcase 3: random ray method

$$\frac{\mathrm{d}}{\mathrm{d}s}\psi_g(s) + \Sigma_{\mathrm{t},g}\psi_g(s) = q_g$$

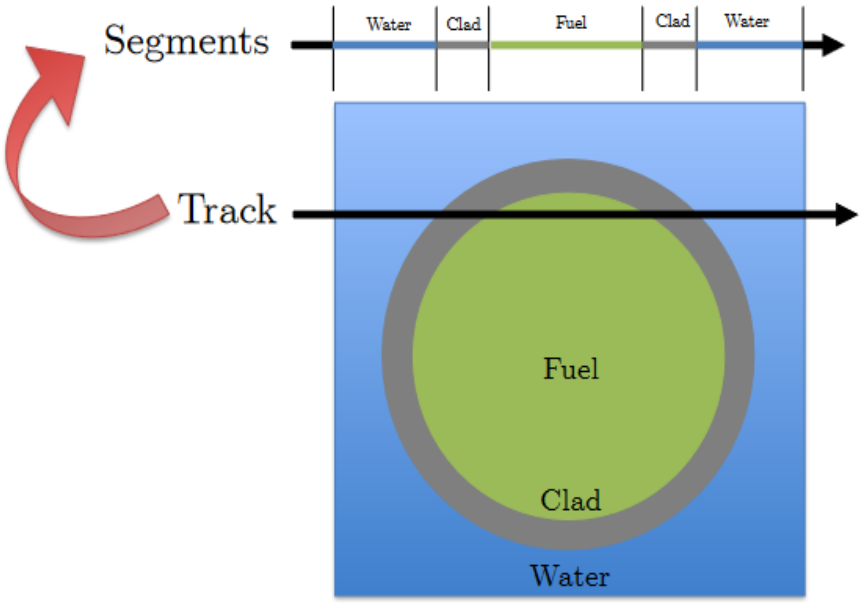

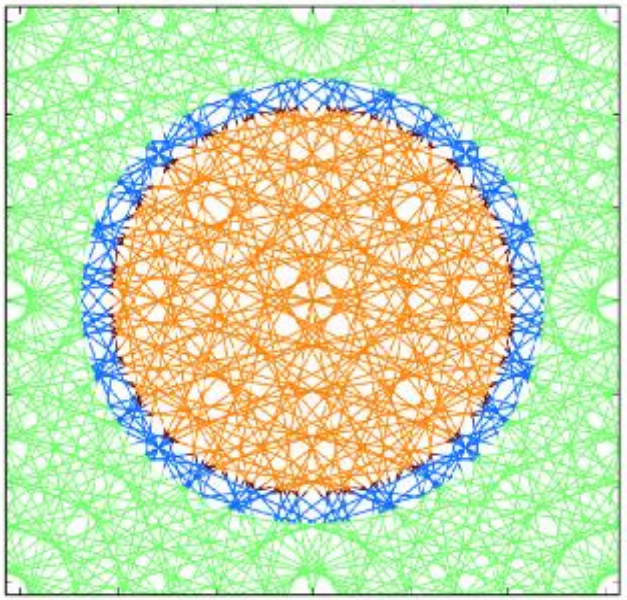

Tramm et al. (2017). "The Random Ray method for neutral particle transport", J. Comp. Phys.

Showcase 3: random ray method

Sampling rays randomly across the geometry has a number of advantages:

- Memory reduction from not storing track lengths or boundary fluxes
- Allowed a much coarser track laydown as the stochastic sample is unbiased (faster iterations)
- Evades ray effects due to continuous angular sampling

On the other hand, fluxes become stochastic, need stochastic estimators, active and inactive cycles… Fits neatly into a Monte Carlo code

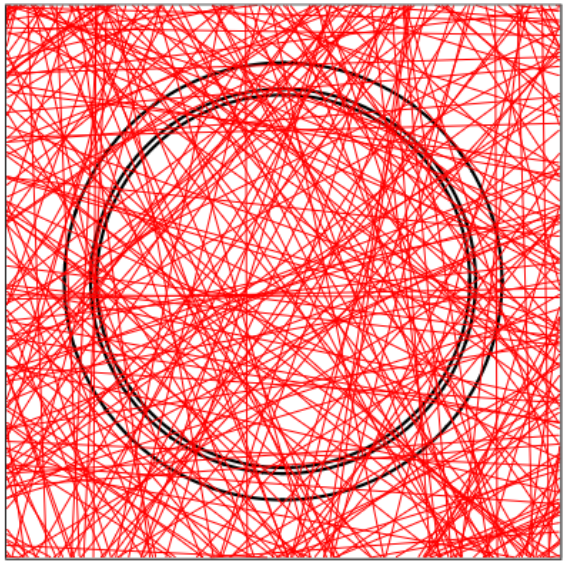

Showcase 3: random ray method

- Uniquely identifying cells
- Allow ‘particle’ to store MG flux
- Writing the algorithm
- Azimuthally divided pins
- Exponential evaluator
- Optional: distance caching (remember distance to boundary at all CSG universe levels)

Algorithm 1 MOC Power Iteration

```
Initialize Scalar Fluxes to 1.0
while K-effective and Scalar Flux Unconverged do
    Normalize Scalar Flux to Fission Source
    Compute Source (Equation 9)
    Flatten Scalar Flux to Zero
    Transport Sweep (Algorithm 2)
    Normalize Scalar Flux to Sum of Ray Distances
    Add Source to Scalar Flux (Equation 10)
    Calculate K-effective
end while
```

Showcase 3: random ray method

C5G7 geometry

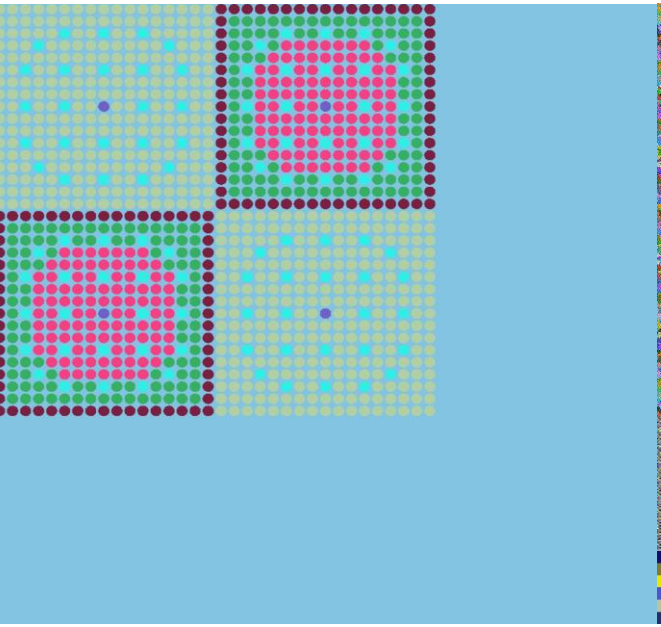

MoC discretisation

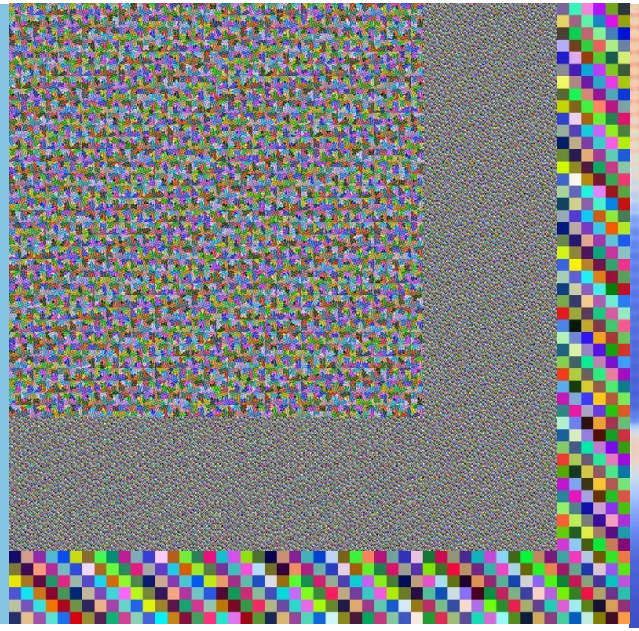

Thermal flux

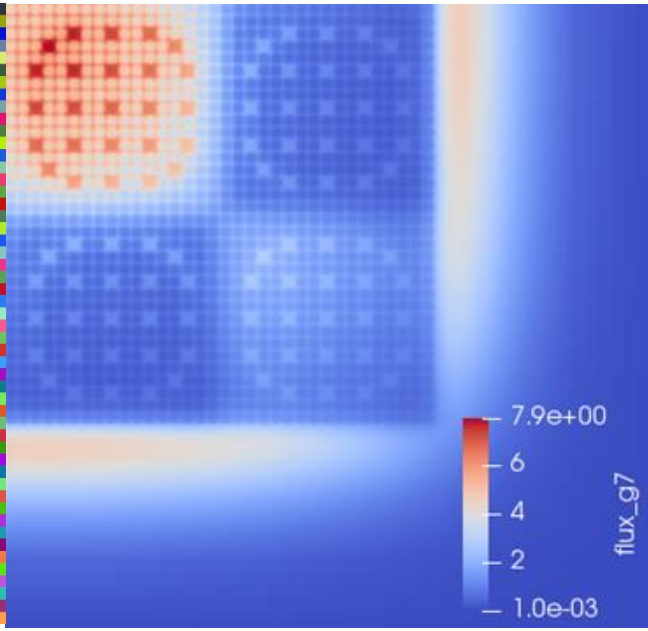

1 minute to run on 40 core 3.1GHz Xeon Gold
Eigenvalue difference of 16pcm, stochastic uncertainty of 15pcm

Showcase 3: random ray method

Which is better: MG MC or TRRM?

Quite similar for C5G7 in error and runtime

With more groups MGMC is actually faster… But that may change with more tallies

However TRRM has a globally flat uncertainty profile: good for deep into shields or reflectors!

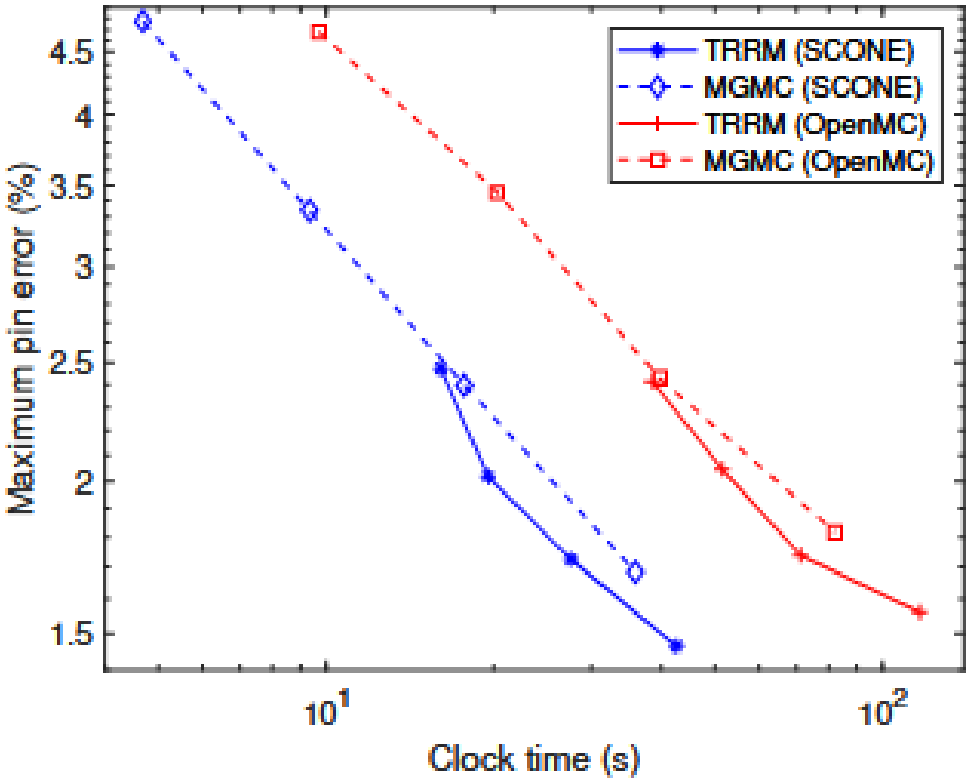

Summary

- SCONE is a Monte Carlo code developed in Cambridge
- Developer team is growing, as are its features and relevance to reactor simulation
- It has been successfully used for several research projects and for enticing students to work on MC methods
- Hopefully it can be useful for others in testing their MC ideas

Thank you for your attention

<*))))><

UNIVERSITY OF CAMBRIDGE

Nuclear fuel behaviour during severe accidents: A CFD perspective

Anuj Dubey

SafeG Workshop - Advanced Modelling Techniques

Outline

- Introduction
- CFD Models and experimental validation
- Severe accident simulations
- Fission gas pressurisation effects
- Conclusions and future scope of work

Background

- Sodium-cooled Fast Reactor (SFR) cores are not designed with most reactive configuration
- Core meltdown followed by fuel compaction can result in prompt-criticality
- Beyond Design Basis Events (BDBEs) studied to mitigate radiological consequences
- Unprotected transient overpower (UTOP) is one of three most conservative BDBEs for SFRs

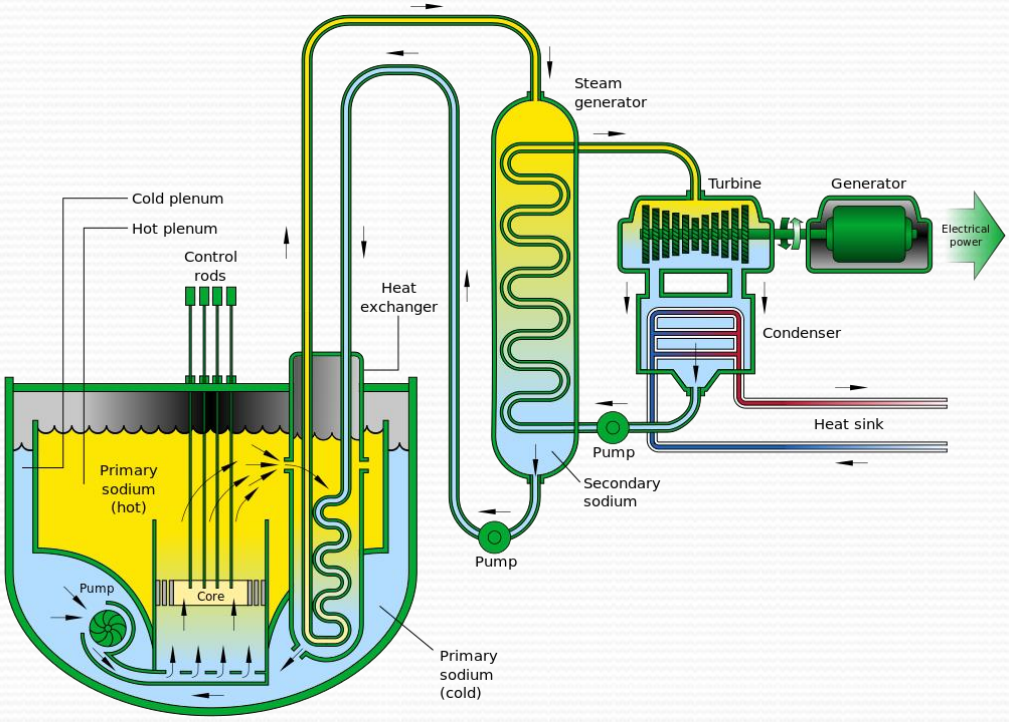

(Schematic of a pool-type SFR)

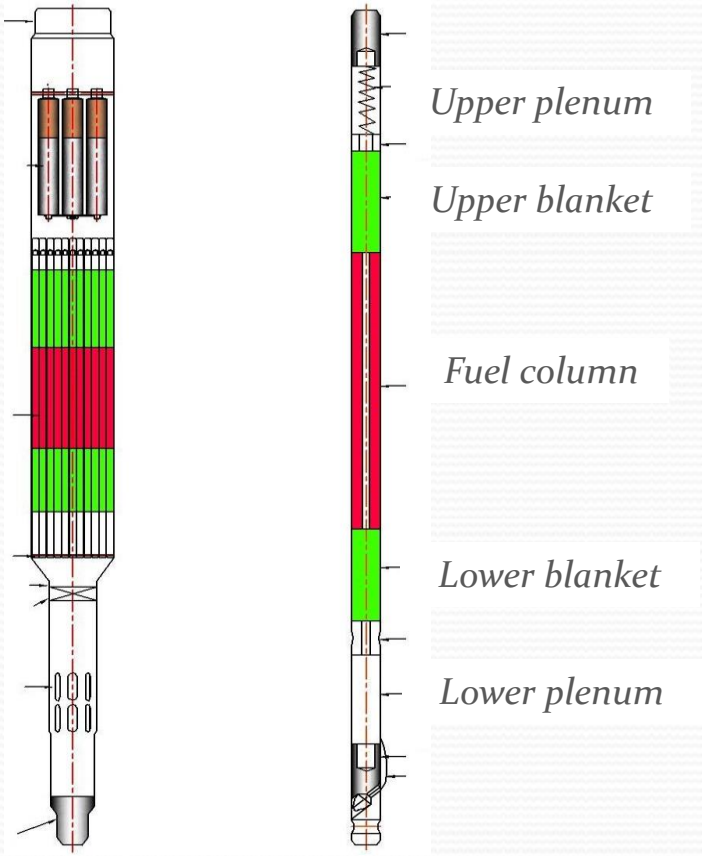

(Typical SFR fuel pin and subassembly)

Fuel melting (Unprotected Transient Overpower)

UTOP - Single control rod withdrawal with simultaneous failure of all shutdown systems.

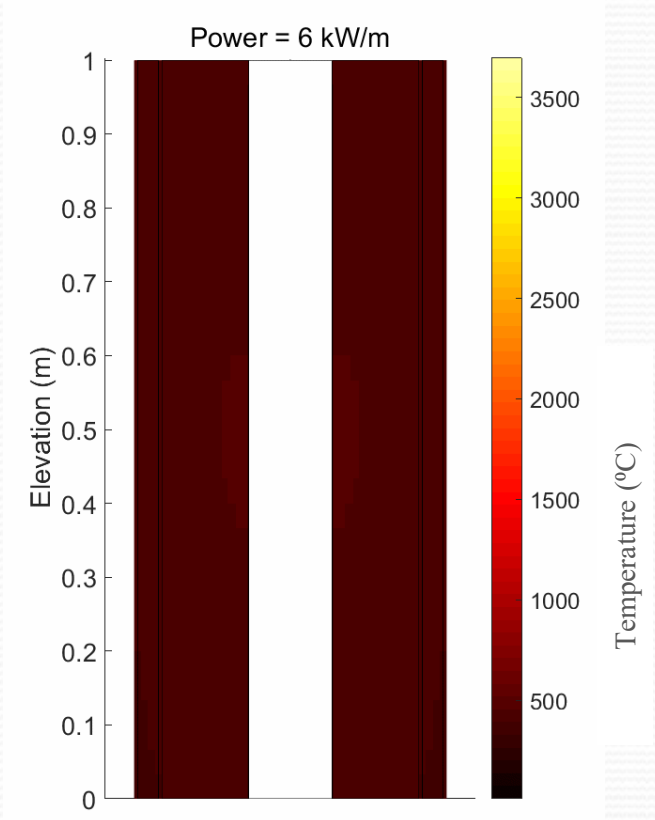

(Thermal map of fuel column)

- **Heat transfer**
  - Heat generation > Heat extraction
  - Clad temperature remains low due to coolant flow
  - Melting begins at inner edge of fuel pellet near core mid-plane
- **Fluid dynamics**
  - Multi-phase flow (*Fluid 1- Molten fuel, Fluid 2- Fission gas mixture*)
  - Movement of molten fuel governed by hydrodynamics *(Gravity, Viscosity, Multi-phase momentum interactions, Pressure perturbations from fission gas release, Surface tension)*

Fuel mass removal - reactivity perturbation worth

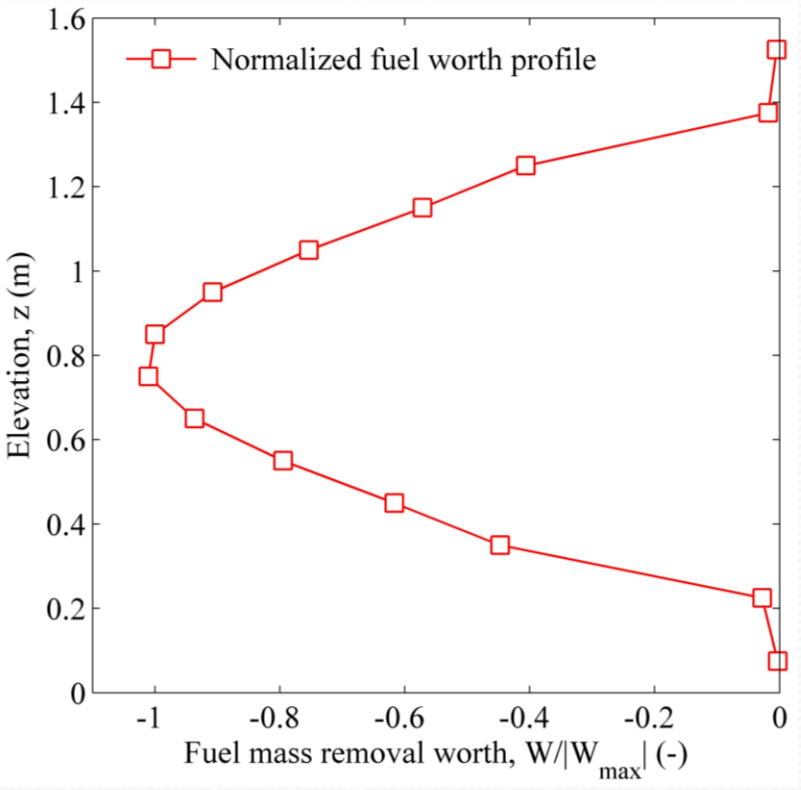

(Fuel mass removal worth profile)

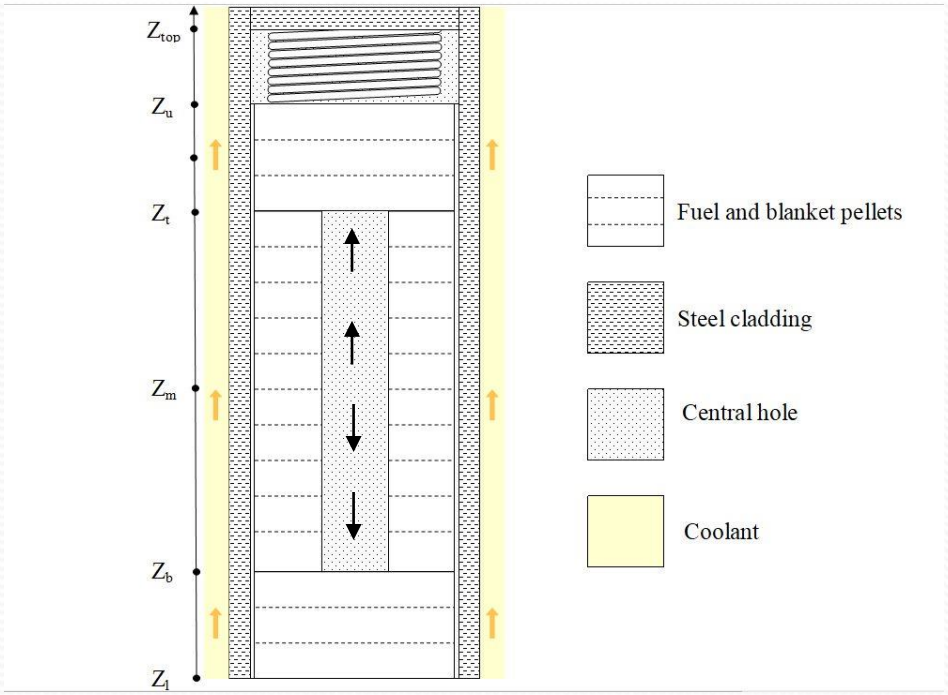

(Fuel and blanket column schematic)

- Large variation in the fuel mass removal worth profile inside fuel column.
- Relocation from high worth to low worth region will improve inherent safety
- Relocation from low to high worth region would result in positive reactivity insertion

Objectives

- Determine the motion of molten nuclear fuel during an unprotected transient overpower (UTOP) accident.
- Predict the consequence of this motion on sodium-cooled fast reactor safety margin.

Problem statement

- SFR fuel pin with solid blanket pellets and annular fuel pellets is subjected to UTOP, resulting in a slow power ramp with continuous coolant flow.
- Melting initiates on the inner surface of fuel pellets.
- Predict the resultant thermal hydraulics and reactor dynamics phenomena?

Challenges

- Phase-change heat transfer is coupled to melt motion
- Multiple hydrodynamic forces (Gravity, Viscosity, Multi-phase drag, Fission gas release induced pressure perturbations, Surface tension)
- Melt motion is dynamically coupled with core reactivity

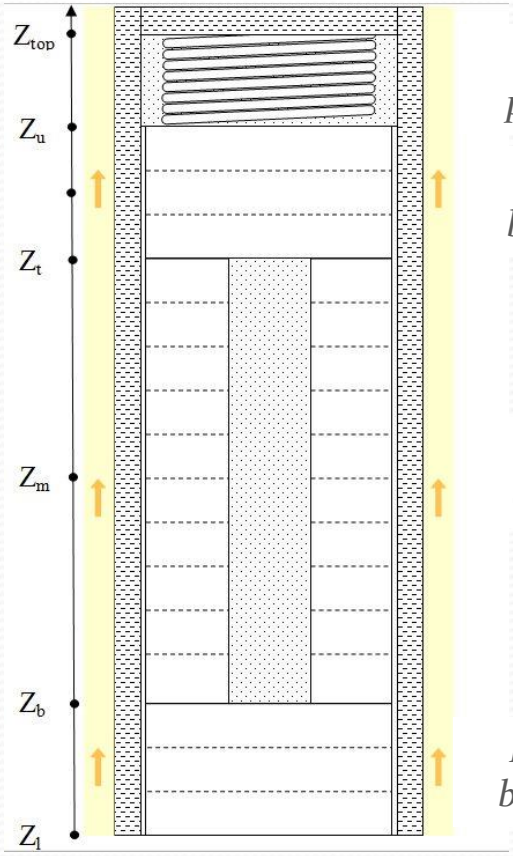

Outline

- Introduction
- **CFD Models and experimental validation**
- Severe accident simulations
- Fission gas pressurisation effects
- Conclusions and future scope of work

Phase-change heat transfer coupling with melt motion

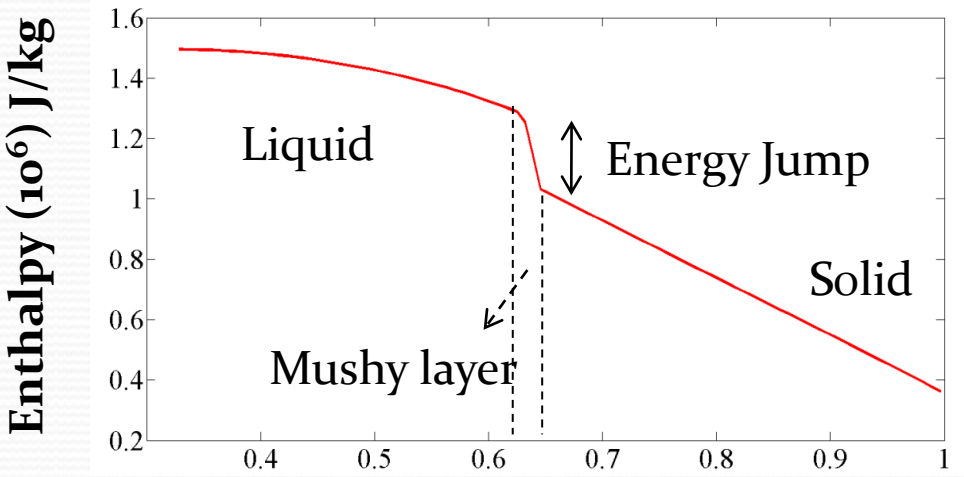

(Phase change in nuclear fuel)

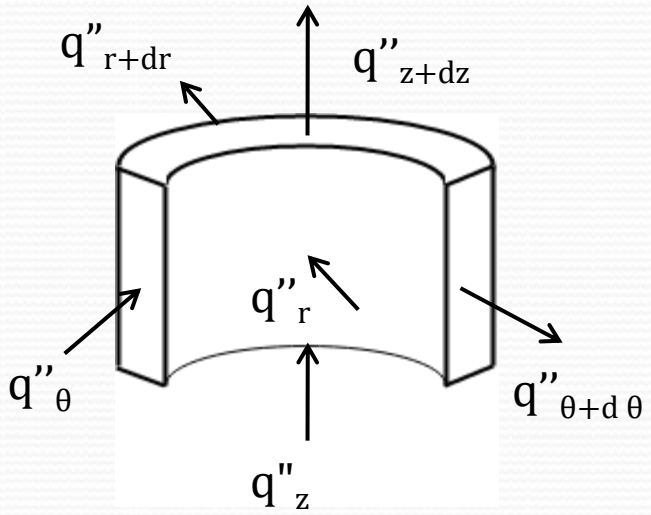

$q''_{\theta}, q''_{\theta+d\theta} = 0$ (axisymmetry)

$$\rho_f(T_f)\frac{\partial H_f}{\partial t} = \dot{Q}(z,t) + \frac{1}{r}\left(\frac{\partial}{\partial r}\left(K_f(T_f) r \frac{\partial T_f}{\partial r}\right)\right) + \frac{\partial}{\partial z}\left(K_f(T_f)\frac{\partial T_f}{\partial z}\right)$$

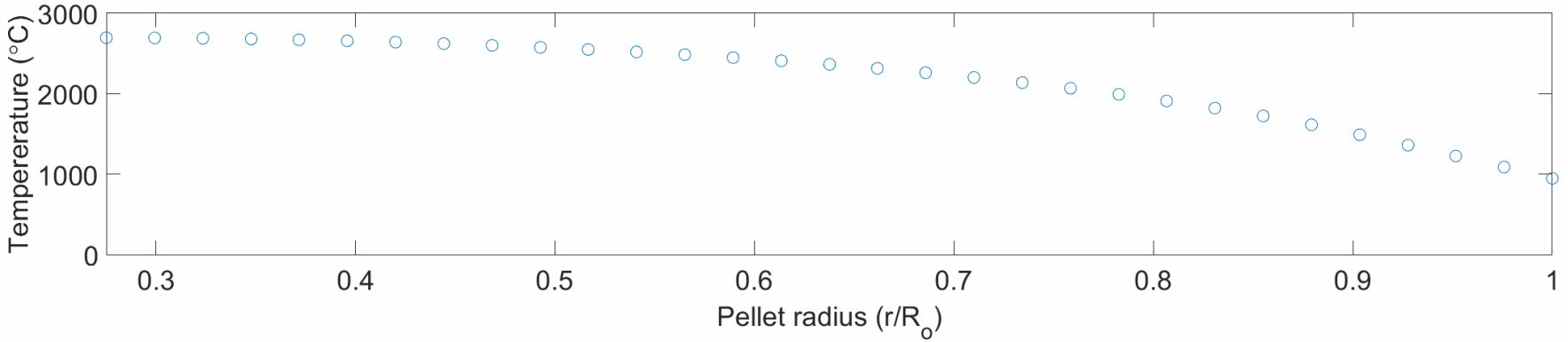

(Melt-interface-fitted coordinate)

Int. J. Therm. Sci, 125: 256-272 (2018)

Fi

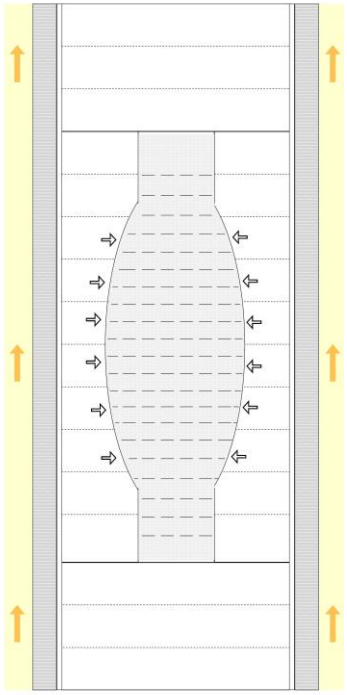

(Schematic

Hydrodynamic

Mass conservation

$$\frac{\partial(\alpha_g \rho_g A)}{\partial t} + \frac{\partial(\rho_g \alpha_g A V_g)}{\partial z} = S_g \quad \text{... (1)}$$

$$\frac{\partial(G_f A)}{\partial t} + \frac{\partial(G_f A V_f)}{\partial z} = S_f \quad \text{... (2)}$$

Energy conservation

$$\alpha_f A \rho_f \frac{\partial H_f}{\partial t} + \frac{\partial(\alpha_f A \rho_f H_f V_f)}{\partial z} = S_f(e_{sf} - H_f) + H_f \frac{\partial(\rho_f \alpha_f A V_f)}{\partial z} - \frac{\partial(\alpha_f A q_f)}{\partial z} + \alpha_f A \rho_f Q_f - q_{f-g} + q_{w,f} \quad \text{... (3)}$$

$$\alpha_g A \rho_g \frac{\partial H_g}{\partial t} + \frac{\partial(\alpha_g A \rho_g H_g V_g)}{\partial z} = S_g(e_{sg} - H_g) + H_g \frac{\partial(\rho_g \alpha_g A V_g)}{\partial z} - \frac{\partial(\alpha_g A q_g)}{\partial z} + q_{f-g} + q_{w,g} \quad \text{... (4)}$$

Momentum conservation

$$\frac{\partial(\alpha_f A \rho_f V_f)}{\partial t} + \frac{\partial(\alpha_f A \rho_f V_f^2)}{\partial z} = -\alpha_f A \frac{\partial P_{cav}}{\partial z} - \alpha_f A \rho_f g - \tau_{w,f} - F_D + F_{vm} \quad \text{... (5)}$$

$$\frac{\partial(\alpha_g A \rho_g V_g)}{\partial t} + \frac{\partial(\alpha_g A \rho_g V_g^2)}{\partial z} = -\alpha_g A \frac{\partial P_{cav}}{\partial z} - \alpha_g A \rho_g g - \tau_{w,g} + F_D - F_{vm} \quad \text{... (6)}$$

$$S_f = \frac{dA_{cav}}{dt} \rho_{f,sol}, \qquad S_g = S_f F_g \quad \text{... (7)}$$

- Melt undergoes significant thermal expansion
- Partially molten fluid is highly viscous
- Melt freezes in relatively cooler pellet surfaces
- Inter-fluid drag and virtual mass forces
- Surface tension attempts to minimize fluid surface area
- Fission gases escape to gas plena

Assumption - Fission gas release does not vary across fuel pellet radius (more on this later)

Melt motion coupling with Reactor Dynamics

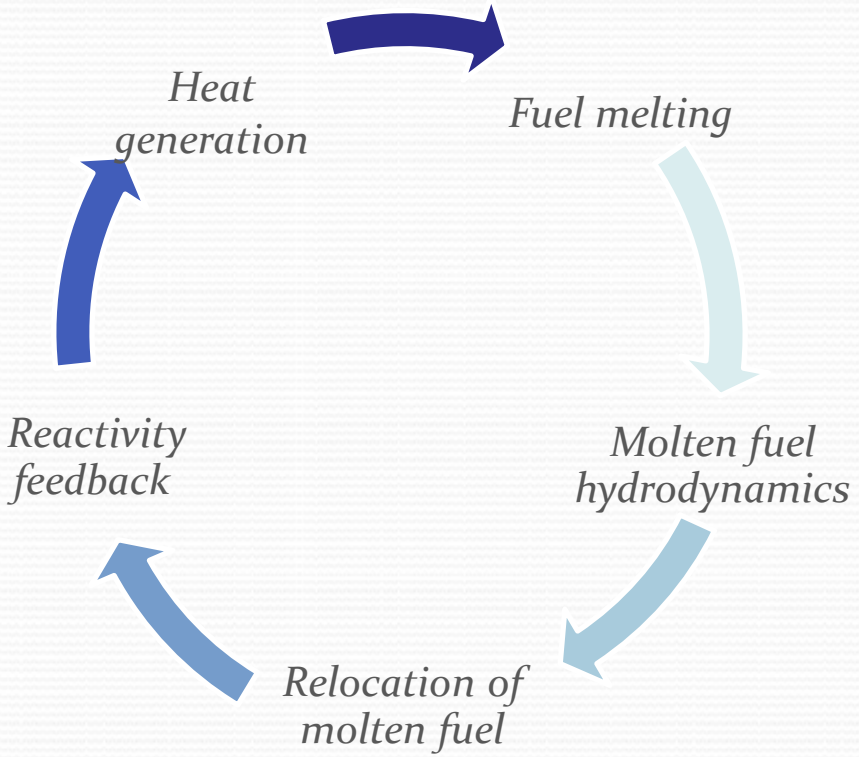

$$\frac{dP(t)}{dt} = \left(\frac{\rho - \beta}{\Lambda}\right) P(t) + \sum_{j=1}^{j=6} \lambda_j C_j(t), \qquad j = 1,2,\ldots 6$$

$$\frac{dC_j(t)}{dt} = \frac{\beta_j}{\Lambda} P(t) - \lambda_j C_j(t), \qquad j = 1,2,\ldots 6$$

$$\rho_{feed} = \rho_{Dop} + \rho_{f,axexp} + \rho_{c,axexp} + \rho_{ct} + \rho_{reloc}$$

$$\rho_{reloc} = \sum \frac{(M_{steady} - M_{transient})}{M_{steady}} (W_k)$$

$$M_{steady} = (M_s + M_l)|_{t=0}$$

$$M_{transient} = (M_s + M_l)|_{t>0}$$

$$M_{sol} = \pi(R_o^2 - R_{int}^2)\Delta z \cdot \rho_{f,s}$$

$$M_{liq} = \alpha_f \cdot \pi R_{int}^2 \Delta z \cdot \rho_{f,l}$$

- Point Kinetics model valid for tightly coupled reactor cores (for e.g., 500 MWe SFR)
- Fuel Doppler, fuel axial expansion, coolant expansion, clad expansion feedbacks
- Fuel relocation feedback (ρ_{reloc}) - generated by axial relocation of molten fuel
- Change in fuel mass $(M_{steady} - M_{transient})$ multiplied with associated fuel mass removal worth (W_k).

Assumption – Control rod driveline expansion, core radial expansion feedbacks neglected for conservative estimate of power rise

Discretization

- **Explicit finite difference solution**
- **Staggered grid for velocity nodes**

Grid independence study

S.NO.	Fuel grid size (axial × radial)	Peak relocation feedback (pcm)	Deviation (%)
1	10 x 10	-2.6523	-
2	20 x 20	-1.823	-31.2
3	30 x 30	-1.9213	5.4
4	40 x 40	-1.9288	0.4

Details of chosen grid

Model region	Δr (mm)	Δy (mm)
Fuel column	0.0625	33.33
Upper/lower blanket column	0.0625	150
Inner cavity	-	33.33
Clad	0.15	33.33/150 (fuel/blanket)

(Selected grid)

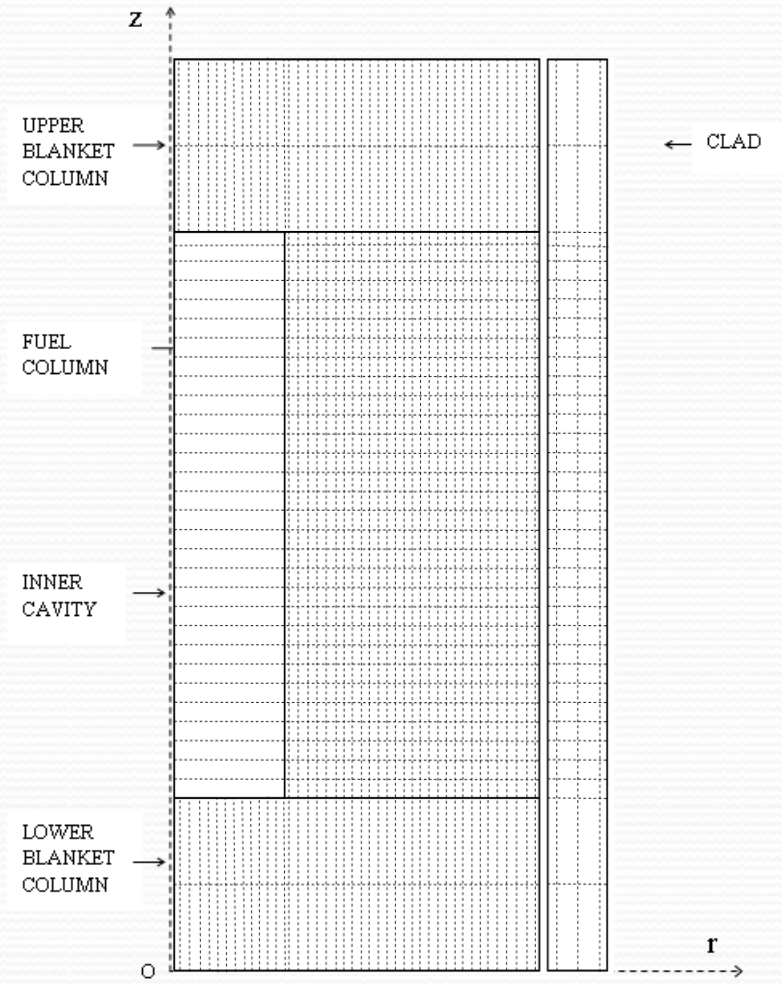

(Cadarache, France)

r built for testing nuclear fuel under severe

spectrum reactor (6 % enriched UO_2, 25 MW).

ne reactor (fissile length = 80 cm).

ntaining Hafnium (23 each).

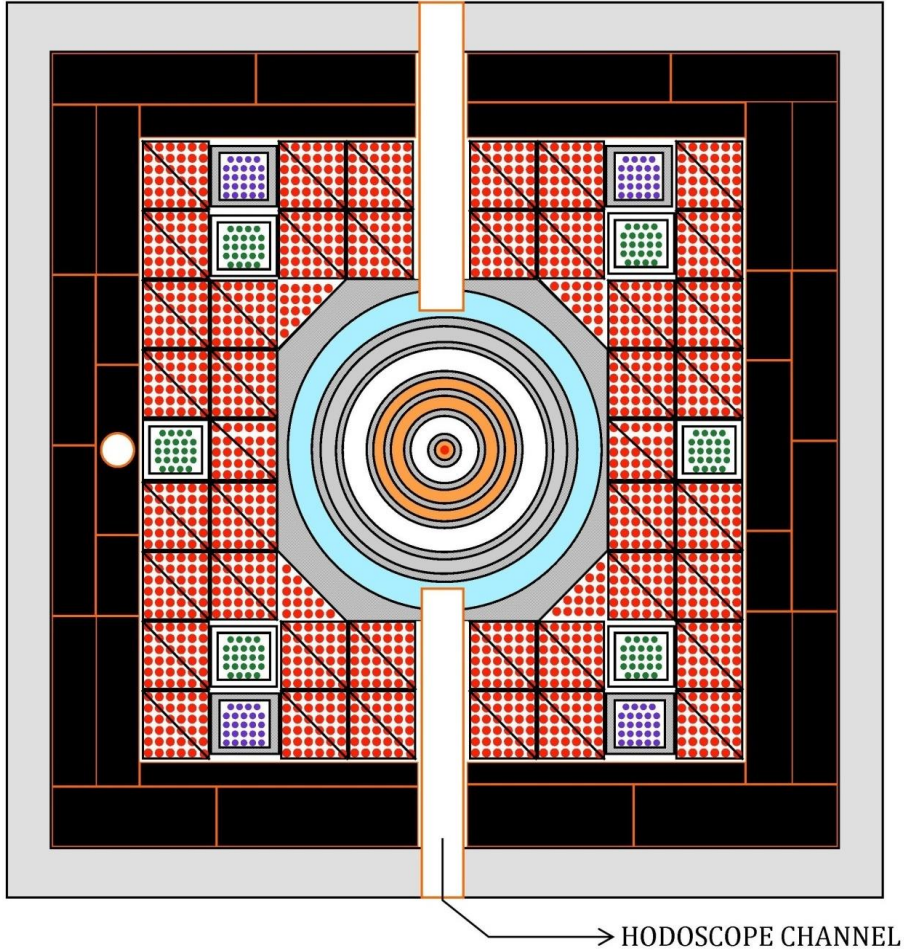

reactor core)

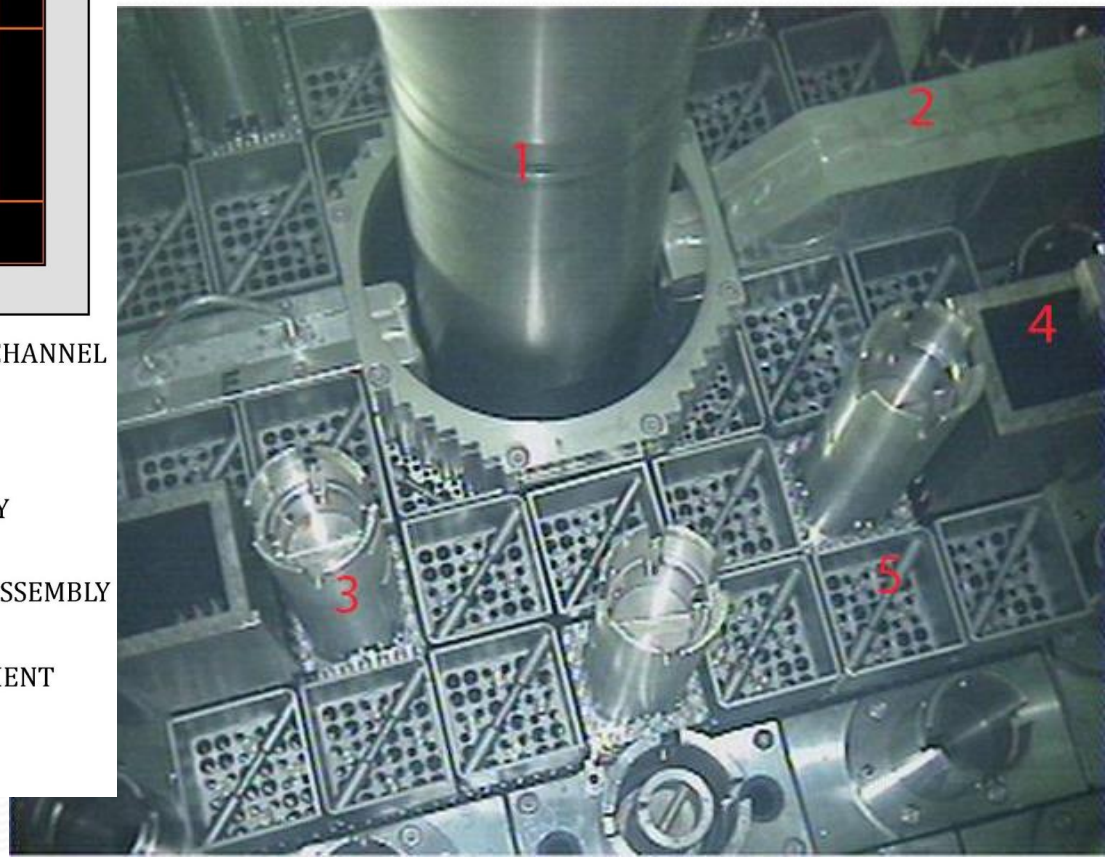

E9bis benchmark test

- CABRI-E9bis test data is used (Charpenel et al., 2000)
- Linear power ramp followed by constant power period and flow coast-down
- Molten fuel movement within the fuel column cannot be detected with on-site hodoscope.
- In the CABRI-E9bis test, the fuel pin contained pre-fractured upper blanket pellets.
- Entry of fuel into the fractured blanket pellets was captured in hodoscope signal (65-69 s).

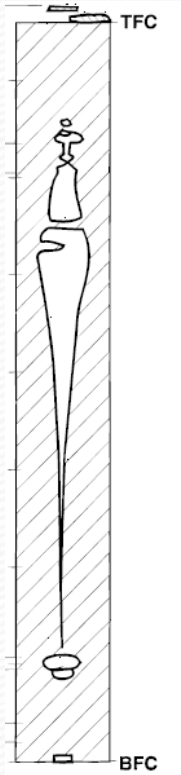

(State of fuel column of E9bis pin in post-test examination)

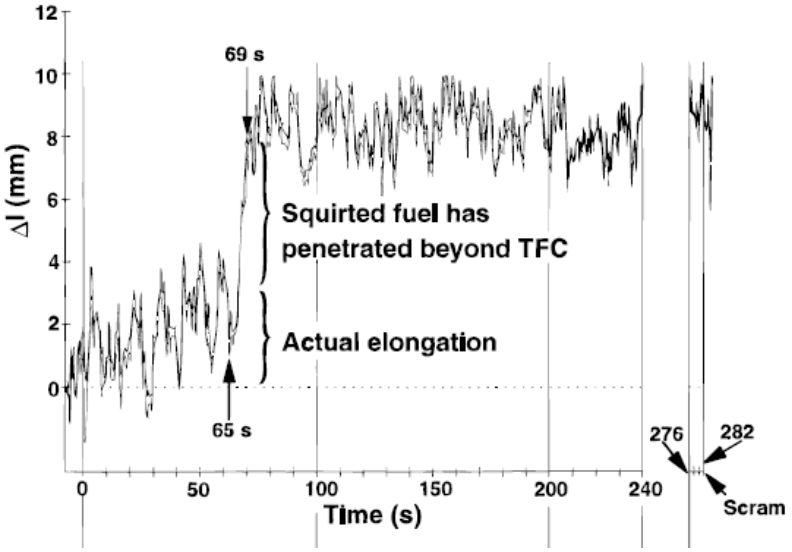

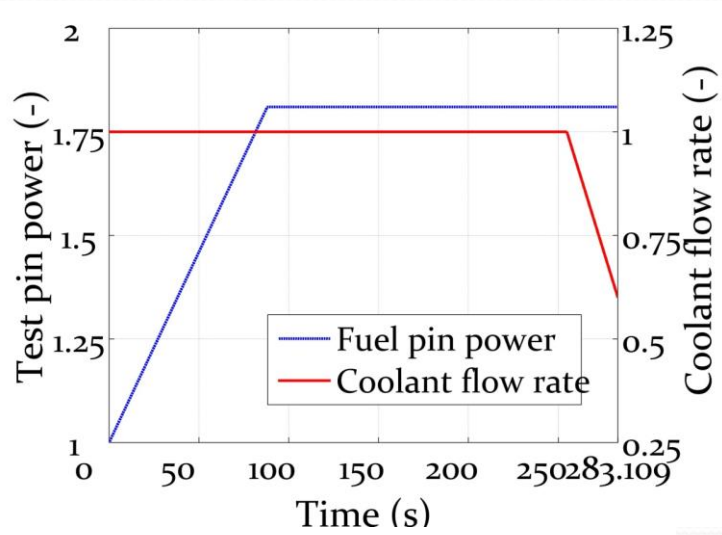

E9bis simulation

Observations

- Top-most node is completely occupied with fuel at t = 65 s
- Molten fuel travels at low speeds (~ 1 cm/s)
- Solidification blockage impedes melt flow
- Melt thermal expansion drives axial relocation
- Melt column axial growth is proportional to amount of melting (quantified by melt mass fraction)
- Thermal parameters in agreement with experimental results

Parameter	***Model***	***Experiment***
Power to melt (kW/m)	*72.4*	*72.7*
Maximum radial melt limits (% R/Ro)	*81.1*	*82±2*
Pin averaged mass melt fraction (%)	*39*	*40-50*
Time of penetration of upper blanket (s)	*67*	*65-69*
Upper axial melt limit (m/BFC)	*0.675*	*0.635*
Lower axial melt limit (m/BFC)	*0.075*	*0.095*

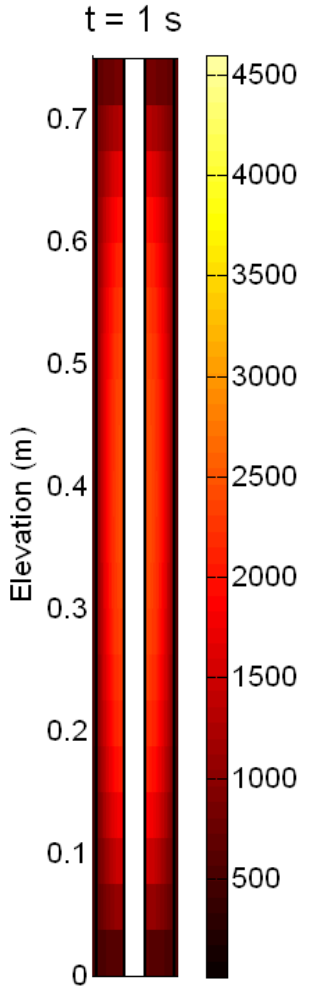

nented towards

Nucl. Eng. Des., 340: 431-446 (2018)

Outline

- Introduction
- CFD Models and experimental validation
- **Severe accident simulations**
- Fission gas pressurisation effects
- Conclusions and future scope of work

SFR core configuration

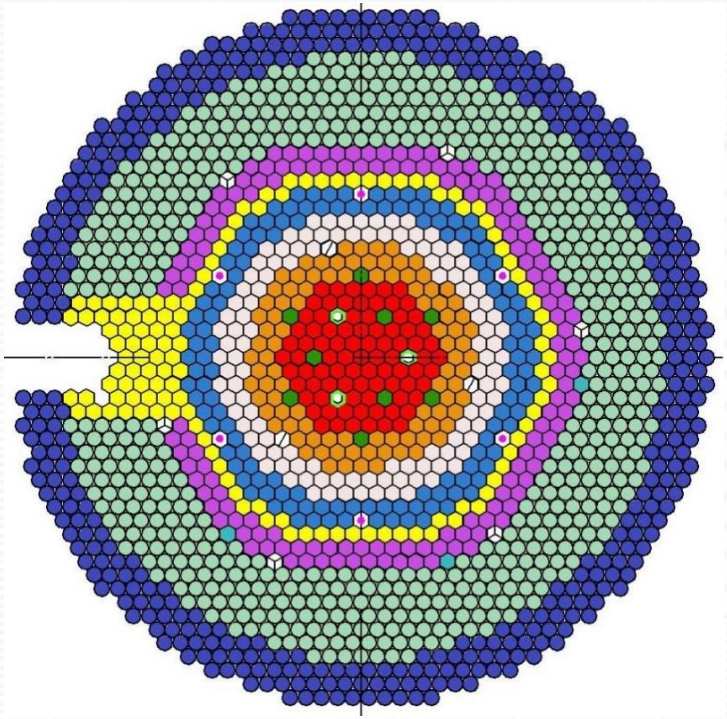

SYMBOL	TYPE OF SUBASS
	FUEL (INNER)
	FUEL (OUTER)
	CONTROL AND SAFETY
	DIVERSE SAFETY ROD
	BLANKET
	SOURCE
	STEEL REFLECTOR
	PURGER
	B_4C SHIELDING (INNE
	STORAGE LOCATION
	STORAGE FOR SOURCE
	FAILED FUEL STORAGE
	STEEL SHIELDING
	B_4C SHIELDING (OUTE

(Core configuration at beginning of equilibrium cycle)

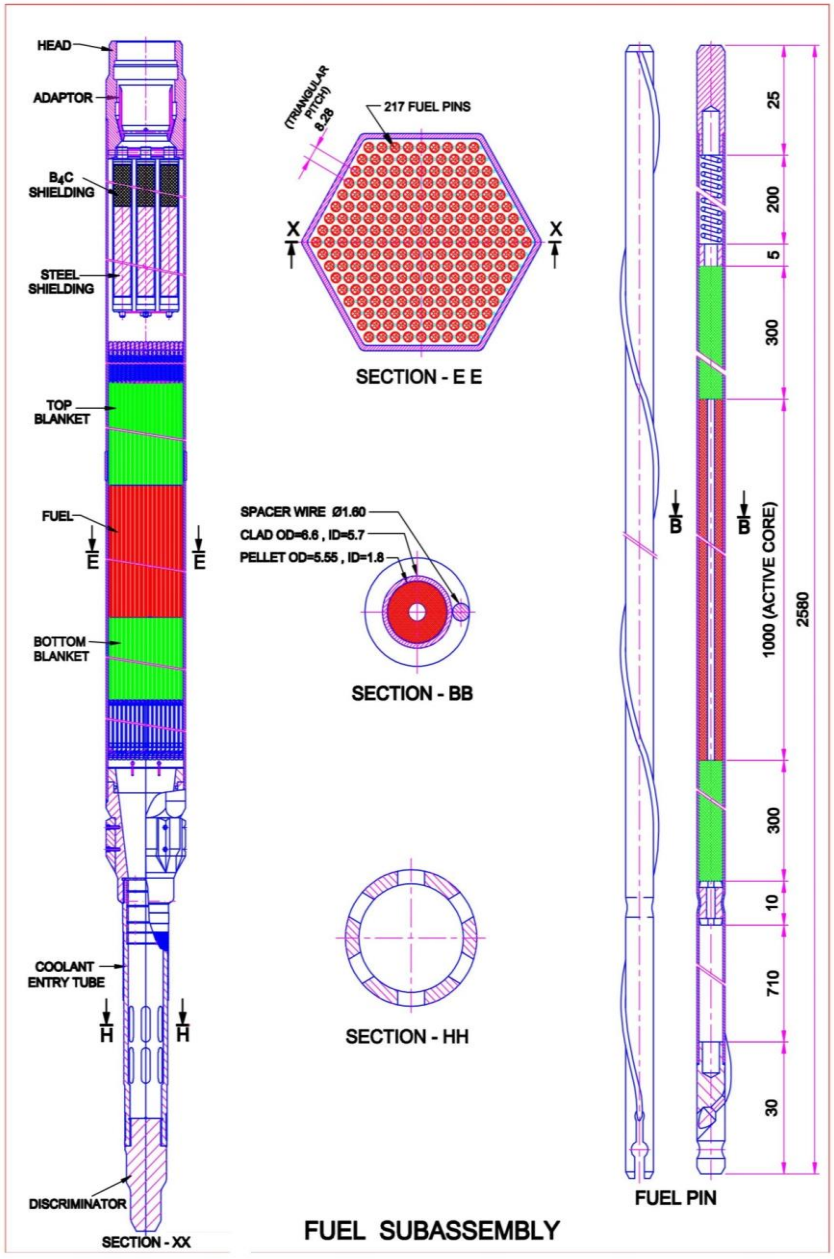

System outline

- Pool-type, liquid sodium cooled, fast breeder rea
- Homogenous core with two fissile enrichment zo

Input data (Fuel parameters)

Fuel subassembly grouping

Zone	FSAs	$(\% X_{max}/X_{max,I})$ BOL	$(\% X_{max}/X_{max,I})$ Equilibrium	$\dot{m}_{ct}$ (kg/s)
I	1	100	100	35.8
II	30	94.3	94.8	35.8
III	24	85.3	86.6	31.4
IV	30	77.9	79.9	28.8
V	30	86.7	90.2	34.1
VI	42	69	72.7	28.8
VII	24	52.1	55.3	20.8

Fuel pin parameters (dual data represents inner/outer core region values)

Parameter	Sign	Value
Fuel inner radius, mm	R_I	0.9
Fuel outer radius, mm	R_O	2.775
Inner clad radius, mm	R_{CI}	2.85
Outer clad radius, mm	R_{CO}	3.3
Fuel column length, m	L	1
Top blanket length, m	L_{TB}	0.3
Bottom blanket length, m	L_{BB}	0.3
Deviation from stoichiometry	x	0.02
Theoretical fuel density (kg/m³)	TD	11063/11097
Fuel pellet density (kg/m³)	ρ_{sol}	10565 (I), 10598 (O)
Length of upper plenum	L_{UP}	0.2
Length of lower plenum	L_{LP}	0.71
Clad material	-	D9

- Zones I-IV and V-VII represent the inner and outer core regions, respectively.
- Peak Linear heat rating (Zone I): 45 kW/m (Beginning-of-life), 41 Kw/m (Equilibrium).
- Hydraulic diameter and length of pellet cavity are 1.8 mm and 1 m, respectively.

Input Data (Control Rod withdrawal worth)

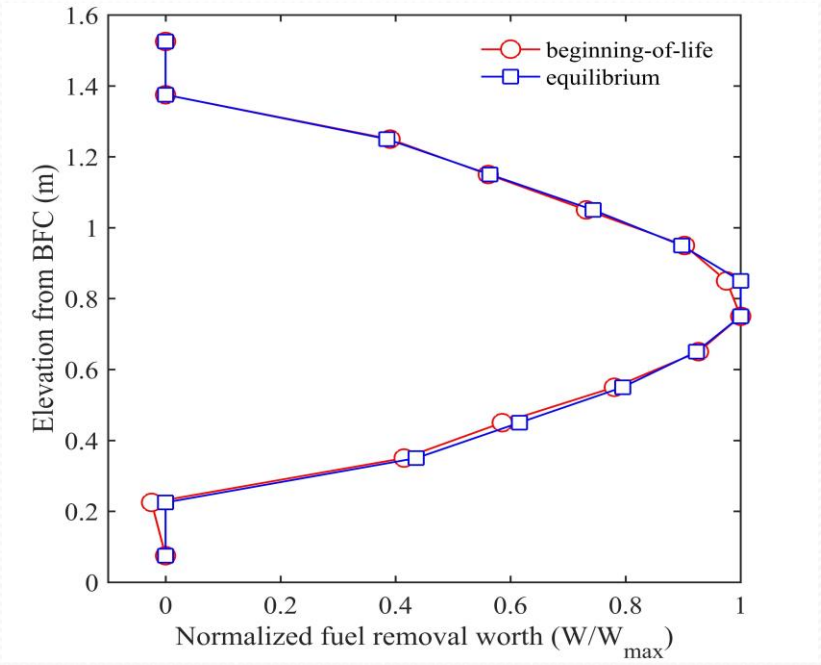

(Axial profile of fuel void worth)

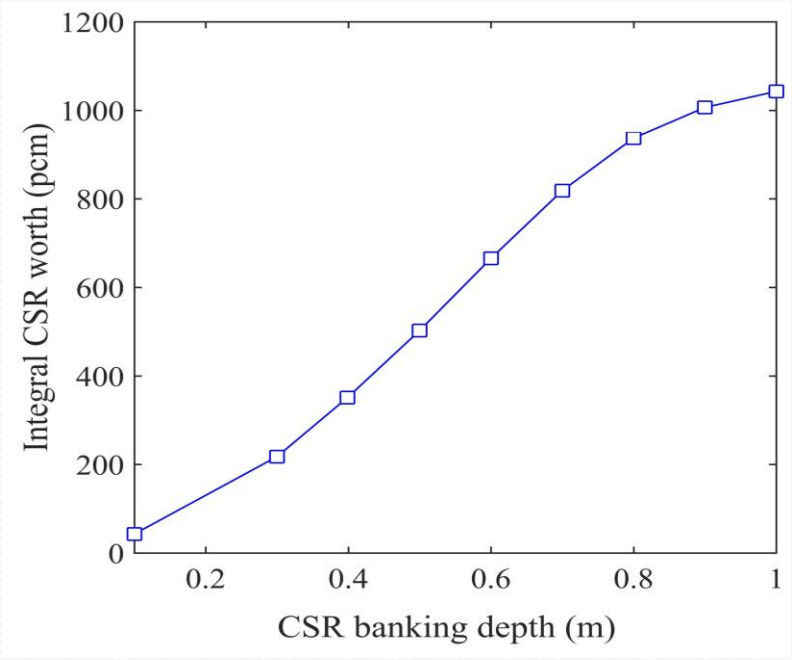

(Integral worth profile for single Control Safety Rod (CSR) withdrawal)

Zone	BOL core	Equilibrium core
I	0.8	0.8
II	22.2	21.2
III	14.3	13.9
IV	15.6	15.4
V	19.4	19.8
VI	19.9	20.6
VII	7.8	8.1

(Zone-wise fuel void worth distribution (% $W_f / \sum W_f$))

Coupled simulations (Reactor Dynamics / Melt hydrodynamics)

- Unprotected transient overpower accident simulations for 500 MWe fast reactor are carried out using validated code.
- Beginning-of-life (BOL) and equilibrium core case studies (best estimate / conservative scenarios). *(Control rod withdrawal during unprotected transient overpower)*

Case study	*Banking depth (cm)*	*Withdrawal time (s)*	*Maximum insertion ($)*	*Steady state peak linear heat rating (kW/m)*
BOL (Best)	*40*	*200*	*0.984*	*45.5*
Equilibrium (Best)	*30*	*150*	*0.57*	*41.6*
BOL (Conservative)	*50*	*250*	*1.48*	*45.5*
Equilibrium (Conservative)	*40*	*200*	*0.98*	*41.6*

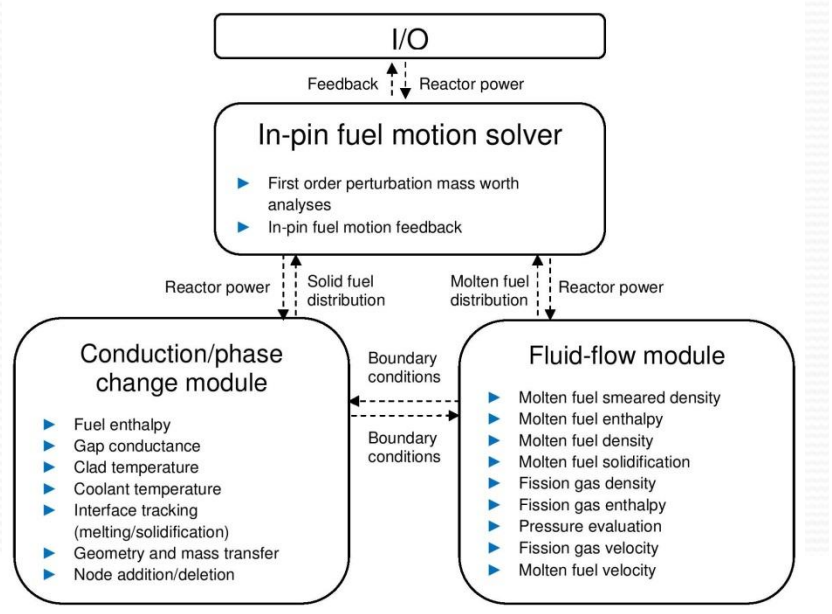

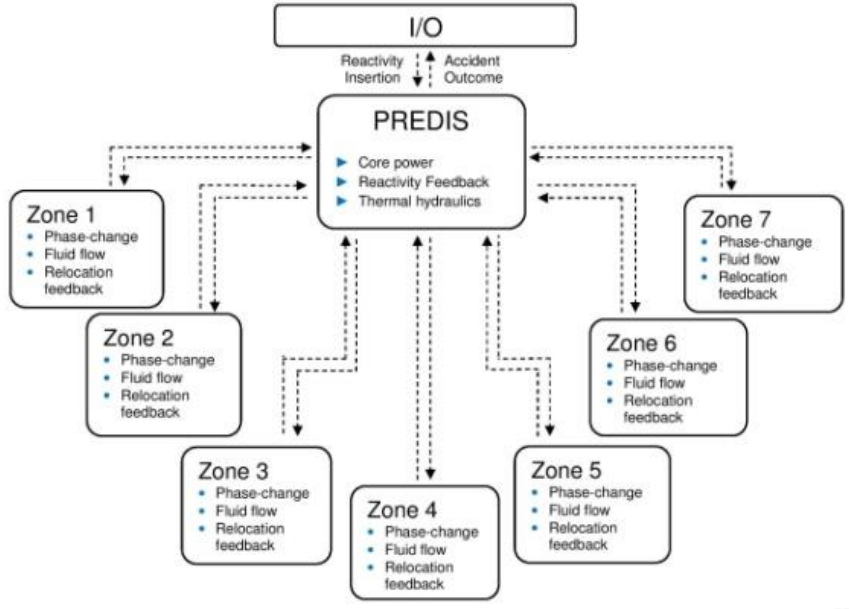

Melt propagation in beginning of life core (best estimate)

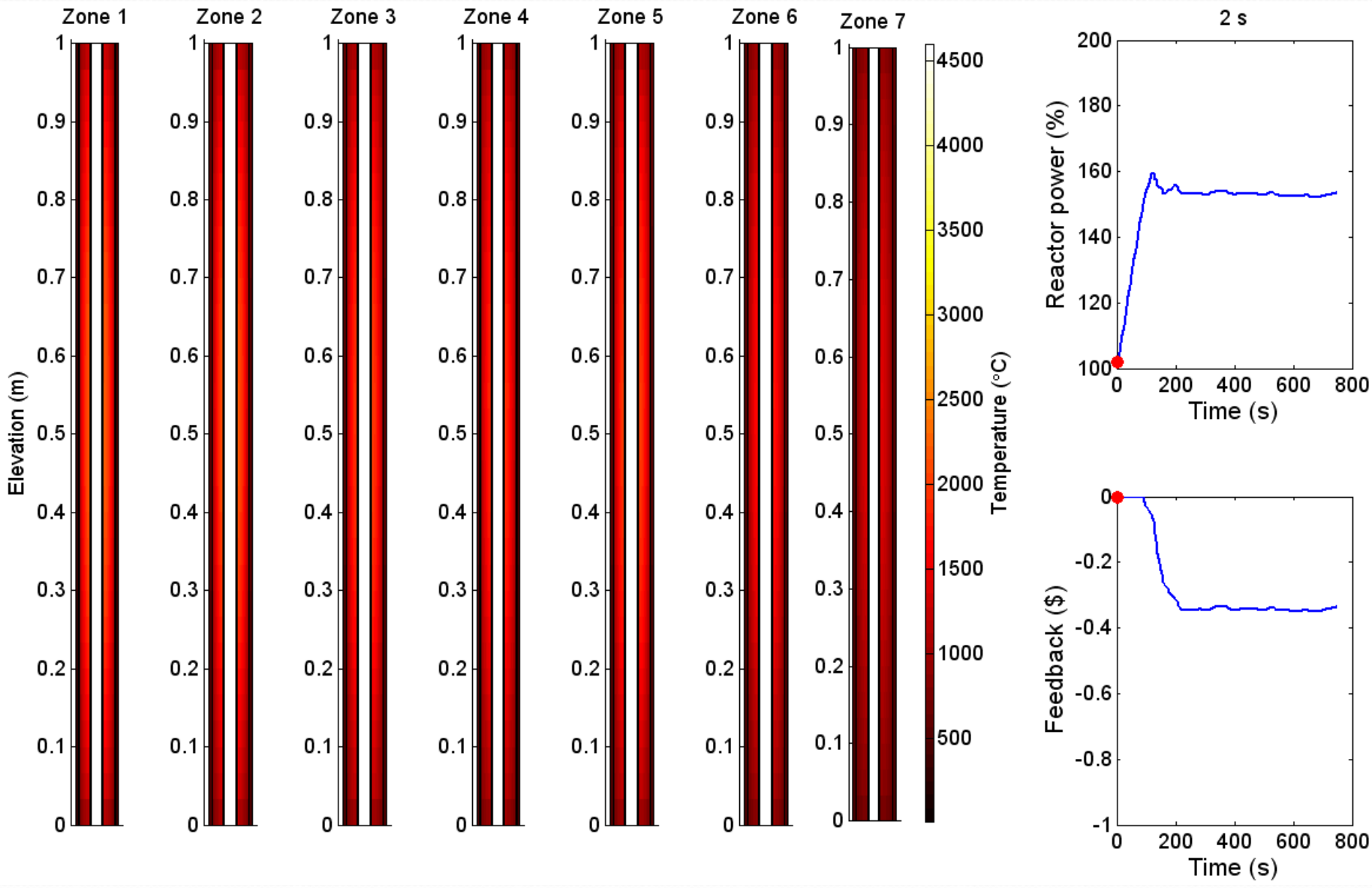

(Melt relocation reactivity feedback as a function of time)

Reactor dynamics (best estimate)

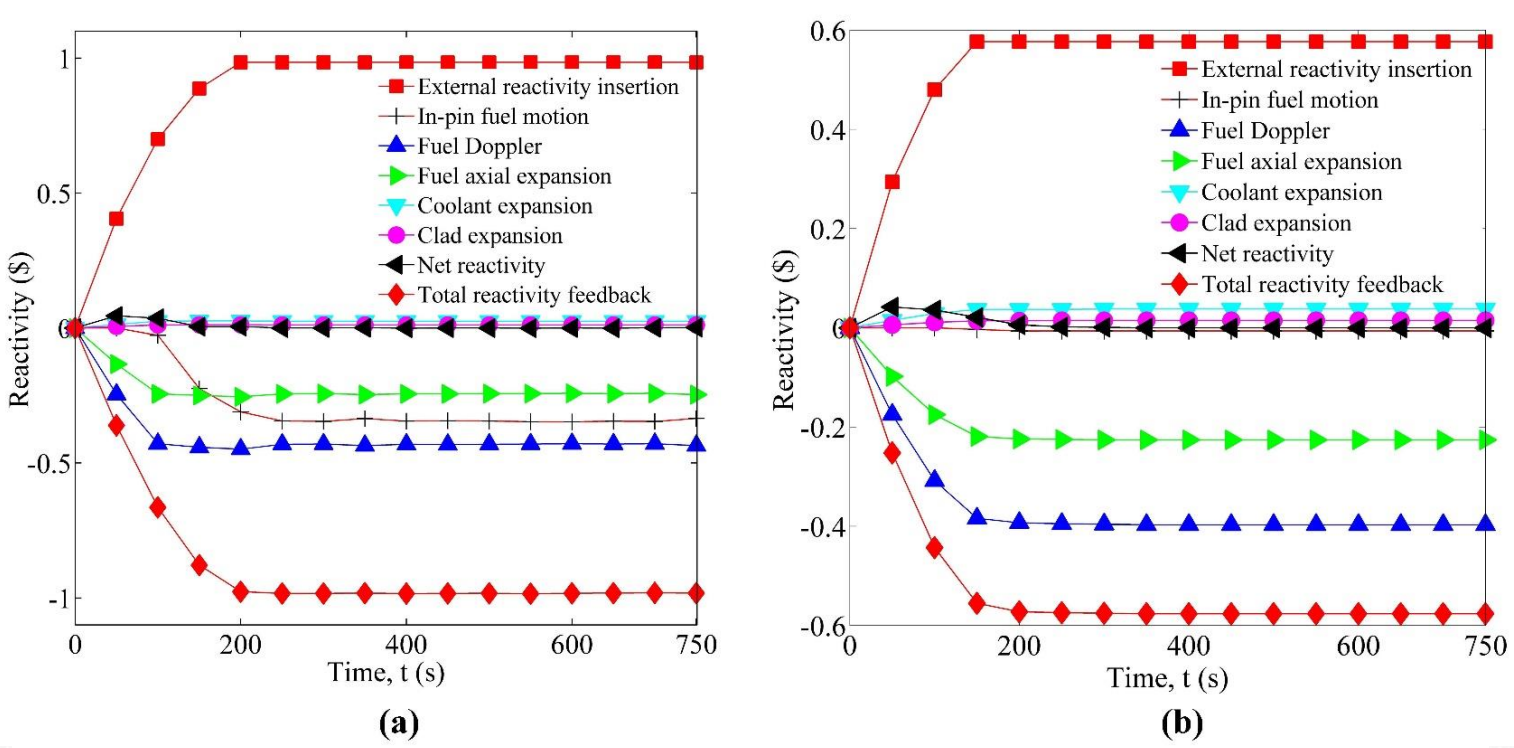

(Reactor dynamics response under best estimate case study. (a) BOL core (b) Equilibrium core)

- Beginning-of-life (BOL) core – melt relocation feedback (–0.35 $) limits the reactor power at 166 % of nominal power (banking depth = 40 cm).
- Equilibrium core – Power rise arrested by fuel axial expansion and Doppler feedbacks, resulting in negligible melting (banking depth = 30 cm).
- Power rise effectively arrested in both cases.

Nucl. Eng. Des., 347: 31-44 (2019)

Reactor dynamics (best estimate)

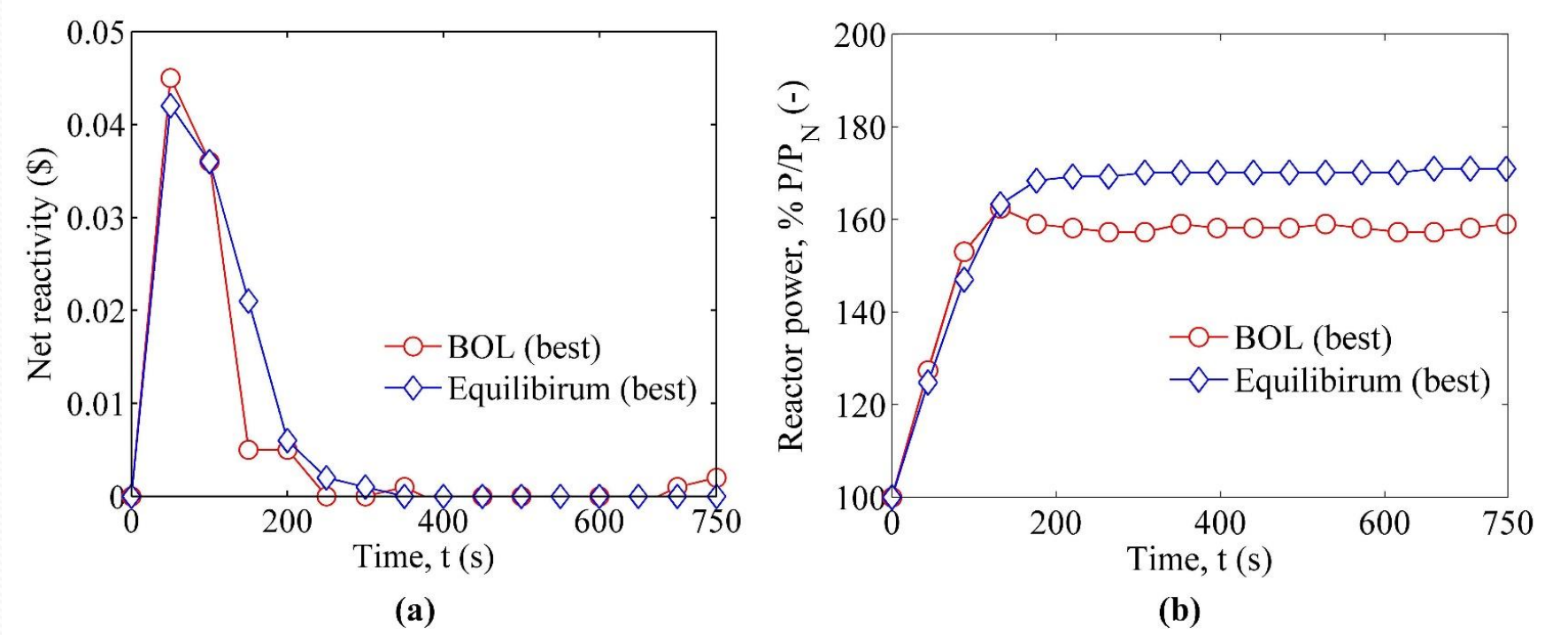

(Transient behaviour of reactor during UTOPA (best estimate). (a) Net reactivity vs. time, (b) Reactor power vs. time)

- Beginning-of-life (BOL) core – Peak reactivity confined to 0.046 $.
- Equilibrium core - Peak reactivity confined to 0.043 $.
- BOL core nominal power = 45 kW/m; Equilibrium core nominal power = 41 Kw/m.

Reactor dynamics (conservative)

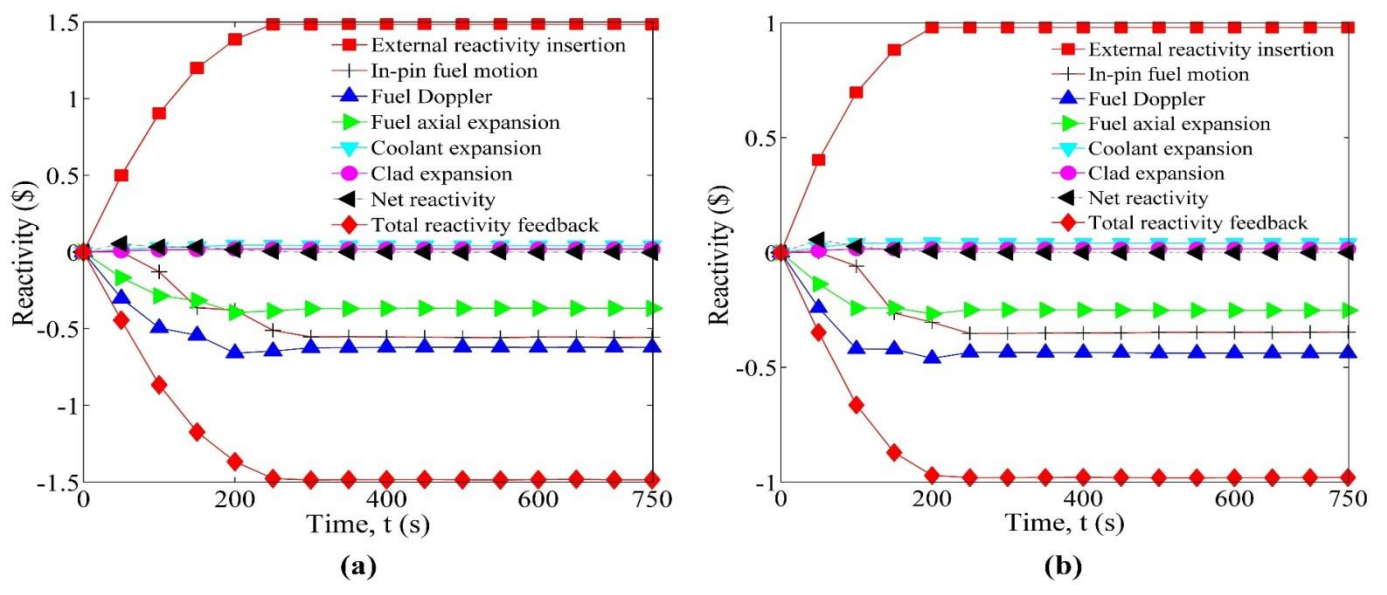

(Reactor dynamics curves for conservative case study. Melt relocation feedback is represented as in-pin fuel motion feedback. (a) Beginning-of-life core (b) Equilibrium core)

- Beginning-of-life (BOL) core - Significant power rise (204% nominal) because of reactivity insertion of 1.4 $.
- Equilibrium core – melt relocation feedback curtails power rise to 182 % nominal with reactor stabilizing at 177 % nominal.
- Melt relocation feedback magnitude increases in proportion to fuel melting.

Reactor dynamics (conservative)

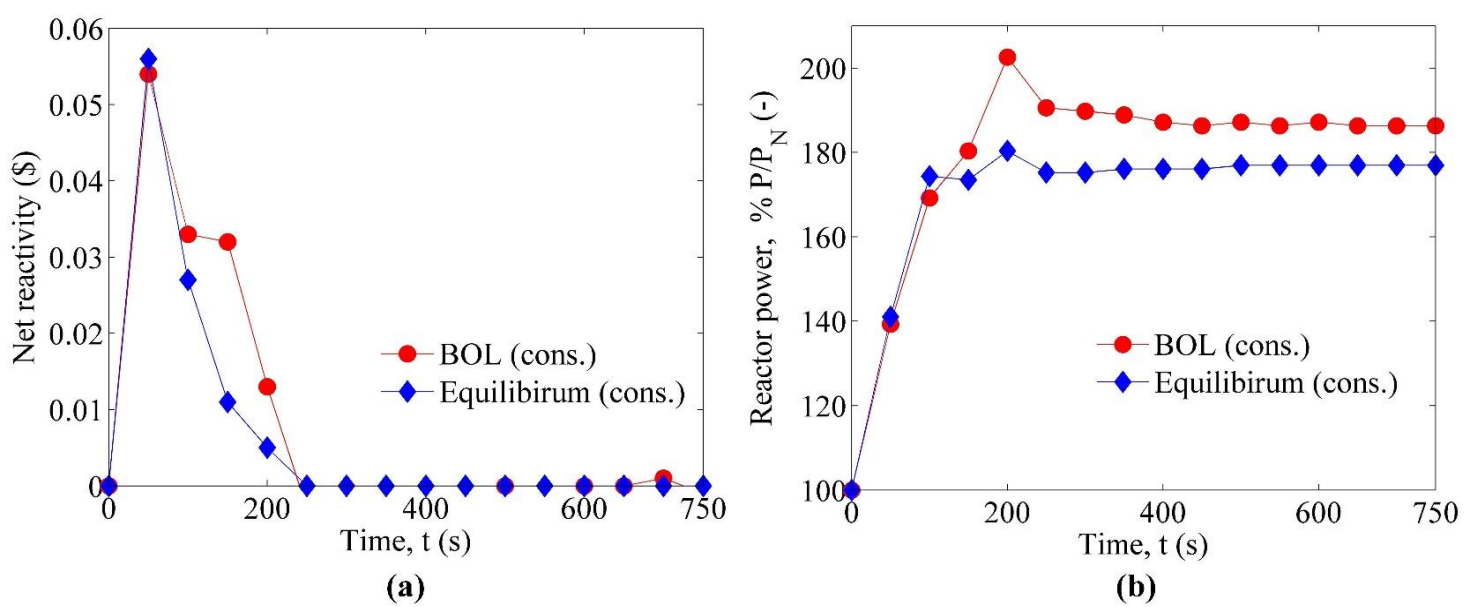

(Transient behaviour of a 500 MWe reactor for unprotected transient (conservative analysis).(a) Net reactivity vs. time, (b) Reactor power vs. time)

- Beginning-of-life (BOL) core - Significant power rise (204% nominal) because of reactivity insertion of 1.4 $.
- Equilibrium core – melt relocation feedback curtails power rise to 182 % nominal with reactor stabilizing at 177 % nominal.
- Melt relocation feedback magnitude increases in proportion to fuel melting.

Impact of fuel relocation feedback

Reactivity feedbacks and peak power levels with and without melt relocation feedback (ρ_{reloc})

	Inclusion of ρ_{reloc}					Exclusion of ρ_{reloc}			
Case	ρ_{peak}	$\frac{P}{P_n}$(%)	ρ_{reloc}	ρ_{Dop}	$\rho_{f,axexp}$	ρ_{peak}	$\frac{P}{P_n}$(%)	ρ_{Dop}	$\rho_{f,axexp}$
Equilibrium (best)	0.042	171	-0.006	-0.397	-0.226	0.042	171	-0.401	-0.229
Beginning-of-life (Best)	0.045	162	-0.345	-0.436	-0.247	0.054	202	-0.657	-0.392
Equilibrium (Conservative)	0.056	182	-0.347	-0.438	-0.252	0.056	223	-0.666	-0.407
Beginning-of-life (Conservative)	0.054	204	-0.556	-0.622	-0.367	0.054	301	-0.983	-0.629

Observations

- Significant reduction in maximum power levels with inclusion of ρ_{reloc}.
- Consequently, other negative feedbacks also smaller in magnitude for corresponding simulations.
- Melt relocation reactivity feedback reduces power excursion during unprotected transient overpower.
- Feedback magnitude comparable with fuel Doppler and axial expansion feedbacks.

Sensitivity to core configuration

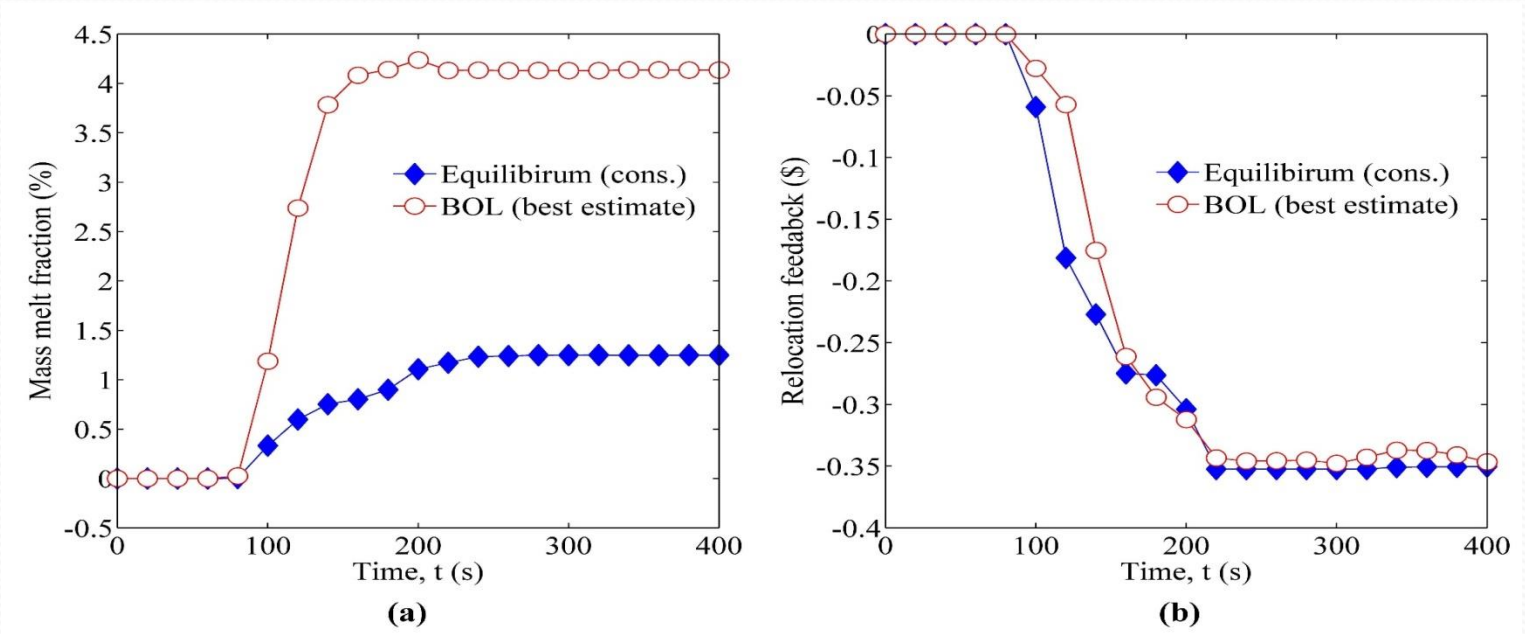

(Comparison between beginning-of-life (best estimate) and equilibrium (conservative) cases (external reactivity insertion is equal for both cases))

- Equivalent reactivity insertion for both cases (~0.98 $)
- Core-averaged melt mass fraction is significantly higher for beginning-of-life (~4 %) core.
- Relocation feedback response for beginning-of-life core is clearly weaker than equilibrium core.
- Could the reason be pressure forces generated by fission gas release in case of equilibrium fuel?

Outline

- Introduction
- CFD Models and experimental validation
- Severe accident simulations
- **Fission gas pressurisation effects**
- Conclusions and future scope of work

ıs release

trix)

$- KC_t + bC_{gb}$

)

tion)

on)

(Gas atom concentration in grain face bubbles)

$$\frac{dn_f}{dt} = (1-F)(1-X)\frac{dn_b}{dt} - \left(\frac{n_f - n_{f1}}{1-F}\right)\frac{dF}{dt} + \frac{n_f}{A_f}\frac{dA_f}{dt}$$

(Gas concentration in grain edge bubbles)

$$\frac{dn_e}{dt} = (1-E)\left((F(1-X)+X)\frac{dn_b}{dt} + \left(\frac{n_f - n_{f1}}{1-F}\right)\frac{dF}{dt} - \frac{n_f}{A_f}\frac{dA_f}{dt}\right) - \left(\frac{n_e - n_{e1}}{1-E}\right)\frac{dE}{dt}$$

(Gas atom concentration released to free volume)

$$\frac{dn_r}{dt} = E\left((F(1-X)+X)\frac{dn_b}{dt} + \left(\frac{n_f - n_{f1}}{1-F}\right)\frac{dF}{dt} - \frac{n_f}{A_f}\frac{dA_f}{dt}\right) + \left(\frac{n_e - n_{e1}}{1-E}\right)\frac{dE}{dt}$$

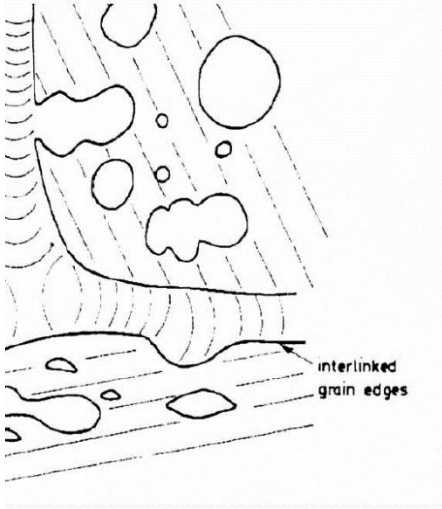

'ge bubbles after inter-linkage)

om concentration in fuel matrix)

$$\frac{\partial}{\partial r}\left(D_g r^2 \frac{\partial C_g}{\partial r}\right) + K_g - D_g K_b^2 C_g - KC_t + bC_{gb}$$

om concentration in bubbles)

$$)_g K_b^2 C_g + KC_t - bC_{gb} - \dot{G}$$

(Total intra-granular gas concentration)

$$C_t = C_g + C_{gb}$$

(Intra-granular bubble concentration)

$$\frac{dC_b}{dt} = KC_t - bC_b - \frac{\dot{G}}{n_b}$$

- ✓ Intra-granular fission gas dynamics
- ✓ Inter-granular fission gas dynamics
- ✓ Release to free volume

Nucl. Eng. Des., 364: 110684 (2020)

Steady state verification

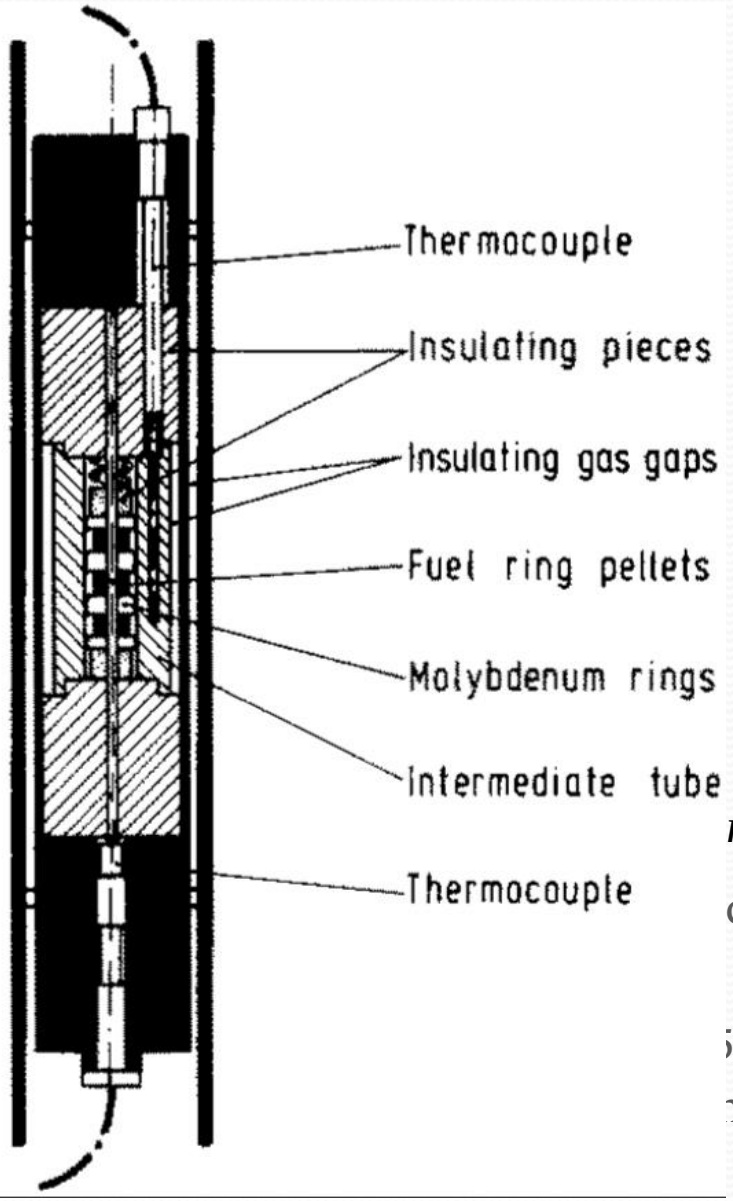

r)

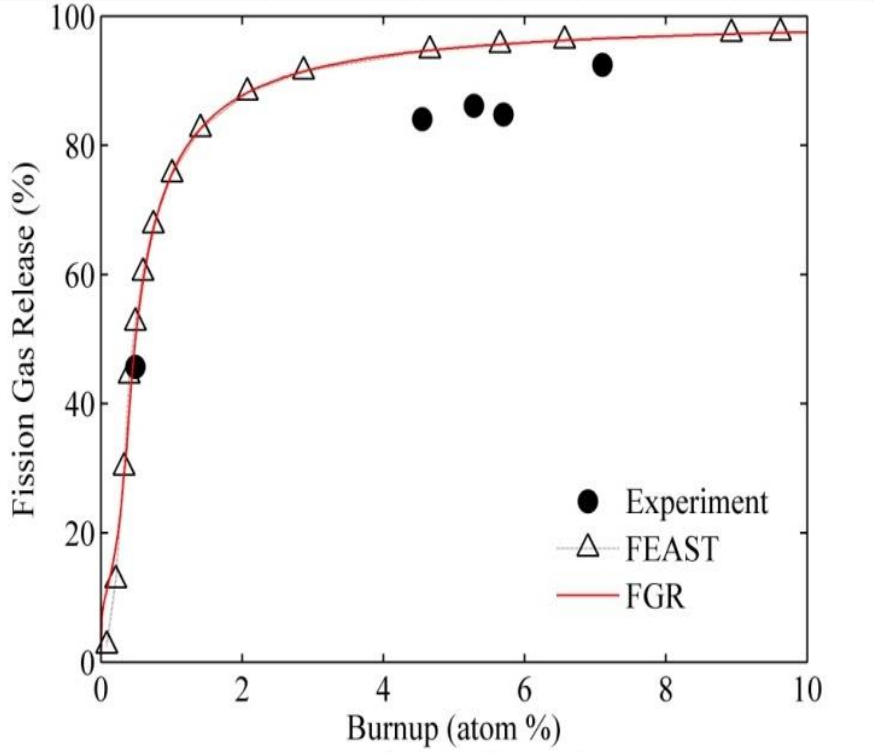

(Fission gas release at 2000 K)

diation tests conducted in FR2 reactor

;o K and 2000 K are verified.

nental data as well as FEAST-OXIDE code

Steady state verification

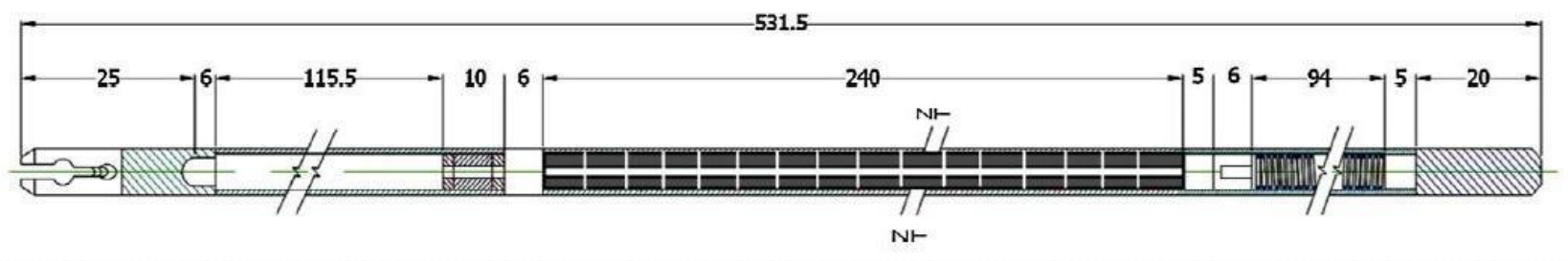

(Sketch of the MOX test fuel pin)

- FGR is used to simulate the fission gas release of MOX fuel pins which were irradiated in FBTR up to burnup level of 112 GWd/t (*Venkiteswaran et. al, 2014*).
- Results are in agreement with test data.

(Comparison of experimental and simulation parameters)

Parameter	***Experiment***	***FGR***
Fission Gas Release (%)	85	83
Pin pressure (MPa, 298 K)	2.4-2.8	2.3

(Characteristics of MOX fuel pin used in FBTR irradiation experiment)

Parameter	***Value***
Outer radius of pellet (m)	*2.78 x 10-3*
Inner radius of pellet (m)	*0.8 x 10-3*
Outer radius of clad (m)	*3.3 x 10-3*
Inner radius of clad (m)	*285 x 10-3*
Peak power (kW/m)	*45*
Plutonium molefraction (%)	*29.0*
Length of fuel pellet cavity (m)	*0.24*
Length of blanket pellet column (m)	*-*
Maximum burnup (at. %)	*11.2*

CABRI-E9 test data

- Annular fuel pin (annular fuel/solid blanket) OPHELIE-6 (from Phenix reactor)
- Slow ramp - 1.1 % (P/Pn)/s
- Experimental data from (Charpenel et. al, 2000) and (Perez-Martin et. al, 2018) is used
- Maximum melt mass fraction = 57 %
- Intact solid blanket pellets prevented fuel relocation beyond the active region.

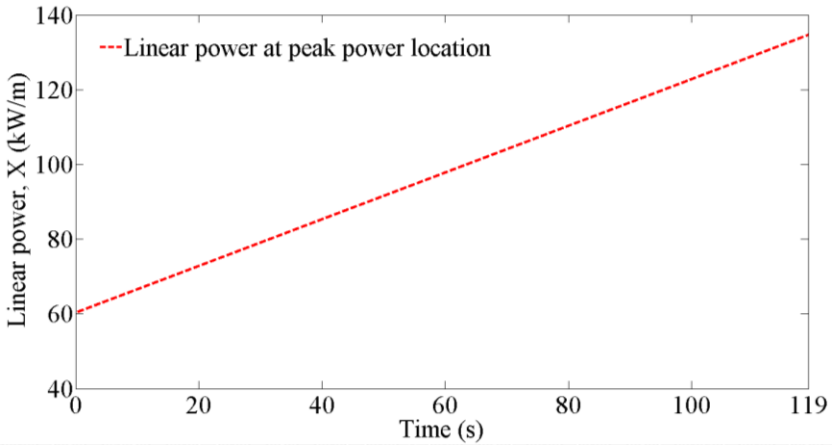

(E9 Power-time history)

(Fuel specifications:- OPHELIE-6)

Parameter	***Value***
Outer radius of pellet (m)	1.0×10^{-3}
Inner radius of pellet (m)	3.635×10^{-3}
Outer radius of clad (m)	4.325×10^{-3}
Inner radius of clad (m)	3.75×10^{-3}
Plutonium mole-fraction (%)	0.145
Length of fuel pellet cavity (m)	0.75
Length of blanket pellet columns (m)	0.2
Maximum burnup (at. %)	4.9

Validation: E9 test

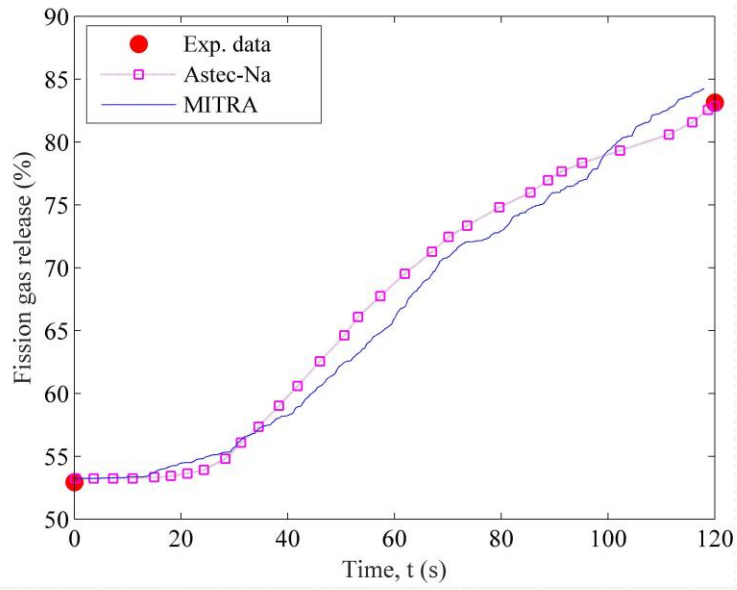

(Comparison of E9 test data with gas release obtained from present simulation)

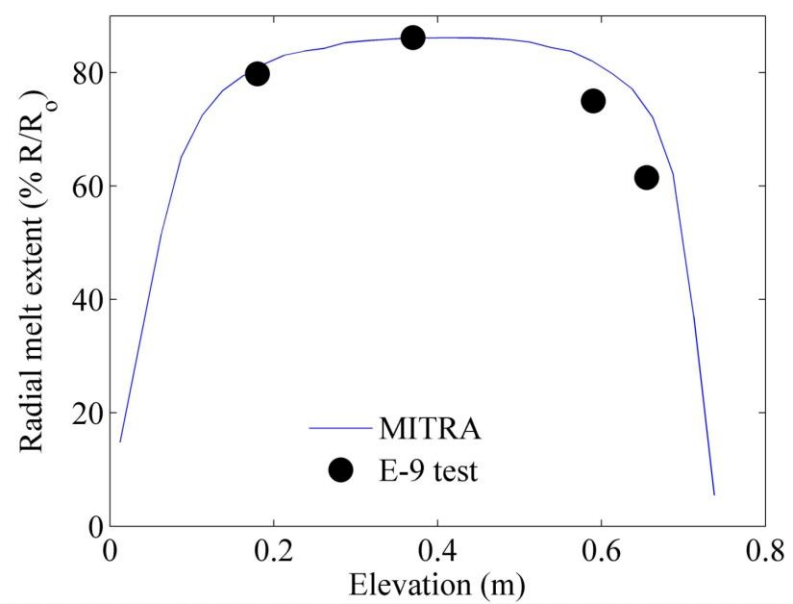

(Comparison of E9 melt radii with present simulation)

PARAMETER	*MITRA*	*EXPERIMENT*
Melt mass fraction, %	54.6	57
Radial melt extent at 0.18 m %	79.8	79.8
Radial melt extent at 0.37 m %	85.4	86.2
Radial melt extent at 0.59 m %	82	75
Upper axial melt extent, m BFC	0.725	0.69
Lower axial melt extent, m BFC	0.025	0.016
Transient fission gas release, %	84	82.6
Power to melt, kW/m	71.5	73

Relocation sensitivity to fuel burnup

- Radial variation in fission gas retention coefficient (F_g) is incorporated in two-phase flow model ($S_g = F_g(r, z) \cdot S_f$).
- Large gas release fraction results in negligible gas retention coefficient in the inner regions (< 65% R/R_o) of fuel pellets.
- Consequently, when melting initiates near inner surface of fuel pellets, $S_g \approx 0$ or $\Delta\rho_g \approx 0$.
- Therefore, pressure perturbations generated by fission gas release ($\Delta P_{cav} = \Delta\rho_g R_g T_g$) result in minimal to no effect on melt motion.

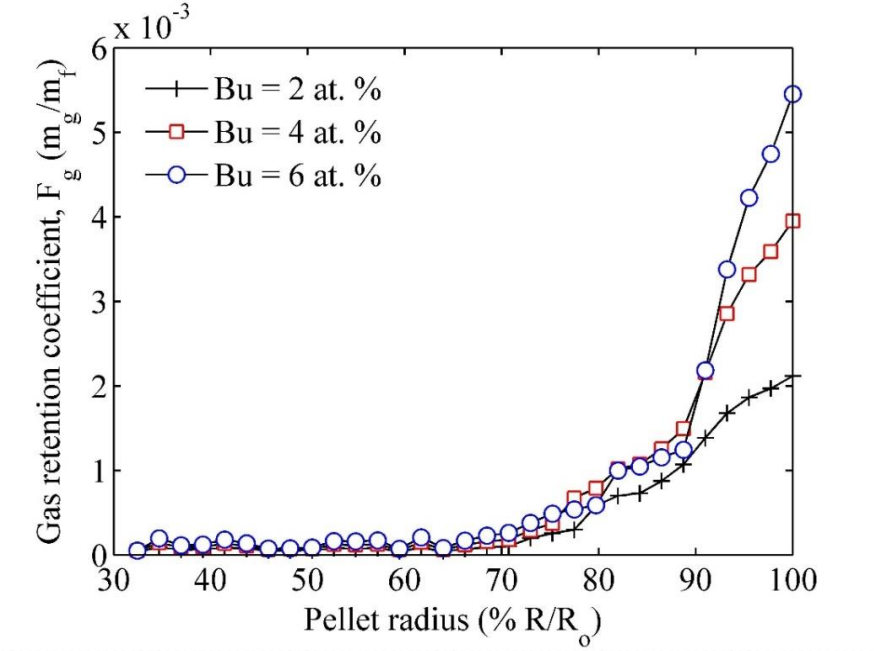

Gas retention coefficient, F_g as a function of radius and fuel burnup level. (peak power location)

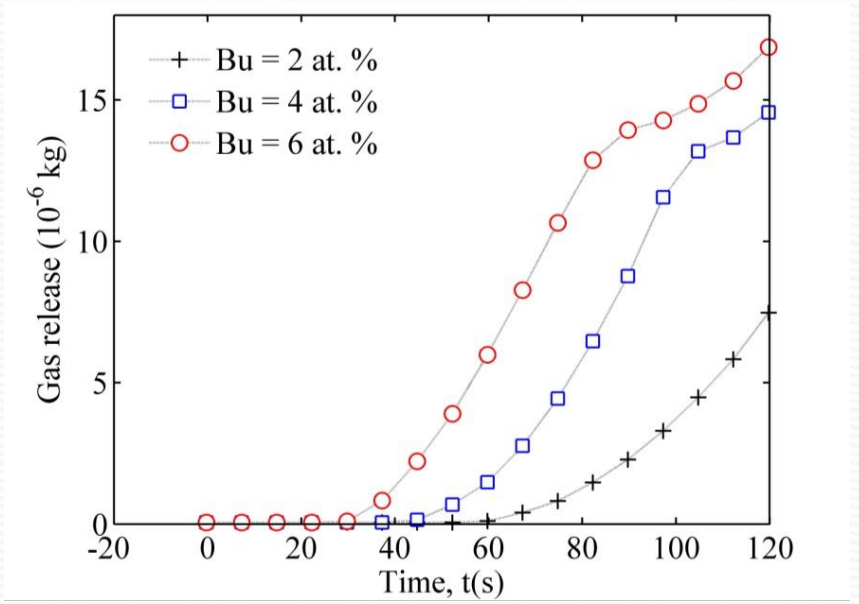

Gas retention coefficient, F_g as a function of radius and fuel burnup level. (peak power location)

Relocation feedback sensitivity to fuel burnup

- Relocation behaviour is approximately similar for three different burnup levels with minor deviation in case of fresh fuel (Bu = 0 at. %).
- Accelerated initial downward melt movement in fresh core is caused by thermal parameters (low gap conductance between pellet outer surface and clad inner surface).

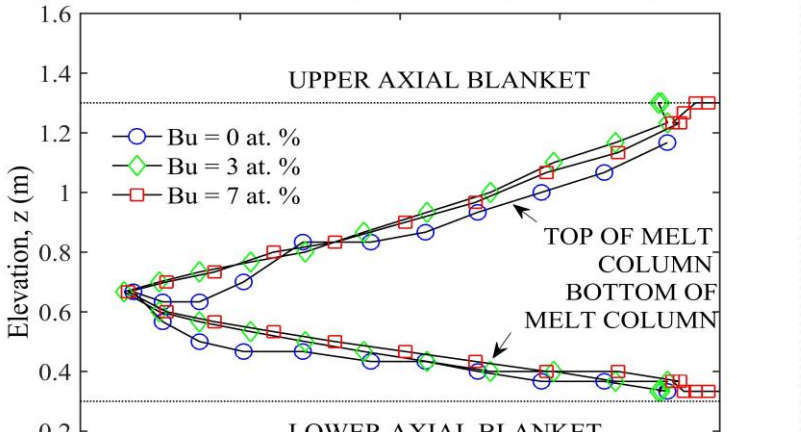

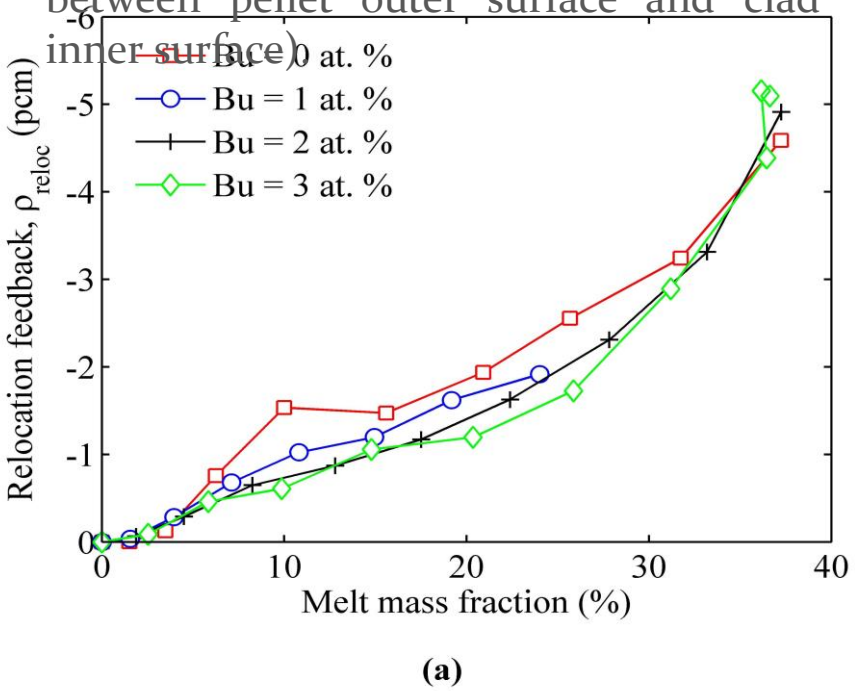

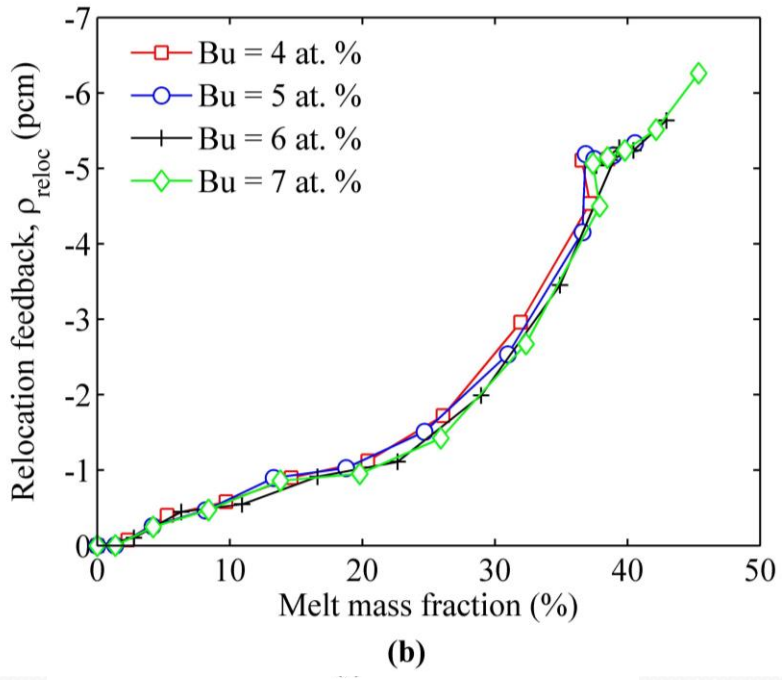

Evolution of the melt column as a function of the melt mass fraction and peak fuel burnup. Melt occupies the region between the top and bottom curves. (Core mid-plane at $z = 0.5\ m$)

Potential of melt removal from fissile region

- Melt motion in upward direction increases with melt mass fraction until it occupies the entire pellet cavity.
- Constraints at top and bottom blanket surfaces stop fuel from relocating further.
- If constraints are removed, would fuel move out of fissile column, resulting in enhanced negative reactivity?

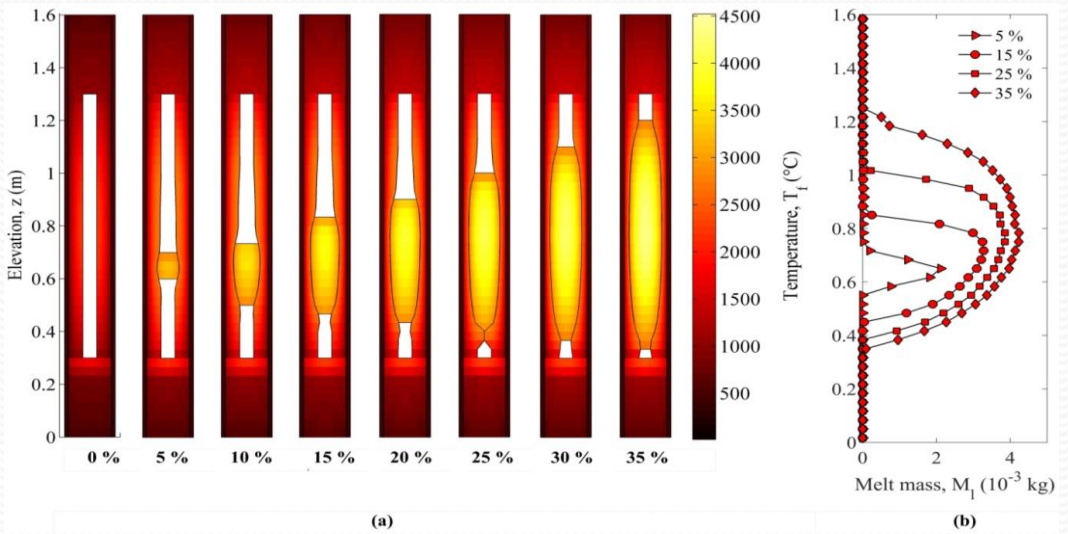

(Melt motion versus melt mass fraction (a) Thermal map (b) Melt mass profile)

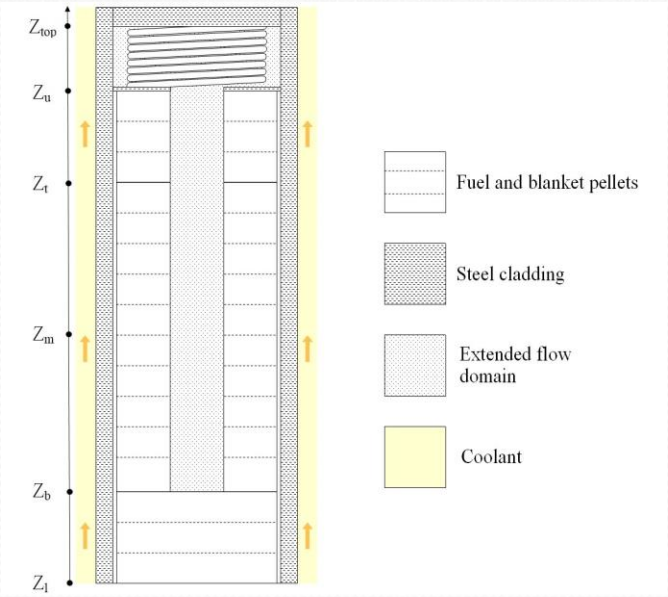

(Modified fuel pin geometry with annular top blanket pellets)

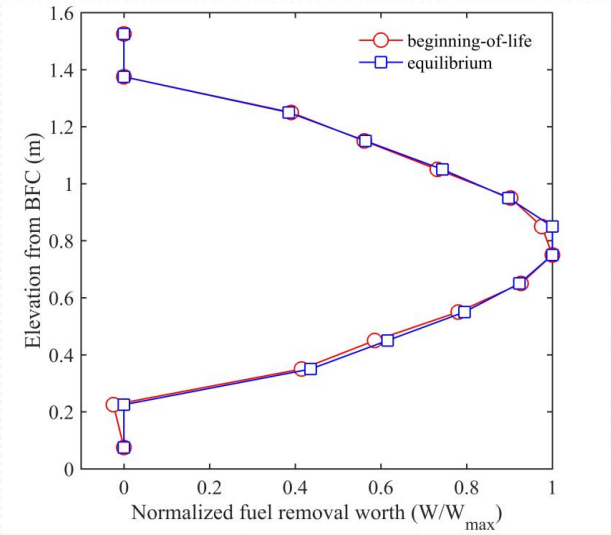

(Axial profile of fuel void worth)

Nucl. Eng. Des., 364: 110684 (2020)

Axial blanket investigation

Relocation in an alternative geometry

- Melt solidification and the resultant viscous resistance continue to constrain the relocation.
- After a threshold melting (34.2 %), the melt enters the top blanket.
- A large enhancement appears in the relocation feedback curve once fuel enters blanket column.

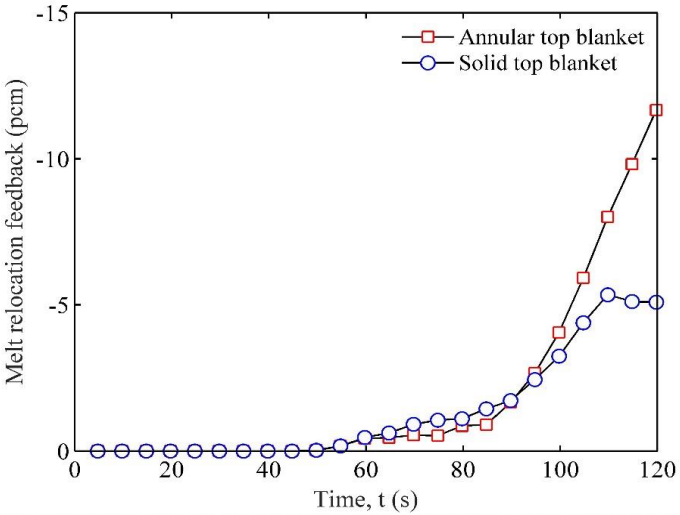

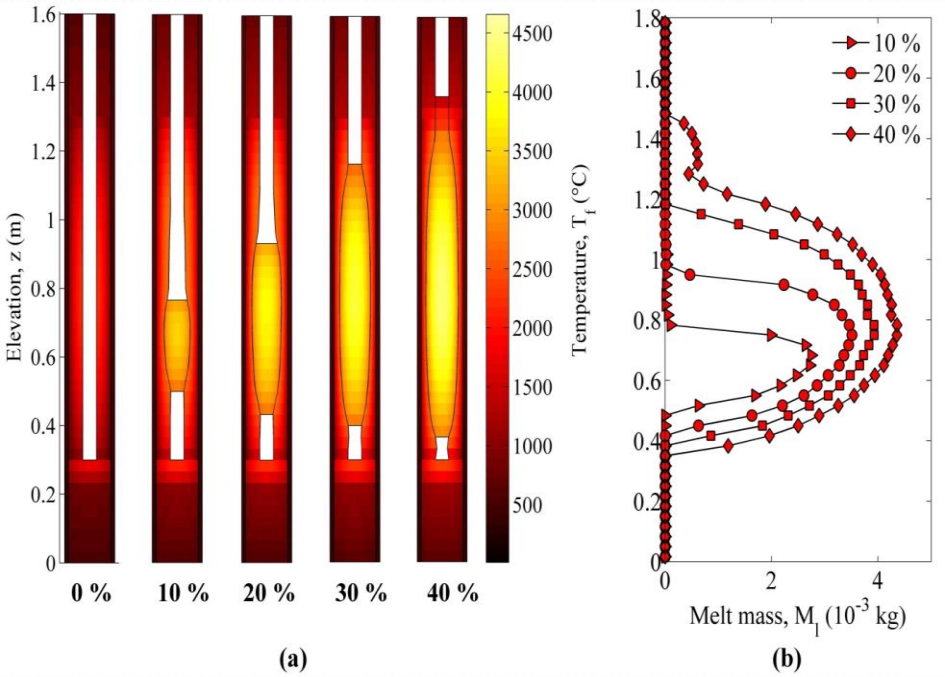

Melt motion in case of annular top blanket (a) Thermal map (b) Melt mass profile

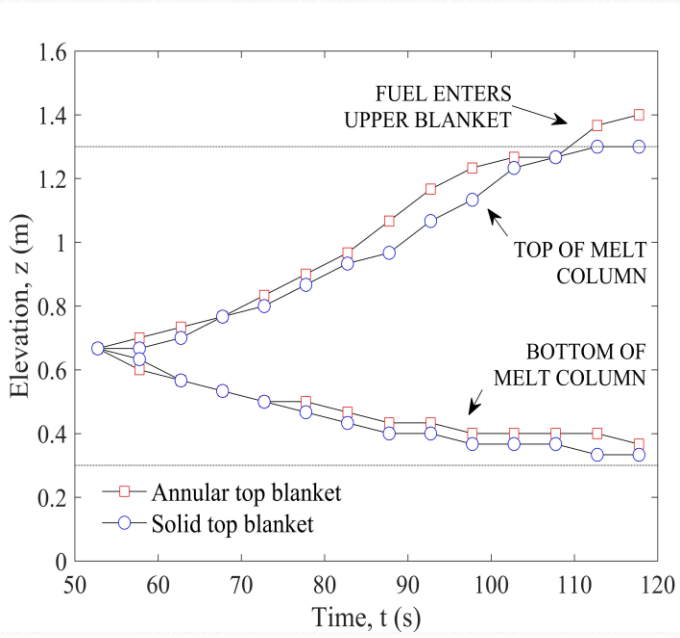

Sensitivity to geometric design variation

Outline

- Introduction
- CFD Models and experimental validation
- Severe accident simulations
- Fission gas pressurisation effects
- **Conclusions and future scope of work**

Conclusions

Objectives

- Determine the motion of molten nuclear fuel during an unprotected transient overpower accident.

✓ Achieved with development of experimentally benchmarked hydrodynamics solver.

- Predict the consequence of this motion on sodium-cooled fast reactor safety margin.

✓ Achieved with dynamically coupled simulations of unprotected transient overpower accident.

Key findings

- Melt motion results in a negative reactivity feedback that improves sodium-cooled fast reactor safety margin.
- Fission gas release does not influence melt motion significantly during such an accident.
- Alternative axial blankets with open flow pathways facilitate melt relocation outside the active core, resulting in further enhancement to fast reactor safety margin.

Features of the developed code

- **Heat-transfer**
- Grid modifications
- Source term evaluation (S_f, S_g)
- Fuel pin temperature distribution

- **Multi-phase flow**
- Melt relocation
- Fission gas flow

- **Fission gas release**
- Radial variations in fission gas retention (F_g)
- Transient fission gas release

- **Friend to point kinetics**
- Melt relocation feedback
- Consolidated data for safety applications

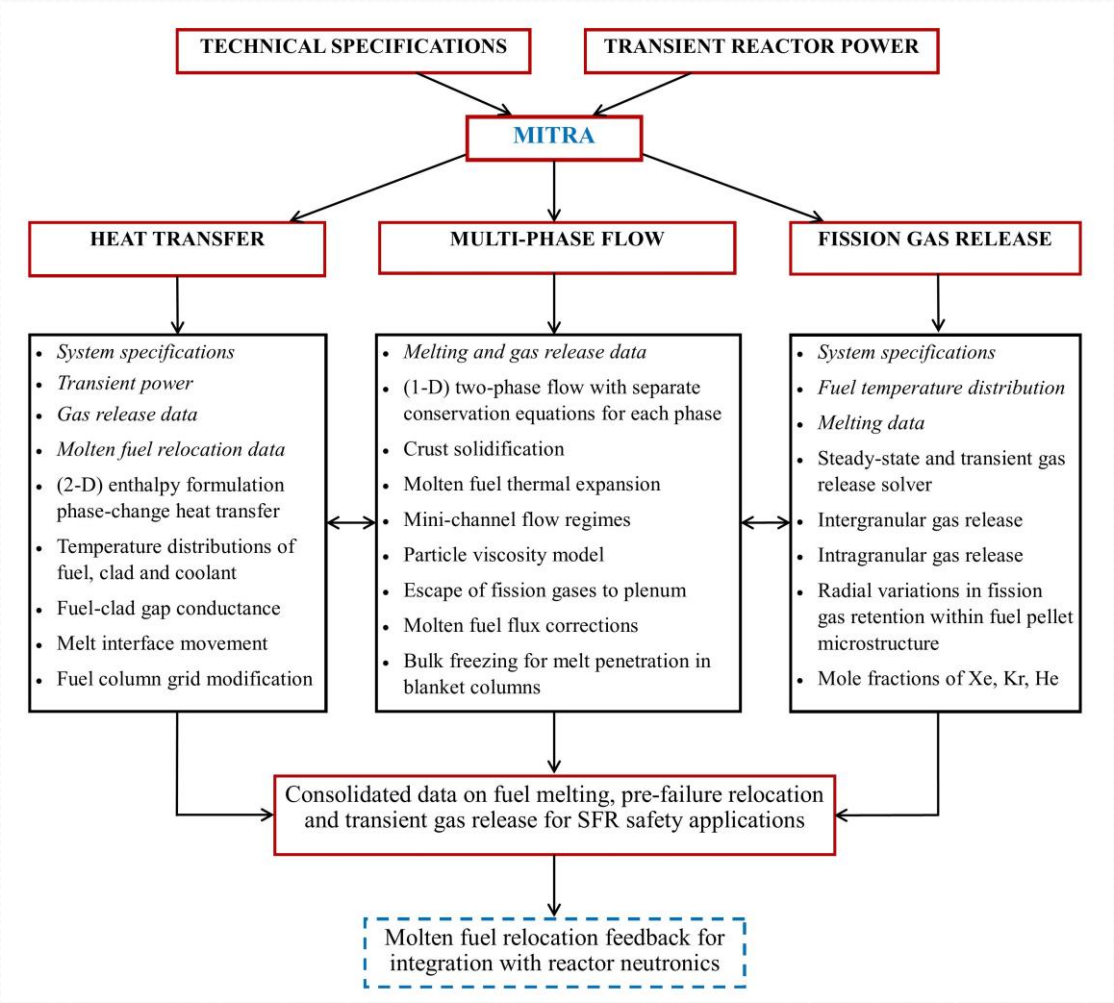

(Salient working description of MITRA)

Future scope of work

- Thermo-mechanical investigation to incorporate elastic / plastic deformations of solid fuel and cladding (during severe accident) in hydrodynamics solver.
- Evidence of melt penetration through solid axial blanket pellets at significantly high overpower (> 300%, MF2 test).
- Code extension to unprotected loss of flow accidents (TP2 test).
- Code extension towards alternative fast reactors and fuel designs.

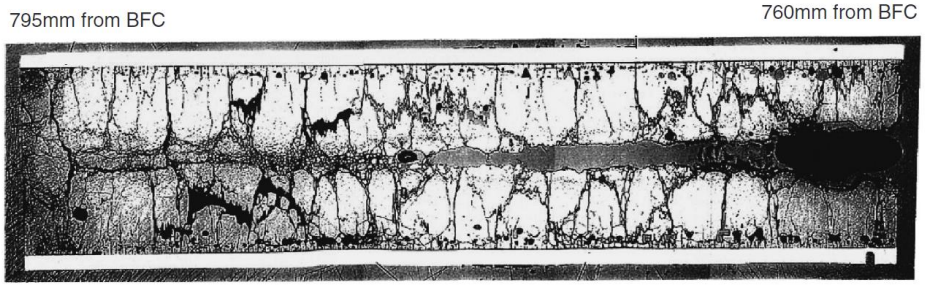

Axial cut of MF2 test fuel pin focused on upper blanket region (molten fuel (dark grey color) is visible between solid blanket pellets

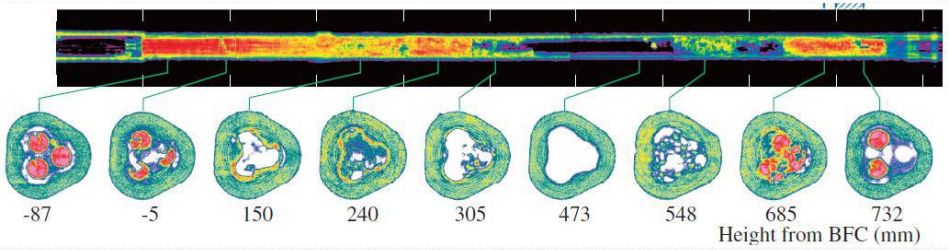

Evidence of molten fuel motion beyond top of fissile column (600 mm) in unprotected loss of flow experiment TP2 (CABRI reactor).

Thank you all for your attention!

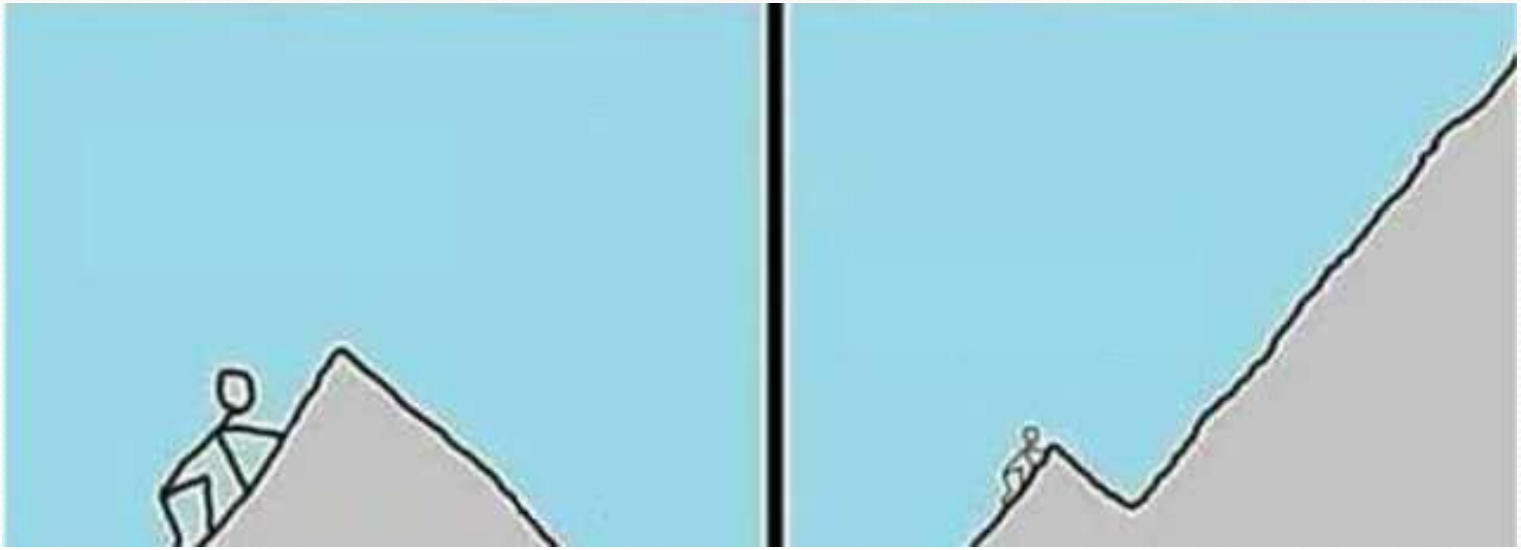

Miles to go….

References

Charpenel J., Sato I., Struwe D., Pfrang W., "Fuel pin behavior under the slow power ramp transients in the CABRI-2 experiments." Nuclear Technology 130 (2000) 252-271.

Fukano Y., Onoda Y., Sato I., Charpenel J., "Fuel Pin Behavior under Slow-Ramp-type Transient-Overpower Conditions in the CABRI-FAST Experiments." Journal of Nuclear Science and Technology 46 (2009) 1049-1058.

Karahan A., Buongiorno J. "Modeling of thermo-mechanical and irradiation behavior of mixed oxide fuel for sodium fast reactors." Journal of Nuclear Materials 396 (2010) 272-282.

Perez-Martin S., Pfrang W., Girault N., Cloarec L., Laborde L., Buck M., Matuzas V., Flores y Flores A., Raison P., Smith A. L., Mozzani N., Feria F., Herranz L., Farges B. "Development and assessment of ASTEC-Na fuel pin thermo-mechanical models performed in the European JASMIN project."Annals of Nuclear Energy 119 (2018) 454-473.

Ozawa T., Abe T. "Development and Verifications of Fast Reactor Fuel Design Code CEPTAR." Nuclear Technology 156 (2006) 39-55.

Zimmermann H., Investigations on swelling and fission gas behaviour in uranium dioxide, Journal of Nuclear Materials 75 (1978) 154-161.

Venkiteswaran C. N. et al., "Irradiation performance of PFBR MOX fuel after 112GWd/t burn-up." Journal of Nuclear Materials 449 (2014) 31-38.

Y. Onoda, Y. Fukano, I. Sato, C. Marquie, B. Duc, Three-Pin Cluster CABRI Tests Simulating the Unprotected Loss-of-Flow Accident in Sodium-Cooled Fast Reactors, Journal of Nuclear Science and Technology 48 (2011) 188.

Publications

- ***Journal Papers***

i. Dubey A., Sharma A. K., 2018. "Melting and multi-phase flow modelling of nuclear fuel in fast reactor fuel rod", **International Journal of Thermal Sciences**, 125: 256-272.

ii. Dubey A., Sathiyasheela T., Sharma A. K., 2018. "Reactor dynamics of in-pin fuel motion in fast breeder reactors" **Nuclear Engineering and Design** 340: 431-446.

iii. Dubey A., Sathiyasheela T., Sharma A. K., 2019. "In-pin fuel motion dynamics for beginning-of-life core in fast breeder reactors" **Nuclear Engineering and Design** 347: 31-44.

iv. Dubey, A., Sharma, A. K., 2020. "Modelling, verifications and safety feedback assessment of annular fast reactor fuel pins with severe accident code MITRA" **Nuclear Engineering and Design** 364: 110684.

v. Sathiyasheela T., John R., Dubey A., Devan K., "A comparative study of reactivity feedbacks including in-pin motion and their impact on UTOPA in a 600 MW fast reactor", **Nuclear Engineering and Design**, 384: 111443.

- ***Book Chapters***

i. Dubey, A., Sathiyasheela, T., Sharma, A. K., (2019) "Reactivity Effects of In-Pin Fuel Motion in Modern Fast Breeder Reactors". Advances in Interdisciplinary Engineering. Lecture Notes in Mechanical Engineering. Springer, Singapore.

Publications

- ***Conference proceedings***

i. Comparisons of feedback under UTOPA with in pin fuel motion dynamics in fast reactors, Sathiyasheela T., Dubey A., Srinivasan G. S., and K. Devan, International Conference on Fast Reactors and Related Fuel Cycles FR22: Sustainable Clean Energy for the Future (CN-291), International Atomic Energy Agency, Vienna, Austria (April 19-22, 2022).

ii. "Modelling and Verifications of Fast Reactor Fuel Melting and Multi-phase Flow Code MITRA", Dubey A., Sathiyasheela T., Sharma A. K., Proceedings of the 25th National and 3rd International Heat and Mass Transfer Conference (IHMTC), IIT Roorkee, India (December 28-31, 2019).

iii. "Reactor Dynamics Analyses of Fuel Melting in Fast Reactors under UTOPA", Dubey A., Sathiyasheela T., Sharma A. K., Proceedings of the 7th International and 45th National Conference on Fluid Mechanics and Fluid Power (FMFP), IIT Bombay, Mumbai, India (December 10-12, 2018).

iv. "Numerical simulation of in-pin fuel motion during transient overpower accident scenario in fast breeder reactors", Dubey A., Sharma A. K., Naga Sivayya D., Proceedings of the 6th International and 43rd National Conference on Fluid Mechanics and Fluid Power (FMFP), MNIT Allahabad, India (December 15-17, 2016).

Improved predictions of UTOP accident

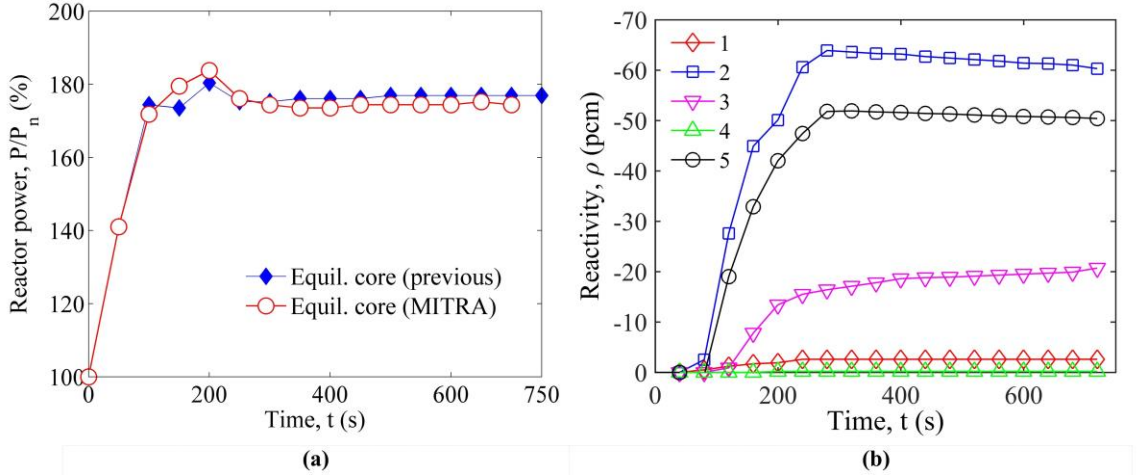

Reactor response a function of time (a) Reactor power history (b) Relocation feedback for zones (1-5). (Equilibrium core (previous) represents results where radial variation in gas retention is neglected; Equilibrium is incorporated)

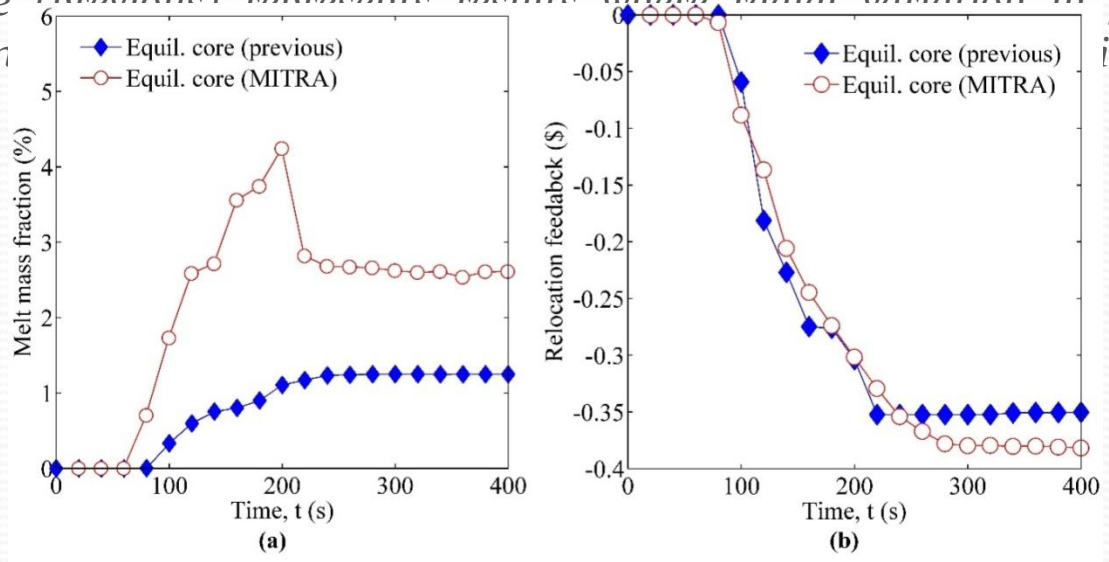

Comparison between earlier and current UTOP simulations; (a) Core averaged melt fraction history (b) Whole core melt feedback history.

Effectiveness of partially annular top blanket columns

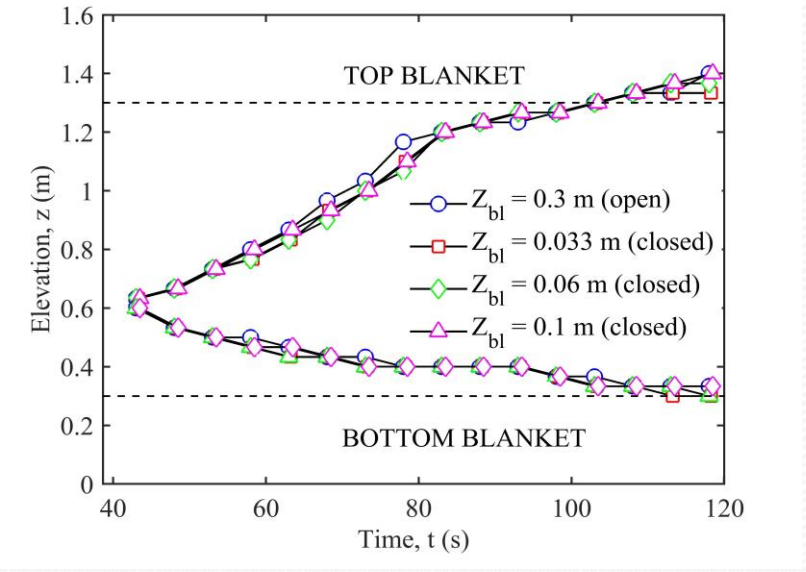

Melt column evolution as a function of the top blanket geometry (Z_{bl}= length of top blanket cavity).

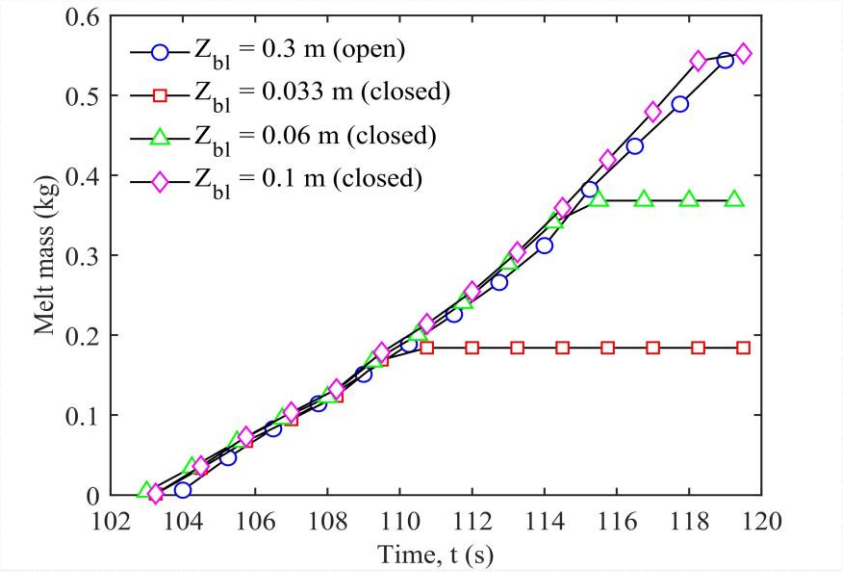

Fuel relocation in top blanket column as a function of top blanket geometry (central subassembly; total fuel mass is 48.8 kg).

Observations

- The pin with ~ 15 annular pellets ($Z_{bl} = 0.1\,m$) in the top blanket removes the same amount of fuel mass from the active core as the pin with fully annular top blanket ($Z_{bl} = 0.3\,m$).
- Improvements in the negative reactivity feedback range between 36-84 % ($Z_{bl} = 0.033 - 0.1\,m$) in comparison with the current annular fuel pin design.

haracteristics

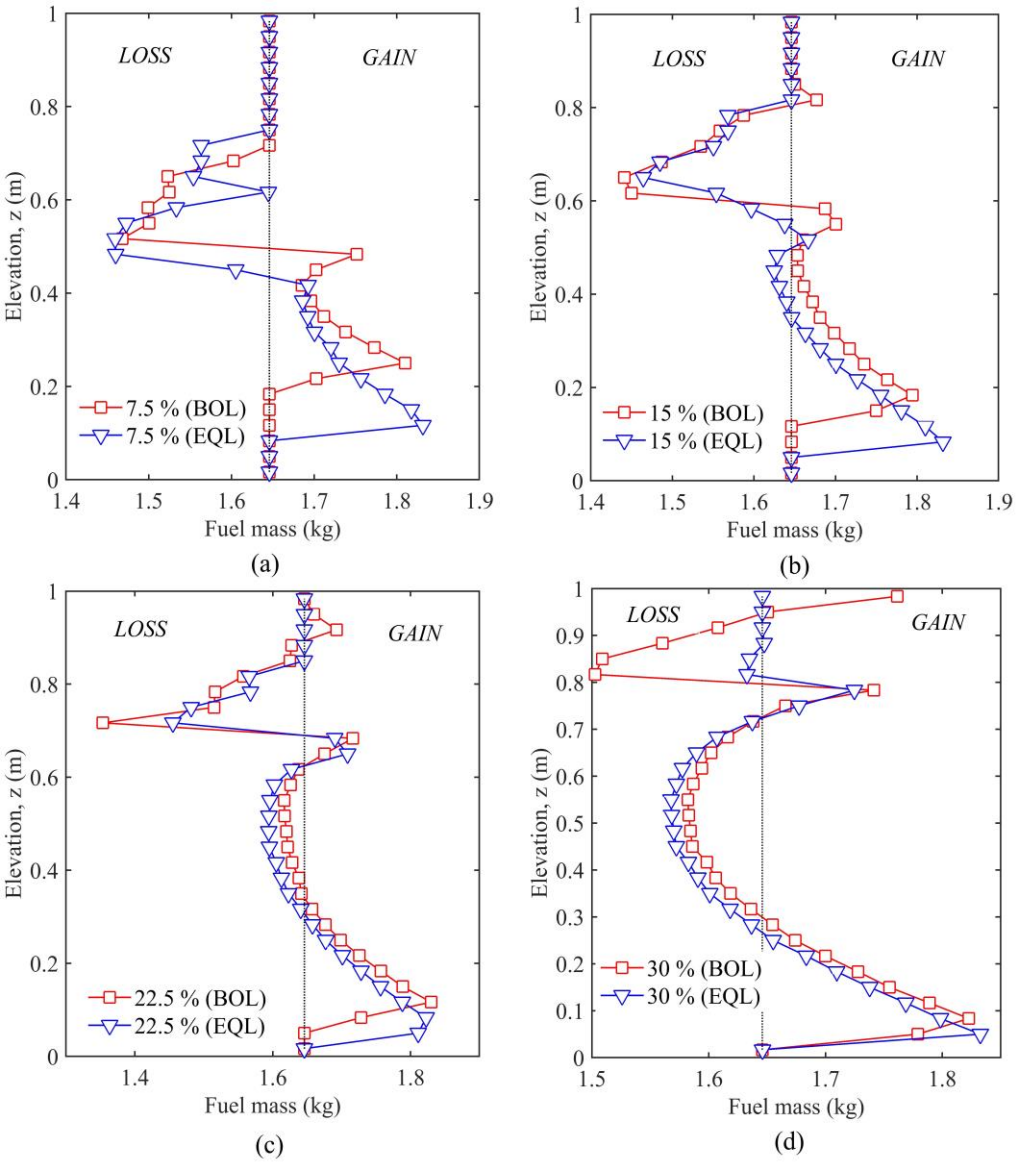

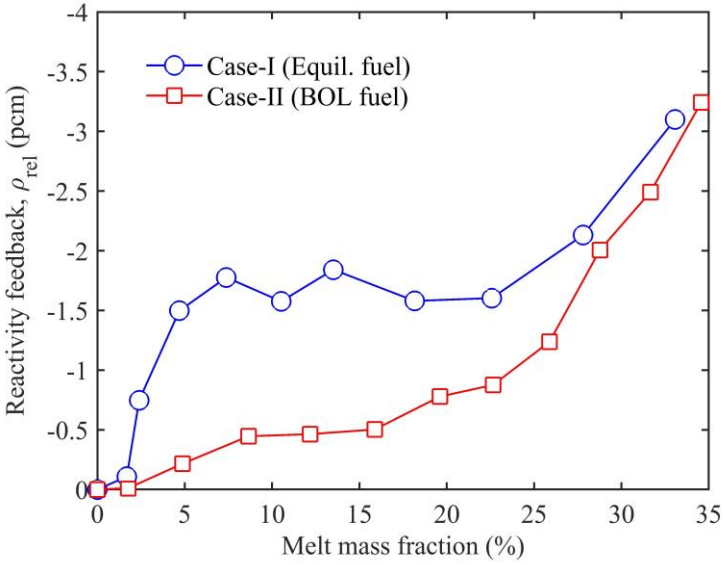

(Melt relocation reactivity feedback characteristics)

						ase-II				
						Δm_{cen}		Δm_{top}	Δm_{bot}	
						0.40		-0.04	0.44	
15	91	79.6	-0.37	-0.41	0.78	64	73.9	-0.20	-0.38	0.58
22.5	99	82.9	-0.30	-0.47	0.77	74	78.6	-0.14	-0.55	0.69
30	106	85.8	-0.67	0.04	0.63	86	84	-0.52	-0.21	0.73

(Table of fuel mass redistribution due to melting and motion (Zone-1, 217 fuel pins). (t = time instant (s); X_{max} = Peak linear power (kW/m)))

Analysis of fuel vapourization

P-H data plots for molten fuel (Saturation vapour curve of molten fuel marks the boundary between liquid and vapour phases)

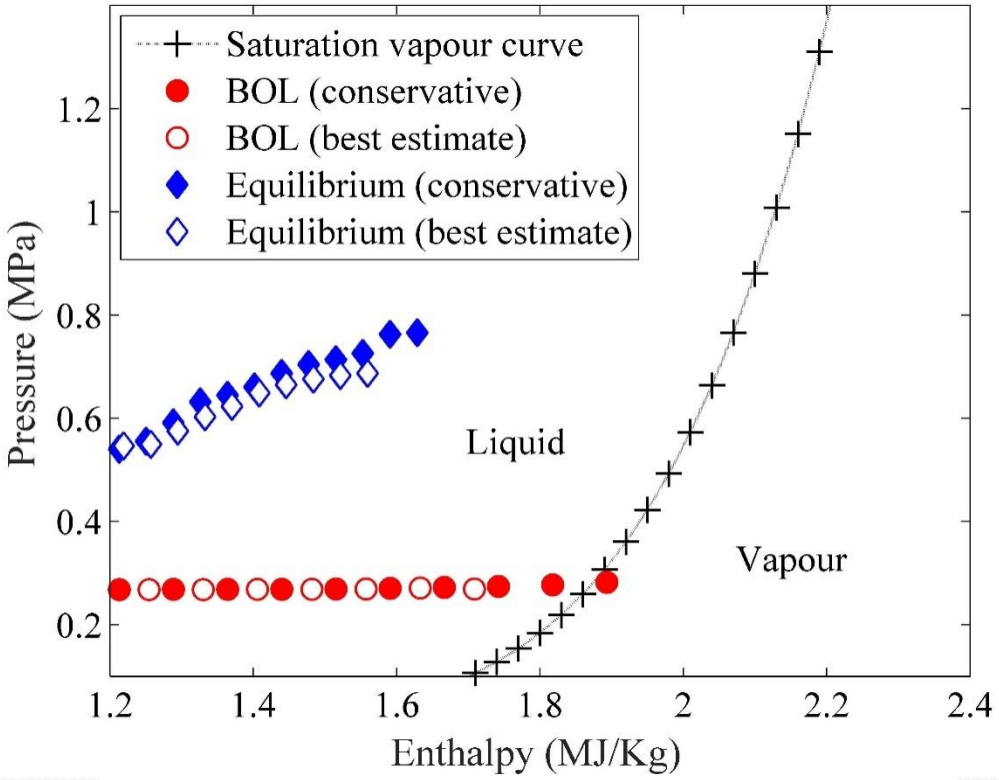

(P-H curves for molten fuel (max. enthalpy points))

- In case of BOL core, the P-H data points cross over in to the vapour zone. The same is not observed in the case of equilibrium core.
- Therefore, there is a greater possibility of fuel vapour formation in the BOL core in comparison with the equilibrium core.
- **There is a greater possibility of fuel vapour formation in the fresh core in comparison with that of equilibrium core.**